PAIN-RELATED NEURAL NETWORKS AND REGULATION MECHANISMS

EDITED BY: Wen Wu, Jie Jia, Fengxian Li, Weiwei Peng and Howe Liu

PUBLISHED IN: Frontiers in Molecular Neuroscience

frontiers Research Topics

ISSN 1664-8714
ISBN 978-2-83250-565-6
DOI 10.3389/978-2-83250-565-6

About Frontiers

Frontiers is more than just an open-access publisher of scholarly articles: it is a pioneering approach to the world of academia, radically improving the way scholarly research is managed. The grand vision of Frontiers is a world where all people have an equal opportunity to seek, share and generate knowledge. Frontiers provides immediate and permanent online open access to all its publications, but this alone is not enough to realize our grand goals.

Frontiers Journal Series

The Frontiers Journal Series is a multi-tier and interdisciplinary set of open-access, online journals, promising a paradigm shift from the current review, selection and dissemination processes in academic publishing. All Frontiers journals are driven by researchers for researchers; therefore, they constitute a service to the scholarly community. At the same time, the Frontiers Journal Series operates on a revolutionary invention, the tiered publishing system, initially addressing specific communities of scholars, and gradually climbing up to broader public understanding, thus serving the interests of the lay society, too.

Dedication to Quality

Each Frontiers article is a landmark of the highest quality, thanks to genuinely collaborative interactions between authors and review editors, who include some of the world's best academicians. Research must be certified by peers before entering a stream of knowledge that may eventually reach the public - and shape society; therefore, Frontiers only applies the most rigorous and unbiased reviews.
Frontiers revolutionizes research publishing by freely delivering the most outstanding research, evaluated with no bias from both the academic and social point of view. By applying the most advanced information technologies, Frontiers is catapulting scholarly publishing into a new generation.

What are Frontiers Research Topics?

Frontiers Research Topics are very popular trademarks of the Frontiers Journals Series: they are collections of at least ten articles, all centered on a particular subject. With their unique mix of varied contributions from Original Research to Review Articles, Frontiers Research Topics unify the most influential researchers, the latest key findings and historical advances in a hot research area! Find out more on how to host your own Frontiers Research Topic or contribute to one as an author by contacting the Frontiers Editorial Office: frontiersin.org/about/contact

PAIN-RELATED NEURAL NETWORKS AND REGULATION MECHANISMS

Topic Editors:
Wen Wu, Southern Medical University, China
Jie Jia, Fudan University, China
Fengxian Li, Southern Medical University, China
Weiwei Peng, Shenzhen University, China
Howe Liu, Allen College, United States

Citation: Wu, W., Jia, J., Li, F., Peng, W., Liu, H., eds. (2022). Pain-Related Neural Networks and Regulation Mechanisms. Lausanne: Frontiers Media SA.
doi: 10.3389/978-2-83250-565-6

Table of Contents

frontiers | Frontiers in Molecular Neuroscience

TYPE Editorial
PUBLISHED 07 October 2022
DOI 10.3389/fnmol.2022.1051335

OPEN ACCESS

EDITED AND REVIEWED BY
Robert John Vandenberg,
The University of Sydney, Australia

*CORRESPONDENCE
Wen Wu
wuwen66@163.com

†These authors have contributed equally to this work and share first authorship

SPECIALTY SECTION
This article was submitted to Pain Mechanisms and Modulators, a section of the journal Frontiers in Molecular Neuroscience

RECEIVED 22 September 2022
ACCEPTED 27 September 2022
PUBLISHED 07 October 2022

CITATION
Wu W, Jia J, Li F, Peng W, Liu H, Chen H and Shi Y (2022) Editorial: Pain-related neural networks and regulation mechanisms. *Front. Mol. Neurosci.* 15:1051335. doi: 10.3389/fnmol.2022.1051335

Editorial: Pain-related neural networks and regulation mechanisms

Wen Wu[1*†], Jie Jia[2†], Fengxian Li[3†], Weiwei Peng[4†], Howe Liu[5†], Hui Chen[1] and Yu Shi[1]

[1]Department of Rehabilitation, Zhujiang Hospital, Southern Medical University, Guangzhou, China, [2]Department of Rehabilitation Medicine, Huashan Hospital, Fudan University, Shanghai, China, [3]Department of Anesthesiology, Zhujiang Hospital, Southern Medical University, Guangzhou, China, [4]School of Psychology, Shenzhen University, Shenzhen, China, [5]Department of Physical Therapy, Allen College, Waterloo, IA, United States

KEYWORDS

pain, neural mechanisms, neural regulation, multiple omics, biomarker, machine learning

Editorial on the Research Topic
Pain-related neural networks and regulation mechanisms

Pain is defined as an unpleasant sensory and emotional experience associated with, or resembling actual or potential tissue damage. However, the pain-related neural networks and regulation mechanisms are still not clearly understood, particularly in the thematic areas of pain biomarkers in multi-omics, molecular mechanism of pain comorbidity, exploration of pain sensitivity, application of machine learning (ML) in solving specific pain problems, and the prospect of research trends in the field of pain. So, we conducted such topical research with a total of 14 articles, including one review, one study protocol, two bibliometric analysis studies, and 10 original quantitative studies.

Biomarkers in pain pathogenesis

The use of high-throughput screening and epigenetic study provides evidence to elucidate the pathogenesis and pathophysiology of disease. Screening biomarkers through multi-omics data is an important approach to study pain-related neural mechanisms. Song et al. explored the effect of swimming exercise on the chronic constriction injury (CCI) rats, and confirmed that exercise can relieve neuropathic pain (NP). They found remarkable differences in the expression of lncRNAs and mRNAs in the CCI rats, and potential biomarkers including Dnah6, Pkd1l2, C3, Adgre1, Plac9, Sgk1, and VGF. Li, Li et al. also studied three diagnostic biomarkers related to immune cell infiltration, and found that five hub genes involved in the pathogenesis might acted as potential genes for target therapy points of lumbar disc herniation as assessed with the bioinformatics analysis. Perhaps we could replicate or conduct with the similar methodology of the aforementioned research to explore more molecular biomarkers

or hub genes to explain the mechanism of pain. In addition, Zhou et al. identified a novel neuron type MAAC (Fxyd7+/Atp1b1+) in dorsal root ganglia of painful diabetic peripheral neuropathy rats with the single-cell RNA sequencing technique, and investigated the transcriptomic characteristics, origin, transition trajectory, regulator and cellular communication. However, this study has not yet thoroughly clarified the role of MAAC in NP.

Neuromorphological approach

Research on the comorbidity of pain, such as emotional disorders and itch, is still in its infancy. Dai et al. exerted significant differences in transcriptomic characteristics between the medial prefrontal cortex (mPFC) and the anterior cingulate cortex (ACC) of mice after spared nerve injury exhibiting acute pain and mild depression. Interestingly, there was sexual dimorphism at the transcriptional level. Furthermore, this study indicated that restoring oligodendrocytes and myelin in the mPFC or extracellular matrix in the ACC may be key to the treatment of pain-depression comorbidity. Overall, this study further highlights the role of the sexually dimorphic brain in neuropsychiatric disorders by examining differences at the neuromorphological and molecular levels. Accordingly, more research studies may be needed to focus on gender differences and its dependent factors, such as sex hormones and genetics, in the pathogenesis and management of pain or its comorbidities. Li, Bai et al. investigated parvalbumin neurons in the in zona incerta that acts as an endogenous negative modulatory center. Up to date, studies have demonstrated that pain, itch, and depression are intricately entangled at anatomical, circuit and molecular levels (Caccavale et al., 2016; Malfliet et al., 2017; Koch et al., 2018; Belinskaia et al., 2019; Roberts et al., 2019; Mihailescu-Marin et al., 2020; Najafi et al., 2021). Therefore, it is very critical to discover the same core pathogenic factors, such as sensory center, among these three symptoms for the future studies.

Study of pain sensitivity

Currently, neuroimaging and neural regulation techniques are widely used in pain study. These techniques may include functional magnetic resonance imaging (fMRI), diffusion tensor imaging (DTI), functional near-infrared spectroscopy (fNIRS), repetitive transcranial magnetic stimulation (rTMS), and transcranial direct current stimulation (tDCS). In this present thematic topic, the pain sensitivity assessed with these techniques seems to be an intriguing point. Zou et al. found that the multi-features (regional homogeneity and connectivity metrics) of multimodal MRI (fMRI and DTI) shows more accurately predictive in anticipating the pain sensitivity. In another study of comparing the effects of three rTMS paradigms on different sensory fibers (Aβ, Aδ, and C fibers) assessed with the fNIRS, Li, Zhang et al. revealed that prolonged continuous theta-burst stimulation can modulate sensitivity on Aβ fibers and affect the activation of dorsolateral prefrontal cortex, frontopolar cortex and other brain regions. Li, Lin et al. directly explored how single session of high-definition tDCS (HD-tDCS) over the primary motor cortex (M1) affects experimental pain sensitivity among healthy participants. Results showed that only anodal HD-tDCS significantly increased cold pain threshold. Interestingly, the effectiveness of anodal HD-tDCS in attenuating pain intensity ratings to suprathreshold pain was dependent upon the level of attentional bias to negative information. It highlights those individual differences in pain-related cognition should be taken into consideration in the clinical applications of tDCS for pain relief.

Disease-specific pain

The neural mechanisms and interventions of specific pain have always been concerned by researchers. Wei, Yang et al. conducted in-depth exploration on migraine without aura (MwoA) and used ML model to study the efficacy of non-steroidal anti-inflammatory drugs (NSAIDs). Their team showed us two high-quality studies on this topic. In Wei, Yang et al., dysfunctional connections within seven networks were observed, including default mode network, executive control network, salience network, sensorimotor network, dorsal attention network, visual network, and auditory network. The support vector machine (SVM) model using the clinical characteristics and functional network connectivity (FNC) abnormalities as features has also proved to be very helpful in predicting efficacy of NSAIDs and improving the decision-making of therapeutic strategy. In Wei, Xu et al., the abnormal functional connectivity (FC) between amygdala and multiple brain regions has been found, which helps to reveal the neural network mechanism of MwoA. At the same time, the multivariable logistic regression (MLR) and SVM models that include disrupted FC patterns from amygdala-based FC analysis and clinical characteristics also show high reliability in verifying the efficacy of NSAIDs, which helps to solve the clinical efficacy problem of MwoA. In other respects, de Souza Moura et al. provided a new study protocol to explore the treatment of head and neck cancer patients under chemoradiation therapy condition with tDCS. The expected results from this proposed study might shed lights on better understanding the neural mechanism of tDCS intervention on the cancer patients.

Pain study in trend

Our topic also focuses on the latest trends in the field of pain to promote research progress. Li, Shu et al. and Du et al. conducted bibliometric analysis on the field of post stroke

pain and diabetic peripheral neuropathic pain, respectively, and provided an analytical method to visualize the trend and frontiers of the above fields. Finally, Yang et al. summarized the research progress of non-invasive brain stimulation (NIBS) in the treatment of different central neuropathic pain (CNP)s and described the effects on alleviating CNPs as well as the underlying mechanisms. It is suggested that the future research should gradually carry out large-scale multi center research to verify the stability and reliability of the analgesic effect induced by NIBS.

To sum up, this paper on the topic "*Neural Networks and Regulatory Mechanisms Associated with Pain*" expands the mechanistic theories, biomarkers and targeted drugs at the neural network and molecular levels in the field of pain.

Author contributions

All authors listed have made a substantial, direct, and intellectual contribution to the work and approved it for publication.

Acknowledgments

We deeply thank all the authors and reviewers who have participated in this Research Topic.

Conflict of interest

The authors declare that the research was conducted in the absence of any commercial or financial relationships that could be construed as a potential conflict of interest.

Publisher's note

References

Belinskaia, D. A., Belinskaia, M. A., Barygin, O. I., Vanchakova, N. P., and Shestakova, N. N. (2019). Psychotropic drugs for the management of chronic pain and itch. *Pharmaceuticals* 12:99. doi: 10.3390/ph12020099

Caccavale, S., Bove, D., Bove, R. M. (2016). Skin and brain: itch and psychiatric disorders. *G. Ital. Dermatol. Venereol.* 151, 525–529. Available online at: https://www.minervamedica.it/en/journals/Ital-J-Dermatol-Venereol/article.php?cod=R23Y2016N05A0525

Koch, S. C., Acton, D., and Goulding, M. (2018). Spinal circuits for touch, pain, and itch. *Annu. Rev. Physiol.* 80, 189–217. doi: 10.1146/annurev-physiol-022516-034303

Malfliet, A., Coppieters, I., Van Wilgen, P., Kregel, J., De Pauw, R., and Dolphens, M., et al. (2017). Brain changes associated with cognitive and emotional factors in chronic pain: a systematic review. *Eur. J. Pain* 21, 769–786. doi: 10.1002/ejp.1003

Mihailescu-Marin, M. M., Mosoiu, D. V., Burtea, V., Sechel, G., Rogozea, L. M., and Ciurescu, D. (2020). Common pathways for pain and Depression-Implications for practice. *Am. J. Ther.* 27, e468–e476. doi: 10.1097/MJT.0000000000001235

Najafi, P., Dufor, O., Ben, S. D., Misery, L., and Carre, J. L. (2021). Itch processing in the brain. *J. Eur. Acad. Dermatol. Venereol.* 35, 1058–1066. doi: 10.1111/jdv.17029

Roberts, C. A., Giesbrecht, T., Stancak, A., Fallon, N., Thomas, A., and Kirkham, T. C. (2019). Where is itch represented in the brain, and how does it differ from pain? An activation likelihood estimation meta-analysis of experimentally-induced itch. *J. Invest. Dermatol.* 139, 2245–2248. doi: 10.1016/j.jid.2019.04.007

frontiers in Molecular Neuroscience

ORIGINAL RESEARCH
published: 24 February 2022
doi: 10.3389/fnmol.2022.819507

Disrupted Functional Connectivity of the Amygdala Predicts the Efficacy of Non-steroidal Anti-inflammatory Drugs in Migraineurs Without Aura

Heng-Le Wei[1†], Chen-Hui Xu[2†], Jin-Jin Wang[1†], Gang-Ping Zhou[1], Xi Guo[1], Yu-Chen Chen[3], Yu-Sheng Yu[1], Zhen-Zhen He[1], Xindao Yin[3], Junrong Li[2] and Hong Zhang[1*]*

[1] Department of Radiology, The Affiliated Jiangning Hospital of Nanjing Medical University, Nanjing, China, [2] Department of Neurology, The Affiliated Jiangning Hospital of Nanjing Medical University, Nanjing, China, [3] Department of Radiology, Nanjing First Hospital, Nanjing Medical University, Nanjing, China

OPEN ACCESS

Edited by:
Weiwei Peng,
Shenzhen University, China

Reviewed by:
Linling Li,
Shenzhen University, China
Xiang Kong,
Nanjing General Hospital of Nanjing Military Command, China
Shuang Qiu,
Institute of Automation (CAS), China

***Correspondence:**
Junrong Li
ljry612@163.com
Hong Zhang
jnyyfsk@126.com

[†] These authors share first authorship

Specialty section:
This article was submitted to Pain Mechanisms and Modulators, a section of the journal Frontiers in Molecular Neuroscience

Received: 21 November 2021
Accepted: 07 February 2022
Published: 24 February 2022

Citation:
Wei H-L, Xu C-H, Wang J-J, Zhou G-P, Guo X, Chen Y-C, Yu Y-S, He Z-Z, Yin X, Li J and Zhang H (2022) Disrupted Functional Connectivity of the Amygdala Predicts the Efficacy of Non-steroidal Anti-inflammatory Drugs in Migraineurs Without Aura. Front. Mol. Neurosci. 15:819507. doi: 10.3389/fnmol.2022.819507

Machine learning (ML) has been largely applied for predicting migraine classification. However, the prediction of efficacy of non-steroidal anti-inflammatory drugs (NSAIDs) in migraine is still in the early stages. This study aims to evaluate whether the combination of machine learning and amygdala-related functional features could help predict the efficacy of NSAIDs in patients with migraine without aura (MwoA). A total of 70 MwoA patients were enrolled for the study, including patients with an effective response to NSAIDs (M-eNSAIDs, n = 35) and MwoA patients with ineffective response to NSAIDs (M-ieNSAIDs, n = 35). Furthermore, 33 healthy controls (HCs) were matched for age, sex, and education level. The study participants were subjected to resting-state functional magnetic resonance imaging (fMRI) scanning. Disrupted functional connectivity (FC) patterns from amygdala-based FC analysis and clinical characteristics were considered features that could promote classification through multivariable logistic regression (MLR) and support vector machine (SVM) for predicting the efficacy of NSAIDs. Further, receiver operating characteristic (ROC) curves were drawn to evaluate the predictive ability of the models. The M-eNSAIDs group exhibited enhanced FC with ipsilateral calcarine sulcus (CAL), superior parietal gyrus (SPG), paracentral lobule (PCL), and contralateral superior frontal gyrus (SFG) in the left amygdala. However, the M-eNSAIDs group showed decreased FC with ipsilateral caudate nucleus (CAU), compared to the M-ieNSAIDs group. Moreover, the M-eNSAIDs group showed higher FC with left pre-central gyrus (PreCG) and post-central gyrus (PoCG) compared to HCs. In contrast, the M-ieNSAIDs group showed lower FC with the left anterior cingulate cortex (ACC) and right SFG. Furthermore, the MwoA patients showed increased FC with the left middle frontal gyrus (MFG) in the right amygdala compared to HCs. The disrupted left amygdala-related FC patterns exhibited significant correlations with migraine characteristics in the M-ieNSAIDs group. The MLR and SVM models discriminated clinical efficacy of NSAIDs with an area under the curve (AUC) of 0.891 and

0.896, sensitivity of 0.971 and 0.833, and specificity of 0.629 and 0.875, respectively. These findings suggest that the efficacy of NSAIDs in migraine could be predicted using ML algorithm. Furthermore, this study highlights the role of amygdala-related neural function in revealing underlying migraine-related neuroimaging mechanisms.

Keywords: migraine, amygdala, functional connectivity, machine learning, non-steroidal anti-inflammatory drugs

INTRODUCTION

Migraine is the leading cause of disability among young women. Moreover, it is the second leading cause of disability worldwide affecting over 15% of the population (GBD 2015 Disease and Injury Incidence and Prevalence Collaborators, 2016). It is a common prevalent neurological disorder characterized by recurrent moderate to severe headaches and is aggravated by physical activity. Non-steroidal anti-inflammatory drugs (NSAIDs), sedatives and opioids, are often used for the management of migraine (Tfelt-Hansen, 2021). In particular, NSAIDs are considered first-line drugs for the treatment of migraine attacks (Ashina, 2020). Nonetheless, NSAIDs have unsatisfactory therapeutic outcomes in a considerable percentage of the patients due to inter-individual variability (Biglione et al., 2020). Moreover, it has been shown that migraineurs who tend to overuse NSAIDs suffer from treatment-resistant headaches and cognitive decline more frequently (Cai et al., 2019). In addition, it was shown in an observational study that migraine patients with or without medication overuse had an increased risk of developing depression. Moreover, migraineurs with medication-overuse had a higher prevalence of depression (Mose et al., 2018). Of note, NSAIDs-induced addiction, cognitive dysfunction and psychiatric disorders are suggestive of central nervous system (CNS) abnormalities in migraine progression, which may lead to unsatisfactory results with the migraine-specific treatments. Furthermore, there is a need to have further understanding of inter-individual variability affecting the response to NSAIDs to allow optimization of therapy.

Endogenous bioactive lipids are critical mediators in hyperalgesia (Patel and Dickenson, 2021). The inhibition of the cyclooxygenase (COX) enzymes and subsequently the synthesis of prostaglandins are the mechanism of action of NSAIDs to tackle the most common forms of hyperalgesia. The COX metabolic hubs are involved in the ascending and descending pathways that modulate nociceptive signaling, including the paraventricular nucleus, prefrontal cortex, amygdala, thalamus, and periaqueductal gray (Buisseret et al., 2019). Due to the complex pathophysiology of migraine, it is described as a disabling neurolimbic pain disorder (Tolner et al., 2019). The amygdala, a core region of the neurolimbic system, plays a crucial role in regulating the top-down nociceptive pathway (Maizels et al., 2012; Minen et al., 2016). On the one hand, seed-based whole-brain functional connectivity (FC) and Granger causality analyses revealed that migraine sufferers exhibit aberrant connectivity between the amygdala and the higher cortex (Wei et al., 2020b; Huang et al., 2021). On the other hand, some studies suggested recurrent nociceptive input could affect the anatomical pattern of the amygdala, and these changes may explain the functional abnormalities in migraine patients (Jia and Yu, 2017). Besides, the amygdala is implicated in analgesic response to NSAIDs. Furthermore, the analgesic effects of NSAIDs are mediated *via* the descending pain inhibitory pathways (Hodkinson et al., 2015). Studies have shown that antinociceptive tolerance to NSAIDs is associated with disrupted amygdala-related FC patterns. However, studies on amygdala-related functional changes for predicting efficacy to NSAIDs in migraine have not been conducted. Multivariable analysis was used to detect group differences. However, neuroimaging-based predictions are required to identify differences at the individual level. Machine learning (ML) provides a complementary strategy to guide individual-level prediction by integrating neuroimaging and clinical features. Although several recent studies used ML methods to investigate migraine-related features, such as classification, frequency, and the efficacy of acupuncture (Chong et al., 2017; Mu et al., 2020; Yin et al., 2020), only a few studies used ML algorithms to predict the efficacy of NSAIDs in migraine.

In this study, the bilateral amygdalae were selected as the seed regions for FC analysis. The study only included patients with migraine without aura (MwoA), the most common subtype, to reduce potential interference due to heterogeneity. We hypothesized that the amygdala-related abnormalities could guide in predicting the efficacy of NSAIDs in MwoA patients. Herein, we established a conventional multivariable logistic regression (MLR) and support vector machine (SVM) models, to predict the efficacy of NSAIDs. These models could help clinicians optimize therapeutic effectiveness of medications used to manage migraine at the individual level.

MATERIALS AND METHODS

Participants

A total of 73 patients diagnosed with episodic MwoA were recruited. A diagnosis of migraine was based on the International Classification of Headache Disorders, 3rd edition (ICHD-3) (Headache Classification Committee of the International Headache Society (IHS), 2013). To reduce potential physiological and pharmacological effects, the inclusion criteria were (1) MwoA patients not taking medications for at least 1 month before enrollment; (2) migraineurs who were headache-free for at least 3 days before and after the scanning. In addition, 33 healthy subjects (all right-handed) matched for age, sex, and education level were recruited as healthy controls (HCs). The exclusion criteria were: (1) comorbidities with other forms of headache; (2) history of psychiatric diseases or severe brain

injury; (3) history of drug use disorders; (4) pregnant women, and (5) any contraindication to magnetic resonance imaging (MRI) examination. Each patient was required to keep a headache diary and complete a semi-structured questionnaire on demographic variables, clinical data, headache profile and past medical history. The study protocol was reviewed and approved by the ethics committee and review boards of the Affiliated Jiangning Hospital of Nanjing Medicine University. All study participants signed a written informed consent.

Clinical Characteristics

All migraineurs underwent cognitive impairment screening using Montreal Cognitive Assessment (MoCA) to evaluate the cognitive condition. All the participants had MoCA scores of above twenty-five. In addition, the severity and impact of headaches were assessed using the Visual Analogue Scale (VAS) and the Headache Impact Test six-item scale (HIT-6). Furthermore, headache-related disability was quantified using the migraine disability assessment (MIDAS). The MwoA patients were instructed to record pain intensity before and 2 h after taking the medicine. Complete, partial, minimal, and no responses were classified as >75, 50–75, 25–50, and <25% reduction in pain intensity, respectively. Response to NSAIDs was defined as a 50% or greater reduction in VAS scores between the pre-treatment level and 2 h after taking medication.

Imaging Data Acquisition

Imaging data were obtained using a 3.0 T MRI scanner (Ingenia) with an eight-channel head coil. The foam padding and earplugs were used to reduce head motion and scanner noise. Structural images were acquired with a three-dimensional turbo fast echo T1-weighted imaging sequence as follows: repetition time (TR)/echo time (TE) = 8.1/3.7 ms; slices = 170; thickness = 1 mm; flip angle (FA) = 8°; acquisition matrix = 256 × 256; field of view (FOV) = 256 mm × 256 mm. Functional images were obtained axially as follows: TR = 2000 ms; TE = 30 ms; slices = 36; thickness = 4 mm; FOV = 240 mm × 240 mm; acquisition matrix = 64 × 64; and FA = 90°. All participants were required to stay awake without thinking anything.

Data Analyses

Data analyses were preprocessed using the resting-state functional MRI (Rs-fMRI) Data Analysis Toolkit plus (RESTplus[1]). The first 10 volumes were discarded to minimize the effect of signal instability. Slice-timing with the middle slice as reference and realignment for head motion correction were performed. Participants with head motion > 2.0 mm translation or a 2.0° rotation in any direction were excluded. Then, the data were spatial normalized to the Montreal Neurological Institute template (resampling voxel size =°3 mm^3 × 3 mm^3 × 3 mm^3). Six head motion parameters and mean time series of white matter (WM) and cerebrospinal fluid (CSF) were included in the regression analysis to eliminate possible effects on the results. Subsequently, detrended, filtered (0.01–0.08 Hz), and smoothed with an isotropic Gaussian kernel [full width at half maximum (FWHM) = 6 mm] were implemented. The WFU_PickAtlas software was used to extract the seed regions of interest (ROIs) of the bilateral amygdalae. The mean time series of each amygdala was computed as a reference time course. After that, Pearson correlation coefficients were calculated between the mean signal change of each ROI and the voxels. Finally, Fisher's z-transformation was applied to improve the normality of the correlation coefficients.

Structural Analysis

Structural images were processed based on the voxel-based morphometry (VBM8) toolbox.[2] Briefly, cerebral tissues were segmented into gray matter (GM), WM, and CSF using the unified segmentation model. GM and WM volumes were calculated by estimating these segments. The brain parenchyma volume was defined as the sum of GM and WM. Subsequently, the GM and WM images were smoothed using a 10-mm FWHM Gaussian kernel. Statistical analysis of the whole-brain GM was performed at the voxel level with family-wise error (FWE) correction for multiple comparisons ($p < 0.05$) or an uncorrected threshold ($p < 0.001$, cluster size > 100), with age, sex, and education as covariates of no interest.

Construction of the Multivariable Logistic Regression and Support Vector Machine Models

Univariable regression analysis was performed using the demographics, clinical characteristics and abnormal FC patterns. Only variables with $p < 0.05$ in the univariate analysis were included in the MLR model to identify independent risk factors affecting NSAIDs efficacy. Additionally, the migraineurs were randomly assigned to the training group (80%) and testing group (20%). The SVM model was constructed based on the demographic variables, clinical features and abnormal amygdala-related FC patterns between the two migraine subgroups through a five-fold cross-validation strategy on the training group. Further, the training group was randomly divided into five equal sized subgroups. Four of these subgroups were used as an intra-training set, whereas, the remaining subgroup was used as an intra-validation set. In each run, four subgroups were used to develop the classifier while the remaining subgroup was used to verify accuracy of the classifier. Subsequently, the SVM model was tested using the testing group. Finally, the receiver operating characteristic (ROC) curves and values of sensitivity, specificity, and area under the curve (AUC) values were obtained.

Statistical Analysis

The SPSS software (version 25.0) was used for statistical analyses. Differences in the demographic and clinical characteristics were analyzed using a one-way analysis of variance (ANOVA) or a two-sample *t*-test for normally distributed data. In addition, the Kruskal-Wallis test or Mann-Whitney *U*-test were used to determine differences in non-normally distributed data. The Chi-square test was used to determine differences in categorical

[1]http://restfmri.net/forum/

[2]http://dbm.neuro.uni-jena.de/vbm

variables. Significant voxel time courses (FWE correction for multiple comparisons, $p < 0.05$) were considered to determine the functional connection of the amygdala-related FC patterns. Age, sex, and education were considered as nuisance covariate. Furthermore, the Pearson correlation was used to analyze the correlation between the amygdala-related dysfunctional connectivity across the three groups and the corresponding clinical characteristics of each migraine subgroups. A p-value of less than 0.05 was considered statistically significant.

RESULTS

Demographics and Clinical Characteristics

Three patients were excluded from the study due to excessive head movement. Therefore, the final cohort included 35 MwoA patients who were effectively managed with NSAIDs (M-eNSAIDs), 35 MwoA patients with ineffective response to NSAIDs (M-ieNSAIDs), and 33 healthy participants. The demographics and clinical characteristics of the study participants are shown in **Table 1**. There were no significant differences in demographic and clinical characteristics observed across the groups ($p > 0.05$).

Voxel Based Morphometry Results

There were no significant differences in total brain volume, including the GM volume, WM volume, and parenchyma volume among the three groups (**Table 1**). Moreover, structural analysis of the GM did not reveal any significant brain region, at a liberal threshold of $p < 0.001$ (uncorrected) or a stringent level of $p < 0.05$ (FWE correction).

Functional Connectivity Between Effective Response to Non-steroidal Anti-inflammatory Drugs and Ineffective Response to Non-steroidal Anti-inflammatory Drugs

The brain regions with increased FC of the left amygdala mainly located in the right superior frontal gyrus (SFG), left calcarine sulcus (CAL), left superior parietal gyrus (SPG) and paracentral lobule (PCL), and these with decreased FC located in the ipsilateral caudate nucleus (CAU) in the M-eNSAIDs patients compared to the M-ieNSAIDs patients. However, the right amygdala did not observe any disruption in FC between the two migraine subgroups (**Figure 1** and **Table 2**).

Functional Connectivity Between Effective Response to Non-steroidal Anti-inflammatory Drugs and Healthy Controls

The brain regions with increased FC of the left amygdala primarily included the left precentral gyrus (PreCG) and post-central gyrus (PoCG), and with increased FC of the right amygdala included the left middle frontal gyrus (MFG) in the M-eNSAIDs patents, compared to the HCs (**Figure 1** and **Table 2**).

Functional Connectivity Between Ineffective Response to Non-steroidal Anti-inflammatory Drugs and Healthy Controls

The study found decreased FC of the left amygdala with the right SFG and left anterior cingulate cortex (ACC), as well as increased FC of the right amygdala with the left MFG in the M-ieNSAIDs patients, compared to the HCs (**Figure 1** and **Table 2**).

Functional Connectivity Between Migraine Without Aura Patients and Healthy Controls

The study found increased FC of the left amygdala with the right middle occipital gyrus (MOG) ($x = 36$, $y = -96$, $z = 6$; cluster size = 77; $t = 4.3239$), as well as increased FC of the right amygdala with the right MOG ($x = 39$, $y = -93$, $z = 6$; cluster size = 60; $t = 3.7749$), left IFG ($x = -48$, $y = 45$, $z = 0$; cluster size = 71; $t = 3.4334$) and left MFG ($x = -51$, $y = 30$, $z = 33$; cluster size = 61; $t = 3.9930$) in the MwoA group, compared to the HCs.

Correlation Analysis

Significant correlations were observed between the FC of the left amygdala-CAL and MIDAS scores ($r = -0.371$, $p = 0.037$) and FC of the amygdala-CAU and VAS scores ($r = 0.438$, $p = 0.012$) in the M-ieNSAIDs group (**Figure 2**). In contrast, there was no significant correlation between the FC of the right amygdala and the clinical characteristics.

Multivariable Logistic Regression and Support Vector Machine Models

The MLR analysis showed that abnormal FC patterns in the left amygdala with ipsilateral CAL and CAU were independent risk factors affecting the efficacy of NSAIDs (**Table 3**). The MLR and SVM models discriminated clinical efficacy of NSAIDs with an area under the curve (AUC) of 0.891 and 0.896, sensitivity of 0.971 and 0.833, and specificity of 0.629 and 0.875, respectively (**Figure 3**).

DISCUSSION

To the best of our knowledge, this was the first study conducted to predict the clinical efficacy of NSAIDs in MwoA patients. The study evaluated abnormal amygdala-related FC patterns between M-eNSAIDs and M-ieNSAIDs groups using the SVM classifier. The study revealed that the SVM classifier demonstrated predictive ability with an accuracy of more than 89%, treating abnormal amygdala-related FC patterns and clinical characteristics as features of interest. The present study demonstrated that the amygdala showed stronger FCs with some higher cognitive regions, including the limbic system, visual cortex and prefrontal cortex in MwoA patients compared

TABLE 1 | The clinical characteristics of the subjects.

	M-eNSAIDs	M-ieNSAIDs	HCs	*F*/*t*/χ2	*P*-value
Age (years)	33.91 ± 10.75	35.69 ± 11.47	36.30 ± 10.38	0.445	0.642
Sex (male/female)	3/32	4/31	2/31	0.669	0.907
Education (years)	13.54 ± 2.81	13.11 ± 3.08	12.39 ± 4.06	1.020	0.364
Disease duration (years)	7.94 ± 6.15	11.60 ± 10.08	/	−1.832	0.071
Frequency (times/month)	4.77 ± 3.15	5.23 ± 5.76	/	−0.412	0.682
Attack duration (hours)	17.31 ± 13.81	17.03 ± 15.05	/	0.083	0.934
VAS score	6.40 ± 1.54	5.97 ± 1.65	/	1.123	0.265
MIDAS score	38.97 ± 32.26	37.29 ± 31.78	/	0.220	0.826
HIT-6 score	57.57 ± 8.86	60.34 ± 9.41	/	−1.269	0.209
Gray matter (mm^3)	613.88 ± 57.32	605.51 ± 47.31	595.21 ± 47.08	1.147	0.322
White matter (mm^3)	516.05 ± 42.63	500.82 ± 54.28	502.22 ± 45.26	1.083	0.343
Parenchyma (mm^3)	1129.93 ± 87.57	1106.33 ± 91.70	1097.43 ± 82.43	1.267	0.286

HCs, healthy controls; HIT, headache impact test; M-eNSAIDs, migraine without aura with effective NSAIDs; M-ieNSAIDs, migraine without aura with ineffective NSAIDs; MIDAS, migraine disability assessment scale; NSAIDs, non-steroidal anti-inflammatory drugs; VAS, visual analogue scale.

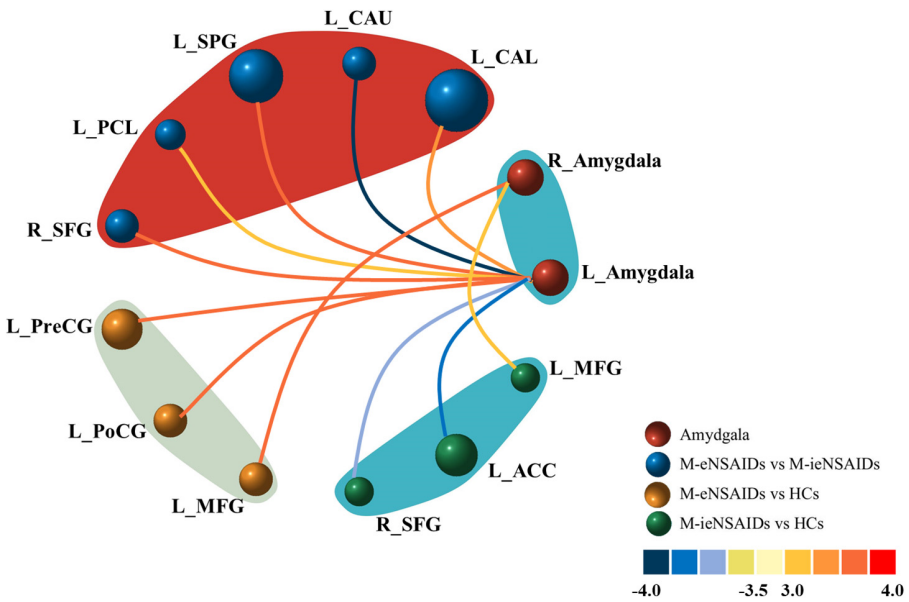

FIGURE 1 | Abnormal functional connectivity of the left amygdala among the three groups. ACC, anterior cingulate cortex; CAL, calcarine sulcus; CAU, caudate nucleus; FC, functional connectivity; HCs, healthy controls; M-eNSAIDs, migraine without aura with effective NSAIDs; M-ieNSAIDs, migraine without aura with ineffective NSAIDs; MFG, middle frontal gyrus; NSAIDs, non-steroidal anti-inflammatory drugs; PCL, paracentral lobule; PoCG, post-central gyrus; PreCG, precentral gyrus; SFG, superior frontal gyrus; SPG, superior parietal gyrus; L, left; R, right.

to the HCs, consistent with previous studies (Wei et al., 2020b; Huang et al., 2021). The higher cognitive regions are involved in the top-down pain control circuit. Therefore, a disrupted circuit may lead to enhanced pain sensitivity. The right lateralization of the amygdala plays a dominant role in the modulation of pain processing and negative emotions (Jiang et al., 2014). In animal models, increased activation of the right amygdala induced by the extracellular signal-regulated kinase triggers hypersensitivity (Carrasquillo and Gereau, 2008). Moreover, blocking the activation of the right amygdala significantly decreases mechanical hypersensitivity (Ji and Neugebauer, 2009). These results suggest that the lateralized activation of the right amygdala mediates the generation and maintenance of pain. In the present study, there was increased left lateralization of the amygdala-related FC in the M-eNSAIDs group compared to the M-ieNSAIDs group. These results suggest that the neural function of the left amygdala plays an important role in determining the effectiveness of NSAIDs. In addition, the findings provide novel insights into the underlying neurophysiological mechanisms in migraine.

Compared to the M-ieNSAIDs group, these findings indicated a significant increase of FC pattern between the left amygdala and ipsilateral CAL in the M-eNSAIDs group. During the interictal and ictal periods, MwoA patients could develop visual, auditory and olfactory hypersensitivity. Photophobia is the most prevalent symptom. Then hyperexcitability of the visual cortex is considered the neural basis of hypersensitivity to light (Mulleners et al., 2001). Generally, the CAL is considered the core region of

TABLE 2 | The regions with changed functional connectivity of amygdala among the three groups.

	Brain regions	MNI coordinates *x, y, z*	Cluster size	*T* value
L_Amygdala				
M-eNSAIDs vs. M-ieNSAIDs	L_CAL	−6, −96, 12	43	3.753
	L_CAU	−6, 15, 9	23	−3.924
	L_SPG	−18, −60, 66	37	3.648
	L_PCL	−6, −36, 72	21	3.242
	R_SFG	21, 42, −18	23	3.712
M-eNSAIDs vs. HCs	L_PreCG	−30, −18, 51	28	3.801
	L_PoCG	−27, −30, 72	23	3.849
M-ieNSAIDs vs. HCs	R_SFG	21, 42, −15	23	−3.647
	L_ACC	−6, 42, 3	20	−3.759
R_Amygdala				
M-eNSAIDs vs. HCs	L_MFG	−54, 30, 27	29	3.525
M-ieNSAIDs vs. HCs	L_MFG	−42, 48, −3	20	3.238

ACC, anterior cingulate cortex; CAL, calcarine sulcus; CAU, caudate nucleus; FC, functional connectivity; HCs, healthy controls; M-eNSAIDs, migraine without aura with effective NSAIDs; M-ieNSAIDs, migraine without aura with ineffective NSAIDs; MFG, middle frontal gyrus; NSAIDs, non-steroidal anti-inflammatory drugs; PCL, paracentral lobule; PoCG, post-central gyrus; PreCG, pre-central gyrus; SFG, superior frontal gyrus; SPG, superior parietal gyrus; L, left; R, right.

the primary visual cortex and is critical in the trigeminovascular pathway, which is essential for the underlying neuromechanism of migraine. Considering the complex functional connection of the dorsal and ventral visual pathways, the CAL may integrate multi-sensory information. Several previous studies revealed functional changes in the visual cortex in migraine patients, which are thought to modulate nociceptive perception (Wei et al., 2019, 2021). In this study, increased amygdala-CAL FC had a negative correlation with the MIDAS scores in M-ieNSAIDs patients. In addition, the MLR model showed amygdala-visual FCs which were shown to positively affect the efficacy of NSAIDs. These findings suggest that amygdala-visual dysfunctional patterns could affect the response to NSAIDs in migraine.

Furthermore, decreased interaction between the left amygdala and ipsilateral striatum region mainly located in CAU was observed in the M-eNSAIDs group. The putamen together with CAU forms the dorsal striatum. Functional neuroimaging studies (Chong et al., 2019) showed that central nervous system mechanisms are critical in understanding the pathophysiology of migraine and indicated the addictive behavior in the brain reward system, including the periaqueductal gray, limbic system and striatum. As a critical region in the reward circuit, the CAU is involved in regulating the transmission of nociceptive inputs to the limbic system from the brainstem. Therefore, abnormal FC patterns in these areas could directly affect the processing of nociceptive information in the reward circuit. Moreover, a previous study employing arterial spin labeling (ASL) (Hodkinson et al., 2015) revealed that hyperactivation of the limbic and striatum regions is involved in the neuro-regulatory mechanism of post-operative analgesia with NSAIDs. Similarly, the current study showed that a dysfunctional amygdala-CAU was an independent risk factor for ineffective treatment response in migraineurs. Moreover, it showed a significant positive correlation with pain severity. This suggests that severe headaches could promote the complexity of migraine treatment and reduce efficacy to NSAIDs. Consequently, ineffective treatment outcomes could increase the risk of using higher drug doses, which may cause medication-overuse headaches. Excessive use of analgesics is associated with some adverse events, such as hepatotoxicity, nephrotoxicity or abnormal striatal function (Fumal et al., 2006). These phenomena influence each other and perpetuate a vicious cycle. In this study, the M-eNSAIDs group showed significantly enhanced FC between the left amygdala and SPG and PCL compared to the M-ieNSAIDs group. The brain regions are located in the trigeminovascular pathway and are involved in the modulation of pain (Russo et al., 2018). Furthermore, MwoA patients receiving acupuncture treatment demonstrated significantly lower FC patterns between the bilateral amygdalae and pain-related regions

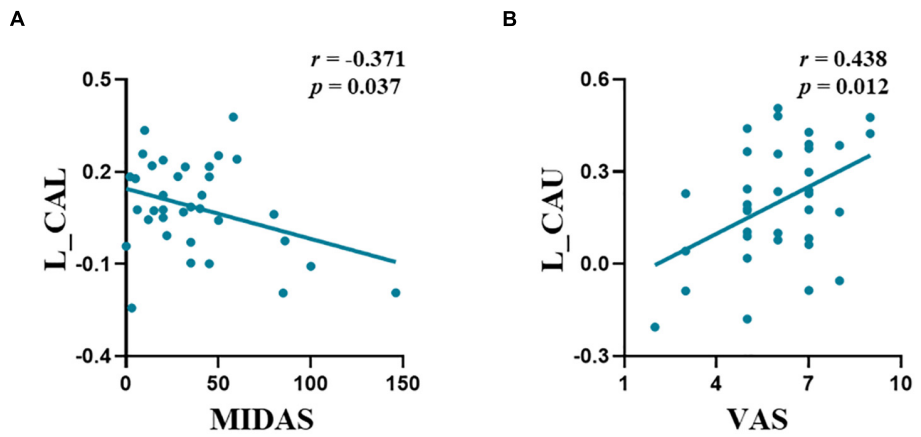

FIGURE 2 | The abnormal functional connectivity patterns of the left amygdala showed significant correlations with migraine characteristics in M-ieNSAIDs **(A,B)**. CAL, calcarine sulcus; CAU, caudate nucleus; M-eNSAIDs, migraine without aura with effective NSAIDs; M-ieNSAIDs, migraine without aura with ineffective NSAIDs; MIDAS, migraine disability assessment scale; NSAIDs, non-steroidal anti-inflammatory drugs; PoCG, post-central gyrus; PreCG, pre-central gyrus; VAS, visual analogue scale; L, left.

TABLE 3 | Univariable and multivariable logistic regression models.

	B	SE	Wald	Unadjusted		Adjusted	
				P	OR (95% CI)	*P*	OR (95% CI)
L_Amygdala–L_CAL	0.680	0.202	11.344	0.001	1.973 (1.329–2.930)	0.012	1.811 (1.139–2.880)
L_Amygdala–L_CAU	−0.656	0.180	13.314	0.000	0.519 (0.365–0.738)	0.002	0.521 (0.347–0.783)
L_Amygdala–R_SFG	0.425	0.136	9.848	0.002	1.530 (1.173–1.996)	/	/
L_Amygdala–L_PCL	0.500	0.159	9.840	0.002	1.649 (1.206–2.253)	/	/
L_Amygdala–L_SPG	0.585	0.176	11.070	0.001	1.796 (1.272–2.535)	/	/

OR, odds ratio; SE, standard deviation. ACC, anterior cingulate cortex; CAL, calcarine sulcus; CAU, caudate nucleus; CI, confidence interval; PCL, paracentral lobule; SFG, superior frontal gyrus; SPG, superior parietal gyrus; L, left; R, right.

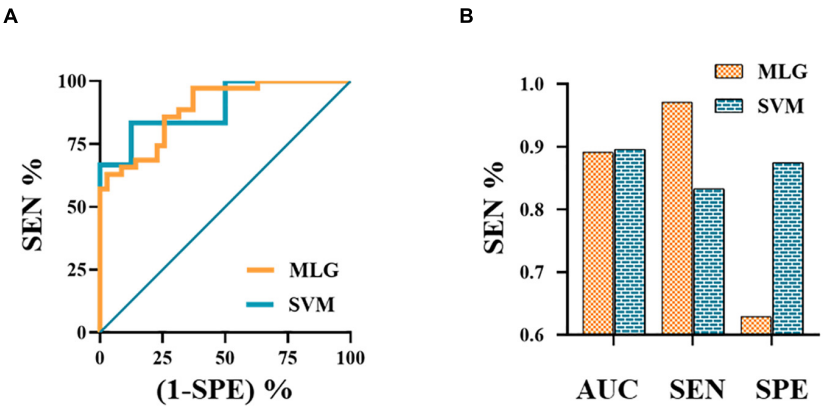

FIGURE 3 | The ROC curves of MLG and SVM models **(A)**. The ROC curve of MLG model based on the anxiety scores and abnormal functional connectivity of the left amygdala with ipsilateral calcarine sulcus and caudate nucleus. The values of AUC, sensitivity and specificity of MLG and SVM were 0.891, 0.971, 0.629 and 0.896, 0.833, 0.875, respectively **(B)**. AUC, area under the curve; MLG, multivariable logistic regression; ROC, receiver operating characteristic; SEN, sensitivity; SPE, specificity; SVM, support vector machine.

(Russo et al., 2018), suggesting that inhibition of functional activity of amygdala-related brain networks could reduce neural hypersensitivity leading to analgesia. Therefore, disruption of amygdala-related FC could be used to develop an effective prediction model for individualizing treatment in MwoA and considered as a potential indicator for developing therapeutic strategies and reduce the side effects.

This study indicated some disrupted brain regions primarily in the executive control network (ECN), salient network (SN), and sensorimotor network (SMN) between migraineurs and HCs. Functional studies have demonstrated coordinated activation of several brain areas in response to somatic and visceral stimuli, including the thalamus, anterior cingulate cortex (ACC), insular cortex, sensory cortices, prefrontal cortex (PFC), basal ganglia, and limbic system (Maizels et al., 2012). This network of brain regions involved in both sensory-discriminative and emotional-affective aspects of pain is termed the "neurolimbic pain matrix." This study demonstrated increased amygdala-functional changes during the resting state with left SFG and MFG in migraineurs. Previous studies showed GABAergic monosynaptic projections from the amygdala to PFC, which could contribute to the affective-motivational aspect of neuropathic pain (Seno et al., 2018; Gadotti et al., 2019). Furthermore, the studies showed amygdala-PFC–periaqueductal gray (PAG)–spinal cord (SC) pathway critical for pain hypersensitivity (Huang et al., 2019). For example, optogenetic and pharmacological studies exhibited that functional activation of the amygdala to PFC inputs was related to loss of descending inhibitory modulation of pain signals (Zhang et al., 2015; Huang et al., 2019; Coppieters et al., 2021). Inhibitory deficit results provide evidence supporting that enhanced input from the amygdala to PFC was a well-received underlying mechanism for the generation and maintenance of neuropathic pain (Cheriyan and Sheets, 2020), consistent with the findings of this study.

The PFC is crucial for executive functioning and pain processing, based on the GABAegic pathway and its dysfunctional connections within the PFC-limbic-PAG circuit (Ong et al., 2019). In line with the susceptibility and negative feedback regulation to stress-related response *via* hypothalamic-pituitary-adrenal (HPA) axis, amygdala activation, and PFC deactivation potentially disrupt the descending pain-inhibitory pathway causing nociceptive experience (Ji and Neugebauer, 2011; Cheriyan and Sheets, 2018). Hodkinson et al. (2015) reported increased cerebral blood flow (CBF) in the midbrain, amygdala and hippocampus, and decreased CBF in the insula, primary sensory cortex and PFC following treatment with analgesics. These differences may be attributed to ongoing pain after surgery. Furthermore, decreased amygdala-related hyperconnectivity has been observed after pain rehabilitation treatment, specifically between the left amygdala and right SFG

and between the right amygdala and left MFG after acupuncture (Simons et al., 2014; Luo et al., 2020). While the above mentioned studies showed that suppressing the input from the amygdala to PFC might modulate the top-down inhibitory circuit. In this study, the M-ieNSAIDs group showed significantly decreased amygdala-PFC and amygdala-ACC connectivity patterns than the M-eNSAIDs group and HCs. The decreased amygdala-related functional connections may lead to ineffective treatment with NSAIDs in M-ieNSAIDs patients, implying other neural pathways may underlie the nociceptive mechanism, including the PFC and ACC. Of note, PFC and ACC are part of the mesolimbic reward circuit modulated by a dopamine neurotransmitter (DosSantos et al., 2017). Thus, decreased connectivity of the left amygdala with PFC and ACC may depict impairment of the reward circuit, which could explain for the ineffective response to NSAIDs treatment.

This study also revealed significantly increased FC between the left amygdala and ipsilateral PreCG and PoCG in the M-eNSAIDs group. The SMN, including the PreCG and PoCG, plays a major role in pain perception and the integration of sensory information. Furthermore, abnormal connections between the amygdala and SMN may partly explain the hypersensitivity in migraineurs to endogenous changes and exogenous stimuli. Besides, previous studies showed that the dysfunction of SMN played an important role in encoding nociceptive information. Moreover, amygdala-SMN connectivity may predict pain-intensity modulation (Gandhi et al., 2020; Wei et al., 2020a). Furthermore, fMRI and positron emission tomography-computed tomography approaches (Qin et al., 2008; Yang et al., 2012) demonstrated that acupuncture was effective in reducing pain intensity by modulating the amygdala-associated brain networks and deactivating the metabolism of SMN. Additionally, cellular mechanisms with increased neuronal excitability in the primary somatosensory cortex have been shown to target these microcircuits *via* inhibiting the SMN activity (Okada et al., 2021), consistent with this study. Therefore, the increased connectivity between the amygdala and SMN in M-eMwoA patients may represent impairment of the inhibitory pathway. Furthermore, these findings may provide insights for developing potential therapeutic targets. Based on the findings of this study, we concluded that alteration of amygdala-related FC patterns with the higher-level sensory cortex and prefrontal cortex were important central pathological features for distinguishing MwoA patients likely to have effective response to NSAIDs from MwoA patients likely to have ineffective response to NSAIDs. These results may help in further elucidating the functional characteristics of migraine and predicting individualized response to NSAIDs.

However, several shortcomings in this study need to be revealed. First, this study was cross-sectional in design and therefore could not reflect the causal relationship between the efficacy of drugs and changes in brain function. In the future, longitudinal studies are needed to verify the causal mechanism. Second, only MwoA patients in the interictal period were included. Therefore, future studies should include patients with other migraine subtypes and in other phases. Third, hormone levels and concomitant psychiatric diseases could potentially exacerbate migraine, influence treatment response and complicate migraine treatment (Yurt and Kaplan, 2018; Radat, 2021). Therefore, future studies should investigate the influence of the hormone profile and psychiatric disorders. Moreover, this study had a small sample size, especially male participants. Therefore, future studies should aim for a large sample size to avoid overfitting. Furthermore, this study did not consider the different distinct effects of each substructure of the amygdala on function. As such, future studies should focus on a more accurate analysis of the anatomical substructures of the amygdala. Finally, the drug history was not comprehensive enough to capture details such as drug dosages or the types of drugs. Therefore, future studies should conduct a comprehensive drug history.

In conclusion, our findings reveal that some amygdala-related FC patterns potentially act as objectively measurable neuroimaging indicators in NSAIDs treatment of MwoA patients. Besides, a combination of the SVM classifier and amygdala-related FC features may represent a valuable strategy for predicting the efficacy of NSAIDs and improving clinical decision-making.

DATA AVAILABILITY STATEMENT

The raw data supporting the conclusions of this article will be made available by the authors, without undue reservation.

ETHICS STATEMENT

The studies involving human participants were reviewed and approved by Affiliated Jiangning Hospital of Nanjing Medicine University. The patients/participants provided their written informed consent to participate in this study. Written informed consent was obtained from the individual(s) for the publication of any potentially identifiable images or data included in this article.

AUTHOR CONTRIBUTIONS

H-LW, JL, and HZ designed the study. J-JW, G-PZ, and XG acquired the data. H-LW, Y-CC, and Z-ZH performed the data analysis. Y-CC, Y-SY, and XY interpreted the results. H-LW and C-HX prepared the manuscript. All authors contributed to manuscript revision and approved the submitted version.

FUNDING

This study was supported by the Science and Technology Development Project of Nanjing (YKK20202) and Science and Technology Development Project of Nanjing Medical University (NMUB2020168).

ACKNOWLEDGMENTS

We thank all participants for their participation.

REFERENCES

Ashina, M. (2020). Migraine. *New Engl. J. Med.* 383, 1866–1876. doi: 10.1056/NEJMra1915327

Biglione, B., Gitin, A., Gorelick, P. B., and Hennekens, C. (2020). Aspirin in the treatment and prevention of migraine headaches: Possible additional clinical options for primary healthcare providers. *Am. J. Med.* 133, 412–416. doi: 10.1016/j.amjmed.2019.10.023

Buisseret, B., Alhouayek, M., Guillemot-Legris, O., and Muccioli, G. G. (2019). Endocannabinoid and prostanoid crosstalk in pain. *Trends Mol. Med.* 25, 882–896. doi: 10.1016/j.molmed.2019.04.009

Cai, X., Xu, X., Zhang, A., Lin, J., Wang, X., He, W., et al. (2019). Cognitive decline in chronic migraine with nonsteroid anti-inflammation drug overuse: A Cross-Sectional study. *Pain Res. Manage.* 2019, 1–8. doi: 10.1155/2019/7307198

Carrasquillo, Y., and Gereau, R. W. (2008). Hemispheric lateralization of a molecular signal for pain modulation in the amygdala. *Mol. Pain* 4, 1744–8069. doi: 10.1186/1744-8069-4-24

Cheriyan, J., and Sheets, P. L. (2018). Altered excitability and local connectivity of mPFC-PAG neurons in a mouse model of neuropathic pain. *J. Neurosci.* 38, 4829–4839. doi: 10.1523/JNEUROSCI.2731-17.2018

Cheriyan, J., and Sheets, P. L. (2020). Peripheral nerve injury reduces the excitation-inhibition balance of basolateral amygdala inputs to prelimbic pyramidal neurons projecting to the periaqueductal gray. *Mol. Brain* 13:100. doi: 10.1186/s13041-020-00638-w

Chong, C. D., Gaw, N., Fu, Y., Li, J., Wu, T., and Schwedt, T. J. (2017). Migraine classification using magnetic resonance imaging resting-state functional connectivity data. *Cephalalgia* 37, 828–844. doi: 10.1177/0333102416652091

Chong, C. D., Schwedt, T. J., and Hougaard, A. (2019). Brain functional connectivity in headache disorders: A narrative review of MRI investigations. *J. Cereb. Blood Flow Metabol.* 39, 650–669. doi: 10.1177/0271678X17740794

Coppieters, I., Cagnie, B., De Pauw, R., Meeus, M., and Timmers, I. (2021). Enhanced amygdala-frontal operculum functional connectivity during rest in women with chronic neck pain: Associations with impaired conditioned pain modulation. *NeuroImage Clin.* 30:102638. doi: 10.1016/j.nicl.2021.102638

DosSantos, M. F., Moura, B. D. S., and DaSilva, A. F. (2017). Reward circuitry plasticity in pain perception and modulation. *Front. Pharmacol.* 8:790. doi: 10.3389/fphar.2017.00790

Fumal, A., Laureys, S., Di Clemente, L., Boly, M., Bohotin, V., Vandenheede, M., et al. (2006). Orbitofrontal cortex involvement in chronic analgesic-overuse headache evolving from episodic migraine. *Brain* 129, 543–550. doi: 10.1093/brain/awh691

Gadotti, V. M., Zhang, Z., Huang, J., and Zamponi, G. W. (2019). Analgesic effects of optogenetic inhibition of basolateral amygdala inputs into the prefrontal cortex in nerve injured female mice. *Mol. Brain* 12:105. doi: 10.1186/s13041-019-0529-1

Gandhi, W., Rosenek, N. R., Harrison, R., and Salomons, T. V. (2020). Functional connectivity of the amygdala is linked to individual differences in emotional pain facilitation. *Pain* 161, 300–307. doi: 10.1097/j.pain.0000000000001714

GBD 2015 Disease and Injury Incidence and Prevalence Collaborators (2016). Global, regional, and national incidence, prevalence, and years lived with disability for 310 diseases and injuries, 1990–2015: A systematic analysis for the Global Burden of Disease Study 2015. *Lancet* 388, 1545–1602. doi: 10.1016/S0140-6736(16)31678-6

Headache Classification Committee of the International Headache Society (IHS) (2013). The International Classification of Headache Disorders, 3rd edition (beta version). *Cephalalgia* 33, 629–808. doi: 10.1177/0333102413485658

Hodkinson, D. J., Khawaja, N., O'Daly, O., Thacker, M. A., Zelaya, F. O., Wooldridge, C. L., et al. (2015). Cerebral analgesic response to nonsteroidal anti-inflammatory drug ibuprofen. *Pain* 156, 1301–1310. doi: 10.1097/j.pain.0000000000000176

Huang, J., Gadotti, V. M., Chen, L., Souza, I. A., Huang, S., Wang, D., et al. (2019). A neuronal circuit for activating descending modulation of neuropathic pain. *Nat. Neurosci.* 22, 1659–1668. doi: 10.1038/s41593-019-0481-5

Huang, X., Zhang, D., Wang, P., Mao, C., Miao, Z., Liu, C., et al. (2021). Altered amygdala effective connectivity in migraine without aura: evidence from resting-state fMRI with Granger causality analysis. *J. Headache Pain* 22:25. doi: 10.1186/s10194-021-01240-8

Ji, G., and Neugebauer, V. (2009). Hemispheric lateralization of pain processing by amygdala neurons. *J. Neurophysiol.* 102, 2253–2264. doi: 10.1152/jn.00166.2009

Ji, G., and Neugebauer, V. (2011). Pain-related deactivation of medial prefrontal cortical neurons involves mGluR1 and GABAA receptors. *J. Neurophysiol.* 106, 2642–2652. doi: 10.1152/jn.00461.2011

Jia, Z., and Yu, S. (2017). Grey matter alterations in migraine: A systematic review and meta-analysis. *NeuroImage Clin.* 14, 130–140. doi: 10.1016/j.nicl.2017.01.019

Jiang, H., Fang, D., Kong, L., Jin, Z., Cai, J., Kang, X., et al. (2014). Sensitization of neurons in the central nucleus of the amygdala *via* the decreased GABAergic inhibition contributes to the development of neuropathic pain-related anxiety-like behaviors in rats. *Mol. Brain* 7:72. doi: 10.1186/s13041-014-0072-z

Luo, W., Zhang, Y., Yan, Z., Liu, X., Hou, X., Chen, W., et al. (2020). The instant effects of continuous transcutaneous auricular vagus nerve stimulation at acupoints on the functional connectivity of amygdala in migraine without aura: A preliminary study. *Neural Plast.* 2020, 1–13. doi: 10.1155/2020/8870589

Maizels, M., Aurora, S., and Heinricher, M. (2012). Beyond neurovascular: Migraine as a dysfunctional neurolimbic pain network. *Headache J. Head Face Pain* 52, 1553–1565. doi: 10.1111/j.1526-4610.2012.02209.x

Minen, M. T., Begasse, De Dhaem, O., Kroon Van Diest, A., Powers, S., Schwedt, T. J., et al. (2016). Migraine and its psychiatric comorbidities. *J. Neurol. Neurosurg. Psychiatry* 87, 741–749. doi: 10.1136/jnnp-2015-312233

Mose, L. S., Pedersen, S. S., Debrabant, B., Jensen, R. H., and Gram, B. (2018). The role of personality, disability and physical activity in the development of medication-overuse headache: A prospective observational study. *J. Headache Pain* 19:39. doi: 10.1186/s10194-018-0863-1

Mu, J., Chen, T., Quan, S., Wang, C., Zhao, L., and Liu, J. (2020). Neuroimaging features of whole-brain functional connectivity predict attack frequency of migraine. *Hum. Brain Mapp.* 41, 984–993. doi: 10.1002/hbm.24854

Mulleners, W. M., Chronicle, E. P., Palmer, J. E., Koehler, P. J., and Vredeveld, J. (2001). Visual cortex excitability in migraine with and without aura. *Headache J. Head Face Pain* 41, 565–572. doi: 10.1046/j.1526-4610.2001.041006565.x

Okada, T., Kato, D., Nomura, Y., Obata, N., Quan, X., Morinaga, A., et al. (2021). Pain induces stable, active microcircuits in the somatosensory cortex that provide a therapeutic target. *Sci. Adv.* 7:d8261. doi: 10.1126/sciadv.abd8261

Ong, W., Stohler, C. S., and Herr, D. R. (2019). Role of the prefrontal cortex in pain processing. *Mol. Neurobiol.* 56, 1137–1166. doi: 10.1007/s12035-018-1130-9

Patel, R., and Dickenson, A. H. (2021). Neuropharmacological basis for multimodal analgesia in chronic pain. *Postgrad. Med.* 2021, 1–15. doi: 10.1080/00325481.2021.1985351

Qin, W., Tian, J., Bai, L., Pan, X., Yang, L., Chen, P., et al. (2008). FMRI connectivity analysis of acupuncture effects on an Amygdala-Associated brain network. *Mol. Pain* 4, 1744–8069. doi: 10.1186/1744-8069-4-55

Radat, F. (2021). What is the link between migraine and psychiatric disorders? From epidemiology to therapeutics. *Rev. Neurol. France* 177, 821–826. doi: 10.1016/j.neurol.2021.07.007

Russo, A., Coppola, G., Pierelli, F., Parisi, V., Silvestro, M., Tessitore, A., et al. (2018). Pain perception and migraine. *Front. Neurol.* 9:576. doi: 10.3389/fneur.2018.00576

Seno, M. D. J., Assis, D. V., Gouveia, F., Antunes, G. F., Kuroki, M., Oliveira, C. C., et al. (2018). The critical role of amygdala subnuclei in nociceptive and depressive-like behaviors in peripheral neuropathy. *Sci. Rep. UK.* 8:13608. doi: 10.1038/s41598-018-31962-w

Simons, L. E., Pielech, M., Erpelding, N., Linnman, C., Moulton, E., Sava, S., et al. (2014). The responsive amygdala: Treatment-induced alterations in functional connectivity in pediatric complex regional pain syndrome. *Pain* 155, 1727–1742. doi: 10.1016/j.pain.2014.05.023

Tfelt-Hansen, P. (2021). Pharmacological strategies to treat attacks of episodic migraine in adults. *Expert Opin. Pharmacol.* 22, 305–316. doi: 10.1080/14656566.2020.1828347

Tolner, E. A., Chen, S., and Eikermann-Haerter, K. (2019). Current understanding of cortical structure and function in migraine. *Cephalalgia* 39, 1683–1699. doi: 10.1177/0333102419840643

Wei, H., Chen, J., Chen, Y., Yu, Y., Guo, X., Zhou, G., et al. (2020a). Impaired effective functional connectivity of the sensorimotor network in interictal episodic migraineurs without aura. *J. Headache Pain* 21:111. doi: 10.1186/s10194-020-01176-5

Wei, H., Chen, J., Chen, Y., Yu, Y., Zhou, G., Qu, L., et al. (2020b). Impaired functional connectivity of limbic system in migraine without aura. *Brain Imaging Behav.* 14, 1805–1814. doi: 10.1007/s11682-019-00116-5

Wei, H., Li, J., Guo, X., Zhou, G., Wang, J., Chen, Y., et al. (2021). Functional connectivity of the visual cortex differentiates anxiety comorbidity from episodic migraineurs without aura. *J. Headache Pain* 22:40. doi: 10.1186/s10194-021-01259-x

Wei, H., Zhou, X., Chen, Y., Yu, Y., Guo, X., Zhou, G., et al. (2019). Impaired intrinsic functional connectivity between the thalamus and visual cortex in migraine without aura. *J. Headache Pain* 20:116. doi: 10.1186/s10194-019-1065-1

Yang, J., Zeng, F., Feng, Y., Fang, L., Qin, W., Liu, X., et al. (2012). A PET-CT study on the specificity of acupoints through acupuncture treatment in migraine patients. *BMC Complem. Altern.* 12:123. doi: 10.1186/1472-6882-12-123

Yin, T., Sun, G., Tian, Z., Liu, M., Gao, Y., Dong, M., et al. (2020). The spontaneous activity pattern of the middle occipital gyrus predicts the clinical efficacy of acupuncture treatment for migraine without aura. *Front. Neurol.* 11:588207. doi: 10.3389/fneur.2020.588207

Yurt, K. K., and Kaplan, S. (2018). As a painkiller: A review of pre- and postnatal non-steroidal anti-inflammatory drug exposure effects on the nervous systems. *Inflammopharmacology* 26, 15–28. doi: 10.1007/s10787-017-0434-0

Zhang, Z., Gadotti, V. M., Chen, L., Souza, I. A., Stemkowski, P. L., and Zamponi, G. W. (2015). Role of prelimbic GABAergic circuits in sensory and emotional aspects of neuropathic pain. *Cell Rep.* 12, 752–759. doi: 10.1016/j.celrep.2015.07.001

Conflict of Interest: The authors declare that the research was conducted in the absence of any commercial or financial relationships that could be construed as a potential conflict of interest.

Publisher's Note: All claims expressed in this article are solely those of the authors and do not necessarily represent those of their affiliated organizations, or those of the publisher, the editors and the reviewers. Any product that may be evaluated in this article, or claim that may be made by its manufacturer, is not guaranteed or endorsed by the publisher.

frontiers in Molecular Neuroscience

ORIGINAL RESEARCH
published: 01 March 2022
doi: 10.3389/fnmol.2022.843754

Parvalbumin Neurons in Zona Incerta Regulate Itch in Mice

Jiaqi Li[1†], Yang Bai[2†], Yi Liang[1†], Yiwen Zhang[3], Qiuying Zhao[1], Junye Ge[1], Dangchao Li[1], Yuanyuan Zhu[1], Guohong Cai[1], Huiren Tao[4], Shengxi Wu[1] and Jing Huang[1]**

[1] Department of Neurobiology, School of Basic Medicine, Fourth Military Medical University, Xi'an, China, [2] Department of Neurosurgery, General Hospital of Northern Theater Command, Shenyang, China, [3] The Cadet Team 6 of School of Basic Medicine, Fourth Military Medical University, Xi'an, China, [4] Department of Spine Surgery, Shenzhen University General Hospital, Shenzhen, China

Pain and itch are intricately entangled at both circuitry and behavioral levels. Emerging evidence indicates that parvalbumin (PV)-expressing neurons in zona incerta (ZI) are critical for promoting nocifensive behaviors. However, the role of these neurons in itch modulation remains elusive. Herein, by combining FOS immunostaining, fiber photometry, and chemogenetic manipulation, we reveal that ZI PV neurons act as an endogenous negative diencephalic modulator for itch processing. Morphological data showed that both histamine and chloroquine stimuli induced FOS expression in ZI PV neurons. The activation of these neurons was further supported by the increased calcium signal upon scratching behavior evoked by acute itch. Behavioral data further indicated that chemogenetic activation of these neurons reduced scratching behaviors related to histaminergic and non-histaminergic acute itch. Similar neural activity and modulatory role of ZI PV neurons were seen in mice with chronic itch induced by atopic dermatitis. Together, our study provides direct evidence for the role of ZI PV neurons in regulating itch, and identifies a potential target for the remedy of chronic itch.

Keywords: zona incerta, parvalbumin, itch, fiber photometry, chemogenetics

OPEN ACCESS

Edited by:
Fengxian Li,
Southern Medical University, China

Reviewed by:
Fang Wang,
Sun Yat-sen University, China
Bo Duan,
University of Michigan, United States

***Correspondence:**
Shengxi Wu
shengxi@fmmu.edu.cn
Jing Huang
jinghuang@fmmu.edu.cn

[†] These authors have contributed equally to this work

Specialty section:
This article was submitted to Pain Mechanisms and Modulators, a section of the journal Frontiers in Molecular Neuroscience

Received: *26 December 2021*
Accepted: *08 February 2022*
Published: *01 March 2022*

Citation:
Li J, Bai Y, Liang Y, Zhang Y, Zhao Q, Ge J, Li D, Zhu Y, Cai G, Tao H, Wu S and Huang J (2022) Parvalbumin Neurons in Zona Incerta Regulate Itch in Mice. Front. Mol. Neurosci. 15:843754. doi: 10.3389/fnmol.2022.843754

INTRODUCTION

Itch is an uncomfortable sensation that triggers the desire to scratch (Davidson and Giesler, 2010). While acute itch protects our body from irritants by scratching, chronic itch, often associated with dermatologic, neuropathic, psychogenic, and systemic disorders, leads to the vicious itch-scratch cycle. Chronic itch, affecting nearly 15% of the population, is the most frequent cause of visits to dermatologists and exerts a huge personal and economic burden (Greaves and Khalifa, 2004; Weisshaar and Matterne, 2016). Despite substantial antipruritics available in the clinic, optimal therapeutic effect is hampered by our inadequate understanding of itch pathophysiology (Tey and Yosipovitch, 2011).

It has long been appreciated that pain and itch are intricately entangled at both circuitry and behavioral levels, and prior efforts have been made to distinguish itch circuitry from that of pain at the level of primary afferents and spinal dorsal horn (SDH) (Dong and Dong, 2018; Koch et al., 2018; Chen, 2021). Accumulating imaging data have indicated that the interwoven network involved in itch processing, including primary sensory cortex (S1), limbic system, and thalamus, mimics the "pain matrix" (Treede et al., 1999; Drzezga et al., 2001; Schweinhardt and Bushnell, 2010; Papoiu et al., 2012). Emerging studies aiming at elucidating supraspinal itch circuitry have also identified the role of the ventral tegmental area (Yuan et al., 2018; Su et al., 2019), central amygdala (Sanders et al., 2019; Samineni et al., 2021), and periaqueductal gray (PAG)

(Gao et al., 2019; Samineni et al., 2019) in itch modulation, all of which are involved in pain regulation (Peters et al., 2021; Tan and Kuner, 2021). Thus, brain mechanisms that signal itch and pain appear remarkably similar.

As an inhibitory subthalamic nucleus, zona incerta (ZI) integrates various sensory modalities and feeds them to a series of downstream areas, including the thalamus, hypothalamus, midbrain, and spinal cord, to modulate behavioral outputs and convey motivational states (Mitrofanis, 2005; Wang et al., 2020b). As yet, ZI has been demonstrated to regulate fear memory (Zhou et al., 2018; Venkataraman et al., 2019), defensive behavior (Chou et al., 2018; Wang et al., 2019), predatory hunting (Zhao et al., 2019), anxiety (Li et al., 2021), and sleep (Liu et al., 2017). Interestingly, ZI is also implicated in pain modulation. Neuropathic pain is related with decreased GABAergic neuronal activity in ZI, and pharmacological activation of ZI improves neuropathic pain behaviors in rats (Masri et al., 2009; Petronilho et al., 2012; Moon et al., 2016; Moon and Park, 2017). Considering that ZI contains heterogeneous groups of cell with diverse functions (Mitrofanis, 2005; Wang et al., 2020b). Wang et al. (2020a) further investigated the role of parvalbumin (PV)-expressing neurons, a neuronal subset mainly residing in the ventral ZI (ZIv), in pain modulation, and observed that these neurons promote nocifensive behaviors. Nevertheless, it still remains unknown how ZI PV neurons encode and modify itch processing. Given the similarity in brain circuitry for pain and itch, we propose this neuronal subpopulation may participate in itch modulation.

Herein, we used morphological and optical imaging approaches, as well as chemogenetic manipulations to identify neural dynamics and functional roles of ZI PV neurons during itch processing in mice. The results showed that activation of these neurons inhibited scratching behaviors in mouse models of acute and chronic itch. Our results highlight novel cellular mechanisms of a diencephalic area underlying itch signaling and brain modulation of itch-related scratching behaviors.

MATERIALS AND METHODS

Experimental Animals

All mice used in this study were adult male with a pure C57BL/6J background. C57BL/6J mice were provided by Experimental Animal Center of the Fourth Military Medical University. PV-IRES-Cre (Stock No: 008069) mice were acquired from the Jackson Laboratory and crossed with wild-type C57BL/6J mice. Mice aged 9–10 weeks were used for FOS immunostaining, while those aged 7–8 weeks received virus injection for photometry recordings and chemogenetic manipulations. All tests were performed during the light phase. The experimenters were blinded to the genotype and experimental conditions. All mice were housed under a 12-h light/dark cycle at 22–25°C with *ad libitum* access to food and water under environmentally controlled conditions. All procedures were approved by the Institutional Animal Care and Use Committee of the Fourth Military Medical University and conformed to the Guide for the Care and Use of Laboratory Animals published by the National Institutes of Health.

Itching Models

For pruritogen-induced acute itch, the mice were shaved on the back of neck and received intradermal injection of histamine (10 μg/μL, Cat#: H7125, Sigma), chloroquine (10 μg/μL, Cat#: C6628, Sigma), or vehicle (saline) into the nape of neck with a total volume of 10 μL. The scratching behaviors were recorded with a digital camera for 30 min and the scratching bouts were counted in a blind manner.

Tropical application of calcipotriol to mouse skin recapitulated features of atopic dermatitis (AD) and was adopted in the present study as the chronic itch model (Kim et al., 2019). As previously reported (Kim et al., 2013), bilateral ear skin were tropically treated with the calcipotriol scalp solution (1.5 mg/30 mL, 30 μL per side, LEO Laboratories Limited, Madison, NJ, United States) or vehicle (ethanol) for three consecutive weeks. Scratching behaviors were video recorded for 30 min after the final drug application to verify successful establishment of the model.

Stereotaxic Surgery

Mice were anesthetized with isoflurane (4% for induction and 1.5% for maintenance) and then mounted in a stereotaxic frame (RWD Life Science Inc., Shenzhen, China). The skull was exposed with a small incision and holes were drilled. Injection into ZIv was performed using a microinjection needle with a 10 μL microsyringe (Shanghai Gaoge Industry and Trade Co., Ltd., Shanghai, China) to deliver the virus at a rate of 30 nL/min using a microsyringe pump (Kd Scientific Inc., Holliston, MA., United States). The microsyringe had a glass pipette of 15–25 μm in diameter at the tip to avoid excessive tissue injury. Following injection, the needle was left in place for another 10 min before retraction. According to the Paxinos and Franklin mouse brain atlas (4th edition), the stereotaxic coordinates for virus injection in ZIv were set as follows: anterior posterior (AP), −2.46; medial lateral (ML), 1.50; and dorsal ventral (DV), −4.25 mm. For fiber photometry, fiber implantation (230 μm OD, 0.5 NA, Newdoon) was performed immediately after viral injection, and the dental acrylic and skull-penetrating screws were used to support the ceramic ferrule. The stereotaxic coordinates for implantation in ZIv were as follows: AP, −2.46; ML, 1.50; and DV, −4.23 mm.

For chemogenetic manipulation of ZI PV neurons, a 200 nL mixture of rAAV-EF1α-DIO-hM3D(Gq)-mCherry-WPREs (titer: 2.36×10^{12} vg/mL; Cat#: PT-0042, BrainVTA, China) or rAAV-EF1α-DIO-hM4D(Gi)-mCherry-WPREs (titer: 2.40×10^{12} vg/mL; Cat#: PT-0043, BrainVTA) was injected bilaterally into the ZI in PV-Cre mice, with rAAV-hSyn-DIO-EGFP-WPRE-hGHpA injected as the control. For recording the activity of ZI PV neurons, 200-nL of rAAV-hSyn-DIO-GCaMP6s-WPREs-pA (titer: 5.40×10^{12} vg/mL; Cat#: PT-0091, BrainVTA) or rAAV-hSyn-DIO-EGFP-WPRE-hGHpA (titer: 2.31×10^{12} vg/mL; Cat#: PT-1103, BrainVTA) was injected into the right ZI of PV-Cre mice.

Chemogenetic Manipulations and Behavioral Tests

The mice were allowed to recover for 3 weeks after chemogenetic virus injection before behavioral experiments. The mice were handled and acclimatized to the testing apparatus for at least 3 days prior to performing behavior tests. For acute itch stimuli, the mice were firstly intraperitoneally injected with 80 μL clozapine N-oxide (CNO, 0.75 mg/mL, dissolved in saline, Cat#: 4936, Tocris, Bristo, United Kingdom). 40 min later, the mice received intradermal injection of histamine or chloroquine, and then were immediately transferred back to the recording cages. Then, the animals were videotaped for at least 30 min. The number of scratching behavior was manually counted. After behavioral tests, the mice were immediately perfused and those with viral expression restricted in the ZI were chosen for statistical analysis. FOS immunostaining was then performed to validate the efficacy of chemogenetics.

For chronic itch stimuli, the establishment of AD model was initiated immediately after viral injection. On the day of behavioral experiments, the mice were treated with CNO, and then placed in the recording cages where the recording started 40 min later and continued for 30 min. Other procedures were the same as those described under the condition of acute itch.

Fiber Photometry

The mice were allowed to recover for 3 weeks after the stereotaxic surgery. The mice were handled and acclimatized to the testing apparatus for at least 3 days prior to experimentation. For acute itch stimuli, the mice received histamine or chloroquine injection and then were immediately transferred back to the recording apparatus on the day of experimentation. For chronic itch stimuli, the establishment of AD model was performed immediately after viral injection. On the day of behavioral test, the mice were placed in the recording apparatus. Fluorescence signals produced by a 473 nm laser (OBIS 488LS; Coherent) was reflected by a dichroic mirror (MD498; Thorlabs, Inc., Newton, MA, United States), focused by a 0.3 NA x10 objective lens (Olympus, Japan), and coupled to an optical commutator (Doris Lenses, Canada). An optical fiber (230 μm OD, 0.5 NA) guided the light between the implanted optical fiber and the commutator. The laser power was adjusted to 0.01–0.02 mW at the tip of the optical fiber for minimizing bleaching of the GCaMP6s probes. The GCaMP6s fluorescence signals were bandpass filtered (MF525-39, Thorlabs, Inc., Newton, MA, United States), and an amplifier was used to convert the CMOS (DCC3240M, Thorlabs, Inc., Newton, MA, United States) current output to a voltage signal. The voltage signal was further filtered through a low-pass filter (40 Hz cutoff, ThinkerTech). The analog voltage signals were digitalized at 50 Hz and recorded by the multichannel fiber photometry recording system (ThinkerTech). The fluorescence signals were recorded continuously during scratching. After behavioral tests, the mice were perfused. Viral injection and fiber implantation were confirmed *post doc*, and animals with incorrect locations were excluded from final analyses.

For data analysis, fluorescence change (ΔF/F) was represented by $(F\text{-}F_0)/F_0$. F_0 referred to the median of the fluorescence values in the baseline period, while F referred to the fluorescence values of each time point. The ΔF/F values of mice in each group were then averaged. To precisely analyze the change in fluorescence values across the scratching train, the baseline period and the post-scratching period were defined as −2 to −1 s relative to the scratching onset and 0–3 s after the onset of scratching behaviors, respectively. The areas under the curve (AUC) of ΔF/F in each time window defined were also adopted to quantify the change of fluorescence values induced by scratching. In addition, permutation tests were performed for analyzing the statistical significance of the event-related fluorescence change (ERF) (Li et al., 2016). Permutation tests with 1000 permutations were used to compare the fluorescence change at each time point of events with the baseline ERF. A series of statistical *P*-values at each time point were then generated and the statistical results were superimposed on the average ERF curve with red segments indicating statistically significant ($P < 0.05$) increase. Non-significant changes were shown as black lines.

Immunofluorescent Staining

The mice were anesthetized with overdose of 2% pentobarbital sodium, and perfused transcardially with 20 ml of 0.01 M phosphate buffer saline (PBS, pH 7.4), followed by 100 ml 4% paraformaldehyde (PFA) fixative solution in 0.1 M phosphate buffer (PB, pH 7.4). After perfusion, their brains were removed, placed in 30% sucrose solution for 24 h at 4°C, and then cut into coronal sections at 30 μm thickness with a cryostat (Leica CM 1950, Leica Microsystems Inc., United States). The sections containing ZI were used for immunostaining. Briefly, the sections were incubated in 10% normal donkey serum (NDS) for 40 min at room temperature (RT) to block non-specific immunoreactivity, and then incubated with primary antibodies at 4°C overnight and secondary antibodies at RT for 4 h in sequence. Finally, the sections were air-dried and cover-slipped with a mixture of 0.1% (v/v) DAPI (Cat#: d9564, Sigma), 50% (v/v) glycerol and 2.5% (w/v) triethylenediamine in 0.01 M PBS. Photomicrographs for injection sites were taken using Olympus VS200 microscope (10×), and confocal images were taken using Olympus FV3000 microscope. Cell counting was carried out manually in a blinded manner.

For examination of FOS expression in the ZI, C57BL/6J mice received intradermal injection of histamine or chloroquine, and then were placed into original rearing cages for 90 min before being perfused. The AD model mice were acclimatized in the rearing cages for 90 min and then sacrificed. The primary antibodies used for double immunofluorescence staining of FOS and PV were mouse anti-PV (1:200, Cat#: p3088, Sigma) and rabbit anti-c-fos (1:500, Cat#: 226008, Synaptic systems). The secondary antibodies were donkey anti-mouse IgG-Alexa 594 (1:500, Cat#: A21203, Invitrogen) and donkey anti-rabbit IgG-Alexa 488 (1:500, Cat#: ab150073, Abcam). For the analysis of FOS expression in different ZI subregions, 10 × confocal images of the ZI area were taken, and the number of FOS-immunoreactive (ir) neurons in the rostral ZI (ZIr), ZIv, the dorsal ZI (ZId), and the caudal ZI (ZIc) was counted from each mouse (three sections for each region per mouse) in different groups. For the analysis of FOS expression in ZI PV

neurons, 20 × confocal images were taken, and the number of neurons expressing FOS or PV were counted from three sections for each mouse.

For verifying the specificity of GCaMP6s expression in PV neurons, PV immunostaining was performed in the ZI from three sections randomly selected from each mouse (n = 3) transduced with the Cre-dependent GCaMP6s protein. The primary antibody and the second antibody were rabbit anti-PV (1:200, Cat#: ab11427, Abcam) and donkey anti-rabbit IgG-Alexa 594 (1:500, Cat#: A21206, Invitrogen), respectively. 20 × confocal images were taken and the number of neurons expressing GCaMP6s-mCherry or PV was counted.

To determine whether hM3Dq was selectively expressed in PV neurons, PV immunostaining was performed in the ZI from three sections randomly selected from each mouse (n = 3) transduced with the Cre-dependent hM3Dq protein. The primary antibody and the second antibody were rabbit anti-PV and donkey anti-rabbit IgG-Alexa 488, respectively. 20 × confocal images were taken and the number of neurons expressing hM3Dq-mCherry or PV was counted.

For verifying the efficacy of chemogenetics, FOS immunostaining was performed in the ZI from three sections randomly selected from each mouse (n = 3) transduced with the Cre-dependent hM3Dq-mCherry or mCherry alone. The primary antibodies used was rabbit anti-c-fos, and the secondary antibody was donkey anti-rabbit IgG-Alexa 488. 20× confocal images were taken and the number of neurons expressing hM3Dq-mCherry or FOS was counted.

Statistical Analysis

All data were expressed as the mean ± SEM. Statistical tests were performed using GraphPad Prism 7 and MATLAB 2018b (MathWorks). The normality test were performed using Kolmogorov–Smirnov test. For the analysis of immunofluorescent and behavioral data, one-way ANOVA with a *post hoc* least significant difference (LSD) test, Kruskal–Wallis test and Nemenyi multiple comparisons tests, or an unpaired t-test was used. For fiber photometry data, repeated measure ANOVA was firstly performed. If significant main effects were found, a simple effect analysis was performed. $P < 0.05$ was considered statistically significant.

RESULTS

Increased FOS Expression in the Ventral ZI Neurons Under the Condition of Acute and Chronic Itch Stimuli

FOS is widely utilized as a biomarker of neuronal activation upon external sensory stimuli (Coggeshall, 2005). Herein, we performed FOS immunostaining in brain sections containing the ZI 90 min after acute itch stimuli, or 21 days after the initiation of calcipotriol administration when the mice exhibited robust spontaneous scratching behavior. The successful establishment of acute (**Supplementary Figures 1A,B**) and chronic (**Supplementary Figures 1C,D**) models was verified by recordings of mouse scratching behavior. Since the ZI is a long diencephalic nucleus along the rostro-caudal axis, we counted the number of FOS-ir neurons in the rostral, dorsal, ventral, and caudal parts of ZI in mice among control, histamine and chloroquine groups. Quantification data showed that acute itch stimuli specifically increased the number of FOS-ir neurons in the ZIv (control: 31.17 ± 8.01, histamine: 69.00 ± 5.68, and chloroquine: 77.50 ± 2.93; P = 0.003) (**Figures 1A,B**), and no change in the number of FOS-expressing neurons was seen in other subregions. For chronic itch stimuli, a significant increase in FOS-expressing neurons was also seen in the ZIv (control: 27.83 ± 3.44, AD: 58.67 ± 5.49; P = 0.009), but not in other parts of ZI (**Figures 1C,D**). These results provide evidence for the activation of the ZIv upon both acute and chronic itch stimuli, laying morphological basis for subsequent investigations of ZI PV neurons in itch processing.

Zona Incerta Parvalbumin Neurons Are Activated During Acute Itch Processing

The ZI has a wealthy cluster of neuro-chemically distinct neurons, among which GABAergic PV neurons are mainly located in the ZIv (Mitrofanis, 2005). The modulatory role of ZI PV neurons in nocifensive behavior has been identified (Wang et al., 2020a). For these reasons, we focused on the role of this neuronal subpopulation in itch processing. A combination of PV and FOS immunostaining was firstly performed to test the activation of ZI PV neurons after introduction of acute itch stimuli. As illustrated in **Figures 2A,C**, the majority of these neurons were accumulated in the ZIv, with a few scattered in the ZId. Notably, a higher proportion of ZI PV neurons expressed FOS under the condition of both histamine and chloroquine stimuli, compared with the control group (control: 1.40 ± 0.72%, histamine: 27.12 ± 7.02%, and chloroquine: 24.14 ± 2.66%; $P < 0.001$).

Next, to quantify physiological activities of these neurons related with acute itch-evoked scratching, we stereotaxically injected rAAVs expressing the Cre-dependent GCaMP6s (AAV-DIO-GCaMP6s) into the ZI of PV-Cre mice, with rAAVs containing only a fluorescent tag served as controls, and implanted an optical fiber with its tip situated in the ZI for long-term recordings of GCaMP6s fluorescence *via* fiber photometry (**Figures 3A–C**). GCaMP6s expression in PV neurons was confirmed *post doc* using PV immunostaining (**Figure 3D**), and 90.66 ± 2.38% GCaMP6s-expressing neurons were labeled by PV. Three weeks after virus injection, the mice were injected with histamine. By aligning GCaMP6s signals in time with scratching trains, we observed that the calcium fluorescence of ZI PV neurons of GCaMP6s group was significantly increased, which initiated at 0.10 ± 2.45 s and continued until 5.13 ± 1.57 s in the post-onset period, compared with that in control group (**Figures 3E–H**). To extend above observations to histamine-independent itch, we investigated the effect of chloroquine injection and obtained similar responses in these neurons. This increase occurred from 0.16 ± 0.28 s to 4.08 ± 0.71 s in the post-scratching period (**Figures 3I–L**). In summary, these data suggest that ZI PV neurons exhibit rapid and strong activation during acute itch-induced scratching.

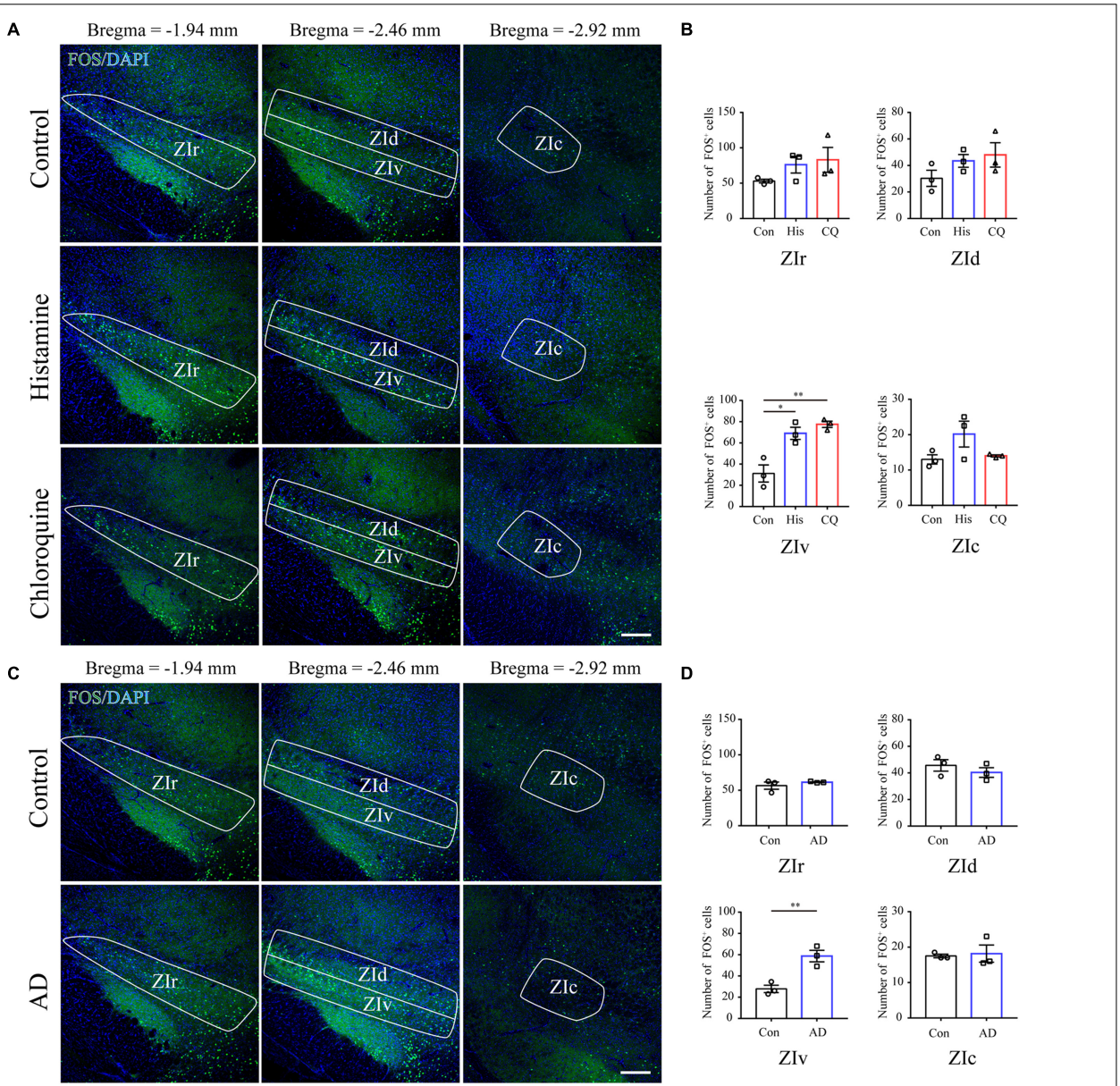

FIGURE 1 | Acute itch stimuli and Chronic itch stimuli increase FOS expression in the ZIv. **(A)** Representative images of FOS staining in the ZI after saline (the upper panel), histamine (the middle panel), and chloroquine (the lower panel) injection. Scale bar = 200 μm. **(B)** Quantification of FOS-expressing neurons in response to saline, histamine, and chloroquine injection showed both histamine and chloroquine stimuli increased FOS expression in the ZIv instead of other ZI subregions. $n = 3$ mice per group, three sections per mouse. One-way ANOVA with *post hoc* LSD test for multiple comparisons. For the analysis in ZIv, $F(2,6) = 17.378$, $P = 0.003$. **(C)** Representative images of FOS staining in the ZI in control (the upper panel) and AD (the lower panel) mice. Scale bar = 200 μm. **(D)** Quantification of FOS-expressing neurons in control and AD mice showed AD increased FOS expression in the ZIv instead of other ZI subregions. $n = 3$ mice per group, three sections per mouse. Unpaired *T*-test. For the analysis in ZIv, $t = -4.759$, $P = 0.009$. ZIr, the rostral ZI; ZIv, the ventral ZI; ZId, the dorsal ZI; ZIc, caudal ZI; AD, atopic dermatitis. $^{*}P < 0.05$, $^{**}P < 0.01$.

Chemogenetic Activation of Zona Incerta Parvalbumin Neurons Attenuates Acute Itch-Induced Scratching

To further characterize the precise role of ZI PV neurons in acute itch processing, chemogenetic manipulations of these neurons were performed. We targeted them by local injection of rAAVs delivering a construct containing excitatory (hM3Dq) or inhibitory (hM4Di) designer receptor fused with EYFP into bilateral ZI of PV-Cre mice. The mice injected with rAAV-DIO-EYFP served as controls (**Figures 4A,B**). Immunostaining results showed that 91.23 ± 3.78% mCherry-labeled neurons expressed PV in the ZI (**Figure 4C**). In addition, CNO treatment

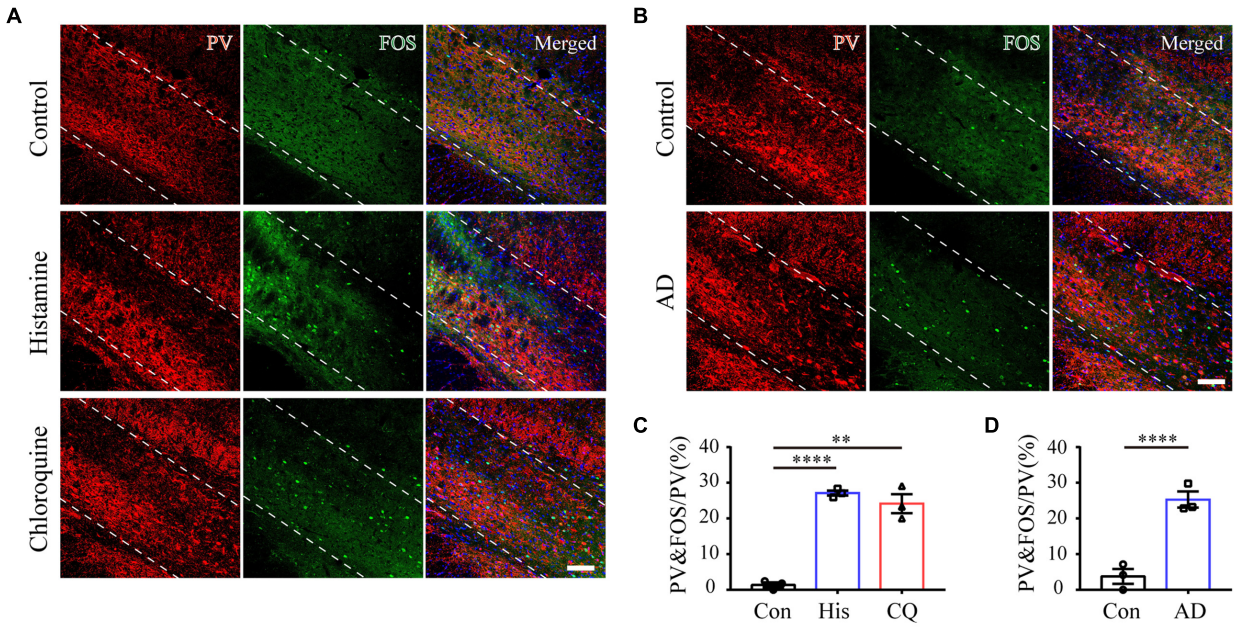

FIGURE 2 | Acute and chronic itch stimuli increase FOS expression in ZI PV neurons. **(A–C)** Representative images of FOS and PV staining in ZI after saline (the upper panel), histamine (the middle panel), and chloroquine (the lower panel) injection. **(B)** Representative images of FOS and PV staining in ZI in control (the upper panel) and AD (the lower panel) mice. Scale bar = 100 μm. **(C)** Quantification of FOS-expressing neurons in response to saline, histamine, and chloroquine injections showed both histamine and chloroquine stimuli increased FOS expression in ZI PV neurons. $n = 3$ mice per group, three sections per mouse. One-way ANOVA with *post hoc* LSD test for multiple comparisons. $F(2,6) = 73.642$, $P < 0.001$. **(D)** Quantification of FOS-expressing neurons in control and AD mice showed chronic itch stimuli increased FOS expression in ZI PV neurons. $n = 3$ mice per group, three sections per mouse. Unpaired T-test. $t = -7.03$, $P = 0.002$. $^{****}P < 0.0001$, $^{**}P < 0.01$.

increased FOS expression in ZI PV neurons of hM3Dq group compared to control group (control: 1.25 ± 0.31%, hM3Dq: 51.14 ± 1.60%; $P < 0.001$) (**Figures 4D,E**). These immunostaining data suggest the reliability and efficiency of modulating the activity of ZI PV neurons with chemogenetics. Behavioral data showed that pharmacogenetic activation of ZI PV neurons greatly attenuated mouse scratching behavior induced by histamine (EYFP group: 71.00 ± 5.54, hM3Dq group: 13.28 ± 4.26, and hM4Di group: 63.17 ± 6.78; $P = 0.001$) and chloroquine (EYFP group: 154.71 ± 23.13, hM3Dq group: 29.00 ± 3.73, and hM4Di group: 171.43 ± 31.82; $P < 0.001$), whereas the inhibition of these neurons exerted no effect on scratching behavior (**Figures 4F,G**). Given above, ZI PV neurons negatively regulate scratching behaviors evoked by acute itch.

Zona Incerta Parvalbumin Neurons Regulate Chronic Itch-Induced Scratching

To further analyze whether ZI PV neurons are also involved in chronic itch, we established a mouse model of AD induced by calcipotriol. Immunostaining results showed that chronic itch stimuli increased FOS expression in ZI PV neurons (control: 3.77 ± 2.07%, AD: 25.29 ± 2.25%; $P = 0.002$) (**Figures 2B,D**). We obtained similar results as in acute itch using fiber photometry, indicating that ZI PV neurons displayed a rapid increase in GCaMP6s fluorescence which closely matched with the onset of each scratching train (from 0.78 ± 0.18 s to 7.36 ± 1.42 s in the post-scratching period) in mice with AD (**Figures 5A–F** and **Supplementary Figure 2A**). As expected, chemogenetic activation of ZI PV neurons induced an apparent decrease in the number of scratching in AD mice, while the inhibition of these neurons did not influence the scratching behavior (EYFP group: 87.00 ± 5.37, hM3Dq group: 14.25 ± 3.95, and hM4Di group: 82.83 ± 8.36; $P < 0.001$) (**Figures 5G–I** and **Supplementary Figures 2B–D**). Taken together, ZI PV neurons also negatively regulate scratching behaviors evoked by chronic itch.

DISCUSSION

Our study showed that ZI PV neurons displayed elevated activity related to acute itch-induced scratching. Chemogenetic activation of ZI PV neurons attenuated scratching behavior induced by both histamine and chloroquine. These phenomena were also seen under the condition of AD-induced chronic itch. These results together suggest that ZI PV neurons act as an endogenous negative modulatory center during itch stimuli.

Pain and itch are two opposing sensations. Pain attenuates itch sensation, and the suppression of pain could enhances itch (Ma, 2010; LaMotte et al., 2014). This was originally attributed to distinct neural circuit mechanisms at the spinal level (Davidson and Giesler, 2010). Then, subsequent evidence identified

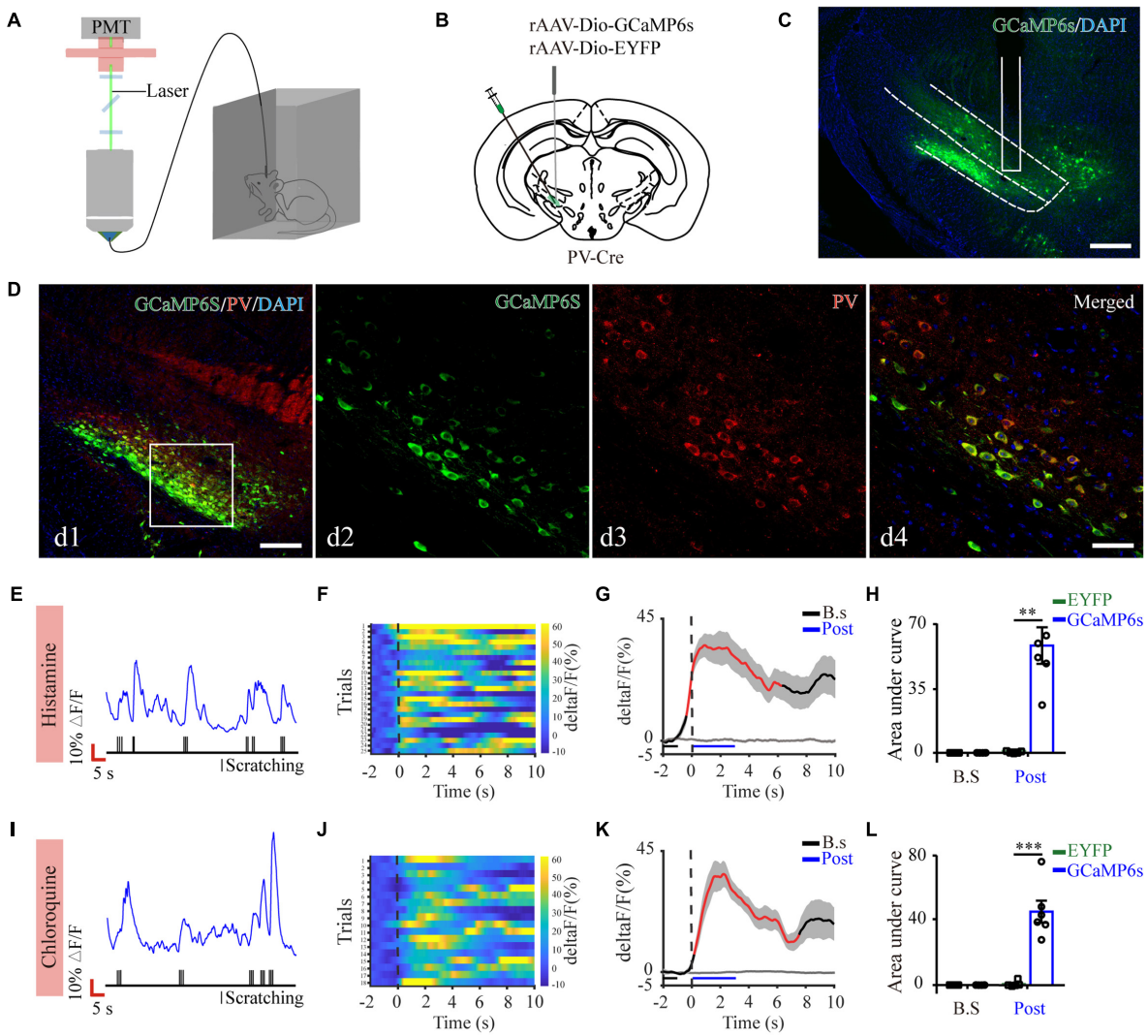

FIGURE 3 | Increased activity of ZI PV neurons during acute itch-induced scratching behavior. **(A)** The fiber photometry setup. **(B)** Schematic showing the viral targeting of AAV-DIO-GCaMP6s-EYFP and AAV-DIO-EYFP into the ZI of PV-Cre mice. **(C)** Histological verification of viral expression (green) and optical fiber implantation in the ZI in a representative mouse. **(D)** Representative photographs showing the expression of PV (red) in GCaMP6s-positive (green) neurons in the ZI of PV-Cre mice. The framed area in d1 was magnified in d2-4. Scale bars represent 100 μm in d1 and 50 μm in d2-4. **(E)** Representative GCaMP6s fluorescence trace (top) and behavioral trace (bottom) recorded simultaneously in ZI PV neurons in response to histamine injection. **(F)** Heatmap illustrating GCaMP6s fluorescence aligned to the beginning of individual scratching trains in all the mice in response to histamine stimuli. Each row represents Ca^{2+} signals corresponding to one scratching train. The color scale at the right indicates ΔF/F. **(G)** Mean fluorescent signal in response to histamine stimuli in all the mice recorded, with shaded areas indicating the SEM. The black and gray lines represent the signals of PV ZI neurons in mice with AAV-GCaMP6s and AAV-EYFP injection, respectively. The red line represents statistically significant increase from the baseline ($P < 0.05$; multivariate permutation test). The vertical dotted line indicates the scratching bout. **(H)** Area under the curve showing fluorescence changes of ZI PV neurons in the mice with AAV-GCaMP6s and AAV-EYFP injection in both pre-scratching and post-scratching periods under the condition of histamine stimuli. Repeated ANOVA followed by simple effects analysis. $n = 5$ mice in EYFP group and 6 mice in GCaMP6s group, $F(1,9) = 27.892$, $P = 0.001$. **(I–L)** Same conventions as **(E–H)** but for recording in response to chloroquine stimuli. $n = 5$ mice in EYFP group and 6 mice in GCaMP6s group, $F(1,9) = 36.586$, $P < 0.001$. ***$P < 0.001$, **$P < 0.01$. PMT, photomultiplier.

several supra-spinal structures related to this phenomenon. Spinal-projecting neurons in the S1 exert inhibitory effects on itch transmission *via* spinal inhibitory interneurons, but facilitate mechanical allodynia *via* spinal excitatory interneurons during neuropathic pain (Liu et al., 2018; Wu et al., 2021). Pain and itch are also subject to opposing descending modulation. The activation of PAG glutamatergic neurons suppresses nociception but facilitates itch (Samineni et al., 2017, 2019). This phenomenon may be owing to the dual modulation of downstream 5-HT signaling in itch and pain during the vicious itch-scratching cycle. Scratching could elicit pain, and consequently result in the activation of 5-HT neurons in the RVM. The released 5-HT acts upon two SDH neuronal subpopulations. Those expressing 5-HT_{1A}R alone

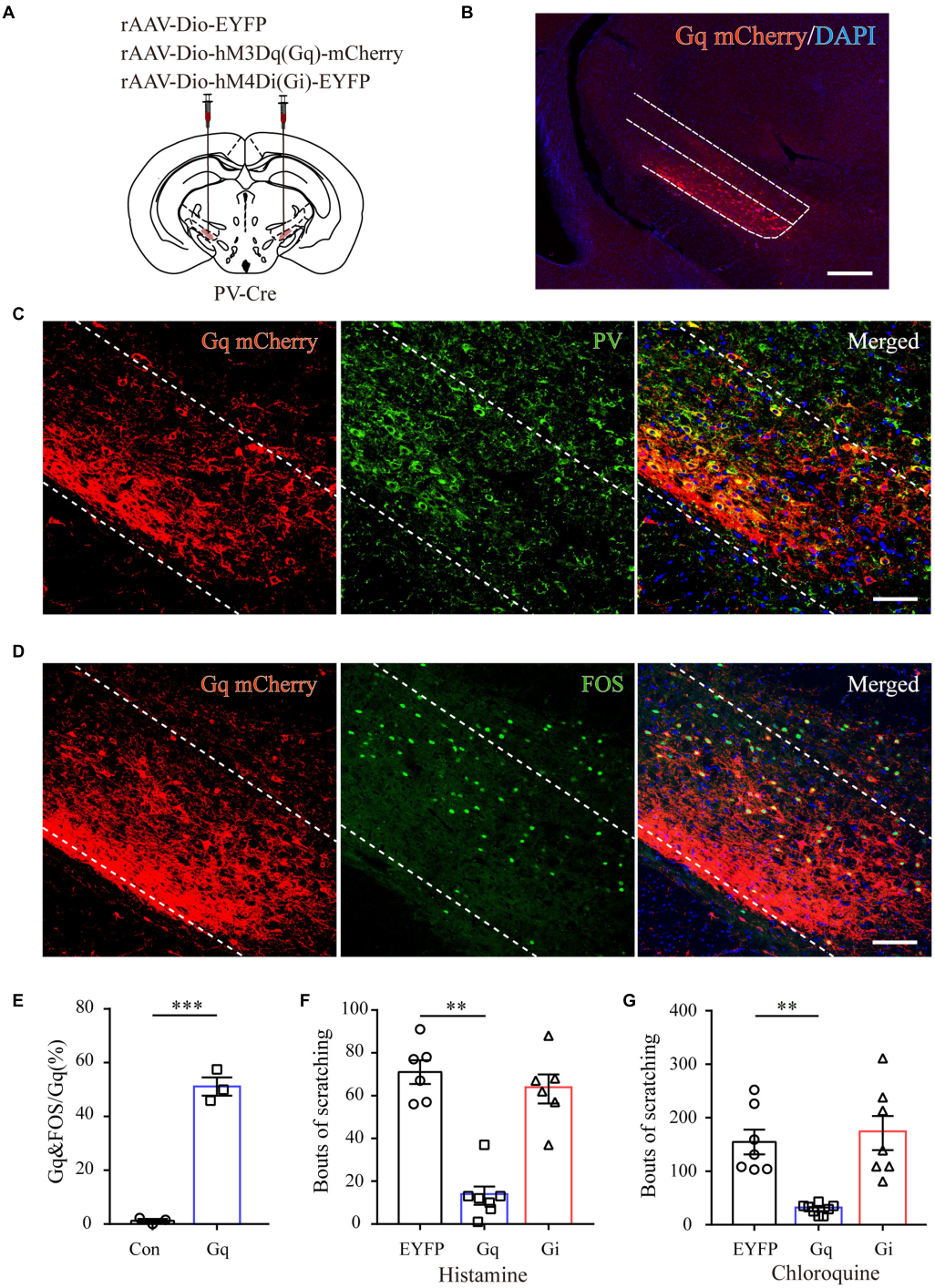

FIGURE 4 | ZI PV neurons negatively regulate scratching behaviors during acute itch. **(A)** Schematic illustration of viral injection for chemogenetic modulation of ZI PV neurons. **(B)** Histological verification of viral expression in the ZI in a representative mouse with AAV-DIO-hM3Dq-mCherry injection. Scale bar = 250 μm. **(C)** Representative photographs showing the expression of PV (green) in hM3Dq-positive (red) neurons in the ZI of PV-Cre mice. **(D)** Representative photographs showing the expression of FOS (green) in hM3Dq-positive (red) neurons in the ZI of PV-Cre mice. **(E)** Quantification of FOS-expressing neurons in mice with AAV-hM3Dq and AAV-mCherry injection showed CNO injection increased FOS expression in ZI PV neurons in the mice in AAV-hM3Dq group. $n = 3$ mice per group, three sections per mouse. Unpaired T-test. $t = -14.44$, $P < 0.001$. **(F,G)** Chemogenetic activation of ZI PV neurons reduces scratching behaviors induced by histamine **(F)** and chloroquine **(G)**, while inhibition of them exerts no effect on scratching behaviors. One-way ANOVA with *post hoc* LSD test for multiple comparisons. For the analysis of histamine-induced itch, $F(2,6) = 10.599$, $P = 0.001$. $n = 6$ mice in EGFP and hM4Di groups and 7 in hM3Dq group. For the analysis of chloroquine-induced itch, $F(2,6) = 13.341$, $P < 0.001$. $n = 6$ mice in EGFP and hM4Di groups and 7 in hM3Dq group. $n = 7$ mice in EGFP and hM4Di groups and 8 in hM3Dq group. $^{***}P < 0.001$, $^{**}P < 0.01$.

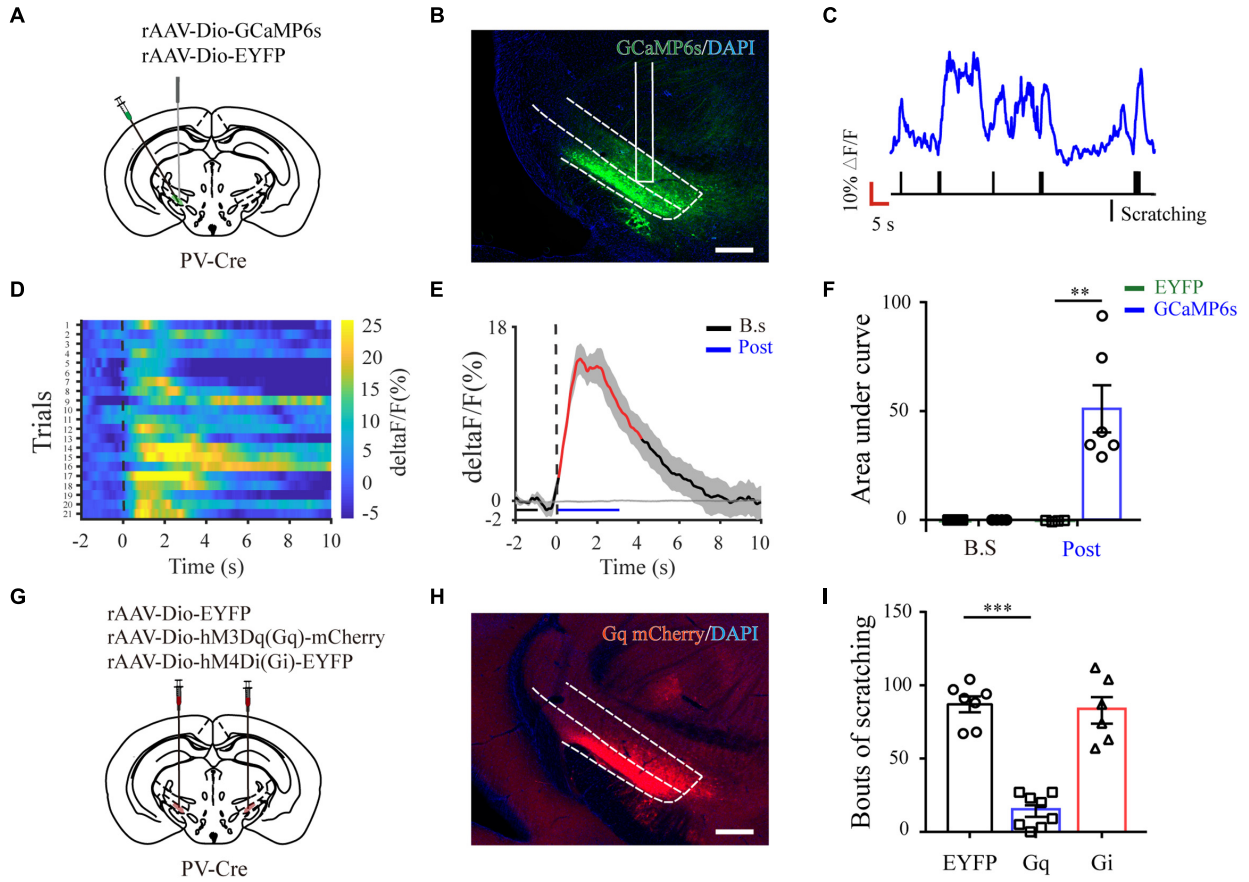

FIGURE 5 | ZI PV neurons negatively regulate scratching behaviors during chronic itch. **(A)** Schematic showing the viral targeting of AAV-DIO-GCaMP6s-EYFP and AAV-DIO-EYFP into the ZI of PV-Cre mice with AD. **(B)** Histological verification of viral expression (green) and optical fiber implantation in the ZI in a representative mouse. **(C)** Representative GCaMP6s fluorescence trace (top) and behavioral trace (bottom) recorded simultaneously in ZI PV neurons in response to calcipotriol injection. **(D)** Heatmap illustrating GCaMP6s fluorescence aligned to the beginning of individual scratching trains in all the mice in response to calcipotriol stimuli. Each row represents Ca^{2+} signals corresponding to one scratching train. **(E)** Mean fluorescent signal in response to calcipotriol stimuli in all the mice recorded, with shaded areas indicating the SEM. The black and gray line represent the signals of PV ZI neurons in mice with AAV-GCaMP6s and AAV-EYFP injection, respectively. The red line represents statistically significant increase from the baseline ($P < 0.05$; multivariate permutation test). **(F)** Area under the curve showing fluorescence changes of ZI PV neurons in mice with AAV-GCaMP6s and AAV-EYFP injection in both pre-scratching and post-scratching periods under the condition of calcipotriol stimuli. Repeated ANOVA followed by simple effects analysis. $n = 4$ mice in EYFP group and 6 mice in GCaMP6s group, $F(1,8) = 14.355$, $P < 0.01$. **(G)** Schematic illustration of viral injection in mice with AD for chemogenetic modulation of ZI PV neurons. **(H)** Histological verification of viral expression within ZI in a representative mouse with AAV-DIO-hM3Dq-mCherry injection. Scale bar = 250 μm. **(I)** Chemogenetic activation of ZI PV neurons reduces scratching behaviors induced by calcipotriol injection, while the inhibition of them exerts no effect on scratching behaviors. One-way ANOVA with *post hoc* LSD test for multiple comparisons. $F(2,6) = 49.27$, $P < 0.001$. $n = 7$, 8, and 6 in EGFP, hM3Dq, and hM4Di group, respectively. ***$P < 0.001$, **$P < 0.01$.

inhibit nociceptive processing, while the others expressing both gastrin releasing peptide receptor and 5-HT_{1A}R facilitate itch transmission (Zhao et al., 2014). Herein, we identify a novel diencephalic area that affects itch and pain in opposing manners, and the activation of ZI PV neurons facilitates nocifensive behaviors (Wang et al., 2020a) but inhibits itch processing as seen in the present study. Distinct downstream neural pathways or postsynaptic neuronal types may mediate these opposing effects.

The unidirectional modulatory effect of ZI PV neurons adds the complexity of neurocircuitry mechanisms underlying itch processing. As shown in the present study, the activation of ZI PV neurons inhibits both histamine and chloroquine induced scratching, however, the inhibition of them fails to enhance scratching behavior. One possible explanation for this phenomenon is that as an exogenous, non-physiological manipulation way during itch stimuli, chemogenetic inhibition of these neurons may recruit other itch-suppressing pathways in a compensatory style, which masked the itch-facilitatory effect induced by decreased ZI PV neuronal activities themselves.

ZI provides massive projections toward various cortical and subcortical regions, including the S1, intra-laminar and higher-order thalamic nuclei, PAG, anterior pretectal nucleus, pontine reticular nucleus, and RVM (Mitrofanis, 2005; Zhao et al., 2019). Among them, the posterior thalamic nucleus (Po) represents a potential target of ZI for pain processing. Incertal neurons participate in a feed forward inhibitory circuit that blocking

sensory transmission through Po, and neuropathic pain is associated with reduced ZI activity and consequently increased Po activity (Trageser and Keller, 2004; Masri et al., 2009). In addition, the activation of ZI-Po pathway mediates the analgesic effects of motor cortex stimulation (Cha et al., 2013). Emerging evidence suggest that Po mediates histaminergic itch (Zhu et al., 2020) and ZIv PV neurons send GABAergic projections to Po (Wang et al., 2020a). Thus, incertal projections toward Po might mediate the anti-pruritus effect of ZIv PV neurons. It is worth mentioning that PAG also receives inputs from ZIv PV neurons (Wang et al., 2020a). It is plausible that the descending PAG-RVM-SDH pathway may subserve the distinct roles of ZIv PV neurons in the modulation of itch and pain.

As a highly heterogenous nucleus, ZI possesses diverse neuronal types with capacity to release neurotransmitters including GABA, glutamate, and neuropeptides (Kolmac and Mitrofanis, 1999; Mitrofanis et al., 2004). ZI GABAergic neurons are abundant in number, which could be further divided by the expression of somatostatin, vasopressin, and PV (Watson et al., 2014). Distinct ZI sectors or neuronal types display diverse connectivity patterns and contribute to multiple roles of ZI in various physiological functions (Mitrofanis, 2005). Despite early studies indicating ZI as an integrative hub for global regulation of physiological behaviors, in-depth dissections of contributions of specific subpopulations were not emphasized until in recent researches with state-of-the-art tract tracing and activity manipulation techniques (Mitrofanis, 2005; Wang et al., 2020b). For instance, the activation of ZIr GABAergic neurons reduced defensive behavior *via* direct projections toward PAG (Chou et al., 2018), which was opposite to that of activating ZIv PV neurons devoid of projections to PAG (Wang et al., 2019). In the domain of pain research, early studies based on non-specific manipulations of ZI activity suggest the antinociceptive role of ZI (Masri et al., 2009; Petronilho et al., 2012; Moon et al., 2016; Moon and Park, 2017), which might be mediated by ZId/r subpopulations that receive glutamatergic inputs from midcingulate cortex (Hu et al., 2019). However, ZI PV neurons positively control nocifensive behavior *via* the incerta-thalamic circuit (Wang et al., 2020a). Herein, although the inhibitory role of ZI PV neurons during itch processing was identified, we did not know whether other subpopulations were engaged in itch behaviors. It would be exciting to explore whether and how (including circuit and molecular mechanisms) other subpopulations are involved in itch regulation in the future.

Chronic itch renders a challenging symptom for clinicians to manage. Although many novel treatments including immunomodulators and drugs targeting at the neural system are identified, frustrated voices concerning its efficacy never diminish, owing to the lack of evidence from large-scale controlled trials as well as adverse effects (e.g., somnolence and weight gain) (Yosipovitch et al., 2018). In the absence of ideal antipruritics, neuromodulation emerges as a promising alternative for refractory itch disorders. Emerging neural targets have been identified along pruritic transmission or modulation pathway, including the spinal cord (Hill and Paraiso, 2015) and the sensorimotor cortex (Knotkova et al., 2013; Nakagawa et al., 2016; Thibaut et al., 2019). There is an ever-growing body of efforts, indicating the importance of ZI stimulation in clinical settings. Deep brain stimulation of ZI has been demonstrated to improve akinesia and bradykinesia in patients with Parkinson's disease (Voges et al., 2002), proximal tremor in patients with multiple sclerosis (Nandi et al., 2002), as well as obsessive symptoms in patients with obsessive compulsive disorder (Mallet et al., 2002). Interestingly, Lu et al. (2021) noticed changes of human perception of experimental heat pain in subthalamic DBS patients, supporting ZI as a potential target for pain modulation. Herein, we showed that ZI PV neurons negatively regulate scratching behaviors evoked by chronic itch. These data may lay preclinical basis for the application of ZI stimulation in the treatment of pharmaco-resistant itch.

This study is not without flaws. Firstly, it is unknown whether pain and itch activate the same population of ZI PV neurons. This issue could be addressed by *in vivo* miniscope, miniature two-photon imaging or multi-channel extracellular recordings (de Groot et al., 2020; Zhang et al., 2021), which helps determine whether individual ZI PV neuron responds to both pain and itch stimuli. In addition, the utilization of the targeted recombination in active populations system in Fos-CreER transgenic mice (Sanders et al., 2019) allows to determine whether selective manipulation of itching-responsive ZI neurons influences pain behaviors. Secondly, nocifensive responses induced by scratching may also activate PV neurons in the ZI. To selectively detect neuronal activity by itch stimuli, a neck collar should be used to avoid scratching-induced activation.

CONCLUSION

In summary, our data revealed a novel role of ZI PV neurons in controlling itch signal processing. These knowledge would extend our understanding of central mechanisms underlying itch sensation and provide clues to intervention strategies for chronic itch.

DATA AVAILABILITY STATEMENT

The raw data supporting the conclusions of this article will be made available by the authors, without undue reservation.

ETHICS STATEMENT

The animal study was reviewed and approved by the Institutional Animal Care and Use Committee of the Fourth Military Medical University.

AUTHOR CONTRIBUTIONS

JH and SW conceived and designed the experiments, conceived the study, analyzed the data, and revised the manuscript. JL, YB, and YL performed the experiments, analyzed the data, and wrote the manuscript. QZ, YWZ, DL, YYZ, and JL assisted with animal studies and histology. JL, JG, and GC performed and interpreted the data and statistical analyses. HT analyzed the data

and revised the manuscript. All authors read and approved the final manuscript.

FUNDING

This work was supported by grants from the National Natural Science Foundation of China (82071235, 82101318, and 81771095), Science and Technology Nova Project of Shaanxi Province (2016KJXX-35), and Outstanding Youth Fund of Shaanxi Province (2021JC-32), and support fund from the Fourth Military Medical University (2020AXJHHJ) and Sanming Project of Medicine in Shenzhen (SZSM201911011).

SUPPLEMENTARY MATERIAL

The Supplementary Material for this article can be found online at: https://www.frontiersin.org/articles/10.3389/fnmol.2022.843754/full#supplementary-material

REFERENCES

Cha, M., Ji, Y., and Masri, R. (2013). Motor cortex stimulation activates the incertothalamic pathway in an animal model of spinal cord injury. *J. Pain* 14, 260–269. doi: 10.1016/j.jpain.2012.11.007

Chen, Z. F. (2021). A neuropeptide code for itch. *Nat. Rev. Neurosci.* 22, 758–776. doi: 10.1038/s41583-021-00526-9

Chou, X. L., Wang, X., Zhang, Z. G., Shen, L., Zingg, B., Huang, J., et al. (2018). Inhibitory gain modulation of defense behaviors by zona incerta. *Nat. Commun.* 9:1151. doi: 10.1038/s41467-018-03581-6

Coggeshall, R. E. (2005). Fos, nociception and the dorsal horn. *Prog. Neurobiol.* 77, 299–352. doi: 10.1016/j.pneurobio.2005.11.002

Davidson, S., and Giesler, G. J. (2010). The multiple pathways for itch and their interactions with pain. *Trends Neurosci.* 33, 550–558. doi: 10.1016/j.tins.2010.09.002

de Groot, A., van den Boom, B. J., van Genderen, R. M., Coppens, J., van Veldhuijzen, J., Bos, J., et al. (2020). NINscope, a versatile miniscope for multi-region circuit investigations. *Elife* 9. doi: 10.7554/eLife.49987

Dong, X., and Dong, X. (2018). Peripheral and Central Mechanisms of Itch. *Neuron* 98, 482–494. doi: 10.1016/j.neuron.2018.03.023

Drzezga, A., Darsow, U., Treede, R. D., Siebner, H., Frisch, M., Munz, F., et al. (2001). Central activation by histamine-induced itch: analogies to pain processing: a correlational analysis of O-15 H2O positron emission tomography studies. *Pain* 92, 295–305. doi: 10.1016/s0304-3959(01)00271-8

Gao, Z. R., Chen, W. Z., Liu, M. Z., Chen, X. J., Wan, L., Zhang, X. Y., et al. (2019). Tac1-Expressing Neurons in the Periaqueductal Gray Facilitate the Itch-Scratching Cycle *via* Descending Regulation. *Neuron* 101, 45.e–59.e. doi: 10.1016/j.neuron.2018.11.010

Greaves, M. W., and Khalifa, N. (2004). Itch: more than skin deep. *Int. Arch. Allergy Immunol.* 135, 166–172. doi: 10.1159/000080898

Hill, A. J., and Paraiso, M. F. (2015). Resolution of Chronic Vulvar Pruritus With Replacement of a Neuromodulation Device. *J. Minim. Invasive Gynecol.* 22, 889–891. doi: 10.1016/j.jmig.2015.02.020

Hu, T. T., Wang, R. R., Du, Y., Guo, F., Wu, Y. X., Wang, Y., et al. (2019). Activation of the Intrinsic Pain Inhibitory Circuit from the Midcingulate Cg2 to Zona Incerta Alleviates Neuropathic Pain. *J. Neurosci.* 39, 9130–9144. doi: 10.1523/jneurosci.1683-19.2019

Kim, B. S., Siracusa, M. C., Saenz, S. A., Noti, M., Monticelli, L. A., Sonnenberg, G. F., et al. (2013). TSLP elicits IL-33-independent innate lymphoid cell responses to promote skin inflammation. *Sci. Transl. Med.* 5:170ra116. doi: 10.1126/scitranslmed.3005374

Kim, D., Kobayashi, T., and Nagao, K. (2019). Research Techniques Made Simple: mouse Models of Atopic Dermatitis. *J. Invest. Dermatol.* 139, 984.e–990.e. doi: 10.1016/j.jid.2019.02.014

Knotkova, H., Portenoy, R. K., and Cruciani, R. A. (2013). Transcranial direct current stimulation (tDCS) relieved itching in a patient with chronic neuropathic pain. *Clin. J. Pain* 29, 621–622. doi: 10.1097/AJP.0b013e31826b1329

Koch, S. C., Acton, D., and Goulding, M. (2018). Spinal Circuits for Touch, Pain, and Itch. *Annu. Rev. Physiol.* 80, 189–217. doi: 10.1146/annurev-physiol-022516-034303

Kolmac, C., and Mitrofanis, J. (1999). Distribution of various neurochemicals within the zona incerta: an immunocytochemical and histochemical study. *Anat. Embryol.* 199, 265–280. doi: 10.1007/s004290050227

LaMotte, R. H., Dong, X., and Ringkamp, M. (2014). Sensory neurons and circuits mediating itch. *Nat. Rev. Neurosci.* 15, 19–31. doi: 10.1038/nrn3641

Li, Y., Zhong, W., Wang, D., Feng, Q., Liu, Z., Zhou, J., et al. (2016). Serotonin neurons in the dorsal raphe nucleus encode reward signals. *Nat. Commun.* 7:10503. doi: 10.1038/ncomms10503

Li, Z., Rizzi, G., and Tan, K. R. (2021). Zona incerta subpopulations differentially encode and modulate anxiety. *Sci. Adv.* 7:eabf6709. doi: 10.1126/sciadv.abf6709

Liu, K., Kim, J., Kim, D. W., Zhang, Y. S., Bao, H., Denaxa, M., et al. (2017). Lhx6-positive GABA-releasing neurons of the zona incerta promote sleep. *Nature* 548, 582–587. doi: 10.1038/nature23663

Liu, Y., Latremoliere, A., Li, X., Zhang, Z., Chen, M., Wang, X., et al. (2018). Touch and tactile neuropathic pain sensitivity are set by corticospinal projections. *Nature* 561, 547–550. doi: 10.1038/s41586-018-0515-2

Lu, C. W., Harper, D. E., Askari, A., Willsey, M. S., Vu, P. P., Schrepf, A. D., et al. (2021). Stimulation of zona incerta selectively modulates pain in humans. *Sci. Rep.* 11:8924. doi: 10.1038/s41598-021-87873-w

Ma, Q. (2010). Labeled lines meet and talk: population coding of somatic sensations. *J. Clin. Invest.* 120, 3773–3778. doi: 10.1172/jci43426

Mallet, L., Mesnage, V., Houeto, J. L., Pelissolo, A., Yelnik, J., Behar, C., et al. (2002). Compulsions, Parkinson's disease, and stimulation. *Lancet* 360, 1302–1304. doi: 10.1016/s0140-6736(02)11339-0

Masri, R., Quiton, R. L., Lucas, J. M., Murray, P. D., Thompson, S. M., and Keller, A. (2009). Zona incerta: a role in central pain. *J. Neurophysiol.* 102, 181–191. doi: 10.1152/jn.00152.2009

Mitrofanis, J. (2005). Some certainty for the "zone of uncertainty"? Exploring the function of the zona incerta. *Neuroscience* 130, 1–15. doi: 10.1016/j.neuroscience.2004.08.017

Mitrofanis, J., Ashkan, K., Wallace, B. A., and Benabid, A. L. (2004). Chemoarchitectonic heterogeneities in the primate zona incerta: clinical and functional implications. *J. Neurocytol.* 33, 429–440. doi: 10.1023/B:NEUR.0000046573.28081.dd

Moon, H. C., Lee, Y. J., Cho, C. B., and Park, Y. S. (2016). Suppressed GABAergic signaling in the zona incerta causes neuropathic pain in a thoracic hemisection spinal cord injury rat model. *Neurosci. Lett.* 632, 55–61. doi: 10.1016/j.neulet.2016.08.035

Moon, H. C., and Park, Y. S. (2017). Reduced GABAergic neuronal activity in zona incerta causes neuropathic pain in a rat sciatic nerve chronic constriction injury model. *J. Pain Res.* 10, 1125–1134. doi: 10.2147/jpr.s131104

Nakagawa, K., Mochizuki, H., Koyama, S., Tanaka, S., Sadato, N., and Kakigi, R. (2016). A transcranial direct current stimulation over the sensorimotor cortex modulates the itch sensation induced by histamine. *Clin. Neurophysiol.* 127, 827–832. doi: 10.1016/j.clinph.2015.07.003

Nandi, D., Chir, M., Liu, X., Bain, P., Parkin, S., Joint, C., et al. (2002). Electrophysiological confirmation of the zona incerta as a target for surgical treatment of disabling involuntary arm movements in multiple sclerosis: use of local field potentials. *J. Clin. Neurosci.* 9, 64–68. doi: 10.1054/jocn.2001.1012

Papoiu, A. D., Coghill, R. C., Kraft, R. A., Wang, H., and Yosipovitch, G. (2012). A tale of two itches. Common features and notable differences in brain activation evoked by cowhage and histamine induced itch. *Neuroimage* 59, 3611–3623. doi: 10.1016/j.neuroimage.2011.10.099

Peters, K. Z., Cheer, J. F., and Tonini, R. (2021). Modulating the Neuromodulators: dopamine, Serotonin, and the Endocannabinoid System. *Trends Neurosci.* 44, 464–477. doi: 10.1016/j.tins.2021.02.001

Petronilho, A., Reis, G. M., Dias, Q. M., Fais, R. S., and Prado, W. A. (2012). Antinociceptive effect of stimulating the zona incerta with glutamate in rats. *Pharmacol. Biochem. Behav.* 101, 360–368. doi: 10.1016/j.pbb.2012.01.022

Samineni, V. K., Grajales-Reyes, J. G., Copits, B. A., O'Brien, D. E., Trigg, S. L., Gomez, A. M., et al. (2017). Divergent Modulation of Nociception by Glutamatergic and GABAergic Neuronal Subpopulations in the Periaqueductal Gray. *eNeuro* 4:ENEURO.0129-16.2017. doi: 10.1523/eneuro.0129-16.2017

Samineni, V. K., Grajales-Reyes, J. G., Grajales-Reyes, G. E., Tycksen, E., Copits, B. A., Pedersen, C., et al. (2021). Cellular, circuit and transcriptional framework for modulation of itch in the central amygdala. *Elife* 10:e68130. doi: 10.7554/eLife.68130

Samineni, V. K., Grajales-Reyes, J. G., Sundaram, S. S., Yoo, J. J., and Gereau, R. W. T. (2019). Cell type-specific modulation of sensory and affective components of itch in the periaqueductal gray. *Nat. Commun.* 10:4356. doi: 10.1038/s41467-019-12316-0

Sanders, K. M., Sakai, K., Henry, T. D., Hashimoto, T., and Akiyama, T. (2019). A Subpopulation of Amygdala Neurons Mediates the Affective Component of Itch. *J. Neurosci.* 39, 3345–3356. doi: 10.1523/jneurosci.2759-18.2019

Schweinhardt, P., and Bushnell, M. C. (2010). Pain imaging in health and disease–how far have we come? *J. Clin. Invest.* 120, 3788–3797. doi: 10.1172/jci43498

Su, X. Y., Chen, M., Yuan, Y., Li, Y., Guo, S. S., Luo, H. Q., et al. (2019). Central Processing of Itch in the Midbrain Reward Center. *Neuron* 102, 858.e–872.e. doi: 10.1016/j.neuron.2019.03.030

Tan, L. L., and Kuner, R. (2021). Neocortical circuits in pain and pain relief. *Nat. Rev. Neurosci.* 22, 458–471. doi: 10.1038/s41583-021-00468-2

Tey, H. L., and Yosipovitch, G. (2011). Targeted treatment of pruritus: a look into the future. *Br. J. Dermatol.* 165, 5–17. doi: 10.1111/j.1365-2133.2011.10217.x

Thibaut, A., Ohrtman, E. A., Morales-Quezada, L., Simko, L. C., Ryan, C. M., Zafonte, R., et al. (2019). Distinct behavioral response of primary motor cortex stimulation in itch and pain after burn injury. *Neurosci. Lett.* 690, 89–94. doi: 10.1016/j.neulet.2018.10.013

Trageser, J. C., and Keller, A. (2004). Reducing the uncertainty: gating of peripheral inputs by zona incerta. *J. Neurosci.* 24, 8911–8915. doi: 10.1523/jneurosci.3218-04.2004

Treede, R. D., Kenshalo, D. R., Gracely, R. H., and Jones, A. K. (1999). The cortical representation of pain. *Pain* 79, 105–111. doi: 10.1016/s0304-3959(98)00184-5

Venkataraman, A., Brody, N., Reddi, P., Guo, J., Gordon Rainnie, D., and Dias, B. G. (2019). Modulation of fear generalization by the zona incerta. *Proc. Natl. Acad. Sci. U.S.A.* 116, 9072–9077. doi: 10.1073/pnas.1820541116

Voges, J., Volkmann, J., Allert, N., Lehrke, R., Koulousakis, A., Freund, H. J., et al. (2002). Bilateral high-frequency stimulation in the subthalamic nucleus for the treatment of Parkinson disease: correlation of therapeutic effect with anatomical electrode position. *J. Neurosurg.* 96, 269–279. doi: 10.3171/jns.2002.96.2.0269

Wang, X., Chou, X. L., Zhang, L. I., and Tao, H. W. (2020b). Zona Incerta: an Integrative Node for Global Behavioral Modulation. *Trends Neurosci.* 43, 82–87. doi: 10.1016/j.tins.2019.11.007

Wang, H., Dong, P., He, C., Feng, X. Y., Huang, Y., Yang, W. W., et al. (2020a). Incerta-thalamic Circuit Controls Nocifensive Behavior *via* Cannabinoid Type 1 Receptors. *Neuron* 107, 538.e–551.e. doi: 10.1016/j.neuron.2020.04.027

Wang, X., Chou, X., Peng, B., Shen, L., Huang, J. J., Zhang, L. I., et al. (2019). A cross-modality enhancement of defensive flight *via* parvalbumin neurons in zona incerta. *Elife* 8:e42728. doi: 10.7554/eLife.42728

Watson, C., Lind, C. R., and Thomas, M. G. (2014). The anatomy of the caudal zona incerta in rodents and primates. *J. Anat.* 224, 95–107. doi: 10.1111/joa.12132

Weisshaar, E., and Matterne, U. (2016). Epidemiology of itch. In: itch: mechanisms and Treatment. *Curr. Probl. Dermatol.* 50, 11–17.

Wu, Z. H., Shao, H. Y., Fu, Y. Y., Wu, X. B., Cao, D. L., Yan, S. X., et al. (2021). Descending Modulation of Spinal Itch Transmission by Primary Somatosensory Cortex. *Neurosci. Bull.* 37, 1345–1350. doi: 10.1007/s12264-021-00713-9

Yosipovitch, G., Rosen, J. D., and Hashimoto, T. (2018). Itch: from mechanism to (novel) therapeutic approaches. *J. Allergy Clin. Immunol.* 142, 1375–1390. doi: 10.1016/j.jaci.2018.09.005

Yuan, L., Liang, T. Y., Deng, J., and Sun, Y. G. (2018). Dynamics and Functional Role of Dopaminergic Neurons in the Ventral Tegmental Area during Itch Processing. *J. Neurosci.* 38, 9856–9869. doi: 10.1523/jneurosci.1483-18.2018

Zhang, C., Zhu, H., Ni, Z., Xin, Q., Zhou, T., Wu, R., et al. (2021). Dynamics of a disinhibitory prefrontal microcircuit in controlling social competition. *Neuron.* doi: 10.1016/j.neuron.2021.10.034

Zhao, Z. D., Chen, Z., Xiang, X., Hu, M., Xie, H., Jia, X., et al. (2019). Zona incerta GABAergic neurons integrate prey-related sensory signals and induce an appetitive drive to promote hunting. *Nat. Neurosci.* 22, 921–932. doi: 10.1038/s41593-019-0404-5

Zhao, Z. Q., Liu, X. Y., Jeffry, J., Karunarathne, W. K., Li, J. L., Munanairi, A., et al. (2014). Descending control of itch transmission by the serotonergic system *via* 5-HT1A-facilitated GRP-GRPR signaling. *Neuron* 84, 821–834. doi: 10.1016/j.neuron.2014.10.003

Zhou, M., Liu, Z., Melin, M. D., Ng, Y. H., Xu, W., and Südhof, T. C. (2018). A central amygdala to zona incerta projection is required for acquisition and remote recall of conditioned fear memory. *Nat. Neurosci.* 21, 1515–1519. doi: 10.1038/s41593-018-0248-4

Zhu, Y. B., Xu, L., Wang, Y., Zhang, R., Wang, Y. C., Li, J. B., et al. (2020). Posterior Thalamic Nucleus Mediates Facial Histaminergic Itch. *Neuroscience* 444, 54–63. doi: 10.1016/j.neuroscience.2020.07.048

Conflict of Interest: The authors declare that the research was conducted in the absence of any commercial or financial relationships that could be construed as a potential conflict of interest.

Publisher's Note: All claims expressed in this article are solely those of the authors and do not necessarily represent those of their affiliated organizations, or those of the publisher, the editors and the reviewers. Any product that may be evaluated in this article, or claim that may be made by its manufacturer, is not guaranteed or endorsed by the publisher.

frontiers in Molecular Neuroscience

ORIGINAL RESEARCH
published: 15 March 2022
doi: 10.3389/fnmol.2022.844146

Combining Regional and Connectivity Metrics of Functional Magnetic Resonance Imaging and Diffusion Tensor Imaging for Individualized Prediction of Pain Sensitivity

*Rushi Zou[1,2,3], Linling Li[1,2,3], Li Zhang[1,2,3], Gan Huang[1,2,3], Zhen Liang[1,2,3], Lizu Xiao[4] and Zhiguo Zhang[1,2,3,5]**

[1] School of Biomedical Engineering, Health Science Center, Shenzhen University, Shenzhen, China, [2] Guangdong Provincial Key Laboratory of Biomedical Measurements and Ultrasound Imaging, Shenzhen University, Shenzhen, China, [3] Marshall Laboratory of Biomedical Engineering, Shenzhen, China, [4] Department of Pain Medicine and Shenzhen Municipal Key Laboratory for Pain Medicine, The Affiliated Shenzhen Sixth Hospital of Guangdong Medical University, Shenzhen, China, [5] Peng Cheng Laboratory, Shenzhen, China

OPEN ACCESS

Edited by:
Wen Wu,
Southern Medical University, China

Reviewed by:
Xianwei Che,
Hangzhou Normal University, China
Ruolei Gu,
Institute of Psychology (CAS), China

***Correspondence:**
Zhiguo Zhang
zgzhang@szu.edu.cn

Specialty section:
This article was submitted to Pain Mechanisms and Modulators, a section of the journal Frontiers in Molecular Neuroscience

Received: *27 December 2021*
Accepted: *22 February 2022*
Published: *15 March 2022*

Citation:
Zou R, Li L, Zhang L, Huang G, Liang Z, Xiao L and Zhang Z (2022) Combining Regional and Connectivity Metrics of Functional Magnetic Resonance Imaging and Diffusion Tensor Imaging for Individualized Prediction of Pain Sensitivity. Front. Mol. Neurosci. 15:844146. doi: 10.3389/fnmol.2022.844146

Characterization and prediction of individual difference of pain sensitivity are of great importance in clinical practice. MRI techniques, such as functional magnetic resonance imaging (fMRI) and diffusion tensor imaging (DTI), have been popularly used to predict an individual's pain sensitivity, but existing studies are limited by using one single imaging modality (fMRI or DTI) and/or using one type of metrics (regional or connectivity features). As a result, pain-relevant information in MRI has not been fully revealed and the associations among different imaging modalities and different features have not been fully explored for elucidating pain sensitivity. In this study, we investigated the predictive capability of multi-features (regional and connectivity metrics) of multimodal MRI (fMRI and DTI) in the prediction of pain sensitivity using data from 210 healthy subjects. We found that fusing fMRI-DTI and regional-connectivity features are capable of more accurately predicting an individual's pain sensitivity than only using one type of feature or using one imaging modality. These results revealed rich information regarding individual pain sensitivity from the brain's both structural and functional perspectives as well as from both regional and connectivity metrics. Hence, this study provided a more comprehensive characterization of the neural correlates of individual pain sensitivity, which holds a great potential for clinical pain management.

Keywords: pain sensitivity, fMRI, DTI, regional-connectivity features, machine learning

INTRODUCTION

Pain is a subjective, complex, and multidimensional sensory experience that exhibits huge inter-subject variability (Rainville, 2002; Nielsen et al., 2009; Coghill, 2010). The study of individual differences in pain sensitivity is of great importance in clinical practice (Werner et al., 2010; Abrishami et al., 2011) and in pharmaceutical research (Chizh et al., 2009; Angst et al., 2012).

For example, pain sensitivity is a predictive factor for the treatment outcome of many clinical diseases (Abrishami et al., 2011; Rehberg et al., 2017). Hence, investigating the underlying neural mechanism of individual differences in pain sensitivity cannot only deepen our understanding of pain sensitivity but can also be used to develop a predictive model of individual pain sensitivity.

With the fast development of neuroimaging technologies and associated data analytics, using neural images and signals, such as magnetic resonance imaging (MRI) and electroencephalography (EEG), to probe the neural mechanisms of pain has been widely adopted in pain researches, which include the studies of momentary (acute or chronic) pain experience (Apkarian et al., 2005) and pain sensitivity (Coghill et al., 2003; Zunhammer et al., 2016). The complex brain activity underlying pain sensitivity plays a major role in the representation and modulation of pain (Rainville, 2002; Apkarian et al., 2005). Several studies have revealed that individual differences in pain sensitivity are reflected in differences in brain structure and function by using different MRI modalities (Geisler et al., 2021; Niddam et al., 2021).

Resting-state functional magnetic resonance imaging (rs-fMRI) uses blood oxygenation level-dependent (BOLD) responses to study spontaneous brain activity in individuals when performing no specific task. A very widely used rs-fMRI feature is Regional Homogeneity (ReHo), which calculates Kendall's coefficient of concordance to measure regional synchronizations of temporal changes in BOLD activities in a voxel-wise manner (Baumgartner et al., 1999). Several studies used ReHo to investigate the local features of spontaneous brain activity in chronic pain such as migraine (Yu et al., 2012; Zhao et al., 2013; Zhang et al., 2016) and headache (Wang et al., 2014). These ReHo-based results showed that patients with chronic pain exhibited increased or decreased ReHo values in certain regions compared to healthy subjects. For example, Yoshino et al. (2017) found that ReHo at the dorsolateral prefrontal cortex significantly decreased in chronic pain patients. Another type of rs-fMRI feature popularly used in pain research is functional connectivity (FC). Unlike ReHo, which measures regional brain activities, FC measures the statistical relationship between BOLD signals of different brain regions. Many studies have demonstrated that FC between some specific regions is related to pain perception and can be used as a neural indicator of individual pain sensitivity. For example, Tu et al. (2019) used multivariate pattern analysis to find that resting-state FC could predict individual pain thresholds with high accuracy (a correlation coefficient of 0.60 between predicted and real values of heat pain thresholds). Meanwhile, they found that the connections within medial-frontal and frontal-parietal networks are the most predictive FC features of pain sensitivity. Another study (Spisak et al., 2020) also identified and validated a pain-free resting-state FC pattern that is predictive of individual differences in pain sensitivity.

Besides rs-fMRI, diffusion tensor imaging (DTI), which maps white matter anatomical connections in the living human brain, is another common MRI modality that has been gradually used to study individual differences in pain sensitivity (Deppe et al., 2013; Porpora et al., 2018). Fractional anisotropy (FA) is the most widely used quantitative DTI measure and it reflects how the diffusion of water is directionally constrained along axons (Alexander et al., 2007). Several DTI studies have found abnormal white matter changes in migraine and other chronic pain conditions (Mansour et al., 2013; Michels et al., 2017). On the other hand, DTI is able to characterize the structural connectivity (SC) based on the fibers connecting each pair of brains regions. DTI-based SC has also been used to investigate the pain-related brain networks. For example, by using the graph analysis of probabilistic tractography based on DTI, one study found that the anterior insula connectivity was related to the individual degree of pain vigilance and awareness (Wiech et al., 2014). Also, studies demonstrated that SC provides new insights into the understanding of chronic pain. For example, Huang et al. (2021) found that patients with chronic prostatitis/chronic pelvic pain syndrome had alterations of SC within the frontal-parietal control network.

However, most of the existing MRI studies regarding pain sensitivity are limited by only using one single modality of MRI (rs-fMRI or DTI) or only using one single type of feature (regional or connectivity features) to explore the relationship between pain sensitivity and MRI features. However, pain has a complicated neural mechanism, which influences and is influenced by the brain's structure and function. Also, both brain patterns within local regions and brain connections among local regions contribute to an individual's sensitivity of pain. Thus, only using one MRI modality or using one type of feature (regional or connectivity) cannot offer a complete characterization of brain patterns related to pain and cannot provide sufficient information to accurately predict the individual pain sensitivity. Accumulated evidence have shown the importance of using multiple MRI modality in the understanding of cognitive functions and the diagnosis of neurological diseases (Michels et al., 2017; Dhamala et al., 2020). For example, Xiao et al. (2021) built a model to predict visual working memory capacity by using voxel-wise multimodal MRI features (amplitude of low-frequency fluctuations from fMRI, gray matter volume from structural MRI, and FA from DTI). On the other hand, MRI studies based on both regional patterns and inter-regional connectivity patterns are also gaining popularity in the research of brain disorders. For example, Luo et al. (2020) used multi-features, including both regional features and connectivity features extracted from fMRI and DTI, to significantly improve the prediction performance of adult outcomes in childhood-onset attention-deficit/hyperactivity disorder compared to using the models based on one type of features. However, combining both regional and connectivity features from both rs-fMRI and DTI in the prediction of pain sensitivity is still lacking. As a result, it remains unclear how the brain's structure, function, and connectivity interact and synergize in the determination of an individual's pain sensitivity.

In the present study, we hypothesize that both regional and connectivity features from both rs-fMRI and DTI are predictive of an individual's pain sensitivity. This hypothesis was proposed based on the following facts. First, scattered evidence has shown that, either regional or connectivity patterns measured from either fMRI or DTI were correlated with an individual's pain threshold (Rogachov et al., 2016; Hsiao et al.,

2020; Geisler et al., 2021). Second, for either fMRI or DTI, its regional patterns and connectivity patterns are associated (Ma et al., 2010; Straathof et al., 2019). Third, because of the brain's structural-functional coupling, fMRI and DTI are also correlated in terms of regional characteristics or connections (Gu et al., 2015; Tang and Bassett, 2018; Straathof et al., 2019). These literature supports will be further elaborated in the Discussion.

To validate this hypothesis, we acquired rs-fMRI and DTI data as well as laser pain threshold from 210 healthy participants and explored the relationship between multi-modal MRI features and individual pain sensitivity. For each participant, we extracted regional and connectivity features from two MRI modalities (ReHo and FC from rs-fMRI; FA and SC from DTI). We used machine learning and feature selection methods to construct prediction models and to identify the most predictive features of pain sensitivity. Furthermore, to examine whether different MRI modalities and different feature types can provide complementary information in predicting an individual's pain thresholds, we established a series of models to fuse various types of MRI features at the decision level and compared their performance.

MATERIALS AND METHODS

Participants

We recruited a total of 210 healthy participants (131 females; age: 20.81 ± 2.93 years) through college and community advertisements and paid for their participation. All the participants were right-handed. Before the experiments, participants were carefully screened to ensure that they had no history of chronic pain, neurological diseases, cerebrovascular diseases, coronary heart disease, and mental disorders, and they had no contraindications to MRI examination. The study was proved by the local ethics committee and all participants gave their written informed consent before participating in the study.

Measurement of Pain Threshold

Pain sensitivity of all the participants was measured as the laser pain threshold in a behavioral experiment before the MRI scan. The laser pain threshold was measured manually using quantitative sensory testing. A series of infrared neodymium yttrium aluminum perovskite (Nd: YAP) laser stimuli were delivered to the back area between the thumb and index finger of a participant's left hand. The measurement started from an energy level at 1 J with a 0.25 J increase at each stimulus. After each stimulus, a participant was asked to report the pain rating from 0 (no pain) to 10 (the worst pain). When a rating of 4 was reported, the corresponding energy level was recorded as the laser pain threshold. For each participant, the laser pain threshold was averaged from two independent measurements conducted in 1 h.

Magnetic Resonance Imaging Acquisition

Multimodal MRI data were acquired using a GE 3.0 T scanner. Resting-state fMRI were collected using the following parameters: 43 oblique slices, thickness/gap = 3/0 mm, acquisition matrix = 64×64, TR = 2,000 ms, TE = 30 ms, flip angle = 90°, field of view = 22×22 mm^2, total volume = 300, acquisition time = 10 min. For the DTI data, the following acquisition parameters were used: 70 axial slices, TR = 8,500 ms, TE = 80.8 ms, 64 optimal non-linear diffusion-weighted directions with b = 1,000 s/mm2 and one additional image without diffusion weighting (i.e., b = 0 s/mm2), 2.0-mm slice thickness, acquisition matrix = 128×128; 2×2 mm in-plane resolution, acquisition time = 10:50 min.

Data Analysis

Functional Magnetic Resonance Imaging Preprocessing

Resting-state fMRI preprocessing was performed with DPABI[1] (Yan et al., 2016) and SPM12 (Statistical Parametric Mapping; Wellcome Department of Imaging Neuroscience, University College London, United Kingdom)[2] running under Matlab R2017b (Mathworks, Sherborn, MA). For each subject, the first 10 volumes of rs-fMRI data were discarded, leaving 290 images pre-processed. The middle slice was used as the reference slice for slice timing correction. Then, fMRI data were realigned to correct the head motion and obtained the 6 rigid body motion parameters. T1 images were co-registered to functional images and segmented into gray matter, white matter, and cerebrospinal fluid. In order to decrease the effects of head motion, the Friston 24-parameter model, 6 head motion parameters, 6 head motion parameters one time point before, and the 12 corresponding squared items (Friston et al., 1996), were used to regress out the head motion parameters. Time points with the head motion parameters larger than 0.2 were scrubbed, and they were modeled as a separate covariable for regression to decrease their influence on the continuity of time. The functional images were then normalized into standard Montreal Neurological Institute (MNI) space, resampled to a 3 × 3 × 3 mm^3 voxel. Finally, a bandpass filter with a frequency window of 0.01–0.1 Hz was used to improve the signal-to-noise ratio of fMRI signals.

Diffusion Tensor Imaging Preprocessing

The DTI data were preprocessed by the PANDA toolbox (Cui et al., 2013)[3] in the FSL diffusion toolkit and MRIcron. The preprocessing steps were performed as follows. Briefly, (a) covert the DICOM files of all subjects into NIfTI images using the MRIcron; (b) estimate the brain mask by extracting the brain tissue and structure; (c) correct for the eddy-current effect; (d) average acquisitions and calculate DTI metrics. In order to get the voxel-based diffusion metrics for the subsequent analysis, the individual diffusion metric images were transformed from the native space into a standard Montreal Neurological Institute (MNI) space (voxel size 1 mm × 1 mm × 1 mm^3) via spatial normalization and smoothed with a 6 mm full width at half-maximum (FWHM) Gaussian kernel.

[1] http://rfmri.org/dpabi/

[2] http://www.fil.ion.ucl.ac.uk/spm

[3] http://www.nitrc.org/projects/panda

Brain Parcellation

In order to better compare the results of different imaging modalities, we used the Automated Anatomical Labeling (AAL) (Tzourio-Mazoyer et al., 2002) atlas, which was commonly adopted in multimodality researches to achieve the whole-brain parcellation on both functional data and structural data (Wee et al., 2012; Ahmed et al., 2017). Cerebellar regions were excluded for incomplete coverage of the cerebellum of several participants. In total 90 regions of interest (ROIs) were defined by the AAL atlas and used in subsequent analyses.

Feature Extraction

We extracted both regional and connectivity metrics from pre-processed fMRI and DTI for the prediction of the laser pain threshold.

fMRI ReHo: For fMRI, individual ReHo maps were generated by calculating Kendall's coefficient concordance of the time series of a given voxel with those of its surrounding 27 voxels (Zang et al., 2004). Then, the data were smoothed with a Gaussian filter of 6 mm FWHM to reduce noise and residual differences in gyral anatomy. These individual maps underwent whole-brain equalization for further analysis. Finally, 55017 ReHo features were extracted for each participant.

fMRI FC: For fMRI FC matrices, Pearson's correlation coefficients (PCC) between BOLD time courses of each pair of ROIs were calculated for each subject. The obtained correlation matrix for each subject was then normalized using Fisher's z-transformation to improve normality. The FC matrix for each individual was a 90×90 symmetric matrix. Only the lower triangular matrix, which has 4005 FC features, was taken for subsequent analysis.

DTI FA: For DTI, the FA matrix, which measures the degree of anisotropy of water diffusion, was calculated in the MNI space for each individual. FA is calculated from the eigenvalues of the diffusion tensor, and its value varies between 0 and 1. FA = 0 means that the diffusion ellipsoid is a sphere (perfect isotropic diffusion). When the eigenvalues become more unequal with progressive diffusion anisotropy, the FA $\rightarrow$ 1. Finally, for each participant, 55017 FA features were extracted for the following analysis.

DTI SC: After the pre-processing of DTI data, probabilistic tractography was used to construct the SC network (Behrens et al., 2007). Briefly, for each defined brain region/node, probabilistic tractography was performed by seeding from all voxels of this region. For each voxel, 5000 fibers were sampled. The connectivity probability from the seed region *i* to another region *j* was defined by the number of fibers passing through region *j* divided by the total number of fibers sampled from region *i*. The connectivity probability of each node to the other nodes within the brain network can be calculated by repeating the tractography procedure for all nodes. This leads to an individual-specific weighted matrix, whose rows and columns represent the brain nodes and whose elements represent the connectivity probability between nodes. The SC matrix for each participant was a 90× 90 matrix.

Prediction of Pain Threshold

After regional features (i.e., ReHo and FA) and connectivity features (i.e., FC and SC) were extracted from fMRI and DTI data, we used feature selection and machine learning techniques to establish models for predicting individual laser pain thresholds. As shown in **Figure 1**, the whole procedure of pain threshold prediction is detailed as follows.

Cross-validation: We selected the features, trained and tested the prediction models based on the leave-one-individual-out cross-validation. At each run, we randomly used one participant's data for testing and the remaining participants' data for training. Because we had a total of 210 participants, the procedure was repeated 210 times to make sure that each participant's data were used as test samples once.

Feature selection: To improve the model accuracy and increase the model interpretability, it is necessary to identify a subset of most predictive features from a high-dimensional feature. We adopt the correlation-based feature selection method for each type of feature (ReHo, FA, FC, or SC) separately. In each run of the cross-validation in regression, PCC between each type of feature and the laser pain thresholds were computed within the training data to make sure the test data were not involved in the step of feature selection. The features with correlation significance beyond a threshold (P = 0.05; P = 0.01; P = 0.001, tested separately for comparison, see **Supplementary Tables 1, 2** for details) were selected and used for the prediction of pain thresholds.

Machine learning algorithms: After feature normalization, four popular and effective ML regression algorithms were used to model the relationship between these MRI features and laser pain threshold, namely, support vector machine regression with linear kernels (SVR-Linear) or Gaussian kernels (SVR-RBF), partial least squares regression (PLSR), and random forest regression (RF). All these algorithms were implemented with the open-source scikit-learn library for python (Pedregosa et al., 2011).

Models with different feature types: We compared the prediction performance of a series of models based on single-modality and single-type features using different machine learning algorithms and different thresholds of feature selection. **Supplementary Tables 1, 2** show the prediction performance of these models. Four models using one type of feature, namely ReHo (SVR-Linear, threshold < 0.001), FA (SVR-RBF, threshold < 0.01), FC (SVR-Linear, threshold < 0.001), and SC (SVR-RBF, threshold < 0.001) models, were determined first because of their better performance than models with other ML algorithms and parameters. Then, features were selected based on above four models using the corresponding feature type. As a result, the fusion process allowed information from multiple modalities to integrate but did not interfere with the feature selection and model selection in each model (ReHo, FA, FC, or SC model). Next, we build five models using different combinations of features: ReHo + FA (regional features), FC + SC (connectivity features), ReHo + FC (fMRI features), FA + SC (DTI features), and all four features. An average of the predicted values of multiple single-type feature models was calculated as the

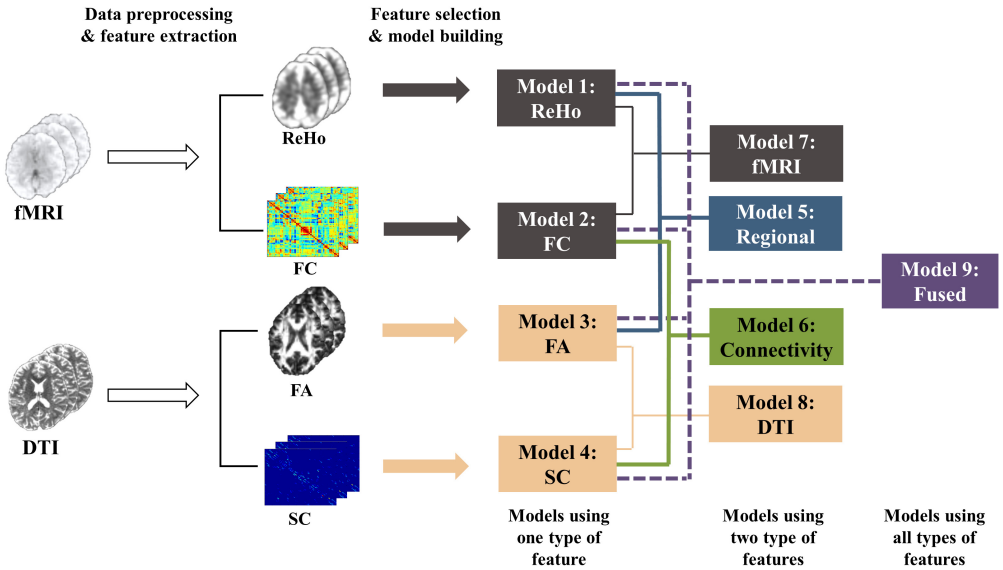

FIGURE 1 | The whole procedure of the pain threshold prediction analysis based on multi-features of multi-modal MRI.

final predicted threshold of each multimodality models. More precisely, we established and compared the following 9 models with different types of features:

1. ReHo Model: using ReHo features;
2. FC Model: using FC features;
3. FA Model: using FA features;
4. SC Model: using SC features;
5. Regional Model: using ReHo (from rs-fMRI) and FA (from DTI) features;
6. Connectivity Model: using FC (from rs-fMRI) and SC (from DTI) features;
7. fMRI Model: using ReHo (regional) and FC (connectivity) features from fMRI;
8. DTI Model: using FA (regional) and SC (connectivity) features from DTI;
9. Fused Model: using all features (ReHo + FA + FC + SC).

Performance evaluation: PCC between the predicted thresholds and the true values across all participants was calculated as the main metric of the performance of these prediction models. Also, we calculated the mean absolute error (MAE), which measured the overall distance between predicted and true values. MAE is calculated as:

$$MAE = \frac{1}{N}\sum_{n=1}^{N}\left|\widehat{y_n} - y_n\right|,$$

where y_n is the measured pain threshold of the n-th participant, $\widehat{y_n}$ is the pain threshold estimated from the prediction model, and N is the total number of participants. The prediction performance in terms of MAE of nine models was compared using paired t-test. The PCCs of any two models were compared using the test for comparing elements of a correlation matrix, as suggested in Steiger (1980). This correlation test was adopted here because the true labels were used in the calculation of all PCCs so that these PCCs were not independent and the conventional t-test could not be used.

Identifying common predictive features: This part is aimed at identifying the brain regions and brain connectivity that are commonly selected across individuals. We calculated the occurrence frequency of each feature across all folds in leave-one-individual-out cross-validation involved in building the models based on one type of feature. For better visualization and interpretation of the features, we only showed those features which were selected more than half of the time in the whole leave-one-individual-out cross-validation procedure. ReHo and FA results were mapped onto the AAL-90 atlas. Connectivity results were visualized by using the Connectivity Visualization Tool[4].

RESULTS

Measurements of Pain Threshold

For all participants, the laser pain thresholds were 2.57 ± 0.53 J (mean ± std). We calculated the PCC between age and pain sensitivity but found no significant relationship (p = 0.98) between age and laser pain threshold. A two-sample t-test revealed that gender had no significant effect on the laser pain threshold (p = 0.49).

Prediction Performance of Different Models

Table 1 shows the prediction performance of nine laser pain threshold prediction models: ReHo Model (PCC = 0.30, $p = 7.64\times10^{-6}$), FC Model (PCC = 0.23, $p = 8.73\times10^{-4}$), FA

[4]https://bioimagesuiteweb.github.io/webapp/connviewer.html

TABLE 1 | Prediction performance of different models using different feature sets.

Feature set	MAE (mean ± std)	PCC (R and *p*-values)
ReHo	0.42 ± 0.33	0.30 (7.64×10^{-6})
FC	0.43 ± 0.32	0.23 (8.73×10^{-4})
FA	0.39 ± 0.29	0.35 (1.61×10^{-7})
SC	0.41 ± 0.32	0.30 (1.36×10^{-5})
fMRI (ReHo + FC)	0.39 ± 0.31	0.35 (2.91×10^{-7})
DTI (FA + SC)	0.37 ± 0.30	0.43 (1.16×10^{-10})
Regional (ReHo + FA)	0.37 ± 0.30	0.42 (3.73×10^{-10})
Connectivity (FC + SC)	0.38 ± 0.30	0.38 (9.54×10^{-9})
Fused (ReHo + FC + FA + SC)	**0.36 ± 0.29**	**0.51** (4.99×10^{-15})

Highlight the best performance of the prediction model.

Model (PCC = 0.35, $p = 1.61\times10^{-7}$), SC Model (PCC = 0.30, $p = 1.36\times10^{-5}$), fMRI Model (PCC = 0.35, $p = 2.91\times10^{-7}$), DTI Model (PCC = 0.43, $p = 1.16\times10^{-10}$), Regional Model (PCC = 0.42, $p = 3.73\times10^{-10}$), Connectivity Model (PCC = 0.38, $p = 9.54\times10^{-9}$), and Fused Model (PCC = 0.51, $p = 4.99\times10^{-15}$). As shown in **Figure 2**, the correlation results of all prediction models are significant. **Figure 3** compares the PCC between predicted and real laser pain thresholds of all the participants among different prediction models. We have the following two major observations from **Table 1** and **Figures 2**, **3**. First, the prediction performances in terms of PCC of the models based on two type features (i.e., Regional Model, Connectivity Model, fMRI Model, and DTI Model) are higher than models which only used one type of feature. Specifically, the correlation result of fMRI Model is significantly better than FC Model ($p = 0.007$), and PCC of DTI Model is significantly better than SC model ($p = 4.19\times10^{-5}$). Also, PCC of Regional Model is significantly better than ReHo model ($p = 6.90\times10^{-5}$), and PCC of Connectivity Model is significantly better than FC model ($p = 0.002$) and SC model ($p = 0.05$). Second, the correlation result of Fused Model is significantly better than all models based on one-type (Fused vs. ReHo, $p = 2.08\times10^{-5}$; Fused vs. FC, $p = 2.67\times10^{-7}$; Fused vs. FA, $p = 0.007$; Fused vs. FT, $p = 4.49\times10^{-4}$) or two type features (Fused vs. fMRI, $p = 3.43\times10^{-6}$; Fused vs. DTI, $p = 0.057$; Fused vs. Regional, $p = 0.011$, Fused vs. Connectivity, $p = 9.29\times10^{-4}$).

Predictive Multimodality Features

Table 2 and **Figure 4** show the common predictive regional feature sets (ReHo or FA, respectively), which were determined

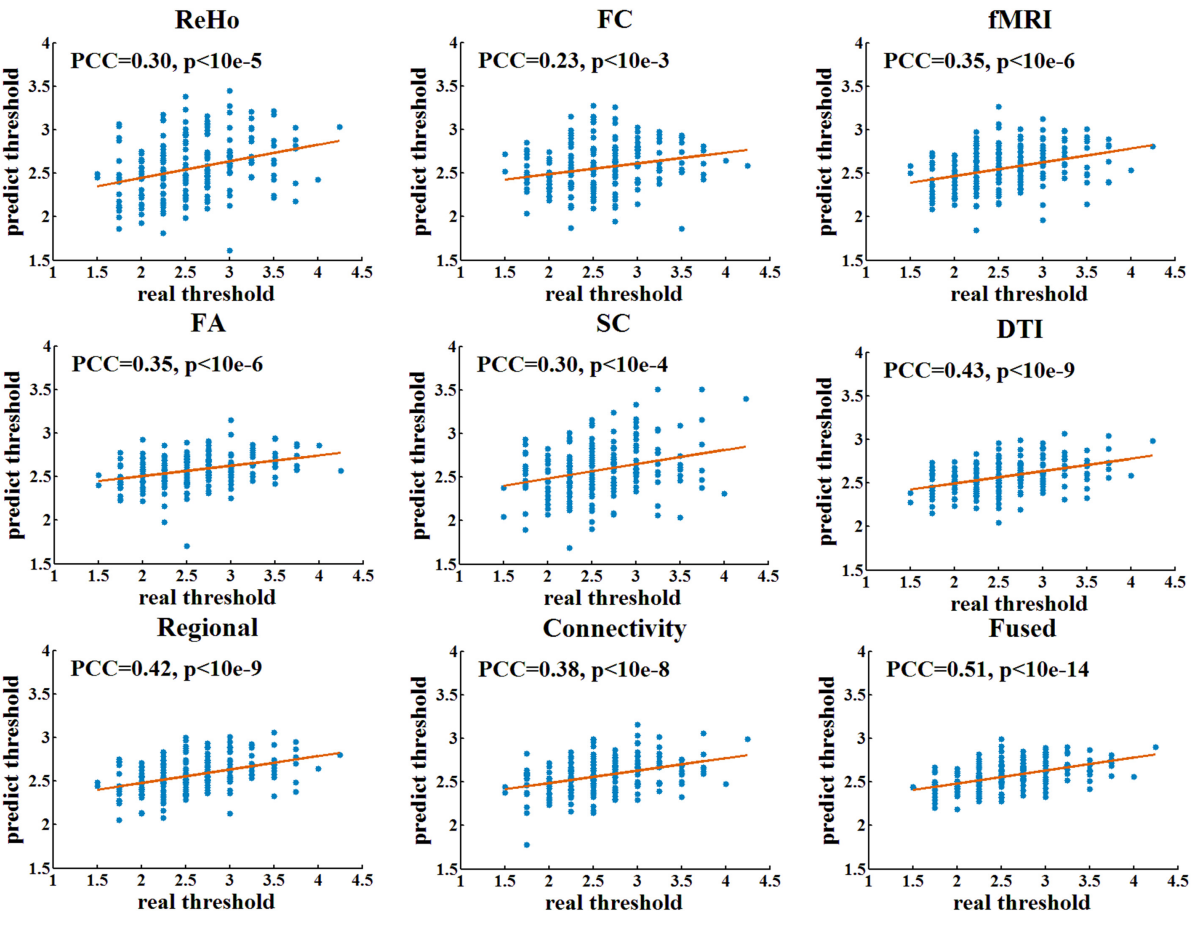

FIGURE 2 | The linear correlation between predicted and real pain thresholds. Each blue dot denotes one participant. Red lines are linear fitting lines.

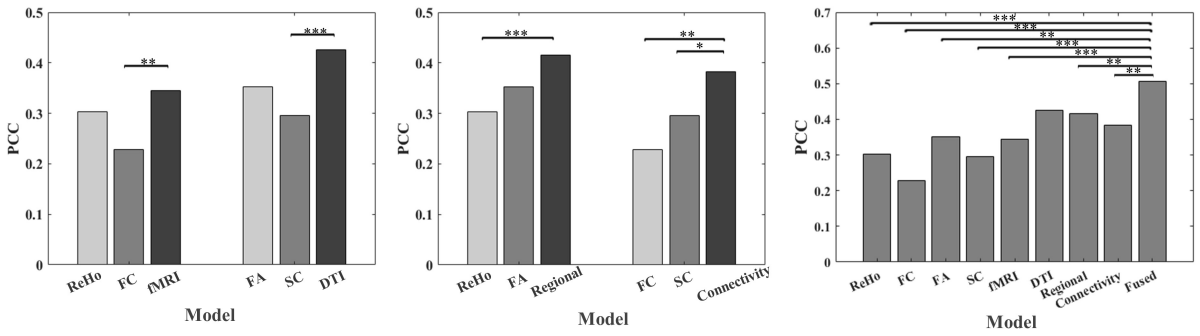

FIGURE 3 | Comparison of PCC between predicted and real laser pain threshold among models using different features. * indicates $p < 0.05$, ** indicates $p < 0.01$, *** indicates $p < 0.001$.

because they were selected for more than half of the time in the leave-one-individual-out cross-validation for the laser pain threshold prediction. Finally, ReHo features of 109 voxels were selected and they were mainly in Parietal_Inf_L, SupraMarginal_L/R, Insula_R, Rolandic_Oper_R, Calcarine_R, Temporal_Mid_R, Precuneus_R, Cingulum_Mid_R. FA features of 668 voxels were selected and they were mainly in Occipital_Inf_R, Temporal_Inf_R, Calcarine_R, Precuneus_R, Insula_L/R, Frontal_Mid_R, Temporal_Pole_Mid_L, Putamen_L/R, Lingual_R. The common regions of ReHo and FA feature sets are Precuneus_R, Insula_R, and Calcarine_R.

As shown in **Table 3** and **Figure 4**, there were 35 common FC features and 2 common SC features were visualized because they were selected for more than half of the time in the leave-one-individual-out cross-validation. These FC features are predominately for the prefrontal-parietal and insula-cingulate networks. For SC, the 2 features are Occipital_Inf_R-Lingual_R, Fusiform_R-Occipital_Sup_R. The common hub of FC and SC is Occipital_Sup_R.

DISCUSSION

In this study, we investigated the predictive capability of multi-features of multi-modal MRI data in the prediction of individual pain sensitivity, as measured by laser pain threshold. The results on 210 healthy subjects demonstrated that fMRI-DTI and regional-connectivity features are capable of accurately predicting an individual's pain threshold. Importantly, the predictive capability of fusing fMRI-DTI and regional-connectivity features is significantly higher than that of using one type of feature from one imaging modality (i.e., ReHo, FA, FC, or SC). These results revealed rich information about individual pain sensitivity from the brain's both structural and functional perspectives as well as from both regional and connectivity brain patterns.

TABLE 2 | List of common predictive regional features for the prediction of laser pain threshold.

Feature set	Regions or connectivity
ReHo	Parietal_Inf_L, SupraMarginal_L/R, Insula_R, Rolandic_Oper_R, Calcarine_R, Temporal_Mid_R, Precuneus_R, Cingulum_Mid_R
FA	Occipital_Inf_R, Temporal_Inf_R, Calcarine_R, Precuneus_R, Insula_L/R, Frontal_Mid_R, Temporal_Pole_Mid_L, Putamen_L/R, Lingual_R
Common regions	Insula_R, Calcarine_R, Precuneus_R

Fused Model Achieves Higher Performance

The fused model that uses fMRI-based ReHo and FC features and DTI-based FA and SC features has the best prediction performance because (1) it uses both regional and connectivity features, and (2) it uses two imaging modalities.

First, the prediction models (i.e., fMRI Model, DTI Model, or Fused Model) which fused the regional features (i.e., ReHo and FA) and brain connectivity features (i.e., FC and SC) outperformed the prediction models which only used one type feature, suggesting that multi-type imaging features embrace richer information than single-type features in the prediction of pain sensitivity. The regional functional feature, ReHo, which reflects the spontaneous brain activity observed in specific regions, serves an important functional role in the efficacy of neural systems. Also, regional structural characteristics like FA reflect the changes in microstructure (Basser and Pierpaoli, 2011). Actually, several previous studies (Erpelding et al., 2012; Emerson et al., 2014; Rogachov et al., 2016; Geisler et al., 2021) have demonstrated the relationship between regional functional signal or structural characteristics and individual pain sensitivity. However, as pain is a complex experience related to a wide network of brain regions, it is also important to explore the relationship between individual pain sensitivity and brain connectivity which reflect the communication between distinct regions. Combining the information of both regional measurement and brain connectivity gives us a more complete understanding of the brain mechanisms underlying pain sensitivity, which may also be the reason for the improvement of the prediction performance after fusion. We will further discuss these predictive regional and connectivity features later in this section.

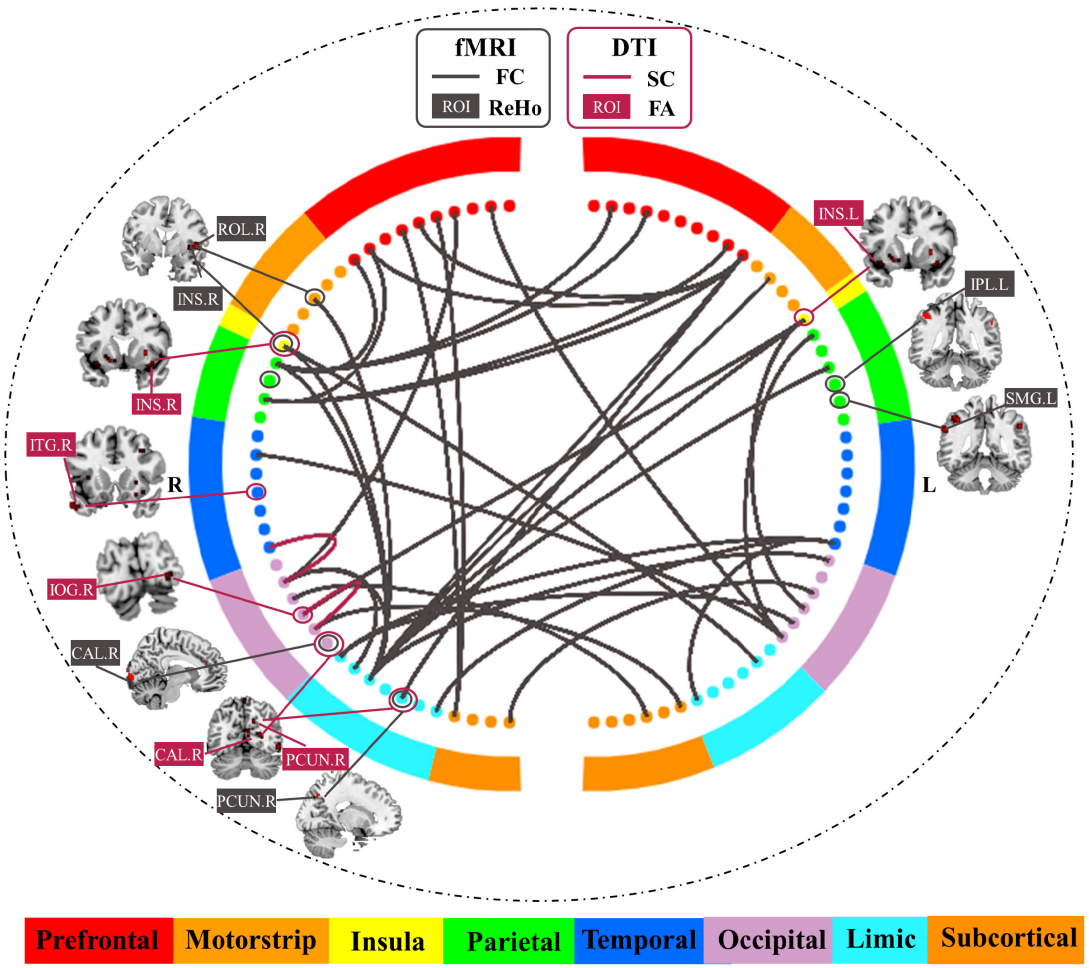

FIGURE 4 | Common predictive regional features and connectivity features for the prediction of laser pain threshold.

Second, we found that models based on both fMRI and DTI features are more predictive than those used single modality only, which implies these two MRI modalities contribute to the determination of pain sensitivity from different perspectives. But the predictive power of fused models is not simply equal to the sum of the power of the related prediction models which only used one MRI modality. This is expected because a wealth of research (Gu et al., 2015; Tang and Bassett, 2018) has shown that white matter microstructure links discreet brain areas and thus regulates brain function. In another word, DTI and fMRI features are correlated because of the brain's structure-function coupling. Therefore, the information provided by fMRI and DTI, on the one hand, complements to each other, while on the other hand, overlaps to some extent. Although little effort has been made on utilizing the multimodal neuroimaging data (fMRI and DTI) for predicting individual pain sensitivity, several studies demonstrated the advantage of integrating DTI and fMRI in the field of cognitive neuroscience and psychiatry (Goble et al., 2012; Sugranyes et al., 2012). For example, Xiao et al. (2021) combined regional features extracted from the whole brain in three modalities (fMRI data, T1-weighted data, and DWI data), achieving a good performance in predicting individual visual working memory capacity.

Functional Magnetic Resonance Imaging Features Predictive of Pain Sensitivity

Our results indicated some relations between the common predictive fMRI regional features and FC features. We found that the selected fMRI regional features are mainly located in the precuneus, insula, and calcarine. As identified in the previous studies, precuneus plays an important role in pain processing (Zhang et al., 2020), possibly with different mechanisms. Precuneus is engaged in continuous information gathering and representation of the self and the external world (co-perception), as well as in the assessment of self-relevant sensations (Johnson et al., 2006), both of which are important aspects of the pain experience. Also, the precuneus is a core constituent of the default-mode network (DMN) (Utevsky et al., 2014), of which the alterations have been well documented to be related to pain progression. In addition, Goffaux et al. (2014) found that pain sensitivity in healthy adults was closely tied to pain-evoked

TABLE 3 | List of common predictive connectivity features for the prediction of laser pain threshold.

Feature set	Regions or connectivity
FC	Frontal_Sup_R- Caudate_R
	Frontal_Sup_Orb_L—Parietal_Sup_R
	Frontal_Mid_Orb_L—Parietal_Sup_R
	Frontal_Mid_Orb_R—Occipital_Sup_R
	Frontal_Inf_Oper_L—Frontal_Inf_Tri_R
	Frontal_Inf_Oper_L—Cingulum_Mid_R
	Frontal_Inf_Oper_L—Parietal_Inf_R
	Frontal_Inf_Oper_L—Precuneus_R
	Frontal_Inf_Oper_R—Parietal_Sup_R
	Frontal_Inf_Tri_L—Parietal_Inf_R
	Frontal_Inf_Tri_R—Parietal_Inf_R
	Rolandic_Oper_L—Cingulum_Mid_R
	Rolandic_Oper_R—Cingulum_Mid_R
	Olfactory_L—Lingual_R
	Frontal_Sup_Medial_R—Caudate_R
	Rectus_R—Calcarine_L
	Insula_L—Cingulum_Mid_R
	Insula_L—Cuneus_L
	Insula_L—Occipital_Inf_R
	Insula_R—Cingulum_Mid_L
	Insula_R—Cingulum_Mid_R
	Cingulum_Ant_R—Occipital_Sup_R
	Cingulum_Mid_R—Occipital_Sup_L
	Cingulum_Mid_R—Occipital_Sup_R
	Cingulum_Mid_R—Parietal_Sup_L
	Cingulum_Mid_R—Parietal_Sup_R
	Hippocampus_R—Lingual_L
	Hippocampus_R—Fusiform_L
	ParaHippocampal_L—Fusiform_L
	ParaHippocampal_R—Fusiform_L
	Calcarine_L—Postcentral_L
	Calcarine_L—Temporal_Pole_Mid_R
	Occipital_Mid_R—Caudate_L
	Occipital_Inf_L—Pallidum_R
	Frontal_Mid_R—Frontal_Inf_Oper_L
SC	Occipital_Inf_R—Lingual_R
	Fusiform_R—Occipital_Sup_R

responses in the contra-lateral precuneus, which was similar to our study. Insula is a part of cortical regions that are related to the affective/motivational aspect of pain (Greenspan et al., 1999; Duerden and Albanese, 2013), and it is also important in the prediction of pain sensitivity.

As for common predictive FC features, a large number of prefrontal-parietal and insula-cingulate connectivity features were identified. Among these connections, we can easily find that some hubs, such as mid-cingulate cortex and insula, were also identified as common predictive regional results, which further showed the important roles of mid-cingulate cortex and insula in the determination of pain sensitivity. A study (Hsiao et al., 2020) has mentioned that pain sensitivity in healthy individuals is associated with the FC in pain-related cortical regions such as the insula. Beyond that, connections between prefrontal cortex and parietal lobe were also found to be the most important predictive connections. This finding is similar to previous studies (Tu et al., 2019), which found the frontal-parietal networks are useful in predicting an individual's pain threshold at both with-session and between-session levels.

Diffusion Tensor Imaging Features Predictive of Pain Sensitivity

For FA, the feature analysis demonstrated the FA features in Occipital_Inf_R, Temporal_Inf_R, Calcarine_R, Precuneus_R, Insula, and Lingual_R are useful for the prediction of laser pain threshold. Importantly, we could find that insula, precuneus, and calcarine are the common predictive regions identified from both fMRI regional features and DTI structural features. Therefore, these results do not only reflect the consistency of structure and function of the brain, but also confirm the key roles of these regions in the determination of pain sensitivity. For SC, occipital-occipital and occipital-temporal connections are predictive for the prediction of pain sensitivity. Actually, till now, only a few studies focused on the relationship between individual pain sensitivity and structural properties of white matter and the findings in these studies are inconsistent. Previous studies suggest that white matter properties are distinct between pain conditions (Mansour et al., 2013; Michels et al., 2017). For example, a DTI study found a negative correlation between FA and migraine duration in the mid-insula and a positive correlation between left mid-insula FA and pain catastrophizing (Mathur et al., 2016). Also, studies have provided evidence that white matter integrity within and between regions of the descending pain modulatory network is critically linked with the individual ability for endogenous pain control (Stein et al., 2012). Our study did not find many predictive DTI SC features in healthy individuals, which may imply that the white matter connectivity is mainly related to pain conditions of chronic patients but not closely related to healthy individuals' pain sensitivity.

Limitations and Future Work

Some limitations of the present study are mentioned here. First, the cerebellum was not included in the feature analysis because a proportion of participants had incomplete coverage of the cerebellum. Previous studies have suggested that the cerebellum has a role in pain and nociceptive processing (Moulton et al., 2010; Tu et al., 2019), so connectivity between the cerebellum and other regions may also be predictive of pain thresholds. Second, AAL atlas was used in our study to extract features in both the fMRI and DTI data. In fact, for each modality, there are more elaborate atlas options. To better compare the features between two modalities' data, we finally chose commonly used AAL atlas to unify the atlas. Third, to some extent, the regional results showed lateralization to the right, which may be influenced by the location of the stimulus. To better validate the hypothesis, the measurement of pain sensitivity can be carried out on both left and right hands/legs. Moreover, pain sensitivity can be measured in many ways. In addition to the pain threshold used in our study, pain tolerance threshold and pain intensity can also be used to assess pain sensitivity. Meanwhile, different painful stimulus could also be used in pain measurement. To better describe subjects' pain sensitivity, different pain measurements should be considered in the future studies. Fourth, the subjects recruited in this study were all young adults, but pain sensitivity and brain structure/function may vary across different ages. Several studies (Cole et al., 2010; El Tumi et al., 2017) have demonstrated that pain sensitivity varies with age. To better study the stability of pain sensitivity and understand the mechanism of pain sensitivity, it will be better to recruit a cohort with a more widely spectrum of ages in further studies. Finally, our finding would be helpful in understanding pain sensitivity in both structural and functional perspectives. However, the correlation

between fMRI and DTI features and the underlying mechanism about how these multimodality features contribute together to affect the individual pain sensitivity remain unclear. Previous studies (Warbrick et al., 2017) have revealed that there is a relationship between fMRI features and DTI features and the relationship is task- and region-dependent. In our study, the relationship between the brain's function and structure in these overlapping regions and how they work together to decide one's pain sensitivity need to be confirmed by further studies. One possibility is that, a brain region's function is (at least partially) determined by its structural characteristics and the brain function reflects complex multisynaptic interactions in structural networks (Suárez et al., 2020).

CONCLUSION

In summary, we combined multi-features from multi-modal MRI data of healthy participants to investigate individual pain sensitivity and found that fusing functional and structural features as well as fusing regional and connectivity features can predict the individual pain threshold more accurately. Moreover, we identified several predictive features to individual pain sensitivity from both functional and structural perspectives as well as regional and connectivity perspectives. This study provides valuable information regarding how the brain's structure, function, and connectivity interact and synergize in the determination of an individual's pain sensitivity.

DATA AVAILABILITY STATEMENT

The orginal contributions presented in the study are included in the article/**Supplementary Material**, further inquires can be directed to the corresponding author/s.

ETHICS STATEMENT

The studies involving human participants were reviewed and approved by the Ethics Committee of the Institute of Psychology, Chinese Academy Sciences, the Ethics Committee of Liaoning Normal University, and the Ethics Committee of Shenzhen University.

AUTHOR CONTRIBUTIONS

RZ, LL, and ZZ contributed to the construction of the study hypothesis. GH and ZL collected the data. RZ analyzed the data. RZ, LL, LZ, and ZZ discussed the results and wrote the manuscript. All authors contributed to the article and approved the submitted version.

FUNDING

This work was supported in part by the National Natural Science Foundation of China under Grant 81871443, in part by the Natural Science Foundation of Guangdong Province, China, under Grant 2021A1515011152, in part by the Shenzhen-Hong Kong Institute of Brain Science-Shenzhen Fundamental Research Institutions under Grant 2021SHIBS0003, in part by the Shenzhen's Sanming Project of Medicine under Grant SZSM202111009, and in part by the Shenzhen Special Project for sustainable Development under Grant KCXFZ20201221173400001.

SUPPLEMENTARY MATERIAL

The Supplementary Material for this article can be found online at: https://www.frontiersin.org/articles/10.3389/fnmol.2022.844146/full#supplementary-material

REFERENCES

Abrishami, A., Chan, J., Chung, F., Wong, J., and Warner, D. S. (2011). Preoperative pain sensitivity and its correlation with postoperative pain and analgesic consumption: a qualitative systematic review. *J. Am. Soc. Anesthesiol.* 114, 445–457. doi: 10.1097/ALN.0b013e3181f85ed2

Ahmed, O. B., Benois-Pineau, J., Allard, M., Catheline, G., Amar, C. B. (2017). Recognition of Alzheimer's disease and Mild Cognitive Impairment with multimodal image-derived biomarkers and Multiple Kernel Learning. *Neurocomputing* 220, 98–110.

Alexander, A. L., Lee, J. E., Lazar, M., and Field, A. S. (2007). Diffusion tensor imaging of the brain. *Neurotherapeutics* 4, 316–329.

Angst, M. S., Phillips, N. G., Drover, D. R., Tingle, M., Ray, A., Swan, G. E., et al. (2012). Pain sensitivity and opioid analgesia: a pharmacogenomic twin study. *Pain* 153, 1397–1409. doi: 10.1016/j.pain.2012.02.022

Apkarian, A. V., Bushnell, M. C., Treede, R.-D., and Zubieta, J.-K. (2005). Human brain mechanisms of pain perception and regulation in health and disease. *Eur. J. Pain* 9, 463–484. doi: 10.1016/j.ejpain.2004.11.001

Basser, P. J., and Pierpaoli, C. (2011). Microstructural and physiological features of tissues elucidated by quantitative-diffusion-tensor MRI. *J. Magnet. Reson.* 213, 560–570.

Baumgartner, R., Somorjai, R., Summers, R., and Richter, W. (1999). Assessment of cluster homogeneity in fMRI data using Kendall's coefficient of concordance. *Magnet. Reson. Imag.* 17, 1525–1532. doi: 10.1016/s0730-725x(99)00101-0

Behrens, T. E., Berg, H. J., Jbabdi, S., Rushworth, M. F., and Woolrich, M. W. (2007). Probabilistic diffusion tractography with multiple fibre orientations: what can we gain? *Neuroimage* 34, 144–155. doi: 10.1016/j.neuroimage.2006.09.018

Chizh, B. A., Priestley, T., Rowbotham, M., and Schaffler, K. (2009). Predicting therapeutic efficacy—experimental pain in human subjects. *Brain Res. Rev.* 60, 243–254. doi: 10.1016/j.brainresrev.2008.12.016

Coghill, R. C. (2010). Individual differences in the subjective experience of pain: new insights into mechanisms and models. *Headache* 50, 1531–1535. doi: 10.1111/j.1526-4610.2010.01763.x

Coghill, R. C., McHaffie, J. G., and Yen, Y.-F. (2003). Neural correlates of interindividual differences in the subjective experience of pain. *Proc. Natl. Acad. Sci.* 100, 8538–8542.

Cole, L. J., Farrell, M. J., Gibson, S. J., and Egan, G. F. (2010). Age-related differences in pain sensitivity and regional brain activity evoked by noxious pressure. *Neurobiol. Aging* 31, 494–503. doi: 10.1016/j.neurobiolaging.2008.04.012

Cui, Z., Zhong, S., Xu, P., Gong, G., and He, Y. (2013). PANDA: a pipeline toolbox for analyzing brain diffusion images. *Front. Hum. Neurosci.* 7:42. doi: 10.3389/fnhum.2013.00042

Deppe, M., Müller, D., Kugel, H., Ruck, T., Wiendl, H., and Meuth, S. G. (2013). DTI detects water diffusion abnormalities in the thalamus that correlate with an extremity pain episode in a patient with multiple sclerosis. *NeuroImag. Clin.* 2, 258–262. doi: 10.1016/j.nicl.2013.01.008

Dhamala, E., Jamison, K., Jaywant, A., Dennis, S., and Kuceyeski, A. (2020). Integrating multimodal connectivity improves prediction of individual cognitive abilities. *biorxiv* [Preprint] doi: 10.1101/2020.06.25.172387

Duerden, E. G., and Albanese, M. C. (2013). Localization of pain-related brain activation: A meta-analysis of neuroimaging data. *Hum. Brain Mapp.* 34, 109–149. doi: 10.1002/hbm.21416

El Tumi, H., Johnson, M., Dantas, P., Maynard, M., and Tashani, O. (2017). Age-related changes in pain sensitivity in healthy humans: A systematic review with meta-analysis. *Eur. J. Pain* 21, 955–964. doi: 10.1002/ejp.1011

Emerson, N. M., Zeidan, F., Lobanov, O. V., Hadsel, M. S., Martucci, K. T., Quevedo, A. S., et al. (2014). Pain sensitivity is inversely related to regional grey matter density in the brain. *Pain* 155, 566–573. doi: 10.1016/j.pain.2013.12.004

Erpelding, N., Moayedi, M., and Davis, K. D. (2012). Cortical thickness correlates of pain and temperature sensitivity. *Pain* 153, 1602–1609. doi: 10.1016/j.pain.2012.03.012

Friston, K. J., Williams, S., Howard, R., Frackowiak, R. S., and Turner, R. (1996). Movement-related effects in fMRI time-series. *Magnet. Reson. Med.* 35, 346–355. doi: 10.1002/mrm.1910350312

Geisler, M., Rizzoni, E., Makris, N., Pasternak, O., Rathi, Y., Bouix, S., et al. (2021). Microstructural alterations in medial forebrain bundle are associated with interindividual pain sensitivity. *Hum. Brain Mapp.* 42, 1130–1137. doi: 10.1002/hbm.25281

Goble, D. J., Coxon, J. P., Van Impe, A., Geurts, M., Van Hecke, W., Sunaert, S., et al. (2012). The neural basis of central proprioceptive processing in older versus younger adults: an important sensory role for right putamen. *Hum. Brain Mapp.* 33, 895–908. doi: 10.1002/hbm.21257

Goffaux, P., Girard-Tremblay, L., Marchand, S., Daigle, K., and Whittingstall, K. (2014). Individual differences in pain sensitivity vary as a function of precuneus reactivity. *Brain Topograph.* 27, 366–374. doi: 10.1007/s10548-013-0291-0

Greenspan, J. D., Lee, R. R., and Lenz, F. A. (1999). Pain sensitivity alterations as a function of lesion location in the parasylvian cortex. *Pain* 81, 273–282. doi: 10.1016/S0304-3959(99)00021-4

Gu, S., Pasqualetti, F., Cieslak, M., Telesford, Q. K., Alfred, B. Y., Kahn, A. E., et al. (2015). Controllability of structural brain networks. *Nat. Commun.* 6:8414.

Hsiao, F.-J., Chen, W.-T., Liu, H.-Y., Wang, Y.-F., Chen, S.-P., Lai, K.-L., et al. (2020). Individual pain sensitivity is associated with resting-state cortical activities in healthy individuals but not in patients with migraine: a magnetoencephalography study. *J Headache Pain* 21:133. doi: 10.1186/s10194-020-01200-8

Huang, X., Chen, J., Liu, S., Gong, Q., Liu, T., Lu, C., et al. (2021). Impaired frontal-parietal control network in chronic prostatitis/chronic pelvic pain syndrome revealed by graph theoretical analysis: A DTI study. *Eur. J. Neurosci.* 53, 1060–1071. doi: 10.1111/ejn.14962

Johnson, M. K., Raye, C. L., Mitchell, K. J., Touryan, S. R., Greene, E. J., and Nolen-Hoeksema, S. (2006). Dissociating medial frontal and posterior cingulate activity during self-reflection. *Soc. Cogn. Affect. Neurosci.* 1, 56–64. doi: 10.1093/scan/nsl004

Luo, Y., Alvarez, T. L., Halperin, J. M., and Li, X. (2020). Multimodal neuroimaging-based prediction of adult outcomes in childhood-onset ADHD using ensemble learning techniques. *NeuroImage. Clin.* 26:102238. doi: 10.1016/j.nicl.2020.102238

Ma, L., Wang, B., Narayana, S., Hazeltine, E., Chen, X., Robin, D. A., et al. (2010). Changes in regional activity are accompanied with changes in inter-regional connectivity during 4 weeks motor learning. *Brain Res.* 1318, 64–76. doi: 10.1016/j.brainres.2009.12.073

Mansour, A. R., Baliki, M. N., Huang, L., Torbey, S., Herrmann, K. M., Schnitzer, T. J., et al. (2013). Brain white matter structural properties predict transition to chronic pain. *Pain* 154, 2160–2168. doi: 10.1016/j.pain.2013.06.044

Mathur, V. A., Moayedi, M., Keaser, M. L., Khan, S. A., Hubbard, C. S., Goyal, M., et al. (2016). High frequency migraine is associated with lower acute pain sensitivity and abnormal insula activity related to migraine pain intensity, attack frequency, and pain catastrophizing. *Front. Hum. Neurosci.* 10:489. doi: 10.3389/fnhum.2016.00489

Michels, L., Christidi, F., Steiger, V. R., Sándor, P. S., Gantenbein, A. R., Landmann, G., et al. (2017). Pain modulation is affected differently in medication-overuse headache and chronic myofascial pain–a multimodal MRI study. *Cephalalgia* 37, 764–779. doi: 10.1177/0333102416652625

Moulton, E. A., Schmahmann, J. D., Becerra, L., and Borsook, D. (2010). The cerebellum and pain: passive integrator or active participator? *Brain Res. Rev.* 65, 14–27. doi: 10.1016/j.brainresrev.2010.05.005

Niddam, D. M., Wang, S.-J., and Tsai, S.-Y. (2021). Pain sensitivity and the primary sensorimotor cortices: a multimodal neuroimaging study. *Pain* 162, 846–855. doi: 10.1097/j.pain.0000000000002074

Nielsen, C. S., Staud, R., and Price, D. D. (2009). Individual differences in pain sensitivity: measurement, causation, and consequences. *J. Pain* 10, 231–237. doi: 10.1016/j.jpain.2008.09.010

Pedregosa, F., Varoquaux, G., Gramfort, A., Michel, V., Thirion, B., Grisel, O., et al. (2011). Scikit-learn: Machine learning in Python. *J. Machine Learn. Res.* 12, 2825–2830. doi: 10.1080/13696998.2019.1666854

Porpora, M. G., Vinci, V., De Vito, C., Migliara, G., Anastasi, E., Ticino, A., et al. (2018). The role of magnetic resonance imaging–diffusion tensor imaging in predicting pain related to endometriosis: a preliminary study. *J. Minim. Invasive Gynecol.* 25, 661–669. doi: 10.1016/j.jmig.2017.10.033

Rainville, P. (2002). Brain mechanisms of pain affect and pain modulation. *Curr. Opin. Neurobiol.* 12, 195–204. doi: 10.1016/s0959-4388(02)00313-6

Rehberg, B., Mathivon, S., Combescure, C., Mercier, Y., and Savoldelli, G. L. (2017). Prediction of acute postoperative pain following breast cancer surgery using the pain sensitivity questionnaire. *Clin. J. Pain* 33, 57–66. doi: 10.1097/AJP.0000000000000380

Rogachov, A., Cheng, J. C., Erpelding, N., Hemington, K. S., Crawley, A. P., and Davis, K. D. (2016). Regional brain signal variability: a novel indicator of pain sensitivity and coping. *Pain* 157, 2483–2492. doi: 10.1097/j.pain.0000000000000665

Spisak, T., Kincses, B., Schlitt, F., Zunhammer, M., Schmidt-Wilcke, T., Kincses, Z. T., et al. (2020). Pain-free resting-state functional brain connectivity predicts individual pain sensitivity. *Nat. Commun.* 11:187. doi: 10.1038/s41467-019-13785-z

Steiger, J. H. (1980). Tests for comparing elements of a correlation matrix. *Psychol. Bull.* 87, 245–251. doi: 10.1037/0033-2909.87.2.245

Stein, N., Sprenger, C., Scholz, J., Wiech, K., and Bingel, U. (2012). White matter integrity of the descending pain modulatory system is associated with interindividual differences in placebo analgesia. *Pain* 153, 2210–2217. doi: 10.1016/j.pain.2012.07.010

Straathof, M., Sinke, M. R., Dijkhuizen, R. M., and Otte, W. M. (2019). A systematic review on the quantitative relationship between structural and functional network connectivity strength in mammalian brains. *J. Cereb. Blood Flow Metabol.* 39, 189–209. doi: 10.1177/0271678X18809547

Suárez, L. E., Markello, R. D., Betzel, R. F., and Misic, B. (2020). Linking structure and function in macroscale brain networks. *Trends Cogn. Sci.* 24, 302–315. doi: 10.1016/j.tics.2020.01.008

Sugranyes, G., Kyriakopoulos, M., Dima, D., O'Muircheartaigh, J., Corrigall, R., Pendelbury, G., et al. (2012). Multimodal analyses identify linked functional and white matter abnormalities within the working memory network in schizophrenia. *Schizophren. Res.* 138, 136–142. doi: 10.1016/j.schres.2012.03.011

Tang, E., and Bassett, D. S. (2018). Colloquium: Control of dynamics in brain networks. *Rev. Modern Phys.* 90:031003.

Tu, Y., Zhang, B., Cao, J., Wilson, G., Zhang, Z., and Kong, J. (2019). Identifying inter-individual differences in pain threshold using brain connectome: a test-retest reproducible study. *Neuroimage* 202:116049. doi: 10.1016/j.neuroimage.2019.116049

Tzourio-Mazoyer, N., Landeau, B., Papathanassiou, D., Crivello, F., Etard, O., Delcroix, N., et al. (2002). Automated anatomical labeling of activations in SPM using a macroscopic anatomical parcellation of the MNI MRI single-subject brain. *Neuroimage* 15, 273–289. doi: 10.1006/nimg.2001.0978

Utevsky, A. V., Smith, D. V., and Huettel, S. A. (2014). Precuneus is a functional core of the default-mode network. *J. Neurosci.* 34, 932–940. doi: 10.1523/jneurosci.4227-13.2014

Wang, P., Du, H., Chen, N., Guo, J., Gong, Q., Zhang, J., et al. (2014). Regional homogeneity abnormalities in patients with tensiontype headache: a resting-state fMRI study. *Neurosci. Bull.* 30, 949–955. doi: 10.1007/s12264-013-1468-6

Warbrick, T., Rosenberg, J., and Shah, N. J. (2017). The relationship between BOLD fMRI response and the underlying white matter as measured by fractional anisotropy (FA): a systematic review. *Neuroimage* 153, 369–381. doi: 10.1016/j.neuroimage.2016.12.075

Wee, C.-Y., Yap, P.-T., Zhang, D., Denny, K., Browndyke, J. N., Potter, G. G., et al. (2012). Identification of MCI individuals using structural and functional connectivity networks. *Neuroimage* 59, 2045–2056. doi: 10.1016/j.neuroimage.2011.10.015

Werner, M. U., Mjöbo, H. N., Nielsen, P. R., Rudin, Å, and Warner, D. S. (2010). Prediction of postoperative pain: a systematic review of predictive experimental pain studies. *J. Am. Soc. Anesthesiol.* 112, 1494–1502. doi: 10.1097/ALN.0b013e3181dcd5a0

Wiech, K., Jbabdi, S., Lin, C., Andersson, J., and Tracey, I. (2014). Differential structural and resting state connectivity between insular subdivisions and other pain-related brain regions. *Pain* 155, 2047–2055. doi: 10.1016/j.pain.2014.07.009

Xiao, Y., Lin, Y., Ma, J., Qian, J., Ke, Z., Li, L., et al. (2021). Predicting visual working memory with multimodal magnetic resonance imaging. *Hum. Brain Mapp.* 42, 1446–1462. doi: 10.1002/hbm.25305

Yan, C.-G., Wang, X.-D., Zuo, X.-N., and Zang, Y.-F. (2016). DPABI: data processing & analysis for (resting-state) brain imaging. *Neuroinformatics* 14, 339–351. doi: 10.1007/s12021-016-9299-4

Yoshino, A., Okamoto, Y., Doi, M., Otsuru, N., Okada, G., Takamura, M., et al. (2017). Regional brain functions in the resting state indicative of potential differences between depression and chronic pain. *Sci. Rep.* 7:3003. doi: 10.1038/s41598-017-03522-1

Yu, D., Yuan, K., Zhao, L., Zhao, L., Dong, M., Liu, P., et al. (2012). Regional homogeneity abnormalities in patients with interictal migraine without aura: a resting-state study. *NMR Biomed.* 25, 806–812. doi: 10.1002/nbm.1796

Zang, Y., Jiang, T., Lu, Y., He, Y., and Tian, L. (2004). Regional homogeneity approach to fMRI data analysis. *Neuroimage* 22, 394–400. doi: 10.1016/j.neuroimage.2003.12.030

Zhang, J., Su, J., Wang, M., Zhao, Y., Yao, Q., Zhang, Q., et al. (2016). Increased default mode network connectivity and increased regional homogeneity in migraineurs without aura. *J. Headache Pain* 17:98. doi: 10.1186/s10194-016-0692-z

Zhang, X., Chen, Q., Su, Y., Meng, J., Qiu, J., and Zheng, W. (2020). Pain in the default mode network: a voxel-based morphometry study on thermal pain sensitivity. *NeuroReport* 31, 1030–1035. doi: 10.1097/WNR.0000000000001512

Zhao, L., Liu, J., Dong, X., Peng, Y., Yuan, K., Wu, F., et al. (2013). Alterations in regional homogeneity assessed by fMRI in patients with migraine without aura stratified by disease duration. *J. Headache Pain* 14:85. doi: 10.1186/1129-2377-14-85

Zunhammer, M., Schweizer, L. M., Witte, V., Harris, R. E., Bingel, U., and Schmidt-Wilcke, T. (2016). Combined glutamate and glutamine levels in pain-processing brain regions are associated with individual pain sensitivity. *Pain* 157, 2248–2256. doi: 10.1097/j.pain.0000000000000634

Conflict of Interest: The authors declare that the research was conducted in the absence of any commercial or financial relationships that could be construed as a potential conflict of interest.

Publisher's Note: All claims expressed in this article are solely those of the authors and do not necessarily represent those of their affiliated organizations, or those of the publisher, the editors and the reviewers. Any product that may be evaluated in this article, or claim that may be made by its manufacturer, is not guaranteed or endorsed by the publisher.

frontiers in Molecular Neuroscience

ORIGINAL RESEARCH
published: 18 March 2022
doi: 10.3389/fnmol.2022.853509

Effects of High-Definition Transcranial Direct Current Stimulation Over the Primary Motor Cortex on Cold Pain Sensitivity Among Healthy Adults

*Xiaoyun Li[1], Xinxin Lin[1], Junjie Yao[1], Shengxiong Chen[2], Yu Hu[2], Jiang Liu[3] and Richu Jin[3]**

[1] School of Psychology, Shenzhen University, Shenzhen, China, [2] Medical Rehabilitation Center, Shenzhen Prevention and Treatment Center for Occupational Diseases, Shenzhen, China, [3] Department of Computer Science and Engineering, Southern University of Science and Technology, Shenzhen, China

Some clinical studies have shown promising effects of transcranial direct current stimulation (tDCS) over the primary motor cortex (M1) on pain relief. Nevertheless, a few studies reported no significant analgesic effects of tDCS, likely due to the complexity of clinical pain conditions. Human experimental pain models that utilize indices of pain in response to well-controlled noxious stimuli can avoid many confounds that are present in the clinical data. This study aimed to investigate the effects of high-definition tDCS (HD-tDCS) stimulation over M1 on sensitivity to experimental pain and assess whether these effects could be influenced by the pain-related cognitions and emotions. A randomized, double-blinded, crossover, and sham-controlled design was adopted. A total of 28 healthy participants received anodal, cathodal, or sham HD-tDCS over M1 (1 mA for 20 min) in different sessions, in which montage has the advantage of producing more focal stimulation. Using a cold pressor test, several indices reflecting the sensitivity to cold pain were measured immediately after HD-tDCS stimulation, such as cold pain threshold and tolerance and cold pain intensity and unpleasantness ratings. Results showed that only anodal HD-tDCS significantly increased cold pain threshold when compared with sham stimulation. Neither anodal nor cathodal HD-tDCS showed significant analgesic effects on cold pain tolerance, pain intensity, and unpleasantness ratings. Correlation analysis revealed that individuals that a had lower level of attentional bias to negative information benefited more from attenuating pain intensity rating induced by anodal HD-tDCS. Therefore, single-session anodal HD-tDCS modulates the sensory-discriminative aspect of pain perception as indexed by the increased pain threshold. In addition, the modulating effects of HD-tDCS on attenuating pain intensity to suprathreshold pain could be influenced by the participant's negative attentional bias, which deserves to be taken into consideration in the clinical applications.

Keywords: high-definition transcranial direct current stimulation (HD-tDCS), primary motor cortex (M1), pain, analgesia, cold pain sensitivity

OPEN ACCESS

Edited by:
Wen Wu,
Southern Medical University, China

Reviewed by:
Shuang Qiu,
Institute of Automation (CAS), China
Jing Meng,
Chongqing Normal University, China

***Correspondence:**
Richu Jin
jinrc@sustech.edu.cn

Specialty section:
This article was submitted to Pain Mechanisms and Modulators, a section of the journal Frontiers in Molecular Neuroscience

Received: *12 January 2022*
Accepted: *17 February 2022*
Published: *18 March 2022*

Citation:
Li X, Lin X, Yao J, Chen S, Hu Y, Liu J and Jin R (2022) Effects of High-Definition Transcranial Direct Current Stimulation Over the Primary Motor Cortex on Cold Pain Sensitivity Among Healthy Adults. Front. Mol. Neurosci. 15:853509. doi: 10.3389/fnmol.2022.853509

INTRODUCTION

Non-invasive brain stimulation techniques, such as transcranial magnetic stimulation and transcranial electrical stimulation, are neuromodulation approaches that can regulate the cortical activity (Nitsche et al., 2008; Lefaucheur et al., 2017). Transcranial direct current stimulation (tDCS) is the most commonly used transcranial electrical stimulation technique, due to its relatively small-size, low-cost, ease-of-use, and safety characteristics (Lefaucheur et al., 2017). The primary mechanism of tDCS is considered to induce polarity-dependent shifts in the resting membrane potentials, thereby, modulating cortical excitability and neuronal spontaneous firing rate (Creutzfeldt et al., 1962; Purpura and McMurtry, 1965). In general, anodal stimulation results in neuronal depolarization and increases cortical excitability, whereas cathodal stimulation causes neuronal hyperpolarization and decreases cortical excitability (Nitsche and Paulus, 2000; Nitsche et al., 2008).

Previous studies have shown tDCS effects on attenuating pain perception in experimental pain and clinical pain conditions, such as neuropathic pain, fibromyalgia, and migraine (Fregni et al., 2007; Lefaucheur et al., 2008; Nitsche et al., 2008; Luedtke et al., 2012b; Mylius et al., 2012). Applying 20-min anodal tDCS over the primary motor cortex (M1) is recommended for pain relief in the evidence-based guidelines (Lefaucheur et al., 2017). Meta-analysis showed that tDCS over M1 has small to moderate analgesic effects on pain threshold in both healthy and chronic pain populations (Vaseghi et al., 2015; Giannoni-Luza et al., 2020). However, some studies reported no significant analgesic effects of tDCS as compared with sham condition (Jürgens et al., 2012; Luedtke et al., 2012a, 2015). For instance, a single-blinded crossover study found that tDCS over M1 was failed to modulate pain threshold and ratings to suprathreshold heat stimuli among healthy volunteers (Jürgens et al., 2012). In addition, anodal tDCS over M1 did not significantly relieve pain and disability for 135 patients with chronic low back pain (Luedtke et al., 2015). These heterogeneous results lead to the question of whether the active tDCS stimulation of M1 is effective for pain modulation.

Most studies that investigated the effects of tDCS over M1 upon pain perception have adopted the conventional montage with the target electrode placed at the M1 and the reference electrode placed at the contralateral supraorbital area. Nevertheless, the spatial distribution of the electrical field for conventional tDCS configurations has been critically discussed. Conventional tDCS stimulation modulates cortical activation in a large cortical area beyond the cortical region underlying the target electrode (Lang et al., 2005; Nitsche et al., 2007). In addition, modeling studies provide evidence that electric fields produced by conventional tDCS montage are highly diffuse, and the target area does not directly receive the largest current density (Datta et al., 2009; Bikson et al., 2010). Relative to conventional tDCS, 4 × 1 high-definition tDCS (HD-tDCS) montage with smaller electrodes allows to restrict the current flow between the central and return electrodes, thereby, providing a more focal stimulation in the target area (Kuo et al., 2013; Villamar et al., 2013). Thus, HD-tDCS seems to overcome one of the main limitations of conventional tDCS by improving the spatial precision of stimulation.

In light of the advantages of HD-tDCS, some studies attempted to assess whether HD-tDCS targeted on M1 can effectively alleviate clinical pain (Villamar et al., 2013; Castillo-Saavedra et al., 2016). For instance, a phase II open-label trial reported that 15 sessions (median number) of HD-tDCS over M1 could achieve a 50% pain reduction in fibromyalgia patients (Castillo-Saavedra et al., 2016). Indeed, there are inevitably some confounding factors in the clinical pain population, such as pain comorbidity of anxiety and depression. Human experimental pain models allow to provide noxious stimuli with standardized intensity and to rigorously measure pain responses with a high level of precision. Noxious stimuli (e.g., cold pressor) of the intensity and modality can be applied in a controlled laboratory setting while other variables of interest are systematically manipulated. In addition, indices of pain perception in response to the well-controlled noxious stimuli can be measured with psychophysical methods. Thus, human experimental pain models are often used to measure pain sensitivity and avoid many confounds presented in the clinical data. A recent study showed that HD-tDCS over M1 was delivered across 3 days among the healthy individuals, but was failed to modulate somatosensory and pain sensitivity (Kold and Graven-Nielsen, 2021). In this study, somatosensory detection and pain thresholds were measured, which mainly reflect the sensory-discriminative aspect of pain perception (Rainville et al., 1992). It remains unclear whether HD-tDCS can modulate the affective-motivation aspect of pain, such as pain tolerance.

Pain perception is greatly dependent upon psychological factors, such as pain-related cognitions and emotions (Bushnell et al., 2013). These psychological factors (e.g., pain catastrophizing and fear of pain) can also predict the outcomes in clinical interventions of clinical pain (Werneke et al., 2009; Mankovsky et al., 2012; Sparkes et al., 2015; Burns et al., 2017; Sharifzadeh et al., 2017). For example, greater pain catastrophizing predicts a worse response to opioid analgesics for patients with chronic low back pain (Burns et al., 2017) and less pain reduction after spinal cord stimulation treatment for patients with chronic neuropathic pain (Sparkes et al., 2015). Moreover, more fear of pain is associated with worse outcomes in physical rehabilitation therapy for patients with low back pain (Werneke et al., 2009). Since the effectiveness of pain intervention is greatly influenced by pain-related cognitions and emotions, it is likely that these psychological factors could influence the analgesic effects of tDCS. Understanding the underlying moderating factors of analgesia induced by tDCS may help to develop tDCS protocols for precision medicine.

Cold pressor pain, induced by submerging a non-dominant hand into cold water, is a well-validated test to mimic clinical pain, because of the more sustained and higher level of pain intensity and unpleasantness that it evokes (Rainville et al., 1992). It shows excellent experimental reliability and validity in assessing cold pain sensitivity (Ehrlich et al., 2003). Here, the present study used the cold pressor test and investigated the effects of single-session HD-tDCS over M1 on cold pain sensitivity among healthy participants. Adopting a randomized,

double-blinded, crossover, and sham-controlled design, pain sensitivity was measured immediately after anodal, cathodal, and sham HD-tDCS targeted on the M1. We hypothesized that when compared with sham stimulation, active HD-tDCS over M1 could increase cold pain threshold and tolerance but decrease pain intensity and unpleasantness ratings. In addition, we hypothesized that the effectiveness of active HD-tDCS on cold pain sensitivity could be influenced by pain-related cognitions and emotions.

MATERIALS AND METHODS

Participants

A priori power analysis using G*Power software was conducted to determine the appropriate sample size for a within-participant design with two factors ($2 \times 3 = 6$ conditions). It yielded a sample size of $n = 28$ to detect a medium effect size of $f = 0.25$ at a standard error probability of $\alpha = 0.05$ with a power of 0.95. Therefore, we recruited 28 participants [14 women; age: mean ± standard error of the mean (SEM) = 23.07 ± 0.34 years) to participate in this study. All participants were right-handed, had a normal or corrected-to-normal vision, and were free from any contraindications for tDCS application. No participant reported any medical condition associated with acute or chronic pain, cardiovascular or neurological diseases, psychiatric disorders, or current use of any medication, or in menstrual period. All participants gave their written informed consent before the experiments according to the Declaration of Helsinki. All experimental procedures were approved by the local research ethics committee.

Questionnaires

Before the experiment, all participants were instructed to complete the pain-related questionnaires that measured their cognitions and emotions to pain. Specifically, the Pain Sensitivity Questionnaire (PSQ) was used to assess subjective pain perception of painful situations in daily life (Ruscheweyh et al., 2009). The Fear of Pain Questionnaire (FPQ; McNeil and Rainwater, 1998) and the Pain Catastrophizing Scale (PCS; Sullivan et al., 1995) were administered to assess their thoughts, attitudes, and beliefs toward pain. The Pain Vigilance and Awareness Questionnaire (PVAQ) was used to measure awareness, consciousness, vigilance, and observation of pain (McCracken, 1997). The Attention to Positive and Negative Information Scale (APNI; Noguchi et al., 2006) was adopted to examine the individual attentional bias to positive or negative information, which consisted of two subscales (Attention to Positive Information, API; Attention to Negative Information, ANI).

General Experimental Procedure

This study was a randomized, double-blinded, crossover, and sham-controlled design. Two experimenters were involved in this study, with one as the tDCS administrator and the other as the pain-test assessor. The tDCS administrator was responsible for the generation of the random allocation sequence and the delivery of the tDCS intervention, who was not involved in any data collection and analysis. As shown in **Figure 1**, each participant attended three sessions and underwent a single session of anodal, cathodal, and sham HD-tDCS targeted on the left or right M1, which were followed by a cold pressor test. Sessions were separated by at least 1 week to prevent any carryover effects. The order and the stimulated site of tDCS intervention were counterbalanced and randomly assigned to the participants. Therefore, each participant received three sessions of HD-tDCS (anodal, cathodal, and sham) with the target region on either left or right M1, which was kept constant across the three sessions.

High-Definition Transcranial Direct Current Stimulation

A 4 × 1 Multichannel Stimulation Adaptor (Model 4 × 1-C3A; Soterix Medical Inc., New York, NY, United States) was employed to deliver 1 mA direct current to the scalp *via* Ag-AgCl sintered ring electrodes (EL-TP-RNG Sintered; Stens Biofeedback Inc., San Rafael, CA, United States) (Minhas et al., 2010). The 4 × 1 ring montage consisted of one central electrode placed at the M1 (C3 or C4) based on the International 10–20 System, and the four return electrodes were surrounded the central electrode at a center-to-center distance of 3.5 cm. When stimulating the

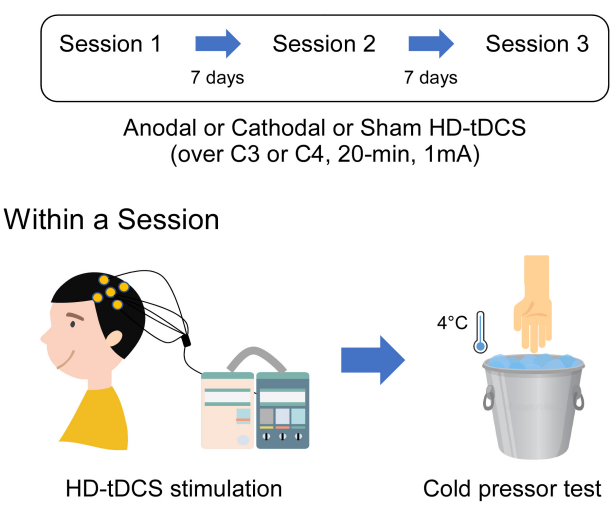

FIGURE 1 | Schematic illustration of the experimental procedures. Each participant visited three sessions which comprised single-session tDCS intervention (1 mA, 20 min) followed by a cold pressor test. Three sessions were separated by 7 days to avoid the possible carryover effects due to the tDCS stimulation. During the tDCS intervention, participants received HD-tDCS targeted on the M1 using anodal, cathodal, or sham stimulation. HD-tDCS electrodes were placed according to the International 10–20 System, with the central electrode placed at C3 or C4 and the return electrodes placed at FC5, FC1, CP1, CP5 or FC6, FC2, CP2, CP6, respectively. During the cold pressor test, sensitivity to cold pain was measured by instructing participants to immerse their both hands (contralateral and ipsilateral to the HD-tDCS target side) into the cold-water apparatus of 4°C.

left M1, the central electrode was placed on C3, while the four return electrodes were placed on FC1, FC5, CP5, and CP1. When stimulating the right M1, the central electrode was placed on C4, and the four return electrodes were placed on FC2, FC6, CP6, and CP2. Previous studies have confirmed that the position of the electrode at C3 or C4 corresponds approximately to the location of the left or right M1 (Edwards et al., 2013). HD-Explore software (Version 2.3, Soterix Medical, New York, NY, United States) was used to confirm the focality of electric fields induced by HD-tDCS (**Figure 2**). The identical montage setting was used for the anodal, cathodal, and sham stimulation. Impedance values were measured for each of the five electrodes and were all verified to be <1 quality unit. For anodal and cathodal stimulations, the current ramped up from 0 to 1 mA in 30 s and was then constantly given for 20 min, with a 30 s ramp-down time period at the end of the stimulation. For sham stimulation, the current ramped up to 1 mA over 30 s, prior to being ramped down over the next 30 s to 0 mA, where its stimulation protocol was still maintained for 20 min. At the end of the stimulation, the current was again ramped up to 1 mA over 30 s. Participants were blinded to the type of HD-tDCS stimulation and the device was kept out of their sight during the experiment. At the end of each session, participants completed a questionnaire regarding blinding efficiency and potential adverse effects caused by the HD-tDCS stimulation, such as itching, pain, or skin irritation (Antal et al., 2010; Brunoni et al., 2011).

Cold Pressor Test

Immediately after HD-tDCS intervention, a cold pressor test was conducted to assess individual cold pain sensitivity. The test was applied to both hands (contralateral and ipsilateral to the HD-tDCS stimulated side), separated by 10 min. The testing order of two hands was counterbalanced and randomly assigned for the participants. Participants were instructed to firstly immerse the hand up to the wrist into a tank with room temperature water at approximately 22°C for 30 s. This was done to ensure that the hand temperature before a cold pressor test was similar across participants. Then, participants were asked to immediately immerse open-hand into a circulating cold-water tank (Type: DX-208, Beijing Changliu Scientific Instrument Co., Ltd.) of 4°C (±0.10). Simultaneously, a stopwatch was activated. Cold pain threshold was defined as the total duration from the onset of hand immersion until the first report of pain perception (in seconds). Cold pain tolerance was defined as the total duration from the onset of hand immersion until the removal of the hand from the cold pressor apparatus (in seconds). Perceived pain intensity and unpleasantness were rated at tolerance, using an 11-point scale ranging from 0 (no pain/unpleasantness) to 10 (unbearable pain/unpleasantness). For the safety concerns, we would instruct the participants to withdraw their hand from the apparatus if the immersion duration reached 3 min. This was not informed to the participants before the cold pressor test.

Statistical Analysis

All statistical analyses were carried out using the IBM SPSS statistical analysis package (version 22; IBM Corp., Armonk, NY, United States). The blinding of tDCS type was examined using a Cochran's *Q*-test, which compared the frequency of yes responses across three sessions. Ratings for adverse effects were investigated using the one-way repeated measures analysis of variance (ANOVA) with a factor of tDCS Type (anodal, cathodal, and sham HD-tDCS). To assess possible effects of HD-tDCS on cold pain sensitivity, measures in the cold pressor test (such as cold pain threshold and tolerance, as well as ratings of perceived pain intensity and unpleasantness) were compared using a two-way repeated measures ANOVA with two within-participant factors of tDCS Type (anodal, cathodal, and sham HD-tDCS) and Stimulation Side (hands ipsilateral and contralateral to the HD-tDCS side). When there was a significant main effect or interaction, we performed *post hoc* comparisons. Bonferroni correction was used for multiple-comparison correction. In addition, the relationship between the analgesic effects of HD-tDCS (active HD-tDCS *minus* sham HD-tDCS) and scores on pain-related questionnaires (i.e., PSQ, FPQ, PCS, PVAQ, and APNI) was assessed using Pearson correlation across all participants. This was done to test whether analgesic effects of HD-tDCS were influenced by pain-related cognitions or emotions.

RESULTS

A total of 28 participants were originally recruited. Three participants failed to complete the three sessions due to either personal issues (n = 1) or the equipment failure (n = 2). To this end, data from 25 participants were included in the data analysis. The demographic information (including age and gender) and psychometric characteristics (including the PSQ, FPQ, PCS, PVAQ, and APNI) are summarized in **Table 1**.

Immediately after tDCS intervention, the blinding of stimulation type was evaluated using the questionnaires. The effectiveness of blinding HD-tDCS (i.e., whether the participant believed that they had received active tDCS or not) was analyzed using a Cochran's *Q*-test. The reports did not differ among the three sessions [χ^2 (2) = 2.00, p = 0.778]. It suggests successful blinding of HD-tDCS. Ratings of adverse events were compared among the three HD-tDCS sessions. As shown in **Table 2**, ratings of adverse events after HD-tDCS are comparable among the three sessions ($p > 0.05$ for all comparisons), except for ratings of burning sensation ($F_{2,46}$ = 5.41, p = 0.010, $\eta_p^2 = 0.191$). *Post hoc* comparisons showed that participants reported greater burning sensations after cathodal stimulation intervention than after anodal stimulation intervention (p = 0.029). Nevertheless, ratings to sham stimulation were not different from anodal or cathodal stimulation (p = 0.575 and p = 0.110, respectively). It suggests that cathodal HD-tDCS causes more adverse effects on eliciting burning sensation.

The duration to cold pain threshold and tolerance and ratings to pain intensity and unpleasantness are displayed in **Figure 3**. Statistics for the effects of HD-tDCS on cold pain sensitivity are summarized in **Table 3**. Analysis of HD-tDCS effects on cold pain threshold showed a significant main effect of tDCS Type

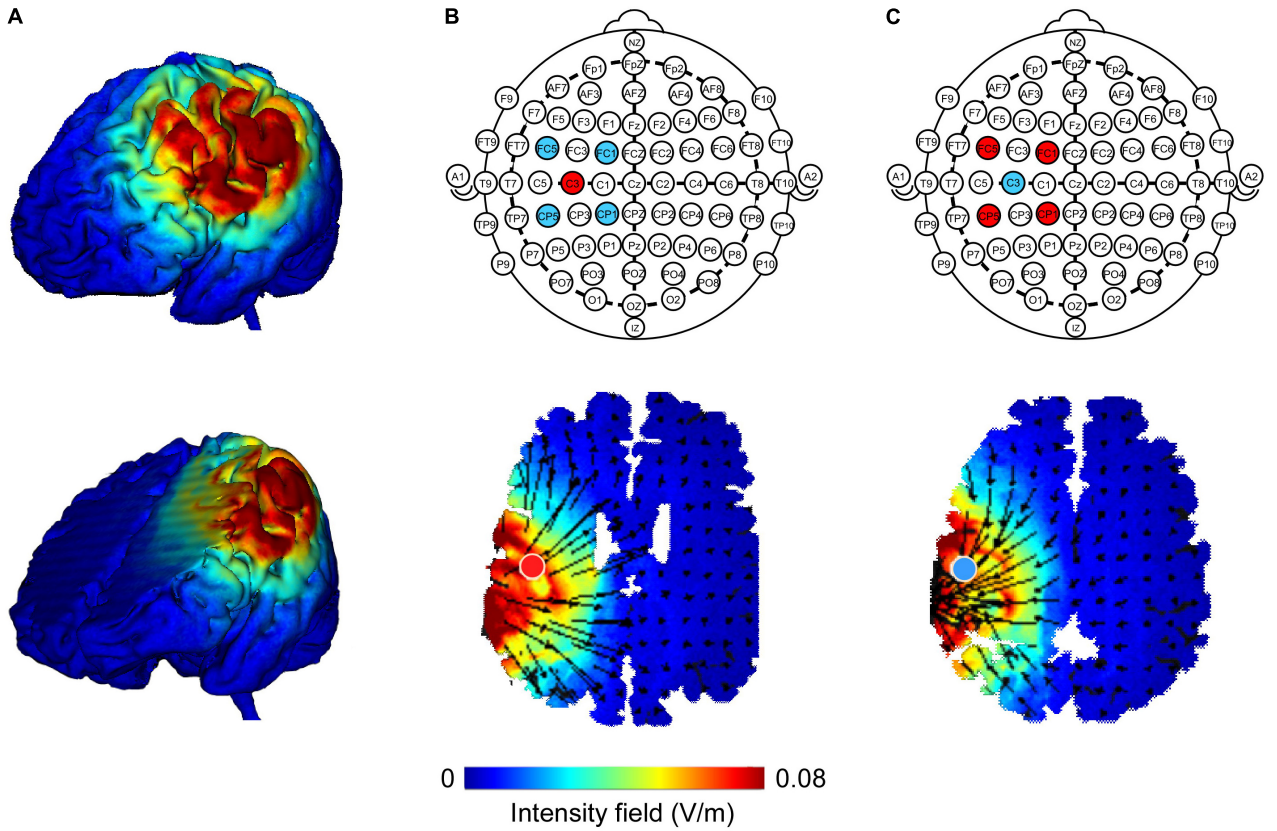

FIGURE 2 | Finite element models of high-definition transcranial direct current (HD-tDCS) of the left M1. Cortical surface and deep brain structure plots illustrate electric field magnitude (**A**; directionless; blue color represents zero electric field and the red color represents peak magnitude). HD-tDCS electrodes were placed according to the International 10–20 System. The central electrode was placed at C3 with surrounding return electrodes that are located at FC1, FC5, CP5, and CP1 (red color represents anode, blue color represents cathode). Anodal **(B)** and cathodal **(C)** modeling showed a similar current field intensity but with current flow in opposite directions. The direction of the current flow is indicated by black arrows. A field intensity range of 0.00–0.08 V/m was used.

($F_{2,48}$ = 3.83, p = 0.035, $\eta_p^2 = 0.138$). *Post hoc* paired-sample t-tests showed that cold pain threshold was greater after anodal HD-tDCS than after sham stimulation (p = 0.008; **Figure 3A**) but was comparable between cathodal and sham stimulation (p = 0.272). The main effect of the Stimulation Side was also significant ($F_{1,24}$ = 7.65, p = 0.011, $\eta_p^2 = 0.242$) such that the cold pain threshold at hand contralateral to the HD-tDCS side was greater than at the ipsilateral side. The interaction was not significant for cold pain threshold ($F_{2,48}$ = 0.08, p = 0.923, $\eta_p^2 = 0.003$). These results suggested that anodal HD-tDCS significantly increased cold pain threshold, in which effect was comparable between hands contralateral or ipsilateral to tDCS target side.

In contrast, repeated measure ANOVA did not show any significant main effects or interaction on pain tolerance, pain intensity, and unpleasantness ratings evoked by cold pressor stimulus ($p > 0.05$ for all comparisons).

Correlation analysis was conducted to determine whether the analgesic effects of HD-tDCS were influenced by pain-related cognitions and emotions. Firstly, cold pain sensitivity measured at hands contralateral and ipsilateral to the HD-tDCS side was grand averaged for each tDCS type (anodal, cathodal, and sham HD-tDCS), thus yielding three values for each pain sensitivity measure and for each participant. Next, the analgesic effects of HD-tDCS were evaluated by calculating the contrast between active and sham stimulation (i.e., anodal *minus* sham or cathodal *minus* sham). A negative value for the pain rating or a positive value for pain threshold and tolerance indicates analgesia induced by active HD-tDCS. Finally, the relationships between the analgesic effects of HD-tDCS and pain-related cognitions/emotions (scores on the PSQ,

TABLE 1 | Demographic and psychometric characteristics of participants (n = 25).

Characteristics	Mean ± SEM
Age (years)	22.92 ± 0.36
Sex (female/male)	13/12
Pain Sensitivity Questionnaire	72.80 ± 4.39
Fear of Pain Questionnaire	101.12 ± 3.24
Pain Catastrophizing Scale	18.2 ± 1.88
Pain Vigilance and Awareness Questionnaire	38.24 ± 1.86
Attention to Positive Information (API)	76.52 ± 0.76
Attention to Negative Information (ANI)	34.72 ± 1.56

TABLE 2 | Reported adverse effects after anodal, cathodal, and sham HD-tDCS stimulation.

	Anodal	Cathodal	Sham	ANOVA
Headache	0.32 ± 0.16	0.72 ± 0.32	0.63 ± 0.37	$F_{2,46} = 0.64$, $p = 0.504$, $\eta_p^2 = 0.027$
Neck pain	0.08 ± 0.08	0.36 ± 0.18	0.13 ± 0.09	$F_{2,46} = 1.33$, $p = 0.274$, $\eta_p^2 = 0.055$
Scalp pain	1.56 ± 0.39	1.44 ± 0.41	1.50 ± 0.33	$F_{2,46} = 0.32$, $p = 0.718$, $\eta_p^2 = 0.014$
Tingling	2.92 ± 0.46	3.24 ± 0.49	2.96 ± 0.59	$F_{2,46} = 0.35$, $p = 0.658$, $\eta_p^2 = 0.015$
Itching	3.24 ± 0.61	3.80 ± 0.59	2.63 ± 0.59	$F_{2,46} = 2.71$, $p = 0.082$, $\eta_p^2 = 0.105$
Burning sensation	0.44 ± 0.19	1.88 ± 0.50	0.88 ± 0.44	$F_{2,46} = 5.41$, $p = 0.010$, $\eta_p^2 = 0.191$
Skin redness	0.16 ± 0.11	0.68 ± 0.33	0.50 ± 0.30	$F_{2,46} = 0.66$, $p = 0.462$, $\eta_p^2 = 0.028$
Sleepiness	2.84 ± 0.40	2.16 ± 0.37	2.92 ± 0.42	$F_{2,46} = 2.49$, $p = 0.107$, $\eta_p^2 = 0.098$
Trouble concentrating	2.24 ± 0.38	2.24 ± 0.49	2.13 ± 0.51	$F_{2,46} = 0.01$, $p = 0.978$, $\eta_p^2 = 0.001$
Acute mood changes	0.44 ± 0.22	0.68 ± 0.34	0.67 ± 0.36	$F_{2,46} = 0.22$, $p = 0.733$, $\eta_p^2 = 0.009$

Data are expressed as mean ± SEM. Statistics were obtained by applying one-way repeated measures ANOVA with one factor of "Type" (anodal, cathodal, and sham HD-tDCS).

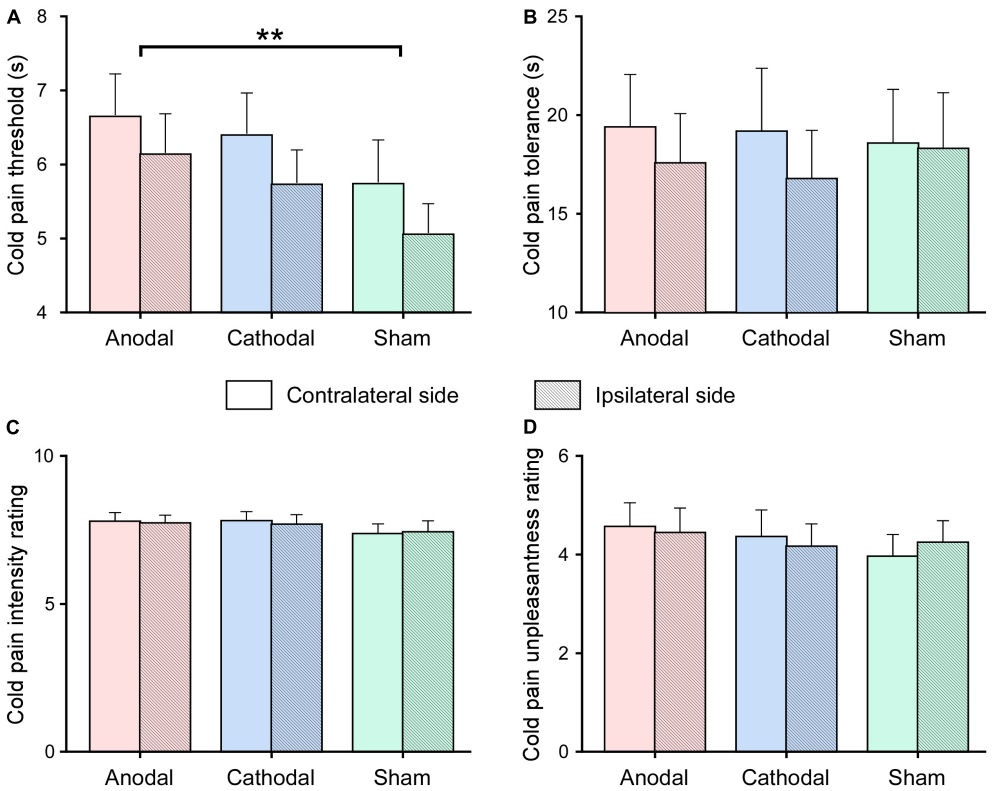

FIGURE 3 | Effects of high-definition transcranial direct current (HD-tDCS) on cold pain sensitivity. Cold pain threshold (measured in seconds; **A**) and tolerance (measured in seconds; **B**), as well as cold pain intensity (measured on the 0–10 scale; **C**) and unpleasantness (measured on the 0–10 scale; **D**) ratings were measured after the application of anodal, cathodal, sham HD-tDCS, for hands contralateral and ipsilateral to the HD-tDCS side. Data are expressed as mean ± SEM. Compared with sham stimulation, the cold pain threshold was significantly increased after anodal HD-tDCS, regardless of whether the cold pain stimulus was delivered to the hand contralateral or ipsilateral to the HD-tDCS side. $^{**}p < 0.01$, paired-sample *t*-test.

FPQ, PCS, PVAQ, and APNI) were estimated using Pearson correlation analysis. As shown in **Figure 4**, the analgesic effect of anodal HD-tDCS on cold pain intensity rating was significantly associated with scores on the ANI ($r = 0.59$, $p = 0.002$). This result suggested that individuals with a lower level of attentional bias to negative information would benefit more from attenuating pain intensity rating induced by anodal HD-tDCS stimulation.

DISCUSSION

The current study evaluated the effects of single-session HD-tDCS over M1 on cold pain sensitivity among the healthy population. Anodal HD-tDCS showed to be effective in increasing cold pain threshold when compared with sham stimulation. Neither anodal nor cathodal HD-tDCS significantly modulated cold pain tolerance and pain intensity

TABLE 3 | Statistics for cold pain sensitivity.

	Stimulation Side	tDCS Type	Stimulation Side × tDCS Type
Cold pain threshold	$F_{1,\ 24} = 7.65^{*}$, $\eta_p^2 = 0.242$	$F_{2,48} = 3.83^{*}$, $\eta_p^2 = 0.138$	$F_{2,48} = 0.08$, $\eta_p^2 = 0.003$
Cold pain tolerance	$F_{1,\ 24} = 1.52$, $\eta_p^2 = 0.059$	$F_{2,48} = 0.19$, $\eta_p^2 = 0.008$	$F_{2,48} = 2.13$, $\eta_p^2 = 0.082$
Pain intensity	$F_{1,\ 24} = 0.13$, $\eta_p^2 = 0.005$	$F_{2,48} = 1.37$, $\eta_p^2 = 0.054$	$F_{2,48} = 0.38$, $\eta_p^2 = 0.016$
Unpleasantness	$F_{1,\ 24} = 0.01$, $\eta_p^2 < 0.001$	$F_{2,48} = 0.42$, $\eta_p^2 = 0.017$	$F_{2,48} = 1.59$, $\eta_p^2 = 0.062$

*Statistics were obtained by applying a two-way repeated measures ANOVA, with two within-participant factors of Stimulation Side (the hands contralateral and ipsilateral to the HD-tDCS side) and tDCS Type (anodal, cathodal, and sham HD-tDCS). *p < 0.05.*

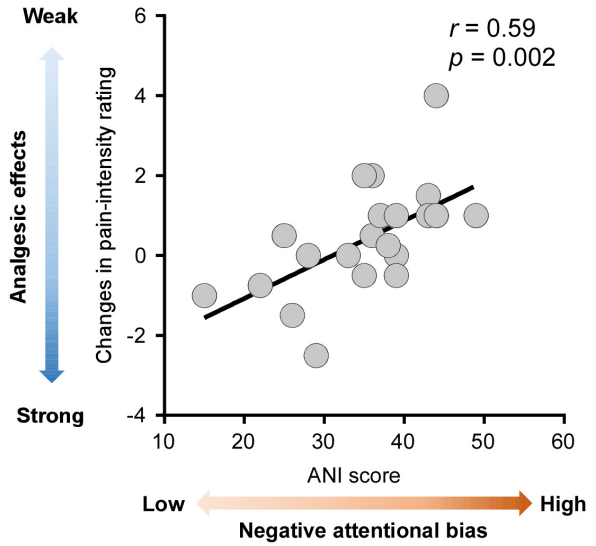

FIGURE 4 | Associations between analgesic effects of anodal high-definition transcranial direct current (HD-tDCS) and negative attentional bias. Analgesic effects of anodal HD-tDCS over M1 on cold pain intensity rating were calculated as the contrast between anodal and sham stimulation condition (anodal HD-tDCS *minus* sham HD-tDCS), with more negative values indicating stronger analgesic effects (colored in darker blue). The negative attentional bias was quantified by the scores on the Attention to Negative Information Scale (ANI), with greater scores on the ANI indicating a higher level of negative attentional bias (colored in darker red). Across all participants, stronger analgesic effects of anodal HD-tDCS were significantly correlated with a lower level of negative attentional bias. Each gray dot in the scatter plots represents a single participant. The black line represents the best linear fit for the data.

and unpleasantness ratings. Analgesic effects of anodal HD-tDCS on cold pain intensity rating could be influenced by the level of attentional bias to negative information. These results suggested that anodal HD-tDCS over M1 can modulate the sensory-discriminative aspect of experimental pain perception and that analgesic effects of anodal HD-tDCS on the perception of suprathreshold pain may be influenced by psychological factors, such as negative attentional bias.

Single-session 20-min anodal HD-tDCS targeted on the M1, relative to sham stimulation, increased cold pain threshold, regardless of whether a painful stimulus was delivered to the hand contralateral or ipsilateral to the tDCS target site. This finding is in line with Zandieh et al. (2013), which reported that the application of conventional anodal tDCS, but not cathodal tDCS, led to an increment in cold pain threshold. Previous meta-analyses also support our findings and show that anodal tDCS stimulation over M1 increases pain threshold in both healthy (Vaseghi et al., 2014) and clinical pain (Giannoni-Luza et al., 2020) population. However, our results are in contrast with previous studies that reported negative effects of tDCS on cold pain threshold among healthy volunteers (Bachmann et al., 2010; Grundmann et al., 2011; Borckardt et al., 2012; Jürgens et al., 2012; Brasil-Neto et al., 2020; Kold and Graven-Nielsen, 2021). Unlike the conventional pad-based tDCS frequently used in previous studies (Bachmann et al., 2010; Grundmann et al., 2011; Jürgens et al., 2012), we used HD-tDCS montage with multiple smaller electrodes that can provide more focal stimulation on the M1, thereby, increasing the credibility of activating M1 (Nitsche et al., 2007; Kuo et al., 2013). A few studies did employ the HD-tDCS stimulation over M1 but also reported little or marginal effect on cold pain threshold (Borckardt et al., 2012; Brasil-Neto et al., 2020; Kold and Graven-Nielsen, 2021). Most of these studies measured cold pain sensitivity before and after the tDCS intervention, which likely induce habituation or sensitization to the noxious stimulus. As the participants were repeatedly exposed to the same assessments with a relatively short interval (i.e., 15–20 min), the novelty and salience of noxious stimulus would be reduced along with the test progress, which may confound with the analgesic effects of tDCS (Kold and Graven-Nielsen, 2021).

Although previous studies have reported analgesic effects of M1-tDCS in both experimental and clinical pain settings (Lefaucheur et al., 2008; Giannoni-Luza et al., 2020), the underlying mechanisms still remain unclear. One of the hypotheses proposes that M1-tDCS induced analgesia through the inhibition of the nociceptive ascending pathway at the spinal cord level by activating the endogenous pain inhibitory pathway (García-Larrea et al., 1999; Giannoni-Luza et al., 2020). Neuroimaging studies provide evidence that motor cortex stimulation triggers activation in the ventral-lateral thalamus, leading to a cascade of events in medial thalamus, anterior cingulate/orbitofrontal cortices, and periaqueductal gray matter, in which regions constitute the endogenous pain inhibitory pathway (García-Larrea et al., 1999; Garcia-Larrea and Peyron, 2007). A meta-analysis reports that non-invasive motor cortex stimulation could effectively modulate pain thresholds and conditioned pain modulation (CPM) efficiency in the healthy and chronic pain populations (Giannoni-Luza et al., 2020). The CPM paradigm is commonly employed to examine the function and integrity of the endogenous pain inhibitory pathway (Bannister and Dickenson, 2017). Indeed, two recent studies confirmed that the single-session HD-tDCS targeted

on the M1 could improve CPM efficiency among healthy populations (Wan et al., 2021; Jiang et al., 2022). Therefore, the observed analgesic effects on pain threshold could have arisen from the top-down modulation of endogenous pain inhibitory pathway *via* HD-tDCS stimulating M1. Nevertheless, we did not measure neurophysiological data that could allow us to assess the mechanisms underlying the analgesic effects. Future neuroimaging studies are recommended to further explore whether and how HD-tDCS over M1 modulates the endogenous pain inhibitory pathway and subjective pain perception.

High-definition tDCS over M1 did not modulate cold pain tolerance and pain intensity and unpleasantness ratings. Human pain is a subjective and multidimensional experience involving sensory-discriminative, affective-motivational, and cognitive-evaluation aspects (Wiech et al., 2008; Tracey, 2011). Although pain threshold, pain tolerance, pain intensity, and unpleasantness ratings are indices of subjective pain perception, they could be reflecting different aspects of pain processing. Pain threshold seems to be determined predominantly by physiological factors, thereby, largely reflecting the sensory-discriminative aspect of pain that is mediated by the primary and secondary somatosensory cortices (Schnitzler and Ploner, 2000; Price et al., 2001; Vierck et al., 2013). Pain tolerance and unpleasantness rating are mainly reflecting the affective-motivational aspect of pain, which is processed in the medial nociceptive system including the anterior cingulate cortex and insula (Peyron et al., 2000; Schnitzler and Ploner, 2000; Bushnell et al., 2013). In contrast, pain intensity rating would be more complex, therefore, encompassing multiple aspects of pain that are encoded in brain regions associated with somatosensory, emotional, attention, and motor processing (Rainville et al., 1992; Coghill et al., 1999). Here, anodal HD-tDCS on M1 increased cold pain threshold but did not significantly affect cold pain tolerance, intensity, and unpleasantness rating. It suggests that HD-tDCS can effectively modulate the sensory-discriminative processes of pain perception, instead of the affective-cognitive aspect of pain perception.

Correlation analysis showed that analgesic effects of anodal HD-tDCS on pain intensity ratings were strongly associated with the participant's negative attentional bias. It is manifested that those healthy participants with a lower level of attentional bias to negative information tend to have greater effects of HD-tDCS on relieving pain intensity. With the knowledge that patients with chronic pain have more negative attitudes and beliefs, such as pain catastrophizing and fear of pain, as well as negative bias toward pain (Vlaeyen and Linton, 2000; Keogh et al., 2004; Bushnell et al., 2013; Meints and Edwards, 2018), the affective turning of the attentional system could direct attention to negatively-valanced information more frequently and consequently, leading to poor responses to pharmacological interventions of pain (Mankovsky et al., 2012; Burns et al., 2017; Sharifzadeh et al., 2017). For instance, chronic pain patients with less pain catastrophizing or fear of pain tend to exhibit better treatment outcomes (Werneke et al., 2009; Sparkes et al., 2015). Consistent with this understanding, hypervigilance to negative information may counteract the pain-relieving effects induced by HD-tDCS. It suggests that the application of tDCS on relieving clinical pain should well consider the patients' cognitions, such as attentional bias. Individuals with less attentional bias to negative information could be the ones that can benefit more from the tDCS intervention. This can help guide more precise tDCS intervention in clinical pain management.

CONCLUSION

In conclusion, relative to sham stimulation, single-session anodal HD-tDCS over M1 increased cold pain threshold in the healthy population. It indicates anodal HD-tDCS targeted on the M1 can effectively modulate the sensory-discriminative aspect of pain perception. In addition, the effectiveness of anodal HD-tDCS in attenuating pain intensity ratings to suprathreshold pain could be influenced by the level of attentional bias to negative information. Our findings support the potential application of HD-tDCS interventions in pain relief among the clinical pain patients and highlight that individual attentional bias to negative information should be well taken into consideration. Given that multiple-session tDCS may be more effective than single-session stimulation (Monte-Silva et al., 2013; Lefaucheur et al., 2017), future studies are recommended to test the effectiveness on relieving clinical pain through applying HD-tDCS with repeated sessions.

DATA AVAILABILITY STATEMENT

The original contributions presented in the study are included in the article/supplementary material, further inquiries can be directed to the corresponding author/s.

ETHICS STATEMENT

The studies involving human participants were reviewed and approved by the Medical Ethics Committee, Health Science Center, Shenzhen University. The patients/participants provided their written informed consent to participate in this study.

AUTHOR CONTRIBUTIONS

XYL and RJ: conception and design of the study and drafting the manuscript. XYL and JY: data acquisition. XYL and XXL: data analysis. XYL, SC, YH, JL, and RJ: writing—reviewing and editing. All authors read and approved the final manuscript.

FUNDING

This study was supported by the Project funded by the China Postdoctoral Science Foundation (2021M691437), the National Natural Science Foundation of China (62101236), the Shenzhen Basic Research Project (20200812113251002), the Guangdong Provincial Department of Education (2020ZDZX3043), the Shenzhen Natural Science Fund (JCYJ20200109140820699), and the Stable Support Plan Program (20200925174052004).

REFERENCES

Antal, A., Terney, D., Kühnl, S., and Paulus, W. (2010). Anodal transcranial direct current stimulation of the motor cortex ameliorates chronic pain and reduces short intracortical inhibition. *J. Pain Symptom Manage.* 39, 890–903. doi: 10.1016/j.jpainsymman.2009.09.023

Bachmann, C. G., Muschinsky, S., Nitsche, M. A., Rolke, R., Magerl, W., Treede, R. D., et al. (2010). Transcranial direct current stimulation of the motor cortex induces distinct changes in thermal and mechanical sensory percepts. *Clin. Neurophysiol.* 121, 2083–2089. doi: 10.1016/j.clinph.2010.05.005

Bannister, K., and Dickenson, A. H. (2017). The plasticity of descending controls in pain: translational probing. *J. Physiol.* 595, 4159–4166. doi: 10.1113/jp274165

Bikson, M., Datta, A., Rahman, A., and Scaturro, J. (2010). Electrode montages for tDCS and weak transcranial electrical stimulation: role of "return" electrode's position and size. *Clin. Neurophysiol.* 121, 1976–1978. doi: 10.1016/j.clinph.2010.05.020

Borckardt, J. J., Bikson, M., Frohman, H., Reeves, S. T., Datta, A., Bansal, V., et al. (2012). A pilot study of the tolerability and effects of high-definition transcranial direct current stimulation (HD-tDCS) on pain perception. *J. Pain* 13, 112–120. doi: 10.1016/j.jpain.2011.07.001

Brasil-Neto, J. P., Iannone, A., Caixeta, F. V., Cavendish, B. A., de Mello Cruz, A. P., and Buratto, L. G. (2020). Acute offline transcranial direct current stimulation does not change pain or anxiety produced by the cold pressor test. *Neurosci. Lett.* 736:135300. doi: 10.1016/j.neulet.2020.135300

Brunoni, A. R., Amadera, J., Berbel, B., Volz, M. S., Rizzerio, B. G., and Fregni, F. (2011). A systematic review on reporting and assessment of adverse effects associated with transcranial direct current stimulation. *Int. J. Neuropsychopharmacol.* 14, 1133–1145. doi: 10.1017/s1461145710001690

Burns, J. W., Bruehl, S., France, C. R., Schuster, E., Orlowska, D., Buvanendran, A., et al. (2017). Psychosocial factors predict opioid analgesia through endogenous opioid function. *Pain* 158, 391–399. doi: 10.1097/j.pain.0000000000000768

Bushnell, M. C., Ceko, M., and Low, L. A. (2013). Cognitive and emotional control of pain and its disruption in chronic pain. *Nat. Rev. Neurosci.* 14, 502–511. doi: 10.1038/nrn3516

Castillo-Saavedra, L., Gebodh, N., Bikson, M., Diaz-Cruz, C., Brandao, R., Coutinho, L., et al. (2016). Clinically effective treatment of fibromyalgia pain with high-definition transcranial direct current stimulation: phase II open-label dose optimization. *J. Pain* 17, 14–26. doi: 10.1016/j.jpain.2015.09.009

Coghill, R. C., Sang, C. N., Maisog, J. M., and Iadarola, M. J. (1999). Pain intensity processing within the human brain: a bilateral, distributed mechanism. *J. Neurophysiol.* 82, 1934–1943. doi: 10.1152/jn.1999.82.4.1934

Creutzfeldt, O. D., Fromm, G. H., and Kapp, H. (1962). Influence of transcortical dc currents on cortical neuronal activity. *Exp. Neurol.* 5, 436–452. doi: 10.1016/0014-4886(62)90056-0

Datta, A., Bansal, V., Diaz, J., Patel, J., Reato, D., and Bikson, M. (2009). Gyri-precise head model of transcranial direct current stimulation: improved spatial focality using a ring electrode versus conventional rectangular pad. *Brain Stimul.* 2, 201–207, 207.e201. doi: 10.1016/j.brs.2009.03.005

Edwards, D., Cortes, M., Datta, A., Minhas, P., Wassermann, E. M., and Bikson, M. (2013). Physiological and modeling evidence for focal transcranial electrical brain stimulation in humans: a basis for high-definition tDCS. *Neuroimage* 74, 266–275. doi: 10.1016/j.neuroimage.2013.01.042

Ehrlich, P. F., Vedulla, G., Cottrell, N., and Seidman, P. A. (2003). Monitoring intraoperative effectiveness of caudal analgesia through skin temperature variation. *J. Pediatr. Surg.* 38, 386–389. doi: 10.1053/jpsu.2003.50113

Fregni, F., Freedman, S., and Pascual-Leone, A. (2007). Recent advances in the treatment of chronic pain with non-invasive brain stimulation techniques. *Lancet Neurol.* 6, 188–191. doi: 10.1016/s1474-4422(07)70032-7

Garcia-Larrea, L., and Peyron, R. (2007). Motor cortex stimulation for neuropathic pain: from phenomenology to mechanisms. *Neuroimage* 37 Suppl 1, S71–S79. doi: 10.1016/j.neuroimage.2007.05.062

García-Larrea, L., Peyron, R., Mertens, P., Gregoire, M. C., Lavenne, F., Le Bars, D., et al. (1999). Electrical stimulation of motor cortex for pain control: a combined PET-scan and electrophysiological study. *Pain* 83, 259–273. doi: 10.1016/s0304-3959(99)00114-1

Giannoni-Luza, S., Pacheco-Barrios, K., Cardenas-Rojas, A., Mejia-Pando, P. F., Luna-Cuadros, M. A., Barouh, J. L., et al. (2020). Noninvasive motor cortex stimulation effects on quantitative sensory testing in healthy and chronic pain subjects: a systematic review and meta-analysis. *Pain* 161, 1955–1975. doi: 10.1097/j.pain.0000000000001893

Grundmann, L., Rolke, R., Nitsche, M. A., Pavlakovic, G., Happe, S., Treede, R. D., et al. (2011). Effects of transcranial direct current stimulation of the primary sensory cortex on somatosensory perception. *Brain Stimul.* 4, 253–260. doi: 10.1016/j.brs.2010.12.002

Jiang, X., Wang, Y., Wan, R., Feng, B., Zhang, Z., Lin, Y., et al. (2022). The effect of high-definition transcranial direct current stimulation on pain processing in a healthy population: a single-blinded crossover controlled study. *Neurosci. Lett.* 767:136304. doi: 10.1016/j.neulet.2021.136304

Jürgens, T. P., Schulte, A., Klein, T., and May, A. (2012). Transcranial direct current stimulation does neither modulate results of a quantitative sensory testing protocol nor ratings of suprathreshold heat stimuli in healthy volunteers. *Eur. J. Pain* 16, 1251–1263. doi: 10.1002/j.1532-2149.2012.00135.x

Keogh, E., Hamid, R., Hamid, S., and Ellery, D. (2004). Investigating the effect of anxiety sensitivity, gender and negative interpretative bias on the perception of chest pain. *Pain* 111, 209–217. doi: 10.1016/j.pain.2004.06.017

Kold, S., and Graven-Nielsen, T. (2021). Effect of anodal high-definition transcranial direct current stimulation on the pain sensitivity in a healthy population: a double-blind, sham-controlled study. *Pain* 162, 1659–1668. doi: 10.1097/j.pain.0000000000002187

Kuo, H. I., Bikson, M., Datta, A., Minhas, P., Paulus, W., Kuo, M. F., et al. (2013). Comparing cortical plasticity induced by conventional and high-definition 4 × 1 ring tDCS: a neurophysiological study. *Brain Stimul.* 6, 644–648. doi: 10.1016/j.brs.2012.09.010

Lang, N., Siebner, H. R., Ward, N. S., Lee, L., Nitsche, M. A., Paulus, W., et al. (2005). How does transcranial DC stimulation of the primary motor cortex alter regional neuronal activity in the human brain? *Eur. J. Neurosci.* 22, 495–504. doi: 10.1111/j.1460-9568.2005.04233.x

Lefaucheur, J. P., Antal, A., Ayache, S. S., Benninger, D. H., Brunelin, J., Cogiamanian, F., et al. (2017). Evidence-based guidelines on the therapeutic use of transcranial direct current stimulation (tDCS). *Clin. Neurophysiol.* 128, 56–92. doi: 10.1016/j.clinph.2016.10.087

Lefaucheur, J.-P., Antal, A., Ahdab, R., de Andrade, D. C., Fregni, F., Khedr, E. M., et al. (2008). The use of repetitive transcranial magnetic stimulation (rTMS) and transcranial direct current stimulation (tDCS) to relieve pain. *Brain Stimul.* 1, 337–344. doi: 10.1016/j.brs.2008.07.003

Luedtke, K., Rushton, A., Wright, C., Geiss, B., Juergens, T. P., and May, A. (2012b). Transcranial direct current stimulation for the reduction of clinical and experimentally induced pain: a systematic review and meta-analysis. *Clin. J. Pain* 28, 452–461. doi: 10.1097/AJP.0b013e31823853e3

Luedtke, K., May, A., and Jürgens, T. P. (2012a). No effect of a single session of transcranial direct current stimulation on experimentally induced pain in patients with chronic low back pain–an exploratory study. *PLoS One* 7:e48857. doi: 10.1371/journal.pone.0048857

Luedtke, K., Rushton, A., Wright, C., Jürgens, T., Polzer, A., Mueller, G., et al. (2015). Effectiveness of transcranial direct current stimulation preceding cognitive behavioural management for chronic low back pain: sham controlled double blinded randomised controlled trial. *BMJ* 350, h1640. doi: 10.1136/bmj.h1640

Mankovsky, T., Lynch, M., Clark, A., Sawynok, J., and Sullivan, M. J. (2012). Pain catastrophizing predicts poor response to topical analgesics in patients with neuropathic pain. *Pain Res. Manag.* 17, 10–14. doi: 10.1155/2012/970423

McCracken, L. M. (1997). Attention to pain in persons with chronic pain: a behavioral approach. *Behav. Ther.* 28, 271–284. doi: 10.1016/S0005-7894(97)80047-0

McNeil, D. W., and Rainwater, A. J. (1998). Development of the fear of pain questionnaire-III. *J. Behav. Med.* 21, 389–410. doi: 10.1023/a:1018782831217

Meints, S. M., and Edwards, R. R. (2018). Evaluating psychosocial contributions to chronic pain outcomes. *Prog. Neuropsychopharmacol. Biol. Psychiatry* 87(Pt B), 168–182. doi: 10.1016/j.pnpbp.2018.01.017

Minhas, P., Bansal, V., Patel, J., Ho, J. S., Diaz, J., Datta, A., et al. (2010). Electrodes for high-definition transcutaneous DC stimulation for applications in drug delivery and electrotherapy, including tDCS. *J. Neurosci. Methods* 190, 188–197. doi: 10.1016/j.jneumeth.2010.05.007

Monte-Silva, K., Kuo, M. F., Hessenthaler, S., Fresnoza, S., Liebetanz, D., Paulus, W., et al. (2013). Induction of late LTP-like plasticity in the human motor

cortex by repeated non-invasive brain stimulation. *Brain Stimul.* 6, 424–432. doi: 10.1016/j.brs.2012.04.011

Mylius, V., Borckardt, J. J., and Lefaucheur, J. P. (2012). Noninvasive cortical modulation of experimental pain. *Pain* 153, 1350–1363. doi: 10.1016/j.pain.2012.04.009

Nitsche, M. A., and Paulus, W. (2000). Excitability changes induced in the human motor cortex by weak transcranial direct current stimulation. *J. Physiol.* 527(Pt 3), 633–639. doi: 10.1111/j.1469-7793.2000.t01-1-00633.x

Nitsche, M. A., Cohen, L. G., Wassermann, E. M., Priori, A., Lang, N., Antal, A., et al. (2008). Transcranial direct current stimulation: state of the art 2008. *Brain Stimul.* 1, 206–223. doi: 10.1016/j.brs.2008.06.004

Nitsche, M. A., Doemkes, S., Karaköse, T., Antal, A., Liebetanz, D., Lang, N., et al. (2007). Shaping the effects of transcranial direct current stimulation of the human motor cortex. *J. Neurophysiol.* 97, 3109–3117. doi: 10.1152/jn.01312.2006

Noguchi, K., Gohm, C. L., and Dalsky, D. J. (2006). Cognitive tendencies of focusing on positive and negative information. *J. Res. Pers.* 40, 891–910. doi: 10.1016/j.jrp.2005.09.008

Peyron, R., Laurent, B., and Garcia-Larrea, L. (2000). Functional imaging of brain responses to pain. A review and meta-analysis (2000). *Neurophysiol. Clin.* 30, 263–288. doi: 10.1016/s0987-7053(00)00227-6

Price, D. D., Riley, J. L., and Wade, J. B. (2001). "Psychophysical approaches to measurement of the dimensions and stages of pain," in *Handbook Of Pain Assessment*, 2nd Edn, eds D. C. Turk and R. Melzack (New York, NY: The Guilford Press), 53–75. doi: 10.1097/PR9.0000000000000821

Purpura, D. P., and McMurtry, J. G. (1965). Intracellular activities and evoked potential changes during polarization of motor cortex. *J. Neurophysiol.* 28, 166–185. doi: 10.1152/jn.1965.28.1.166

Rainville, P., Feine, J. S., Bushnell, M. C., and Duncan, G. H. (1992). A psychophysical comparison of sensory and affective responses to four modalities of experimental pain. *Somatosens. Mot. Res.* 9, 265–277. doi: 10.3109/08990229209144776

Ruscheweyh, R., Marziniak, M., Stumpenhorst, F., Reinholz, J., and Knecht, S. (2009). Pain sensitivity can be assessed by self-rating: development and validation of the Pain Sensitivity Questionnaire. *Pain* 146, 65–74. doi: 10.1016/j.pain.2009.06.020

Schnitzler, A., and Ploner, M. (2000). Neurophysiology and functional neuroanatomy of pain perception. *J. Clin. Neurophysiol.* 17, 592–603. doi: 10.1097/00004691-200011000-00005

Sharifzadeh, Y., Kao, M. C., Sturgeon, J. A., Rico, T. J., Mackey, S., and Darnall, B. D. (2017). Pain catastrophizing moderates relationships between pain intensity and opioid prescription: nonlinear sex differences revealed using a learning health system. *Anesthesiology* 127, 136–146. doi: 10.1097/aln.0000000000001656

Sparkes, E., Duarte, R. V., Mann, S., Lawrence, T. R., and Raphael, J. H. (2015). Analysis of psychological characteristics impacting spinal cord stimulation treatment outcomes: a prospective assessment. *Pain Phys.* 18, E369–E377.

Sullivan, M. J., Bishop, S. R., and Pivik, J. (1995). The pain catastrophizing scale: development and validation. *Psychol. Assess.* 7, 524–532. doi: 10.1037/1040-3590.7.4.524

Tracey, I. (2011). Can neuroimaging studies identify pain endophenotypes in humans? *Nat. Rev. Neurol.* 7, 173–181. doi: 10.1038/nrneurol.2011.4

Vaseghi, B., Zoghi, M., and Jaberzadeh, S. (2014). Does anodal transcranial direct current stimulation modulate sensory perception and pain? A meta-analysis study. *Clin. Neurophysiol.* 125, 1847–1858. doi: 10.1016/j.clinph.2014.01.020

Vaseghi, B., Zoghi, M., and Jaberzadeh, S. (2015). A meta-analysis of site-specific effects of cathodal transcranial direct current stimulation on sensory perception and pain. *PLoS One* 10:e0123873. doi: 10.1371/journal.pone.0123873

Vierck, C. J., Whitsel, B. L., Favorov, O. V., Brown, A. W., and Tommerdahl, M. (2013). Role of primary somatosensory cortex in the coding of pain. *Pain* 154, 334–344. doi: 10.1016/j.pain.2012.10.021

Villamar, M. F., Volz, M. S., Bikson, M., Datta, A., Dasilva, A. F., and Fregni, F. (2013). Technique and considerations in the use of 4x1 ring high-definition transcranial direct current stimulation (HD-tDCS). *J. Vis. Exp.* 77:e50309. doi: 10.3791/50309

Vlaeyen, J. W. S., and Linton, S. J. (2000). Fear-avoidance and its consequences in chronic musculoskeletal pain: a state of the art. *Pain* 85, 317–332. doi: 10.1016/s0304-3959(99)00242-0

Wan, R., Wang, Y., Feng, B., Jiang, X., Xu, Y., Zhang, Z., et al. (2021). Effect of high-definition transcranial direct current stimulation on conditioned pain modulation in healthy adults: a crossover randomized controlled trial. *Neuroscience* 479, 60–69. doi: 10.1016/j.neuroscience.2021.10.019

Werneke, M. W., Hart, D. L., George, S. Z., Stratford, P. W., Matheson, J. W., and Reyes, A. (2009). Clinical outcomes for patients classified by fear-avoidance beliefs and centralization phenomenon. *Arch. Phys. Med. Rehabil.* 90, 768–777. doi: 10.1016/j.apmr.2008.11.008

Wiech, K., Ploner, M., and Tracey, I. (2008). Neurocognitive aspects of pain perception. *Trends Cogn. Sci.* 12, 306–313. doi: 10.1016/j.tics.2008.05.005

Zandieh, A., Parhizgar, S. E., Fakhri, M., Taghvaei, M., Miri, S., Shahbabaie, A., et al. (2013). Modulation of cold pain perception by transcranial direct current stimulation in healthy individuals. *Neuromodulation* 16, 345–348; discussion348. doi: 10.1111/ner.12009

Conflict of Interest: The authors declare that the research was conducted in the absence of any commercial or financial relationships that could be construed as a potential conflict of interest.

Publisher's Note: All claims expressed in this article are solely those of the authors and do not necessarily represent those of their affiliated organizations, or those of the publisher, the editors and the reviewers. Any product that may be evaluated in this article, or claim that may be made by its manufacturer, is not guaranteed or endorsed by the publisher.

frontiers in Molecular Neuroscience

ORIGINAL RESEARCH
published: 30 March 2022
doi: 10.3389/fnmol.2022.865310

Long Non-coding RNA and mRNA Expression Change in Spinal Dorsal Horn After Exercise in Neuropathic Pain Rats

Ge Song[1], Wei-Ming Zhang[1], Yi-Zu Wang[1], Jia-Bao Guo[2], Yi-Li Zheng[3], Zheng Yang[4], Xuan Su[3], Yu-Meng Chen[3], Qing Xie[1] and Xue-Qiang Wang[3,5]**

[1] Department of Rehabilitation Medicine, Ruijin Hospital, Shanghai Jiao Tong University School of Medicine, Shanghai, China, [2] The Second Clinical Medical School, Xuzhou Medical University, Xuzhou, China, [3] Department of Sport Rehabilitation, Shanghai University of Sport, Shanghai, China, [4] Department of Rehabilitation Medicine, Shanghai Jiao Tong University Affiliated Sixth People's Hospital, Shanghai, China, [5] Department of Rehabilitation Medicine, Shanghai Shangti Orthopaedic Hospital, Shanghai, China

OPEN ACCESS

Edited by:
Wen Wu,
Southern Medical University, China

Reviewed by:
Qiuhua Yu,
Sun Yat-sen University, China
Farinaz Nasirinezhad,
Iran University of Medical Sciences, Iran
Junhao Huang,
Guangzhou Sport University, China

***Correspondence:**
Qing Xie
ruijin_xq@163.com
Xue-Qiang Wang
wangxueqiang@sus.edu.cn

Specialty section:
This article was submitted to Pain Mechanisms and Modulators, a section of the journal Frontiers in Molecular Neuroscience

Received: *29 January 2022*
Accepted: *07 March 2022*
Published: *30 March 2022*

Citation:
Song G, Zhang W-M, Wang Y-Z, Guo J-B, Zheng Y-L, Yang Z, Su X, Chen Y-M, Xie Q and Wang X-Q (2022) Long Non-coding RNA and mRNA Expression Change in Spinal Dorsal Horn After Exercise in Neuropathic Pain Rats. Front. Mol. Neurosci. 15:865310. doi: 10.3389/fnmol.2022.865310

Exercise can help inhibition of neuropathic pain (NP), but the related mechanism remains being explored. In this research, we performed the effect of swimming exercise on the chronic constriction injury (CCI) rats. Compared with CCI group, the mechanical withdrawal threshold of rats in the CCI-Swim group significantly increased on the 21st and 28th day after CCI surgery. Second-generation RNA-sequencing technology was employed to investigate the transcriptomes of spinal dorsal horns in the Sham, CCI, and CCI-Swim groups. On the 28th day post-operation, 306 intersecting long non-coding RNAs (lncRNAs) and 173 intersecting mRNAs were observed between the CCI vs Sham group and CCI-Swim vs CCI groups. Then, the biological functions of lncRNAs and mRNAs in the spinal dorsal horn of CCI rats were then analyzed. Taking the results together, this study could provide a novel perspective for the treatment for NP.

Keywords: swim, spinal dorsal horn, sequencing, neuropathic pain, lncRNA, mRNA

INTRODUCTION

Neuropathic pain (NP) is a primary lesion or disease of the somatosensory system, the symptoms and signs of which include spontaneous pain, allodynia, hyperalgesia, and paresthesia (Jensen and Finnerup, 2014; Colloca et al., 2017; Cavalli et al., 2019). Long-term pain not only reduces the sleep quality of NP patients, but also leads to decreased quality of life and psychological state (Colloca et al., 2017; Wu et al., 2019). Epidemiological surveys show that the prevalence of NP is 7–10% (van Hecke et al., 2014). Global aging has rendered NP a major public health issue and socioeconomic burden (Colloca et al., 2017; Bouhassira, 2019). Previous studies have found that the majority of available NP treatments have mild effects or dose-limiting side effects, and many NP patients have pain that cannot be properly treated (Attal and Bouhassira, 2015; Cooper et al., 2016; Gierthmühlen and Baron, 2016). Therefore, exploring safe and effective treatments for NP is necessary.

Exercise is widely used in the medical field as a therapeutic method and as a new approach to relieve various painful conditions (Dobson et al., 2014; Cooper et al., 2016; Kami et al., 2017; Palandi et al., 2020; Zhao et al., 2020; Zhou et al., 2020; Zheng et al., 2021; Peng et al., 2022; Wu et al., 2022). Previous studies have reported that swimming and treadmill running could significantly

improve mechanical allodynia, cold allodynia, and heat hyperalgesia, while suppress the level of inflammatory cytokines in animal NP models (Cooper et al., 2016; Kami et al., 2017). Swimming, as an effective method of reducing pain in rats, is an attractive form of exercise for patients with NP. Swimming can relieve the load on the aching limbs and coordination problems affected by pain in most patients, especially in the elderly (Cooper et al., 2016; Kami et al., 2017). However, the exact mechanism by which swimming alleviates NP is insufficiently understood and requires further exploration.

Recent developments in RNA-sequencing (RNA-seq) technology have enabled the screening of differentially expressed genes (DEGs) in the NP process and improved the understanding of the mechanism of NP (St John Smith, 2018). Long non-coding RNAs (lncRNAs), as non-protein coding RNAs with more than 200 nucleotides in length, have gene regulation functions. Earlier research established the participation of lncRNAs in the pathological process of NP by modulating pain-associated genes and altering neuronal excitability (Zhou et al., 2017a,b; Wu et al., 2019). Published studies also found that the spinal dorsal horn is the site of greatest concern in basic researches on NP. The spinal dorsal horn is the first station for the central nervous system to receive pain afferent signals (Cohen and Mao, 2014; Tsuda, 2016). After preliminary integration, the information is uploaded to the thalamus, and then the information is further transmitted to the cerebral cortex, thus causing pain. The dorsal horn of spinal cord is an important node for upward transmission of pain signals (Guo and Hu, 2014). However, no study evaluating the function of exercise in spinal dorsal horn transcriptomes in an NP animal model has yet been published. Therefore, in this research, we demonstrate the effect of swimming on the transcriptome of chronic constriction injury (CCI) rats, and utilized RNA-seq technology analyzing DEGs with their biological function. The genetic changes induced by exercise afford potential intervention targets for the development of NP.

MATERIALS AND METHODS

Animals and Exercise Training

The SLAC Laboratory (Shanghai, China) afforded us with Sprague Dawley rats. The rats were all 6-week-old males weighing between 180 and 200 g. The rats were given standard water and rat chow. Their ambient temperature was controlled at 24 ± 1°C and the light and dark cycle was 12/12 h. All experimental processes were authorized by the Ethics Committee of Scientific Research of Shanghai University of Sport.

The rats (n = 18) were grouped randomly into three groups: the Sham group (n = 6), the CCI group (n = 6), and the CCI-Swim group (n = 6). Adaptive feeding was conducted for 1 week. The rats in Sham and CCI groups were routinely fed and did not participate in swimming exercise, while rats in the CCI-Swim group were adapted to swim for 1 week preoperatively. Swimming time gradually increased from 10 min on day 1 to 60 min on day 6. On the third day after the CCI operation, rats in the CCI-Swim group were made to swim for a total of 19 sessions, and the swimming time was gradually increased. The first and second sessions involved swimming for 30 min each day, the third and fourth sessions involved swimming for 40 min each day, and the fifth and sixth sessions involved swimming for 50 min each day. In the seventh to ninth sessions, the rats swam for 60 min each time (**Figure 1**). This swimming training program is based on a previously published animal swimming exercise program that was improved by our research group. The rats were made to swim in a plastic box (82 cm × 60 cm × 59 cm) at a temperature of 35–37°C. After swimming, the rats are caught and dried with a heat blower (Almeida et al., 2015).

Chronic Constriction Injury Models

We performed CCI on the sciatic nerve of the rats on the basis of a previous study (Jaggi et al., 2011). First, we anesthetized the animal with 5% isoflurane. Then, the skin of the rats' right lower limb was cut, and the muscle and connective tissue were bluntly dissected to locate the sciatic nerve. Four chromic catguts

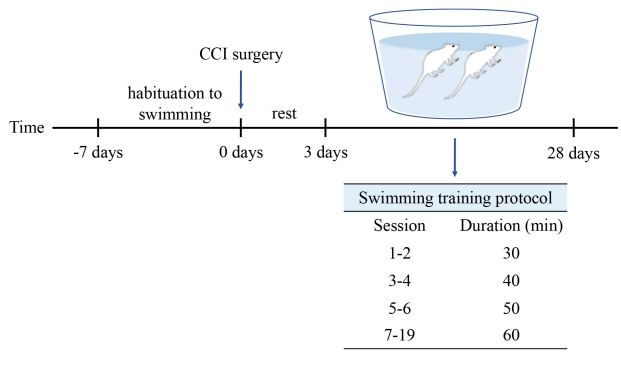

FIGURE 1 | Protocol for swimming exercise. Swimming was included 1-week habituation before CCI surgery and 4-week formal training after CCI surgery.

TABLE 1 | The primers utilized in qRT-PCR.

Primer	Forward	Reverse
XLOC_274480	AGATACCAGTCATCCT ACCTGC	CGAGACATCGTATCATG GAGTCA
XLOC_105980	CGGTCTCCAGCTAGTTA TCCAC	GGCAACCGGAGAAAGAA TTGAAC
XLOC_134372	AGTGAAATACATTGCTGT CCTGTC	CACTGGGAGGATATGG TAAGGCA
AABR07047899.1	TGATCCAAAAGCTGC CCGACA	GAACAGAATCTCCTTGC GACA
C3	TCTTGTCACTGCCC ATCACT	GAGTCCTTCACAT CCACCCA
Sgk1	CTCAGTAACAAAACCC GAGGC	ATTCCCGGTCAAGAA ATGCTC
Dnah7	ATGATACCCGTTCTG CACCA	TGACGAGGGTGCT TCTGAAA
Vwa3a	TCCACGAGAAGGCA ATGGTA	TATCTGCACAGCTT TCCCGA
U6	CTCGCTTCG GCAGCACA	AACGCTTCACGAA TTTGCGT
β-Actin	TGTCACCAACTGG GACGATA	GGGGTGTTGAAGGT CTCAAA

(4.0 silk) were ligated on the sciatic nerve at an interval of approximately 1 mm. The sciatic nerve of rats in the Sham group was exposed but not ligated. The skin was then sewn with 5.0 silk sutures, and the rats were allowed a recovery period after the operation.

Mechanical Withdrawal Threshold

We performed mechanical withdrawal threshold (MWT) tests before and after CCI at 3, 7, 14, 21, and 28 days. The rats were placed in transparent glass boxes for 20 min to acclimatize before each behavioral test. The MWT test was performed by harmless stimulation to the posterior plantar of the rats. Von Frey wires (4–180 g, Aesthesio, Danmic Global, United States) were applied to the right hind paw, and the intensity of the Von Frey wires increased from small to large until the rats exhibited the desired behavior. Each rat was tested at least three times, at 5 min intervals.

Histological Examination

On the 28th day after CCI operation, three rats in each group (i.e., Sham, CCI, and CCI-Swim groups) were killed, and the spinal cord was collected for histopathological analysis. The spinal cord was fixed in 4% paraformaldehyde solution at 4°C for 90 min. After phosphate-buffered saline (PBS) cleaning for 15 min, the samples were then respectively soaked in 15 and 30% sucrose solution for 24 and 48 h. The tissue samples were placed in compound compounds (SAKURA, 4583), sliced (14 μm thick), and dyed with hematoxylin and eosin (HE). The slices were rinsed with PBS for 5 min, soaked in hematoxylin staining solution (Servicebio, G1005-1) for 4 min, and then washed under running water for 20 min. After washing, 1% hydrochloric acid solution was used for differentiation for 3 s. Rinsing was repeated for 15 min. The slides were kept in 0.1% eosin staining solution (Servicebio, G1005-2) for 3 min and then soaked in 85, 95, and 100% alcohol solutions for 1 min in sequence. After soaking in xylene I and xylene II for 1 min, the tissue samples were sealed with neutral resin and then observed under an Olympus BX53 microscope (Tokyo, Japan).

Sample Collection and RNA-Sequencing

On the 28th day after surgery, the remaining rats (n = 9, three in each group) were anesthetized with 3% pentobarbital sodium and instilled with saline (250 mL, 4°C) via the aorta. The corresponding positions of L4–L6 were located on the surgical side of the spine, and the spinal canal was opened to remove the L4–L6 spinal dorsal horn. TRIzol reagent was utilized to extract total RNA from the spinal dorsal horn. RNA quantification and qualification were conducted prior to sequencing. We established sequencing libraries through NEBNext® Ultra™ RNA Library Prep Kit for Illumina® (NEB, United States) and appended the index code to attribute sequence of each sample. Then, the PCR products were purified by AMPure XP system, and the library quality was evaluated on Agilent Bioanalyzer 2100 system. Finally, the library preparation was sequenced by Illumina Hiseq platform.

Differentially Expressed Genes and Bioinformatics Analysis

The DESeq2 R package (1.10.1) was utilized to analyze the identified DEGs. DEG selection criteria is P-values < 0.05 and $|\log2$ Fold Change (FC)$| > 1$.

Gene Ontology (GO) analysis was executed by the clusterProfiler R package. The KEGG database allows for genome deciphering, which enables a better understanding and analysis of the interactions, reactions, and relational networks of biomolecules produced by sequencing experimental techniques.[1] The ClusterProfiler R package was utilized to detect DEGs enrichment in KEGG pathways. The significant enrichment criterion for GO analysis and KEGG pathway analyses was $P < 0.05$.

Validation by Quantitative Real-Time PCR

Quantitative real-time PCR (qRT-PCR) was used to detect the DEGs to verify the accuracy of the sequencing results. Total RNA was reverse transcribed into cDNA by Evo M-MLV RT Kit with gDNA Clean for qPCR II (Cat. No. AG11711). The qRT-PCR was executed by SYBR® Green Premix Pro Taq HS qPCR Kit II (Cat. No. AG11702) and run in a real-time system (Thermo Fisher Scientific, CA, United States). U6 and β-actin were identified as internal controls for lncRNAs and mRNAs, respectively, and the $2^{-\Delta\Delta Ct}$ approach was applied to describe relative expression ratios. The specific primer sequences in this work are listed **Table 1**.

Statistics

Two-way repeated-measures analysis of variance with Tukey's *post hoc* analysis was conducted to evaluate the results of

[1]http://www.genome.jp/kegg/

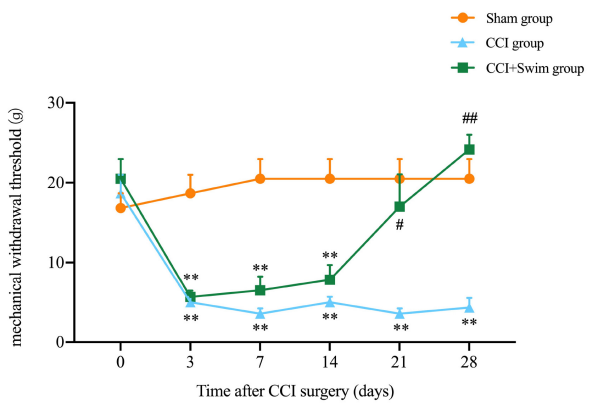

FIGURE 2 | Effect of exercise therapy on mechanical allodynia induced by chronic constrictive injury (CCI). Analyses was adopted by two-way repeated measures analysis of variance (ANOVA) with Tukey's *post hoc* analysis. The average is denoted by mean ± standard error of mean (SEM), N = 6 per group. $^{**}p < 0.01$, for comparisons of the Sham group vs the CCI group or CCI-Swim group. $^{\#}p < 0.05$, $^{\#\#}p < 0.01$ for comparisons of the CCI-Swim group vs the CCI group.

weight measurement and behavioral tests. The results of qRT-PCR were determined by independent-sample *t*-tests. All of the data were analyzed by Graphpad Prism 9.0 and presented as mean ± standard error of the mean (SEM). The standard of statistical significance was $P < 0.05$.

RESULTS

Chronic Constriction Injury Model Identification and Mechanical Withdrawal Threshold Analysis

In this study, the NP model of rats involved CCI on the right hind limb. MWT test was performed in all three groups before and after operation (**Figure 2**). No significant difference in body weight among the three groups. Contrast to rats in the Sham group, animals in CCI group showed higher mechanical allodynia sensitivity from day 3 to 28 after CCI surgery; the CCI-Swim group also exhibited higher MWT on days 3, 7, and 14 after surgery. MWT was significantly improved in the CCI-Swim group on the day 21 and 28 after operation in contrast to the CCI group.

Histological Examination of the Spinal Dorsal Horn

The HE staining results showed that the spinal dorsal horn neurons in the Sham group were intact, regular, and orderly and that the nucleolus *in vivo* was distinct. In the CCI group,

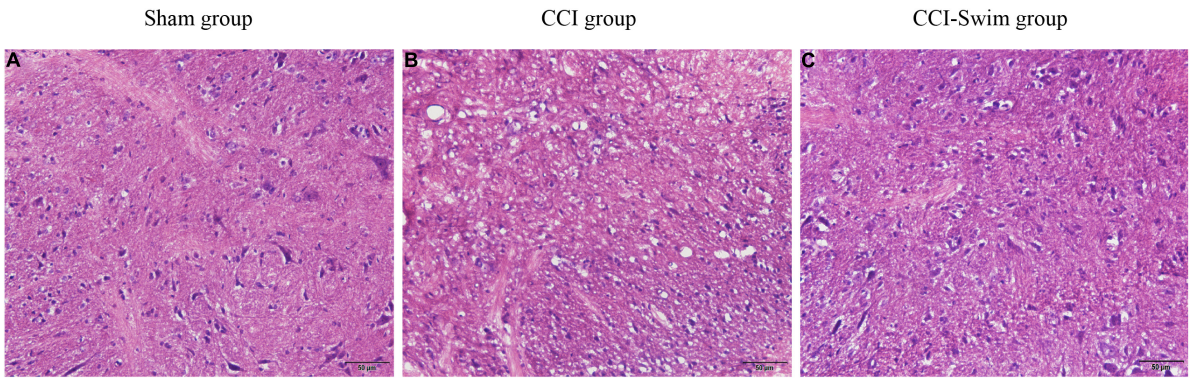

FIGURE 3 | Histological examination of spinal dorsal horn. The hematoxylin-eosin (HE) staining of spinal dorsal horn tissue were observed under light microscopy (×200, bar = 50 μm). Sham group **(A)**, CCI group **(B)**, and CCI-Swim group **(C)**.

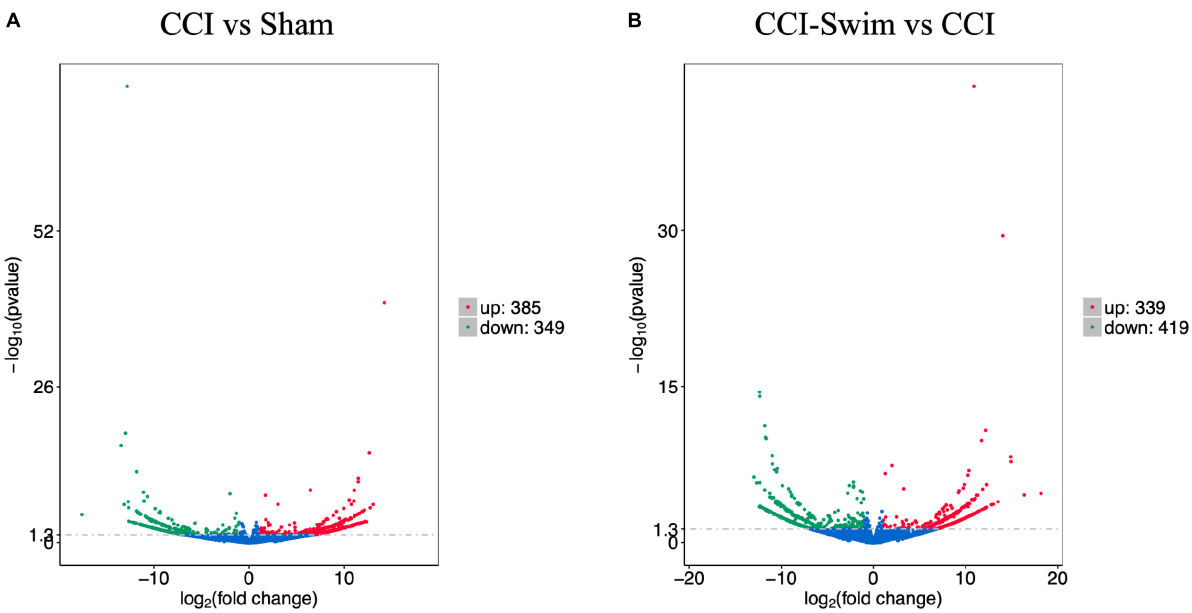

FIGURE 4 | Volcano plots of RNA-sequencing data exhibited the differentially expressed lncRNAs in the spinal dorsal horn between rats in the comparisons of CCI group vs Sham group **(A)**, and CCI-Swim group vs CCI group **(B)**. The red part is significantly upregulated lncRNAs, the green part is significantly downregulated lncRNAs, and the blue part is not significantly expressed lncRNAs.

the spinal dorsal horn neurons were damaged and denatured, with pyknosis, fragmentation, and dissolution of the nucleus, as well as loose surrounding tissues. These features indicate that the CCI model had been successfully prepared. Compared with the CCI group, the CCI-Swim group showed a slightly irregular arrangement of sensory neurons in the spinal dorsal horn and relatively dense surrounding tissues. In general, the histological features of the spinal cord in this group were better than those of the CCI group overall (**Figure 3**).

TABLE 2 | The top 20 DE lncRNAs in CCI group vs Sham group.

Gene name	Log_2FC	*P*-value	Regulation
AABR07015080.2	−12.81	<0.001	Down
XLOC_097393	14.21	<0.001	Up
XLOC_309240	−13.00	<0.001	Down
XLOC_176078	−13.45	<0.001	Down
XLOC_314732	12.62	<0.001	Up
XLOC_085264	−11.83	<0.001	Down
XLOC_234469	11.47	<0.001	Up
XLOC_173719	11.46	<0.001	Up
1700066B19Rik	6.44	<0.001	Up
XLOC_189377	11.04	<0.001	Up
XLOC_239191	−11.10	<0.001	Down
XLOC_274480	−2.01	<0.001	Down
XLOC_002354	1.71	<0.001	Up
XLOC_011654	−10.70	<0.001	Down
XLOC_122558	10.52	<0.001	Up
XLOC_305707	−11.04	<0.001	Down
LOC102546683	11.01	<0.001	Up
AABR07053749.1	−12.70	<0.001	Down
XLOC_244676	10.74	<0.001	Down
AABR07058158.1	3.02	<0.001	Up

DE, differentially expressed; FC, fold change.

TABLE 3 | The top 20 DE lncRNAs in CCI-Swim group vs CCI group.

Gene name	Log_2FC	*P*-value	Regulation
AABR07015080.2	10.90	<0.001	Up
XLOC_309240	14.03	<0.001	Up
LOC108348298	−12.39	<0.001	Down
XLOC_025354	−12.35	<0.001	Down
AABR07067076.1	−11.79	<0.001	Down
XLOC_312531	12.16	<0.001	Up
XLOC_032459	−11.70	<0.001	Down
XLOC_033171	−11.65	<0.001	Down
XLOC_096101	11.72	<0.001	Up
XLOC_189377	−10.99	<0.001	Down
AABR07062823.1	14.90	<0.001	Up
XLOC_243724	14.93	<0.001	Up
XLOC_212511	−10.98	<0.001	Down
XLOC_274480	2.01	<0.001	Up
XLOC_044460	−10.43	<0.001	Down
XLOC_097273	−10.72	<0.001	Down
XLOC_244676	10.36	<0.001	Up
AABR07071299.1	−10.51	<0.001	Down
AABR07015078.1	1.27	<0.001	Up
XLOC_119427	10.25	<0.001	Up

DE, differentially expressed; FC, fold change.

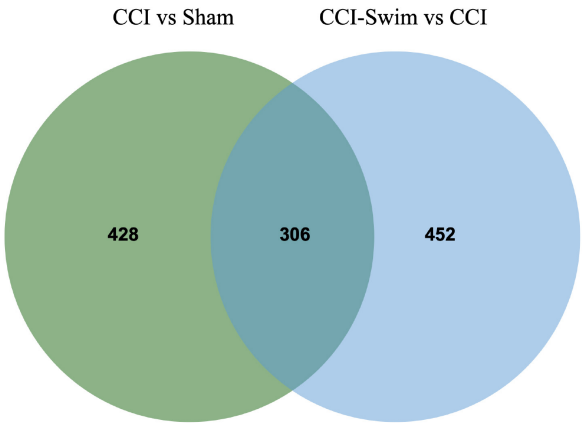

FIGURE 5 | Venn diagram of lncRNAs. The figure shows the intersection of differential expressed lncRNAs between the CCI vs Sham group and the CCI-Swim vs CCI group.

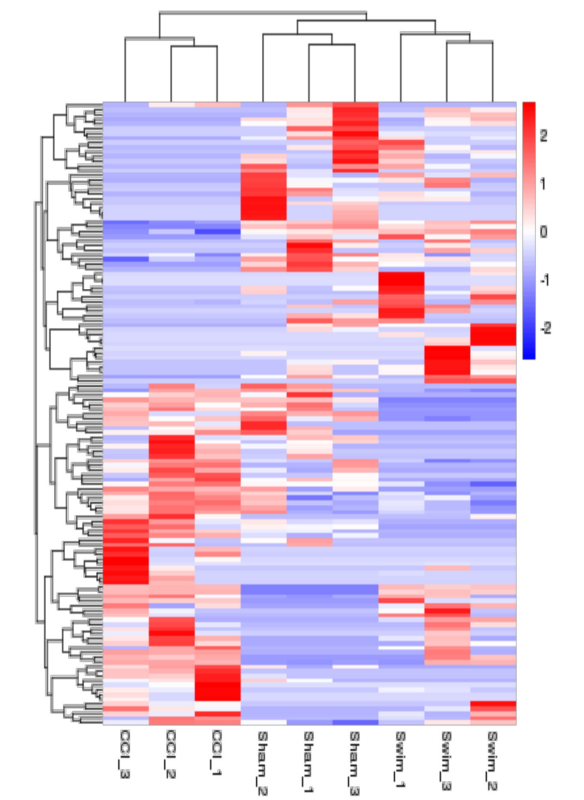

FIGURE 6 | The hierarchical cluster analysis diagram shows the clustering patterns of the Sham, CCI, and CCI-Swim groups of differentially expressed lncRNAs. The red part represents the upregulated lncRNAs and the blue part represents the downregulated lncRNAs.

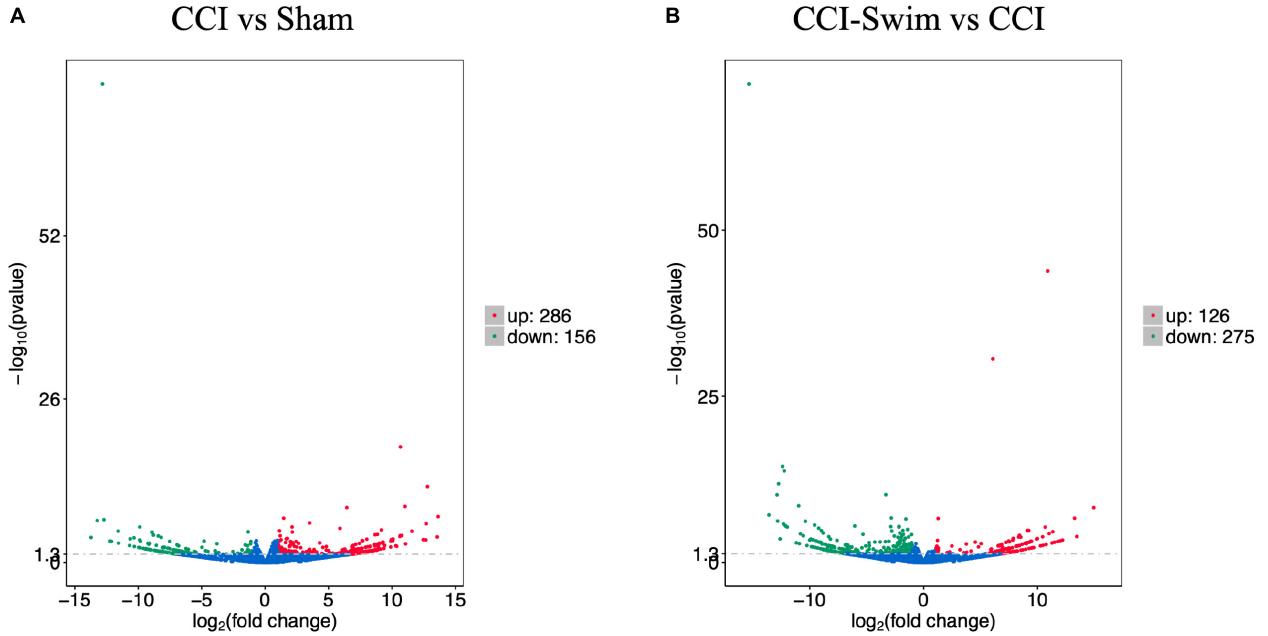

FIGURE 7 | Volcano plots of RNA-sequencing data exhibited the differentially expressed mRNAs in the spinal dorsal horn between rats in the comparisons of CCI group vs Sham group **(A)**, and CCI-Swim group vs CCI group **(B)**. The red part is significantly upregulated lncRNAs, the green part is significantly downregulated lncRNAs, and the blue part is not significantly expressed lncRNAs.

Differentially Expressed Gene Expression in the Spinal Dorsal Horn

The quality of the RNA-seq results was evaluated. Comparison of the Sham and CCI groups (**Figure 4A**) revealed a total of 734 DE lncRNAs, among which 385 lncRNAs were upregulated and 349 were downregulated. The top 20 DE lncRNAs in the Sham vs CCI group are shown in **Table 2**. There were 758 DE lncRNAs were noted in the CCI-Swim vs CCI group (**Figure 4B**) and the top 20 DE are listed in **Table 3**. The Venn diagram indicated 306 intersecting lncRNAs in the two comparisons (**Figure 5**). Hierarchical cluster analysis revealed the clustering patterns of the three groups of DE lncRNAs (**Figure 6**).

Figure 7 shows differences in mRNA expression among the three groups. Compared with the Sham group, 442 mRNAs were significantly changed in the CCI group, including 286 upregulated mRNAs and 156 downregulated mRNAs (**Figure 7A**). The top 20 DE mRNAs in the Sham and CCI groups are listed in **Table 4**. A total of 401 DE mRNAs were observed in the CCI-Swim and CCI groups (126 upregulated and 275 downregulated; **Figure 7B**). The top 20 DE mRNAs in the CCI vs CCI-Swim group are detailed in **Table 5**. The Venn diagram obtained showed 173 intersecting mRNAs, which are listed in **Figure 8**. Hierarchical clustering analysis of the three groups of DE mRNAs revealed their clustering patterns (**Figure 9**).

Gene Ontology Functional Analysis

Gene Ontology analysis was conducted on the target genes with significant changes in DE lncRNAs. Between the CCI and Sham groups, the target genes were enriched in biological process (BP) terms such as muscle structure development, positive regulation of BP, and muscle organ development ($P < 0.05$). The cellular component (CC) terms were significantly related to Z disc, I band, and sarcomere ($P < 0.05$). Molecular functions (MFs) were

TABLE 4 | The top 20 DE mRNAs in CCI group vs Sham group.

Gene name	Log_2FC	*P*-value	Regulation
AABR07015080.2	−12.81	<0.001	Down
LOC100910708	10.66	<0.001	Up
Trdn	12.79	<0.001	Up
LOC685716	11.02	<0.001	Up
1700066B19Rik	6.44	<0.001	Up
LOC100910990	13.64	<0.001	Up
C3	1.47	<0.001	Up
AABR07053749.1	−12.70	<0.001	Down
Senp1	−13.23	<0.001	Down
LOC100910270	3.51	<0.001	Up
LOC100910021	12.69	<0.001	Up
AABR07051731.1	−9.88	<0.001	Down
Clrn3	2.12	<0.001	Up
AABR07043288.1	5.90	<0.001	Up
LOC685699	9.17	<0.001	Up
Adgre1	1.13	<0.001	Up
AABR07017658.1	−11.57	<0.001	Down
Themis	11.57	<0.001	Up
Sgk1	−1.34	<0.001	Down
Vgf	2.15	<0.001	Up

DE, differentially expressed; FC, fold change.

TABLE 5 | The top 20 DE mRNAs in CCI-Swim group vs CCI group.

Gene name	Log_2FC	*P*-value	Regulation
LOC100910882	−15.35	< 0.001	down
AABR07015080.2	10.90	<0.001	Up
Fam111a	6.08	<0.001	Up
LOC108348298	−12.39	<0.001	Down
Tex11	−12.25	<0.001	Down
Trdn	−12.74	<0.001	Down
Myo3b	−3.32	<0.001	Down
Rgs13	−12.87	<0.001	Down
LOC685716	−10.97	<0.001	Down
LOC100910143	14.94	<0.001	Up
LOC100910990	−13.59	<0.001	Down
Ak7	−2.84	<0.001	Down
Senp1	13.26	<0.001	Up
AABR07015078.1	1.27	<0.001	Up
Pik3c2g	−1.56	<0.001	Down
LOC103690114	−12.83	<0.001	Down
AABR07052585.1	−10.39	<0.001	Down
Nhp2	−12.31	<0.001	Down
Noxred1	−9.58	<0.001	Down
AABR07042937.1	−12.16	<0.001	Down

DE, differentially expressed; FC, fold change.

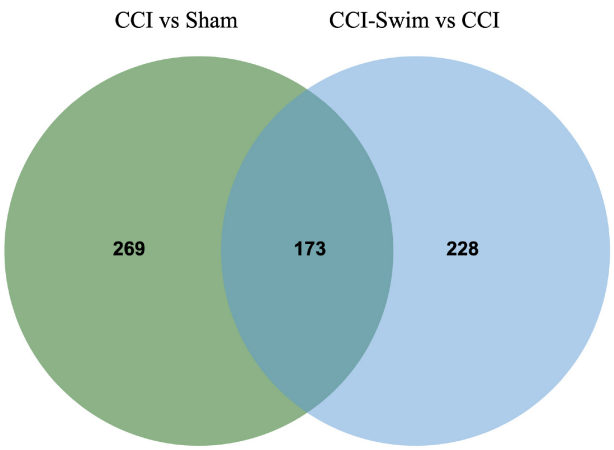

FIGURE 8 | Venn diagram of mRNAs. The figure shows the intersection of differential expressed mRNAs between the CCI vs Sham group and the CCI-Swim vs CCI group.

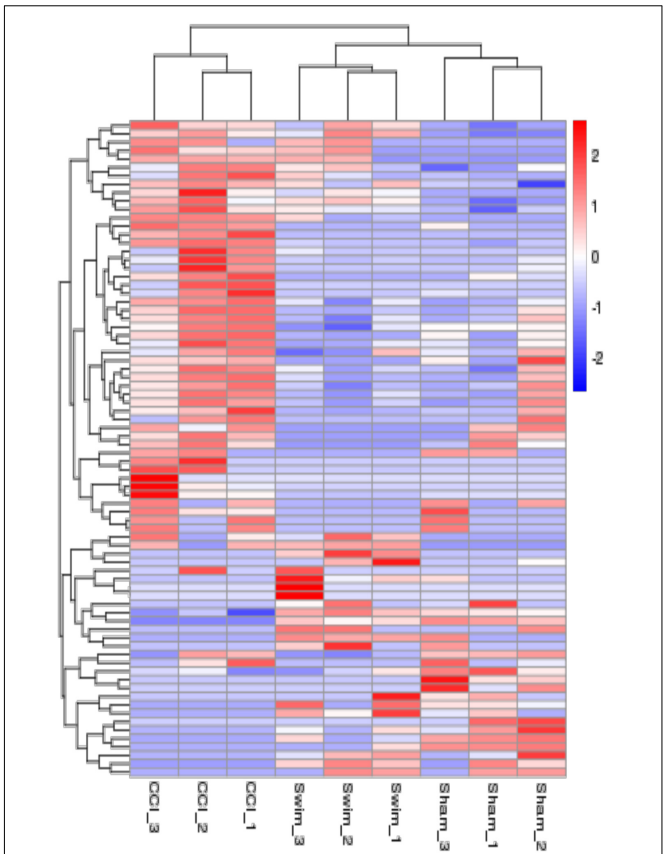

FIGURE 9 | The hierarchical cluster analysis diagram shows the clustering patterns of the Sham, CCI, and CCI-Swim groups of differentially expressed mRNAs. The red part represents the upregulated mRNAs and the blue part represents the downregulated mRNAs.

enriched in terms such as acid phosphatase activity, structural constituent of muscle, and protein binding ($P < 0.05$). The target genes of DE lncRNAs in the CCI-Swim and CCI groups were concentrated in BP terms such as muscle system process, positive regulation of immune system process, and positive regulation of immune response ($P < 0.05$). The most enriched CCs were Z disc, I band, and sarcomere ($P < 0.05$). MF terms were focused on acid phosphatase activity, structural constituent of muscle, and phosphatase activity ($P < 0.05$).

Gene Ontology analysis was also applied to the DE mRNAs of two groups, and the results are shown in **Figure 10** ($P < 0.05$). DE mRNAs in the CCI and Sham groups were enriched in BP terms such as positive T cell selection, negative T cell selection, and membrane fusion; DE mRNAs were also enriched in CC terms such as proteasome core complex, beta-subunit complex, proteasome core complex, and COP9 signalosome ($P < 0.05$). The most enriched MF terms were sarcosine oxidase activity, oxidoreductase activity, and threonine-type endopeptidase activity ($P < 0.05$). The DEGs of mRNAs in the CCI vs CCI-Swim group were focused on BPs terms such as nucleoside triphosphate biosynthetic process, sodium ion export from cell, and establishment or maintenance of transmembrane electrochemical gradient ($P < 0.05$). The CC terms were enriched in the sodium:potassium-exchanging ATPase complex. Finally, DE mRNAs were significantly enriched in MF terms such as cation-transporting ATPase activity, ATPase activity, coupled to transmembrane movement of ions, and sodium:potassium-exchanging ATPase activity ($P < 0.05$; **Figure 11**).

KEGG Pathway Enrichment Analysis

Figure 12 shows the KEGG pathways of the target genes of DE lncRNAs in the CCI vs Sham groups. The top five KEGG pathways were hypertrophic cardiomyopathy (HCM), dilated

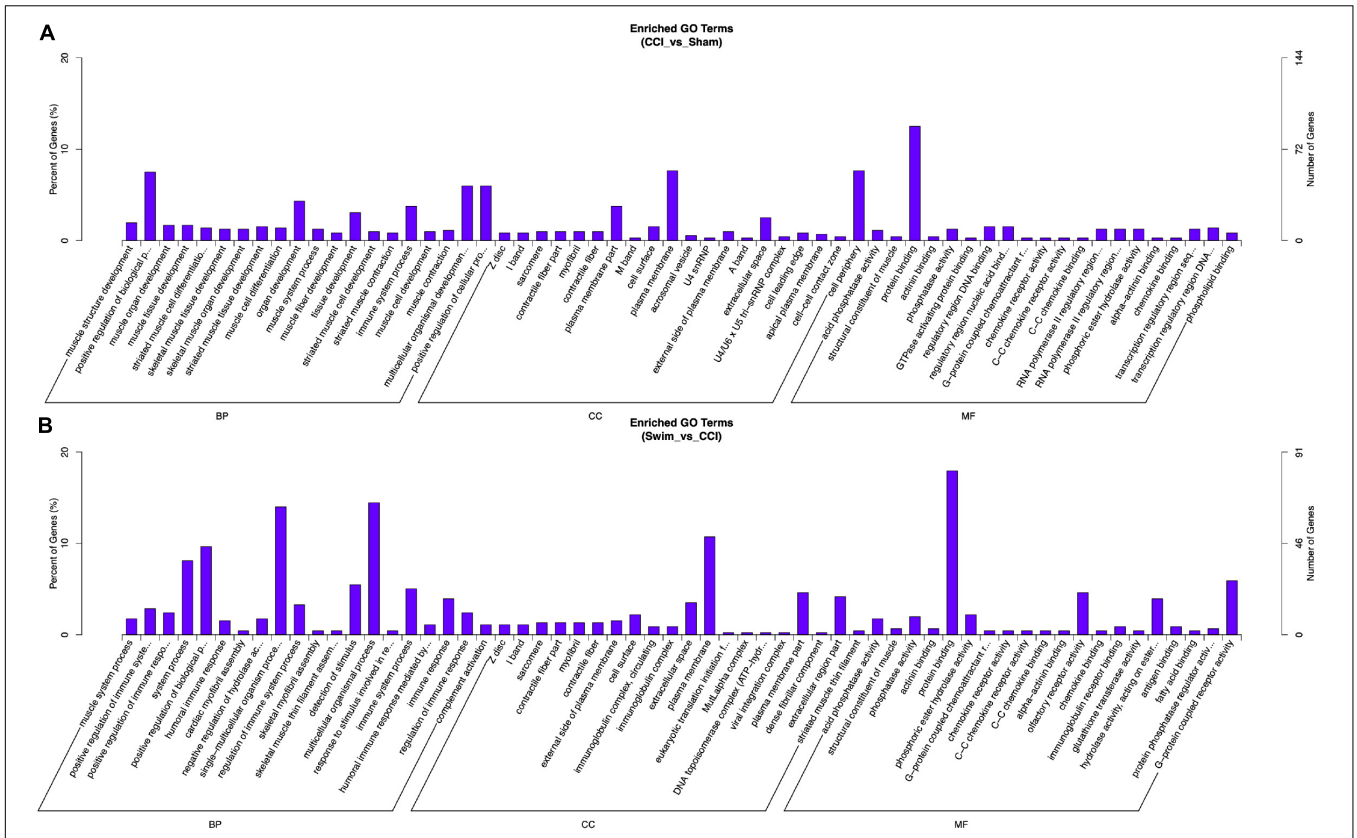

FIGURE 10 | Gene Ontology analysis on target genes of lncRNA. **(A)** CCI group vs Sham group, and **(B)** CCI-Swim group vs CCI group. *N* = 3 per group.

cardiomyopathy, ribosome, asthma, and PPAR signaling pathway ($P < 0.05$). In the CCI-Swim vs CCI groups, the top five enriched KEGG pathways were HCM, dilated cardiomyopathy, olfactory transduction, ribosome, and cytokine–cytokine receptor interaction ($P < 0.05$). For mRNAs, DEGs in the CCI and Sham groups focused on aldosterone-regulated sodium reabsorption and B cell receptor signaling pathway. DE mRNAs in the CCI-Swim and CCI groups were significantly enriched in the KEGG pathways of metabolic pathways, oxidative phosphorylation, Parkinson's disease, proximal tubule bicarbonate reclamation, glycosylphosphatidylinositol–anchor biosynthesis, and cAMP signaling pathway ($P < 0.05$; **Figure 13**).

Quantitative Real-Time PCR Analysis

We verified four lncRNAs (i.e., XLOC_274480, XLOC_105980, XLOC_137372, and AABR07047899.1) and four mRNAs (i.e., C3, Sgk1, Dnah7, and Vwa3a) to demonstrate the accuracy of the RNA-seq results. According to **Figures 14**, **15**, the expression changes of the eight DEGs were consistent with the RNA-seq result.

DISCUSSION

In this study, we found remarkable differences in the expression of lncRNAs and mRNAs in the spinal dorsal horn of rats in the Sham, CCI, and CCI-Swim groups. We also predicted the potential functions of these DEGs by GO and KEGG pathway analyses. The findings are helpful in further explorations of the potential therapeutic targets of NP.

Previous studies demonstrated that the potential mechanisms of NP include abnormal heterotopic activity of the injurious nerve, peripheral and central sensitization, impaired inhibitory regulation, and pathological activation of microglia (Meacham et al., 2017; Inoue and Tsuda, 2018; Tozaki-Saitoh and Tsuda, 2019; Finnerup et al., 2021). The current treatment methods for NP mainly include pharmacology, non-pharmacology and interventional therapy (Nijs et al., 2015; Macone and Otis, 2018). However, most existing treatments are limited in their effectiveness in controlling pain (Gilron et al., 2015; Xu et al., 2016; Szok et al., 2019). Therefore, exploring new alternative treatment methods for NP remains an urgent necessity.

Given the increasing popularity of exercise in the field of medicine, the treatment of NP by exercise has become a research hotspot (Safakhah et al., 2017; Guo et al., 2019; Ma et al., 2019; Palandi et al., 2020). Kuphal et al. (2007) demonstrated that in NP model mice, swimming for 7 days can significantly increase the pain threshold of thermal hyperalgesia, while swimming for 18–20 days can significantly improve the thermal hyperalgesia and cold allodynia in CCI rats. Farzad et al. (2018) reported that after 4 weeks of swimming training could significantly decrease allodynia and hyperalgesia in rats with NP. The authors thus

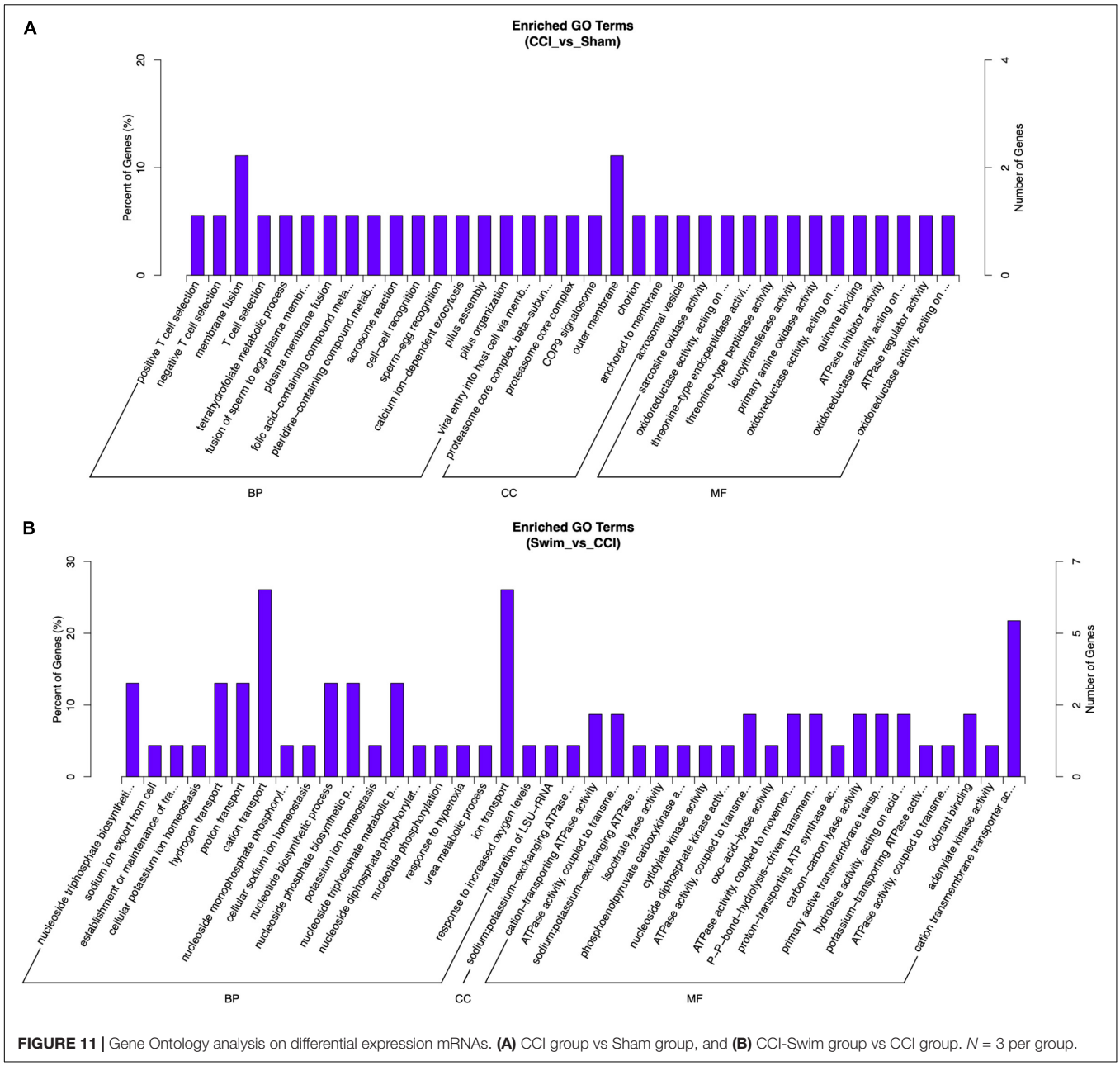

FIGURE 11 | Gene Ontology analysis on differential expression mRNAs. **(A)** CCI group vs Sham group, and **(B)** CCI-Swim group vs CCI group. *N* = 3 per group.

believed that the improvement of pain tests was associate with GAD65 (Farzad et al., 2018). Another study demonstrate the expressions of inflammatory cytokines IL-4, IL-1RA, and IL-5DE were upregulated in the spinal cord of mice with peripheral nerve injury. Two weeks of treadmill exercise could significantly suppress the expression of inflammatory factors and improve pain behaviors (Bobinski et al., 2018). The results of our own research presented that the mechanical pain threshold of CCI rats significantly increased on day 21 and day 28 after swimming training. These studies have confirmed that exercise has a positive effect on NP.

Previous research showed that lncRNAs participated in the processes of NP and regulate NP-related gene expression (Li et al., 2019; Wu et al., 2019). Zhou et al. (2017a) utilized the second-generation sequencing method to observe the expressions of lncRNA and mRNA in the spinal cord of SNI rats at different time points. The authors' results showed that lncRNAs and mRNAs in rats changed significantly at each measuring time point measured. The authors then explored the profiles of DEGs in the spinal cord of NP rats through GO and KEGG analyses (Zhou et al., 2017a). Another article employed microarray analysis to show the level of DEGs in the spinal cord of spinal nerve ligation (SNL) rats. A total of 511 DEGs of lncRNAs and 493 DEGs of mRNAs were observed on the 10th day after SNL surgery. Functional analysis indicated that the DEGs most enriched in SNL included immune response,

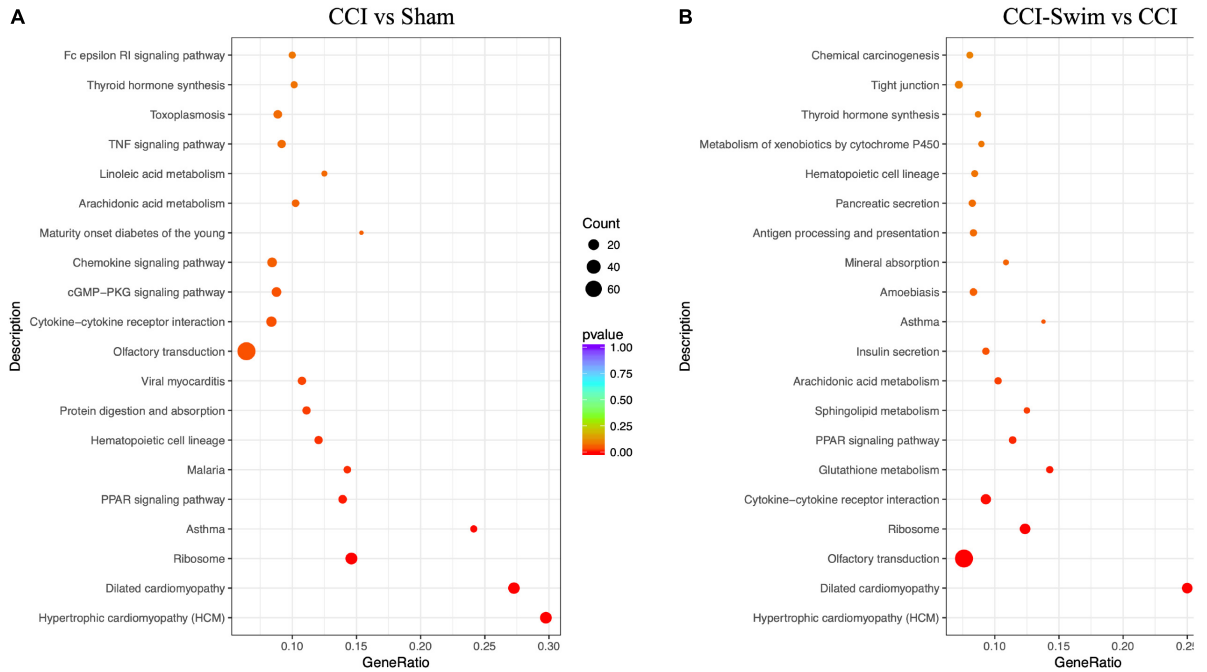

FIGURE 12 | KEGG pathways of the target genes of lncRNAs. **(A)** CCI group vs Sham group, and **(B)** CCI-Swim group vs CCI group. *N* = 3 per group.

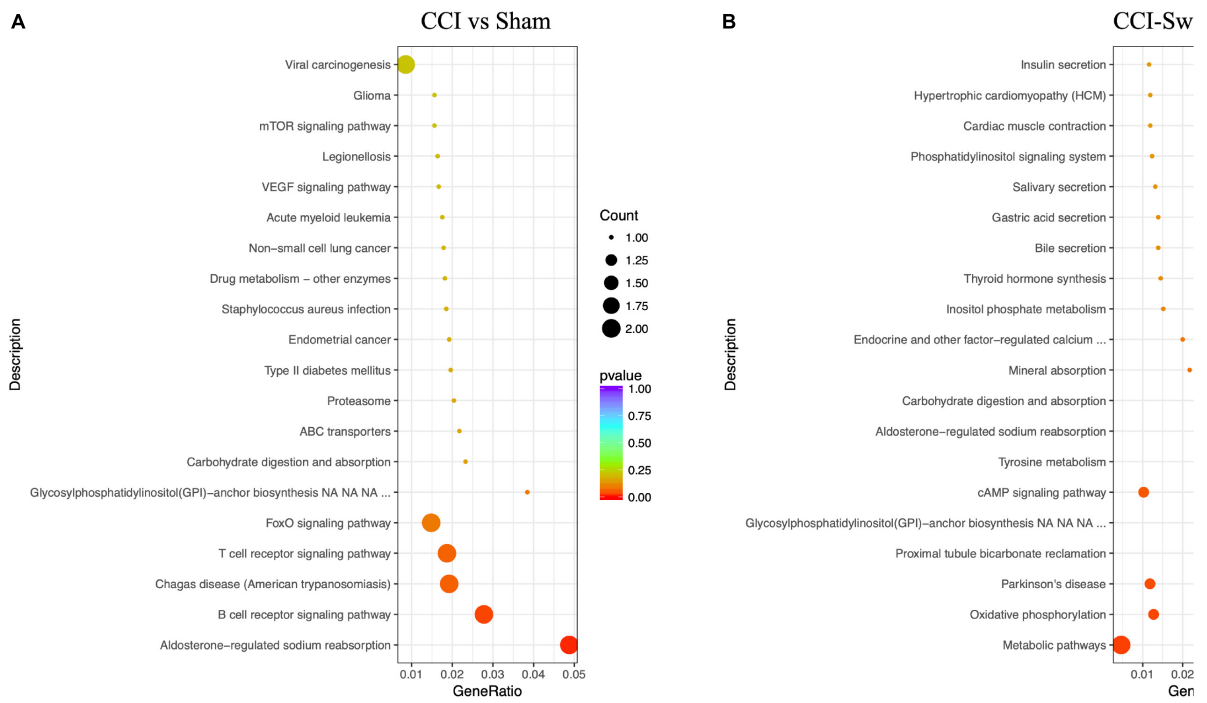

FIGURE 13 | KEGG pathways of the differential expression mRNAs. **(A)** CCI group vs Sham group, and **(B)** CCI-Swim group vs CCI group. *N* = 3 per group.

defense response, and inflammatory response, thus revealing the potential mechanisms in NP (Jiang et al., 2015).

Some existing studies have explored DEGs in NP through gene sequencing and gene functional analysis. However, there was few literatures analyzing the potential mechanisms of the improvement of NP through exercise. Hence, we explored DE lncRNAs and mRNAs by means of second-generation sequencing and conducted further functional analysis. Among the two

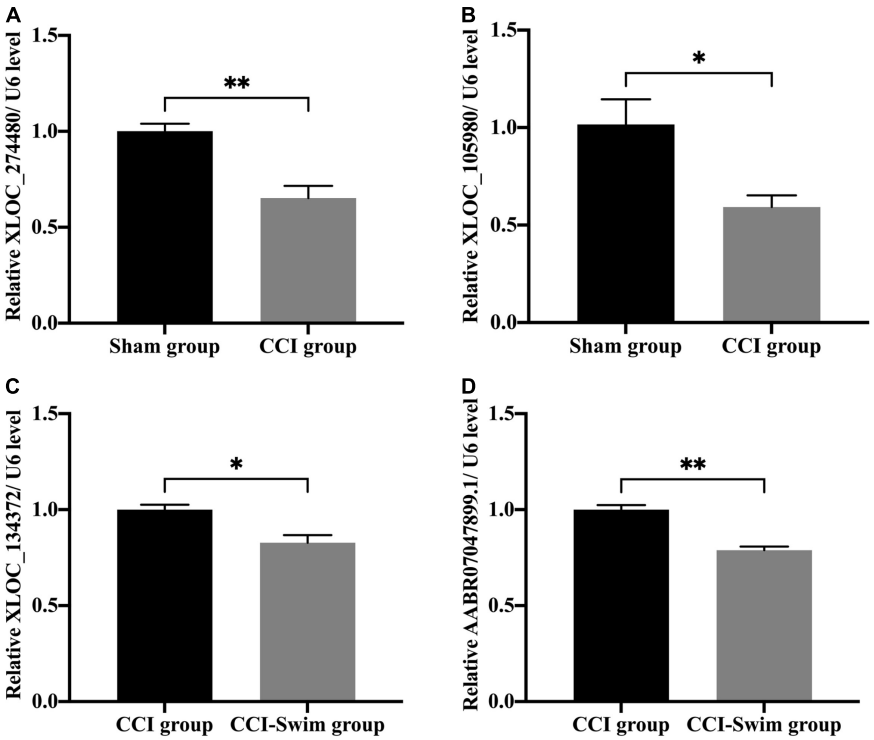

FIGURE 14 | Quantitative real-time PCR validation. The expression levels of lncRNAs **(A)** XLOC_274480, **(B)** XLOC_105980, **(C)** XLOC_134372, and **(D)** AABR07047899.1 in the spinal cord of CCI rats at 28 days post operation. Data was analyzed by independent-samples *t*-test. Values are denoted by mean ± SEM, $N = 3$ per group. $^{*}p < 0.05$, $^{**}p < 0.01$.

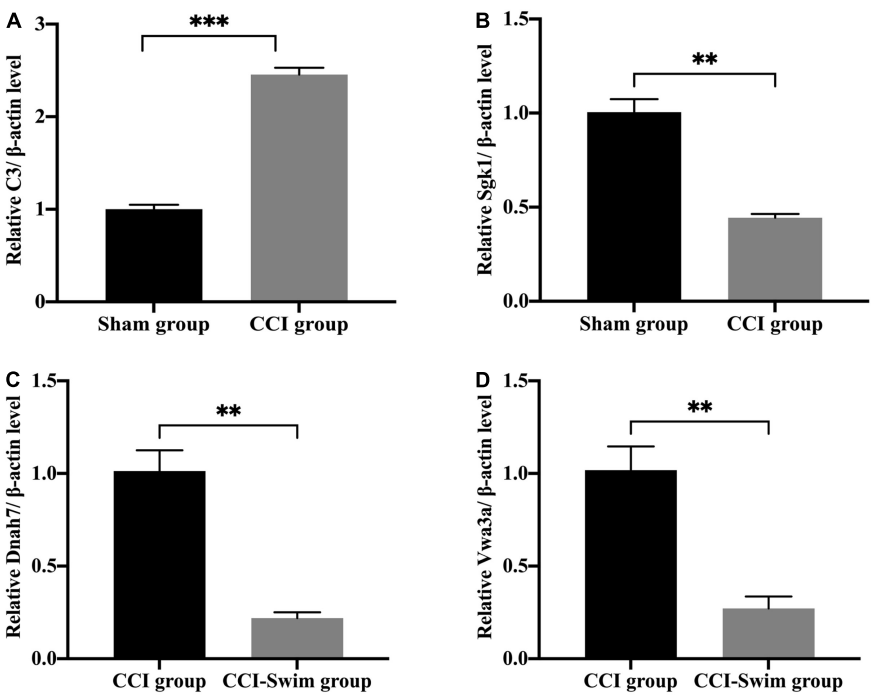

FIGURE 15 | Quantitative real-time PCR validation. The expression levels of mRNAs **(A)** C3, **(B)** Sgk1, **(C)** Dnah7, and **(D)** Vwa3a in the spinal cord of CCI rats at 28 days post operation. Data was analyzed by independent-samples *t*-test. Values are denoted by mean ± SEM, $N = 3$ per group. $^{**}p < 0.01$, $^{***}p < 0.001$.

comparison groups, we revealed 173 intersecting mRNAs. In these intersecting mRNAs, Dnah6 was significantly upregulated in the CCI vs Sham group but downregulated in the CCI-Swim vs CCI group. Similarly, Zhou et al. (2017a) demonstrated that the expression of Dnah6 is significantly increased in the NP model rats, which is consistent with our results. The mRNAs Pkd1l2, C3, Adgre1, and Plac9 have showed in previous RNA-seq literatures related with NP, and their significant alterations are consistent with our results (Zhou et al., 2017a,b; Du et al., 2018). Changes in the DE of these mRNAs were consistent with our sequencing results, which means they could be potential target genes for the development of NP. In addition, we found that some significantly altered mRNA such as C3, Sgk1, and VGF were associated with NP. Studies have revealed that C3 levels are positively correlated with the degree of neurological impairment in a variety of neurodegenerative diseases (Aeinehband et al., 2015). Sgk1 is genetically regulated by cellular stress and several hormones. It can activate a variety of ion channels and participate in BPs (Arteaga et al., 2008; Lang and Shumilina, 2013). VGF is selectively expressed in neuroendocrine cells and neurons, including central and peripheral nervous systems (Ferri et al., 2011). These mRNAs may be biomarkers for the treatment of NP, and future studies can focus on these mRNAs for further research.

The results of GO analysis of DE lncRNA target genes revealed the GO terms, such as extracellular space, plasma membrane, phosphatase activity, and protein binding, consistent with previous NP related studies (Zhou et al., 2017a,b; Du et al., 2018; Mao et al., 2018; Wang et al., 2019; Li et al., 2021). These GO terms were significantly expressed among the two group comparisons, thus suggesting that they may be the potential pathways of the effects of exercise on NP.

In the CCI vs Sham group and the CCI-Swim vs CCI group, the KEGG pathway enriched by lncRNA target genes showed significant changes in cytokine–cytokine receptor interaction, Asthma, Ribosome, and PPAR signaling pathway. The enrichment degree of these pathways in the CCI vs Sham group was significantly changed, which was in accordance with existing researches (Zhou et al., 2017a; Du et al., 2018; Wang et al., 2019; Li et al., 2021). In addition, these enrichment pathways changed significantly again after swimming in the CCI-Swim group, suggesting that they may be a potential pathway for exercise to improve NP.

In clinical work, medical workers may recommend appropriate exercise for NP patients to improve the symptoms of pain, which has guiding significance for the clinical treatment of NP. Although we investigated the underlying mechanism of exercise therapy for NP by sequencing, there are still some limitations in our study. For example, the results showed significant improvements in the pain behavior of rats in the CCI-Swim vs CCI groups on days 21 and 28 postoperatively. However, RNA-seq was only performed on the 28th day after CCI surgery; thus, future studies should also conduct RNA-seq on the 21st day to explore more NP-related DEGs. Moreover, whereas swimming is usually a voluntary exercise in humans, it is a forced exercise in rats. Therefore, future studies on the role of exercise in improving NP may include forms of exercises considered voluntary in animals, such as autonomous wheel exercise.

CONCLUSION

In this study, we demonstrated that swimming exercise can relieve NP. RNA-seq analysis was utilized to identify the DEGs of lncRNAs and mRNAs among Sham, CCI, and CCI-Swim groups. The DEGs obtained may be potential treatment targets for NP. We also conducted bioinformatics analysis of dysregulated lncRNAs and mRNAs and obtained information that could lead to a better understanding of the mechanism of exercise in improving NP.

DATA AVAILABILITY STATEMENT

The raw data have been uploaded to the Sequence Read Archive (SRA) database of NCBI under accession number PRJNA768994.

ETHICS STATEMENT

The animal study was reviewed and approved by the Ethics Committee of Scientific Research of Shanghai University of Sport.

AUTHOR CONTRIBUTIONS

X-QW, QX, and GS contributed to conception and design of the study. GS, J-BG, and Y-LZ organized the related experiments. ZY, XS, and Y-MC performed the statistical analysis. GS and X-QW wrote the first draft of the manuscript. QX, J-BG, W-MZ, Y-ZW, and Y-LZ wrote sections of the manuscript. All authors contributed to manuscript revision, read, and approved the submitted version.

FUNDING

This work was supported by the National Natural Science Foundation of China (81871844), Shuguang Program supported by Shanghai Education Development Foundation and Shanghai Municipal Education Commission (18SG48), the Shanghai Key Lab of Human Performance (Shanghai University of Sport) (11DZ2261100), and Shanghai Clinical Research Center for Rehabilitation Medicine (21MC1930200).

SUPPLEMENTARY MATERIAL

The Supplementary Material for this article can be found online at: https://www.frontiersin.org/articles/10.3389/fnmol.2022.865310/full#supplementary-material

REFERENCES

Aeinehband, S., Lindblom, R. P. F., Nimer, F. A., Vijayaraghavan, S., Sandholm, K., Khademi, M., et al. (2015). Complement component C3 and butyrylcholinesterase activity are associated with neurodegeneration and clinical disability in multiple sclerosis. *PLoS One* 10:e0122048. doi: 10.1371/journal.pone.0122048

Almeida, C., DeMaman, A., Kusuda, R., Cadetti, F., Ravanelli, M. I., Queiroz, A. L., et al. (2015). Exercise therapy normalizes BDNF upregulation and glial hyperactivity in a mouse model of neuropathic pain. *Pain* 156, 504–513. doi: 10.1097/01.j.pain.0000460339.23976.12

Arteaga, M. F., Coric, T., Straub, C., and Canessa, C. M. (2008). A brain-specific SGK1 splice isoform regulates expression of ASIC1 in neurons. *Proc. Natl. Acad. Sci. U.S.A.* 105, 4459–4464. doi: 10.1073/pnas.0800958105

Attal, N., and Bouhassira, D. (2015). Pharmacotherapy of neuropathic pain: which drugs, which treatment algorithms? *Pain* 156(Suppl. 1), S104–S114. doi: 10.1097/01.j.pain.0000460358.01998.15

Bobinski, F., Teixeira, J. M., Sluka, K. A., and Santos, A. R. S. (2018). Interleukin-4 mediates the analgesia produced by low-intensity exercise in mice with neuropathic pain. *Pain* 159, 437–450. doi: 10.1097/j.pain.0000000000001109

Bouhassira, D. (2019). Neuropathic pain: definition, assessment and epidemiology. *Rev. Neurol.* 175, 16–25. doi: 10.1016/j.neurol.2018.09.016

Cavalli, E., Mammana, S., Nicoletti, F., Bramanti, P., and Mazzon, E. (2019). The neuropathic pain: an overview of the current treatment and future therapeutic approaches. *Int. J. Immunopathol. Pharmacol.* 33:2058738419838383. doi: 10.1177/2058738419838383

Cohen, S. P., and Mao, J. (2014). Neuropathic pain: mechanisms and their clinical implications. *BMJ* 348:f7656. doi: 10.1136/bmj.f7656

Colloca, L., Ludman, T., Bouhassira, D., Baron, R., Dickenson, A. H., Yarnitsky, D., et al. (2017). Neuropathic pain. *Nat. Rev. Dis. Primers* 3:17002. doi: 10.1038/nrdp.2017.2

Cooper, M. A., Kluding, P. M., and Wright, D. E. (2016). Emerging relationships between exercise, sensory nerves, and neuropathic pain. *Front. Neurosci.* 10:372. doi: 10.3389/fnins.2016.00372

Dobson, J. L., McMillan, J., and Li, L. (2014). Benefits of exercise intervention in reducing neuropathic pain. *Front. Cell Neurosci.* 8:102. doi: 10.3389/fncel.2014.00102

Du, H., Shi, J., Wang, M., An, S., Guo, X., and Wang, Z. (2018). Analyses of gene expression profiles in the rat dorsal horn of the spinal cord using RNA sequencing in chronic constriction injury rats. *J. Neuroinflamm.* 15:280. doi: 10.1186/s12974-018-1316-0

Farzad, B., Rajabi, H., Gharakhanlou, R., Allison, D. J., Hayat, P., and Jameie, S. B. (2018). Swimming training attenuates allodynia and hyperalgesia induced by peripheral nerve injury in an adult male rat neuropathic model: effects on irisin and GAD65. *Pain Med.* 19, 2236–2245. doi: 10.1093/pm/pnx294

Ferri, G. L., Noli, B., Brancia, C., D'Amato, F., and Cocco, C. (2011). VGF: an inducible gene product, precursor of a diverse array of neuro-endocrine peptides and tissue-specific disease biomarkers. *J. Chem. Neuroanat.* 42, 249–261. doi: 10.1016/j.jchemneu.2011.05.007

Finnerup, N. B., Kuner, R., and Jensen, T. S. (2021). Neuropathic pain: from mechanisms to treatment. *Physiol. Rev.* 101, 259–301. doi: 10.1152/physrev.00045.2019

Gierthmühlen, J., and Baron, R. (2016). Neuropathic pain. *Semin. Neurol.* 36, 462–468. doi: 10.1055/s-0036-1584950

Gilron, I., Baron, R., and Jensen, T. (2015). Neuropathic pain: principles of diagnosis and treatment. *Mayo Clin. Proc.* 90, 532–545. doi: 10.1016/j.mayocp.2015.01.018

Guo, D., and Hu, J. (2014). Spinal presynaptic inhibition in pain control. *Neuroscience* 283, 95–106. doi: 10.1016/j.neuroscience.2014.09.032

Guo, J. B., Chen, B. L., Wang, Y., Zhu, Y., Song, G., Yang, Z., et al. (2019). Meta-analysis of the effect of exercise on neuropathic pain induced by peripheral nerve injury in rat models. *Front. Neurol.* 10:636. doi: 10.3389/fneur.2019.00636

Inoue, K., and Tsuda, M. (2018). Microglia in neuropathic pain: cellular and molecular mechanisms and therapeutic potential. *Nat. Rev. Neurosci.* 19, 138–152. doi: 10.1038/nrn.2018.2

Jaggi, A. S., Jain, V., and Singh, N. (2011). Animal models of neuropathic pain. *Fundam. Clin. Pharmacol.* 25, 1–28. doi: 10.1111/j.1472-8206.2009.00801.x

Jensen, T. S., and Finnerup, N. B. (2014). Allodynia and hyperalgesia in neuropathic pain: clinical manifestations and mechanisms. *Lancet Neurol.* 13, 924–935. doi: 10.1016/s1474-4422(14)70102-4

Jiang, B. C., Sun, W. X., He, L. N., Cao, D. L., Zhang, Z. J., and Gao, Y. J. (2015). Identification of lncRNA expression profile in the spinal cord of mice following spinal nerve ligation-induced neuropathic pain. *Mol. Pain* 11:43. doi: 10.1186/s12990-015-0047-9

Kami, K., Tajima, F., and Senba, E. (2017). Exercise-induced hypoalgesia: potential mechanisms in animal models of neuropathic pain. *Anat. Sci. Int.* 92, 79–90. doi: 10.1007/s12565-016-0360-z

Kuphal, K. E., Fibuch, E. E., and Taylor, B. K. (2007). Extended swimming exercise reduces inflammatory and peripheral neuropathic pain in rodents. *J. Pain* 8, 989–997. doi: 10.1016/j.jpain.2007.08.001

Lang, F., and Shumilina, E. (2013). Regulation of ion channels by the serum- and glucocorticoid-inducible kinase SGK1. *FASEB J.* 27, 3–12. doi: 10.1096/fj.12-218230

Li, Y., Yin, C., Liu, B., Nie, H., Wang, J., Zeng, D., et al. (2021). Transcriptome profiling of long noncoding RNAs and mRNAs in spinal cord of a rat model of paclitaxel-induced peripheral neuropathy identifies potential mechanisms mediating neuroinflammation and pain. *J. Neuroinflamm.* 18:48. doi: 10.1186/s12974-021-02098-y

Li, Z., Li, X., Chen, X., Li, S., Ho, I. H. T., Liu, X., et al. (2019). Emerging roles of long non-coding RNAs in neuropathic pain. *Cell Prolif.* 52:e12528. doi: 10.1111/cpr.12528

Ma, X. Q., Qin, J., Li, H. Y., Yan, X. L., Zhao, Y., and Zhang, L. J. (2019). Role of exercise activity in alleviating neuropathic pain in diabetes *via* inhibition of the pro-inflammatory signal pathway. *Biol. Res. Nurs.* 21, 14–21. doi: 10.1177/1099800418803175

Macone, A., and Otis, J. A. D. (2018). Neuropathic pain. *Semin. Neurol.* 38, 644–653. doi: 10.1055/s-0038-1673679

Mao, P., Li, C. R., Zhang, S. Z., Zhang, Y., Liu, B. T., and Fan, B. F. (2018). Transcriptomic differential lncRNA expression is involved in neuropathic pain in rat dorsal root ganglion after spared sciatic nerve injury. *Braz. J. Med. Biol. Res.* 51:e7113. doi: 10.1590/1414-431x20187113

Meacham, K., Shepherd, A., Mohapatra, D. P., and Haroutounian, S. (2017). Neuropathic pain: central vs. peripheral mechanisms. *Curr. Pain Headache Rep.* 21:28. doi: 10.1007/s11916-017-0629-5

Nijs, J., Apeldoorn, A., Hallegraeff, H., Clark, J., Smeets, R., Malfliet, A., et al. (2015). Low back pain: guidelines for the clinical classification of predominant neuropathic, nociceptive, or central sensitization pain. *Pain Phys.* 18, E333–E346.

Palandi, J., Bobinski, F., de Oliveira, G. M., and Ilha, J. (2020). Neuropathic pain after spinal cord injury and physical exercise in animal models: a systematic review and meta-analysis. *Neurosci. Biobehav. Rev.* 108, 781–795. doi: 10.1016/j.neubiorev.2019.12.016

Peng, M. S., Wang, R., Wang, Y. Z., Chen, C. C., Wang, J., Liu, X. C., et al. (2022). Efficacy of therapeutic aquatic exercise vs physical therapy modalities for patients with chronic low back pain: a randomized clinical trial. *JAMA Netw. Open* 5:e2142069. doi: 10.1001/jamanetworkopen.2021.42069

Safakhah, H. A., Moradi Kor, N., Bazargani, A., Bandegi, A. R., Gholami Pourbadie, H., Khoshkholgh-Sima, B., et al. (2017). Forced exercise attenuates neuropathic pain in chronic constriction injury of male rat: an investigation of oxidative stress and inflammation. *J. Pain Res.* 10, 1457–1466. doi: 10.2147/jpr.S135081

St John Smith, E. (2018). Advances in understanding nociception and neuropathic pain. *J. Neurol.* 265, 231–238. doi: 10.1007/s00415-017-8641-6

Szok, D., Tajti, J., Nyári, A., and Vécsei, L. (2019). Therapeutic approaches for peripheral and central neuropathic pain. *Behav. Neurol.* 2019:8685954. doi: 10.1155/2019/8685954

Tozaki-Saitoh, H., and Tsuda, M. (2019). Microglia-neuron interactions in the models of neuropathic pain. *Biochem. Pharmacol.* 169:113614. doi: 10.1016/j.bcp.2019.08.016

Tsuda, M. (2016). Microglia in the spinal cord and neuropathic pain. *J. Diabetes Investig.* 7, 17–26. doi: 10.1111/jdi.12379

van Hecke, O., Austin, S. K., Khan, R. A., Smith, B. H., and Torrance, N. (2014). Neuropathic pain in the general population: a systematic review of epidemiological studies. *Pain* 155, 654–662. doi: 10.1016/j.pain.2013.11.013

Wang, Q., Ai, H., Liu, J., Xu, M., Zhou, Z., Qian, C., et al. (2019). Characterization of novel lnc RNAs in the spinal cord of rats with lumbar disc herniation. *J. Pain Res.* 12, 501–512. doi: 10.2147/jpr.S164604

Wu, B., Zhou, L. L., Chen, C. C., Wang, J., and Wang, X. Q. (2022). Effects of exercise-induced hypoalgesia and its neural mechanisms. *Med. Sci. Sports Exerc.* 54, 220–231. doi: 10.1249/MSS.0000000000002781

Wu, S., Bono, J., and Tao, Y. X. (2019). Long noncoding RNA (lncRNA): a target in neuropathic pain. *Expert Opin. Ther. Targets* 23, 15–20. doi: 10.1080/14728222.2019.1550075

Xu, L., Zhang, Y., and Huang, Y. (2016). Advances in the treatment of neuropathic pain. *Adv. Exp. Med. Biol.* 904, 117–129. doi: 10.1007/978-94-017-7537-3_9

Zhao, L. N., Yang, Y. Q., Wang, W. W., Li, Q., and Xiao, H. (2020). The effects of traditional Chinese medicine combined with chemotherapy on immune function and quality of life in patients with non-small cell lung cancer: a protocol for systematic review and meta-analysis. *Medicine* 99:e22859. doi: 10.1097/md.0000000000022859

Zheng, K. Y., Chen, C. C., Yang, S. Y., and Wang, X. Q. (2021). Aerobic exercise attenuates pain sensitivity: an event-related potential study. *Front. Neurosci.* 15:735470. doi: 10.3389/fnins.2021.735470

Zhou, J., Fan, Y., and Chen, H. (2017a). Analyses of long non-coding RNA and mRNA profiles in the spinal cord of rats using RNA sequencing during the progression of neuropathic pain in an SNI model. *RNA Biol.* 14, 1810–1826. doi: 10.1080/15476286.2017.1371400

Zhou, J., Xiong, Q., Chen, H., Yang, C., and Fan, Y. (2017b). Identification of the spinal expression profile of non-coding RNAS involved in neuropathic pain following spared nerve injury by sequence analysis. *Front. Mol. Neurosci.* 10:91. doi: 10.3389/fnmol.2017.00091

Zhou, J., Ren, Y., Tan, L., Song, X., Wang, M., Li, Y., et al. (2020). Norcantharidin: research advances in pharmaceutical activities and derivatives in recent years. *Biomed. Pharmacother.* 131:110755. doi: 10.1016/j.biopha.2020.110755

Conflict of Interest: The authors declare that the research was conducted in the absence of any commercial or financial relationships that could be construed as a potential conflict of interest.

frontiers | Frontiers in Molecular Neuroscience

ORIGINAL RESEARCH
published: 12 April 2022
doi: 10.3389/fnmol.2022.887426

Prolonged Continuous Theta Burst Stimulation Can Regulate Sensitivity on Aβ Fibers: An Functional Near-Infrared Spectroscopy Study

*Chong Li†, Nannan Zhang†, Qiong Han, Lifang Zhang, Shuo Xu, Shuting Tu, Yong Xie and Zhiyong Wang**

Department of Rehabilitation Medicine, First Affiliated Hospital of Fujian Medical University, Fujian, China

OPEN ACCESS

Edited by:
Jie Jia,
Huashan Hospital Affiliated to Fudan University, China

Reviewed by:
Shiliu Tian,
Shanghai University of Sport, China
Xiangyun Liu,
Shanghai Frontiers Sciences Research Base of Exercise and Metabolic Health, China
Qi Zhang,
Huashan Hospital, Fudan University, China

***Correspondence:**
Zhiyong Wang
fjykdxwzy@163.com

†These authors have contributed equally to this work and share the first authorship

Specialty section:
This article was submitted to Pain Mechanisms and Modulators, a section of the journal Frontiers in Molecular Neuroscience

Received: *01 March 2022*
Accepted: *16 March 2022*
Published: *12 April 2022*

Citation:
Li C, Zhang N, Han Q, Zhang L, Xu S, Tu S, Xie Y and Wang Z (2022) Prolonged Continuous Theta Burst Stimulation Can Regulate Sensitivity on Aβ Fibers: An Functional Near-Infrared Spectroscopy Study. Front. Mol. Neurosci. 15:887426. doi: 10.3389/fnmol.2022.887426

Objective: High-frequency repetitive transcranial magnetic stimulation (rTMS) induces analgesic effects in both experimental pain and clinical pain conditions. However, whether rTMS can modulate sensory and pain thresholds on sensory fibers is still unclear. Here, we compared the effects of three rTMS paradigms on sensory and pain thresholds conducted by different sensory fibers (Aβ, Aδ, and C fibers) with sham stimulation and investigate the potential brain activation using functional near-infrared spectroscopy (fNIRS).

Methods: Forty right-handed healthy subjects were randomly allocated into one of four groups. Each subject received one session rTMS [prolonged continuous theta-burst stimulation (pcTBS), intermittent theta-burst stimulation (iTBS), 10 Hz rTMS or sham]. Current perception threshold (CPT), pain tolerance threshold (PTT), and fNIRS were measured at baseline, immediately after stimulation, and 1 h after stimulation, respectively.

Results: Significant differences between treatments were observed for changes for CPT 2,000 Hz between baseline and 1 h after rTMS ($F = 6.551$, $P < 0.001$): pcTBS versus sham ($P = 0.004$) and pcTBS versus 10 Hz rTMS ($P = 0.007$). There were significant difference in average HbO μm in the right frontopolar cortex (FPC) [channel 23: $P = 0.030$ (pcTBS versus sham: $P = 0.036$)], left dorsolateral prefrontal cortex (DLPFC) [channel 7: $P = 0.006$ (pcTBS versus sham: $P = 0.004$)], left FPC [channel 17: $P = 0.014$ (pcTBS versus sham: $P = 0.046$), channel 22: $P = 0.004$ (pcTBS versus sham: $P = 0.004$)] comparing four group in 1 h after stimulation in PTT 2000 Hz (Aβ-fiber).

Conclusion: Prolonged continuous theta-burst stimulation can regulate sensitivity on Aβ fibers. In addition, single-session pcTBS placed on left M1 can increase the excitability of DLPFC and FPC, indicating the interaction between M1 and prefrontal cortex may be a potential mechanism of analgesic effect of rTMS. Studies in patients with central post-stroke pain are required to confirm the potential clinical applications of pcTBS.

Keywords: repetitive transcranial magnetic stimulation, theta-burst stimulation, pain, sensory fiber, functional near-infrared spectroscopy

INTRODUCTION

For the revised International Association for the Study of Pain definition, pain is termed as an unpleasant sensory and emotional experience associated with, or resembling that associated with, actual or potential tissue damage (Raja et al., 2020). Pain is mainly transmitted by sensory nerve fibers. According to morphological, electrophysiological, and functional characteristics, sensory nerve fibers can be divided into three main subgroups: large myelinated sensory nerve fibers (Aβ fibers), small myelinated sensory nerve fibers (Aδ fibers), and unmyelinated sensory nerve fibers (C fibers) (Lynn and Carpenter, 1982). In the peripheral nerves, vibration sensation, tactile sensation, and light pressure sensation are mainly conducted by Aβ fibers. Temperature sensation, rapid pain sensation, and pressure sensation are mainly conducted by Aδ fibers. Warmth, slow pain, and various forms of nociceptive sensation are mainly conducted by C fibers (Schmelz, 2011; Paricio-Montesinos et al., 2020; Gomatos and Rehman, 2022). Pain is a subjective emotional experience that may be due to many different diseases or conditions, and there are few effective treatments. At present, the application of analgesic drugs is the main way to relieve pain (Finnerup et al., 2015, 2021). However, long-term use of analgesic drugs is not only prone to addiction, but also has many side effects (Koob, 2021).

Transcranial magnetic stimulation (TMS) is a biological stimulation technology that uses the time-varying magnetic field to act on the cerebral cortex to generate induced current and change the action potential of cortical nerve cells, thus affecting brain metabolism and nerve electrical activity (Cárdenas-Morales et al., 2010; Lefaucheur, 2019). Repeated transcranial magnetic stimulation (rTMS) refers to the process of giving repeated stimulation to a specific cortical area. As a painless, safe, and non-invasive brain stimulation technology, rTMS is gradually applied to pain therapy caused by various conditions (Lefaucheur et al., 2014, 2020; Klein et al., 2015). It has been shown that high frequency (>5 Hz) rTMS applied over the primary motor cortex (M1) can induce analgesic effects against both experimental pain (Summers et al., 2004; Nahmias et al., 2009; Houzé et al., 2013) and chronic pain (André-Obadia et al., 2008; Young et al., 2014; Attia et al., 2021). Studies indicated that the analgesic effect of 10 Hz rTMS is better than that of other frequencies (André-Obadia et al., 2008; Young et al., 2014; Attia et al., 2021). In addition, studies have shown that rTMS may relieve pain by regulating neural plasticity, influencing cerebral blood flow changes, and mediating pain circuits (Hoogendam et al., 2010; Dall'Agnol et al., 2014; Park et al., 2017).

In addition to the classic rTMS, new rTMS parameters have been described. Theta burst stimulation (TBS) consists of bursts of three pulses at 50 Hz, repeated five times per second. Intermittent TBS (iTBS) with 600 pulses and prolonged continuous TBS (pcTBS) with 1,200 pulses induce facilitation of cortical excitability (Huang et al., 2005; Gamboa et al., 2010; Moisset et al., 2015). Such stimulation sessions are much shorter than classical high-frequency rTMS sessions, which can optimize medical resources. Existing studies mainly focused on the effects of different parameters of rTMS on different experimental pain (such as cold pain, hot pain, tenderness, etc.) and clinically related pain, such as post-stroke pain. However, the analgesic effect of rTMS with different parameters on sensory fibers remains unclear.

Therefore, we hypothesized that pcTBS and/or iTBS would yield analgesic effects and modulate sensitivity on sensory fibers similar to or, stronger than classical 10 Hz rTMS. We carried out a double-blind, randomized controlled study in healthy volunteers to prove our hypothesis. The purpose of this study is twofold: first, to compare the effects of the three rTMS paradigms on pain thresholds conducted by different sensory fibers; and second, to investigate the potential mechanisms of action of these stimulation paradigms using functional near-infrared spectroscopy (fNIRS).

MATERIALS AND METHODS

Study Design

This was a double-blind, four-group randomized controlled trial comparing three types of rTMS with sham stimulation on sensory and pain threshold in healthy volunteers. The protocol involved four experimental sessions, in which we compared the effects of pcTBS, iTBS, 10 Hz rTMS, and sham stimulation on sensory and pain thresholds. In each session, the stimulation administered targeted the left primary motor cortex. This study was conducted at the first affiliated hospital of Fujian Medical University (Fujian, China) from November 2021 to January 2022 and was approved by the Institutional Review Board of Huashan Hospital, Fudan University (KY2021-815).

Participants

Forty healthy volunteers were recruited in this study. The inclusion criteria were: (1) right-handed non-smokers; (2) aged between 20 and 40; and (3) free of pain during the past 6 months. The exclusion criteria included: (1) a history of chronic pain or recent acute pain; (2) on medication at the time of testing or during the previous; (3) serious medical conditions; (4) pregnancy or breastfeeding; (5) sensory impairment. All of the participants gave written informed consent after inclusion.

Experimental Procedures

A blinded evaluator performed assessments for all participants. All participants were assessed sensory and pain thresholds after inclusion. An independent researcher not involved in the study created a blocked randomization sequence using a computerized program (Microsoft Excel). Block randomization ensured equal numbers of participants for group allocation. Allocation assignments were placed in sequentially numbered, opaque, and sealed envelopes by an offsite officer not involved in the study. Participants were blind regarding the intervention received. Once the participant completed the baseline assessment, an independent person would open an envelope and reveal the group allocation.

After giving informed consent, participants were allocated to one of four groups receiving one session of rTMS stimulation. The evaluator would assess sensory and pain thresholds for

all participants immediately after stimulation and 1 h after stimulation (**Figure 1**).

Transcranial Magnetic Stimulation

A magnetic therapy device (Model CCY-II; Wuhan Yiruide Medical Equipment Co., Ltd., Wuhan, China, YZB-20142211249) was used. rTMS was applied over the left M1 using a figure-of-eight-shaped coil (70 mm diameter) positioned tangentially to the scalp and horizontally in the posterior-anterior direction, which proved to be effective in pain relief (Andre-Obadia et al., 2018).

Resting motor threshold (RMT) was determined experimentally as the lowest stimulation intensity that produced motor evoked potentials (MEP) $\geq$ 50 μV in 50% of trials (Rossini et al., 1994). In addition, we also recorded the cortical latency of the subjects.

Repetitive transcranial magnetic stimulation was applied at 80% of the RMT, as in previous studies in which that was sufficient to induce pain analgesia in healthy volunteers (Nahmias et al., 2009; de Andrade et al., 2011). Three active and one sham stimulation were applied randomly, with only one type of stimulation applied for each participant. pcTBS consisted of three pulses at 50 Hz repeated 400 times at intervals of 200 ms (1,200 pulses, 1 min and 40 s). iTBS consisted of three pulses at 50 Hz repeated 10 times at intervals of 200 ms (600 pulses, 3 min and 20 s). The 10 Hz rTMS pattern consisted of 15 trains of 10 s with an interval of 50 s (1,500 pulses, 15 min).

Outcome Measures

Sensory and Pain Thresholds Assessments

Painless current perception threshold (CPT) and pain tolerance threshold (PTT) were evaluated using Neurometer® device (the UAS). The Neurometer® generates a constant current stimulus which evokes responses that quantify the functional integrity of each of the three major sub-populations of sensory nerve fibers. Specifically, Aβ, Aδ, and C fiber groups are selectively stimulated by sinusoid waveform currents of 2,000, 250, and 5 Hz respectively. Using small surface electrodes, this test generated discrete double-blinded CPT measures ($P < 0.006$). After the start of the test, the subjects were placed in a comfortable position and a pair of electrodes were fixed to the tip of the index finger of the subject's right hand with adhesive tape (**Figure 2**).

For the CPT test, the Neurometer® device emits stimuli of three different frequencies. Subjects need to distinguish between "true" and "false" stimuli randomly generated by the detector. After a sufficient number of consistent tests are conducted for each stimulus frequency, the detector determines the current sensing threshold of the frequency test.

When the intensity of Neurometer® stimulation exceeds the painless CPT value, it will induce pain. Under the self-control of the subjects, the maximum intensity that can tolerate nerve selective electrical stimulation is defined as the pain tolerance threshold. The PTT was tested combined with the functional near-infrared test.

Functional Near-Infrared Spectroscopy Neuroimaging and Probe Localization

We used an fNIRS system (BS-3000, Wuhan Znion Technology Co., Ltd., Wuhan, China) with wavelengths of 695 and 830 nm. The fNIRS cap setup included 12 emitters of near-infrared light and 12 detectors spaced 3 cm apart, yielding 37 data channels deployed at the prefrontal area according to the EEG-10-20 system (**Figures 3A,B**). The system used a chin strap to secure

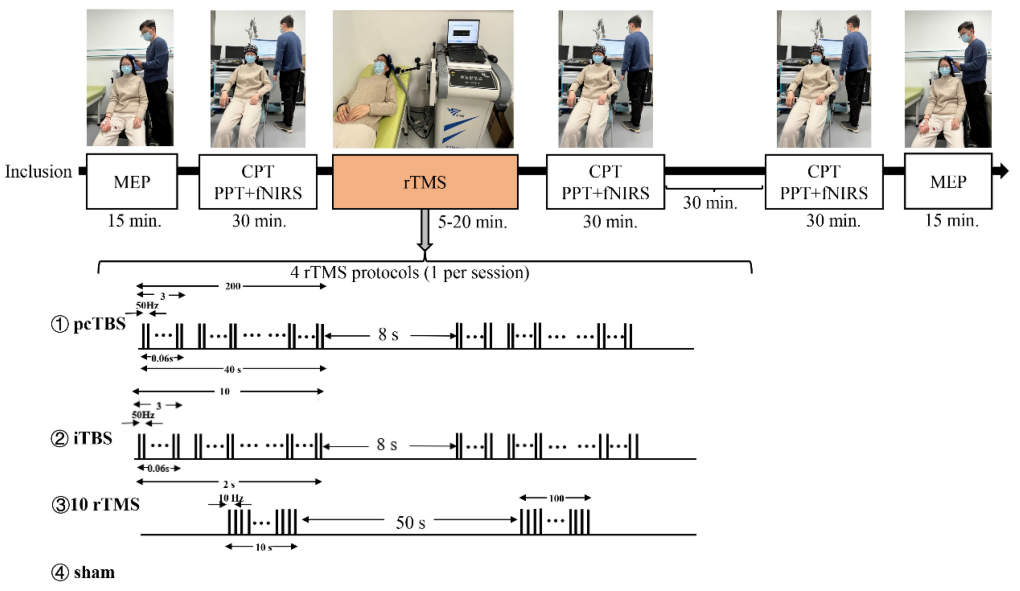

FIGURE 1 | Schematic overview of the whole study. MEP means motor evoked potentials, CPT means current perception thresholds, PTT means pain tolerance threshold, fNIRS means functional near-infrared spectroscopy. Prolonged continuous theta-burst stimulation (pcTBS) consisted of three pulses at 50 Hz repeated 400 times at intervals of 200 ms (1,200 pulses, 1 min and 40 s). Intermittent theta-burst stimulation (iTBS) consisted of three pulses at 50 Hz repeated 10 times at intervals of 200 ms (600 pulses, 3 min and 20 s). 10 Hz rTMS consisted of 15 trains of 10 s with an interval of 50 s (1,500 pulses, 15 min).

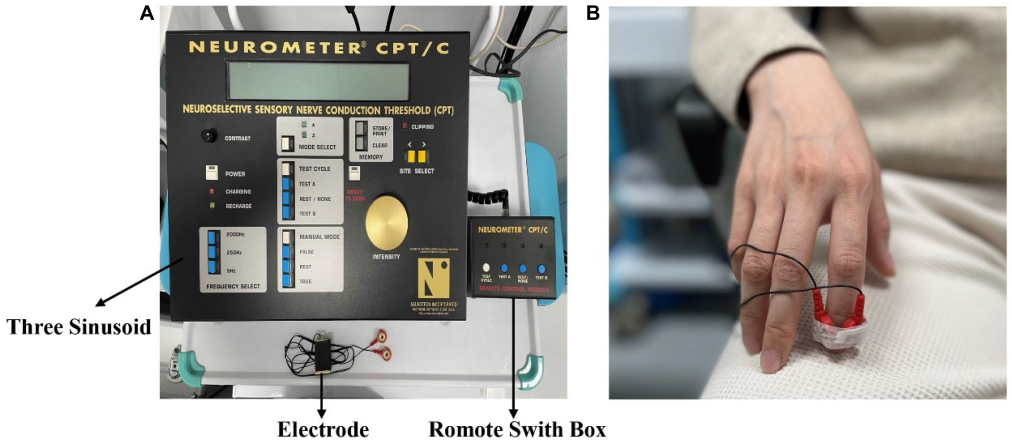

FIGURE 2 | (A) The Neurometer® device. **(B)** The electrode is placed on the fingertip of the right index finger.

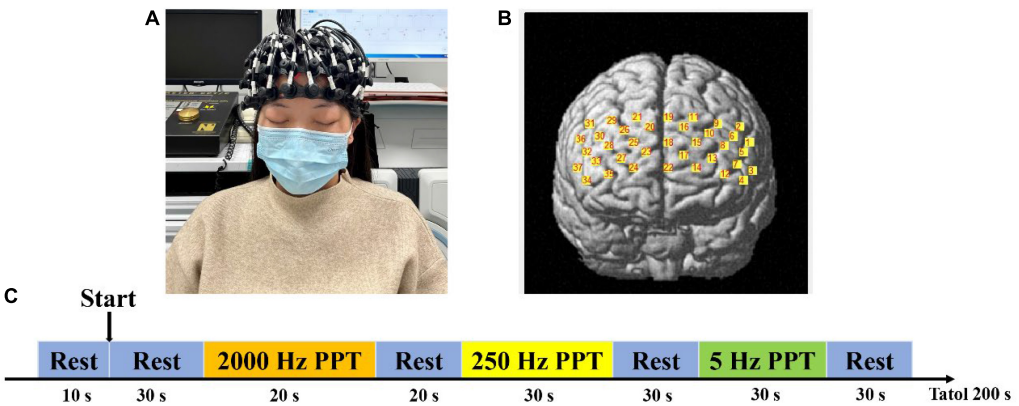

FIGURE 3 | Illustration of fNIRS testing. **(A)** Wearing method of functional near-infrared spectroscopy cap. **(B)** Brain localization schema of channels. **(C)** fNIRS testing procedure. PTT means pain tolerance threshold.

the cap in place to reduce cap movement. A NIR gain quality check was performed to ensure data acquisition before recording. Neuroimaging data were collected at a sampling rating of 20 Hz throughout the entire experiment.

For each fNIRS testing, participants were asked to rest for 30 s, followed by the PTT tests (20 s 2,000 Hz PTT test and 20 s rest, 30 s 250 Hz PTT test and 30 s rest, and 30 s 5 Hz PTT test and 30 s rest) (**Figure 3C**). Using fNIRS, we observed the activation of different parameters of rTMS applied on the left M1 in the prefrontal cortex (Broca's area, dorsolateral prefrontal cortex, frontopolar area, and orbitofrontal area).

Statistical Analysis

Statistical analysis was performed in IBM SPSS Statistics (version 26). Data were confirmed to have a normal distribution using the Shapiro–Wilk normality test since the sample size was small. A repeated-measures analysis of variance (ANOVA) with the factors "time," "stimulation," and the "time × stimulation" interaction was used for the comparison of CPT, PTT. If there was a significant "time × stimulation," simple main effects were calculated for "time" and "stimulation" and paired *t*-tests with Bonferroni's correction for multiple comparisons. One-way ANOVA was used for comparison between four groups. For categorical variables, we use Fisher exact test to compare differences between groups.

In order to minimize motion artifact and ambient light noise for fNIRS data, a low pass filter was used to filtered the detected signals. Modified Beer-Lambert Law (MBLL) was used to calculate hemodynamic changes for each of the 37 channels. To demonstrate the differences in the prefrontal cortex activity, NIRS_SPM and Homer_2 were used the make topographical maps. A repeated-measures ANOVA was used to calculate difference for intra-group comparison. One-way ANOVA was used to calculate difference for inter-group comparison. Statistical significance was established at $P < 0.05$.

RESULTS

Forty healthy volunteers were included in the study (mean age: 24.7 ± 4.43 years, 26 men and 14 women) to receive

different rTMS parameters applied to the left M1. None volunteer withdrew from the study. The participants' baseline demographic characteristics are shown in **Table 1**. No significant differences were observed between the groups regarding gender, age, RMT, MEP-latency, CPT, and PTT ($P > 0.05$).

Effect of Left M1 Repetitive Transcranial Magnetic Stimulation on Sensory Threshold

Sensory thresholds and pain thresholds were determined for the right index fingertip, which represented the global effect of stimulation. Significant differences between treatments were observed for changes in CPT 2K Hz between baseline and 1 h after rTMS ($F = 6.551$, $P < 0.001$): pcTBS versus sham ($P = 0.004$) and pcTBS versus 10 Hz rTMS ($P = 0.007$) (**Figure 5A**). There was a significant difference for changes in CPT 250 Hz between baseline and 1 h after stimulation ($F = 3.809$, $P = 0.018$): pcTBS versus 10 Hz rTMS ($P = 0.018$) (**Figure 5B**). No significant effect of treatments was observed for CPT 2K Hz (F(time × stimulation) = 3.127, $P = 0.058$), CPT 250 Hz (F(time × stimulation) = 2.286, $P = 0.082$), CPT 5 Hz (F(time × stimulation) = 1.312, $P = 0.268$) (**Table 2** and **Figures 4A–C**).

Effect of Left M1 Repetitive Transcranial Magnetic Stimulation on Pain Threshold

There was no significant difference on pain threshold for the test stimulation for PTT 2K Hz [F(stimulation) = 0.072, $P = 0.974$], PTT 250 Hz [F(stimulation) = 0.214, $P = 0.886$], and PTT 5Hz [F(stimulation) = 0.556, $P = 0.649$] (**Figures 4D–F**). Neither effect of change for PTT 2K Hz ($F = 0.706$, $P = 0.554$), PTT 250 Hz ($F = 1.085$, $P = 0.368$), PTT 2K Hz ($F = 0.751$, $P = 0.529$) between baseline and 1 h after stimulation.

TABLE 1 | Baseline information for four groups.

Variable	pcTBS	iTBS	10 Hz rTMS	sham	F/X^2	*P*-value
Age (years)	26.9 ± 6.45	24.7 ± 4.19	24.5 ± 3.53	22.7 ± 1.88	1.573	0.213
Gender, *n*					0.424	0.737
Man/Female	3/7	4/6	4/6	3/7		
BMI (kg/m^2)	20.97 ± 3.52	21.94 ± 3.75	21.95 ± 3.36	22.69 ± 3	0.441	0.932
RMT (percentage)	38 ± 13.3	39 ± 7.3	36 ± 10.4	34 ± 7	0.452	0.717
MEP-latency (ms)	24.34 ± 1.71	25.02 ± 2.01	24.95 ± 3.62	23.25 ± 1.94	1.120	0.354
CPT-2 kHz	147.40 ± 36.13	144.40 ± 30.32	134.60 ± 27.62	155.30 ± 22.44	0.839	0.482
CPT-250 Hz	65.60 ± 24.41	51 ± 17.49	55 ± 13.36	64.9 ± 20.81	1.395	0.260
CPT-5 Hz	37.4 ± 17.31	29.9 ± 13.15	28.8 ± 11.81	37.5 ± 17.23	0.971	0.417
PTT-2 kHz	11.3 ± 4.11	10.3 ± 4.54	10.5 ± 3.81	11.1 ± 5.15	0.115	0.951
PTT-250 Hz	7.3 ± 2.79	7.8 ± 4.8	6.9 ± 2.99	7.23 ± 3.23	0.163	0.921
PTT-5 Hz	12.7 ± 5.31	10.3 ± 5.22	10.7 ± 5.18	11.5 ± 5.64	0.392	0.760

Data are presented as mean ± SD. pcTBS, prolonged continuous theta-burst stimulation; iTBS, intermittent theta-burst stimulation; rTMS, repetitive transcranial magnetic stimulation; BMI, body mass index; RMT, resting motor thresholds; MEP, motor evoked potential; CPT, current perception threshold; PTT, pain tolerance threshold.

TABLE 2 | Comparison of outcomes in the four groups in post-stimulation and 1 h after stimulation.

Variable	pcTBS	iTBS	10Hz rTMS	sham	F/X^2	*P*-value
RMT-1 h (percentage)	35 ± 11.6	38 ± 7.4	34 ± 10.1	34 ± 6.3	0.384	0.765
MEP-latency 1 h	22.73 ± 1.93	22.50 ± 1.27	24.41 ± 2.77	23.04 ± 1.89	1.757	0.173
CPT-2K Hz post	168.2 ± 35.24	147 ± 33.57	145.7 ± 28.56	157.5 ± 21.94	1.201	0.323
CPT-2K Hz 1h	180.2 ± 42.2	166.3 ± 26.82	136.6 ± 28.39	157.4 ± 20.7	3.577	0.023*
CPT-250 Hz post	69.9 ± 24.76	48.7 ± 22.86	52.1 ± 13.45	65 ± 20.07	2.391	0.085
CPT-250 Hz 1 h	77.4 ± 28.99	50.5 ± 17.27	50.9 ± 10.96	65.1 ± 20.38	3.964	0.015*
CPT-5 Hz post	43.4 ± 31.91	26.3 ± 15.03	31.1 ± 11.35	38.2 ± 18.39	1.335	0.278
CPT-5 Hz 1 h	36.6 ± 20.7	22.7 ± 8.09	25.1 ± 12.04	37.6 ± 17.85	2.473	0.077
PTT-2K Hz post	11.3 ± 5.2	10.4 ± 4.27	11 ± 5.05	11 ± 5.22	0.058	0.981
PTT-2K Hz 1 h	12.7 ± 6.32	12 ± 5.37	11.4 ± 5.08	10.9 ± 5.04	0.201	0.895
PTT-250 Hz post	7.5 ± 2.99	7.7 ± 4.64	7.6 ± 4.55	6.7 ± 2.75	0.142	0.934
PTT-250 Hz 1 h	9.2 ± 5.18	8.2 ± 4.36	8 ± 4.57	7 ± 2.49	0.446	0.722
PTT-5 Hz post	12.8 ± 4.87	10.7 ± 4.49	10.4 ± 4.57	10.9 ± 6.22	0.455	0.715
PTT-5 Hz 1 h	13.9 ± 6.91	10 ± 4.66	11.7 ± 5.16	11.3 ± 6.03	0.792	0.506

Data are presented as mean ± SD. pcTBS, prolonged continuous theta-burst stimulation; iTBS, intermittent theta-burst stimulation; rTMS, repetitive transcranial magnetic stimulation; RMT, resting motor thresholds; MEP, motor evoked potential; CPT, current perception threshold; PTT, pain tolerance threshold.
**P < 0.05.*

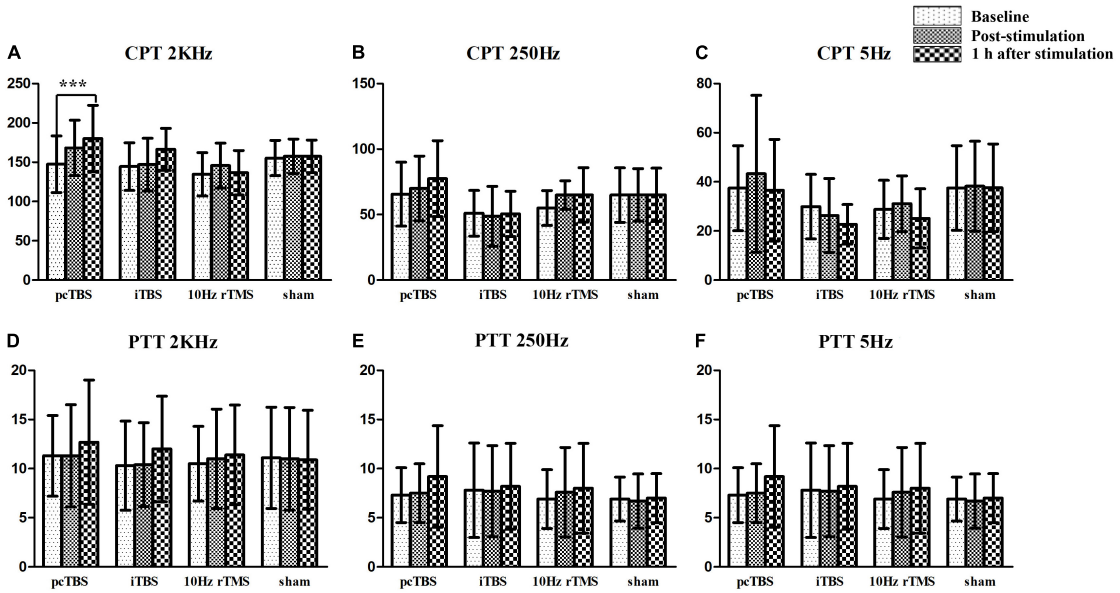

FIGURE 4 | Sensory and pain thresholds measurements. CPT means current perception threshold and PTT means pain tolerance threshold. pcTBS, prolonged continuous theta-burst stimulation; iTBS, intermittent theta-burst stimulation; rTMS, repetitive transcranial magnetic stimulation. ***$P < 0.001$.

Effect of Left M1 Repetitive Transcranial Magnetic Stimulation on Left M1 Cortical Excitability

The mean baseline RMT was 37 ± 9.6% of the stimulator maximum output power [F(stimulation) = 0.452, P = 0.717]. There was no significant change after stimulation (F = 1.420, P = 0.253) (**Table 2**). The latency of the RMT was 24.39 ± 2.459 ms at baseline [F(stimulation) = 1.120, P = 0.354]. Significant difference was observed for change for latency (F = 4.260, P = 0.011): iTBS versus sham (P = 0.017) (**Figure 5C**).

Effect of Left M1 Repetitive Transcranial Magnetic Stimulation on Brain Activation

There were no significant differences in average oxygenated hemoglobin (HbO) among four groups in baseline ($P > 0.05$). There was significant difference in average HbO μm in the right dorsolateral prefrontal cortex (DLPFC) [P = 0.037 (pcTBS versus sham: P = 0.041)] and left DLPFC [P = 0.0058 (pcTBS versus iTBS: P = 0.005, pcTBS versus 10 Hz rTMS: P = 0.034)] when performing PTT 2,000 Hz task immediately after stimulation (**Figure 6A**). Significant difference was found in average HbO μm in left DLPFC [P = 0.039 (iTBS versus sham: P = 0.024)] when performing PTT 5 Hz task immediately after stimulation (**Figure 6B**). There was significant difference in average HbO μm in the right DLPFC [channel 32: P = 0.038 (10 Hz rTMS versus sham: P = 0.032), channel 34: P = 0.020 (10 Hz rTMS versus sham: P = 0.013)], right frontopolar cortex (FPC) [channel 23: P = 0.030 (pcTBS versus sham: P = 0.036), channel 35: P = 0.008 (10 Hz rTMS versus sham: P = 0.005)], left DLPFC [channel 7: P = 0.006 (pcTBS versus sham: P = 0.004)], left FPC [channel 17: P = 0.014 (pcTBS versus sham: P = 0.046), channel 22: P = 0.004 (pcTBS versus sham: P = 0.004)] (**Figure 6C**) comparing four group in 1 h after stimulation of PTT 2K Hz. When comparing the changes of PPT 2K Hz between 1 h after stimulation and baseline, significant difference was found in average HbO um in left DLPFC (F = 3.9727, P = 0.038): pcTBS versus sham: P = 0.029 (**Figure 6D**).

Adverse Effects

Mild headaches occurred in one subject after pcTBS and one subject after iTBS stimulation. No serious adverse effects occurred.

DISCUSSION

This study aimed to identify the sensory thresholds, pain thresholds, and functional brain activity changes by comparing three rTMS paradigms with sham stimulation. The results of this study indicate that pcTBS can modulate sensitivity on Aβ fibers compared with 10 Hz rTMS and sham stimulation. In addition, pcTBS applied to left M1 can activate DLPFC and FPC after stimulation compared with iTBS, 10 Hz rTMS, and sham stimulation. However, no significant changes were found in pain tolerance threshold from behavioral data.

Acute Sensory and Pain Threshold Change After rTMS Stimulation

Our results revealed that one-session pcTBS can modulate sensitivity on Aβ fibers compared with 10 Hz rTMS and sham stimulation. In addition, on-session pcTBS can modulate sensitivity on Aδ fibers compared with iTBS. This result is congruent with the statement that doubling the stimulation

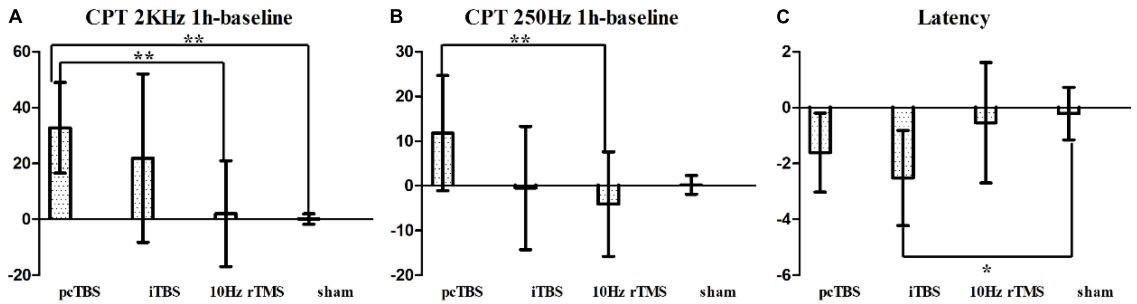

FIGURE 5 | (A) Changes in current perception threshold of 2,000 Hz between baseline and 1 h after stimulation. **(B)** Changes in current perception threshold of 250 Hz between baseline and 1 h after stimulation. **(C)** Changes of latency in MEP between baseline and 1 h after stimulation. pcTBS, prolonged continuous theta-burst stimulation; iTBS, intermittent theta-burst stimulation; rTMS, repetitive transcranial magnetic stimulation. $^{*}P < 0.05$; $^{**}P < 0.001$ (not significant otherwise).

duration of the cTBS can convert inhibitory cTBS into facilitatory pcTBS (Gamboa et al., 2010; De Martino et al., 2019). In addtion, one study indicated that 1 Hz rTMS over M1 had significant modulatory effects on pain perception (Tamura et al., 2004a). Our study found that pcTBS (50 Hz) can increase the Aβ-fiber threshold, which can support the previous studies. pcTBS has some potential advantages over other parameters. On the one hand, pcTBS can promote cortical excitability in a short time. On the other hand, pcTBS needs less stimulation time than iTBS and 10Hz rTMS, which can greatly improve the efficiency of therapeutic instruments.

No significant changes were found for pain thresholds after one-session high-frequency rTMS stimulation, which supports the results reported in previously published studies (Antal and Paulus, 2010; Borckardt et al., 2011; Klírová et al., 2020). Klírová et al. found that pcTBS of the motor cortex can modulate cortical excitability but not pain perception. Antal and Paulus, and Borckardt et al. found that iTBS of the motor cortex did not induce a significant reduction in acute pain perception. However, most studies indicated that one-session high-frequency rTMS can decrease pain sensitivity (Ciampi et al., 2014; Moisset et al., 2015; De Martino et al., 2019; Liu et al., 2021). An explanation could be related to differences in the methodology used to assess pain thresholds. Most of the studies were conducted with pain induction tests using capsaicin, cold pain, heat pain, and pressure pain. Our study directly measures the pain tolerance threshold on sensory fibers of participants. Another explanation could be related to parameters of rTMS. A systematic review indicated the changes of MEP suppression in 30 Hz TBS were more persistent compared with 50 Hz TBS (Chung et al., 2016). In addition, one study found that three sessions of pcTBS to the left dorsolateral prefrontal cortex increased heat, cold, and pressure pain thresholds (De Martino et al., 2019). Therefore, frequency may be a key fact for rTMS to relieve pain.

Acute Brain Activation Change After rTMS Stimulation

Although our behavioral data showed that one-session high-frequency rTMS can not increase the pain threshold of healthy subjects, fNIRS showed that high-frequency rTMS applied over left M1 can activate the DLPFC immediately after stimulation. After 1 h of stimulation, it can diffuse to the bilateral DLPFC and FPC. In addition, pcTBS can significantly activate DLPFC and FPC on A-fibers compared with iTBS, 10 Hz rTMS, and sham stimulation, which indicates that pcTBS has a potential analgesic effect. This result is in line with one study (Tupak et al., 2013). The authors indicated that iTBS applied to the left PFC can decrease prefrontal oxygenation. Other studies also used fNIRS to investigate acute neural adaptation after high-frequency rTMS on M1. However, decreased functional connectivity within PFC (Li et al., 2019) and reduction in HbO concentration from both motor and prefrontal cortices (Rihui et al., 2017) were observed during rTMS. The possible explanation is that these two studies applied rTMS over 1–2 cm lateral from the vertex rather than M1.

The analgesic effect of rTMS is still unclear. fMRI showed that rTMS can directly activate the thalamus through cortical-thalamic projection and inhibit the transmission of sensory information through the spinothalamic pathway, thus relieving pain (Cioni and Meglio, 2007). In addition, electrophysiological studies have shown that high-frequency rTMS can increase the excitability of the M1 area and cause cumulative plasticity changes of brain nerve tissue (Pridmore et al., 2005). Furthermore, studies indicated that chronic pain is accompanied by the decrease of blood perfusion in the thalamus and other parts, while low-frequency rTMS can reduce blood flow in the stimulated ipsilateral side and increase blood flow compensation in the contralateral brain (Tamura et al., 2004b). Our results indicate that single-session pcTBS placed on M1 can increase the excitability of DLPFC and FPC compared with iTBS, 10 Hz rTMS, sham stimulation. In addition, high-frequency rTMS can increase blood flow compensation in the prefrontal lobe. This result indicates that rTMS applied to the left M1 may play an analgesic effect by regulating DLPFC and FPC in the frontal lobe. More research is needed in the future to identify the interaction between M1 and the prefrontal cortex in pain research.

Potential Clinical Application of pcTBS

One study examined the nociceptive threshold in the hind paws using the Neurometer in the bilateral carotid artery occlusion (BCAO) mouse model. The results found that the sensitivity of C

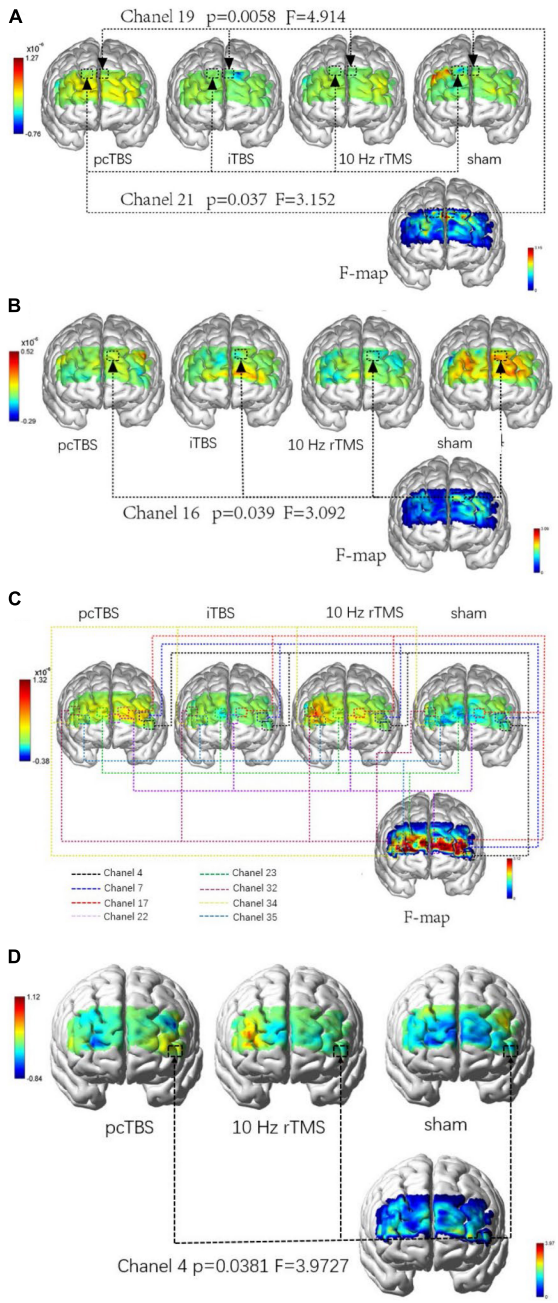

FIGURE 6 | (A) Comparison of difference in brain activation when performing PTT 2,000 Hz task immediately after stimulation. **(B)** Comparison of difference in brain activation when performing PTT 5 Hz task immediately after stimulation. **(C)** Comparison of difference in brain activation when performing PTT 2,000 Hz task 1 h after stimulation. **(D)** Comparison of difference in changes between 1 h after stimulation and baseline in brain activation when performing PTT 2,000 Hz. pcTBS, prolonged continuous theta-burst stimulation; iTBS, intermittent theta-burst stimulation; rTMS, repetitive transcranial magnetic stimulation.

and Aβ fibers (at stimulation of 5 and 2KHz, respectively) were significantly decreased in the 30 min BCAO group compared with those before BCAO, which were closely related to the development of the hyperalgesia component of central post-stroke pain (P) (Tamiya et al., 2013). Another study examined alterations of the current stimulation threshold of primary neurons using the Neurometer in mice receiving left middle cerebral artery occlusion (MCAO). The data showed that the sensitivity of Aδ and Aβ fibers (at 2 kHz and 250 Hz stimulation, respectively) was significantly decreased on day 3 after MCAO, which may contribute to the allodynia for CPSP (Takami et al., 2011). This study indicated that Aβ fiber damage may be the key to cause CPSP.

Our data show that pcTBS can modulate the sensitivity of Aβ fibers more effectively than 10 Hz rTMS and sham stimulation, which means that pcTBS may be used as a potential treatment for CPSP. In the future, multicenter, large-sample randomized controlled trials are needed to prove its effectiveness.

Limitations

There are a few limitations in this study. Due to the limitation of research conditions, this study is the absence of a neuronavigation system that can target the left M1 according to the functional imaging examination. In addition, due to the limited number of fNIRS channels, we did not monitor the neuroplastic changes in the left M1. Therefore, we were unable to analyze the changes of brain functional connections between motor areas and the prefrontal cortex. In addition, sensory sensitivity may change at different ages. We only recruited subjects around 24 years old which may cause the results not stability across other age cohorts. Another limitation is that the sample of the study ($n = 40$) actually can be considered as a small sample, which can also limit the extrapolation of the results.

CONCLUSION

In conclusion, our data demonstrate the advantages of pcTBS over 10 Hz rTMS and sham stimulation on Aβ fibers, opening new avenues of research concerning the clinical application of pcTBS for the treatment of CPSP. In addition, single-session pcTBS placed on left M1 can increase the excitability of DLPFC and FPC compared with iTBS, 10 Hz rTMS, and sham stimulation, indicating the interaction between M1 and prefrontal cortex may be a potential mechanism of analgesic effect of rTMS.

DATA AVAILABILITY STATEMENT

The raw data supporting the conclusions of this article will be made available by the authors, without undue reservation.

ETHICS STATEMENT

The studies involving human participants were reviewed and approved by the Institutional Review Board of Huashan Hospital, Fudan University. The patients/participants provided

their written informed consent to participate in this study. Written informed consent was obtained from the individual(s) for the publication of any potentially identifiable images or data included in this article.

AUTHOR CONTRIBUTIONS

CL, NZ, and ZW designed the experiment. CL, QH, LZ, and SX conducted the experiment. CL reduced and analyzed the data. CL and NZ wrote the manuscript. ZW revised the manuscript. All authors contributed to the article and approved the submitted version.

FUNDING

This work was supported by the Key National Research and Development Program (No. 2018YFC2002300), National Nature Innovation Research Group Project (No. 82021002), National Nature Integration Project (No. 91948302), and Natural Science Foundation of Fujian Province (No. 2021J01709).

ACKNOWLEDGMENTS

We wish to thank all the subjects for their participation in this study.

REFERENCES

Andre-Obadia, N., Magnin, M., Simon, E., and Garcia-Larrea, L. (2018). Somatotopic effects of rTMS in neuropathic pain? a comparison between stimulation over hand and face motor areas. *Eur. J. Pain* 22, 707–715. doi: 10.1002/ejp.1156

André-Obadia, N., Mertens, P., Gueguen, A., Peyron, R., and Garcia-Larrea, L. (2008). Pain relief by rTMS: differential effect of current flow but no specific action on pain subtypes. *Neurology* 71, 833–840. doi: 10.1212/01.wnl.0000325481.61471.f0

Antal, A., and Paulus, W. (2010). Effects of transcranial theta-burst stimulation on acute pain perception. *Restor Neurol Neurosci.* 28, 477–484. doi: 10.3233/RNN-2010-0555

Attia, M., McCarthy, D., and Abdelghani, M. (2021). Repetitive transcranial magnetic stimulation for treating chronic neuropathic pain: a systematic review. *Curr. Pain Headache Rep.* 25:48. doi: 10.1007/s11916-021-00960-5

Borckardt, J. J., Reeves, S. T., Beam, W., Jensen, M. P., Gracely, R. H., Katz, S., et al. (2011). A randomized, controlled investigation of motor cortex transcranial magnetic stimulation (TMS) effects on quantitative sensory measures in healthy adults: evaluation of TMS device parameters. *Clin. J. Pain* 27, 486–494. doi: 10.1097/AJP.0b013e31820d2733

Cárdenas-Morales, L., Nowak, D. A., Kammer, T., Wolf, R. C., and Schönfeldt-Lecuona, C. (2010). Mechanisms and applications of theta-burst rTMS on the human motor cortex. *Brain Topogr.* 22, 294–306. doi: 10.1007/s10548-009-0084-7

Chung, S. W., Hill, A. T., Rogasch, N. C., Hoy, K. E., and Fitzgerald, P. B. (2016). Use of theta-burst stimulation in changing excitability of motor cortex: a systematic review and meta-analysis. *Neurosci. Biobehav. Rev.* 63, 43–64. doi: 10.1016/j.neubiorev.2016.01.008

Ciampi, D. A. D., Mhalla, A., Adam, F., Texeira, M. J., and Bouhassira, D. (2014). Repetitive transcranial magnetic stimulation induced analgesia depends on N-methyl-D-aspartate glutamate receptors. *Pain* 155, 598–605. doi: 10.1016/j.pain.2013.12.022

Cioni, B., and Meglio, M. (2007). Motor cortex stimulation for chronic non-malignant pain: current state and future prospects. *Acta Neurochir. Suppl.* 97, 45–49. doi: 10.1007/978-3-211-33081-4_5

Dall'Agnol, L., Medeiros, L. F., Torres, I. L., Deitos, A., Brietzke, A., Laste, G., et al. (2014). Repetitive transcranial magnetic stimulation increases the corticospinal inhibition and the brain-derived neurotrophic factor in chronic myofascial pain syndrome: an explanatory double-blinded, randomized, sham-controlled trial. *J. Pain* 15, 845–855. doi: 10.1016/j.jpain.2014.05.001

de Andrade, D. C., Mhalla, A., Adam, F., Texeira, M. J., and Bouhassira, D. (2011). Neuropharmacological basis of rTMS-induced analgesia: the role of endogenous opioids. *Pain* 152, 320–326. doi: 10.1016/j.pain.2010.10.032

De Martino, E., Fernandes, A. M., Galhardoni, R., De Oliveira, S. C., Ciampi De Andrade, D., Graven-Nielsen, T., et al. (2019). Sessions of prolonged continuous theta burst stimulation or high-frequency 10 hz stimulation to left dorsolateral prefrontal cortex for 3 days decreased pain sensitivity by modulation of the efficacy of conditioned pain modulation. *J. Pain* 20, 1459–1469. doi: 10.1016/j.jpain.2019.05.010

Finnerup, N. B., Attal, N., Haroutounian, S., McNicol, E., and Baron, R. (2015). Pharmacotherapy for neuropathic pain in adults: a systematic review and meta-analysis. *Lancet Neurol.* 14, 162–173. doi: 10.1016/S1474-4422(14)70251-0

Finnerup, N. B., Kuner, R., and Jensen, T. S. (2021). Neuropathic pain: from mechanisms to treatment. *Physiol. Rev.* 101, 259–301. doi: 10.1152/physrev.00045.2019

Gamboa, O. L., Antal, A., Moliadze, V., and Paulus, W. (2010). Simply longer is not better: reversal of theta burst after-effect with prolonged stimulation. *Exp. Brain Res.* 204, 181–187. doi: 10.1007/s00221-010-2293-4

Gomatos, E. L., and Rehman, A. (2022). "Sensory neuropathy," in *StatPearls [Internet]* (Treasure Island, FL: StatPearls Publishing).

Hoogendam, J. M., Ramakers, G. M., and Di Lazzaro, V. (2010). Physiology of repetitive transcranial magnetic stimulation of the human brain. *Brain Stimul.* 3, 95–118. doi: 10.1016/j.brs.2009.10.005

Houzé, B., Bradley, C., Magnin, M., and Garcia-Larrea, L. (2013). Changes in sensory hand representation and pain thresholds induced by motor cortex stimulation in humans. *Cereb. Cortex* 23, 2667–2676. doi: 10.1093/cercor/bhs255

Huang, Y. Z., Edwards, M. J., Rounis, E., Bhatia, K. P., and Rothwell, J. C. (2005). Theta burst stimulation of the human motor cortex. *Neuron* 45, 201–206. doi: 10.1016/j.neuron.2004.12.033

Klein, M. M., Treister, R., Raij, T., Pascual-Leone, A., Park, L., Nurmikko, T., Lenz, F., Lefaucheur, J. P. et al. (2015). Transcranial magnetic stimulation of the brain: guidelines for pain treatment research. *Pain* 156, 1601–1614. doi: 10.1097/j.pain.0000000000000210

Klírová, M., Hejzlar, M., Kostýlková, L., Mohr, P., Rokyta, R., Novák, T. et al. (2020). Prolonged continuous theta burst stimulation of the motor cortex modulates cortical excitability but not pain perception. *Front. Syst. Neurosci.* 14:27. doi: 10.3389/fnsys.2020.00027

Koob, G. F. (2021). Drug addiction: hyperkatifeia/Negative reinforcement as a framework for medications development. *Pharmacol. Rev.* 73, 163–201. doi: 10.1124/pharmrev.120.000083

Lefaucheur, J. P. (2019). Transcranial magnetic stimulation. *Handb. Clin. Neurol.* 160, 559–580.

Lefaucheur, J. P., Aleman, A., Baeken, C., Benninger, D. H., Brunelin, J., Di Lazzaro, V. et al. (2020). Evidence-based guidelines on the therapeutic use of repetitive transcranial magnetic stimulation (rTMS): an update (2014-2018). *Clin. Neurophysiol.* 131, 474–528. doi: 10.1016/j.clinph.2019.11.002

Lefaucheur, J. P., André-Obadia, N., Antal, A., Ayache, S. S., Baeken, C., Benninger, D. H. et al. (2014). Evidence-based guidelines on the therapeutic use of repetitive transcranial magnetic stimulation (rTMS). *Clin. Neurophysiol.* 125, 2150–2206. doi: 10.1016/j.clinph.2014.05.021

Li, R., Potter, T., Wang, J., Shi, Z., Wang, C., Yang, L. et al. (2019). Cortical hemodynamic response and connectivity modulated by sub-threshold high-Frequency repetitive transcranial magnetic stimulation. *Front. Hum. Neurosci.* 13:90. doi: 10.3389/fnhum.2019.00090

Liu, Y., Yu, L., Che, X., and Yan, M. (2021). Prolonged continuous theta burst stimulation to demonstrate a larger analgesia as well as cortical excitability

changes dependent on the context of a pain episode. *Front. Aging Neurosci.* 13:804362. doi: 10.3389/fnagi.2021.804362

Lynn, B., and Carpenter, S. E. (1982). Primary afferent units from the hairy skin of the rat hind limb. *Brain Res.* 238, 29–43. doi: 10.1016/0006-8993(82)90768-5

Moisset, X., Goudeau, S., Poindessous-Jazat, F., Baudic, S., Clavelou, P., Bouhassira, D. et al. (2015). Prolonged continuous theta-burst stimulation is more analgesic than 'classical' high frequency repetitive transcranial magnetic stimulation. *Brain Stimul.* 8, 135–141. doi: 10.1016/j.brs.2014.10.006

Nahmias, F., Debes, C., de Andrade, D. C., Mhalla, A., and Bouhassira, D. (2009). Diffuse analgesic effects of unilateral repetitive transcranial magnetic stimulation (rTMS) in healthy volunteers. *Pain* 147, 224–232. doi: 10.1016/j.pain.2009.09.016

Paricio-Montesinos, R., Schwaller, F., Udhayachandran, A., Rau, F., Walcher, J., Evangelista, R. et al. (2020). The sensory coding of warm perception. *Neuron* 106, 830–841. doi: 10.1016/j.neuron.2020.02.035

Park, E., Kang, M. J., Lee, A., Chang, W. H., Shin, Y. I., Kim, Y. H. et al. (2017). Real-time measurement of cerebral blood flow during and after repetitive transcranial magnetic stimulation: a near-infrared spectroscopy study. *Neurosci. Lett.* 653, 78–83. doi: 10.1016/j.neulet.2017.05.039

Pridmore, S., Oberoi, G., Marcolin, M., and George, M. (2005). Transcranial magnetic stimulation and chronic pain: current status. *Australas Psychiatry* 13, 258–265. doi: 10.1080/j.1440-1665.2005.02197.x

Raja, S. N., Carr, D. B., Cohen, M., Finnerup, N. B., Flor, H., Gibson, S. et al. (2020). The revised international association for the study of pain definition of pain: concepts, challenges, and compromises. *Pain* 161, 1976–1982. doi: 10.1097/j.pain.0000000000001939

Rihui, L., Chushan, W., Kairong, H., Zhixi, S., Wang, J., Zhang Y. et al. (2017). Blood oxygenation changes resulting from subthreshold high frequency repetitive transcranial magnetic stimulation. *Annu Int Conf IEEE Eng. Med. Biol. Soc.* 2017, 1513–1516. doi: 10.1109/EMBC.2017.8037123

Rossini, P. M., Barker, A. T., Berardelli, A., Caramia, M. D., Daskalakis, Z., Di Iorio, R., et al. (1994). Non-invasive electrical and magnetic stimulation of the brain, spinal cord and roots: basic principles and procedures for routine clinical application. Report of an IFCN committee. *Electroencephalogr. Clin. Neurophysiol.* 91, 79–92. doi: 10.1016/0013-4694(94)90029-9

Schmelz, M. (2011). Neuronal sensitivity of the skin. *Eur. J. Dermatol.* 21(Suppl. 2), 43–47. doi: 10.1684/ejd.2011.1265

Summers, J., Johnson, S., Pridmore, S., and Oberoi, G. (2004). Changes to cold detection and pain thresholds following low and high frequency transcranial magnetic stimulation of the motor cortex. *Neurosci. Lett.* 368, 197–200. doi: 10.1016/j.neulet.2004.07.008

Takami, K., Fujita-Hamabe, W., Harada, S., and Tokuyama, S. (2011). Aβ and Aδ but not C-fibres are involved in stroke related pain and allodynia: an experimental study in mice. *J. Pharm. Pharmacol.* 63, 452–456. doi: 10.1111/j.2042-7158.2010.01231.x

Tamiya, S., Yoshida, Y., Harada, S., Nakamoto, K., and Tokuyama, S. (2013). Establishment of a central post-stroke pain model using global cerebral ischaemic mice. *J. Pharm. Pharmacol.* 65, 615–620. doi: 10.1111/jphp.12007

Tamura, Y., Hoshiyama, M., Inui, K., Nakata, H., Qiu, Y., Ugawa, Y., et al. (2004a). Facilitation of a[delta]-fiber-mediated acute pain by repetitive transcranial magnetic stimulation. *Neurology* 62, 2176–2181. doi: 10.1212/01.wnl.0000130081.96533.85

Tamura, Y., Okabe, S., Ohnishi, T., N Saito, D., Arai, N., Mochio, S., et al. (2004b). Effects of 1-Hz repetitive transcranial magnetic stimulation on acute pain induced by capsaicin. *Pain* 107, 107–115. doi: 10.1016/j.pain.2003.10.011

Tupak, S. V., Dresler, T., Badewien, M., Hahn, T., Ernst, L. H., Herrmann, M. J. et al. (2013). Inhibitory transcranial magnetic theta burst stimulation attenuates prefrontal cortex oxygenation. *Hum. Brain Mapp.* 34, 150–157. doi: 10.1002/hbm.21421

Young, N. A., Sharma, M., and Deogaonkar, M. (2014). Transcranial magnetic stimulation for chronic pain. *Neurosurg. Clin. N. Am.* 25, 819–832. doi: 10.1016/j.nec.2014.07.007

Conflict of Interest: The authors declare that the research was conducted in the absence of any commercial or financial relationships that could be construed as a potential conflict of interest.

Publisher's Note: All claims expressed in this article are solely those of the authors and do not necessarily represent those of their affiliated organizations, or those of the publisher, the editors and the reviewers. Any product that may be evaluated in this article, or claim that may be made by its manufacturer, is not guaranteed or endorsed by the publisher.

frontiers | Frontiers in Molecular Neuroscience

ORIGINAL RESEARCH
published: 13 April 2022
doi: 10.3389/fnmol.2022.854000

The Last Decade Publications on Diabetic Peripheral Neuropathic Pain: A Bibliometric Analysis

Shu-Hao Du[1], Yi-Li Zheng[1], Yong-Hui Zhang[1], Ming-Wen Wang[2] and Xue-Qiang Wang[1,2]**

[1] Department of Sport Rehabilitation, Shanghai University of Sport, Shanghai, China, [2] Department of Rehabilitation Medicine, Shanghai Shangti Orthopaedic Hospital, Shanghai, China

Background: Diabetic peripheral neuropathic pain (DPNP) is a usual complication of diabetes with a high incidence and mortality. Many diabetes-related studies have been published in various journals. However, bibliometrics and visual analyses in the domain of DPNP research are still lacking. The study aimed to offer a visual method to observe the systematic overview of global research in this field from 2011 to 2021.

Methods: The publications from the Science Citation Index Expanded in Web of Science (WOS) in the past 11 years (from 2011 to 2021) were collected and sorted out, and those related to DPNP were extracted and analyzed. The article language was limited in English. Then, CiteSpace V was used for the bibliometric analysis of the extracted literature.

Results: A total of 1,422 articles met the inclusion criteria. A continuous but unstable growth in the amounts of papers published on DPNP was observed over the last 11 years. The subject sort of the 1,422 papers mainly concentrates on *Endocrinology Metabolism*, *Clinical neurology* and *Neurosciences* from the WOS. According to the research contribution in the field of DPNP, the United States occupies a leading position, with the highest amounts of publications, citations, open access, and the H- index.

Conclusion: This study provides a visual analysis method for the trend of DPNP, and offers some hidden serviceable information that may define new directions for future research.

Keywords: diabetic, neuropathic pain, trend, visual analysis, bibliometric

OPEN ACCESS

Edited by:
Howe Liu,
University of North Texas Health Science Center, United States

Reviewed by:
Qiang Gao,
Sichuan University, China
Francisco Lopez-Munoz,
Camilo José Cela University, Spain

****Correspondence:***
Ming-Wen Wang
wengmingwang@126.com
Xue-Qiang Wang
wangxueqiang@sus.edu.cn

Specialty section:
This article was submitted to Pain Mechanisms and Modulators, a section of the journal Frontiers in Molecular Neuroscience

Received: *13 January 2022*
Accepted: *07 March 2022*
Published: *13 April 2022*

Citation:
Du S-H, Zheng Y-L, Zhang Y-H, Wang M-W and Wang X-Q (2022) The Last Decade Publications on Diabetic Peripheral Neuropathic Pain: A Bibliometric Analysis. Front. Mol. Neurosci. 15:854000. doi: 10.3389/fnmol.2022.854000

INTRODUCTION

Diabetes mellitus refers to a series of metabolic diseases distinguished by high blood sugar, which is mainly caused by lack of insulin secretion, defective action, or both (Abbott et al., 2011). According to the reports, diabetes accounted for the largest share among 155 conditions of United States health care spending in 2013, with an estimated amount of $101.4 billion, including 57.6% spent on medical drugs and 23.5% on outpatient care (Dieleman et al., 2016). Diabetic peripheral neuropathic pain (DPNP) is a common diabetic peripheral neuropathy, and about 20–30% of patients with diabetes experience peripheral neuropathic pain during their lifetime (Baba et al., 2019). Moreover, more than half of the diabetic patients may admit peripheral neuropathic pain

(Calcutt, 2010). Most studies found that it developed before pre-diabetes (Tesfaye et al., 2010). There is evidence that DPNP reduces health-related quality of life and increases health-care expenditures (Gore et al., 2006; Stewart et al., 2007; Ritzwoller et al., 2009). Furthermore, DPNP is closely associated with some depressive symptoms, anxiety, and lower rates of optimal sleep (Sadosky et al., 2013).

Due to the high morbidity and family burden of DPNP, an increasing number of studies have been involved in the field of DPNP, and relevant literature has been published in academic journals. Some studies have explored the mechanisms of pain relief by non-pharmacological interventions (Zheng et al., 2021; Peng et al., 2022; Wu et al., 2022). However, only a few large-scale systematic global reviews of DPNP have been published (Çakici et al., 2016).

Bibliometric analysis is an important quantitative analysis method for literature on a specific topic (Bornmann and Leydesdorff, 2014). The purpose of this work is to offer a classified analysis of this research on DPNP from 2011 to 2021, including quantitative information by authors, countries, institutions, and co-citations (Chen and Wang, 2020). Bibliometrics analyzes the numbers of articles published, keywords, citations, and cooperation in recent years to better understand the current trends and the knowledge structure of research. WOS is a database from which relevant literature can be extracted, and CiteSpace V is used for the in-depth analysis of visualization (Yao et al., 2020). Moreover, we can know which places occupy the international leading positions in this field so far and which one has a significant impact on this discipline through the analysis of publishing states, authors, and institutions (Chen et al., 2012, 2014; Li et al., 2020). Visual analysis extracts useful information from big data through data mining technology and presents it clearly for readers to understand the development of the discipline more intuitively (Liao et al., 2018; Weng et al., 2020). Bibliometrics and visual analysis have been widely used in various fields, such as mathematics (Sabermahani and Ordokhani, 2021), medicine (Weng et al., 2020), artificial intelligence (Xieling et al., 2021), big data financial decision-making (Nobanee, 2021) and economics (Liang et al., 2017). According to these researches, this study explored the characteristics of articles in the field of DPNP through bibliometrics and visual analysis. Specific influential literature can be found to evaluate the current research status of diabetic neuropathy and predict the future research direction through the association among different literature and citations. The study also provided valuable reference information for researchers and promoted the cooperation among various institutions (Weng et al., 2020).

MATERIALS AND METHODS

Source and Search Strategy

We retrieved and downloaded all published literature in the past 11 years (from 2011 to 2021) from the Science Citation Index Expanded (SCI-Expanded) of WOS. The keywords "pain" and "diabetes" and its disparate utterances were used as the subject to search correlative paper (Weng et al., 2020). All fundamental information about each article, such as authors, countries, institutions, citation, key words, and references, was collected (Weng et al., 2020). The specific search strategy can be found in the Supplementary.

Inclusion Criteria

The included paper should meet the following standards: (1) Articles published in various journals over the last 11 years (from 2011 to 2021); (2) Articles in English; and (3) literature on pain and diabetic.

Analysis Tool

Microsoft Office Excel was used to extract the literature downloaded from WOS. The extracted relevant data included the amounts of publications and citations from different countries/regions, and institutions; keywords; journals; references; and H-index. Two documents named "Date" and "Project" were created to extract the data downloaded from the WOS. CiteSpace V, a superb bibliometric analysis instrument, was used for the bibliometric analysis of extracted literature. We diagrammed co-citation diagrams of authors, countries, and institutions that contributed the most to diabetic peripheral neuralgia. The top 25 keywords with the strongest citation bursts and the top 10 citations paper were drawn. The numbers of publications, citations, and H-indexes for different years were also summarized and an annual bar chart was plotted. Meanwhile, a regional world diagram was drawn using Microsoft Office Excel. The red areas represented the regions with the highest amounts of posts, followed by orange, purple, yellow, and blue. The gray area represented a region that had no published literature. Cluster analysis and citation bursts were performed and a large node circle indicated a high occurrence frequency.

RESULTS

The Number and Growth Trend of Annual Publications

A total of 1,422 articles met the inclusion criteria. We summarized the amounts of publications and citations from 2011 to 2021 and charted the growth trend (**Figure 1**). The numbers of papers published each year has risen from 103 in 2011 to 127 in 2021 (**Figure 1A**). Overall, the number of published papers showed a continuous but unstable growth trend, which can be roughly divided into two stages. In the first stage, the number of published papers increased steadily from 103 in 2015 to 151 in2015. From 2015 to 2016, with the number of published papers dropping from 151 to 126, was a turning point. The period from 2016 to 2021 was the second stage, showing a fluctuating growth and a relatively slow growth rate, with an average annual publication volume of 135. The 1,422 papers were cited 16.620 times. The numbers of citations have decrease from 2,893 in 2011 to 138 in 2021 (**Figure 1B**). Considering the impact of publication year, the absence of high amounts of citations in recent years was normal. In the last five 2-year periods (2011–2012, 2013–2014, 2015–2016, 2017–2018, 2019–2020, and 2021), the largest

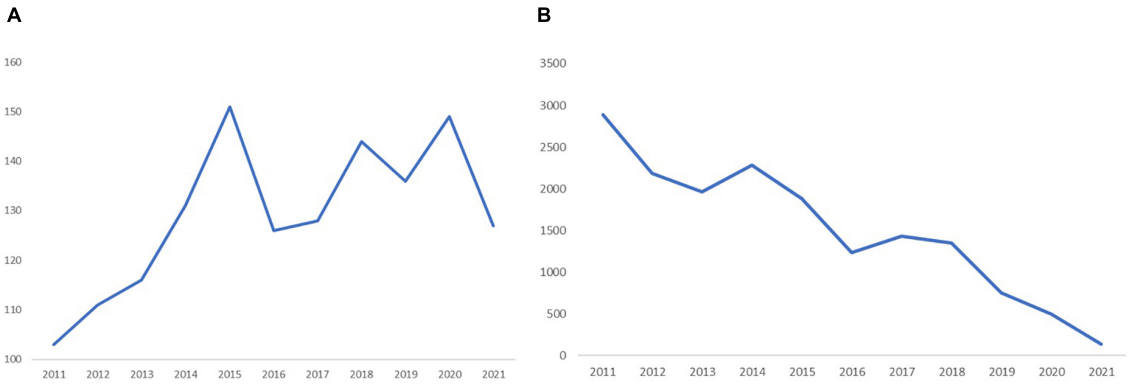

FIGURE 1 | The amounts of papers and citations published. **(A)** The annual amounts of publications on DPNP research from 2011 to 2021. **(B)** The annual amounts of citations on DPNP research from 2011 to 2021.

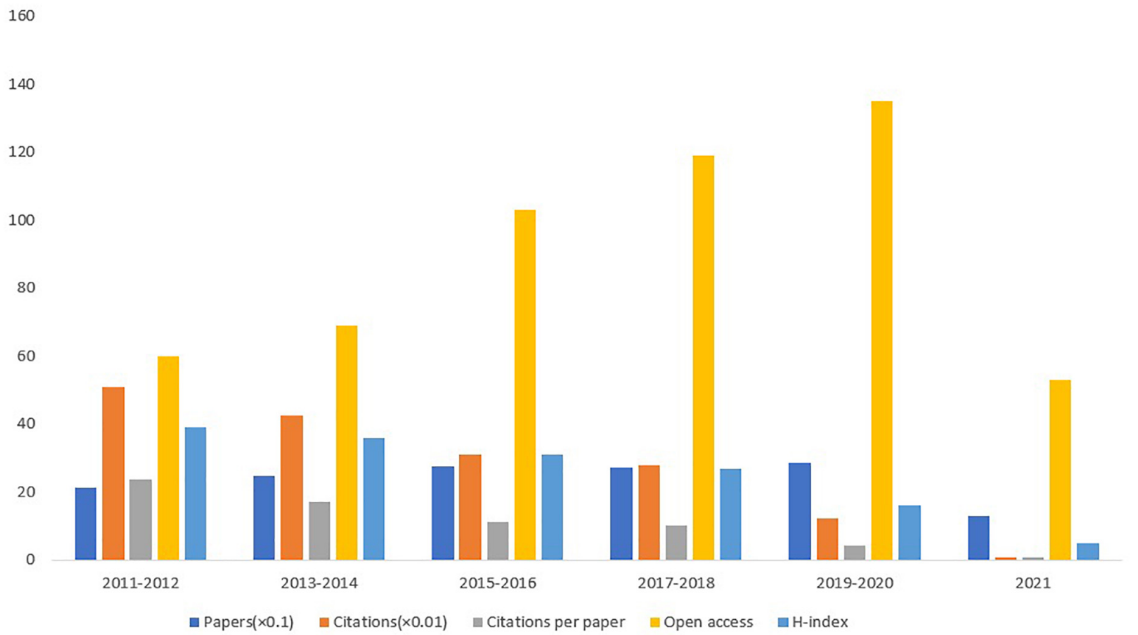

FIGURE 2 | Amounts of publications, citations, citations per paper, open access paper, H-index, and citations for each 2-year time period.

average numbers of citations per paper (23.74), citations (5,080), and the highest H-index (39) occurred in 2011–2012. In 2019–2020, the highest numbers of published papers and open access values were 285 and 135, respectively (**Figure 2**). The amounts of papers published and open access in the domain of DPNP increased continuously but unstably, while the citation per paper and H-index decreased.

Different Subject Sort of Web of Science

The top 10 subject sorts on DPNP, including publications, citations, open access, and H-index, were demonstrated in **Figure 3**. Among the top 10 discipline sorts, *Endocrinology Metabolism* published most papers, with amount of 347. However, *Neurosciences* had the highest amounts of citations, the open access papers, and the H-index, being 4,771, 96, and 36, respectively. *Anesthesiology* had the highest amounts of citations per paper of 27.22. According to statistical analysis, the top 10 subject sorts calculated by the amounts of publications were *Endocrinology Metabolism, Clinical neurology, Neurosciences, Pharmacology pharmacy, Medicine general internal, Anesthesiology, Medicine research experimental, Biochemistry molecular biology, Health care sciences services,* and *Health policy services.*

Distribution by Different Journals

The **Table 1** demonstrated the top 10 journals in the field of DPNP. In the top 10 journals, *Diabetes*, *Diabetologia*, and *Diabetic medicine* contributed the most to the amounts of

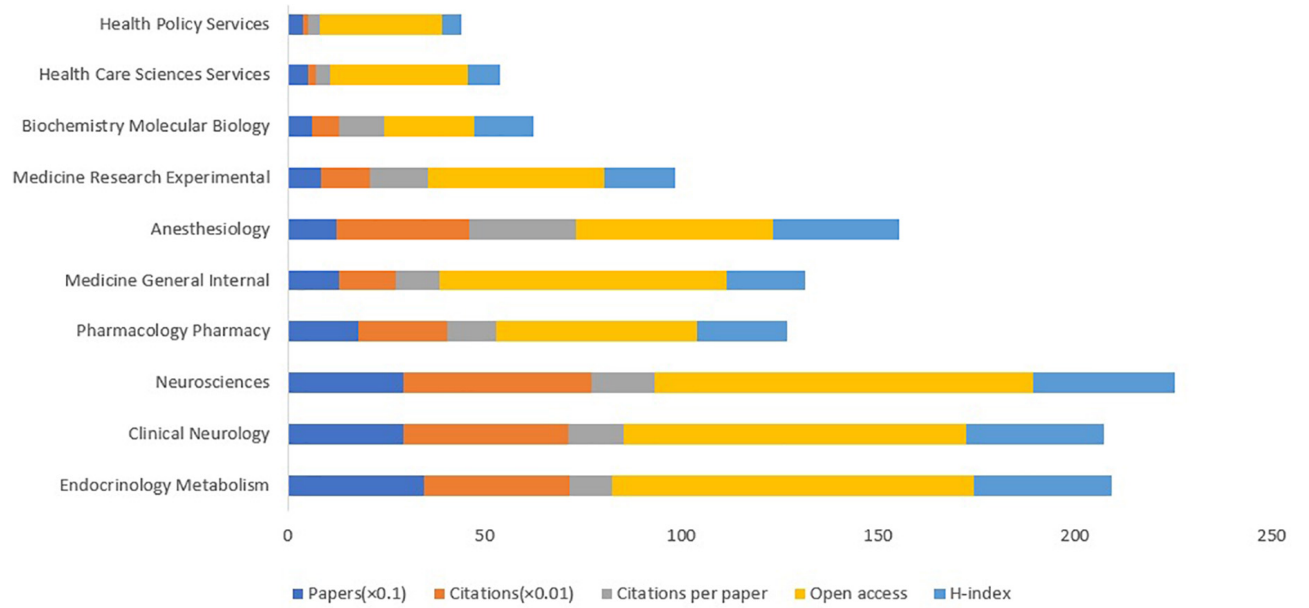

FIGURE 3 | The amounts of papers, citations, citations per paper, open access papers, and H-index of the top 10 subject sort of Web of Science.

TABLE 1 | The top 10 journals in the field of DPNP.

Journals	Papers	Number of papers about neurpathic pain/total number of papers	Citations (WOS)	Citations per paper	Open access	WOS sort	IF (2020)	Quartile	H-index
Diabetes	65	65/1422	241	3.71	8	ENDOCRINOLOGY & METABOLISM	9.461	Q1	7
Diabetologia	59	59/1422	75	1.27	3	ENDOCRINOLOGY & METABOLISM	10.122	Q1	2
Diabetic medicine	42	7/237	295	7.02	4	CLINICAL NEUROLOGY; NEUROSCIENCES	4.359	Q3	7
Journal of the peripheral nervous system	39	13/474	13	0.33	0	ENDOCRINOLOGY & METABOLISM	3.494	Q3	3
Value in health	32	32/1422	8	0.25	27	ECONOMICS; HEALTH CARE SCIENCES & SERVICES; HEALTH POLICY & SERVICES	5.728	Q2	1
Pain	31	31/1422	1638	52.84	10	CLINICAL NEUROLOGY; NEUROSCIENCES	6.961	Q1; Q2	19
Journal of pain	30	5/237	290	9.67	10	ANESTHESIOLOGY; CLINICAL NEUROLOGY; NEUROSCIENCES	5.828	Q2	6
Neurology	26	13/711	399	15.35	4	CLINICAL NEUROLOGY	9.91	Q1	4
Pain medicine	26	13/711	427	16.42	22	ANESTHESIOLOGY; MEDICINE, GENERAL & INTERNAL	3.75	Q3	13
Diabetes care	17	17/1422	1131	66.53	16	ENDOCRINOLOGY & METABOLISM	19.112	Q1	13

published papers, with the papers of 65, 59, and 42 respectively. *Pain* showed the most citations and the highest H-index, being 1,638 and 19, respectively. *Diabetes care* had the largest average per paper citations and the highest impact factor, which were 66.53 and 19.112, respectively. *Value in health* presented the highest open access value of 27 to the public free of charge. Among the top 10 journals, 45.45% were Q1 (Q1 on behalf of the top 25% of 3-year average IF of various journals), 27.27% journals

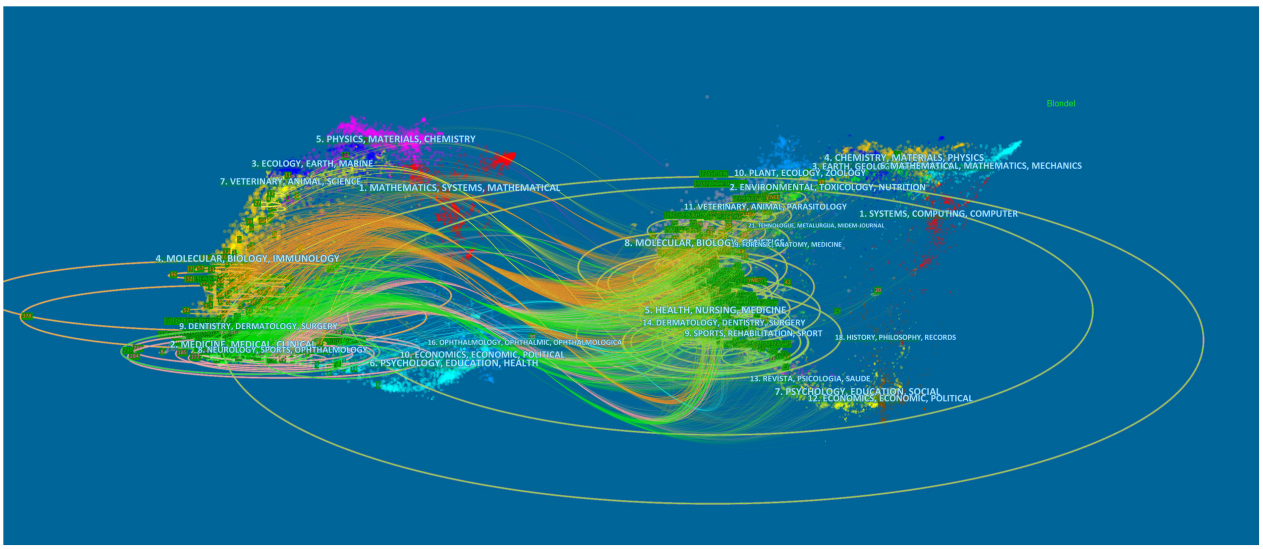

FIGURE 4 | The dual-diagram overlay of journals related to DPNP research.

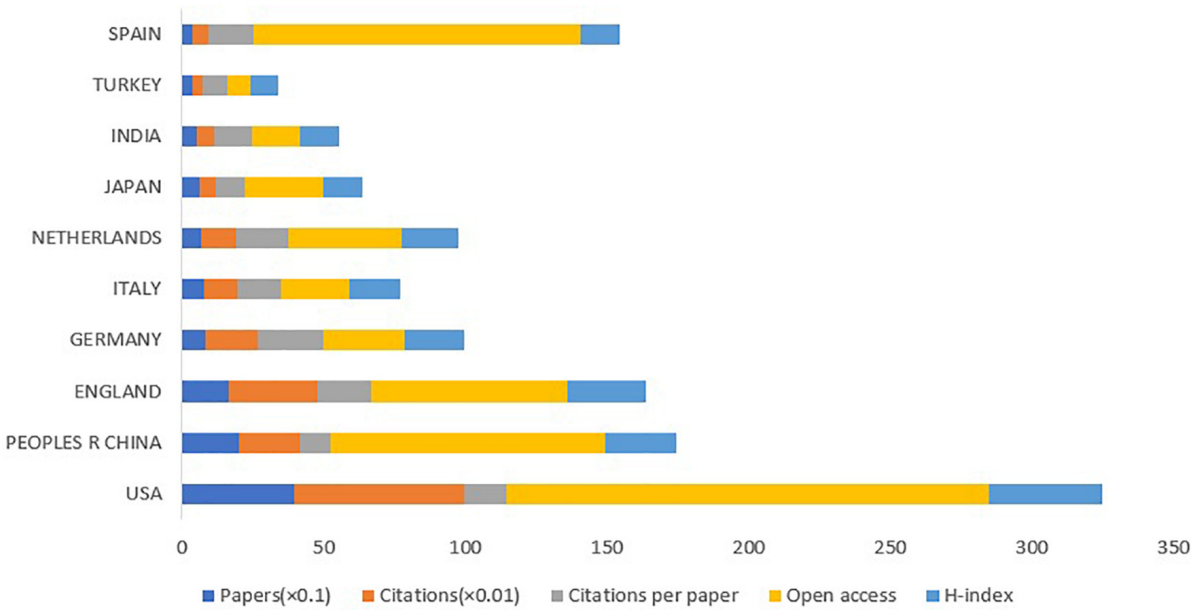

FIGURE 5 | The amounts of papers, citations, citations per paper, open access papers, and H-index of the top 10 countries.

were Q2 (Q2 on behalf of the 25–50% of average IF distribution), and 27.27% journals were Q3 (Q3 on behalf of the 50–75% of average IF distribution).

Figure 4 depicted the dual diagram of citing and cited of different journals, with the diagram on the left and right sides representing the citing journals and cited journals, respectively. The line between the citing and cited journals represented communication and connection between the two and the node tags meant the disciplines wrapped by the different journals. The ellipse's aclinic axis represented the numbers of relevant authors, while the perpendicular axis was the amounts of journals published. Based on the diagram, the journals that contributed the most were mainly from the fields of *mathematic, medicine*, and *ecology*, while the journals cited the most were mainly from the fields of *systems*, *environmental*, and *earth*.

Distribution by Different Countries and Institutions

The **Figure 5** showed the top 10 countries in terms of the numbers of publications on DPNP, with total 1,166 papers. The highest amounts of publications, citations, open access value, and the H-index was reported in United States, being 394, 6,003,

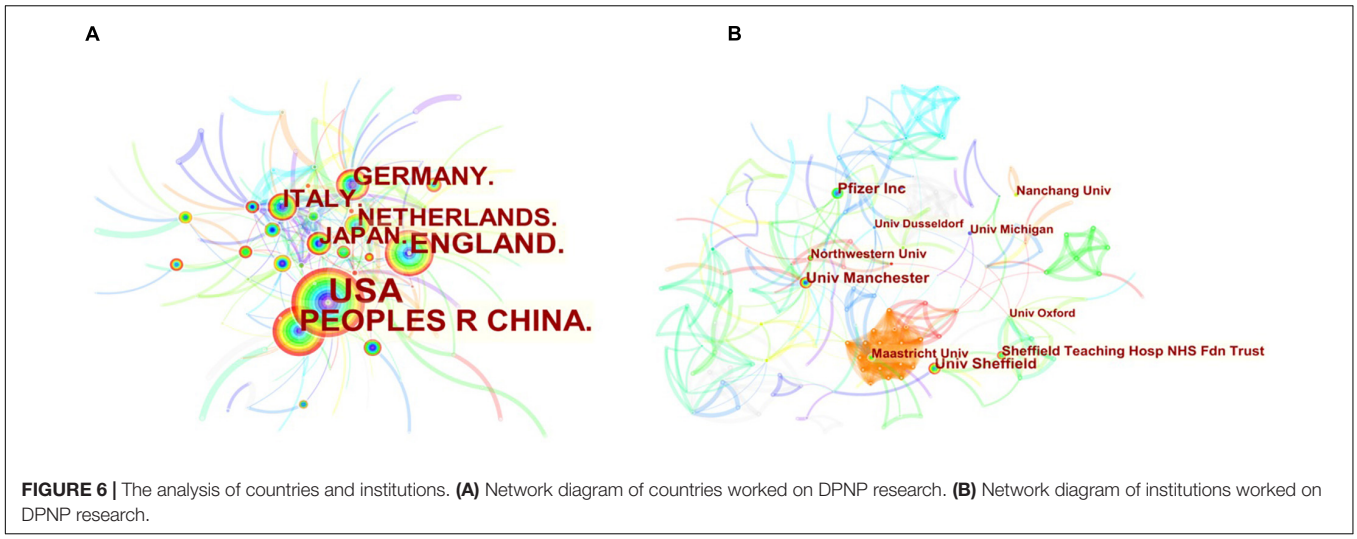

FIGURE 6 | The analysis of countries and institutions. **(A)** Network diagram of countries worked on DPNP research. **(B)** Network diagram of institutions worked on DPNP research.

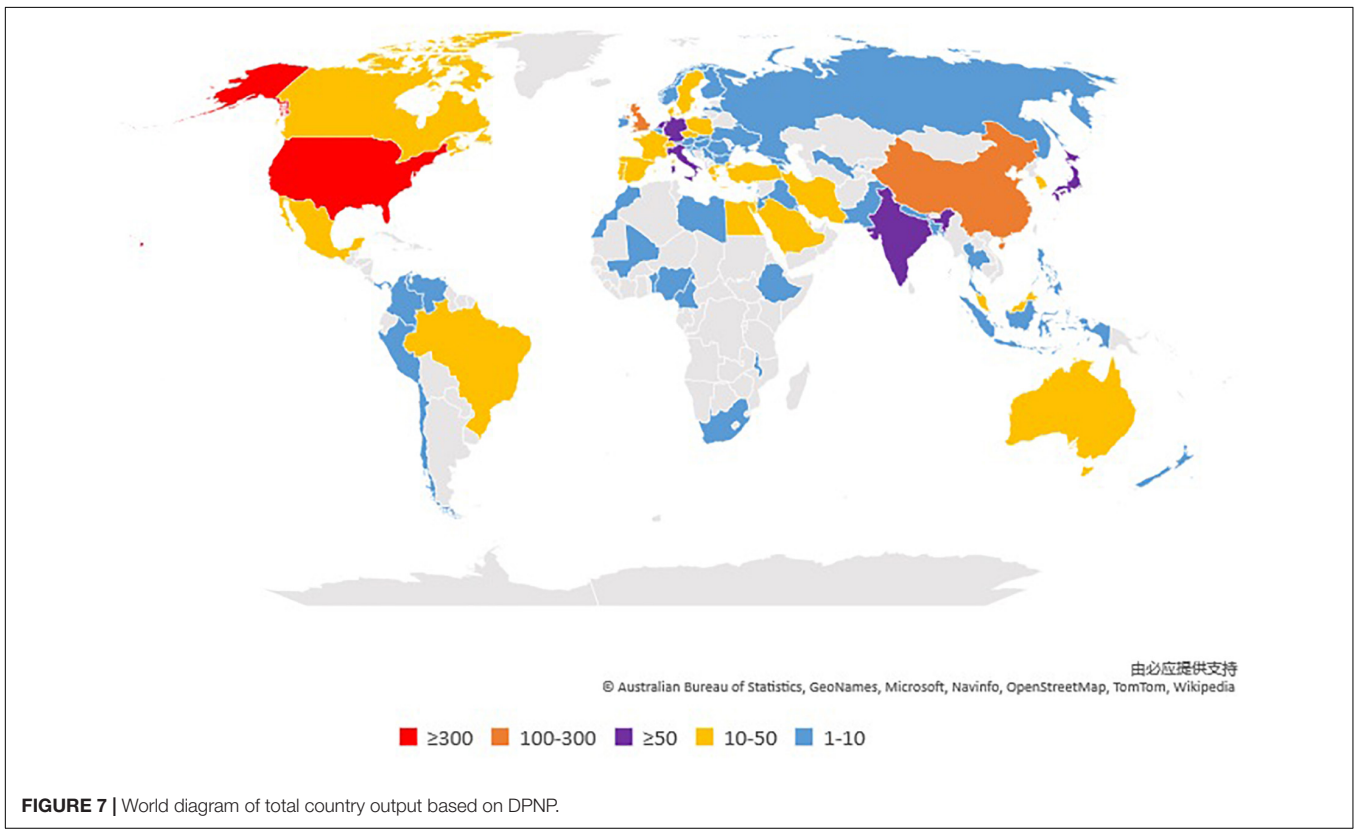

FIGURE 7 | World diagram of total country output based on DPNP.

170, and 40, respectively; followed by China (200 publications); England (165 publications); and Germany (80 publications). **Figure 6A** showed the cooperation among various countries. The Czech Republic had the maximum centrality (0.50), which was followed by Switzerland (0.35) and India (0.33). According to the relevant definition of centrality, these countries indicated close cooperative links with other countries and represented some academic influence. Combining publication and centrality analysis, United States and China were in the dominant positions. The United States, England, Japan, and China have established extensive cooperative relationship and radiate outwards. A world diagram was created with the amounts of published papers to provide a clearer picture of the 1,422 published papers in each country (**Figure 7**). In this map, the Americas was in the ascendancy, with the United States leading the way.

The top 10 institutions by amounts of published papers were shown in **Figure 8**, which contributed 326 papers in the domain of DPNP. The Pfizer had the largest publications with the amount of 53. Although the Pfizer had the highest H-index value of 17, the University of Manchester had the

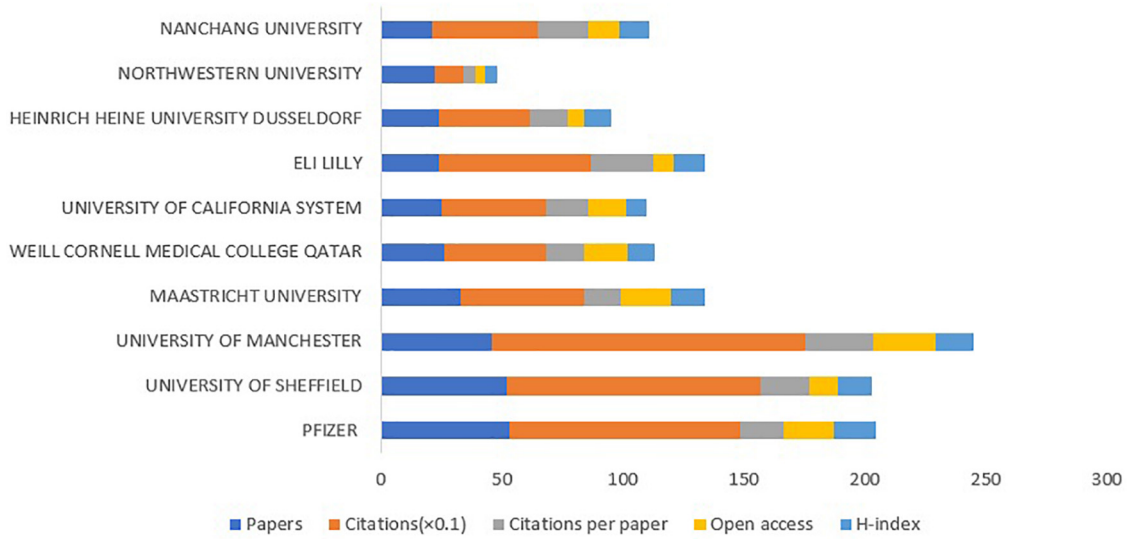

FIGURE 8 | The amounts of papers, citations, citations per paper, open access papers, and H-index of the top 10 institutions.

TABLE 2 | The top 10 authors, co-cited authors, and co-cited references on DPNP research.

Author	Published articles	Cocited author	Cited times	Cocited reference	Cited times
TESFAYE S	63	TESFAYE S	271	Painful diabetic peripheral neuropathy: consensus recommendations on diagnosis, assessment and management?	181
SELVARAJAH D	53	ZIEGLER D	166	The Pain in Neuropathy Study (PiNS): a cross-sectional observational study determining the somatosensory phenotype of painful and painless diabetic neuropathy?	133
WILKINSON ID	29	BOULTON AJM	160	A new look at painful diabetic neuropathy	49
PARSONS B	27	ABBOTT CA	143	Healthcare utilization and costs in diabetes relative to the clinical spectrum of painful diabetic peripheral neuropathy	56
MALIK RA	25	DWORKIN RH	137	Prevalence and characteristics of painful diabetic neuropathy in a large community-based diabetic population in the united kingdom	411
GANDHI R	21	BRIL V	135	Microvascular perfusion abnormalities of the thalamus in painful but not painless diabetic polyneuropathy a clue to the pathogenesis of pain in type 1 diabetes	47
GAO Y	20	DAVIES M	130	LncRNA NON-RATT021972 siRNA regulates neuropathic pain behaviors in type 2 diabetic rats through the P2X (7) receptor in dorsal root ganglia	74
ZIEGLER D	20	FINNERUP NB	119	From guideline to patient: a review of recent recommendations for pharmacotherapy of painful diabetic neuropathy?	61
FABER CG	16	GORE M	118	Spinal cord stimulation and pain relief in Painful diabetic peripheral neuropathy: a prospective two-center randomized controlled trial?	82
GREIG M	15	VINIK AI	110	Painful and painless diabetic neuropathies: what is the difference?	36

most citations, citations per paper, and open access at 1,291, 28.07, and 26, respectively. **Figure 6B** depicted the cooperation and communication among various institutions. The Aarhus University showed maximum centrality (0.18), followed by University of Michigan (0.17) and Weill Cornell Medical College Qatar (0.15). These institutions exhibited extensive cooperative relationships and strong academic influence. Based on the analysis of the number and centrality of publications, Pfizer, Northwestern University and University of Manchester showed relatively close cooperative relationship.

Distribution by Different Authors

The top 10 authors, co-cited authors, and co-cited references on DPNP research were listed in **Table 2**. Among the top 10 authors, Tesfaye S had the most publications (63 publications), followed by Selvarajah D (53 publications), and Wilkinson ID (29 publications). From perspective of co-cited authors, Tesfaye S also had the most cited times (271 cited times), followed by Ziegler D (166 cited times), and Boulton AJM (160 cited times). The collaboration among different authors was demonstrated in **Figure 9**.

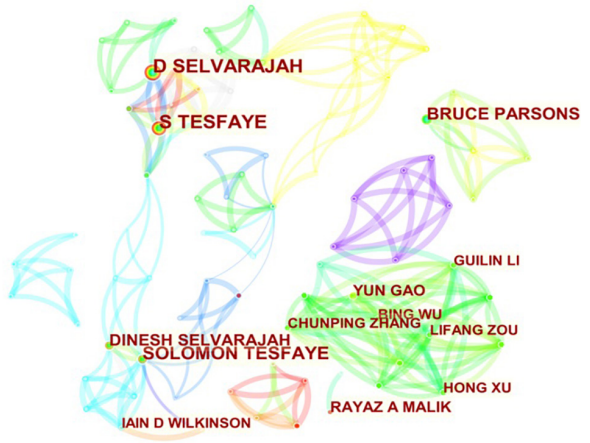

FIGURE 9 | The analysis of authors. Network diagram of influential authors devoted to DPNP research.

Analysis by Different References

Figure 10 showed the time plot of the first 16 co-citation references in the cluster analysis. The modularity Q value was 0.8304 (higher than 0.5), which indicated the network was compatibly distributed to loosely coupled clusters. The largest cluster #0 was "*skin biopsy*", followed by "*diabetic neuropathic pain*" (#1), "*abt-894*" (#2), and "*7*" (#3) (Chen and Wang, 2020).

Analysis by Different Keywords

The top 25 keywords with the strongest citation bursts from 2011 to 2021 was depicted in **Figure 11**. The strongest citation bursts of keyword since 2011 was *symptomatic treatment*. By the end of 2021, the keywords with the most outbreaks of cited literature included "*inflammation*" (2017–2021), "*activation*" (2018–2021), "*phenotype*" (2018–2021), "*phenotype*" (2018–2021), "*adult*" (2018–2021), and "*receptor*" (2019–2021) among the top 25 keywords (*inflammation, randomized controlled trial, placebo, activation, phenotype, adult, natural history, in vitro, open label, obesity, disease, receptor, EFNS guideline, pharmacological treatment, management, pathogenesis, controlled trial, sensory neuron, mice, placebo controlled trial, multicenter, recommendation, microglia, injury, and symptomatic treatment*).

Analysis by the 10 Most Frequently Cited Papers

The top 10 frequently cited papers on DPNP were listed in **Table 3**. The most cited paper (411 citations) by Abbott with

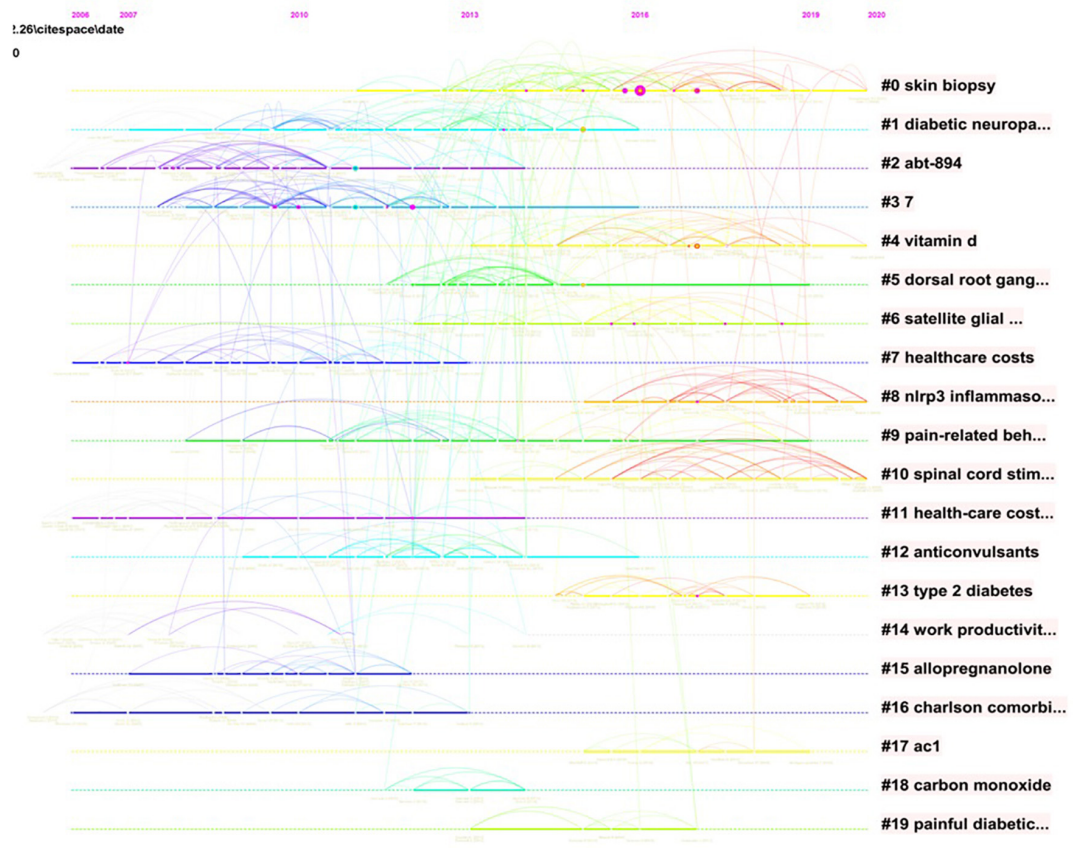

FIGURE 10 | The analysis of references. Co-citation diagram (timeline view) of references from publications on DPNP research.

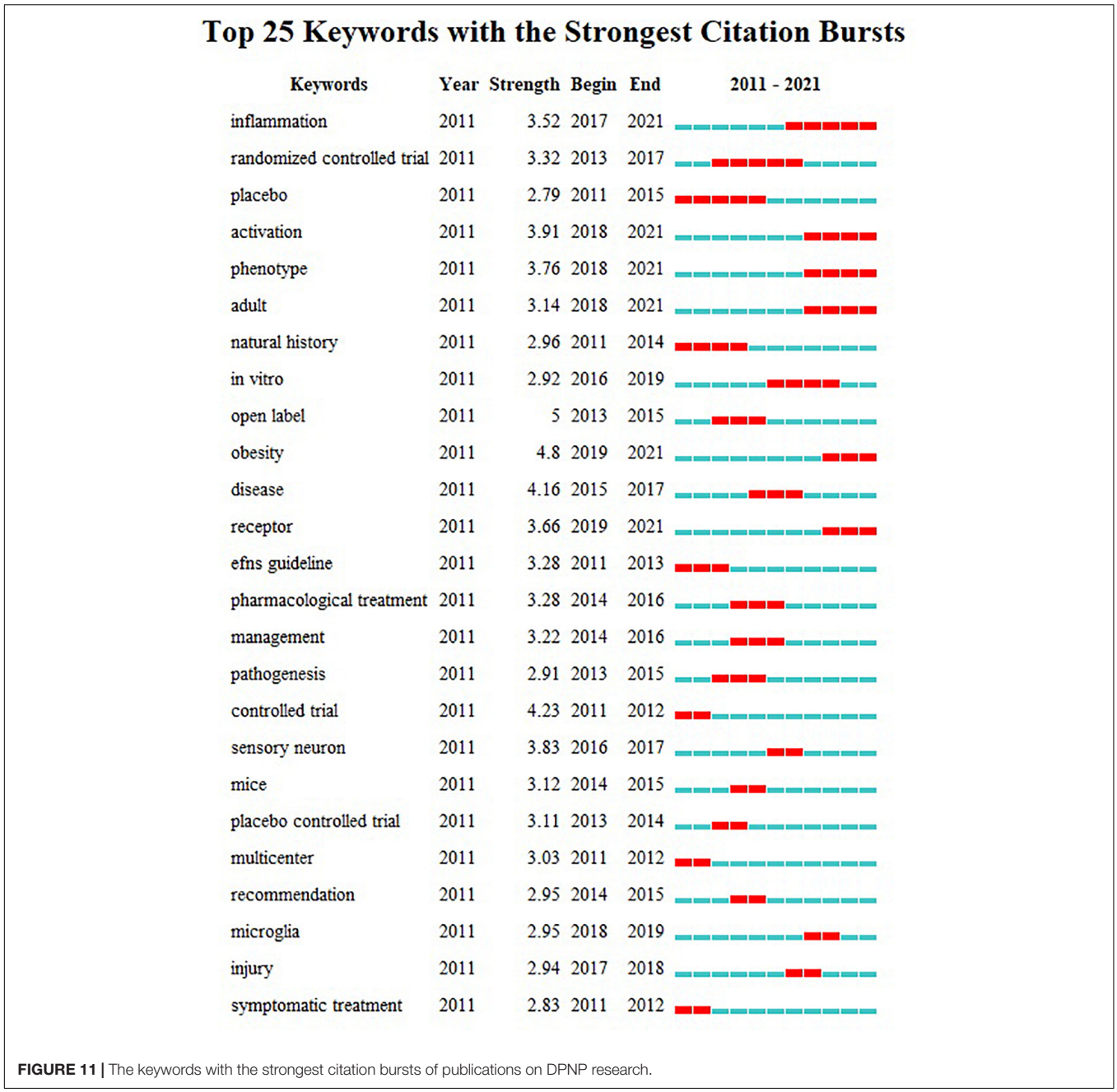

FIGURE 11 | The keywords with the strongest citation bursts of publications on DPNP research.

the title "*Prevalence and Characteristics of Painful Diabetic Neuropathy in a Large Community-Based Diabetic Population in the United Kingdom*" (Abbott et al., 2011) was published in 2011 in *Diabetes care*. Out of the top 10 citations, three of them were published in the journals with IF $\geq$ 10 (*Neuron* and *Diabetes care*) (Abbott et al., 2011; Tesfaye et al., 2013a; Feldman et al., 2017), four in journals with 5 $\leq$ IF $<$ 10 (*Neurology* and *Pain*) (Bril et al., 2011; Yarnitsky et al., 2012; Tesfaye et al., 2013b; Themistocleous et al., 2016), one in journal with 3 $\leq$ IF $<$ 5 (*Diabetes-Metabolism research and reviews*) (Tesfaye et al., 2011), and two in journals with 2 $\leq$ IF $<$ 3 (*Current Medical research and opinion* and *Fitoterapia*) (Schwartz et al., 2011; Kandhare et al., 2012).

DISCUSSION

Global Development Tendency of Diabetic Peripheral Neuropathic Pain Research

This bibliometric analysis provided a scientific review of DPNP over the past 11 years (Chen and Wang, 2020). The numbers of publications correlated with DPNP have showed a continuous but unstable growth trend yearly, with the most obvious growth trend from 2014 to 2015. However, the numbers of citations have been drawn from 2,893 in 2011 to 138 in 2021. Notably,

TABLE 3 | The top 10 papers with the most citations on DPNP research.

Title	First author	Journal	IF (2019)	Year	Citations (WOS)	WOS sort	Category ranking
Prevalence and characteristics of painful diabetic neuropathy in a large community-based diabetic population in the United Kingdom	Abbott, CA	DIABETES CARE	19.112	2011	411	Endocrinology & metabolism	4/143
Conditioned pain modulation predicts duloxetine efficacy in painful diabetic neuropathy	Yarnitsky, D	PAIN	6.961	2012	320	Anesthesiology; Clinical Neurology; Neurosciences	6/32;25/204;43/272
Evidence-based guideline: Treatment of painful diabetic neuropathy	Bril, V	NEUROLOGY	9.91	2011	289	Clinical Neurology	10/204
New Horizons in diabetic neuropathy: mechanisms, bioenergetics, and pain	Feldman, EL	NEURON	17.173	2017	288	Neurosciences	6/272
Painful diabetic peripheral neuropathy: consensus recommendations on diagnosis, assessment and management	Tesfaye, S	DIABETES-METABOLISM RESEARCH AND REVIEWS	4.876	2011	181	Endocrinology & Metabolism	64/143
Mechanisms and management of diabetic painful distal symmetrical polyneuropathy	Tesfaye, S	DIABETES CARE	19.112	2013	170	Endocrinology & Metabolism	4/143
Safety and efficacy of tapentadol ER in patients with painful diabetic peripheral neuropathy: results of a randomized-withdrawal, placebo-controlled trial	Schwartz, S	CURRENT MEDICAL RESEARCH AND OPINION	2.58	2011	168	Medicine, General & Internal; Medicine, Research & Experimental	61/165;93/139
Duloxetine and pregabalin: High-dose monotherapy or their combination? The "COMBO-DN study" - a multinational, randomized, double-blind, parallel-group study in patients with diabetic peripheral neuropathic pain	Tesfaye, S	PAIN	6.961	2013	145	Anesthesiology; Clinical Neurology; Neurosciences	6/32;25/204;43/272
Neuroprotective effect of naringin by modulation of endogenous biomarkers in streptozotocin induced painful diabetic neuropathys	Kandhare, AD	FITOTERAPIA	2. 882	2012	136	Chemistry, Medicinal; Pharmacology & Pharmacy	38/61;152/271
The pain in neuropathy study (PiNS): a cross-sectional observational study determining the somatosensory phenotype of painful and painless diabetic neuropathy	Themistocleous, AC	PAIN	6.961	2016	133	Anesthesiology; Clinical Neurology; Neurosciences	6/32;25/204;43/272

the increased amounts of published articles do not mean the improvement of the literature quality, and the decreased amounts of citations are not equal to the decline of quality. Considering the factor of year, the amounts of citations in the last 2 years are not as high as those in previous years, which is a normal phenomenon (Wang et al., 2020). The highest amounts of published papers and open access values are in 2019–2020, which are 285 and 135, respectively. Moreover, the year 2011–2012 has the highest number of citations (5,080) and H-index (39). These results indicate that DPNP is receiving increasing attention, and the papers published between 2011 and 2013 are of high-quality.

With regards of journals, *Diabetes* (65 publications), *Diabetologia* (59 publications), and *Diabetic medicine* (42 publications) contributed the most to the numbers of published papers. Among the top 10 journals, 45.45% of them were Q1, 27.27% were Q2, and 27.27% were Q3. IFs of 70% of the journals were more than 5. These results indicated that the *Diabetes* was the most influential journal in the field. Most of the top 10 journals had high IFs though some of them located in Q2 and Q3, which might imply that more exploration is required in this domain.

According to the numbers of papers published in the field of DPNP, the United States ranked first (394 publications), far

ahead of China (200 publications), England (165 publications), Germany (80 publications), and other countries. The six European countries, three Asian countries, one North American country composed the top 10 countries. **Figure 6** depicted a wide range of cooperative relationships that have been established between various countries/regions and institutions. From the top 10 institutions, 80% were the world-renowned universities. These results demonstrated that universities were a major front in the field of DPNP, with some American and European universities having a relatively large influence in this field. Pfizer, Northwestern University, and University of Manchester have relatively close cooperative relationship, meaning that the University and the company have established a wide cooperative relationship, which can play a certain positive role in the transformation from scientific research into clinical practice.

Research Focusing on Diabetic Peripheral Neuropathic Pain

According to the subject sort of DPNP, the research mainly focused on *Endocrinology Metabolism*, *Clinical Neurology,* and *Neurosciences*. The prevention and education of diabetes have been emphasized based on the concept of *Endocrinology and Metabolism* (Sanjari et al., 2021). However, the largest amounts of citations, open access papers, and H-index were found in *Neurosciences*, being 4,771, 96, and 36, respectively. In terms of co-cited references, the largest cluster #0 was "*skin biopsy*", followed by "*diabetic neuropathic pain*" (#1), "*abt-894*" (#2), and "*7*" (#3). Based on the analysis of keywords, while the strongest citation bursts of keyword since 2011 was *symptomatic treatment*, the keywords by the end of 2021 included "*inflammation*" (2017–2021), "*activation*" (2018–2021), "*phenotype*" (2018–2021), "*adult*" (2018–2021), and "*receptor*" (2019–2021). This change may represent that the focuses of research about DPNP have transferred from the superficial symptoms to the possible pathogenesis, which probably indicates that future research should further explore the mechanism of diabetes.

Benefits and Limitations

This paper is the first to present a visual analysis of global trends and feasibility in the domain of DPNP over the last 11 years. The included publications are from different academic journals in the SCI-Expanded of WOS to obtain richer data and draw more convincing conclusions (Chen and Wang, 2020). Furthermore, some high-quality journals, such as *Diabetes care* (IF = 19.112), *Diabetologia* (IF = 10.122), and *Neurology* (IF = 9.91), are also included in this study. Moreover, this study contains a more comprehensive analysis, including the number and growth trend of annual publications, different subject sort of WOS, relationship among different journals, authors, countries and institutions, analysis by different references, citations, and keywords.

However, this study still has a few limitations. First of all, we only collected the English publications from SCI-expanded, which might neglect high-quality literature in other languages. In addition, some literatures use specific indicators of bibliometrics, such as Price's Law, Lotka's Law, and Bradford's Law (López-Muñoz et al., 2013, 2015; Redondo et al., 2017), which could accurately reflect the changes in this field. Finally, the figure illustrating the links among different countries and institutions is hard to read due to the close and complicated cooperation among various states and institutions in this field.

CONCLUSION

The study extracted some hidden and useful information from the 2011 to 2021 study of DPNP. The tendency of publications each year increased from 103 in 2011 to 127 in 2021, showing a continuous but unstable growth trend. *Endocrinology Metabolism* and *Clinical Neurology* were the two most popular subject sorts in this domain. The United States has occupied a leading position in this field and has established contacts with Italy, Japan, and other countries. The Pfizer had the largest publications with the amounts of 53. Tesfaye S published the most amounts of studies. The recent emerging burst keywords included "*inflammation,*" "*activation,*" "*phenotype,*" "*adult,*" and "*receptor*." The study provided some valuable information for follow-up researchers, such as development trend and direction, influential journals, and cooperation among different regional institutions.

DATA AVAILABILITY STATEMENT

The original contributions presented in the study are included in the article/**Supplementary Material**, further inquiries can be directed to the corresponding author/s.

AUTHOR CONTRIBUTIONS

S-HD performed the data analyses and wrote the manuscript. Y-LZ helped perform the analysis with constructive discussions. Y-HZ and M-WW helped further revise and rewrote the manuscript. X-QW contributed to the conception of the study. All authors contributed to the article and approved the submitted version.

FUNDING

This work was supported by Fok Ying-Tong Education Foundation of China (161092). The scientific and technological research program of the Shanghai Science and Technology Committee (Fund number: 19080503100) and the Shanghai Key Lab of Human Performance (Shanghai University of Sport) (11DZ2261100).

SUPPLEMENTARY MATERIAL

The Supplementary Material for this article can be found online at: https://www.frontiersin.org/articles/10.3389/fnmol.2022.854000/full#supplementary-material

REFERENCES

Abbott, C. A., Malik, R. A., van Ross, E. R., Kulkarni, J., and Boulton, A. J. (2011). Prevalence and characteristics of painful diabetic neuropathy in a large community-based diabetic population in the U.K. *Diabetes Care* 34, 2220–2224. doi: 10.2337/dc11-1108

Baba, M., Matsui, N., Kuroha, M., Wasaki, Y., and Ohwada, S. (2019). Mirogabalin for the treatment of diabetic peripheral neuropathic pain: a randomized, double-blind, placebo-controlled phase III study in Asian patients. *J. Diabetes Investig.* 10, 1299–1306. doi: 10.1111/jdi.13013

Bornmann, L., and Leydesdorff, L. (2014). Scientometrics in a changing research landscape. *EMBO Rep.* 15, 1228–1232. doi: 10.15252/embr.201439608

Bril, V., England, J. D., Franklin, G. M., Backonja, M., Cohen, J. A., Del Toro, D. R., et al. (2011). Evidence-based guideline: treatment of painful diabetic neuropathy–report of the American Association of Neuromuscular and Electrodiagnostic Medicine, the American Academy of Neurology, and the American Academy of Physical Medicine & Rehabilitation. *Muscle Nerve* 43, 910–917. doi: 10.1002/mus.22092

Çakici, N., Fakkel, T. M., van Neck, J. W., Verhagen, A. P., and Coert, J. H. (2016). Systematic review of treatments for diabetic peripheral neuropathy. *Diabet. Med.* 33, 1466–1476. doi: 10.1111/dme.13083

Calcutt, N. (2010). Tolerating diabetes: an alternative therapeutic approach for diabetic neuropathy. *ASN Neuro* 2:e00042. doi: 10.1042/an20100026

Chen, C., Dubin, R., and Kim, M. C. (2014). Emerging trends and new developments in regenerative medicine: a scientometric update (2000 - 2014). *Expert Opin. Biol. Ther.* 14, 1295–1317. doi: 10.1517/14712598.2014.920813

Chen, C., Hu, Z., Liu, S., and Tseng, H. (2012). Emerging trends in regenerative medicine: a scientometric analysis in CiteSpace. *Expert Opin. Biol. Ther.* 12, 593–608. doi: 10.1517/14712598.2012.674507

Chen, Y., and Wang, X. (2020). Bibliometric Analysis of Exercise and Neuropathic Pain Research. *J. Pain Res.* 13, 1533–1545. doi: 10.2147/jpr.S258696

Dieleman, J. L., Baral, R., Birger, M., Bui, A. L., Bulchis, A., Chapin, A., et al. (2016). US Spending on Personal Health Care and Public Health, 1996-2013. *JAMA* 316, 2627–2646. doi: 10.1001/jama.2016.16885

Feldman, E. L., Nave, K. A., Jensen, T. S., and Bennett, D. L. H. (2017). New Horizons in Diabetic Neuropathy: mechanisms, Bioenergetics, and Pain. *Neuron* 93, 1296–1313. doi: 10.1016/j.neuron.2017.02.005

Gore, M., Brandenburg, N. A., Hoffman, D. L., Tai, K. S., and Stacey, B. (2006). Burden of illness in painful diabetic peripheral neuropathy: the patients' perspectives. *J. Pain* 7, 892–900. doi: 10.1016/j.jpain.2006.04.013

Kandhare, A. D., Raygude, K. S., Ghosh, P., Ghule, A. E., and Bodhankar, S. L. (2012). Neuroprotective effect of naringin by modulation of endogenous biomarkers in streptozotocin induced painful diabetic neuropathy. *Fitoterapia* 83, 650–659. doi: 10.1016/j.fitote.2012.01.010

Li, C., Zhong, H., and Zhang, W. (2020). A Scientometric Analysis of Recent Literature on Arsenic Bioaccumulation and Biotransformation in Marine Ecosystems. *Bull. Environ. Contam. Toxicol.* 104, 551–558. doi: 10.1007/s00128-020-02849-2

Liang, Y. D., Li, Y., Zhao, J., Wang, X. Y., Zhu, H. Z., and Chen, X. H. (2017). Study of acupuncture for low back pain in recent 20 years: a bibliometric analysis *via* CiteSpace. *J. Pain Res.* 10, 951–964. doi: 10.2147/jpr.S132808

Liao, H., Tang, M., Luo, L., Li, C., Chiclana, F., and Zeng, X.-J. (2018). A Bibliometric Analysis and Visualization of Medical Big Data Research. *Sustainability* 10:166. doi: 10.3390/su10010166

López-Muñoz, F., Sanz-Fuentenebro, J., Rubio, G., García-García, P., and Álamo, C. (2015). Quo Vadis Clozapine? A Bibliometric Study of 45 Years of Research in International Context. *Int. J. Mol. Sci.* 16, 23012–23034. doi: 10.3390/ijms160923012

López-Muñoz, F., Shen, W. W., Pae, C. U., Moreno, R., Rubio, G., Molina, J. D., et al. (2013). Trends in scientific literature on atypical antipsychotics in South Korea: a bibliometric study. *Psychiatry Investig.* 10, 8–16. doi: 10.4306/pi.2013.10.1.8

Nobanee, H. (2021). A Bibliometric Review of Big Data in Finance. *Big Data* 9, 73–78. doi: 10.1089/big.2021.29044.edi

Peng, M. S., Wang, R., Wang, Y. Z., Chen, C. C., Wang, J., Liu, X. C., et al. (2022). Efficacy of therapeutic aquatic exercise vs physical therapy modalities for patients with chronic low back pain: a randomized clinical trial. *JAMA Netw. Open* 5:e2142069. doi: 10.1001/jamanetworkopen.2021.42069

Redondo, M., Leon, L., Povedano, F. J., Abasolo, L., Perez-Nieto, M. A., and López-Muñoz, F. (2017). A bibliometric study of the scientific publications on patient-reported outcomes in rheumatology. *Semin. Arthr. Rheum.* 46, 828–833. doi: 10.1016/j.semarthrit.2016.12.002

Ritzwoller, D. P., Ellis, J. L., Korner, E. J., Hartsfield, C. L., and Sadosky, A. (2009). Comorbidities, healthcare service utilization and costs for patients identified with painful DPN in a managed-care setting. *Curr. Med. Res. Opin.* 25, 1319–1328. doi: 10.1185/03007990902864749

Sabermahani, S., and Ordokhani, Y. (2021). General Lagrange-hybrid functions and numerical solution of differential equations containing piecewise constant delays with bibliometric analysis. *Appl. Math. Comput.* 395:13. doi: 10.1016/j.amc.2020.125847

Sadosky, A., Schaefer, C., Mann, R., Bergstrom, F., Baik, R., Parsons, B., et al. (2013). Burden of illness associated with painful diabetic peripheral neuropathy among adults seeking treatment in the US: results from a retrospective chart review and cross-sectional survey. *Diabetes Metab. Syndr. Obes.* 6, 79–92. doi: 10.2147/dmso.S37415

Sanjari, M., Aalaa, M., Mehrdad, N., Atlasi, R., Amini, M., Esfehani, E. N., et al. (2021). Endocrinology and metabolism research institute educational achievements on diabetes at a glance: conventional review and Scientometrics. *J. Diabetes Metab. Disord.* doi: 10.1007/s40200-021-00755-w

Schwartz, S., Etropolski, M., Shapiro, D. Y., Okamoto, A., Lange, R., Haeussler, J., et al. (2011). Safety and efficacy of tapentadol ER in patients with painful diabetic peripheral neuropathy: results of a randomized-withdrawal, placebo-controlled trial. *Curr. Med. Res. Opin.* 27, 151–162. doi: 10.1185/03007995.2010.537589

Stewart, W. F., Ricci, J. A., Chee, E., Hirsch, A. G., and Brandenburg, N. A. (2007). Lost productive time and costs due to diabetes and diabetic neuropathic pain in the US workforce. *J. Occup. Environ. Med.* 49, 672–679. doi: 10.1097/JOM.0b013e318065b83a

Tesfaye, S., Boulton, A., Dyck, P., Freeman, R., Horowitz, M., Kempler, P., et al. (2010). Diabetic neuropathies: update on definitions, diagnostic criteria, estimation of severity, and treatments. *Diabetes Care* 33, 2285–2293. doi: 10.2337/dc10-1303

Tesfaye, S., Boulton, A. J., and Dickenson, A. H. (2013a). Mechanisms and management of diabetic painful distal symmetrical polyneuropathy. *Diabetes Care* 36, 2456–2465. doi: 10.2337/dc12-1964

Tesfaye, S., Wilhelm, S., Lledo, A., Schacht, A., Tölle, T., Bouhassira, D., et al. (2013b). Duloxetine and pregabalin: high-dose monotherapy or their combination? The "COMBO-DN study"–a multinational, randomized, double-blind, parallel-group study in patients with diabetic peripheral neuropathic pain. *Pain* 154, 2616–2625. doi: 10.1016/j.pain.2013.05.043

Tesfaye, S., Vileikyte, L., Rayman, G., Sindrup, S. H., Perkins, B. A., Baconja, M., et al. (2011). Painful diabetic peripheral neuropathy: consensus recommendations on diagnosis, assessment and management. *Diabetes Metab. Res. Rev.* 27, 629–638. doi: 10.1002/dmrr.1225

Themistocleous, A. C., Ramirez, J. D., Shillo, P. R., Lees, J. G., Selvarajah, D., Orengo, C., et al. (2016). The Pain in Neuropathy Study (PiNS): a cross-sectional observational study determining the somatosensory phenotype of painful and painless diabetic neuropathy. *Pain* 157, 1132–1145. doi: 10.1097/j.pain.0000000000000491

Wang, R., Weng, L., Peng, M., and Wang, X. (2020). Exercise for low back pain: a bibliometric analysis of global research from 1980 to 2018. *J. Rehabilit. Med.* 52:jrm00052. doi: 10.2340/16501977-2674

Weng, L., Zheng, Y., Peng, M., Chang, T., Wu, B., and Wang, X. (2020). A Bibliometric Analysis of Nonspecific Low Back Pain Research. *Pain Res. Manag.* 2020, 5396734. doi: 10.1155/2020/5396734

Wu, B., Zhou, L., Chen, C., Wang, J., Hu, L. I., and Wang, X. (2022). Effects of exercise-induced hypoalgesia and its neural mechanisms. *Med. Sci. Sports Exerc.* 54, 220–231. doi: 10.1249/mss.0000000000002781

Xieling, C., Di, Z., Haoran, X., and Lee, W. F. (2021). Past, present, and future of smart figurelearning: a topic-based bibliometric analysis. *Int. J. Educ. Technol. Higher Educ.* 18:2.

Yao, L., Hui, L., Yang, Z., Chen, X., and Xiao, A. (2020). Freshwater microplastics pollution: detecting and visualizing emerging trends based on

Citespace II. *Chemosphere* 245:125627. doi: 10.1016/j.chemosphere.2019.125627

Yarnitsky, D., Granot, M., Nahman-Averbuch, H., Khamaisi, M., and Granovsky, Y. (2012). Conditioned pain modulation predicts duloxetine efficacy in painful diabetic neuropathy. *Pain* 153, 1193–1198. doi: 10.1016/j.pain.2012.02.021

Zheng, K., Chen, C., Yang, S., and Wang, X. (2021). Aerobic exercise attenuates pain sensitivity: an event-related potential study. *Front. Neurosci.* 15:735470. doi: 10.3389/fnins.2021.735470

Conflict of Interest: The authors declare that the research was conducted in the absence of any commercial or financial relationships that could be construed as a potential conflict of interest.

Publisher's Note: All claims expressed in this article are solely those of the authors and do not necessarily represent those of their affiliated organizations, or those of the publisher, the editors and the reviewers. Any product that may be evaluated in this article, or claim that may be made by its manufacturer, is not guaranteed or endorsed by the publisher.

frontiers | Frontiers in Molecular Neuroscience

ORIGINAL RESEARCH
published: 21 April 2022
doi: 10.3389/fnmol.2022.846554

Computational Analysis of the Immune Infiltration Pattern and Candidate Diagnostic Biomarkers in Lumbar Disc Herniation

Kai Li†, Shijue Li†, Haojie Zhang, Di Lei, Wai Leung Ambrose Lo and Minghui Ding**

Department of Rehabilitation Medicine, The First Affiliated Hospital, Sun Yat-sen University, Guangzhou, China

Objectives: Lumbar disc herniation (LDH) is a musculoskeletal disease that contributes to low back pain, sciatica, and movement disorder. Existing studies have suggested that the immune environment factors are the primary contributions to LDH. However, its etiology remains unknown. We sought to identify the potential diagnostic biomarkers and analyze the immune infiltration pattern in LDH.

Methods: The whole-blood gene expression level profiles of GSE124272 and GSE150408 were downloaded from the Gene Expression Omnibus (GEO) database, including that of 25 patients with LDH and 25 healthy volunteers. After merging the two microarray datasets, Differentially Expressed Genes (DEGs) were screened, and a functional correlation analysis was performed. The Least Absolute Shrinkage and Selection Operator (LASSO) logistic regression algorithm and support vector machine recursive feature elimination (SVM-RFE) were applied to identify diagnostic biomarkers by a cross-validation method. Then, the GSE42611 dataset was used as a validation dataset to detect the expression level of these diagnostic biomarkers in the nucleus pulposus and evaluate their accuracy. The hub genes in the network were identified by the CIBERSORT tool and the Weighted Gene Coexpression Network Analysis (WGCNA). A Spearman correlation analysis between diagnostic markers and infiltrating immune cells was conducted to further illustrate the molecular immune mechanism of LDH.

Results: The azurophil granule and the systemic lupus erythematosus pathway were significantly different between the healthy group and the LDH group after gene enrichment analysis. The XLOC_l2_012836, lnc-FGD3-1, and scavenger receptor class A member 5 were correlated with the immune cell infiltration in various degrees. In addition, five hub genes that correlated with LDH were identified, including AQP9, SIRPB2, SLC16A3, LILRB3, and HSPA6.

Conclusion: The XLOC_l2_012836, lnc-FGD3-1, and SCARA5 might be adopted for the early diagnosis of LDH. The five identified hub genes might have similar pathological mechanisms that contribute to the degeneration of the lumbar disc. The identified hub genes and immune infiltrating pattern extend the knowledge on the potential functioning mechanisms, which offer guidance for the development of therapeutic targets of LDH.

Keywords: lumbar disc herniation, GEO dataset, diagnostic biomarkers, immune cell infiltration, pain

OPEN ACCESS

Edited by:
Wen Wu,
Southern Medical University, China

Reviewed by:
Qingquan Kong,
Sichuan University, China
Wei Wei,
Affiliated Hospital of Shandong University of Traditional Chinese Medicine, China

****Correspondence:***
Wai Leung Ambrose Lo
luowliang@mail.sysu.edu.cn
Minghui Ding
dingmh@mail.sysu.edu.cn

† These authors have contributed equally to this work

Specialty section:
This article was submitted to Pain Mechanisms and Modulators, a section of the journal Frontiers in Molecular Neuroscience

Received: *31 December 2021*
Accepted: *21 February 2022*
Published: *21 April 2022*

Citation:
Li K, Li S, Zhang H, Lei D, Lo WLA and Ding M (2022) Computational Analysis of the Immune Infiltration Pattern and Candidate Diagnostic Biomarkers in Lumbar Disc Herniation. Front. Mol. Neurosci. 15:846554. doi: 10.3389/fnmol.2022.846554

INTRODUCTION

Low back pain (LBP) affects approximately 1.71 billion people worldwide and is the main contributor to the global burden of musculoskeletal conditions (Cieza et al., 2021). Lumbar disc herniation (LDH) is a pathology that causes LBP, sciatica, and movement disorders (Clark and Horton, 2018). LDH causes LBP symptoms by mechanical compression, chemical radiculitis, and autoimmunity. However, the exact pathological immune mechanism of LDH remains unknown. A study illustrated that immune environment factors are a contributing factor to inflammation and pain exacerbation for patients with LDH. Until now, no effective medical therapy has been available for LDH. Therefore, identifying the vital biomarkers and revealing the relationship is of great significance to developing effective treatment strategies for patients with LDH.

The intervertebral disc is a fibrocartilage that connects two adjacent vertebrae. The disc consists of the outer annulus fibrosus (AF), inner nucleus pulposus (NP), and cartilage endplate (CEP). A previous study reported that intervertebral disc degeneration and aging are crucial factors that contribute to the dehydration of the NP, consequently weakening the AF (Gorth et al., 2019). As the cartilage endplate becomes weak, fissures will appear in the AF, and its shock-absorbing ability will be limited and will eventually contribute to LDH. An increasing number of studies suggest that the immune environment plays an important role in the occurrence and deterioration of LDH. Sun et al. (2020) showed that the damage of the blood-NP barrier (BNB), an immune privilege of the intervertebral disc, plays a significant role in the whole process of LDH. Therefore, identifying the differential gene expression will assist the clarification of the molecular mechanism that underpins LDH and develops new immunotherapy targets. To date, only a few studies that have investigated the molecular immune mechanism of the development of LDH were found.

MATERIALS AND METHODS

Selecting and Preprocessing Data

In the Gene Expression Omnibus (GEO) database[1], intervertebral disc degeneration and lumbar disc herniation were set as the retrieval condition. Based on the sample size and retrieval condition of the lumbar disc, the datasets GSE124272 (Wang et al., 2019) and GSE150408 (Wang et al., 2021) were selected. Whole-blood RNA-seq transcriptome data were obtained from eight patients in the GSE124272 dataset and 17 patients in the GSE150408 dataset. In addition, the patients with treatment were excluded from the transcriptome data in the GSE150408 dataset. Healthy group data were obtained from eight healthy volunteers in the GSE124272 dataset and 17 healthy volunteers in the GSE150408 dataset.

The "R" software (R v4.1.1)[2] was adopted for the analysis. The Practical Extraction and Report Language (Perl)[3] was applied to accurately handle the text formats that were required for the R package analysis. **Figure 1** shows the analysis steps in this study. Two gene expression matrices were merged, and the inter-batch differences were removed for next-stage analysis. The "ggplot2" package (Skidmore et al., 2016) was applied to draw the two-dimensional PCA cluster plot and to visualize the effect after data normalization.

Processing Data and Analyzing Enrichment

The "limma" package (Ritchie et al., 2015) was adopted to screen differentially expressed genes (DEGs), and the "ConsensusClusterPlus" package (Wilkerson and Hayes, 2010) was applied to cluster the LDH dataset into different groups on account of the expression similarity. Then, the "pheatmap" package and the "ggplot2" package (Steenwyk and Rokas, 2021) were applied to visualize the expression of DEGs. The selection criteria were $|\log2\ FC| > 1$, and false discovery rate (FDR) was < 0.05.

The "clusterProfiler," (Yu et al., 2012) "org.Hs.eg.db," "enrichplot," and "ggplot2" packages were applied to perform Gene Ontology (GO) (Gene Ontology Consortium, 2015) and Kyoto Encyclopedia of Genes and Genomes (KEGG) (Kanehisa and Goto, 2000; Kanehisa et al., 2017). Then, the "GSEABase" package and the "DOSE" were applied to analyze Disease Ontology (DO) (Yu et al., 2015) enrichment on DEGs. The GO analysis consisted of biological process (BP), molecular function (MF), and cellular component (CC). The KEGG analysis was adopted to identify the pathways of biological molecular interaction. The DO analysis was applied to explore the similarity of diseases. The level of FDR < 0.25 and $p < 0.05$ were chosen to find out the significant function enrichment.

The "clusterProfiler" package was adopted to perform Gene Set Enrichment Analysis (GSEA) (Reimand et al., 2019) on the gene expression matrix. The "c2.cp.kegg.v7.0.symbols.gmt" and "c5.go.v7.4.symbols.gmt" were applied to analyze significant enrichment between the healthy group and LDH group. Subsequently, the results were illustrated in the enrichment plot by applying the "enrichplot" package. The GSEA is another enrichment analysis to identify significant biological changes in the microarray datasets. Net enrichment score (NES), gene ratio, and p-value in the GSEA analysis were applied to verify the GO and KEGG enrichment results.

Abbreviations: LDH, Lumbar disc herniation; GEO, Gene Expression Omnibus; DEGs, Differentially Expressed Genes; LASSO, Least Absolute Shrinkage and Selection Operator; WGCNA, Weighted Gene Coexpression Network Analysis; LBP, Low back pain; AF, Annulus fibrous; NP, Nucleus pulposus; BNB, Blood-NP barrier; GO, Gene Ontology; KEGG, Kyoto Encyclopedia of Genes and Genomes; DO, Disease Ontology; BP, Biological process; MF, Molecular function; CC, Cellular component; FDR, False discovery rate; GSEA, Gene Set Enrichment Analysis; ROC, Receiver operating characteristic; TOM, Topological Overlap Matrix; GS, Gene significance; MM, Module membership; PPI, Protein-protein interaction; ICCs, Infiltrating immune cells; BPI, Bactericidal permeability-increasing protein; HRASLS, The H-RAS-like suppressor; CTSG, Cathepsin G; AQP9, Aquaporin 9; SIRPB2, Signal Regulatory Protein Beta 2; LILRB3, Leukocyte immunoglobulin-like receptor subfamily B member 3; HSPA6, Heat Shock Protein 6.

[1]https://www.ncbi.nlm.nih.gov/geo/

[2]https://www.r-project.org/

[3]https://www.perl.org/get.html

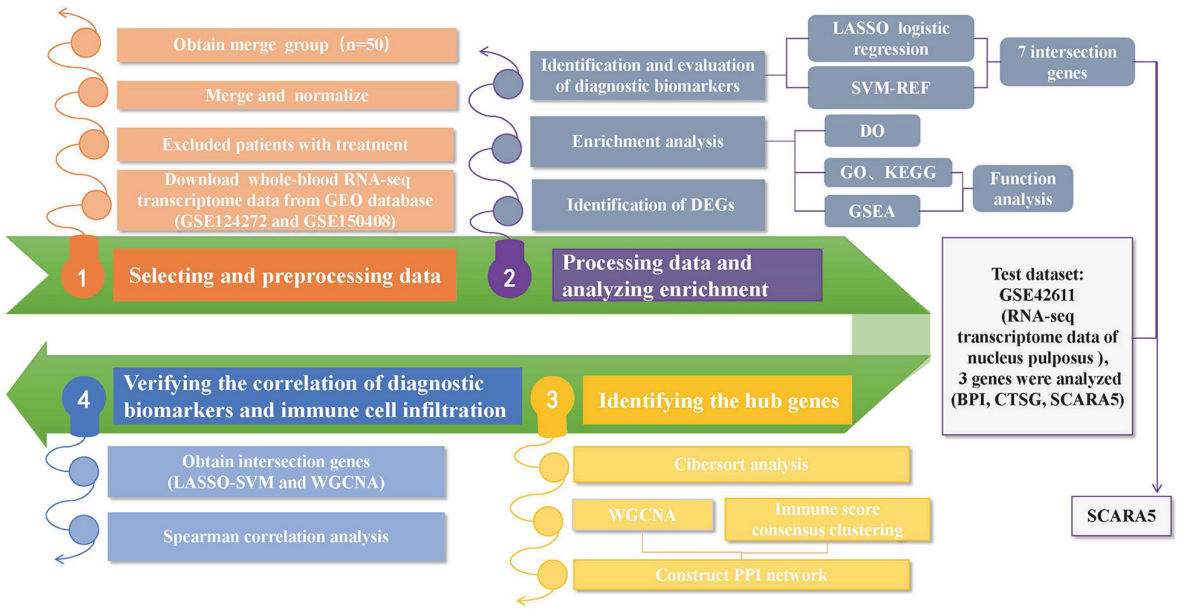

FIGURE 1 | A flow-process diagram showing the analysis steps in this study (GEO: Gene Expression Omnibus; DEGs: Differentially Expressed Genes; ROC: Receiver operating characteristic; LASSO: Least Absolute Shrinkage and Selection Operator; SVM-RFE: the support vector machine recursive feature elimination; GO: Gene Ontology; KEGG: Kyoto Encyclopedia of Genes and Genomes; DO: Disease Ontology; GSEA: Gene Set Enrichment Analysis; WGCNA: Weighted Gene Coexpression Network Analysis; PPI: Protein-protein interaction).

Screening and Verifying Diagnostic Biomarkers

The "glmnet" package was applied to analyze DEGs by the application of the Least Absolute Shrinkage and Selection Operator (LASSO) logistic regression algorithm. The feature sorting method of support vector machine recursive feature elimination (SVM-RFE) (Zhang et al., 2018) was conducted to improve the accuracy of identifying the diagnostic biomarkers by analyzing appropriate datasets selected by the LASSO algorithm to obtain biomarkers. The "e1071" package, "kernlab" package, and "caret" package were applied to identify DEGs from whole-blood gene expression profiles by applying SVM-RFE. The "VennDiagram" package was applied to draw a Venn plot which shows the screened intersection genes after using the LASSO algorithm and SVM-RFE method to analyze the gene expression profiles. The GSE42611 dataset was used as a validation dataset to detect the gene expression level of intersection genes in the nucleus pulposus. The "pROC" package was adopted to draw receiver operating characteristic (ROC) curves (Mandrekar, 2010), calculate AUC, and evaluate values of diagnostic biomarkers.

Identifying the Hub Genes

The "CIBERSORT" method (Newman et al., 2015) was applied to analyze the level of immune cell infiltration. Then, the "e1071" package was adopted to calculate the relative ratio of immune cells and immunity score (Chen et al., 2018). Moreover, the "corrplot" package was used to draw the correlation graph of 22 types of infiltrating immune cells. Due to the sample size of DEGs, the merged group was chosen to analyze and filter out the low expression data. Based on the gene difference analysis, the "ConsensusClusterPlus" package was applied to cluster the "merge" data set into different groups for gene expression similarity. Then, the "ggpubr" package was applied to analyze the immune infiltration of DEGs between the healthy group and the LDH group. Besides, the "ggplot2" package was adopted to draw a boxplot to show the difference in infiltrating immune cells.

The immune cell infiltration-related genes were identified by the Weighted Gene Coexpression Network Analysis (WGCNA) (Langfelder and Horvath, 2008), revealing the correlation between immune cell infiltration-related genes and exploring the phenotype and hub genes in the network. Total samples were clustered by average linkage and Pearson correlation value. $\beta = 4$ (scale free $R^2 = 0.9$) was chosen to construct a scale-free network (**Figure 5C**). Then, a hierarchical clustering tree was constructed by the dynamic hybrid cutting technology to construct gene modules (minimum gene number of gene modules is 50). Branches represent a series of genes with similar expression data, and each leaf represents a gene in the tree (**Figure 5D**). In addition, six modules (**Figure 5E**) were built into the analysis. A heatmap was used to show the gene expression in six modules and two groups. Afterward, cluster analysis was carried out on gene modules and the modules were merged into a new dynamic tree. Gene significance (GS) and module membership (MM) were calculated. The relationship between gene expression and sample trait (including immune cell infiltration score) was determined. Lastly, the "VennDiagram" package (Chen and Boutros, 2011) was used to draw a Venn plot and show the intersection of DEGs and gene modules. Intersection genes were analyzed using the

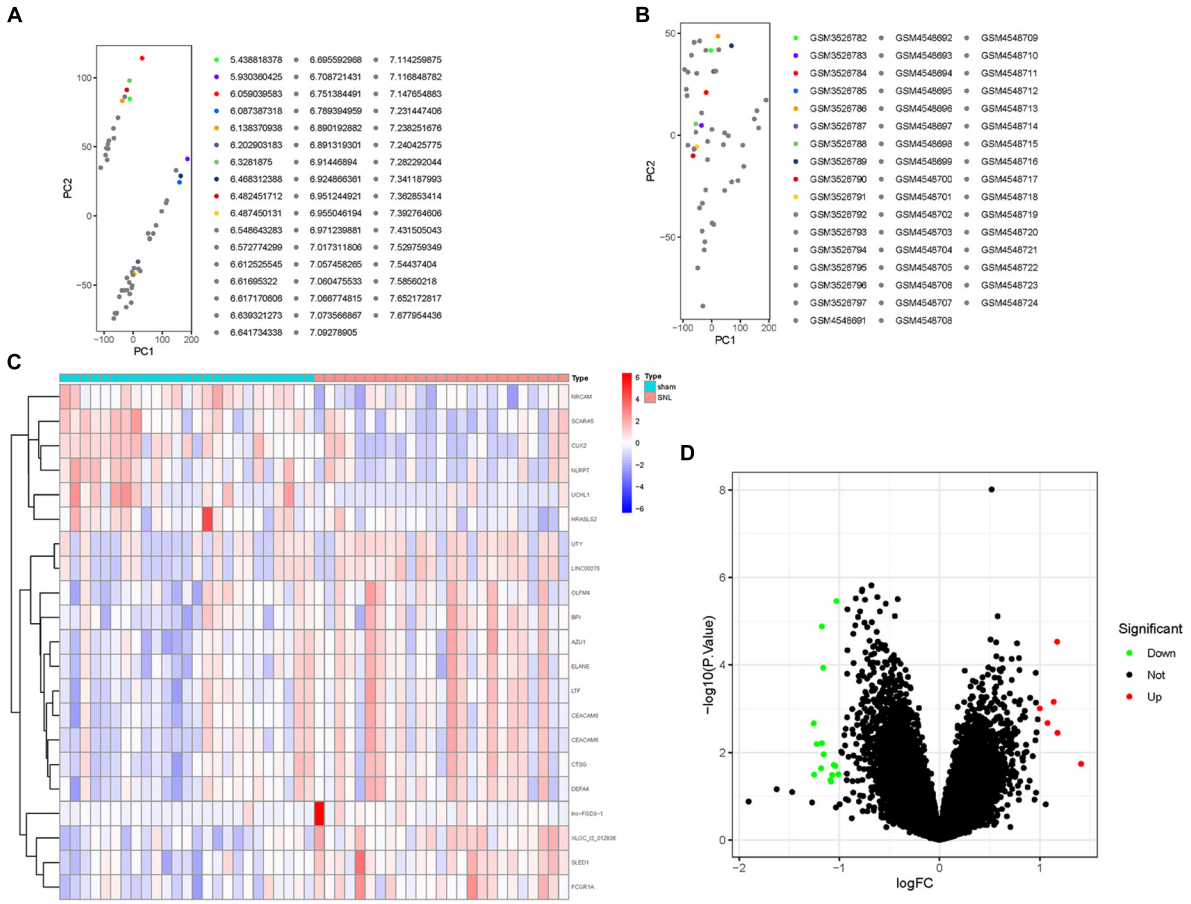

FIGURE 2 | The distribution of RNA in lumbar disc herniation (LDH) after merging the GSE124272 and the GSE150408 datasets. **(A)** In the two-dimensional PCA cluster plot of the merged dataset before normalization, with each point representing a sample. **(B)** In the two-dimensional PCA cluster plot of the merged dataset after normalization, with each point representing a sample. **(C)** The expression level of RNA in LDH. The higher the level of expression, the darker the color (red represents upregulated, green represents downregulated). The tree on the left showed the clustering results of significant RNA in different samples. The grid on the right indicated the groups (red represented normal group and blue represented LDH group). **(D)** Volcano map of differentially expressed genes (DEGs); red represents upregulated differentially expressed genes (DGEs), gray represents no significant DGEs, and green represents downregulated DGEs.

online tool STRING[4] to construct a protein-protein interaction (PPI) network (Miryala et al., 2018), and Cytoscape software (Reimand et al., 2019) was employed to investigate the interaction and identify the hub genes.

Verifying the Correlation of Diagnostic Biomarkers and Immune Cell Infiltration

The "corrplot" package was adopted to analyze the correlation of the 22 types of immune cells. In addition, intersection genes were filtered from the genes of LASSO logistic regression and significant gene modules. The "VennDiagram" package was applied to draw a Venn plot and show the intersection genes. The "ggpubr" package and the "ggExtra" package were applied to perform Spearman correlation analysis on diagnostic markers and infiltrating immune cells. Then, a lollipop drawing was applied to visualize the analysis results.

[4]https://string-db.org

RESULTS

Selecting and Preprocessing Data

The inter-batch differences between GSE124272 and GSE150408 datasets were eliminated after the two datasets merged. The clustering of the two datasets was evenly distributed after data normalization (**Figures 2A,B**), indicating a reliable sample source.

Processing Data and Analyzing Enrichment

A total of 21 DEGs between the healthy and LDH groups were identified from the merging gene expression matrix. **Figures 2C,D** illustrate the expression of DEGs. Six upregulated genes and 15 downregulated genes were found in the merging dataset.

Figure 3 illustrates the results of functional correlation analysis of GO, KEGG, and DO. The results of GO analysis

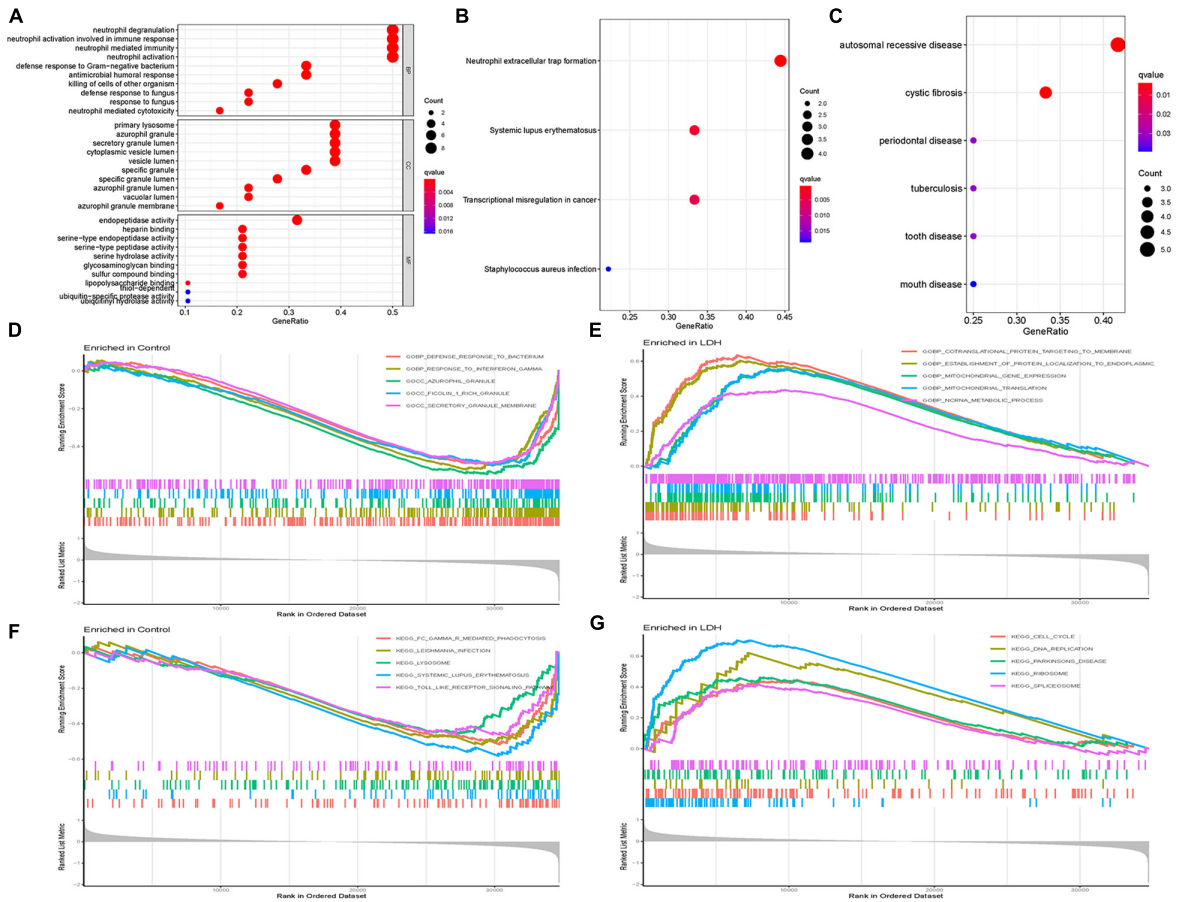

FIGURE 3 | Functional correlation analysis. **(A)** Gene Ontology (GO) enrichment analysis, where the circle size represents the count of DEGs (the larger the circle size, the more count of DEGs), and the color represents *p*-value (the redder the color, the smaller the value). GO analyses consisted of biological process (BP), molecular function (MF), and cellular component (CC). **(B)** Kyoto Encyclopedia of Genes and Genomes (KEGG) enrichment analysis, where the circle size represents the count of DEGs, and the color represents *p*-value. **(C)** Disease Ontology (DO) enrichment analysis, where the circle size represents the count of DEGs, and the color represents *p*-value. **(D)** Gene Set Enrichment Analysis (GSEA) in the normal group using annotation information of GO. **(E)** GSEA in the LDH group using annotation information of GO. **(F)** GSEA in the normal group using annotation information of KEGG. **(G)** GSEA in the LDH group using annotation information of KEGG [Net enrichment score (NES), gene ratio, and *p*-value in GSEA analysis were used to verify the GO and KEGG enrichment results].

(**Figure 3A**) suggest that DEGs are mainly involved in 3 cellular functions: BP, CC, and MF. The primary variations in BP are neutrophil degranulation, neutrophil activation in immune response, neutrophil-mediated immunity, and neutrophil activation. The main differences in CC were the primary lysosome, azurophil granule, secretory granule lumen, cytoplasmic vesicle lumen, and vesicle lumen. The most variation in MF was the endopeptidase activity. **Figure 3B** illustrates the results of the KEGG pathway analysis. It shows that DEGs were significantly enriched in neutrophil extracellular trap formation, systemic lupus erythematosus, transcriptional misregulation in cancer, and staphylococcus aureus infection. DO analysis (**Figure 3C**) revealed that DEGs were primarily related to autosomal recessive disease, cystic fibrosis, periodontal disease, tuberculosis, tooth disease, and mouth disease.

Gene Set Enrichment Analysis (GSEA) and GO analysis (**Figures 3D,E**) showed that azurophil granules were significantly different between the healthy and LDH groups. The GSEA enrichment results showed the top five significant results in the healthy and LDH group. In addition, GSEA and KEGG analysis (**Figures 3F,G**) indicated that systemic lupus erythematosus was significantly different between the healthy and LDH groups.

Screening and Verifying Diagnostic Biomarkers

Figure 4A illustrates gene numbers after using LASSO logistic regression algorithm to screen genes. **Figure 4B** presents the gene numbers after using SVM-RFE to screen genes. The ROC curves (**Figure 4E**) indicated the accuracy of five diagnostic biomarkers distinguishing the healthy and LDH patients, including XLOC_l2_012836 (AUC = 0.690), HRASLS2 (AUC = 0.736), scavenger receptor class A member 5 (SCARA5; AUC = 0.722), LINC00278 (AUC = 0.693), and lnc-FGD3-1 (AUC = 0.557). **Figure 4C** presents the seven intersection genes screened by both the LASSO and SVM-RFE methods.

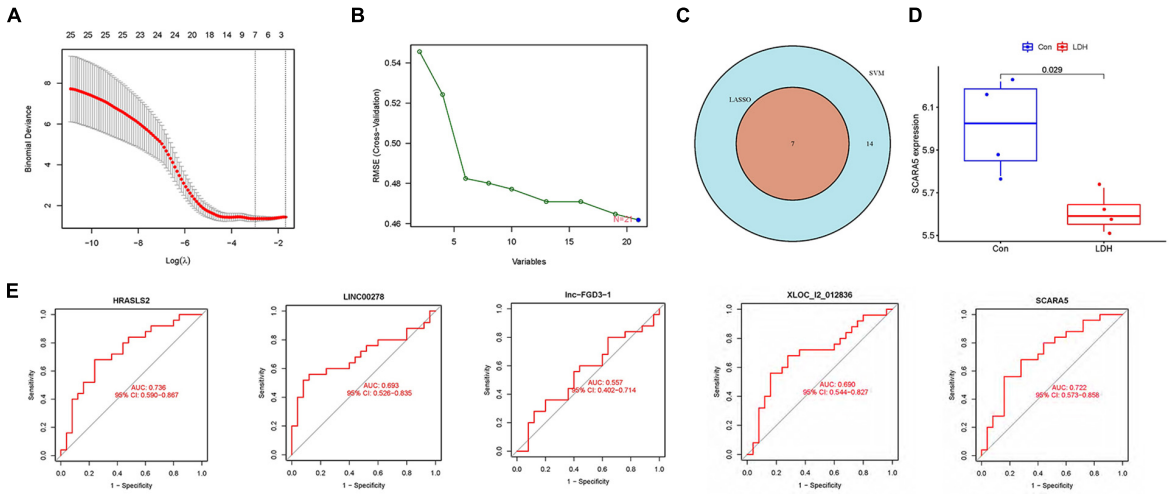

FIGURE 4 | Identification of diagnostic biomarkers in LDH. **(A)** The gene numbers screened by the LASSO. **(B)** The gene numbers screened by the support vector machine recursive feature elimination (SVM-RFE). **(C)** The Venn plot was adopted to show the intersection genes between LASSO and SVM-RFE. **(D)** The distribution of scavenger receptor class A member 5 (SCARA5) between healthy and LDH group in GSE42611 dataset. **(E)** Receiver operating characteristic (ROC) curves showed the prediction efficiency of diagnostic markers.

According to the result of the gene expression levels of three intersection genes in the GSE42611 dataset, the expression of SCARA5 was different in the nucleus pulposus (**Figure 4D**), while the expressions of Bactericidal permeability-increasing protein (BPI) and Cathepsin G (CTSG) were not significantly different.

Identifying the Hub Genes

Figure 5 illustrates the results of the WGCNA analysis. Within the six of the merged modules, two gene modules were significantly associated with LDH. Among them, the yellow module is positively correlated with LDH, and the brown module is negatively correlated with LDH. The yellow module consists of 287 genes, while the brown module consists of 384 genes. Venn plot was constructed to show the intersection genes between the two clustering groups (**Figure 5G**) and the two modules. Subsequently, 11 intersection genes were obtained between the yellow module and the clustering genes (**Figure 5G**), including ADCY4, AQP9, ATG16L2, ECEL1P2, HSPA6, LILRB3, lnc-F8A2-2, LOC101928948 (lncRNA), LOC729040 (lncRNA), SIRPB2, and SLC16A3. **Figures 6A,B** illustrate the results of the PPI network of intersection genes. As a result, five significant hub genes were identified (**Figures 6A,B**), namely, AQP9, LILRB3, HSPA6, SIRPB2, and SLC16A3. The ADCY4, AQP9, ECEL1P2, HSPA6, LILRB3, lnc-F8A2-2, LOC101928948, LOC729040, SIRPB2, and SLC16A3, all of which were found to have upregulated gene expressions. On the other hand, ATG16L2 was found to have downregulated gene expression in LDH.

Verifying the Correlation of Biomarkers and Immune Cell Infiltration

The relationships between the 22 types of immune cells of DEGs in the LDH group were analyzed (**Figure 6C**). It was found that resting natural killer (NK) cells were positively related to plasma cells and CD4 memory-activated T cells. The heatmap revealed that neutrophils had a positive relation with plasma cells, CD4-naive T cells, macrophages M0, macrophages M1, and activated mast cells while having a negative correlation with CD8 T cells, CD4 memory-activated T cells, and monocytes. Then, the boxplot of immune infiltration (**Figure 6D**) revealed that naive B cells, resting NK cells, neutrophils, and immune scores have a significant difference between the healthy and LDH groups. Subsequently, Venn plots were applied to identify diagnostic markers and perform Spearman correlation analysis. Consequently, the lnc-FGD3-1 was identified when screening intersection genes in brown modules and genes obtained by LASSO logistic regression (**Figure 6E**). The XLOC_l2_012836 (lncRNA) was also identified when screening intersection genes in yellow modules and genes obtained by LASSO logistic regression (**Figure 6E**). **Figures 6F–H** illustrate the relationship between diagnostic biomarkers and immune cell infiltration. The expression level of lnc-FGD3-1 was negatively correlated with naive B cells ($r = -0.313$, $p = 0.027$) (**Figure 6F**). In addition, the expression level of XLOC_l2_012836 was positively correlated with neutrophils ($r = 0.561$, $p < 0.001$), macrophages M0 ($r = 0.426$, $p = 0.002$), activated mast cells ($r = 0.313$, $p = 0.027$), and CD4-naive T cells ($r = 0.295$, $p = 0.038$). The expression level of XLOC_l2_012836 was negatively related with naive B cells ($r = -0.324$, $p = 0.022$) and CD8 T cells ($r = -0.346$, $p = 0.014$) (**Figure 6G**). The expression level of SCARA5 was negatively correlated with neutrophils ($r = -0.298$, $p = 0.036$) and activated mast cells ($r = -0.309$, $p = 0.029$) (**Figure 6H**).

DISCUSSION

This study aimed to identify the vital diagnostic biomarkers and hub genes and to analyze the immune cell infiltration

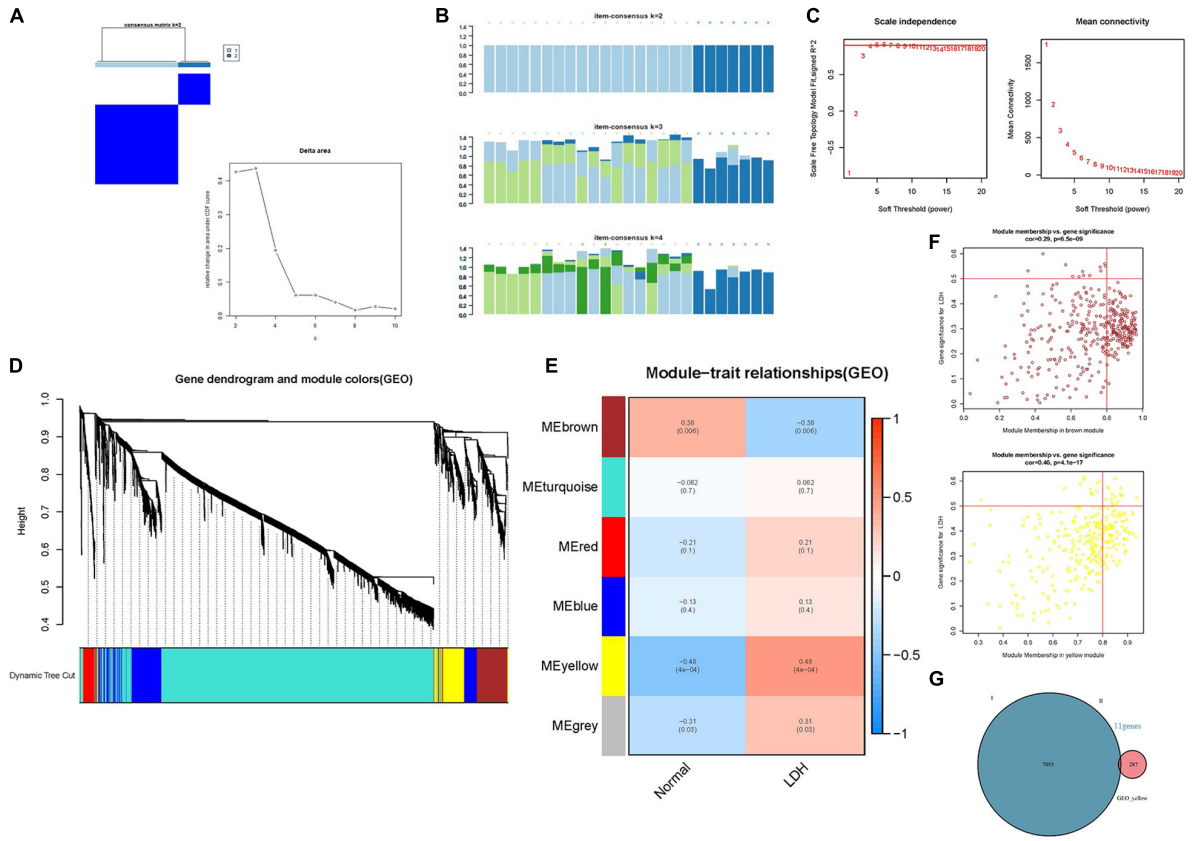

FIGURE 5 | Identification of the hub genes in LDH. **(A)** Consensus clustering matrix for k = 2 in LDH dataset [Consensus clustering cumulative distribution function (CDF) for k = 2 to 9]; **(B)** Consensus clustering matrix (Each bar represents a grid, where the more complete the bar color, the better the clustering degree); **(C)** β = 4 (scale free R^2 = 0.9) was chosen to construct a scale-free network; **(D)** A cluster tree of co-representation network modules based on 1-Tom matrix is constructed. **(E)** Module-trait relationships, where different colors represent different modules in two groups (each row corresponds to a module, and each unit includes a correlation coefficient and a *p*-value). **(F)** Module-gene relationships: each plot includes a correlation coefficient and a *p*-value. **(G)** Venn plot: identification of intersection genes between cluster genes and module genes.

patterns in the LDH population. It is observed that the genes XLOC_l2_012836, lnc-FGD3-1, and SCARA5 correlated with the immune cell infiltration to various extents, which may, therefore, act as potential diagnostic biomarkers of LDH. Five hub genes were identified that correlated with LDH, including AQP9, SIRPB2, SLC16A3, LILRB3, and HSPA6. The new hub genes and immune infiltrating pattern identification extend the knowledge of the potential lumbar disc degeneration mechanisms.

In the present study, the GSEA and GO analysis (**Figures 3D,E**) showed that azurophil granule in the LDH and healthy group was significantly different. Azurophil granules released cytotoxic and digestive agents when neutrophils were guided to the site of infection (Cowland and Borregaard, 2016). The result supports the recent theory that inflammation plays a role in the cause of LDH. In addition, the GSEA and KEGG analysis (**Figures 3F,G**) indicated that the systemic lupus erythematosus pathway was significantly different between the LDH and the healthy group. A recent study suggested that NP cells could transform into fibroblast-like cells after the injury of the intervertebral disc (Au et al., 2020). Besides, a previous study found that systemic lupus erythematosus (SLE) was associated with the proliferation of fibrous tissue cells (Yamamoto et al., 2005). Though no study had provided firm evidence to support that SLE is correlated with the development of LDH, it is reasonable to speculate that SLE may contribute to the development of LDH by promoting the transformation of NP cells in the interverbal disc.

The LASSO logistic regression determines variables by looking for optional λ when the classification error is minimal. The SVM-RFE was used to achieve better performance by analyzing the appropriate dataset selected by the LASSO algorithm to obtain biomarkers. The intersection genes from the two modules of WGCNA and LASSO logistic regression identified significant differences in lnc-FGD3-1 and XLOC_l2_012836 between the LDH and healthy groups (**Figure 6E**). A long non-coding RNA (lncRNA) was found to play a vital role in the development of LDH by regulating cell proliferation and metastasis (Tang et al., 2020). Faciogenital dysplasia 3 (FGD3) has a presumed guanine nucleotide exchange factor which plays an important role in cell migration (Hayakawa et al., 2008). The FDG3 is found in the growth plate cartilage of the femurs of mice, which is associated with articular cartilage and growth plates (Takasuga et al., 2015).

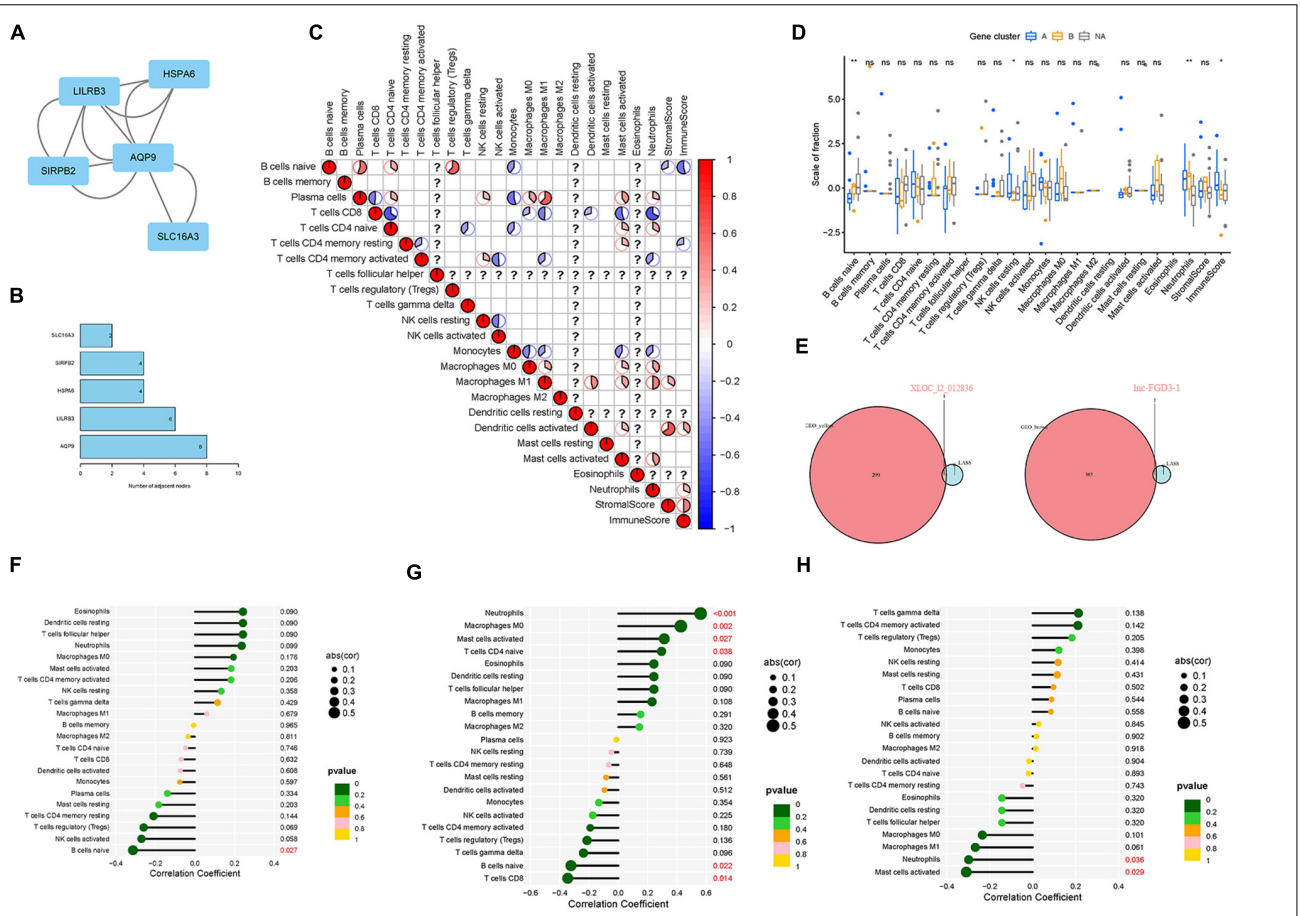

FIGURE 6 | Identification of the hub genes in LDH and verification of the correlation between diagnostic biomarkers and immune cell infiltration. **(A)** The protein-protein interaction (PPI) network was constructed to identify the hub genes; **(B)** The number of adjacent nodes correlated with protein of hub genes; **(C)** analysis of the relationship between 22 types of immune cells of DEGs in LDH; **(D)** box plot: identification of significant immune cells between normal groups and LDH group (symbol "*," "**," and "ns," respectively, stand for *p*-value under.05, *p*-value under.01, and non-significance.); **(E)** Venn plot: identification of intersection genes between biomarkers and module genes; **(F)** Expression level correlation between lnc-FGD3-1 and infiltrating immune cells; **(G)** Expression level correlation between XLOC_l2_012836 and infiltrating immune cells. **(H)** Expression level correlation between SCARA5 and infiltrating immune cells (The larger the circle size, the stronger the correlation; The color of the dots represents the *p*-value, and $p < 0.05$ was considered statistically significant).

Therefore, it is reasonable to speculate that lnc-FGD3-1 may promote the degeneration of the intervertebral disc by regulating FDG3 expression and inhibiting the growth of the cartilage endplate. In addition, XLOC_l2_012836 (lncRNA) was positively correlated with neutrophils, M0 macrophages, activated mast cells, and CD4-naive T cells, while negatively correlated with naive B cells and CD8 T cells (**Figure 6G**). A previous study (Peng et al., 2006) suggested that macrophages and mast cells may play a vital role in repairing damaged AF and subsequent disc degeneration. This is given some support by a study that reported that imbalanced counts of CD4 + T and CD4 + /CD8 + lymphocytes were correlated with LDH-related back pain. Therefore, it could be proposed that XLOC_l2_012836 promotes the development of LDH by stimulating neutrophils, M0 macrophages, activated mast cells, and CD4-naive T cells, reducing naive B cells, and CD8 T cells. It is reasonable to speculate that XLOC_l2_012836 might play a vital role in the immune response in LDH. It is also reasonable to take SCARA5 into a relationship analysis between diagnostic biomarkers and immune cells after using the external validation of the GSE42611 dataset. The expression level of SCARA5 was negatively correlated with the expression of neutrophils ($r = -0.298$, $p = 0.036$) and activated mast cells ($r = -0.309$, $p = 0.029$) (**Figure 6H**). A previous study found that the downregulation expression of SCARA5 is correlated with the proliferation of synovial (de Seny et al., 2021) and cancer cells (Yan et al., 2012). From the result of the present study, the downregulated expression of SCARA5 might promote the proliferation of the nucleus pulposus to some extent and correlate with the occurrence of inflammation. More studies are needed to further analyze the function of lncRNA.

The hub genes of AQP9, SIRPB2, SLC16A3, LILRB3, and HSPA6 were significantly different between the LDH and healthy groups (**Figures 6A,B**). Aquaporin-9 (AQP9) is a hydroglycerin channel protein that promotes water movement between cerebrospinal fluid and brain parenchyma (Badaut et al.,

2001). A study showed that AQP9 might be involved in chronic inflammation disease (Mesko et al., 2010). The downregulation of AQP9 was observed in the cartilage cells, which would cause the decomposition-related genes of stimulating the IL-1β that is down-expressed in osteoarthritis (Piccio et al., 2005). It is reasonable to suspect that the increased expression of AQP9 would promote the inflammation of CEP in the intervertebral disc, which subsequently contributes to LDH. Another potential theory is that owing to the lack of local blood supply, the NP cells settle in hypoxic conditions, which, thereby produces an increased amount of lactic acid and promotes the high expression of AQP9 (Badaut et al., 2001). Signal-regulatory protein beta 2 (SIRPB2), a transmembrane glycoprotein, is found to be expressed in the immune and central nervous system (Piccio et al., 2005). A recent study showed that the CD47 on antigen-presenting cells that engage with SIRPB2 on T cells could promote the proliferation of antigen-specific T-cells (Veillette and Chen, 2018). Therefore, the SIRPB2 might play a significant role in the immune response. The solute carrier family 16 member 3 (SLC16A3, also called MCT4), which is mainly affected by HIF-1α in NP cells at hypoxic conditions, plays a significant role in maintaining the stability of the intervertebral disc (Silagi et al., 2020). It is possible that due to the lack of blood supply, prolonged hypoxia could stimulate the increased expression of SLC16A3 and induce NP cell death. Leukocyte immunoglobulin-like receptor subfamily B member 3 (LILRB3, also called PIR-B) is found to be associated with the neutrophil activation and antibacterial effect function (Zhao et al., 2020). It might be reasonable to regard LILRB3 as an immune-induced treatment point since it can effectively inhibit immune response *in vitro* (Yeboah et al., 2020). The heat shock 70 kDa protein 6 (HSPA6) involves cell repairment and cell protection (Hageman et al., 2011). Becirovic and Brown (2017) illustrated that HSPA6 is involved in the post-stress transcriptional recovery in neurodegenerative diseases. Therefore, HSPA6 might be associated with the cell protection of LDH when facing stress. To date, there is no conclusive evidence confirming the above hub genes have the same pathological mechanism that contributes to the development of LDH. However, these genes are associated with the same factors, such as hypoxia or injury that promote the development of LDH. It might be a possible means to produce targeted therapy using these genes as the starting points.

LIMITATIONS

In the present study, the cross-validation between LASSO logistic regression algorithm and SVM-RFE was applied to identify significant genes, followed by functional enrichment analysis to identify the mechanism. The data was then analyzed using the CIBERSORT method to explore the pattern of immune cells infiltration. However, there are still limitations about the effect of diagnostic markers in LDH. First, the present research is a retrospective study. Although external validation was added in the present study, there was no clinical trial to verify the accuracy of biomarker identification. Therefore, the functional impact of these RNAs in the occurrence and development of LDH ought to be assessed by knocking out or importing studies in animal models and cell lines. Second, the present study is a secondary analysis based on the originally published dataset. Although the results were broadly consistent with previous studies, the validity of the results should be examined with reasonable doubt. Moreover, the effect of treatment on the expression of RNA was not appraised. Despite the two chosen datasets being from the same research institute to minimize the error, the small sample size may contain bias.

CONCLUSION

The present study identifies XLOC_l2_012836 (lncRNA), lnc-FGD3-1, and SCARA5 as potential genes for target therapy points. Their involvement in the development of LDH are potentially related to the immune response or inhibiting growth of cartilage endplate. The five identified hub genes are associated with the same factors of hypoxia or injury. The azurophil granule and the SLE pathway are significantly different between the healthy group and the LDH group after gene enrichment analysis. The findings of the present study provide some guidance for future research on the pathogenesis and treatment of LDH.

DATA AVAILABILITY STATEMENT

Publicly available datasets were analyzed in this study. These data can be found here: https://www.ncbi.nlm.nih.gov/geo/query/acc.cgi?acc=GSE124272; https://www.ncbi.nlm.nih.gov/geo/query/acc.cgi?acc=GSE150408; https://www.ncbi.nlm.nih.gov/geo/query/acc.cgi?acc=GSE42611.

AUTHOR CONTRIBUTIONS

KL and SL contributed to the literature search and design of the study protocol, drafted the manuscript, data collection, and data analysis. HZ and DL contributed to the data analysis and drafting of the manuscript. WL and MD managed the research and adjudicate any dispute, contributed to the funding acquisition and study management. All authors had read and approved the final manuscript, fulfilled the four authorship criteria, in addition, involved in a specific aspect of the study.

FUNDING

The present study was financially supported by the National Natural Science Foundation of China (81971224) and the Guangzhou Science and Technology Project (201803010083).

ACKNOWLEDGMENTS

We would like to thank the Gene Expression Omnibus (GEO) network for its generous sharing of large amounts of data. We also would like to thank Dr. Zhen Hua Liu for the constructive feedback, scientific advise, profound discussion and revision of the manuscript.

REFERENCES

Au, T. Y. K., Lam, T. K., Peng, Y., Wynn, S. L., Cheung, K. M. C., Cheah, K. A. E., et al. (2020). Transformation of resident notochord-descendent nucleus pulposus cells in mouse injury-induced fibrotic intervertebral discs. *Aging Cell* 19:e13254. doi: 10.1111/acel.13254

Badaut, J., Hirt, L., Granziera, C., Bogousslavsky, J., Magistretti, P. J., and Regli, L. (2001). Astrocyte-specific expression of aquaporin-9 in mouse brain is increased after transient focal cerebral ischemia. *J. Cereb. Blood Flow Metab.* 21, 477–482. doi: 10.1097/00004647-200105000-00001

Becirovic, L., and Brown, I. R. (2017). Targeting of Heat Shock Protein HSPA6 (HSP70B') to the periphery of nuclear speckles is disrupted by a transcription inhibitor following thermal stress in human neuronal cells. *Neurochem. Res.* 42, 406–414. doi: 10.1007/s11064-016-2084-9

Chen, B., Khodadoust, M. S., Liu, C. L., Newman, A. M., and Alizadeh, A. A. (2018). Profiling tumor infiltrating immune cells with CIBERSORT. *Methods Mol. Biol.* 1711, 243–259. doi: 10.1007/978-1-4939-7493-1_12

Chen, H., and Boutros, P. C. (2011). VennDiagram: a package for the generation of highly-customizable Venn and Euler diagrams in R. *BMC Bioinformatics* 12:35. doi: 10.1186/1471-2105-12-35

Cieza, A., Causey, K., Kamenov, K., Hanson, S. W., Chatterji, S., and Vos, T. (2021). Global estimates of the need for rehabilitation based on the Global Burden of Disease study 2019: a systematic analysis for the Global Burden of Disease study 2019. *Lancet* 396, 2006–2017. doi: 10.1016/S0140-6736(20)32340-0

Clark, S., and Horton, R. (2018). Low back pain: a major global challenge. *Lancet* 391:2302. doi: 10.1016/S0140-6736(18)30725-6

Cowland, J. B., and Borregaard, N. (2016). Granulopoiesis and granules of human neutrophils. *Immunol. Rev.* 273, 11–28. doi: 10.1111/imr.12440

de Seny, D., Baiwir, D., Bianchi, E., Cobraiville, G., Deroyer, C., Poulet, C., et al. (2021). New Proteins contributing to immune cell infiltration and pannus formation of synovial membrane from arthritis diseases. *Int. J. Mol. Sci.* 23:434. doi: 10.3390/ijms23010434

Gene Ontology Consortium (2015). Gene Ontology Consortium: going forward. *Nucleic Acids Res.* 43, D1049–D1056. doi: 10.1093/nar/gku1179

Gorth, D. J., Shapiro, I. M., and Risbud, M. V. A. (2019). New understanding of the role of IL-1 in age-related intervertebral disc degeneration in a murine model. *J. Bone Miner. Res.* 34, 1531–1542. doi: 10.1002/jbmr.3714

Hageman, J., van Waarde, M. A., Zylicz, A., Walerych, D., and Kampinga, H. H. (2011). The diverse members of the mammalian HSP70 machine show distinct chaperone-like activities. *Biochem. J.* 435, 127–142. doi: 10.1042/BJ20101247

Hayakawa, M., Matsushima, M., Hagiwara, H., Oshima, T., Fujino, T., Ando, K., et al. (2008). Novel insights into FGD3, a putative GEF for Cdc42, that undergoes SCF(FWD1/beta-TrCP)-mediated proteasomal degradation analogous to that of its homologue FGD1 but regulates cell morphology and motility differently from FGD1. *Genes Cells* 13, 329–342. doi: 10.1111/j.1365-2443.2008.01168.x

Kanehisa, M., and Goto, S. (2000). KEGG: kyoto encyclopedia of genes and genomes. *Nucleic Acids Res.* 28, 27–30.

Kanehisa, M., Furumichi, M., Tanabe, M., Sato, Y., and Morishima, K. (2017). KEGG: new perspectives on genomes, pathways, diseases and drugs. *Nucleic Acids Res.* 45, D353–D361. doi: 10.1093/nar/gkw1092

Langfelder, P., and Horvath, S. (2008). WGCNA: an R package for weighted correlation network analysis. *BMC Bioinformatics* 9:559. doi: 10.1186/1471-2105-9-559

Mandrekar, J. N. (2010). Receiver operating characteristic curve in diagnostic test assessment. *J. Thorac. Oncol.* 5, 1315–1316. doi: 10.1097/JTO.0b013e3181ec173d

Mesko, B., Poliska, S., Szegedi, A., Szekanecz, Z., Palatka, K., Papp, M., et al. (2010). Peripheral blood gene expression patterns discriminate among chronic inflammatory diseases and healthy controls and identify novel targets. *BMC Med. Genomics* 3:15. doi: 10.1186/1755-8794-3-15

Miryala, S. K., Anbarasu, A., and Ramaiah, S. (2018). Discerning molecular interactions: a comprehensive review on biomolecular interaction databases and network analysis tools. *Gene* 642, 84–94. doi: 10.1016/j.gene.2017.11.028

Newman, A. M., Liu, C. L., Green, M. R., Feng, W., Xu, Y., Hoang, C. D., et al. (2015). Robust enumeration of cell subsets from tissue expression profiles. *Nat. Methods* 12, 453–457. doi: 10.1038/nmeth.3337

Peng, B., Hao, J., Hou, S., Wu, W., Jiang, D., Fu, X., et al. (2006). Possible pathogenesis of painful intervertebral disc degeneration. *Spine* 31, 560–566. doi: 10.1097/01.brs.0000201324.45537.46

Piccio, L., Vermi, W., Boles, K. S., Fuchs, A., Strader, C. A., Facchetti, F., et al. (2005). Adhesion of human T cells to antigen-presenting cells through SIRPbeta2-CD47 interaction costimulates T-cell proliferation. *Blood* 105, 2421–2427. doi: 10.1182/blood-2004-07-2823

Reimand, J., Isserlin, R., Voisin, V., Kucera, M., Tannus-Lopes, C., Rostamianfar, A., et al. (2019). Pathway enrichment analysis and visualization of omics data using g:Profiler, GSEA, Cytoscape and EnrichmentMap. *Nat. Protoc.* 14, 482–517. doi: 10.1038/s41596-018-0103-9

Ritchie, M. E., Phipson, B., Wu, D., Hu, Y., Law, C. W., Shi, W., et al. (2015). limma powers differential expression analyses for RNA-sequencing and microarray studies. *Nucleic Acids Res.* 43:e47. doi: 10.1093/nar/gkv007

Silagi, E. S., Novais, E. J., Bisetto, S., Telonis, A. G., Snuggs, J., Le Maitre, C. L., et al. (2020). Lactate efflux from intervertebral disc cells is required for maintenance of spine health. *J. Bone Miner. Res.* 35, 550–570. doi: 10.1002/jbmr.3908

Skidmore, Z. L., Wagner, A. H., Lesurf, R., Campbell, K. M., Kunisaki, J., Griffith, O. L., et al. (2016). GenVisR: genomic visualizations in R. *Bioinformatics* 32, 3012–3014. doi: 10.1093/bioinformatics/btw325

Steenwyk, J. L., and Rokas, A. (2021). ggpubfigs: colorblind-Friendly color palettes and ggplot2 graphic system extensions for publication-quality scientific figures. *Microbiol. Resour. Announc.* 10:e0087121. doi: 10.1128/MRA.00871-21

Sun, Z., Liu, B., and Luo, Z. J. (2020). The immune privilege of the intervertebral disc: implications for intervertebral disc degeneration treatment. *Int. J. Med. Sci.* 17, 685–692. doi: 10.7150/ijms.42238

Takasuga, A., Sato, K., Nakamura, R., Saito, Y., Sasaki, S., Tsuji, T., et al. (2015). Non-synonymous FGD3 variant as positional candidate for disproportional tall stature accounting for a carcass weight QTL (CW-3) and skeletal dysplasia in Japanese black cattle. *PLoS Genet.* 11:e1005433. doi: 10.1371/journal.pgen.1005433

Tang, N., Dong, Y., Xiao, T., and Zhao, H. (2020). LncRNA TUG1 promotes the intervertebral disc degeneration and nucleus pulposus cell apoptosis though modulating miR-26a/HMGB1 axis and regulating NF-kappaB activation. *Am. J. Transl. Res.* 12, 5449–5464.

Veillette, A., and Chen, J. (2018). SIRPalpha-CD47 immune checkpoint blockade in anticancer therapy. *Trends Immunol.* 39, 173–184. doi: 10.1016/j.it.2017.12.005

Wang, Y., Dai, G., Jiang, L., Liao, S., and Xia, J. (2021). Microarray analysis reveals an inflammatory transcriptomic signature in peripheral blood for sciatica. *BMC Neurol.* 21:50. doi: 10.1186/s12883-021-02078-y

Wang, Y., Dai, G., Li, L., Liu, L., Jiang, L., Li, S., et al. (2019). Transcriptome signatures reveal candidate key genes in the whole blood of patients with lumbar disc prolapse. *Exp. Ther. Med.* 18, 4591–4602. doi: 10.3892/etm.2019.8137

Wilkerson, M. D., and Hayes, D. N. (2010). ConsensusClusterPlus: a class discovery tool with confidence assessments and item tracking. *Bioinformatics* 26, 1572–1573. doi: 10.1093/bioinformatics/btq170

Yamamoto, T., Sumi, K., Yokozeki, H., and Nishioka, K. (2005). Multiple cutaneous fibrous histiocytomas in association with systemic lupus erythematosus. *J. Dermatol.* 32, 645–649. doi: 10.1111/j.1346-8138.2005.tb00815.x

Yan, N., Zhang, S., Yang, Y., Cheng, L., Li, C., Dai, L., et al. (2012). Therapeutic upregulation of Class A scavenger receptor member 5 inhibits tumor growth and metastasis. *Cancer Sci.* 103, 1631–1639. doi: 10.1111/j.1349-7006.2012.02350.x

Yeboah, M., Papagregoriou, C., Jones, D. C., Chan, H. T. C., Hu, G., McPartlan, J. S., et al. (2020). LILRB3 (ILT5) is a myeloid cell checkpoint that elicits profound immunomodulation. *JCI Insight* 5:e141593. doi: 10.1172/jci.insight.141593

Yu, G., Wang, L. G., Han, Y., and He, Q. Y. (2012). clusterProfiler: an R package for comparing biological themes among gene clusters. *OMICS* 16, 284–287. doi: 10.1089/omi.2011.0118

Yu, G., Wang, L. G., Yan, G. R., and He, Q. Y. (2015). DOSE: an R/Bioconductor package for disease ontology semantic and enrichment analysis. *Bioinformatics* 31, 608–609. doi: 10.1093/bioinformatics/btu684

Zhang, Y., Deng, Q., Liang, W., and Zou, X. (2018). An efficient feature selection strategy based on multiple support vector machine technology with gene expression data. *Biomed. Res. Int.* 2018:7538204. doi: 10.1155/2018/7538204

Zhao, Y., van Woudenbergh, E., Zhu, J., Heck, A. J. R., van Kessel, K. P. M., de Haas, C. J. C., et al. (2020). The orphan immune receptor LILRB3 modulates fc receptor-mediated functions of neutrophils. *J. Immunol.* 204, 954–966. doi: 10.4049/jimmunol.1900852

Conflict of Interest: The authors declare that the research was conducted in the absence of any commercial or financial relationships that could be construed as a potential conflict of interest.

Publisher's Note: All claims expressed in this article are solely those of the authors and do not necessarily represent those of their affiliated organizations, or those of the publisher, the editors and the reviewers. Any product that may be evaluated in this article, or claim that may be made by its manufacturer, is not guaranteed or endorsed by the publisher.

frontiers | Frontiers in Molecular Neuroscience

ORIGINAL RESEARCH
published: 13 May 2022
doi: 10.3389/fnmol.2022.905679

Research Hotspots and Frontiers in Post Stroke Pain: A Bibliometric Analysis Study

Chong Li[1,2,3], *Xiaoyi Shu*[1,2,3] *and Xiangyun Liu*[1,2,3]*

[1] School of Kinesiology, Shanghai University of Sport, Shanghai, China, [2] Shanghai Key Laboratory of Sports Ability Support and Development, Shanghai, China, [3] Shanghai Frontiers Science Research Base of Exercise and Metabolic Health, Shanghai, China

Background: Pain is a common complication after stroke with a high incidence and mortality rate. Many studies in the field of pain after stroke have been published in various journals. However, bibliometric analysis in the domain of pain after stroke is still lacking. This study aimed to deliver a visual analysis to analyze the global trends in research on the comorbidity of pain after stroke in the last 12 years.

Methods: The publications from the Web of Science (WoS) in the last 12 years (from 2010 to 2021) were collected and retrieved. CiteSpace software was used to analyze the relationship of publication year with countries, institutions, journals, authors, references, and keywords.

Results: A total of 322 publications were included in the analysis. A continuous but unstable growth in the number of articles published on pain after stroke was observed over the last 12 years. The Peoples' R China (65), Chang Gung University (10), and *Topic in Stroke Rehabilitation* (16) were the country, institution, and journal with the highest number of publications, respectively. Analysis of keywords showed that shoulder pain after stroke and central post-stroke pain were the research development trends and focus in this research field.

Conclusion: This study provides a visual analysis method for the trend and frontiers of pain research after stroke. In the future, large sample, randomized controlled trials are needed to identify the potential treatments and pathophysiology for pain after stroke.

Keywords: pain, stroke, CiteSpace, visual analysis, bibliometric

OPEN ACCESS

Edited by:
Jie Jia,
Huashan Hospital Affiliated to Fudan University, China

Reviewed by:
Mengchen Yin,
Shanghai University of Traditional Chinese Medicine, China
Hao Liu,
JORU Rehabilitation Hospital, China

***Correspondence:**
Xiangyun Liu
liuxy_666666@126.com

Specialty section:
This article was submitted to Pain Mechanisms and Modulators, a section of the journal Frontiers in Molecular Neuroscience

Received: *27 March 2022*
Accepted: *06 April 2022*
Published: *13 May 2022*

Citation:
Li C, Shu X and Liu X (2022) Research Hotspots and Frontiers in Post Stroke Pain: A Bibliometric Analysis Study. Front. Mol. Neurosci. 15:905679. doi: 10.3389/fnmol.2022.905679

INTRODUCTION

Pain is a common complication of stroke, reported in 10–45.8% of patients with stroke (Yang and Chang, 2021; Zhang et al., 2021a). Pain after stroke can hinder the progress of rehabilitation and decrease the quality of life in stroke survivors (Payton and Soundy, 2020; Wang and Liu, 2021; Zhang et al., 2021b). However, due to cognitive impairment or lack of communication, pain after stroke is frequently overlooked. Pain is often missed clinically due to a low disclosure rate. The main subtypes of pain after stroke include central post-stroke pain (CPSP), complex regional pain syndrome (CRPS), shoulder pain, and spasticity-related pain (Delpont et al., 2018; Torres-Parada et al., 2020; Yang and Chang, 2021). Many patients persistently experience at least one subtype. Pain after stroke is not always responsive to conventional painkillers (Choi et al., 2021; Haslam et al., 2021). In

addition, owing to unclear pathophysiology, effective methods for the treatment of pain after stroke are still limited.

Given the high incidence of post-stroke pain, an increasing number of researchers have studied pain after stroke, and related articles have been published in academic journals (Elias et al., 2020; Scuteri et al., 2020; Chiu et al., 2021; Zhang et al., 2021b). Some studies have investigated non-drug interventions to relieve pain after stroke (Kadono et al., 2021; Malfitano et al., 2021; Zhao et al., 2021). However, a quantitative analysis of publications on pain after stroke has not yet been conducted.

Data visualization is a technology that uses computer graphics and image processing technology to convert data into graphics and display them on the screen and process them interactively (Chen, 2004). Based on co-citation analysis theory and pathfinding network algorithm, CiteSpace software can analyze literature of specific disciplines or fields from multiple perspectives and draw visual maps to explore the critical paths, research hotspots, and frontiers of the evolution of this discipline or field (Chen and Song, 2019). In recent years, using CiteSpace software combined with relevant authoritative databases to visually analyze the literature of a certain discipline or field has become a hot research topic for scholars all over the world (Yin et al., 2020, 2021; Wang et al., 2021; Wu et al., 2021; Yuan et al., 2021).

To address the weakness of quantitative analysis for studies involved in pain after stroke, the objective of this study is to perform bibliometric analysis for the global scientific research on pain after stroke using CiteSpace. The results of the present study would provide valuable reference information for researchers and promote cooperation among various countries and institutions.

METHODS AND MATERIALS

Data Source and Search Strategy

A bibliometric literature search was performed from 01 January 2010 to 31 December 2021 on the core collection database of Web of Science (WoS). For the search, two Medical Subject Heading (MeSH) terms were used. Term A was "stroke." Term B was "pain." The search terms were as follows: TS = (stroke) AND TS = (pain).

Inclusion and Exclusion Criteria

Studies related to pain after stroke were selected after screening the title and abstract. Only articles and reviews were included. Other document types, such as letters, commentaries, and meeting abstracts, were excluded. In addition, the publication language was limited to English. The flow chart of the inclusion is shown in **Figure 1**. Finally, 322 records (276 articles and 46 reviews) were identified for final analysis.

Analytic Methods

Software Parameter Settings

CiteSpace is a visualization software developed by Professor Chen Chaomei (Drexel University, USA) for bibliometric analysis. We used CiteSpace 5.8.R3 to analyze the final records. The 'Time Sliding' value was set to 1 year. The type of node was selected according to the purpose of the analysis.

Interpretation of Main Parameters in Visualization Map

Cluster view and burst detection: cluster view is carried out on the generated map, and each cluster is labeled by citing the title, keywords, and subject headings in the abstract of the citing reference. The function of burst detection is to detect the situation where there is a great change in the number of citations in a certain period. Thus, it can be used to find the decline or rise of keywords.

Dual-map overlaps: dual-map overlaps are a new method to display the distribution and citation trajectory of articles in various disciplines. As a result, there is a distribution of citing journals on the left side and a distribution of cited journals on the right side. The curve is the citation line, which completely shows the context of the citation.

RESULTS

Publication Outputs Analysis

A total of 322 articles were included in the analysis. **Figure 2A** shows the distribution of annual publication of pain after stroke from 2010 to 2021. The overall trend of publications is positively increasing, and the time trend of publications indicated a significant correlation ($R^2 = 0.5518$, $p<0.01$) between the annual

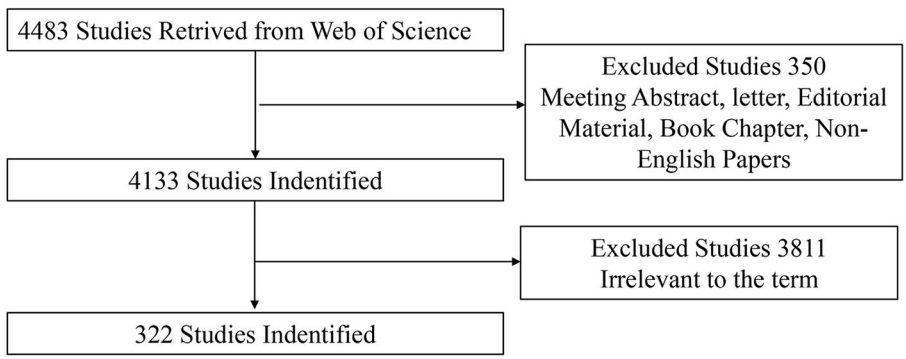

FIGURE 1 | Flowchart of studies inclusion.

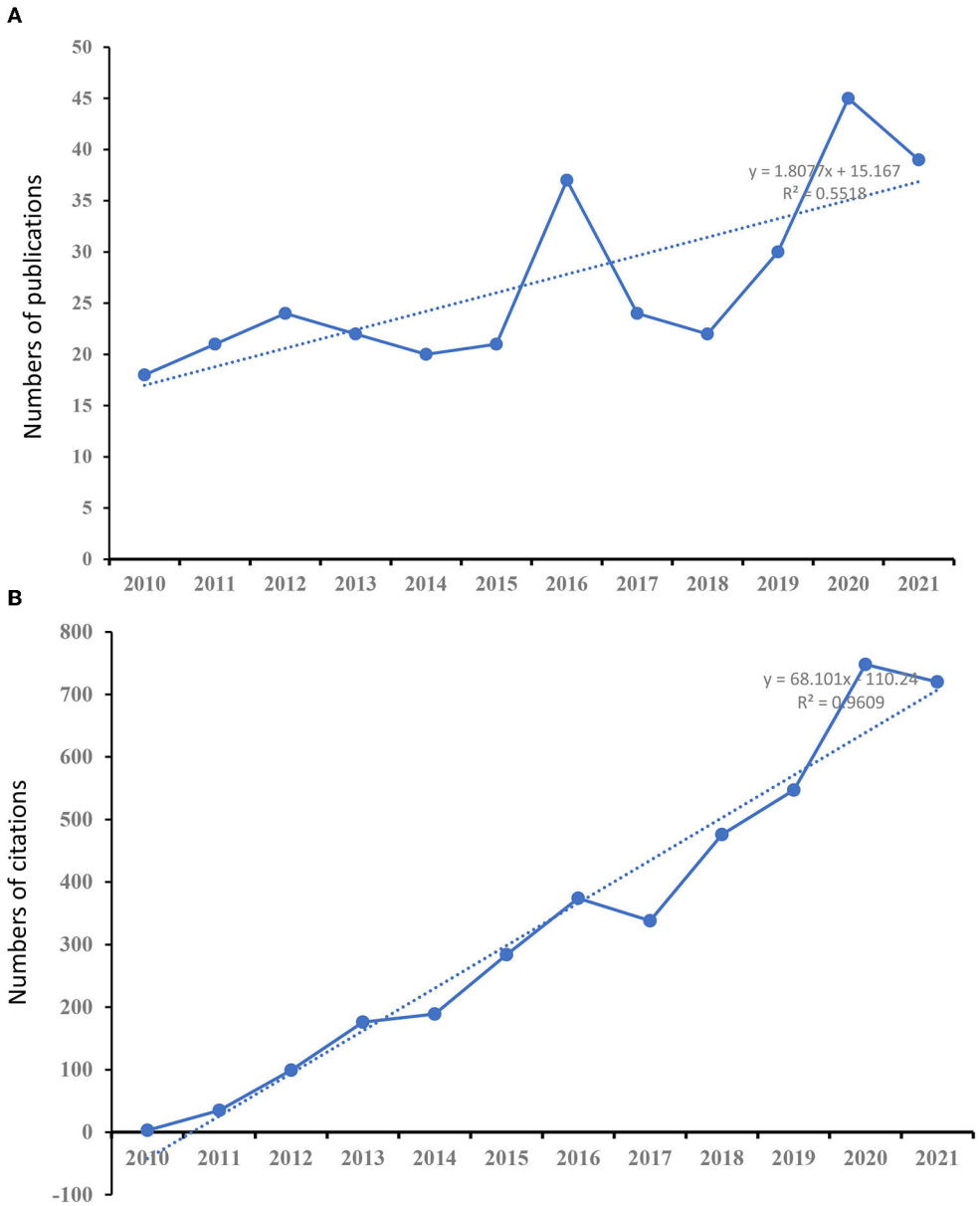

FIGURE 2 | The number of publications and citations. **(A)** The number of annual publications on studies of pain after stroke from 2010 to 2021. **(B)** The number of annual citations on studies of pain after stroke research from 2010 to 2021.

publication outputs and the years in the last 12 years. **Figure 2B** shows the distribution of annual citations of included studies. The number of citations increased from 3 in 2010 to 720 in 2021. The overall trend is positive and the time trend of citations indicated a significant correlation ($R^2 = 0.9609$, $p<0.001$). The highest average number of citations per article (33.83), citations (711) occurred in 2011. The highest H-index was found in 2012, and the most published articles (45) were recorded in 2020 (**Figure 3**).

Authoritative Journals Analysis

The included 322 studies were published in 156 academic journals. The information of the top 15 journals is shown in **Table 1**. In the top 15 journals, *Topic in Stroke Rehabilitation* contributed the most published articles (16), followed by *Pain* (12) and *Frontiers in Neurology* (9). *Pain* showed the most citations (335). *Stroke* had the highest average per article citations (45.8) and impact factor (IF = 7.914). *Frontiers in Neurology* presented with the greatest open access value of 9.

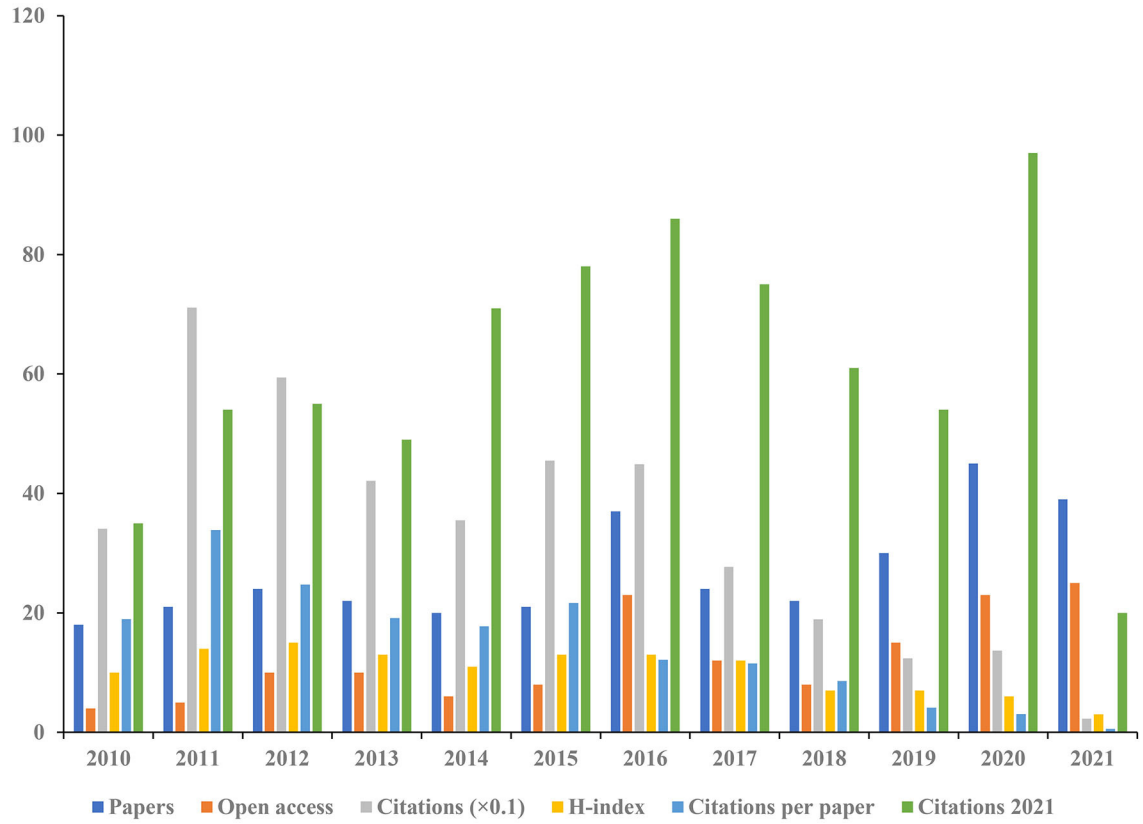

FIGURE 3 | The number of articles, open-access articles, citations, citations per article, citations in 2021, and H-index for each year.

Based on the Blondel algorithm, dual-map overlaps of journals are displayed in **Figure 4**. The citing journals of 322 studies were mainly from the fields of Medicine, Medical, Neurology, and Sports. The cited journals were mainly from the fields of Health, Medicine, Sports, and Rehabilitation.

Subject Categories of WoS Analysis

We classified the 322 papers into 45 subject categories of WoS. The top 15 categories are demonstrated in **Figure 5**. Among the top 15 subject categories, *Clinical Neurology* ranked the largest number of articles (109), open-access articles (45), citations (1864), and the highest H-index value (24). *Peripheral Vascular Disease* had the largest number of citations per article (27.43).

References Analysis

The clustered research categories of reference co-citation analysis were divided into 13 groups (#0–12). The timeline view of clusters is shown in **Figure 6**, which presents the characteristics of the time-span citation information for the cluster domains. The largest cluster (#0) has 42 members, which is labeled as *hemiplegic shoulder pain* by Latent Semantic Indexing (LSI). The most relevant citer to the cluster is "Persistent shoulder pain in the first 6 months after stroke: results of a prospective cohort study" (Roosink et al., 2011). The second-largest cluster (#1) has 34 members labeled as *central post-stroke pain* by LSI. The most relevant citer to the cluster is "Prevalence and management challenges in central post-stroke neuropathic pain: a systematic review and meta-analysis" (Liampas et al., 2020).

The Sigma value can be used to identify innovative references. Five innovative references are summarized in **Table 2**. Three articles are observational studies and two articles are reviews.

Authoritative Countries and Institutions Analysis

Figure 7 shows the top 15 countries in terms of the number of publications on pain after stroke. The highest numbers of publications (65) and open access value (37) were reported in China. The United States had the highest number of citations (941) and H-index (18). Denmark ranked the highest numbers of citation per article (40.71).

Figure 8 shows the top 15 institutions based on the number of publications on pain after stroke. The highest amounts of publications (10), open access value (7), and H-index (7) were reported at Chang Gung University. The University of Verona had the highest number of citations (281) and citations per article (46.83). **Figure 9** indicates the collaborations between countries and institutions.

TABLE 1 | The top 15 journals of articles in pain after stroke.

Journals	Papers	Citations (WOS)	Citations per Paper	Open access	WoS Categories	IF (2021)	Quartile	*H*-index
European Journal of Neurology	4	73	18.25	0	Clinical neurology; neurosciences	6.089	Q2; Q2	3
Stroke	5	229	45.8	5	Clinical neurology; peripheral vascular disease	7.914	Q1; Q1	5
Journal of Stroke Cerebrovascular Diseases	5	16	3.2	1	Neurosciences; peripheral vascular disease	2.136	Q4; Q4	3
Clinical Rehabilitation	5	71	14.2	2	Rehabilitation	3.477	Q2	4
BMC Neurology	5	57	11.4	5	Clinical neurology	2.474	Q4	3
PM R	6	65	10.83	3	Rehabilitation; sport sciences	2.298	Q4; Q4	3
Journal of Pain Research	6	47	7.83	6	Clinical neurology	3.133	Q4	4
Journal of Rehabilitation Medicine	7	134	19.14	7	Rehabilitation; sport sciences	2.912	Q3; Q3	5
Archives of Physical Medicine and Rehabilitation	7	180	25.71	1	Rehabilitation; sport sciences	3.966	Q1; Q2	7
American Journal of Physical Medicine Rehabilitation	7	224	32	2	Rehabilitation; sport sciences	2.159	Q4; Q4	7
Medicine	8	47	5.88	8	Medicine	1.889	Q4	4
Journal of Physical Therapy Science	8	58	7.25	7	Sport sciences	\	\	5
Frontiers in Neurology	9	49	5.44	9	Clinical Neurology; Neurosciences	4.003	Q3; Q3	4
Pain	12	335	27.92	1	Anesthesiology; Clinical Neurology	6.961	Q2; Q2	8
Topic in Stroke Rehabilitation	16	199	12.44	1	Rehabilitation	2.119	Q4	9

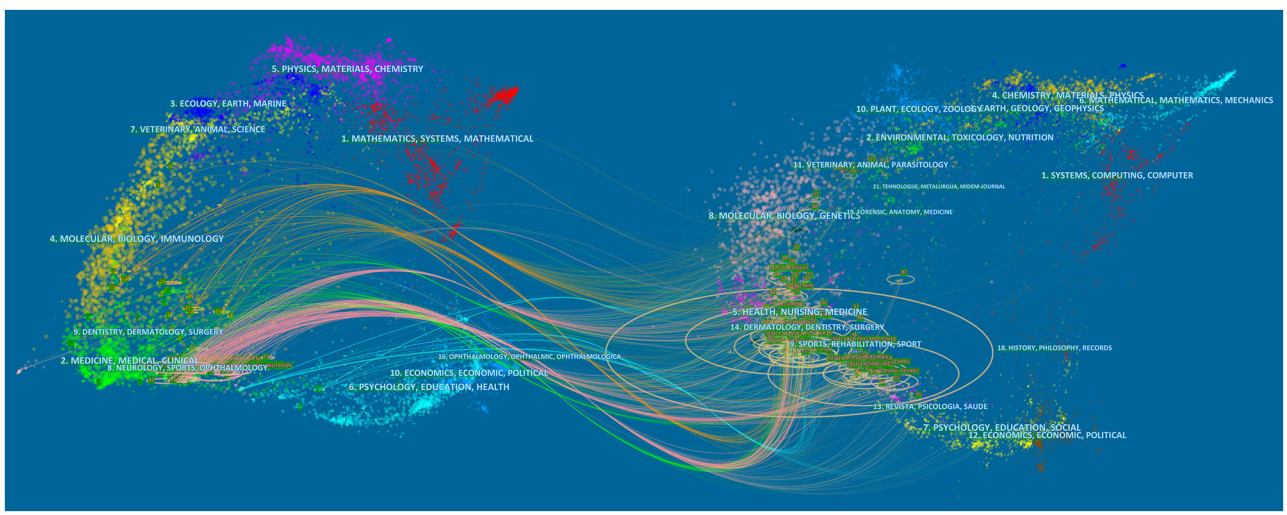

FIGURE 4 | Visualization of dual-map overlays of citing journals and cited journals of 322 studies published from 2010 to 2021. The colored curve indicates the path of citation, which originates from 11 fields of the citing journals on the left and points to 14 fields of the cited journals on the right.

Authoritative Authors Analysis

The 322 papers were contributed by 1,437 authors. The top 15 authors and co-cited authors were ranked in terms of the number of journals published (**Table 3**). In terms of publications, Shyu BC ranked first (8), followed by Huang YC (7) and Finnerup NB (6). Klit H was co-cited 139 times, followed by Lindgren I (67) and Andersen G (67).

Keywords Analysis

The top 25 keywords with the strongest citations bursts from 2010 to 2021 are shown in **Figure 10**. The strongest citation burst of keywords since 2010 was *central pain*. By the end of 2021, the keywords with the most outbreaks of cited literature included *spinal cord* (2019–2021), *impact* (2019–2021), *chronic pain* (2020–2021), *quality* (2020–2021), *frequency*

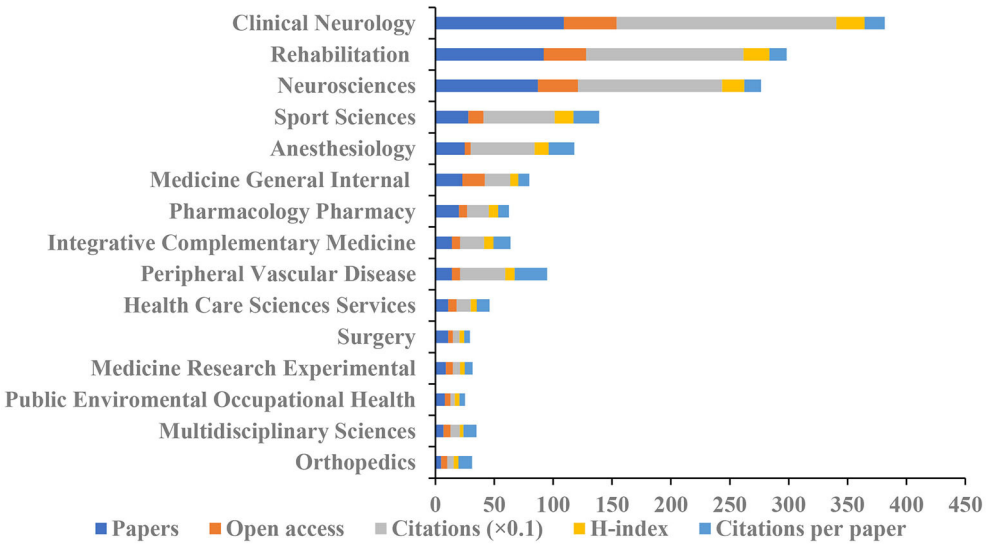

FIGURE 5 | The number of articles, open-access articles, citations, H-index, and citations per article of the top 15 subject categories of Web of Science (WoS).

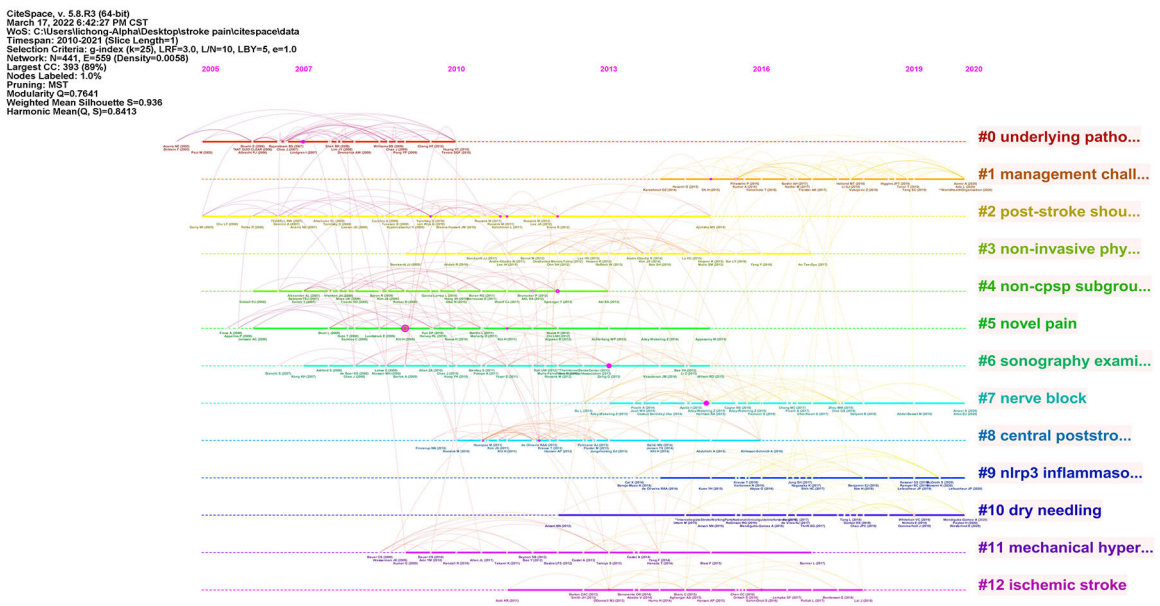

FIGURE 6 | A timeline view of reference co-citation analysis.

(2020–2021), and *systematic review* (2020–2021) among the top 25 keywords.

The Most Frequently Cited Articles Analysis

The top 10 frequently cited articles on pain after stroke are listed in **Table 4**. The most cited article (95 citations) by Harrison et al. with the title "*Post Stroke Pain: Identification, Assessment, and Therapy*" was published in 2015 in *Cerebrovascular Diseases*. Among the top 10 cited articles, one of them was published in the journals with IF $\geq$ 10 (*Brain*), five in journals with 5 $\leq$ IF $\leq$10 (*Stroke* and *Pain*), and four in journals with IF < 5.

DISCUSSION

Global Research Trends on Pain After Stroke

This study presents a bibliometric analysis of pain after stroke over the last 12 years. The number of citations has shown a continuous but unstable growth trend yearly, with the most

TABLE 2 | Five innovative studies about the pain after stroke research among the cited references of the included 322 studies.

Study	Sigma*	Journal	Study type	Sample	Intervention	Outcomes	Highlights
Adey-Wakeling et al., 2015	0.24	Archives of physical medicine and rehabilitation	A prospective population-based study	301	NA	Subjective reports of onset, severity, and aggravating factors for pain and 3 passive range-of-motion measures	The frequency of poststroke shoulder pain is almost 30%.
Zeilig et al., 2013	0.21	Pain	An observational study	30	NA	The thresholds of warmth, cold, heat-pain, touch, and graphesthesia	The more prominent sensory alterations in the shoulder region suggest that neuropathic factors play a role in hemiplegic shoulder pain.
Sprenger et al., 2012	0.17	Brain	An observational study	10	NA	Magnetic resonance imaging	The ventral posterior nucleus-pulvinar border zone is crucial in the pathogenesis of thalamic pain.
Kalichman and Ratmansky, 2011	0.17	American journal of physical medicine and rehabilitation	Review	NA	NA	NA	The authors categorized the possible underlying pathologies of hemiplegic shoulder pain into three categories: (1) impaired motor control (muscle tonus changes), (2) soft-tissue lesions, and (3) altered peripheral and central nervous activity.
Oh and Seo, 2015	0.17	Pain management nursing	Review	NA	NA	NA	Nurses should be knowledgeable of central post-stroke pain (CPSP), provide precise information to patients and their families, and develop effective nursing care plans that improve outcomes and quality of life for patients with CPSP.

**Sigma = (centrality+1) burstness (burstness on the index) to identify innovative reference.*

obvious growth trend from 2015 to 2016. The highest amount of published articles (45 publications) was in 2020. The highest numbers of citations and citations per article are in 2011, which are 711 and 33.86, respectively. In addition, the highest H-index (15) value occurred in 2012. These results indicate that studies involved in pain after stroke attracting more and more attention from all over the world.

In terms of authoritative journals, *Topic in Stroke Rehabilitation* (16 publications), *Pain* (12 publications), and *Frontiers in Neurology* (nine publications) contributed the most to the number of published papers. Among the top 15 journals, 13.33% of them were Q1, 20% were Q2, and 13.33% were Q3, indicating the quality of studies on pain after a stroke still needed to strengthen. *Stroke* had the highest number of citations per article (45.8 times). *Pain* had the highest amounts of citations (335 times). The highest H-index value (9) occurred in *Topic in Stroke Rehabilitation*. According to the Journal Citation Reports (2021 edition), none of the top 15 journals had an IF of more than 10. Seven journals had an IF value of 1–3 (*Journal of Stroke Cerebrovascular Diseases*, *BMC Neurology*, *PM &R*, *Journal of Rehabilitation Medicine*, *American Journal of Physical Medicine Rehabilitation*, *Medicine*, and *Topic in Stroke Rehabilitation*), four journals had an IF value of 3–5 (*Clinical Rehabilitation*, *Journal of Pain Research*, *Archives of Physical Medicine and Rehabilitation*, and *Frontiers in Neurology*), three journals had an IF value of 5–10 (*European Journal of Neurology*, *Stroke*, and *Pain*). These results indicate that high-quality research should be carried out in the future.

In terms of authoritative countries, China had a dominating contribution to the numbers of published articles (65), followed by the United States (57) and South Korea (38). The top 15 countries are composed of eight European countries, four Asia-Pacific countries, and three American countries. In terms of authoritative institutions, 73% of the top 15 institutions were world-renowned universities. According to international cooperation, the United States and the Chang Gung University

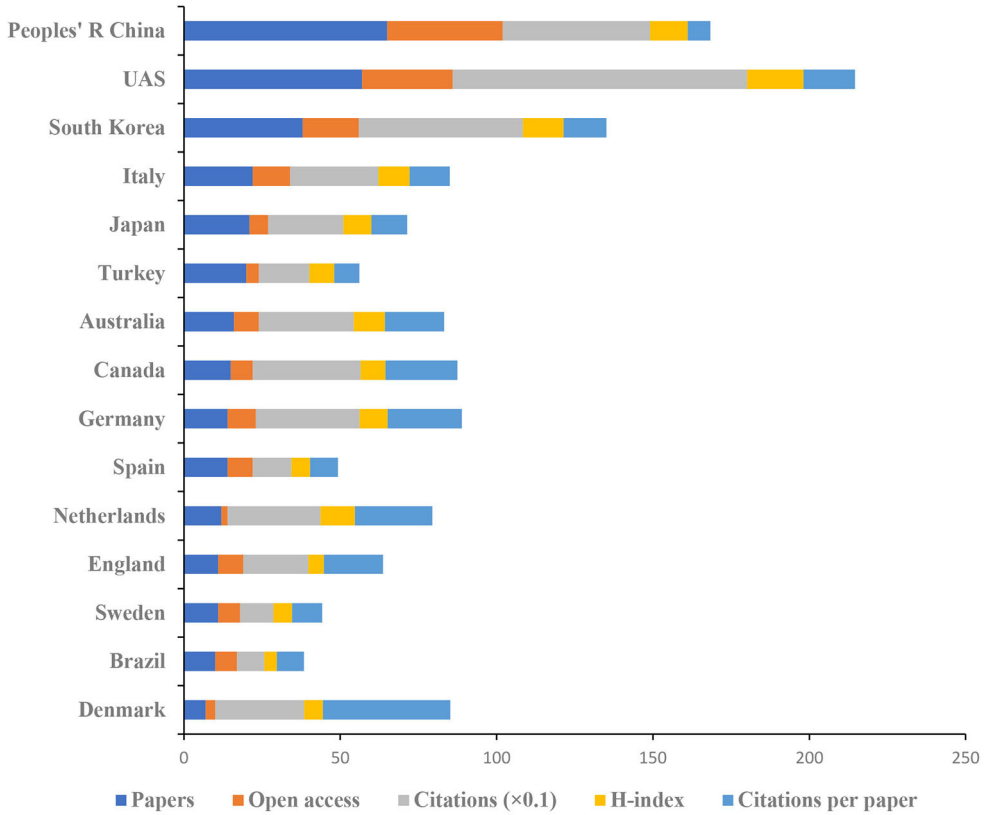

FIGURE 7 | The number of articles, citations, citations per article, and open-access articles, and H-index of the top 15 countries.

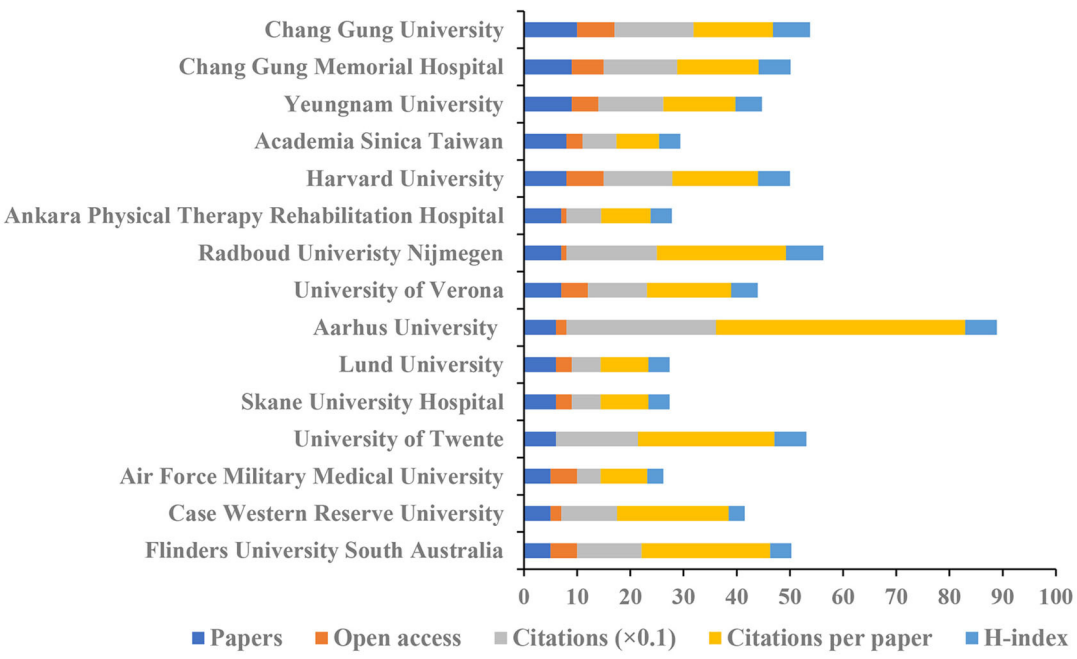

FIGURE 8 | The number of articles, citations, citations per articles, and open-access articles, and H-index of the top 15 institutions.

FIGURE 9 | The analysis of countries and institutions. **(A)** Network map of countries engaged in pain after stroke. **(B)** Network map of institutions engaged in pain after stroke.

TABLE 3 | The top 15 authors, co-cited authors, and co-cited references in pain after stroke.

Author	Papers	Co-cited author	Cited times	Cocited reference	Cited times
Shyu Bc	8	Klit H	139	Klit H, 2009, LANCENT NEUROL, V8, P857, DOI 10.1016/S1474-4422(09)70176-0	37
Huang YC	7	Lindgren I	67	Klit H, 2011, PAIN, V152, P818, DOI 10.1016/j.pain.2010.12.030	21
Finnerup NB	6	Andersen G	67	Sprenger T, 2012, BRAIN, V135, P2536, DOI 10.1093/brain/aws153	20
Huang ACW	6	Bowsher D	64	Lindgren I, 2007, STROKE, V16, P343, DOI 10.1161/01.STR.0000254598.16739.4e	20
Ijzerman MJ	6	Kumar B	60	Hansen AP, 2012, EUR J PAIN, V16, P1128, DOI 10.1002/j.1532-2149.2012.00123.x	20
Renzenbrink GJ	6	Kim JS	58	Harrison RA, 2015, CEREBROVASC DIS, V39, P190, DOI 10.1159/000375397	19
Roosink M	6	Jonsson AC	57	Paolucci S, 2016, PAIN MED, V17, P924, DOI 10.1093/pm/pnv019	19
Brogardh C	5	Widar M	55	Kumar B, 2009, ANESTH ANALG, V108, P1645, DOI 10.1213/ane.0b013e31819d644c	17
Fernandez-de-las penas C	5	Chae J	55	Adey-Wakeling Z, 2015, ARCH PHYS MED REHAB, V96, P241, DOI 10.1016/j.apmr.2014.09.007	16
Jang SH	5	Gamble GE	54	Krause T, 2012, J NEUROL NEUROSUR PS, V83, P776, DOI 10.1136/jnnp-2011-301936	14
Jensen TS	5	Vestergaard K	53	Kim JS, 2011, PAIN, V152, P1018, DOI 10.1016/j.pain.2010.12.023	14
Kit H	5	Leijon G	50	Kalichman L, 2011, AM J PHYS MED REHAB, V90, P768, DOI 10.1097/PHM.0b013e318214e976	13
Leong CP	5	Bohannon RW	44	Dromerick AW, 2008, ARCH PHYS MED REHAB, V89, P1589, DOI 10.1016/j.apmr.2007.10.051	13
Lindgren I	5	Roosink M	43	Klit H, 2010, PLOS ONE, V6, P0, DOI 10.1371/journal.pone.0027607	13
Tokuyama S	5	Boivie J	42	Naess H, 2010, J NEUROL, V257, P1446, DOI 10.1007/s00415-010-5539-y	12

TABLE 4 | The top 10 articles with the most citation frequency in pain after stroke.

Title	First author	Journal	Impact factor	Year	Citations (WoS)	WoS categories	Category ranking
Post Stroke Pain: Identification, Assessment, and Therapy	Harrison	Cerebrovascular Diseases	2.762	2015	95	Peripheral vascular disease; clinical neurology	39/65; 133/208
Botulinum Toxin for the Upper Limb After Stroke (BoTULS) Trial Effect on Impairment, Activity Limitation, and Pain	Shaw	Stroke	7.914	2011	89	Peripheral vascular disease; clinical neurology	6/65; 16/208
Central poststroke pain: A population-based study	Klit	Pain	6.961	2011	88	Anesthesiology; clinical neurology; neurosciences	4/33; 23/208; 39/273
Pain following stroke: A prospective study	Hansen	European Journal of Pain	3.931	2012	85	Anesthesiology; clinical neurology; neurosciences	13/33; 75/208; 121/273
Safety and efficacy of pregabalin in patients with central post-stroke pain	Kim	Pain	6.961	2011	75	Anesthesiology; clinical neurology; neurosciences	4/33; 23/208; 39/273
Duloxetine in patients with central neuropathic pain caused by spinal cord injury or stroke: A randomized, double-blind, placebo-controlled trial	Vranken JH	Pain	6.961	2011	71	Anesthesiology; clinical neurology; neurosciences	4/33; 23/208; 39/273
Underlying Pathology and Associated Factors of Hemiplegic Shoulder Pain	Kalichman	American Journal of Physical Medicine & Rehabilitation	2.159	2011	71	Rehabilitation	40/68
Assessing the risk of central post-stroke pain of thalamic origin by lesion mapping	Sprenger	Brain	13.501	2012	68	Clinical neurology; neurosciences	6/208; 10/273
Chronic Pain Syndromes After Ischemic Stroke PRoFESS Trial	O'Donnell	Stroke	7.914	2013	65	Peripheral vascular disease; clinical neurology	6/65; 16/208
Injury of the Spino-Thalamo-Cortical Pathway Is Necessary for Central Post-Stroke Pain	Hong JH	European Neurology	1.710	2010	60	Clinical neurology; neurosciences	179/208; 248/273

had relatively close collaborations with others. Though a wide range of cooperative relationships has been established between various countries and institutions, future studies involved in pain after stroke should focus on international cooperation to carry out multi-center, large sample studies.

Research Hotspots and Frontiers on Pain After Stroke

According to the subject categories of articles on pain after stroke, *Clinical Neurology* (109) was the most prolific research field, followed by *Rehabilitation* (90) and *Neurosciences* (87). The top 15 subject categories were *Clinical Neurology*, *Rehabilitation, Neurosciences*, *Sport Sciences*, *Anesthesiology*, *Medicine General Internal*, *Pharmacology Pharmacy, Integrative Complementary Medicine*, *Peripheral Vascular Disease*, *Health Care Sciences Services*, *Surgery, Medicine Research Experimental*, *Public Environmental Occupational Health*, *Multidisciplinary Sciences*, *and Orthopedics*, indicating pain after stroke is a complex issue that needed multi-disciplinary intervention. *Clinical Neurology* had the highest numbers of open access (45), citations (1864), and H-index value (24).

In terms of reference analysis, the most relevant citer to the largest cluster is "Persistent shoulder pain in the first 6 months after stroke: results of a prospective cohort study." The authors found that the association of persistent poststroke shoulder pain with restricted, passive, pain-free range of motion, and signs indicative of somatosensory sensitization may implicate a vicious cycle of repetitive trauma that can establish itself rapidly after stroke (Roosink et al., 2011). Therefore, intervention for post-stroke shoulder pain should be focused on maintaining and restoring joint ROM as well as preventing injury and somatosensory sensitization. Future research should investigate different interventions to relieve poststroke shoulder pain.

The evolution of a knowledge domain can be reflected by keywords. Therefore, keyword analysis can reveal emerging trends and provide directions for future research. In terms of count numbers, *shoulder pain* (55) ranked first, followed by *central post-stroke pain* (44). Shoulder pain is one of the most common nociceptive pain syndromes after stroke (Anwer and Alghadir, 2020). The pathophysiology of shoulder pain is thought to be a multifactorial factor, such as glenohumeral subluxation, impingement, rotator cuff tears, glenohumeral capsulitis, and weakness and spasticity are thought to be involved (Precerutti et al., 2010; Chang, 2017). The treatment of shoulder pain after stroke includes pharmacological (antispasmodic medications, Nonsteroidal anti-inflammatory drugs et al.), and

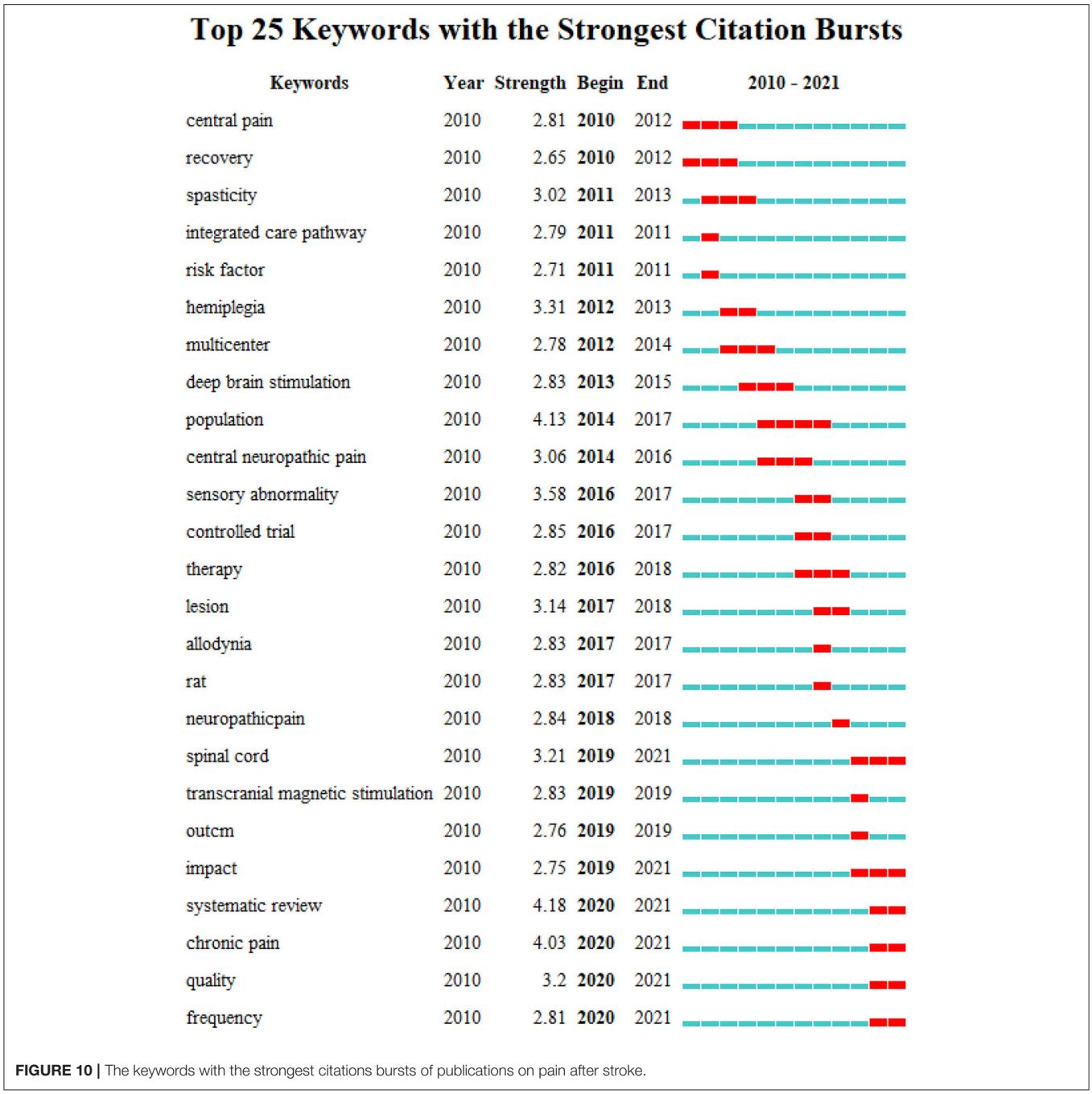

FIGURE 10 | The keywords with the strongest citations bursts of publications on pain after stroke.

nonpharmacological (passive range-of-motion exercises et. al) interventions (Dyer et al., 2020; Souza et al., 2021). In recent years, noninvasive brain stimulation has been proven as a potentially effective intervention to relieve shoulder pain after stroke (Choi and Chang, 2018; de Souza et al., 2019). CPSP is a type of central neuropathic pain. While the pathophysiology of the occurrence of CPSP has not yet been elucidated, some possible mechanisms include hyperexcitability of the spinothalamic tract and central sensitization (Park et al., 2021). Oral medications and non-drug treatments are used to treat CPSP (Ramger et al., 2019; Choi et al., 2021). Recently, a study indicated that prolonged continuous burst stimulation could be a potential treatment for CPSP. Among the top 25 keywords with the strongest citation bursts, *spinal cord* had the strongest strength from 2019 to 2021. A study published in 2020 indicated that perispinal etanercept can provide significant benefits for chronic post-stroke pain (Ralph et al., 2020). Therefore, the current studies on post-stroke pain mainly focus on post-stroke shoulder pain and post-stroke central pain. Future research should focus on well-designed pharmacological and

non-pharmacological interventions aiming to relieve pain after stroke. In addition, more studies should focus on the potential pathophysiology of pain after stroke.

Strengths and Limitations

To the best of our knowledge, this study is the first visual analysis of global trends of pain after stroke based on literature published from 2010 to 2021. In addition, this study contains a comprehensive analysis, such as the number and growth trend of annual publications, different subject sorts of WoS, the relationship among different journals, authors, countries, and institutions, and analysis by different references, citations, and keywords. Nevertheless, this work has some limitations. Because of a limitation of the CiteSpace software, we only analyzed references in the WoS database. Some articles could inevitably have been missed. In addition, large-sample randomized controlled data are lacking.

CONCLUSION

In conclusion, this study may help investigators discover the publication patterns and emerging trends of pain after stroke from 2010 to 2021. The most influential author, institutions, journals, and countries were Shyu Bc, Chang Gung University, *Topic in Stroke Rehabilitation*, and the Peoples' R China. The visual map shows the hot research directions of research on pain after stroke in recent years, such as shoulder pain and CPSP. Our bibliometric analysis of 322 studies using CiteSpace software is in line with current clinical studies of research on pain after stroke, indicating that the methodology is valid. In the future, large sample, randomized controlled trials are needed to carry out for pain after stroke.

DATA AVAILABILITY STATEMENT

The original contributions presented in the study are included in the article/supplementary material, further inquiries can be directed to the corresponding author.

AUTHOR CONTRIBUTIONS

LXY contributed to the conception of the study. LC performed the data analyses and wrote the manuscript. SXY and LXY revised the manuscript. All authors contributed to the article and approved the submitted version.

REFERENCES

Adey-Wakeling, Z., Arima, H., Crotty, M., Leyden, J., Kleinig, T., Anderson, C. S., et al. (2015). Incidence and associations of hemiplegic shoulder pain poststroke: prospective population-based study. *Arch Phys Med Rehabil.* 96, 241–247. doi: 10.1016/j.apmr.2014.09.007

Anwer, S., and Alghadir, A. (2020). Incidence, prevalence, and risk factors of hemiplegic shoulder pain: a systematic review. *Int. J. Environ. Res.* 17. doi: 10.3390/ijerph17144962

Chang, M. C. (2017). The effects of ultrasound-guided corticosteroid injection for the treatment of hemiplegic shoulder pain on depression and anxiety in patients with chronic stroke. *Int. J. Neurosci.* 127, 958–964. doi: 10.1080/00207454.2017.1281274

Chen, C. (2004). Searching for intellectual turning points: Progressive knowledge domain visualization. *Proc. Natl. Acad. Sci. U S A.* 1, 5303–5310. doi: 10.1073/pnas.0307513100

Chen, C., and Song, M. (2019). Visualizing a field of research: a methodology of systematic scientometric reviews. *PLoS ONE.* 14, e223994. doi: 10.1371/journal.pone.0223994

Chiu, Y. H., Chang, K. V., Wu, W. T., Hsu, P. C., and Ozcakar, L. (2021). Comparative effectiveness of injection therapies for hemiplegic shoulder pain in stroke: a systematic review and network meta-analysis. *Pharmaceuticals.* 14. doi: 10.3390/ph14080788

Choi, G. S., and Chang, M. C. (2018). Effects of high-frequency repetitive transcranial magnetic stimulation on reducing hemiplegic shoulder pain in patients with chronic stoke: a randomized controlled trial. *Int. J. Neurosci.* 128, 110–116. doi: 10.1080/00207454.2017.1367682

Choi, H. R., Aktas, A., and Bottros, M. M. (2021). Pharmacotherapy to manage central post-stroke pain. *CNS Drugs.* 35, 151–160. doi: 10.1007/s40263-021-00791-3

de Souza, J. A., Corrêa, J., Agnol, L. D., Dos, S. F., Gomes, M., and Corrêa, F. I. (2019). Effects of transcranial direct current stimulation on the rehabilitation of painful shoulder following a stroke: protocol for a randomized, controlled, double-blind, clinical trial. *Trials.* 20, 165. doi: 10.1186/s13063-019-3266-y

Delpont, B., Blanc, C., Osseby, G. V., Hervieu-Begue, M., Giroud, M., and Bejot, Y. (2018). Pain after stroke: a review. *Revue Neurologique.* 174, 671–674. doi: 10.1016/j.neurol.2017.11.011

Dyer, S., Mordaunt, D. A., and Adey-Wakelin, Z. (2020). Interventions for post-stroke shoulder pain: an overview of systematic reviews. *Int. J. Gen. Med.* 13, 1411–1426. doi: 10.2147/IJGM.S200929

Elias, G., De Vloo, P., Germann, J., Boutet, A., Gramer, R. M., Joel, S. E., et al. (2020). Mapping the network underpinnings of central poststroke pain and analgesic neuromodulation. *Pain.* 161, 2805–2819. doi: 10.1097/j.pain.0000000000001998

Haslam, B. S., Butler, D. S., Kim, A. S., and Carey, L. M. (2021). Chronic pain following stroke: current treatment and perceived effect. *Disabil Health J.* 14. doi: 10.1016/j.dhjo.2020.100971

Kadono, Y., Koguchi, K., Okada, K., Hosomi, K., Hiraishi, M., Ueguchi, T., et al. (2021). Repetitive transcranial magnetic stimulation restores altered functional connectivity of central poststroke pain model monkeys. *Sci. Rep.* 11. doi: 10.1038/s41598-021-85409-w

Kalichman, L., and Ratmansky, M. (2011). Underlying pathology and associated factors of hemiplegic shoulder pain. *Am. J. Phys. Med. Rehabil.* 90, 768–780. doi: 10.1097/PHM.0b013e318214e976

Liampas, A., Velidakis, N., Georgiou, T., Vadalouca, A., Varrassi, G., Hadjigeorgiou, G. M., et al. (2020). Prevalence and management challenges in central Post-Stroke neuropathic pain: a systematic review and meta-analysis. *Adv. Therapy.* 37, 3278–3291. doi: 10.1007/s12325-020-01388-w

Malfitano, C., Rossetti, A., Scarano, S., Malloggi, C., and Tesio, L. (2021). Efficacy of repetitive transcranial magnetic stimulation for acute central post-stroke pain: a case study. *Front. Neurol.* 12. doi: 10.3389/fneur.2021.742567

Oh, H., and Seo, W. (2015). A comprehensive review of central post-stroke pain. *Pain Manag. Nurs.* 16, 804–818. doi: 10.1016/j.pmn.2015.03.002

Park, J. G., Hong, B. Y., Park, H. Y., Yoo, Y. J., Yoon, M. J., Kim, J. S., et al. (2021). Alteration of white matter in patients with central Post-Stroke pain. *J. Pers. Med.* 11. doi: 10.3390/jpm11050417

Payton, H., and Soundy, A. (2020). The experience of Post-Stroke pain and the impact on quality of life: an integrative review. *Behav. Sci.* 10. doi: 10.3390/bs10080128

Precerutti, M., Garioni, E., Madonia, L., and Draghi, F. (2010). US anatomy of the shoulder: Pictorial essay. *J. Ultrasound.* 13, 179–187. doi: 10.1016/j.jus.2010.10.005

Ralph, S. J., Weissenberger, A., Bonev, V., King, L. D., Bonham, M. D., Ferguson, S., et al. (2020). Phase I/II parallel double-blind randomized

controlled clinical trial of perispinal etanercept for chronic stroke: improved mobility and pain alleviation. *Expert. Opin. Investig. Drugs*. 29, 311–326. doi: 10.1080/13543784.2020.1709822

Ramger, B. C., Bader, K. A., Davies, S. P., Stewart, D. A., Ledbetter, L. S., Simon, C. B., et al. (2019). Effects of Non-Invasive brain stimulation on clinical pain intensity and experimental pain sensitivity among individuals with central Post-Stroke pain: A systematic review. *J. Pain Res.* 12, 3319–3329. doi: 10.2147/JPR.S216081

Roosink, M., Renzenbrink, G. J., Buitenweg, J. R., Van Dongen, R. T., Geurts, A. C., and IJzerman, M. J. (2011). Persistent shoulder pain in the first 6 months after stroke: results of a prospective cohort study. *Arch. Phys. Med. Rehabil.* 92, 1139–1145. doi: 10.1016/j.apmr.2011.02.016

Scuteri, D., Mantovani, E., Tamburin, S., Sandrini, G., Corasaniti, M. T., Bagetta, G., et al. (2020). Opioids in post-stroke pain: A systematic review and Meta-Analysis. *Frontiers in Pharmacology* 11. doi: 10.3389/fphar.2020.587050

Souza, I., De Souza, R. F., Barbosa, F., Scipioni, K., Aidar, F. J., and Zanona, A. D. (2021). Protocols used by occupational therapists on shoulder pain after stroke: systematic review and meta-analysis. *Occup. Ther. Int.* 2021. doi: 10.1155/2021/8811721

Sprenger, T., Seifert, C. L., Valet, M., Andreou, A. P., Foerschler, A., Zimmer, C., et al. (2012). Assessing the risk of central post-stroke pain of thalamic origin by lesion mapping. *Brain.* 135, 2536–2545. doi: 10.1093/brain/aws153

Torres-Parada, M., Vivas, J., Balboa-Barreiro, V., and Marey-Lopez, J. (2020). Post-stroke shoulder pain subtypes classifying criteria: towards a more specific assessment and improved physical therapeutic care. *Braz. J. Phys. Ther.* 24, 124–134. doi: 10.1016/j.bjpt.2019.02.010

Wang, K. R., and Liu, H. (2021). Association between widespread pain and dementia, Alzheimer's disease and stroke: a cohort study from the Framingham Heart Study. *Reg. Anesth. Pain Med.* 46, 879–885. doi: 10.1136/rapm-2021-102733

Wang, Y. Z., Wu, C. C., and Wang, X. Q. (2021). Bibliometric study of pain after spinal cord injury. *Neural. Plast.* 2021, 6634644. doi: 10.1155/2021/6634644

Wu, C. C., Wang, Y. Z., Hu, H. Y., and Wang, X. Q. (2021). Bibliometric analysis of research on the comorbidity of cancer and pain. *J. Pain Res.* 14, 213–228. doi: 10.2147/JPR.S291741

Yang, S., and Chang, M. C. (2021). Poststroke pain. *Semin. Neurol.* 41, 67–74. doi: 10.1055/s-0040-1722641

Yin, M., Xu, C., Ma, J., Ye, J., and Mo, W. (2021). A bibliometric analysis and visualization of current research trends in the treatment of cervical spondylotic myelopathy. *Global Spine J.* 11, 988–998. doi: 10.1177/2192568220948832

Yin, M. C., Wang, H. S., Yang, X., Xu, C. Q., Wang, T., Yan, Y. J., et al. (2020). A bibliometric analysis and visualization of current research trends in chinese medicine for osteosarcoma. *Chin. J. Integr. Med*. doi: 10.1007/s11655-020-3429-4

Yuan, G., Shi, J., Jia, Q., Shi, S., Zhu, X., Zhou, Y., et al. (2021). Cardiac rehabilitation: a bibliometric review from 2001 to 2020. *Front. Cardiovasc. Med.* 8, 672913. doi: 10.3389/fcvm.2021.672913

Zeilig, G., Rivel, M., Weingarden, H., Gaidoukov, E., and Defrin, R. (2013). Hemiplegic shoulder pain: Evidence of a neuropathic origin. *Pain.* 154, 263–271. doi: 10.1016/j.pain.2012.10.026

Zhang, Q., Chen, D. N., Shen, Y. X., Bian, M. J., Wang, P., and Li, J. (2021a). Incidence and prevalence of poststroke shoulder pain among different regions of the world: A systematic review and meta-analysis. *Front. Neurol.* 12. doi: 10.3389/fneur.2021.724281

Zhang, Y. H., Wang, Y. C., Hu, G. W., Ding, X. Q., Shen, X. H., Yang, H., et al. (2021b). The effects of gender, functional condition, and ADL on pressure pain threshold in stroke patients. *Front. Neurosci.* 15. doi: 10.3389/fnins.2021.705516

Zhao, C. G., Sun, W., Ju, F., Jiang, S., Wang, H., Sun, X. L., et al. (2021). Analgesic effects of navigated repetitive transcranial magnetic stimulation in patients with acute central poststroke pain. *Pain Therapy.* 10, 1085–1100. doi: 10.1007/s40122-021-00261-0

Conflict of Interest: The authors declare that the research was conducted in the absence of any commercial or financial relationships that could be construed as a potential conflict of interest.

Publisher's Note: All claims expressed in this article are solely those of the authors and do not necessarily represent those of their affiliated organizations, or those of the publisher, the editors and the reviewers. Any product that may be evaluated in this article, or claim that may be made by its manufacturer, is not guaranteed or endorsed by the publisher.

frontiers | Frontiers in Molecular Neuroscience

ORIGINAL RESEARCH
published: 18 May 2022
doi: 10.3389/fnmol.2022.886916

Sex-Specific Transcriptomic Signatures in Brain Regions Critical for Neuropathic Pain-Induced Depression

Weiping Dai[1,2,3†], Shuying Huang[1,2,3†], Yuan Luo[3,4], Xin Cheng[1,2,3], Pei Xia[1,2,3], Mengqian Yang[1,2,3], Panwu Zhao[1,2,3], Yingying Zhang[1,2,3], Wei-Jye Lin[3,4] and Xiaojing Ye[1,2,3*]*

[1] Faculty of Forensic Medicine, Zhongshan School of Medicine, Sun Yat-sen University, Guangzhou, China, [2] Guangdong Province Translational Forensic Medicine Engineering Technology Research Center, Sun Yat-sen University, Guangzhou, China, [3] Guangdong Province Key Laboratory of Brain Function and Disease, Zhongshan School of Medicine, Sun Yat-sen University, Guangzhou, China, [4] Guangdong Provincial Key Laboratory of Malignant Tumor Epigenetics and Gene Regulation, Guangdong-Hong Kong Joint Laboratory for RNA Medicine, Medical Research Center, Sun Yat-sen Memorial Hospital, Sun Yat-sen University, Guangzhou, China

OPEN ACCESS

Edited by:
Weiwei Peng,
Shenzhen University, China

Reviewed by:
Marcos Fabio DosSantos,
Federal University of Rio de Janeiro, Brazil
Hongrui Zhan,
Southern Medical University, China

***Correspondence:**
Xiaojing Ye
yexiaoj8@mail.sysu.edu.cn
Wei-Jye Lin
linwj26@mail.sysu.edu.cn

[†] These authors have contributed equally to this work

Specialty section:
This article was submitted to Pain Mechanisms and Modulators, a section of the journal Frontiers in Molecular Neuroscience

Received: 01 March 2022
Accepted: 19 April 2022
Published: 18 May 2022

Citation:
Dai W, Huang S, Luo Y, Cheng X, Xia P, Yang M, Zhao P, Zhang Y, Lin W-J and Ye X (2022) Sex-Specific Transcriptomic Signatures in Brain Regions Critical for Neuropathic Pain-Induced Depression. Front. Mol. Neurosci. 15:886916. doi: 10.3389/fnmol.2022.886916

Neuropathic pain is a chronic debilitating condition with a high comorbidity with depression. Clinical reports and animal studies have suggested that both the medial prefrontal cortex (mPFC) and the anterior cingulate cortex (ACC) are critically implicated in regulating the affective symptoms of neuropathic pain. Neuropathic pain induces differential long-term structural, functional, and biochemical changes in both regions, which are thought to be regulated by multiple waves of gene transcription. However, the differences in the transcriptomic profiles changed by neuropathic pain between these regions are largely unknown. Furthermore, women are more susceptible to pain and depression than men. The molecular mechanisms underlying this sexual dimorphism remain to be explored. Here, we performed RNA sequencing and analyzed the transcriptomic profiles of the mPFC and ACC of female and male mice at 2 weeks after spared nerve injury (SNI), an early time point when the mice began to show mild depressive symptoms. Our results showed that the SNI-induced transcriptomic changes in female and male mice were largely distinct. Interestingly, the female mice exhibited more robust transcriptomic changes in the ACC than male, whereas the opposite pattern occurred in the mPFC. Cell type enrichment analyses revealed that the differentially expressed genes involved genes enriched in neurons, various types of glia and endothelial cells. We further performed gene set enrichment analysis (GSEA), which revealed significant de-enrichment of myelin sheath development in both female and male mPFC after SNI. In the female ACC, gene sets for synaptic organization were enriched, and gene sets for extracellular matrix were de-enriched after SNI, while such signatures were absent in male ACC. Collectively, these findings revealed region-specific and sexual dimorphism at the transcriptional levels induced by neuropathic pain, and provided novel therapeutic targets for chronic pain and its associated affective disorders.

Keywords: neuropathic pain, sex-differences, depression, medial prefrontal cortex, anterior cingulate cortex, RNA sequencing

INTRODUCTION

Neuropathic pain, which is defined as "pain caused by a lesion or disease of the somatosensory system," affects 6–8% of the population worldwide (Treede et al., 2008; Bannister et al., 2020; Finnerup et al., 2021). As a debilitating medical condition, neuropathic pain severely impairs the quality of life of patients due to the difficulty in clinical management of the disease (Treede et al., 2008). Over 60% of patients with neuropathic pain have depression, which is characterized by persistent depressed mood as well as loss in pleasure and motivation (Bair et al., 2003; de Heer et al., 2014). Such high comorbidity with depression in patients suffering from neuropathic pain exacerbates the severity of pain sensation and leads to worsening prognosis (Williams et al., 2003; Walker et al., 2014; Tappe-Theodor and Kuner, 2019). However, the mechanisms underlying the dynamic interactions of neuropathic pain and depression remain poorly understood. Moreover, although pain and depression can occur in both sexes, women generally show higher prevalence of physical pain and depression than men, while the underlying mechanisms remain underexplored (Ruau et al., 2012; Altemus et al., 2014; Vetvik and MacGregor, 2017; Mogil, 2020; Bangasser and Cuarenta, 2021).

The experience of pain, a combination of sensory and emotional components, is thought to arise from collaborative activities of multiple brain regions (Bushnell et al., 2013; Tan and Kuner, 2021). The brain regions most commonly activated by painful stimuli are often referred to as the "pain-related regions." The medial prefrontal cortex (mPFC) and the anterior cingulate cortex (ACC) are considered as two hub regions (Tracey and Johns, 2010; Ong et al., 2019; Kummer et al., 2020). Both the mPFC and the ACC are associative cortices, with vast connectivity with other cortical and subcortical regions involved in the processing of pain and/or emotion (Etkin et al., 2011; Ong et al., 2019; Tan and Kuner, 2021; Pizzagalli and Roberts, 2022). These two regions are close in location, extensively connected with each other, and both can be activated by various types of acute pain (Bliss et al., 2016; Seminowicz and Moayedi, 2017; Tan and Kuner, 2021).

Chronic pain, including neuropathic pain, modifies the structures and functions of the mPFC and the ACC differently. Both human and animal studies have shown that chronic pain reduces the volume of gray matter as well as the activity of mPFC (Rodriguez-Raecke et al., 2009; Bushnell et al., 2013; Fritz et al., 2016; Phelps et al., 2021). The reduced mPFC activity is accompanied by increased GABAergic tone and decreased glutamatergic currents (Zhang et al., 2015; Kelly et al., 2016; Kummer et al., 2020). Pharmacologic or optogenetic rescue of mPFC activity alleviates nociceptive responses as well as pain-associated depression, suggesting that both the sensory and affective aspects of pain can be processed by the mPFC (Millecamps et al., 2007; Zhang et al., 2015; Hare and Duman, 2020; Tan and Kuner, 2021; Yan and Rein, 2021). Chronic pain also results in reduced gray matter volume in the ACC (Rodriguez-Raecke et al., 2009; Bushnell et al., 2013). However, a hyperactive phenotype of ACC was observed in human functional magnetic resonance imaging (fMRI) studies and confirmed by electrophysiological recording in the animal models of chronic pain (Buffington et al., 2005; Bliss et al., 2016). Prolonged pain induces long-term changes in synaptic plasticity, leading to persistently increased excitatory and decreased inhibitory synaptic transmission in the ACC (Li et al., 2010; Bliss et al., 2016). Lesion or inactivation of ACC relieves neuropathic pain-induced depression, but the effects on nociception are mixed (Barthas et al., 2015; Tan and Kuner, 2021; Zhu et al., 2021). In the reversed fashion, electrical or optogenetic activation of ACC lowers mechanical pain threshold as well as induces aversion to the place where it is delivered (Navratilova and Porreca, 2014; Bliss et al., 2016; Zhang et al., 2017; Tan and Kuner, 2021). Therefore, in contrast to the impairment of the mPFC, chronic pain induces abnormal elevation of the ACC activity to increase pain sensitivity and drive depression. However, the differential mechanisms underlying acute pain-induced activation of both the mPFC and the ACC, and the opposite changes induced by prolonged pain in these two brain regions, remain to be explored.

The comorbidity of neuropathic pain and depression engages long-lasting functional and structural modifications of the mPFC and the ACC, which in turn often involve changes in gene expression that are functionally associated with both diseases (Bliss et al., 2016; Descalzi et al., 2017; Li et al., 2021; Tan and Kuner, 2021). In this study, we aimed to compare differences in the transcriptomic profiles of the mPFC and the ACC in both female and male mice induced by spared nerve injury (SNI), a classical model of neuropathic pain (Decosterd and Woolf, 2000; Guida et al., 2020; Sadler et al., 2022). Our results revealed that more robust transcriptomic changes were induced at 2 weeks after SNI in the ACC of female mice than that of male mice, whereas the opposite pattern was observed in the mPFC. Further analyses revealed brain region-specific and sexual dimorphic changes in the transcriptional profiles after SNI. These findings are of value to advance the understanding of the mechanisms underlying cortical processing of pain and its affective aspects, and to suggest novel therapeutic targets for the treatment of neuropathic pain and its associated affective disorders.

MATERIALS AND METHODS

Animals

A total of 2–3 months old female and male C57BL/6J mice were obtained from the Institute of Experimental Animals of Sun Yat-sen University or Guangdong Medical Laboratory Animal Center (Guangzhou, China). The mice were housed in groups of 5 and maintained on a 12 h light/dark cycle in a specific pathogen free (SPF) facility. All mice were allowed *ad libitum* access to food and water. The experiments were performed during the light cycle. The animals were randomly assigned to different experimental groups and were handled for 2 min per day for 4 days before behavioral testing. All animal studies were approved by the Institutional Animal Care and Use Committee of Sun Yat-sen University. A total number of 132 animals were used in the study.

Spared Nerve Injury Surgery

Mice were anesthetized with 1.5% isoflurane at an oxygen flow rate of 0.4 L/min (RWD Life Science, Shenzhen, China). After

shaving the fur and sterilizing the incision site, incisions were made in the skin and muscle on the left hind leg at the mid-thigh level to expose the sciatic nerve and its branches. The common peroneal and sural nerves were ligated with 5.0 silk suture (Shanghai Pudong Jinhuan Medical Instrument, Shanghai, China), transected, and a 1–2 mm sections of each nerve were removed. The tibial nerve was left intact. Afterward, the skin was sutured. The mice were allowed to recover on a heating pad before returning to their home-cage. The control mice were sham operated, exposed to the same surgery procedure without injury of the nerves.

von Frey Test

The sensitivity to mechanical pain threshold was measured following the up-down method using the von Frey hairs (Aesthesio Precise Tactile Sensory Evaluator Kit, DanMic Global Danmic, United States) (Hansson, 2003; Deuis et al., 2017). Mice were habituated to a transparent chamber with a metal mesh floor for 30–60 min before testing. The plantar surface of the hind paw was stimulated with von Frey hairs and a quick withdrawal of the paw upon the stimulation was indicative of a nociceptive response. von Frey hairs with forces ranging from 0.04 to 2 g were applied in an ascending manner, and each hair was applied for five consecutive times. The lowest force to evoke a paw withdrawal 50% of the time was recorded as the threshold for mechanical pain (Chaplan et al., 1994). von Frey test was performed by an investigator who was blinded to the experimental conditions.

Behavioral Tests

Depression-like behaviors were assessed over 2 and 4 weeks after the surgery of SNI, as previously described (Cryan et al., 2005; Jiang et al., 2019; Vuralli et al., 2019). The animals were acclimated to the testing room for 1–2 h prior to testing. The behavioral testing apparatus were cleaned with 75% ethanol between animals. Behavioral analyses were performed by an investigator who was blinded to the experimental conditions.

The splash test (ST) was carried out in a normal mouse home-cage under red-light. The mouse was allowed to habituate in the cage for 1 min, after which the dorsal coat of mouse was sprayed with a 10% sucrose solution. The test process was videotaped, and the grooming time in the first 5 min after the application of sucrose solution was scored by a researcher blinded to the experimental groups.

The tail suspension test (TST) was carried out by suspending the individual mouse by its tail from a ledge with an adhesive tape (approximately 1 cm from the tip of the tail). The immobile time during the 5 min of the test were videotaped and analyzed offline by a researcher blinded to the experimental groups. The mice were considered immobile only when they were hung passively and completely motionless.

The forced swim test (FST) was carried out by placing the mice into a 5 L glass beaker containing 3.5 L of water (24–25°C) under white light, and videotaped for 6 min. The water in the cylinder was replaced after each animal. The immobile time during the last 4 min of the 6 min test were analyzed offline by a researcher blinded to the experimental groups. The mice were defined as immobile as absence of any movement except that necessary for them to keep their heads above water.

The open field test (OFT) was used to assess the general locomotor activity of the mice. The mice were placed onto a corner of a 40 × 40 cm arena illuminated with red-light. The total distance traveled in the 5-min test were tracked and analyzed by the DigBehv system (Ji-Liang, Shanghai, China).

Tissue Dissection and RNA Extraction and Sequencing

Two weeks after SNI surgery or sham operation, mice were sacrificed by rapid cervical dislocation. Their brains were sliced into 1 mm sections on a brain matrix (RWD Life Science, Shenzhen, China) in ice-cold dissection buffer (2.6 mM KCl, 1.23 mM NaH_2PO_4, 26.2 mM $NaHCO_3$, 5 mM kynurenic acid, 212.7 mM sucrose, 10 mM dextrose, 0.5 mM $CaCl_2$, 1 mM $MgCl_2$). The mPFC and ACC were dissected out with a 15G puncher and snap-frozen on dry ice. Total RNA was isolated using RNAeasy Micro Kit following the manufacturer's protocol (Qiagen, Hilden, Germany). The RNA samples were submitted to the MAGIGENE (Guangzhou, China) for quality control using Agilent 4200 Bioanalyzer. All samples have RNA integrity numbers (RINs) > 8. The samples further underwent library construction and sequenced by an Illumina NovaSeq 6000 system as paired-end 150 bp reads.

RNA Sequencing Alignment, Read Counting and Differential Gene Expression Analysis

Raw data of fastq format was processed by Trimmomatic (version 0.36) to acquire the clean reads, which were then mapped to NCBI Rfam databases, to remove the rRNA sequences by Bowtie2 (version 2.33). The reads were mapped to the mouse reference genome[1] using the Hisat2 (version 2.1.0) (Anders et al., 2015; Lachmann et al., 2020). HTSeq-count (version 0.9.1) was used to obtain the read count and function information of each gene. The count tables were normalized based on their library size using trimmed mean of *M*-values (TMM) normalization implemented in R/Bioconductor EdgeR (version 3.34.0) (Robinson et al., 2010; McDermaid et al., 2019). Normalized read counts were fitted to a negative binomial distribution with a quasilikelihood *F*-test. Principal component analysis (PCA) was performed for the regularized log transform (rlog) of the normalized counts using plotPCA tools with default parameters (Mi et al., 2019; Yoo et al., 2021). Differential gene expression analysis was further carried out using EdgeR. The transcripts were considered as differentially expressed genes (DEGs) at false discovery rate (FDR) < 0.1 with Benjamini–Hochberg correction for multiple testing. Volcano plots, Venn plot and heatmaps were generated using VennDiagram (version 1.6.20), plot, and pheatmap (version 1.0.12) packages in R/Bioconductor (Wang et al., 2021; Yoo et al., 2021).

[1] https://cloud.biohpc.swmed.edu/index.php/s/grcm38/download

Cell Type-Specificity Analyses

To identify cell type-enriched transcripts, we compared our DEGs to a database of cell type-specific mRNA expression published by Zhang et al. (2014), which established selectively enriched transcripts in neurons, glia, and vascular cells of mouse cerebral cortex. Using FPKM numbers for astrocyte, endothelial cell, neuron, microglia, and oligodendrocyte, we calculated the enrichment scores of the transcripts as follows: enrichment score in cell type X = FPKM of transcripts expressed in cell type X/FPKM of transcripts expressed in all other cell types. The DEGs with enrichment scores >1.5 in a given cell type were considered as cell-type enriched.

Validation of RNA Sequencing Data by Quantitative PCR

The quantitative PCR (qPCR) primers were selected from the PrimerBank[2] or designed using Primer-BLAST.[3] The specificity of the primers was further confirmed with BLAST[4] and melting curve analysis, and the amplification efficient of the primers were examined by qPCR using series dilutions of a cDNA template. The sequences of the primers are listed in **Supplementary Table 1**. The cDNAs were synthesized using the NovoScript Plus All-in-on Strand cDNA Synthesis Supermix (Novoprotein, Suzhou, China) following the manufacturer's instructions. The qPCR was performed using a CFX96 Touch Real-Time PCR Detection System (Bio-Rad) with the NovoStart SYBR qPCR SuperMix Plus (Novoprotein, Suzhou, China). For each sample, 2 or 8 ng of cDNA was amplified using one initial denaturation step at 95°C for 1 min, followed by 40 cycles at 95°C for 20 s, 60°C for 20 s, and 72°C for 30 s. Triplicates of each sample were analyzed by qPCR, and the mean cycle quantification (Cq) value was used for calculating the relative expression of target mRNAs using the ΔΔCt method, using the mRNA level of *Gapdh* as the internal control for normalization.

Analyses of Protein–Protein Interaction Networks

STRING (version 11.5) was used to identify potential protein–protein interactions between the DEGs. The cytoHubba's Maximal Clique Centrality (MCC) score were used to identify top hub DEGs and their sub-networks (Chin et al., 2014; Szklarczyk et al., 2019; Pan et al., 2021). The data were visualized by Cytoscape (version 3.9.1).

Gene Set Enrichment Analysis

Gene set enrichment analysis (GSEA) (Broad Institute, version 4.2.2) analysis was performed to identify changes in functional enrichments of the transcriptomic profiles, using the gene set databases for Gene Ontology (GO, c5.go.bp.v7.51.symbols.gmt, c5.go.mf.v7.51.symbols.gmt, and c5.go.cc.v7.51.symbols.gmt) and KEGG pathways (c2.cp.kegg.v7.51.symbols.gmt). Gene set size filters were set at minimum of 5 and maximum of 1000. FDR for the enrichment score of the gene set were calculated based on 1000 gene set permutations. The top gene sets enriched in each group were plotted with ggplot2 (version 3.3.5) in R.

Statistical Analyses

The statistical analyses of the RNA sequencing (RNAseq) data were described in the sections above. Two-way ANOVA followed by Sidak's or Tukey's multiple comparisons tests were used for comparing the behavioral or von Frey test results for the sham versus SNI groups of female and male mice. Unpaired Student's *t*-test was used for qPCR analyses to validate gene expression changes by SNI. The statistical analyses were performed in GraphPad Prism for windows (version 8.0.0). Data were presented as mean ± SEM and $p < 0.05$ was considered as statistically significant.

RESULTS

Spared Nerve Injury Induces Depression-Like Behaviors in Both Female and Male Mice

To explore the temporal course for the development of depressive symptoms after SNI, a classic model of neuropathic pain, we measured behavioral changes at different time points after SNI surgery in both female and male mice. The von Frey test was used to measure mechanical pain sensitivity. The ST, TST, and the FST were used to assess depressive-like behaviors. The OFT was used to evaluate general locomotion (**Figure 1A**). The results showed that, after SNI, mice of both sexes developed robust mechanical allodynia as early as 1 week post-surgery, which persisted for at least 4 weeks. The decrease in mechanical pain threshold measured by the von Frey test was relatively larger in the female mice than that in the male mice (**Figures 1B,C**). At 2 weeks after SNI surgery, the female mice exhibited significantly less grooming time in the ST and trends toward increased immobility in the TST and the FST. Similarly, the male mice also showed depressive phenotypes at 2 weeks post-SNI surgery, including significantly decreased grooming time in the ST and increased immobility in the TST and FST (**Figures 1D–F**). At 4 weeks after SNI surgery, both female and male mice showed robust depression-like behaviors (**Figures 1G–I**). The decreased grooming and increased immobility in the tests above were unlikely due to the impairment in the general locomotion of these mice after SNI surgery, as for both time points, the total distance of mice traveled in the OFT was not altered (**Figures 1J,K**).

Thus, these data reveal that SNI induces chronic pain and depression-like behaviors in both female and male mice.

Sex-Specific Transcriptional Signatures in the Medial Prefrontal Cortex and the Anterior Cingulate Cortex of Mice After Spared Nerve Injury Surgery

We next sought to identify transcriptional changes that may contribute to the development of depressive symptoms induced by neuropathic pain. Previous studies have reported

[2]https://pga.mgh.harvard.edu/primerbank/

[3]https://www.ncbi.nlm.nih.gov/tools/primer-blast/index.cgi

[4]https://blast.ncbi.nlm.nih.gov/Blast.cgi

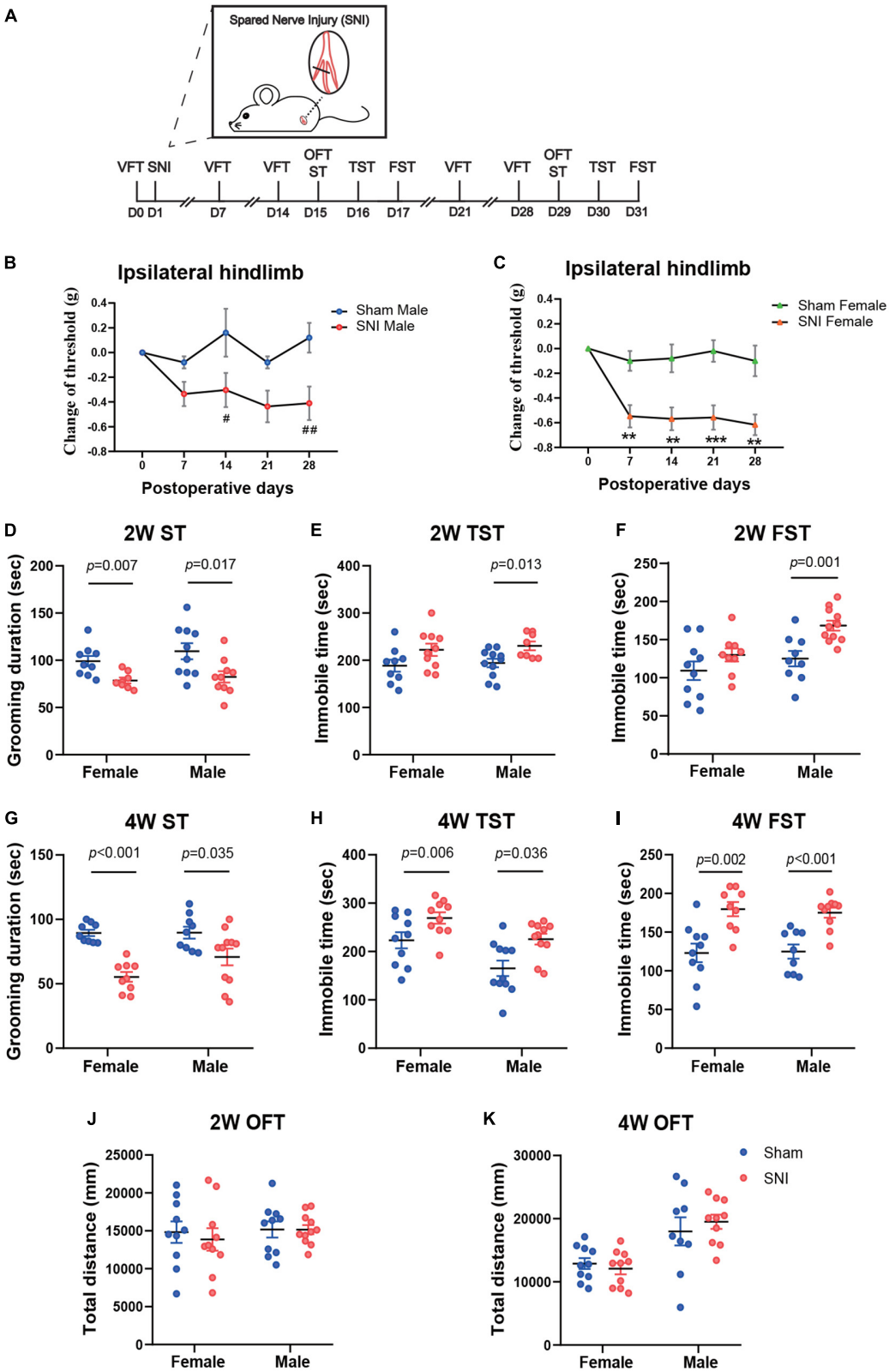

FIGURE 1 | The spared nerve injury (SNI) model of neuropathic pain induces mechanical allodynia and depression-like behaviors in both female and male mice at 2 and 4 weeks after surgery. **(A)** The schema for SNI and the experimental timeline showing the sequence of surgery and behavioral tests. **(B,C)** Changes in the

(Continued)

FIGURE 1 | mechanical withdrawal threshold of the ipsilateral hindlimb over 4 weeks after surgery, compared to the threshold measured before surgery by von Frey test (VFT). Data are presented as mean ± SEM and analyzed by two-way ANOVA followed by Tukey's multiple comparisons test. $^{\#}p < 0.05$, $^{\#\#}p < 0.01$ for SNI male group versus Sham male group **(B)**; $^{**}p < 0.01$, $^{***}p < 0.001$ for SNI female group versus Sham female group **(C)**. *N* = 10 (sham female), 10 (SNI female), 5 (Sham male), and 11 (SNI male). The time spent in grooming during the 5 min splash test (ST) at 2 weeks **(D)** and 4 weeks **(G)** after SNI surgery. The time spent immobile during the 5 min tail suspension test (TST) at 2 weeks **(E)** and 4 weeks **(H)** after SNI surgery. The time spent immobile during the last 4 min of the 6 min forced swim test (FST) at 2 weeks **(F)** and 4 weeks **(I)** after SNI surgery. The total distance traveled during the open field test (OFT) at 2 weeks **(J)** and 4 weeks **(K)** after SNI surgery. **(D–K)** *N* = 9–11 mice per group. Data are analyzed by two-way ANOVA followed by Sidak's multiple comparisons test, and presented as mean ± SEM.

transcriptomic changes in the brains after SNI but at much later time points (2.5–6 months post-surgery) (Alvarado et al., 2013; Berta et al., 2017; Descalzi et al., 2017; Li et al., 2021). Since the mPFC and the ACC are two brain regions critical for regulating both the affective symptoms of neuropathic pain and depression (Bliss et al., 2016; Descalzi et al., 2017; Li et al., 2021; Tan and Kuner, 2021), we chose to examine the transcriptomic profiles of the mPFC and the ACC at 2 weeks post-SNI, a time point when the mice started to show mild depressive phenotypes, to identify the potential molecular signatures that are involved in the emergence of depressive phenotypes during the progression of neuropathic pain.

The mPFC and the ACC were harvested from female and male mice at 2 weeks after SNI surgery or sham operation. The RNAs from both groups were extracted in parallel and underwent quality checks. Afterward, RNAseq were performed on three independent pools of samples from each sex and brain region (4–5 animals were mixed as one biological pool) (**Figure 2A**). The principal component analysis (PCA) revealed striking separation between the mPFC and the ACC transcriptomes, as well as between the female and male transcriptomes (**Figure 2B**). In general, more differentially expressed genes between the sham and the SNI groups (DEGs, FDR < 0.1 by edgeR) were observed in the mPFC than the ACC (**Figure 2C** and **Supplementary Table 2**). Interestingly, for the mPFC, more DEGs were identified in the male mice (211 total) than the female mice (48 total). In contrast, for the ACC, more DEGs were identified in the female mice (59 total), whereas only 8 DEGs were identified in the male mice (**Figure 2C**).

Of note, among the top transcripts upregulated by SNI in the mPFC of SNI female mice, *Snhg14* encodes a long non-coding RNA that regulates the expression of ubiquitin protein ligase E3A (*Ube3a*), which is known to critically implicate in the social interaction dysfunction in Angelman's syndrome (Stanurova et al., 2016; Chung et al., 2020). The top transcripts downregulated in the mPFC of SNI female mice involved *Gdf1*, which encodes growth differentiation factor 1, a secreted ligand of the TGF-beta superfamily (Tanaka et al., 2007), and *Myh14*, which encodes the heavy chain of myosin, a motor protein (Donaudy et al., 2004; **Figure 2D**). For the mPFC of SNI male mice, the most noticeable signatures included downregulation of *Mal* (myelin and lymphocyte protein), *Mbp* (myelin basic protein), and *Cnp* (2′,3′-cyclic nucleotide 3′-phosphodiesterase), genes that are known for their roles in myelin formation (Fulton et al., 2010; Cao et al., 2013; **Figure 2E**). The noteworthy transcriptomic changes in the ACC of female mice included upregulation of *Syt6* and *Syt2*, which encode presynaptic protein synaptotagmins and are important for neurotransmitter release (Wolfes and Dean, 2020), and downregulation of *Col3a1* and *Col1a1*, two transcripts that encode type I and type III collagens, components of the extracellular matrix (Fujiwara et al., 2010; Santoro Belangero et al., 2018; **Figure 2F** and **Supplementary Table 2**). The eight DEGs identified in the ACC of male mice were mostly pseudogenes whose functions remain unclear, except *Gcat*, which encodes glycine C-acetyltransferase that is involved in the synthesis of glycine and acetyl-CoA (Ravichandran et al., 2018; **Figure 2G**).

Further comparison of the DEGs between different groups revealed little commonality between brain regions and between different sexes. In comparison of the mPFC and the ACC, we identified two common DEGs in the female mice (*Gm26723* and *Tmem267*) and no common DEGs in the male mice. By comparing female and male mice, we found two common DEGs in the mPFC (*B430305J03Rik* and *Unc5b*) and one common DEG in the ACC (*Gm5641*) (**Figure 3A**). We combined the DEGs from both sexes to generate the heatmaps, and the results revealed that part of the DEGs exhibited similar directions of changes in both sexes but with greater magnitudes in one sex over the other, while the other DEGs showed sex-specific changes and even changes in opposite directions in different sexes (**Figures 3B,C**).

We further evaluated the cell-type specificity of the identified DEGs by comparing our data to a cell-type specific mouse brain RNAseq repository (Zhang et al., 2014). For the DEGs in the female mPFC, 13 were identified to be enriched in specific brain cell-types, including astrocytes, endothelial cells, neuron and oligodendrocytes (**Figure 3D**). For the male mPFC, a noteworthy signature was downregulation of DEGs enriched in the oligodendrocytes (**Figure 3E**). For the DEGs in the ACC of female mice, the downregulated DEGs were found mainly enriched in astrocytes, endothelial cells, and oligodendrocytes, whereas the upregulated DEGs were found mainly enriched in neurons (**Figure 3F**). For the eight DEGs identified in the male ACC, one of those was enriched in oligodendrocytes (**Figure 3G**). Thus, SNI modifies the transcriptomic profiles across multiple cell-types in the mPFC and the ACC in both sexes.

To validate the RNAseq results, we performed qPCR analyses using independent sets of individual RNA samples. Eight mPFC-specific DEGs were chosen for the subsequent qPCR validation, which included *Gdf1* (growth differentiation factor 1), *Snhg14* (small nucleolar RNA host gene 14), *Myh14* (myosin heavy chain 14), *Tmem267* (transmembrane protein 267), *Trf* (transferrin), *Gfap* (glial fibrillary acidic protein), *Mbp* (myelin basic protein), and *Cnp* (2′,3′-cyclic nucleotide 3′ phosphodiesterase) (**Figure 4A**). Similarly, seven ACC-specific DEGs were assessed,

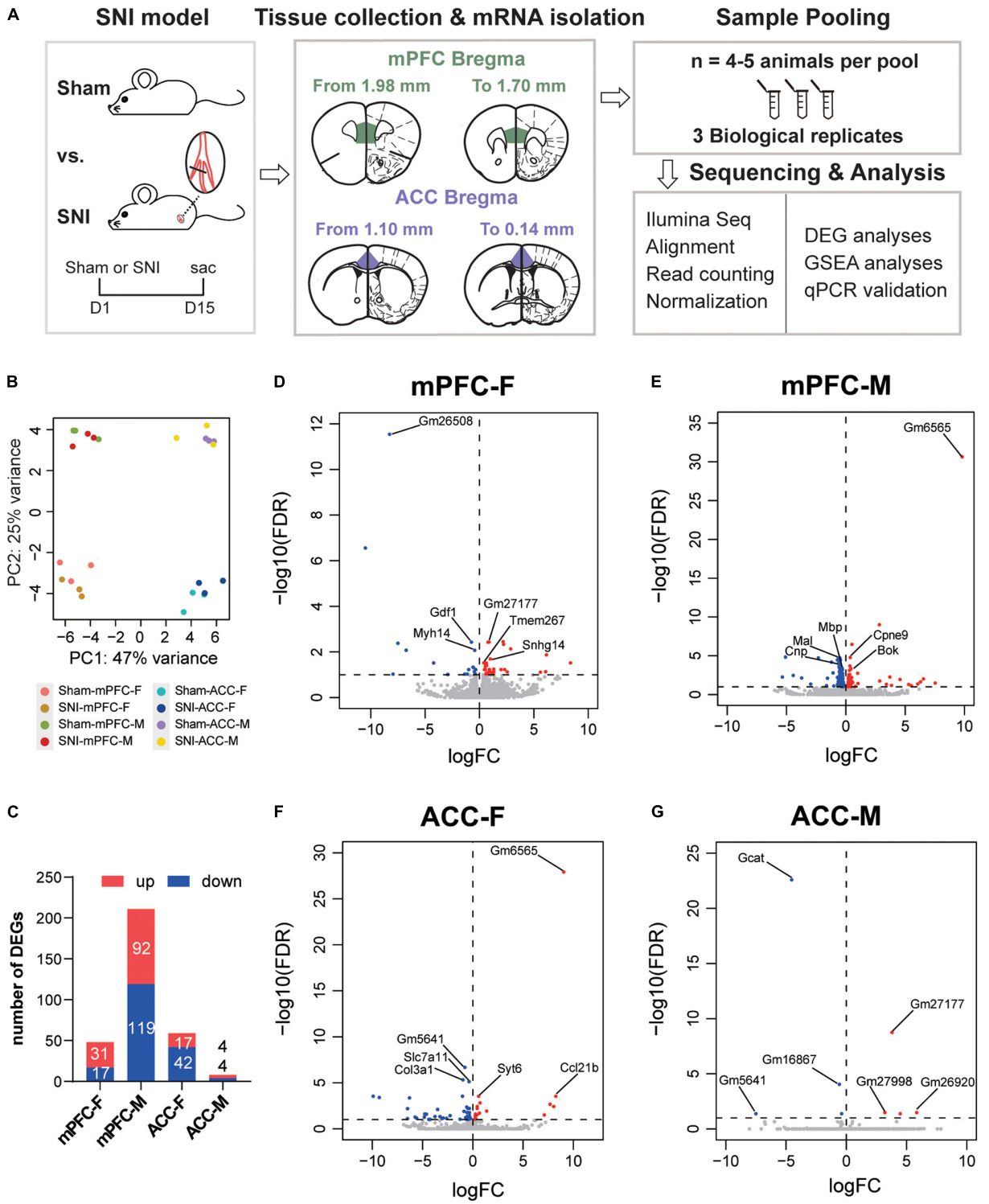

FIGURE 2 | Differentially expressed genes in the mPFC and the ACC of female and male mice at 2 weeks after SNI surgery, compared to the sham group. **(A)** Experimental design and the workflow of the RNAseq and analyses. **(B)** Principal component analysis (PCA) plot of the sham versus the SNI groups, depicting the clustering of samples: the mPFC versus the ACC, female versus male, and the sham group versus the SNI group. **(C)** The numbers of the significantly upregulated or downregulated differentially expressed genes (DEGs) by SNI. mPFC-F, the mPFC of female mice; mPFC-M, the mPFC of male mice; ACC-F, the ACC of female mice; ACC-M, the ACC of male mice. The volcano plots of the DEGs in the mPFC of female (mPFC-F, **D**) and male mice (mPFC-M, **E**), as well as in the ACC of female (ACC-F, **F**) and male mice (ACC-M, **G**), with horizontal lines at the $-\log_{10}$ (false discovery rate, FDR) = 1 and vertical lines at $\log_2$ (fold change, FC) = 0, delineating positive versus negative regulation. Blue dots represent downregulated DEGs, and red dots represent upregulated DEGs.

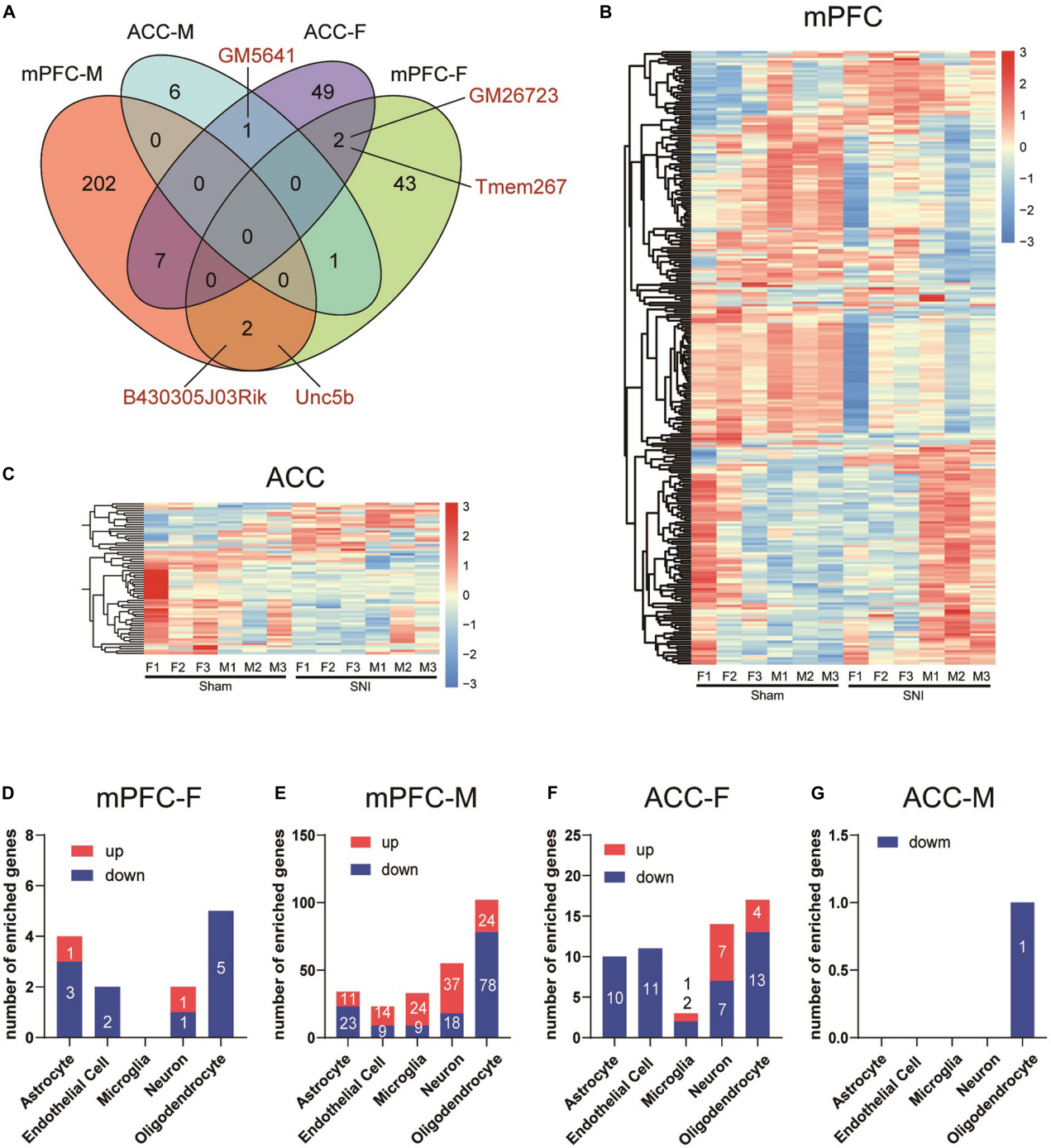

FIGURE 3 | Differential transcriptomic profiles and cell-type enrichment of the DEGs induced in the mPFC and the ACC of mice of different sexes by SNI. **(A)** Venn diagram depicting limited overlaps of the DEGs between the mPFC and the ACC, as well as between different sexes. mPFC-F, the mPFC of female mice; mPFC-M, the mPFC of male mice; ACC-F, the ACC of female mice; ACC-M, the ACC of male mice. Hierarchical clustered heatmaps of the mPFC **(B)** and the ACC **(C)**, showing relative expression of the DEGs across the sham and the SNI groups in different sexes (F, female; M, male). Color scales represent standardized rlog-transformed values across samples. **(D–G)** The numbers of DEGs enriched in different cell types in the mPFC and the ACC of female and male mice, comparing the sham versus the SNI groups, as determined from a database of cell type-specific transcripts in the mouse cortex by Zhang et al. (2014).

which included *Scn4b* (sodium voltage-gated channel beta subunit 4), *Syt2* (synaptotagmin 2), *Acta2* (actin alpha 2), *Col1a1* (collagen type I alpha 1 chain), *Gm27177*, *Gm5641*, and *Gcat* (glycine C-acetyltransferase) (**Figure 4D**). The results of qPCR analysis confirmed the findings of the RNAseq (**Figures 4B,C,E,F**).

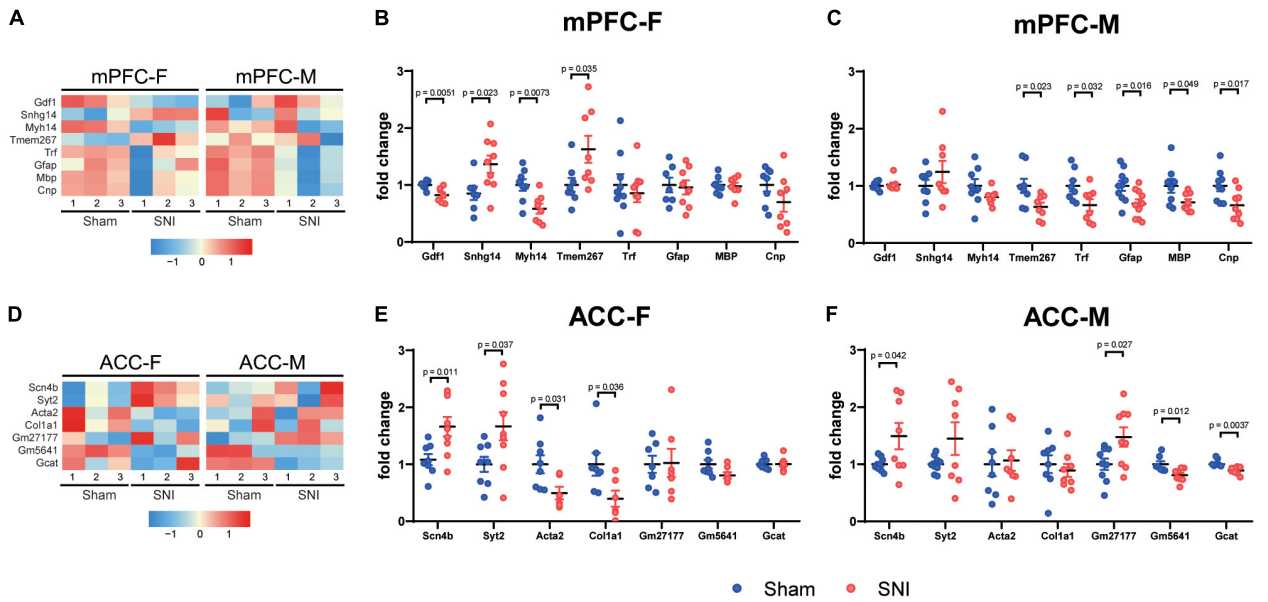

FIGURE 4 | Quantitative PCR validation of the DEGs between the sham and the SNI groups in the mPFC and the ACC of mice of different sexes. Heatmaps showing relative expression levels of the selected upregulated and downregulated DEGs in the mPFC **(A)** and the ACC **(D)** of female and male mice, comparing the sham versus SNI groups. mPFC-F, the mPFC of female mice; mPFC-M, the mPFC of male mice; ACC-F, the ACC of female mice; ACC-M, the ACC of male mice. Color scales represent standardized rlog-transformed values across samples. qPCR validation results of the selected upregulated and downregulated transcripts in the mPFC **(B,C)** and ACC **(E,F)**. *N* = 6–9 mice per group. Data are analyzed by unpaired Student's *t*-test, and presented as mean ± SEM.

Collectively, our data showed that highly distinct and sex-specific changes in the transcriptomic profiles occurred in the mPFC and the ACC at 2 weeks after SNI surgery.

Analysis of Protein–Protein Interaction Network Identifies Hub Genes Related to Spared Nerve Injury in the Male Medial Prefrontal Cortex and the Female Anterior Cingulate Cortex

To explore the molecular interactions and the potential key drivers of the identified DEGs in the mPFC and the ACC of female and male mice after SNI surgery, we performed network analysis based on the STRING Protein–Protein Interaction database (Szklarczyk et al., 2019). Analysis of the DEGs generated a network of 105 nodes and 249 edges in male mPFC, and 20 nodes and 30 edges in female ACC (**Figures 5A,B**). We did not observe any network structure for the female mPFC and the male ACC, likely due to the limited number of DEGs identified in these two conditions. We further used the cytoHubba's MCC score to identify top hub DEGs and their sub-networks (Chin et al., 2014; Li and Xu, 2019). For the male mPFC, the top 20 hub DEGs constituted a sub-network, collectively engaged in nervous system development and axon ensheathment (**Figure 5A**). For the female ACC, the top eight hub DEGs formed a sub-network, encoding the components of extracellular matrix (**Figure 5B**).

Of note, among the top hub DEGs in the network for male mPFC, *Mal* (myelin and lymphocyte protein), *Cnp* (2′,3′-cyclic nucleotide 3′-phosphodiesterase), *Plp1* (proteolipid protein 1), *Mobp* (myelin associated oligodendrocyte basic protein), *Mbp* (myelin basic protein), and *Mog* (myelin oligodendrocyte glycoprotein) were functionally related to the myelination process and also among the top 20 DEGs whose expression was most significantly downregulated after SNI. Similarly, in the female ACC network, the hub DEGs, including *Col3a1* (collagen type III alpha 1 chain) and *Dcn* (decorin), were important components of the extracellular matrix and they were also among the top 20 DEGs whose expression was most significantly downregulated after SNI. These data suggest that decreased myelination in the male mPFC and disruption of extracellular matrix in the female ACC are likely the key factors involved in the pathological development of the comorbidity of SNI-induced neuropathic pain and depressive phenotype.

Gene Set Enrichment Analysis of Spared Nerve Injury Versus Sham Groups Reveals Sex-Dependent Signatures in the Medial Prefrontal Cortex and the Anterior Cingulate Cortex

In order to gain functional insights of the transcriptomic changes in the mPFC and the ACC at 2 weeks after SNI surgery, we performed GSEA analysis, which does not rely on the DEGs selected by arbitrary imposed statistical cut-off parameters, but instead uses the entire list of genes ranked according to a combinational score of the fold change and the adjusted *p*-value. Thus, GSEA analysis is a sensitive method for GO/KEGG enrichment of genes with modest but coordinated changes (Subramanian et al., 2005).

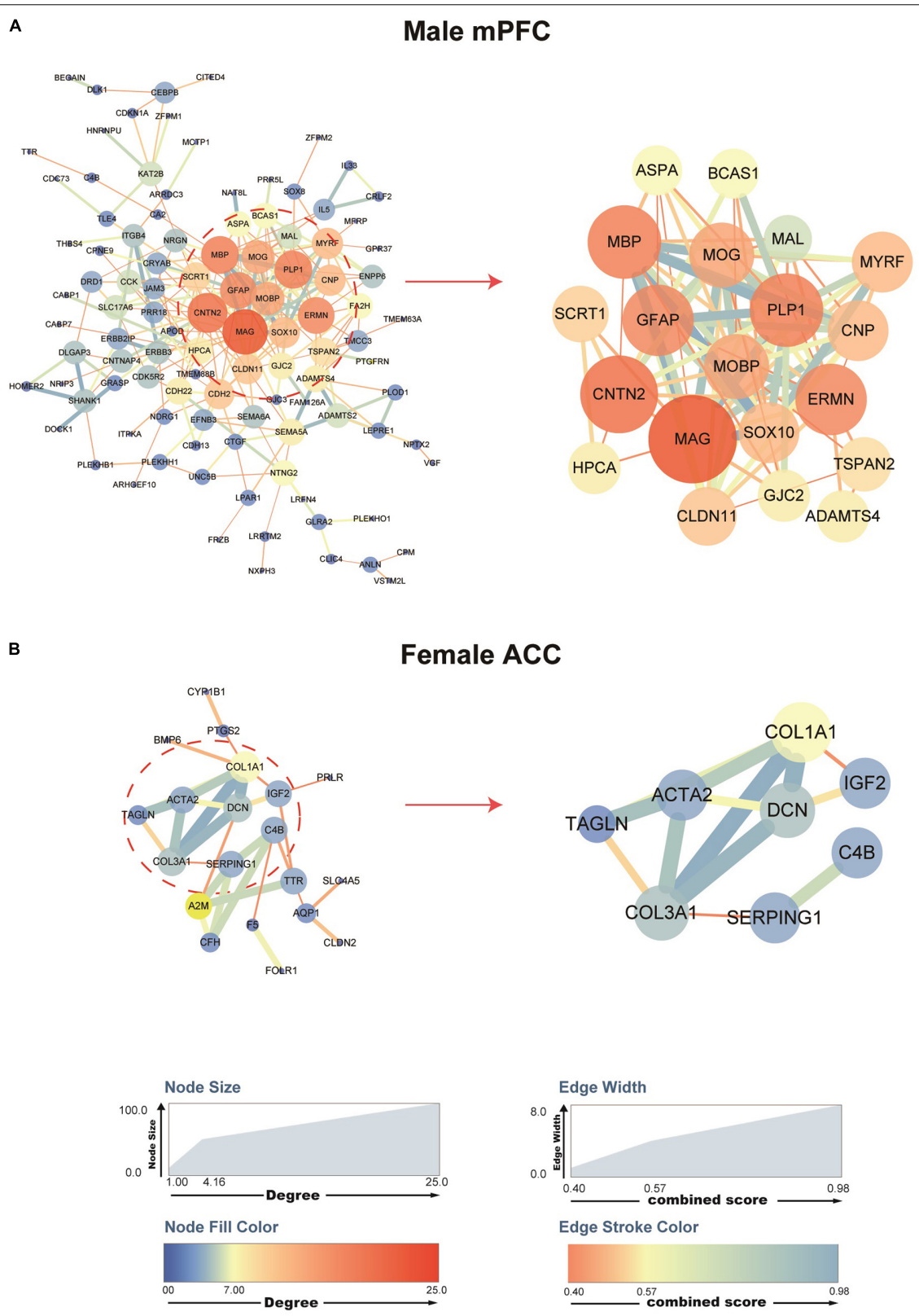

FIGURE 5 | Protein–protein interaction (PPI) networks of the DEGs in the male mPFC and female ACC, comparing the sham versus the SNI groups. STRING PPI networks depicting the potential interactions of the DEGs in the mPFC **(A)** and the ACC **(B)** at 2 weeks after SNI. The color and size of the nodes are relative to the degree of the connectivity, and the color and size of the edges are relative to the combined score of the interactions.

We combined the GO and KEGG terms that were most significantly different between sham versus SNI groups to generate the list of top 10 gene sets for each condition (**Figure 6**). The results showed that for the female mPFC, the most significantly regulated gene sets included oligodendrocyte differentiation, semaphoring plexin signaling pathway, negative regulation of gliogenesis, neuron fate commitment, intrinsic component of external side of plasma membrane, and germ cell nucleus (**Figure 6A**), which were all de-enriched after SNI. For the male mPFC, the gene sets that emerged as the most significant changes by SNI included enrichment of RNA splicing, mitochondrion organization, glutamatergic synapse, voltage gated potassium channel activity, and nucleoside triphosphatase regulator activity; de-enrichment of positive regulation of interferon gamma production and myelin sheath (**Figure 6B**). Of note, most of the identified gene sets were significantly enriched in one sex, but showed no or minimal enrichment in the other sex. The exceptions were myelin sheath and germ cell nucleus in the SNI group, which showed similar degree of de-enrichment in the mPFC of both sexes (**Figures 6A,B** and **Supplementary Table 3**).

For the ACC, the GSEA results revealed that the most significant changes by SNI in the female included enrichment of mitochondrial respiratory chain complex assembly, RNA splicing *via* transesterification reactions, main axon and neuron to neuron synapse; and de-enrichment of collagen fibril organization, collagen trimer, extracellular matrix structural constituent, and serine type endopeptidase inhibitor activity (**Figure 6C**). In the male ACC, the top list included enrichment of triglyceride lipase activity; and de-enrichment of regulation of translational initiation, respirasome, ribosome, spliceosomal complex, graft versus host disease, and Parkinson's disease (**Figure 6D**). Similar to the observation in the mPFC, the gene sets in the ACC also showed sex-divergent patterns (**Figures 6C,D** and **Supplementary Table 3**).

Taken together, these data suggest that the GO and signaling pathways of the transcriptomic changes of the mPFC and the ACC at 2 weeks after SNI are also largely sex-specific.

The Transcriptomic Profiles Between the Medial Prefrontal Cortex and the Anterior Cingulate Cortex Are Partially Distinct and Have Sex-Specific Properties in the Non-spared Nerve Injury Condition

We next wondered whether the brain area and sex-specific differences existed in the transcriptomic changes regulated by SNI in the sham (non-SNI) group of mice. Toward that end, we first compared the transcriptomic profiles between the mPFC and the ACC in the same sex of the sham groups. The DEG analyses identified 1630 transcripts in female mice and 950 transcripts in male mice that were significantly enriched in the mPFC, among which 597 were shared DEGs in both sexes. For the transcripts significantly enriched in the ACC, 2071 in female and 1294 in male mice were found, among which 708 DEGs were shared by both sexes (**Figure 7A** and **Supplementary Table 4**). Overall, more DEGs were identified in the female than the male mice, and similar amounts of DEGs were enriched in the mPFC versus the ACC (**Figures 7B,C**). Of note, between the mPFC and the ACC, *Dio3* (iodothyronine deiodinase 3) was among the most significantly enriched transcripts in the mPFC of both sexes (**Figures 7D,E**). It encodes an enzyme catalyzing the inactivation of thyroid hormone, and is involved in regulating aggressive and maternal behaviors (Stohn et al., 2016, 2018). The top DEGs enriched in the ACC and shared by both sexes included *Npnt* (nephronectin), a member of the epidermal growth factor-like superfamily; *Pvalb* (parvalbumin), the marker for fast-spiking inhibitory neurons regulating the excitability of the targeted neurons; and *Kcnab3* (potassium voltage-gated channel subfamily a regulatory beta subunit 3), a component of potassium channel (**Figures 7D,E**). The identified DEGs were enriched across multiple cell types in both sexes, with the highest enrichment in oligodendrocytes and neurons (**Figures 7F,G**). Further GSEA analyses revealed that the most significantly enriched gene sets in the mPFC of both sexes were related with mating, grooming behavior, microtubule formation, neuropeptide receptor activity, axon guidance and notch signaling pathway (**Figure 7H**). On the other hand, the top gene sets enriched in the ACC of both sexes were related with mitochondrial function, potassium channel regulator activity, extracellular matrix, Parkinson's disease, oxidative phosphorylation as well as complement and coagulation cascades (**Figure 7I** and **Supplementary Table 5**). Of note, the gene sets of mitochondrial function, potassium channel regulator activity, extracellular matrix and Parkinson's disease were also among the most significant ones regulated by SNI, indicating that the differences in transcriptomic changes after SNI in the mPFC versus the ACC are at least in part due to the distinct patterns of transcriptomes between these two regions at baseline.

To further characterize sex-dependent transcriptomic signatures in the brain regions of interest, we performed DEG analyses of the female versus male transcriptomes in the mPFC and the ACC of the sham groups. The results showed that the expression levels of 61 transcripts of the mPFC and 41 transcripts of the ACC were higher in the female than the male mice. Ten of these transcripts were shared by the mPFC and the ACC, among which *Xist*, *Eif2s3x*, and *Ddx3x* are located within the X chromosome (**Figure 8A**). The expression levels of 97 transcripts in the mPFC and 37 transcripts in the ACC were significantly higher in the male than the female mice. Seven of these transcripts were shared by the mPFC and the ACC, among which *Ddx3y*, *Eif2s3y*, *Uty*, and *Uba1y* are located within the Y chromosome (**Figure 8A** and **Supplementary Table 6**). More DEGs between female and male mice were identified in the mPFC than the ACC. In the mPFC, more DEGs were enriched in the male than female mice, whereas similar amounts of DEGs were enriched in the female and male ACC (**Figures 8B,C**). Beyond the genes located in X or Y chromosomes, the noticeable top enriched transcripts in the female mPFC included *Myh7*, which encodes myosin heavy chain 7, and *Col6a1*, which encodes collagen type VI alpha 1 chain, the basic structural unit of collagen VI. The most significantly enriched transcripts in the male mPFC included *Tpt1-ps3* (tumor protein, translationally controlled, pseudogene 3) and *Krt17*

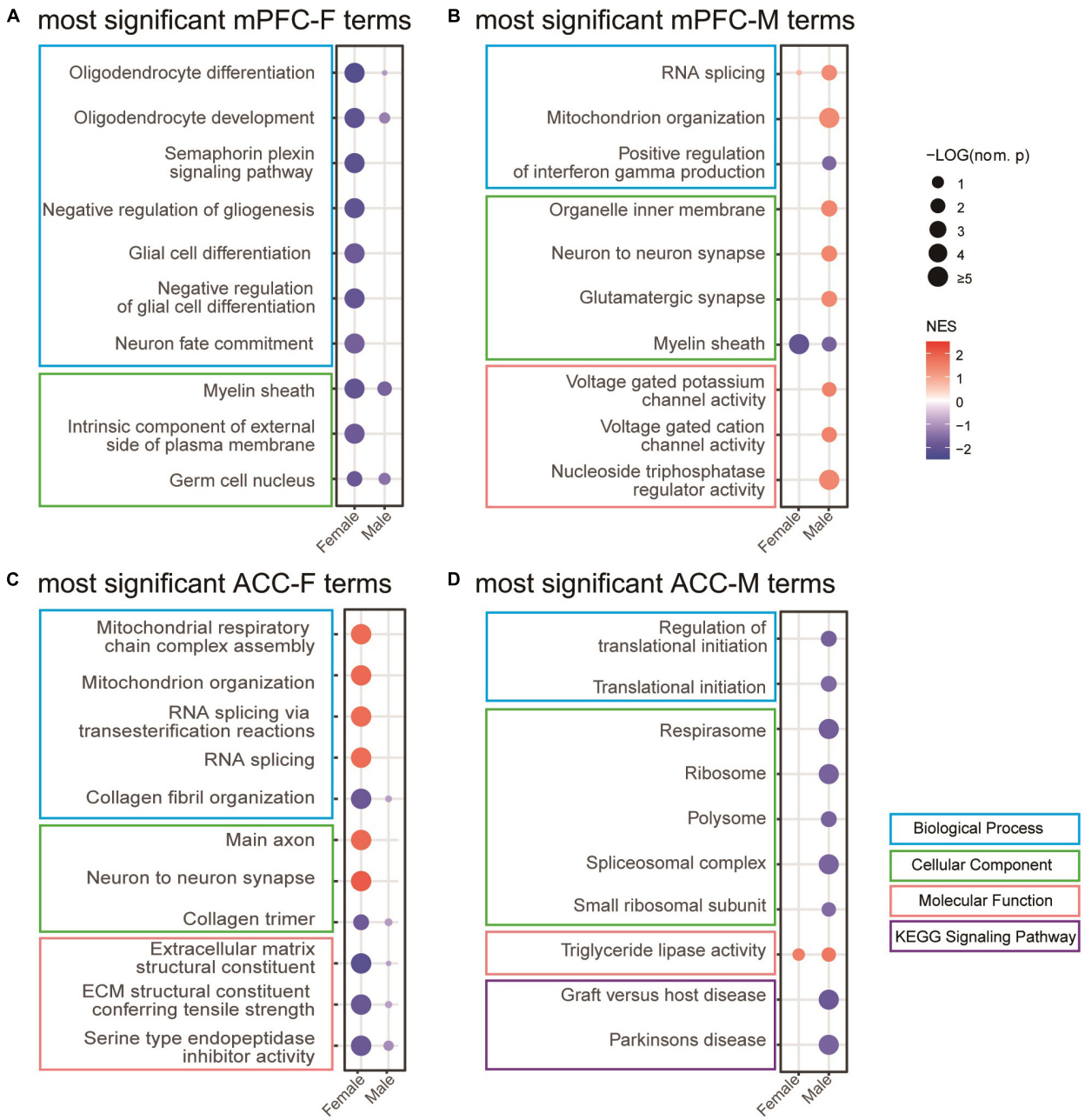

FIGURE 6 | Gene set enrichment analysis (GSEA) of the transcriptomic changes in the mPFC and the ACC of female and male mice at 2 weeks after SNI. Most significantly regulated gene sets in the mPFC of female (mPFC-F, **A**) and male (mPFC-M, **B**) mice, as well as in the ACC of female (ACC-F, **C**) and male (ACC-M, **D**) mice, comparing the sham versus SNI groups. The size of the dots indicates the $-\log_{10}$ (nominal *p*) values, and the color indicates the normalized enrichment scores (NES).

(keratin 17), both of which regulate tumorigenesis (Fiucci et al., 2003; Yang et al., 2019; **Figure 8D**). The noteworthy sex-different transcripts in the ACC included *Ide* (insulin degrading enzyme; female > male), which regulates the catabolism of insulin and β-amyloid (Tundo et al., 2013); and *Irs2* (insulin receptor substrate 2, male > female), which provides an alternative route for insulin signaling (Copps and White, 2012; **Figure 8E**). The differential expression of *Ide* and *Irs2* indicates the possibility of distinct responses to insulin in the female versus male ACC. The identified DEGs were enriched across multiple cell types in the mPFC and the ACC (**Figures 8F,G**). We further performed GSEA analyses to compare female versus male mPFC and ACC. We found sex-differences across multiple domains of GO and KEGG signaling pathways in both brain regions. The sex-specific gene sets in the sham groups were partially overlapped with the most significantly altered gene sets in

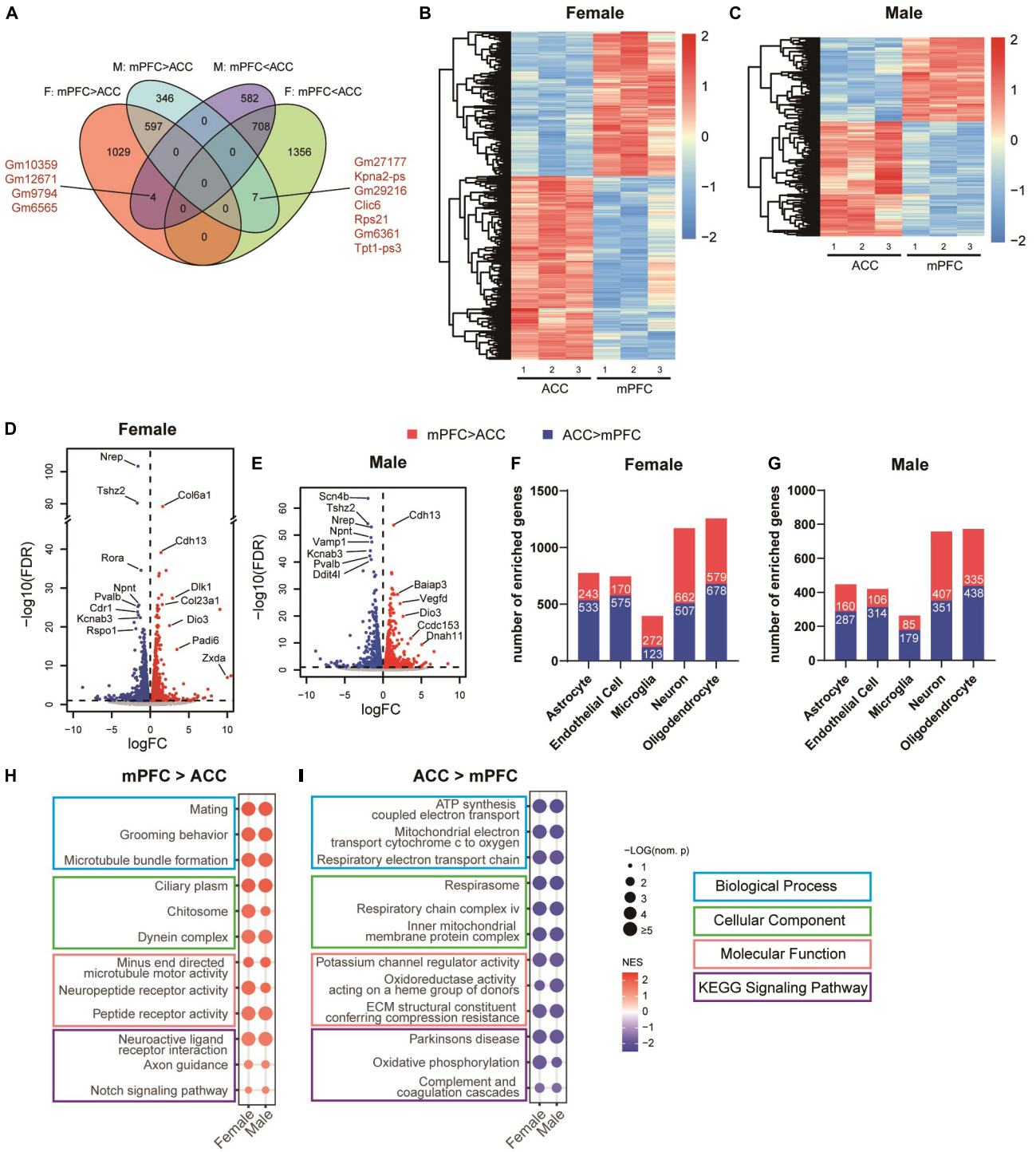

FIGURE 7 | Differences between the transcriptomic profiles of the mPFC versus the ACC of female and male mice in the sham group. **(A)** Venn diagram depicting partial overlaps of the DEGs comparing the mPFC versus the ACC between the female and male mice. F, female; M, male. mPFC > ACC: transcripts expressed significantly more in the mPFC than in the ACC; mPFC < ACC: transcripts expressed significantly more in the ACC than in the mPFC. Hierarchical clustered heatmaps showing relative expression of the DEGs comparing the ACC versus the mPFC in the female **(B)** and male **(C)** mice from the sham group. Color scales represent standardized rlog-transformed values across samples. The volcano plots of the DEGs in the female **(D)** and male **(E)** mice, with horizontal lines at the $-\log_{10}$ (false discovery rate, FDR) = 1 and vertical lines at $\log_2$ (fold change, FC) = 0. Blue dots represent transcripts expressed significantly more in the ACC than the mPFC, and the red dots represent transcripts expressed significantly more in the mPFC than the ACC. The numbers of DEGs enriched in different cell types in the female **(F)** and male **(G)** mice, comparing the mPFC versus the ACC. Top differentially enriched gene sets in the mPFC **(H)** versus the ACC **(I)**. The size of the dots indicates the $-\log_{10}$ (nominal *p*) values, and the color indicates the normalized enrichment scores (NES).

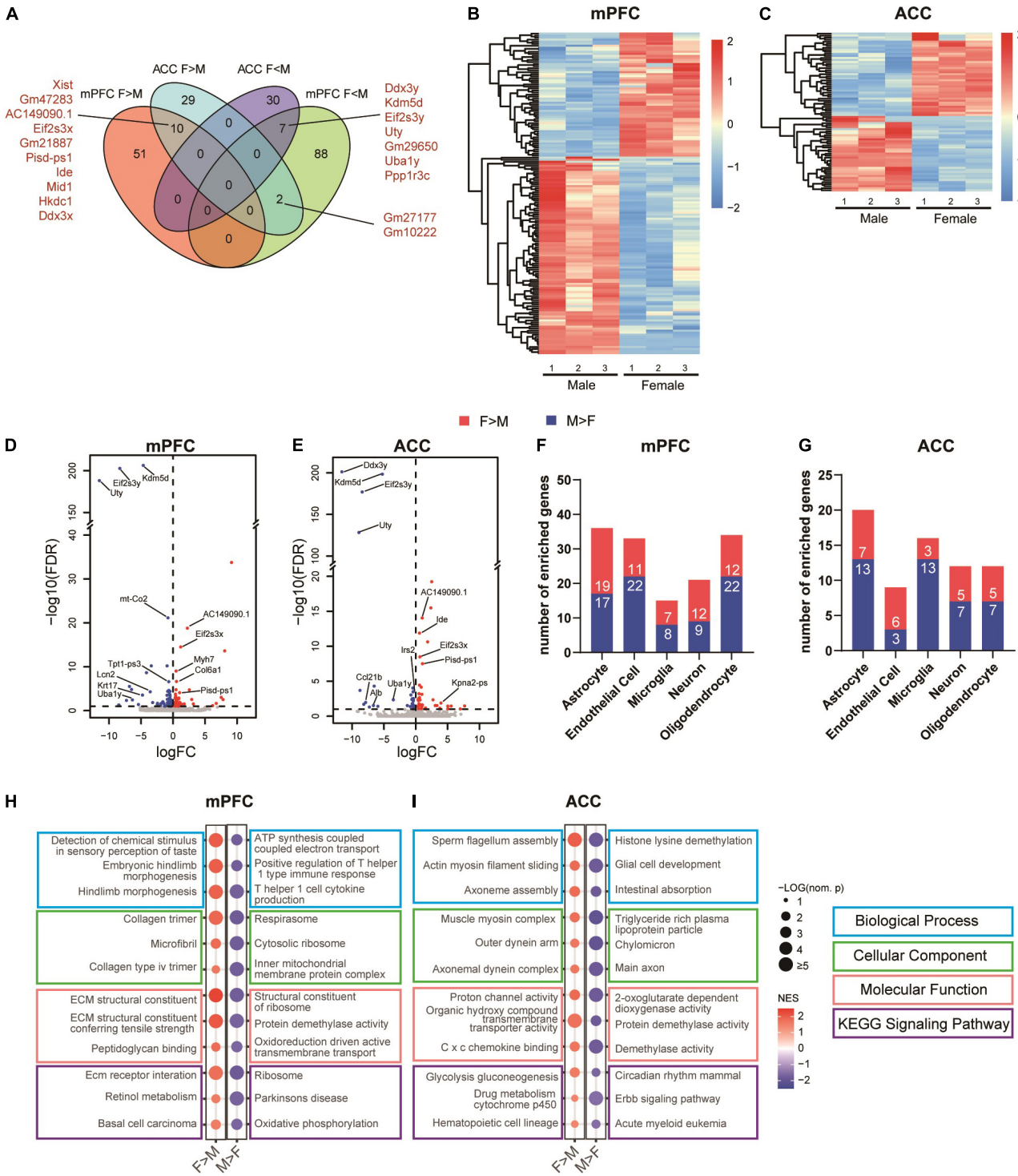

FIGURE 8 | Sex differences in the transcriptomic profiles of the mPFC and the ACC in the sham group. **(A)** Venn diagram depicting partial overlaps of the sex-specific DEGs between the mPFC and the ACC. F > M: transcripts expressed significantly more in the female than in the male mice; F < M: transcripts expressed significantly more in the male than in the female mice. Hierarchical clustered heatmaps showing relative expression of the sex-specific DEGs in the mPFC **(B)** and the ACC **(C)** from the sham group. Color scales represent standardized rlog-transformed values across samples. The volcano plots of the sex-specific DEGs in the mPFC **(D)** and the ACC **(E)**, with horizontal lines at the $-\log_{10}$ (false discovery rate, FDR) = 1 and vertical lines at $\log_2$ (fold change, FC) = 0. Blue dots represent transcripts expressed significantly more in the male than in the female mice, and the red dots represent transcripts expressed significantly more in the female than in the male mice. The numbers of specific DEGs enriched in different cell types in the mPFC **(F)** and the ACC **(G)**. Top sex-specific differentially enriched gene sets in the mPFC **(H)** and the ACC **(I)**. The size of the dots indicates the $-\log_{10}$ (nominal *p*) values, and the color indicates the normalized enrichment scores (NES).

different sexes by SNI (**Figures 6A–D**, **8H,I** and **Supplementary Table 7**).

Collectively, these findings suggest the already existed difference of transcriptomic profiles between the mPFC and the ACC of non-SNI sham group in a sex-specific manner, which may contribute to the region- and sex-specific alternations in the transcriptomic profiles induced by SNI.

DISCUSSION

In summary, the current study reveals the distinct nature of the transcriptomic profiles of the mPFC and the ACC in a sex-specific manner at 2 weeks after SNI, an early time point when mice began to show mild depression-like phenotypes. Given that sex difference exists in susceptibility to both pain and depression (Bartley and Fillingim, 2013; Altemus et al., 2014), and that the mPFC and the ACC are known brain regions for their critical but opposite roles in the comorbidity of pain and depression (Barthas et al., 2015; Sellmeijer et al., 2018; Kummer et al., 2020), our findings provide a valuable resource for elucidating the molecular mechanisms underlying the differential regulation of the mPFC and the ACC in different sexes during early development of the comorbidity of pain and depression. In addition, these findings should pave the way for the development of targeted therapeutics for the treatment of chronic pain and its affective disorders.

Several epidemiological studies of chronic pain have well documented that the prevalence of chronic pain and depression is higher in women than men (Williams et al., 2003; Fillingim et al., 2009; Ruau et al., 2012; Vetvik and MacGregor, 2017). Although social and cultural factors may contribute to the differences (Meints and Edwards, 2018; Mills et al., 2019), biological factors cannot be ignored. However, the preclinical studies of pain and its associated affective disorders have been largely relied on male rodents. Direct comparison of the similarity and differences between sexes have rarely been reported (Mogil, 2020). In the current study, we first compared the mechanical pain and depression-like behaviors in female and male mice after SNI surgery, which, however, did not exhibit significant sex differences, except that the decrease in mechanical pain threshold was relatively larger in the female mice than in the male mice. We reason that several factors may contribute to the lack of sex-differences in our behavioral tests. First, SNI is a procedure that generates robust and persistent stimulation to pain fibers, which is hard to tolerant (Decosterd and Woolf, 2000; Guida et al., 2020), whereas sex-differential sensitivity to pain may be more relevant to lower magnitudes of painful stimuli. Second, the sex differences in tolerance to chronic pain and development of associated depressive phenotypes are likely due to in part the differential adaptation to chronic pain conditions. The current study only examined behavioral changes over the first 4 weeks after SNI, but sex-contributed phenotypic difference may require more time to emerge. Third, we cannot exclude the possibility that the behavioral tests used in this study weren't sensitive enough to reveal the sex differences.

Despite limited differences at the behavioral level were detected, robust sex differences were observed at the transcriptional level after SNI. Interestingly, comparing the sham group versus the SNI group, more DEGs were identified for the male mice than the female mice in the mPFC, whereas the opposite patterns occurred in the ACC, indicating differential modulation of the two brain regions in different sexes. Consistent with this notion, Jones and Sheets reported that SNI selectively increased the excitability and the excitatory synaptic currents of the parvalbumin-expressing (PV^+) inhibitory neurons in the layer 5 of the mPFC of male mice but not female mice (Jones and Sheets, 2020). As PV^+ neurons are critical for controlling the excitability of the targeted pyramidal neurons (Hu et al., 2014), the change mentioned above may lead to greater reduction of overall excitability in the mPFC of the male mice than female mice, which in turn is thought to contribute to greater attention deficits in male and female individuals with chronic pain (Shiers et al., 2018; Jones and Sheets, 2020). On the other hand, women but not men with chronic low back pain showed alterations in the functional connectivity of the subgenual ACC (sgACC) (Osborne et al., 2021). It would be of interest to examine how the sex-specific and distinct changes in the transcriptomic profiles of the mPFC and the ACC may be related to their functional alterations during neuropathic pain.

In addition to the differences in the numbers of DEGs, we found that the DEGs induced by SNI in the mPFC and the ACC showed little overlaps between female and male mice. The GSEA results further revealed largely distinct enrichment of transcriptomes in the GO and signaling pathways induced by SNI in female versus male mice. These findings are consistent with the emerging evidences, suggesting that clear differences existed in the mechanisms underlying chronic pain processing and the development of affective disorders during chronic pain progression at the system, cellular, and molecular levels (Barthas et al., 2015; Zhu et al., 2021). Such mechanistic differences may contribute to the differential sensitivity and tolerance of chronic pain and susceptibility to pain-induced depression, as well as differential treatment options for female and male patients (Bartley and Fillingim, 2013; Meints and Edwards, 2018). By directly comparing female and male transcriptomes in the two brain hub regions for the comorbidity of pain and depression, our study provides a useful resource for further dissecting and understanding the mechanisms contributing to the dynamic interaction of neuropathic pain and depression.

The sex-differences in the transcriptomic changes of the mPFC and the ACC after SNI were partially overlapped with the sex-differences in the transcriptomes of the two regions in the sham group. These findings suggest that the already existed biological differences in the female and male brains, which may be due to genetic, genomic imprinting, and hormonal differences in different sexes (Ngun et al., 2011; Mogil, 2012; Choleris et al., 2018), may contribute to their differential responses and adaption to chronic pain and its affective disorders like depression.

While the mPFC and the ACC are both activated by acute pain, chronic pain leads to opposite phenotypes in the two regions: hypoactive mPFC and hyperactive ACC accompanied by long-lasting changes in synaptic plasticity (Bliss et al., 2016; Sellmeijer et al., 2018; Tan and Kuner, 2021). However, direct comparison of the mechanisms underlying the divergent

alterations of the mPFC versus the ACC by chronic pain remains under-investigated. Here, we showed that the transcriptomic profiles between the mPFC and the ACC were dramatically different in the sham condition and after SNI. Interestingly, after SNI, the most noticeable changes in the mPFC involved the downregulation of transcripts related to myelin formation, glia development, and axonal transportation. These processes are known to be prerequisite for the establishment and maintenance of proper functions of neural circuits during developmental stages and in the adulthood (Almeida and Lyons, 2017; Monje, 2018; Stadelmann et al., 2019). Therefore, we speculate that the impairment of these processes during early phase of neuropathic pain likely weakens the functional connectivity of the mPFC, which then contributes to the development of hypoactive phenotype. On the other hand, the most significantly upregulated transcripts in the ACC include *Syt6* and *Syt2*, two genes that encode different subtypes of synaptotagmins. Synaptotagmin-2 is one of three major synaptotagmins that are required for fast synchronous neurotransmitter release from presynaptic terminals, which also play important roles in long-term potentiation (LTP) and short-term synaptic plasticity of excitatory synapses (Chen et al., 2017; Wolfes and Dean, 2020). Synaptotagmin-6 is a key component of the acrosomal exocytosis process, which involves in exocytosis of neuropeptides such as BDNF (Dean et al., 2009). The upregulation of the *Syt6* and *Syt2* expression in the ACC after SNI may be involved in the regulation of LTP and hyperactivity of ACC neurons. However, it should be emphasized that increasing evidences have suggested that chronic pain induces distinct changes in diverse subtypes of neurons (including excitatory and different types of inhibitory neurons) in different layers of the mPFC and the ACC (Bliss et al., 2016; Tan and Kuner, 2021). Therefore, it is important to investigate in the next steps which neuronal populations are most affected by the key transcriptomic changes induced by SNI in the mPFC and the ACC.

How are changes at the transcriptional level in the mPFC at 2 weeks after SNI surgery related to the pathological development of depression during neuropathic pain? It has been reported previously that the PFC in patients with depression exhibits a hypoactive feature (Kupfer et al., 2012; Li et al., 2016). The PFC and the nucleus accumbens (NAc) receive dopaminergic innervation from the ventral tegmental area (VTA), also known as the brain's reward circuits that are involved in the regulation of the susceptibility of depressive phenotypes, pain perception, and addictive behaviors (Russo and Nestler, 2013; Navratilova and Porreca, 2014). Optogenetic activation of glutaminergic projection of mPFC-to-NAc resulted in increased resilience to stress-induced depressive phenotypes (Bagot et al., 2015), while optogenetic suppression of VTA-to-mPFC neurons promoted susceptibility (Chaudhury et al., 2013), results that are in agreement with the numerous literatures on human and animal studies that support a general function of the mPFC to render individual resistance to stress and other negative stimuli, whereas dysfunction of mPFC can result in increased susceptibility to depression (Gomes and Grace, 2017; Hare and Duman, 2020). Importantly, elevation of the mPFC activity in the animal models, which also affect the reward circuits as mentioned above, can alleviate depression-like behaviors as well as hyperalgesia, suggesting that the mPFC acts as a hub which can regulate both pain and depression (Kummer et al., 2020; Liang et al., 2020). It is worth noting that in the clinical settings, repeated, non-invasive electrical or magnetic field stimulation targeting the mPFC has been found to ameliorate chronic pain as well as depressive symptoms, at least for a subset of patients who showed altered mPFC activity and connectivity (Borckardt et al., 2017; Ong et al., 2019; Hare and Duman, 2020; Scangos et al., 2021; Tan and Kuner, 2021). Ketamine, a fast-acting antidepressant, also appears to rapidly induce elevation of mPFC activity (Berman et al., 2000; Hare and Duman, 2020). These findings highlight the mPFC as an intercepted region for developing the comorbidity of pain and depression, and the importance of elucidating the molecular signatures and their underlying mechanisms that may contribute to the regulation of the neuronal activity of mPFC and its connecting strength to other brain regions in the reward circuits.

How does the mPFC become hypoactive in both chronic pain and depression? A growing number of studies have suggested the potential involvement of non-neuronal brain cells in depression. During the early pathogenesis of depression, alterations of non-neuronal brain cells may precede and lead to neuronal dysfunction (Cathomas et al., 2022). In line with this notion, we found in the current study that downregulation of myelination was the most striking change in the mPFC of both female and male mice at 2 weeks after SNI, when depressive-like behaviors began to emerge. In the mPFC of male mice after SNI, more than half of the downregulated transcripts were enriched in the oligodendrocytes. The myelin-related and oligodendrocyte-enriched genes, such as *Mal*, *Cnp*, *Plp1*, *Mobp*, *Mbp*, and *Mog* were among the most downregulated genes as well as the most strongly associated hub genes in the PPI network in the male mPFC. On the other hand, for the mPFC in female mice after SNI, we observed modest changes in the expression of individual genes enriched in oligodendrocytes and engaged in myelination, but highly coordinated expressional changes across multiple genes in the related gene sets. These led to the findings from our GSEA analysis that downregulation of gene sets involved in oligodendrocyte development and myelin sheath were the most prominent features after SNI. Thus, although gene expression patterns differ greatly between female and male mice after SNI, dysfunction of myelination process emerged to be the most pronounced alteration in the mPFC in both sexes. Interestingly, recent studies have also found decreases in oligodendrocytes and impairment of myelin in the mPFC after several types of stress that produce depressive phenotypes (Liu et al., 2012; Makinodan et al., 2012; Bonnefil et al., 2019). Selective demyelination of the mPFC induced by focal injection of lysolecithin reduced social interaction, a depression-related phenotype in mice, whereas clemastine, a compound that induced oligodendrocyte differentiation in the mPFC, alleviated depressive-like social avoidance induced by prolonged social isolation (Liu et al., 2016; Bonnefil et al., 2019). Oligodendrocytes in the mPFC have also been reported to play an important role in pain management. Downregulation of myelin-related proteins and oligodendrocyte apoptosis were observed

in rats with fentanyl-induced hyperalgesia, whereas prophylactic blockage of oligodendrocyte apoptosis in the mPFC prevented hyperalgesia to occur (Wang et al., 2022). Together with these findings, our study suggests that restoring oligodendrocytes and myelin in the mPFC may be key to the treatment of comorbidity of pain and related depression.

In addition to the mPFC, the ACC has also been identified as a critical region in the pathological development of depression, particularly in the context of chronic pain (Barthas et al., 2015; Tan and Kuner, 2021). Abnormally increased activities in the sgACC and the perigenual ACC (pgACC) have been observed in patients with major depressive disorder and has been correlated with anhedonia, a typical symptom of depression (Philippi et al., 2015; Rupprechter et al., 2021; Pizzagalli and Roberts, 2022). The fast-acting antidepressant ketamine reduced sgACC and pgACC activity. Importantly, this reduction was associated with an anti-anhedonia effect at the behavioral level (Alexander et al., 2021). In neuropathic pain, lesion or inactivation of ACC reduced pain-related depressive symptoms, whereas activation of the ACC induced aversion to the place of its administration (Barthas et al., 2015; Zhang et al., 2017). Therefore, the ACC is also a key brain region at the interface between pain and depression.

In the present study, the transcriptome of ACC was significantly altered by SNI in the female mice, while only a limited numbers of DEGs were detected in the ACC of male mice. Given the importance of ACC in depression (Etkin et al., 2011; Pizzagalli and Roberts, 2022), and female subjects being more prone to depression than male subjects (Altemus et al., 2014; Bangasser and Cuarenta, 2021), we speculate that the sex-differences in transcriptional changes in the ACC after SNI may contribute to the differential prevalence of depression as neuropathic pain progresses. This speculation, however, awaits further experimental testing. In the ACC of female mice after SNI, besides upregulation of the synaptotagmins, the most notable change was the reduction of genes encoding extracellular matrix components. These genes also constituted the central sub-network of hub genes in the PPI network of the DEGs in the female ACC after SNI. Furthermore, GSEA analysis of the ACC transcriptome of female mice showed that downregulation of collagen fibril organization, collagen trimer, extracellular matrix structural constituent, and serine type endopeptidase inhibitor activity were the most prominent changes after SNI. Collectively, these findings reveal that the disruption of extracellular matrix in the ACC of female mice is a major event accompanying the early development of depressive-like phenotypes at 2 weeks after SNI surgery.

Extracellular matrix, which accounts for 20% of the brain's volume, not only provides a supporting scaffold for other brain cells, but also acts as the first messengers for transmission of extracellular signals to modulate neuronal functions (Dityatev et al., 2010; Barros et al., 2011; Laham and Gould, 2021). Formation of extracellular matrix at the end of the "critical period" during visual cortex development serves as an essential mechanism to restrain structural plasticity (Hensch, 2005; de Vivo et al., 2013). In the adulthood, it has been reported that remodeling of extracellular matrix is required for *de novo* synapse formation, various forms of synaptic plasticity, and fear memory erasure (Tajerian et al., 2018; Laham and Gould, 2021). In the context of neuropathic pain, Kawasaki et al. (2008) reported the distinct roles of acutely up-regulated matrix metalloproteases-9 and delayed induction of matrix metalloproteases-2, two proteases involved in the breakdown of extracellular matrix and cytokines, in the dorsal root ganglion for the development of early- and late-phase neuropathic pain indued by spinal nerve ligation. Inhibition of matrix metalloproteases-9 and matrix metalloproteases-2 by pharmacological or siRNA-based strategies effectively produced anti-allodynic effect (Kawasaki et al., 2008). Li et al. (2021) reported that SNI reduced the expression of LAMB1, a major component of extracellular matrix in the ACC. Knockdown of LAMB1 in the ACC increased the release probability of neurotransmitters and led to abnormal postsynaptic spine remodeling, which in turn increased pain sensitivity and caused depression-like behaviors (Li et al., 2021). Our findings now showed that the decrease of extracellular matrix is a major event in the early development of depressive phenotypes after SNI, further highlight the restoration of extracellular matrix in the ACC as a potential therapeutic strategy for the treatment of pain and depression comorbidity.

In conclusion, our study reveals that at 2 weeks after SNI, an early time point when the mice began to show mild depressive symptoms, the transcriptomic changes in the mPFC and the ACC are highly distinct and sex-specific. Female mice exhibited stronger transcriptomic changes in the ACC than male mice, while the opposite was observed in the mPFC. The transcriptomic changes occurred across multiple brain cell types. We further identified downregulation of myelin-related transcripts in the mPFC of both sexes, as well as upregulation of synaptotagmins and downregulation of extracellular matrix components in the female ACC as the most prominent changes induced by SNI. Taken together, these findings demonstrate the transcriptional dimorphism in both sexes and brain areas induced by neuropathic pain, suggesting potential therapeutic targets for the treatment of chronic pain and its related affective disorders.

DATA AVAILABILITY STATEMENT

The datasets presented in this study can be found in online repositories. The names of the repository/repositories and accession number(s) can be found below: https://www.ncbi.nlm.nih.gov/geo/, GSE197233.

ETHICS STATEMENT

The animal study was reviewed and approved by the Institutional Animal Care and Use Committee of Sun Yat-sen University.

AUTHOR CONTRIBUTIONS

XY and W-JL designed the study. WD, SH, XC, and YZ carried out the RNAseq analyses. WD, YL, PZ, PX, and MY carried out

the experiments. XY, W-JL, SH, and WD wrote the manuscript. All authors contributed to the article and approved the submitted version.

FUNDING

This work was supported by grants from the National Key R&D Program of China (No. 2021ZD0202000 to XY), National Natural Science Foundation of China (Nos. 81873797 to XY and 81972967 to W-JL), Natural Science Foundation of Guangdong Province (Nos. 2019A1515011483 to XY and 2019A1515011754 to W-JL), the Fundamental Research Funds for the Central Universities (No. 19ykzd40 to XY), Guangdong Project (No. 2019QN01Y202 to XY), Science and Technology Program of Guangzhou (No. 202007030001 to XY and W-JL), and Guangdong Science and Technology Department (Nos. 2020B1212060018 and 2020B1212030004 to W-JL).

ACKNOWLEDGMENTS

We thank the animal facility and the core facility of the Zhongshan School of Medicine, Sun Yat-sen University. We also thank all members of the Ye Lab and the Lin Lab for discussion and technical assistance during the execution of this project.

SUPPLEMENTARY MATERIAL

The Supplementary Material for this article can be found online at: https://www.frontiersin.org/articles/10.3389/fnmol.2022.886916/full#supplementary-material

Supplementary Table 1 | List of primers used in the qPCR validation of RNAseq results.

Supplementary Table 2 | List of the DEGs in the mPFC and the ACC of female and male mice, comparing the sham versus the SNI groups.

Supplementary Table 3 | Gene set enrichment analysis results for the mPFC and the ACC of female and male mice, comparing the sham versus the SNI groups.

Supplementary Table 4 | List of the DEGs comparing the mPFC versus the ACC in the female and male mice of the sham groups.

Supplementary Table 5 | Gene set enrichment analysis results for the female and male mice, comparing the mPFC versus the ACC in the sham groups.

Supplementary Table 6 | List of the DEGs in the mPFC and the ACC, comparing female and male mice of the sham groups.

Supplementary Table 7 | Gene set enrichment analysis results for the mPFC and the ACC, comparing female and male mice of the sham groups.

REFERENCES

Alexander, L., Jelen, L. A., Mehta, M. A., and Young, A. H. (2021). The anterior cingulate cortex as a key locus of ketamine's antidepressant action. *Neurosci. Biobehav. Rev.* 127, 531–554. doi: 10.1016/j.neubiorev.2021.05.003

Almeida, R. G., and Lyons, D. A. (2017). On myelinated axon plasticity and neuronal circuit formation and function. *J. Neurosci.* 37, 10023–10034. doi: 10.1523/JNEUROSCI.3185-16.2017

Altemus, M., Sarvaiya, N., and Neill Epperson, C. (2014). Sex differences in anxiety and depression clinical perspectives. *Front. Neuroendocrinol.* 35:320–330. doi: 10.1016/j.yfrne.2014.05.004

Alvarado, S., Tajerian, M., Millecamps, M., Suderman, M., Stone, L. S., and Szyf, M. (2013). Peripheral nerve injury is accompanied by chronic transcriptome-wide changes in the mouse prefrontal cortex. *Mol. Pain* 9:21. doi: 10.1186/1744-8069-9-21

Anders, S., Pyl, P. T., and Huber, W. (2015). HTSeq–a Python framework to work with high-throughput sequencing data. *Bioinformatics* 31, 166–169. doi: 10.1093/bioinformatics/btu638

Bagot, R. C., Parise, E. M., Pena, C. J., Zhang, H. X., Maze, I., Chaudhury, D., et al. (2015). Ventral hippocampal afferents to the nucleus accumbens regulate susceptibility to depression. *Nat. Commun.* 6:7062. doi: 10.1038/ncomms8062

Bair, M. J., Robinson, R. L., Katon, W., and Kroenke, K. (2003). Depression and pain comorbidity: a literature review. *Arch. Intern. Med.* 163, 2433–2445. doi: 10.1001/archinte.163.20.2433

Bangasser, D. A., and Cuarenta, A. (2021). Sex differences in anxiety and depression: circuits and mechanisms. *Nat. Rev. Neurosci.* 22, 674–684. doi: 10.1038/s41583-021-00513-0

Bannister, K., Sachau, J., Baron, R., and Dickenson, A. H. (2020). Neuropathic pain: mechanism-based therapeutics. *Annu. Rev. Pharmacol. Toxicol.* 60, 257–274. doi: 10.1146/annurev-pharmtox-010818-021524

Barros, C. S., Franco, S. J., and Muller, U. (2011). Extracellular matrix: functions in the nervous system. *Cold Spring Harb. Perspect. Biol.* 3:a005108. doi: 10.1101/cshperspect.a005108

Barthas, F., Sellmeijer, J., Hugel, S., Waltisperger, E., Barrot, M., and Yalcin, I. (2015). The anterior cingulate cortex is a critical hub for pain-induced depression. *Biol. Psychiatry* 77, 236–245. doi: 10.1016/j.biopsych.2014.08.004

Bartley, E. J., and Fillingim, R. B. (2013). Sex differences in pain: a brief review of clinical and experimental findings. *Br. J. Anaesth.* 111, 52–58. doi: 10.1093/bja/aet127

Berman, R. M., Cappiello, A., Anand, A., Oren, D. A., Heninger, G. R., Charney, D. S., et al. (2000). Antidepressant effects of ketamine in depressed patients. *Biol. Psychiatry* 47, 351–354. doi: 10.1016/s0006-3223(99)00230-9

Berta, T., Perrin, F. E., Pertin, M., Tonello, R., Liu, Y. C., Chamessian, A., et al. (2017). Gene expression profiling of cutaneous injured and non-injured nociceptors in SNI animal model of neuropathic pain. *Sci. Rep.* 7:9367. doi: 10.1038/s41598-017-08865-3

Bliss, T. V., Collingridge, G. L., Kaang, B. K., and Zhuo, M. (2016). Synaptic plasticity in the anterior cingulate cortex in acute and chronic pain. *Nat. Rev. Neurosci.* 17, 485–496. doi: 10.1038/nrn.2016.68

Bonnefil, V., Dietz, K., Amatruda, M., Wentling, M., Aubry, A. V., Dupree, J. L., et al. (2019). Region-specific myelin differences define behavioral consequences of chronic social defeat stress in mice. *Elife* 8:e40855. doi: 10.7554/eLife.40855

Borckardt, J. J., Reeves, S. T., Milliken, C., Carter, B., Epperson, T. I., Gunselman, R. J., et al. (2017). Prefrontal versus motor cortex transcranial direct current stimulation (tDCS) effects on post-surgical opioid use. *Brain Stimul.* 10, 1096–1101. doi: 10.1016/j.brs.2017.09.006

Buffington, A. L., Hanlon, C. A., and McKeown, M. J. (2005). Acute and persistent pain modulation of attention-related anterior cingulate fMRI activations. *Pain* 113, 172–184. doi: 10.1016/j.pain.2004.10.006

Bushnell, M. C., Ceko, M., and Low, L. A. (2013). Cognitive and emotional control of pain and its disruption in chronic pain. *Nat. Rev. Neurosci.* 14, 502–511. doi: 10.1038/nrn3516

Cao, J., Wang, J., Dwyer, J. B., Gautier, N. M., Wang, S., Leslie, F. M., et al. (2013). Gestational nicotine exposure modifies myelin gene expression in the brains of adolescent rats with sex differences. *Transl. Psychiatry* 3:e247. doi: 10.1038/tp.2013.21

Cathomas, F., Holt, L. M., Parise, E. M., Liu, J., Murrough, J. W., Casaccia, P., et al. (2022). Beyond the neuron: role of non-neuronal cells in stress disorders. *Neuron* 110, 1116–1138. doi: 10.1016/j.neuron.2022.01.033

Chaplan, S. R., Bach, F. W., Pogrel, J. W., Chung, J. M., and Yaksh, T. L. (1994). Quantitative assessment of tactile allodynia in the rat paw. *J. Neurosci. Methods* 53, 55–63. doi: 10.1016/0165-0270(94)90144-9

Chaudhury, D., Walsh, J. J., Friedman, A. K., Juarez, B., Ku, S. M., Koo, J. W., et al. (2013). Rapid regulation of depression-related behaviours by control of midbrain dopamine neurons. *Nature* 493, 532–536. doi: 10.1038/nature11713

Chen, C., Arai, I., Satterfield, R., Young, S. M. Jr., and Jonas, P. (2017). Synaptotagmin 2 is the fast Ca(2+) sensor at a central inhibitory synapse. *Cell Rep.* 18, 723–736. doi: 10.1016/j.celrep.2016.12.067

Chin, C. H., Chen, S. H., Wu, H. H., Ho, C. W., Ko, M. T., and Lin, C. Y. (2014). cytoHubba: identifying hub objects and sub-networks from complex interactome. *BMC Syst. Biol.* 8(Suppl. 4):S11. doi: 10.1186/1752-0509-8-S4-S11

Choleris, E., Galea, L. A. M., Sohrabji, F., and Frick, K. M. (2018). Sex differences in the brain: Implications for behavioral and biomedical research. *Neurosci. Biobehav. Rev.* 85, 126–145. doi: 10.1016/j.neubiorev.2017.07.005

Chung, M. S., Langouet, M., Chamberlain, S. J., and Carmichael, G. G. (2020). Prader-Willi syndrome: reflections on seminal studies and future therapies. *Open Biol.* 10, 200195. doi: 10.1098/rsob.200195

Copps, K. D., and White, M. F. (2012). Regulation of insulin sensitivity by serine/threonine phosphorylation of insulin receptor substrate proteins IRS1 and IRS2. *Diabetologia* 55, 2565–2582. doi: 10.1007/s00125-012-2644-8

Cryan, J. F., Mombereau, C., and Vassout, A. (2005). The tail suspension test as a model for assessing antidepressant activity: review of pharmacological and genetic studies in mice. *Neurosci. Biobehav. Rev.* 29, 571–625. doi: 10.1016/j.neubiorev.2005.03.009

de Heer, E. W., Gerrits, M. M., Beekman, A. T., Dekker, J., van Marwijk, H. W., de Waal, M. W., et al. (2014). The association of depression and anxiety with pain: a study from NESDA. *PLoS One* 9:e106907. doi: 10.1371/journal.pone.0106907

de Vivo, L., Landi, S., Panniello, M., Baroncelli, L., Chierzi, S., Mariotti, L., et al. (2013). Extracellular matrix inhibits structural and functional plasticity of dendritic spines in the adult visual cortex. *Nat. Commun.* 4:1484. doi: 10.1038/ncomms2491

Dean, C., Liu, H., Dunning, F. M., Chang, P. Y., Jackson, M. B., and Chapman, E. R. (2009). Synaptotagmin-IV modulates synaptic function and long-term potentiation by regulating BDNF release. *Nat. Neurosci.* 12, 767–776. doi: 10.1038/nn.2315

Decosterd, I., and Woolf, C. J. (2000). Spared nerve injury: an animal model of persistent peripheral neuropathic pain. *Pain* 87, 149–158. doi: 10.1016/S0304-3959(00)00276-1

Descalzi, G., Mitsi, V., Purushothaman, I., Gaspari, S., Avrampou, K., Loh, Y. E., et al. (2017). Neuropathic pain promotes adaptive changes in gene expression in brain networks involved in stress and depression. *Sci. Signal.* 10:eaaj1549. doi: 10.1126/scisignal.aaj1549

Deuis, J. R., Dvorakova, L. S., and Vetter, I. (2017). Methods used to evaluate pain behaviors in rodents. *Front. Mol. Neurosci.* 10:284. doi: 10.3389/fnmol.2017.00284

Dityatev, A., Schachner, M., and Sonderegger, P. (2010). The dual role of the extracellular matrix in synaptic plasticity and homeostasis. *Nat. Rev. Neurosci.* 11, 735–746. doi: 10.1038/nrn2898

Donaudy, F., Snoeckx, R., Pfister, M., Zenner, H. P., Blin, N., Di Stazio, M., et al. (2004). Nonmuscle myosin heavy-chain gene MYH14 is expressed in cochlea and mutated in patients affected by autosomal dominant hearing impairment (DFNA4). *Am. J. Hum. Genet.* 74, 770–776. doi: 10.1086/383285

Etkin, A., Egner, T., and Kalisch, R. (2011). Emotional processing in anterior cingulate and medial prefrontal cortex. *Trends Cogn. Sci.* 15, 85–93. doi: 10.1016/j.tics.2010.11.004

Fillingim, R. B., King, C. D., Ribeiro-Dasilva, M. C., Rahim-Williams, B., and Riley, J. L. III (2009). Sex, gender, and pain: a review of recent clinical and experimental findings. *J. Pain* 10, 447–485. doi: 10.1016/j.jpain.2008.12.001

Finnerup, N. B., Kuner, R., and Jensen, T. S. (2021). Neuropathic pain: from mechanisms to treatment. *Physiol. Rev.* 101, 259–301. doi: 10.1152/physrev.00045.2019

Fiucci, G., Lespagnol, A., Stumptner-Cuvelette, P., Beaucourt, S., Duflaut, D., Susini, L., et al. (2003). Genomic organization and expression of mouse Tpt1 gene. *Genomics* 81, 570–578. doi: 10.1016/s0888-7543(03)00047-8

Fritz, H. C., McAuley, J. H., Wittfeld, K., Hegenscheid, K., Schmidt, C. O., Langner, S., et al. (2016). Chronic back pain is associated with decreased prefrontal and anterior insular gray matter: results from a population-based cohort study. *J. Pain* 17, 111–118. doi: 10.1016/j.jpain.2015.10.003

Fujiwara, K., Jindatip, D., Kikuchi, M., and Yashiro, T. (2010). In situ hybridization reveals that type I and III collagens are produced by pericytes in the anterior pituitary gland of rats. *Cell Tissue Res.* 342, 491–495. doi: 10.1007/s00441-010-1078-1

Fulton, D., Paez, P. M., and Campagnoni, A. T. (2010). The multiple roles of myelin protein genes during the development of the oligodendrocyte. *ASN Neuro* 2:e00027. doi: 10.1042/AN20090051

Gomes, F. V., and Grace, A. A. (2017). Prefrontal cortex dysfunction increases susceptibility to schizophrenia-like changes induced by adolescent stress exposure. *Schizophr. Bull.* 43, 592–600. doi: 10.1093/schbul/sbw156

Guida, F., De Gregorio, D., Palazzo, E., Ricciardi, F., Boccella, S., Belardo, C., et al. (2020). Behavioral, biochemical and electrophysiological changes in spared nerve injury model of neuropathic pain. *Int. J. Mol. Sci.* 21:3396. doi: 10.3390/ijms21093396

Hansson, P. (2003). Difficulties in stratifying neuropathic pain by mechanisms. *Eur. J. Pain* 7, 353–357. doi: 10.1016/S1090-3801(03)00051-X

Hare, B. D., and Duman, R. S. (2020). Prefrontal cortex circuits in depression and anxiety: contribution of discrete neuronal populations and target regions. *Mol. Psychiatry* 25, 2742–2758. doi: 10.1038/s41380-020-0685-9

Hensch, T. K. (2005). Critical period plasticity in local cortical circuits. *Nat. Rev. Neurosci.* 6, 877–888. doi: 10.1038/nrn1787

Hu, H., Gan, J., and Jonas, P. (2014). Interneurons. Fast-spiking, parvalbumin(+) GABAergic interneurons: from cellular design to microcircuit function. *Science* 345:1255263. doi: 10.1126/science.1255263

Jiang, C., Lin, W. J., Labonte, B., Tamminga, C. A., Turecki, G., Nestler, E. J., et al. (2019). VGF and its C-terminal peptide TLQP-62 in ventromedial prefrontal cortex regulate depression-related behaviors and the response to ketamine. *Neuropsychopharmacology* 44, 971–981. doi: 10.1038/s41386-018-0277-4

Jones, A. F., and Sheets, P. L. (2020). Sex-specific disruption of distinct mPFC inhibitory neurons in spared-nerve injury model of neuropathic pain. *Cell Rep.* 31:107729. doi: 10.1016/j.celrep.2020.107729

Kawasaki, Y., Xu, Z. Z., Wang, X., Park, J. Y., Zhuang, Z. Y., Tan, P. H., et al. (2008). Distinct roles of matrix metalloproteases in the early- and late-phase development of neuropathic pain. *Nat. Med.* 14, 331–336. doi: 10.1038/nm1723

Kelly, C. J., Huang, M., Meltzer, H., and Martina, M. (2016). Reduced glutamatergic currents and dendritic branching of layer 5 pyramidal cells contribute to medial prefrontal cortex deactivation in a rat model of neuropathic pain. *Front. Cell. Neurosci.* 10:133. doi: 10.3389/fncel.2016.00133

Kummer, K. K., Mitric, M., Kalpachidou, T., and Kress, M. (2020). The medial prefrontal cortex as a central hub for mental comorbidities associated with chronic pain. *Int. J. Mol. Sci.* 21:3440. doi: 10.3390/ijms21103440

Kupfer, D. J., Frank, E., and Phillips, M. L. (2012). Major depressive disorder: new clinical, neurobiological, and treatment perspectives. *Lancet* 379, 1045–1055. doi: 10.1016/S0140-6736(11)60602-8

Lachmann, A., Clarke, D. J. B., Torre, D., Xie, Z., and Ma'ayan, A. (2020). Interoperable RNA-Seq analysis in the cloud. *Biochim. Biophys. Acta Gene Regul. Mech.* 1863:194521. doi: 10.1016/j.bbagrm.2020.194521

Laham, B. J., and Gould, E. (2021). How stress influences the dynamic plasticity of the brain's extracellular matrix. *Front. Cell. Neurosci.* 15:814287. doi: 10.3389/fncel.2021.814287

Li, C. T., Chen, M. H., Lin, W. C., Hong, C. J., Yang, B. H., Liu, R. S., et al. (2016). The effects of low-dose ketamine on the prefrontal cortex and amygdala in treatment-resistant depression: a randomized controlled study. *Hum. Brain Mapp.* 37, 1080–1090. doi: 10.1002/hbm.23085

Li, C., and Xu, J. (2019). Feature selection with the Fisher score followed by the Maximal Clique Centrality algorithm can accurately identify the hub genes of hepatocellular carcinoma. *Sci. Rep.* 9:17283. doi: 10.1038/s41598-019-53471-0

Li, X. Y., Ko, H. G., Chen, T., Descalzi, G., Koga, K., Wang, H., et al. (2010). Alleviating neuropathic pain hypersensitivity by inhibiting PKMzeta in the anterior cingulate cortex. *Science* 330, 1400–1404. doi: 10.1126/science.1191792

Li, Z. Z., Han, W. J., Sun, Z. C., Chen, Y., Sun, J. Y., Cai, G. H., et al. (2021). Extracellular matrix protein laminin beta1 regulates pain sensitivity and anxiodepression-like behaviors in mice. *J. Clin. Invest.* 131:e146323. doi: 10.1172/JCI146323

Liang, H. Y., Chen, Z. J., Xiao, H., Lin, Y. H., Hu, Y. Y., Chang, L., et al. (2020). nNOS-expressing neurons in the vmPFC transform pPVT-derived chronic pain signals into anxiety behaviors. *Nat. Commun.* 11:2501. doi: 10.1038/s41467-020-16198-5

Liu, J., Dietz, K., DeLoyht, J. M., Pedre, X., Kelkar, D., Kaur, J., et al. (2012). Impaired adult myelination in the prefrontal cortex of

socially isolated mice. *Nat. Neurosci.* 15, 1621–1623. doi: 10.1038/nn.3263

Liu, J., Dupree, J. L., Gacias, M., Frawley, R., Sikder, T., Naik, P., et al. (2016). Clemastine enhances myelination in the prefrontal cortex and rescues behavioral changes in socially isolated mice. *J. Neurosci.* 36, 957–962. doi: 10.1523/JNEUROSCI.3608-15.2016

Makinodan, M., Rosen, K. M., Ito, S., and Corfas, G. (2012). A critical period for social experience-dependent oligodendrocyte maturation and myelination. *Science* 337, 1357–1360. doi: 10.1126/science.1220845

McDermaid, A., Monier, B., Zhao, J., Liu, B., and Ma, Q. (2019). Interpretation of differential gene expression results of RNA-seq data: review and integration. *Brief. Bioinform.* 20, 2044–2054. doi: 10.1093/bib/bby067

Meints, S. M., and Edwards, R. R. (2018). Evaluating psychosocial contributions to chronic pain outcomes. *Prog. Neuropsychopharmacol. Biol. Psychiatry* 87(Pt. B), 168–182. doi: 10.1016/j.pnpbp.2018.01.017

Mi, J. X., Zhang, Y. N., Lai, Z., Li, W., Zhou, L., and Zhong, F. (2019). Principal component analysis based on nuclear norm minimization. *Neural Netw.* 118, 1–16. doi: 10.1016/j.neunet.2019.05.020

Millecamps, M., Centeno, M. V., Berra, H. H., Rudick, C. N., Lavarello, S., Tkatch, T., et al. (2007). D-cycloserine reduces neuropathic pain behavior through limbic NMDA-mediated circuitry. *Pain* 132, 108–123. doi: 10.1016/j.pain.2007.03.003

Mills, S. E. E., Nicolson, K. P., and Smith, B. H. (2019). Chronic pain: a review of its epidemiology and associated factors in population-based studies. *Br. J. Anaesth.* 123, e273–e283. doi: 10.1016/j.bja.2019.03.023

Mogil, J. S. (2012). Sex differences in pain and pain inhibition: multiple explanations of a controversial phenomenon. *Nat. Rev. Neurosci.* 13, 859–866. doi: 10.1038/nrn3360

Mogil, J. S. (2020). Qualitative sex differences in pain processing: emerging evidence of a biased literature. *Nat. Rev. Neurosci.* 21, 353–365. doi: 10.1038/s41583-020-0310-6

Monje, M. (2018). Myelin plasticity and nervous system function. *Annu. Rev. Neurosci.* 41, 61–76. doi: 10.1146/annurev-neuro-080317-061853

Navratilova, E., and Porreca, F. (2014). Reward and motivation in pain and pain relief. *Nat. Neurosci.* 17, 1304–1312. doi: 10.1038/nn.3811

Ngun, T. C., Ghahramani, N., Sanchez, F. J., Bocklandt, S., and Vilain, E. (2011). The genetics of sex differences in brain and behavior. *Front. Neuroendocrinol.* 32:227–246. doi: 10.1016/j.yfrne.2010.10.001

Ong, W. Y., Stohler, C. S., and Herr, D. R. (2019). Role of the prefrontal cortex in pain processing. *Mol. Neurobiol.* 56, 1137–1166. doi: 10.1007/s12035-018-1130-9

Osborne, N. R., Cheng, J. C., Rogachov, A., Kim, J. A., Hemington, K. S., Bosma, R. L., et al. (2021). Abnormal subgenual anterior cingulate circuitry is unique to women but not men with chronic pain. *Pain* 162, 97–108. doi: 10.1097/j.pain.0000000000002016

Pan, Y., Wu, L., He, S., Wu, J., Wang, T., and Zang, H. (2021). Identification of hub genes in thyroid carcinoma to predict prognosis by integrated bioinformatics analysis. *Bioengineered* 12, 2928–2940. doi: 10.1080/21655979.2021.1940615

Phelps, C. E., Navratilova, E., and Porreca, F. (2021). Cognition in the chronic pain experience: preclinical insights. *Trends Cogn. Sci.* 25, 365–376. doi: 10.1016/j.tics.2021.01.001

Philippi, C. L., Motzkin, J. C., Pujara, M. S., and Koenigs, M. (2015). Subclinical depression severity is associated with distinct patterns of functional connectivity for subregions of anterior cingulate cortex. *J. Psychiatr. Res.* 71, 103–111. doi: 10.1016/j.jpsychires.2015.10.005

Pizzagalli, D. A., and Roberts, A. C. (2022). Prefrontal cortex and depression. *Neuropsychopharmacology* 47, 225–246. doi: 10.1038/s41386-021-01101-7

Ravichandran, M., Priebe, S., Grigolon, G., Rozanov, L., Groth, M., Laube, B., et al. (2018). Impairing L-threonine catabolism promotes healthspan through methylglyoxal-mediated proteohormesis. *Cell Metab.* 27, 914–925.e915. doi: 10.1016/j.cmet.2018.02.004

Robinson, M. D., McCarthy, D. J., and Smyth, G. K. (2010). edgeR: a Bioconductor package for differential expression analysis of digital gene expression data. *Bioinformatics* 26, 139–140. doi: 10.1093/bioinformatics/btp616

Rodriguez-Raecke, R., Niemeier, A., Ihle, K., Ruether, W., and May, A. (2009). Brain gray matter decrease in chronic pain is the consequence and not the cause of pain. *J. Neurosci.* 29, 13746–13750. doi: 10.1523/JNEUROSCI.3687-09.2009

Ruau, D., Liu, L. Y., Clark, J. D., Angst, M. S., and Butte, A. J. (2012). Sex differences in reported pain across 11,000 patients captured in electronic medical records. *J. Pain* 13, 228–234. doi: 10.1016/j.jpain.2011.11.002

Rupprechter, S., Stankevicius, A., Huys, Q. J. M., Series, P., and Steele, J. D. (2021). Abnormal reward valuation and event-related connectivity in unmedicated major depressive disorder. *Psychol. Med.* 51, 795–803. doi: 10.1017/S0033291719003799

Russo, S. J., and Nestler, E. J. (2013). The brain reward circuitry in mood disorders. *Nat. Rev. Neurosci.* 14, 609–625. doi: 10.1038/nrn3381

Sadler, K. E., Mogil, J. S., and Stucky, C. L. (2022). Innovations and advances in modelling and measuring pain in animals. *Nat. Rev. Neurosci.* 23, 70–85. doi: 10.1038/s41583-021-00536-7

Santoro Belangero, P., Antonio Figueiredo, E., Cohen, C., de Seixas Alves, F., Hiromi Yanaguizawa, W., Cardoso Smith, M., et al. (2018). Changes in the expression of matrix extracellular genes and TGFB family members in rotator cuff tears. *J. Orthop. Res.* 36, 2542–2553. doi: 10.1002/jor.23907

Scangos, K. W., Makhoul, G. S., Sugrue, L. P., Chang, E. F., and Krystal, A. D. (2021). State-dependent responses to intracranial brain stimulation in a patient with depression. *Nat. Med.* 27, 229–231. doi: 10.1038/s41591-020-01175-8

Sellmeijer, J., Mathis, V., Hugel, S., Li, X. H., Song, Q., Chen, Q. Y., et al. (2018). Hyperactivity of anterior cingulate cortex areas 24a/24b drives chronic pain-induced anxiodepressive-like consequences. *J. Neurosci.* 38, 3102–3115. doi: 10.1523/JNEUROSCI.3195-17.2018

Seminowicz, D. A., and Moayedi, M. (2017). The dorsolateral prefrontal cortex in acute and chronic pain. *J. Pain* 18, 1027–1035. doi: 10.1016/j.jpain.2017.03.008

Shiers, S., Pradhan, G., Mwirigi, J., Mejia, G., Ahmad, A., Kroener, S., et al. (2018). Neuropathic pain creates an enduring prefrontal cortex dysfunction corrected by the type II diabetic drug metformin but not by gabapentin. *J. Neurosci.* 38, 7337–7350. doi: 10.1523/JNEUROSCI.0713-18.2018

Stadelmann, C., Timmler, S., Barrantes-Freer, A., and Simons, M. (2019). Myelin in the central nervous system: structure, function, and pathology. *Physiol. Rev.* 99, 1381–1431. doi: 10.1152/physrev.00031.2018

Stanurova, J., Neureiter, A., Hiber, M., de Oliveira Kessler, H., Stolp, K., Goetzke, R., et al. (2016). Angelman syndrome-derived neurons display late onset of paternal UBE3A silencing. *Sci. Rep.* 6:30792. doi: 10.1038/srep30792

Stohn, J. P., Martinez, M. E., and Hernandez, A. (2016). Decreased anxiety- and depression-like behaviors and hyperactivity in a type 3 deiodinase-deficient mouse showing brain thyrotoxicosis and peripheral hypothyroidism. *Psychoneuroendocrinology* 74, 46–56. doi: 10.1016/j.psyneuen.2016.08.021

Stohn, J. P., Martinez, M. E., Zafer, M., Lopez-Espindola, D., Keyes, L. M., and Hernandez, A. (2018). Increased aggression and lack of maternal behavior in Dio3-deficient mice are associated with abnormalities in oxytocin and vasopressin systems. *Genes Brain Behav.* 17, 23–35. doi: 10.1111/gbb.12400

Subramanian, A., Tamayo, P., Mootha, V. K., Mukherjee, S., Ebert, B. L., Gillette, M. A., et al. (2005). Gene set enrichment analysis: a knowledge-based approach for interpreting genome-wide expression profiles. *Proc. Natl. Acad. Sci. U.S.A.* 102, 15545–15550. doi: 10.1073/pnas.0506580102

Szklarczyk, D., Gable, A. L., Lyon, D., Junge, A., Wyder, S., Huerta-Cepas, J., et al. (2019). STRING v11: protein-protein association networks with increased coverage, supporting functional discovery in genome-wide experimental datasets. *Nucleic Acids Res.* 47, D607–D613. doi: 10.1093/nar/gky1131

Tajerian, M., Hung, V., Nguyen, H., Lee, G., Joubert, L. M., Malkovskiy, A. V., et al. (2018). The hippocampal extracellular matrix regulates pain and memory after injury. *Mol. Psychiatry* 23, 2302–2313. doi: 10.1038/s41380-018-0209-z

Tan, L. L., and Kuner, R. (2021). Neocortical circuits in pain and pain relief. *Nat. Rev. Neurosci.* 22, 458–471. doi: 10.1038/s41583-021-00468-2

Tanaka, C., Sakuma, R., Nakamura, T., Hamada, H., and Saijoh, Y. (2007). Long-range action of Nodal requires interaction with GDF1. *Genes Dev.* 21, 3272–3282. doi: 10.1101/gad.1623907

Tappe-Theodor, A., and Kuner, R. (2019). A common ground for pain and depression. *Nat. Neurosci.* 22, 1612–1614. doi: 10.1038/s41593-019-0499-8

Tracey, I., and Johns, E. (2010). The pain matrix: reloaded or reborn as we image tonic pain using arterial spin labelling. *Pain* 148, 359–360. doi: 10.1016/j.pain.2009.11.009

Treede, R. D., Jensen, T. S., Campbell, J. N., Cruccu, G., Dostrovsky, J. O., Griffin, J. W., et al. (2008). Neuropathic pain: redefinition and a grading system for

clinical and research purposes. *Neurology* 70, 1630–1635. doi: 10.1212/01.wnl.0000282763.29778.59

Tundo, G. R., Sbardella, D., Ciaccio, C., Bianculli, A., Orlandi, A., Desimio, M. G., et al. (2013). Insulin-degrading enzyme (IDE): a novel heat shock-like protein. *J. Biol. Chem.* 288, 2281–2289. doi: 10.1074/jbc.M112.393108

Vetvik, K. G., and MacGregor, E. A. (2017). Sex differences in the epidemiology, clinical features, and pathophysiology of migraine. *Lancet Neurol.* 16, 76–87. doi: 10.1016/S1474-4422(16)30293-9

Vuralli, D., Wattiez, A. S., Russo, A. F., and Bolay, H. (2019). Behavioral and cognitive animal models in headache research. *J. Headache Pain* 20:11. doi: 10.1186/s10194-019-0963-6

Walker, A. K., Kavelaars, A., Heijnen, C. J., and Dantzer, R. (2014). Neuroinflammation and comorbidity of pain and depression. *Pharmacol. Rev.* 66, 80–101. doi: 10.1124/pr.113.008144

Wang, W., Lyu, C., Wang, F., Wang, C., Wu, F., Li, X., et al. (2021). Identification of potential signatures and their functions for acute lymphoblastic leukemia: a study based on the cancer genome Atlas. *Front. Genet.* 12:656042.

Wang, X. X., Cui, L. L., Gan, S. F., Zhang, Z. R., Xiao, J., Li, C. H., et al. (2022). Inhibition of oligodendrocyte apoptosis in the prelimbic medial prefrontal cortex prevents fentanyl-induced hyperalgesia in rats. *J. Pain* S1526-5900(22)00003-7. doi: 10.1016/j.jpain.2021.12.012

Williams, L. S., Jones, W. J., Shen, J., Robinson, R. L., Weinberger, M., and Kroenke, K. (2003). Prevalence and impact of depression and pain in neurology outpatients. *J. Neurol. Neurosurg. Psychiatry* 74, 1587–1589. doi: 10.1136/jnnp.74.11.1587

Wolfes, A. C., and Dean, C. (2020). The diversity of synaptotagmin isoforms. *Curr. Opin. Neurobiol.* 63, 198–209. doi: 10.1016/j.conb.2020.04.006

Yan, Z., and Rein, B. (2021). Mechanisms of synaptic transmission dysregulation in the prefrontal cortex: pathophysiological implications. *Mol. Psychiatry* 27, 445–465. doi: 10.1038/s41380-021-01092-3

Yang, L., Zhang, S., and Wang, G. (2019). Keratin 17 in disease pathogenesis: from cancer to dermatoses. *J. Pathol.* 247, 158–165. doi: 10.1002/path.5178

Yoo, Y. E., Lee, S., Kim, W., Kim, H., Chung, C., Ha, S., et al. (2021). Early chronic memantine treatment-induced transcriptomic changes in wild-type and Shank2-mutant mice. *Front. Mol. Neurosci.* 14:712576. doi: 10.3389/fnmol.2021.712576

Zhang, Q., Manders, T., Tong, A. P., Yang, R., Garg, A., Martinez, E., et al. (2017). Chronic pain induces generalized enhancement of aversion. *Elife* 6:e25302. doi: 10.7554/eLife.25302

Zhang, Y., Chen, K., Sloan, S. A., Bennett, M. L., Scholze, A. R., O'Keeffe, S., et al. (2014). An RNA-sequencing transcriptome and splicing database of glia, neurons, and vascular cells of the cerebral cortex. *J. Neurosci.* 34, 11929–11947. doi: 10.1523/JNEUROSCI.1860-14.2014

Zhang, Z., Gadotti, V. M., Chen, L., Souza, I. A., Stemkowski, P. L., and Zamponi, G. W. (2015). Role of prelimbic GABAergic circuits in sensory and emotional aspects of neuropathic pain. *Cell Rep.* 12, 752–759. doi: 10.1016/j.celrep.2015.07.001

Zhu, X., Tang, H. D., Dong, W. Y., Kang, F., Liu, A., Mao, Y., et al. (2021). Distinct thalamocortical circuits underlie allodynia induced by tissue injury and by depression-like states. *Nat. Neurosci.* 24, 542–553. doi: 10.1038/s41593-021-00811-x

Conflict of Interest: The authors declare that the research was conducted in the absence of any commercial or financial relationships that could be construed as a potential conflict of interest.

Publisher's Note: All claims expressed in this article are solely those of the authors and do not necessarily represent those of their affiliated organizations, or those of the publisher, the editors and the reviewers. Any product that may be evaluated in this article, or claim that may be made by its manufacturer, is not guaranteed or endorsed by the publisher.

frontiers | Frontiers in Molecular Neuroscience

REVIEW
published: 19 May 2022
doi: 10.3389/fnmol.2022.879909

Non-invasive Brain Stimulation for Central Neuropathic Pain

Qi-Hao Yang[1], Yong-Hui Zhang[1], Shu-Hao Du[1], Yu-Chen Wang[1], Yu Fang[2] and Xue-Qiang Wang[1,3]**

[1] Department of Sport Rehabilitation, Shanghai University of Sport, Shanghai, China, [2] School of Mechanical and Automotive Engineering, Shanghai University of Engineering Science, Shanghai, China, [3] Department of Rehabilitation Medicine, Shanghai Shangti Orthopaedic Hospital, Shanghai, China

The research and clinical application of the noninvasive brain stimulation (NIBS) technique in the treatment of neuropathic pain (NP) are increasing. In this review article, we outline the effectiveness and limitations of the NIBS approach in treating common central neuropathic pain (CNP). This article summarizes the research progress of NIBS in the treatment of different CNPs and describes the effects and mechanisms of these methods on different CNPs. Repetitive transcranial magnetic stimulation (rTMS) analgesic research has been relatively mature and applied to a variety of CNP treatments. But the optimal stimulation targets, stimulation intensity, and stimulation time of transcranial direct current stimulation (tDCS) for each type of CNP are still difficult to identify. The analgesic mechanism of rTMS is similar to that of tDCS, both of which change cortical excitability and synaptic plasticity, regulate the release of related neurotransmitters and affect the structural and functional connections of brain regions associated with pain processing and regulation. Some deficiencies are found in current NIBS relevant studies, such as small sample size, difficulty to avoid placebo effect, and insufficient research on analgesia mechanism. Future research should gradually carry out large-scale, multicenter studies to test the stability and reliability of the analgesic effects of NIBS.

Keywords: rTMS, tDCS, central neuropathic pain, analgesic mechanism, analgesic effects

OPEN ACCESS

Edited by:
Fengxian Li,
Southern Medical University, China

Reviewed by:
Ulf Strauss,
Charité – Universitätsmedizin Berlin, Germany
Muhammad Abul Hasan,
NED University of Engineering and Technology, Pakistan

****Correspondence:***
Yu Fang
fangyu_hit@126.com
Xue-Qiang Wang
wangxueqiang@sus.edu.cn

Specialty section:
This article was submitted to Pain Mechanisms and Modulators, a section of the journal Frontiers in Molecular Neuroscience

Received: *20 February 2022*
Accepted: *04 May 2022*
Published: *19 May 2022*

Citation:
Yang Q-H, Zhang Y-H, Du S-H, Wang Y-C, Fang Y and Wang X-Q (2022) Non-invasive Brain Stimulation for Central Neuropathic Pain. Front. Mol. Neurosci. 15:879909. doi: 10.3389/fnmol.2022.879909

INTRODUCTION

Neuropathic pain (NP) was defined by the International Association for the Study of Pain (IASP) in 2008 as "pain caused by a lesion or disease of the somatosensory nervous system" (Beydoun, 2003). And the prevalence of NP was about 3.3%–8.2% (Haanpää et al., 2011). According to the anatomical location of the injury or disease, NP can be classified as central NP (CNP), which is due to lesions or diseases of the spinal cord or brain, and peripheral neuropathic pain (PNP), which includes diabetic neuropathy, nerve damage, facial pain, phantom limb pain, cancer pain, and deformity (Colloca et al., 2017). The most common CNP syndromes include NP associated with spinal cord injury (SCI), post-stroke pain (PSP), NP associated with multiple sclerosis (MS), and Parkinson's disease (PD) (Finnerup et al., 2016; Zhang et al., 2021; **Figure 1**). The appearance and aggravation of pain symptoms often occur within a few days after the lesion or disease. CNP has no specific treatment at present (Dworkin et al., 2013; Cruccu et al., 2016), and patients suffer from chronic pain for a

long time, which seriously affects their quality of life. The aversive experience of pain is activated by the temporal and spatial coordination of a neural network called the pain matrix after a nociceptive stimulus (Garcia-Larrea and Bastuji, 2018). Pain matrix is mainly distributed in the cerebral cortex and subcortical regions, including thalamus, insula, cingulate cortex, prefrontal cortex, and frontal-orbitofrontal cortex (Mouraux et al., 2011). Responses during NP exhibit reproducible patterns, in particular hypoactivity of the thalamus contralateral to the pain area and deficit in reactiveness of the prefrontal cortices during NP (Garcia-Larrea and Peyron, 2013). Common pharmacological treatments for NP include calcium channel modulators, opioid analgesics, and antidepressants, while non-pharmacological treatments include exercise, noninvasive brain stimulation (NIBS), spinal cord stimulation (SCS), radiofrequency ablation (RFA), and nerve block (Baron et al., 2010; Reimer et al., 2014; Zheng et al., 2021; Peng et al., 2022; Wu et al., 2022). Since there is no specific drug for NP at present, non-drug therapy has been gradually accepted by NP patients because of its no side effects, no drug resistance, and strong pertinence (Moisset et al., 2020). NIBS has been applied in the rehabilitation of various brain dysfunction to regulate cortical excitability and neuroplasticity and has attracted wide attention because of its noninvasiveness, tolerability, and portability (Chisari et al., 2014). In basic and clinical settings, two approaches have become the pillars of NIBS: repetitive transcranial magnetic stimulation (rTMS) and transcranial direct current stimulation (tDCS) with a painless current (current intensities ± 1–2 mA) applied to the scalp. Both techniques are effective in reducing pain as measured by the visual analog scale (VAS) and numerical rating scale (NRS) (Ayache et al., 2016b; Nardone et al., 2017). rTMS focuses on neuromodulation sequelae through magnetic fields (Hallett, 2007). tDCS is applied to the scalp by a weak current to produce neuromodulation (Terney et al., 2008). In terms of different types of pain, NP response to NIBS is better than non-neurotic pain (Knotkova et al., 2021). NIBS is a promising therapeutic technique for resolving the dynamic neurological changes caused by NP (Costa et al., 2019).

REPETITIVE TRANSCRANIAL MAGNETIC STIMULATION FOR CENTRAL NEUROPATHIC PAIN

Based on the principles of electromagnetic induction and electromagnetic conversion, TMS, including single-pulse TMS and rTMS, alters the motor potential of cortical nerve cells by stimulating the magnetic field generated by coil transients, which affects intra-brain metabolism and neuroelectric activity (Hallett, 2007). Compared with the chronic implantation procedure, rTMS is a safe, noninvasive, easy to tolerate, and effective therapeutic intervention pattern that continuously distributes multiple pulses at a fixed frequency and is more widely used in clinical applications (Gu and Chang, 2017; Choi et al., 2018). The main limitation of rTMS is the short-term analgesic effects (Hemond and Fregni, 2007). Low-frequency rTMS (LF-rTMS, ≤1 Hz) can inhibit the metabolism of nerve cells and reduce cortical excitability, whereas high-frequency rTMS (HF-rTMS, ≥1 Hz) has the opposite effect (Wagner et al., 2007). The reduction in VAS and NRS scores with HF-rTMS (10–20 Hz) is much greater than that with LF-rTMS (≤1 Hz) under conditions for analgesia (Lefaucheur et al., 2001; Canavero et al., 2002; Lefaucheur, 2006; Leo and Latif, 2007; Borckardt et al., 2011). Therefore, HF-rTMS is often used in the clinical treatment of NP. More research information about the effect of rTMS on CNP is shown in **Table 1**.

The guidelines of the International Federation of Clinical Neurophysiology and the European Federation of Neurological Societies supported the specific analgesic effect of HF-rTMS stimulation in the primary motor cortex (M1) of NP (Cruccu et al., 2007; Lefaucheur et al., 2020). Moreover, a longer course of treatment and continuous treatment was more conducive to the analgesic effect and therefore included in the grade A recommendation. Stimulation of the frontal lobes, particularly the dorsolateral prefrontal cortex (DLPFC), was associated with improved depression and cognitive impairment, but its effect on NP improvement was clinically controversial and not addressed in the guidelines. In the studies included in the guidelines, rTMS was often used to stimulate the contralateral M1 of NP at a frequency of 5–10 Hz; approximately 80%–90% resting motor threshold (RMT) and 5–10 sessions of treatment can usually have a definite analgesic effect (Lefaucheur et al., 2020).

Repetitive Transcranial Magnetic Stimulation for Post-stroke Pain

Pain was common and present in 10%–45.8% of stroke cases (Paolucci et al., 2016; Choi-Kwon et al., 2017). PSP impeded recovery, affects the mental state of patients with stroke, and further impairs the quality of life of patients (Lundström et al., 2009; Naess et al., 2012). The common variants of PSP are central poststroke pain (CPSP), complex regional pain syndrome (CRPS), shoulder pain, spasticity-related pain, and headache (Treister et al., 2017; Delpont et al., 2018). CPSP was a CNP disorder that affected 10%–35% of the post-stroke population (Flaster et al., 2013). The properties of pain included searing or freezing pain or numbness, and pain intensity was reported as a VAS score of nearly 8 out of 10 (Oh et al., 2015). Some studies that focused on the analgesic effect of rTMS on PSP showed that HF- rTMS (5–20 Hz) can produce effective immediate pain relief in patients after stroke, and multiple sessions and a long duration of intervention can make the analgesic effects last (Ohn et al., 2012; Hosomi et al., 2013; Matsumura et al., 2013; Hasan et al., 2014; Kobayashi et al., 2015; Ramger et al., 2019). Most patients with CPSP responded positively to rTMS (Ohn et al., 2012; Matsumura et al., 2013; Kobayashi et al., 2015). Pain relief was more pronounced in the rTMS group than in the sham stimulation group as measured by VAS and NRS. They also found a time-course effect on pain relief after 1 and 3 weeks of stimulation that lasted for up to 12 weeks and peaked at around 8 weeks.

The influence of the site of the stimuli around the motor cortex on the analgesic effect is also the focus of research (Saitoh and Yoshimine, 2007). M1 is the stimulus area selected by most

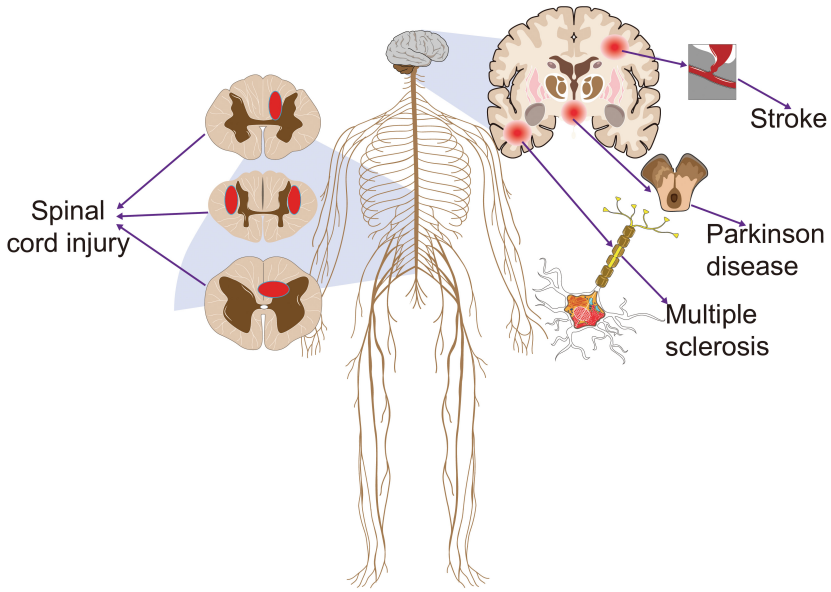

FIGURE 1 | The common diseases that cause central neuropathic pain. Stroke, Parkinson's disease, multiple sclerosis, and spinal cord injury often lead to central neuropathic pain that persists throughout the recovery cycle. This pain clearly has a negative effect on the prognosis of patients.

studies and has achieved a good analgesic effect on PSP (Saitoh and Yoshimine, 2007; Ohn et al., 2012; Hosomi et al., 2013; Matsumura et al., 2013; Hasan et al., 2014; Sacco et al., 2014; Kobayashi et al., 2015; Ramger et al., 2019). In addition, two studies (Khedr et al., 2005; Zhao et al., 2021) selected the upper limb and hand regions of the motor cortex as stimulation sites and found that CPSP is effectively alleviated by intervention at these sites. By contrast, DLPFC and anterior cingulate cortex (ACC) were also selected for stimulation in some studies but did not produce analgesic effects compared with the stimulation of the motor cortex (de Oliveira et al., 2014; Galhardoni et al., 2019; Attal et al., 2021). In addition to common PSP, Choi and Chang (2018) found that rTMS could be used as an effective therapeutic tool for managing post-stroke shoulder pain, and this pain relief could be maintained for about 4 weeks after 10 sessions of HF-rTMS (10 Hz) treatment.

Repetitive Transcranial Magnetic Stimulation for Central Neuropathic Pain Associated With Spinal Cord Injury

Central neuropathic pain is a common and disabling symptom in individuals with SCI; it affects 75%–81% of SCI patients, and one-third reported severe pain that worsens their mood state (Margot-Duclot et al., 2009). CNP affects the quality of life, rehabilitation, and recovery of more than two-thirds of SCI cases (Rekand et al., 2012). CNP following SCI is resistant to common pharmacologic treatments (Moreno-Duarte et al., 2014). rTMS has been developed to offer a safe and reliable approach to pain management (Quesada et al., 2018). Most of the stimulation sites were located in M1, as well as the premotor cortex (PMC) and limb cortex areas depending on the pain site (Lefaucheur et al., 2004; Sun et al., 2019). One study found analgesic effects when stimulating the vertex (Defrin et al., 2007). HF-rTMS (5–20 Hz) can produce effective pain relief for NP following SCI (Kang et al., 2009; Yılmaz et al., 2014; Zhao et al., 2020). Zhao et al. (2020) found that 10 Hz rTMS over the hand area of the motor cortex could relieve acute CNP during the early stage of SCI. Some studies indicated that rTMS has no early pain relief after SCI but has a better intermediate analgesic effect compared with sham rTMS (Shen et al., 2020). Regarding the management of intractable NP by rTMS in cases with SCI, Yılmaz et al. (2014) found that the middle-term (over 6 weeks) analgesic effect of rTMS (10 Hz) was encouraging. Sun et al. (2019) found that rTMS (10 Hz, 6 weeks with 1-day interval per week) showed more analgesic effect on NP following SCI at 2–6 weeks. rTMS applied over the hand or leg motor cortex can relieve NP, improve spasm, and therefore reduce pain in patients with incomplete SCI (Kumru et al., 2010; Jetté et al., 2013). Pain relief caused by single rTMS treatment may be due to placebo, but patients with SCI may benefit from multiple rTMS sessions (Defrin et al., 2007).

Repetitive Transcranial Magnetic Stimulation for Central Neuropathic Pain Associated With Parkinson's Disease

Parkinson's disease is a common chronic progressive neurodegenerative disease among middle-aged and elderly people and is characterized by motor and non-motor symptoms. More than 90% of patients with PD experienced non-motor symptoms; among which, the most common was pain with an incidence of 40%–85%, and it seriously affected the quality of life of patients (Elefant et al., 2012; Young Blood et al., 2016). The current rTMS protocol did not pose a substantial risk to patients with PD (Vonloh et al., 2013). Most current research on rTMS in PD focused on motor symptoms, such as gait, motor retardation,

TABLE 1 | Major findings of Repetitive transcranial magnetic stimulation (rTMS) in central neuropathic pain (CNP) studies.

Author, year	Study type	CNP type	Sample (size, sex, age)	rTMS site	Frequency/Intensity	Duration	Analgesic effect
de Oliveira et al., 2014	Prospective cohort	CPSP	21, 10M, 11F, Real: 55 ± 9.67, Sham: 57.8 ± 11.86	M1/DLPFC	10 Hz/120%RMT	10 days	No effective pain relief by VAS
Zhao et al., 2021	Randomized control	Acute CPSP	38, 21M, 7F, Real: 50.1 ± 11.34, Sham: 48.9 ± 11.51	Upper limb area of the motor cortex	10 Hz/80%RMT	3 weeks	Significant pain relief by NRS and MPQ
Khedr et al., 2005	Randomized parallel	PSP	24, 14M, 10F, 52.3 ± 10.3	Hand area of the motor cortex	20 Hz/80%RMT	5 days	Pain relief by VAS and LANSS scales
Hosomi et al., 2013	Cross-over	PSP	57, Gender not, 60.7 ± 10.6	M1	5 Hz/90%RMT	10 sessions	Modest pain relief by VAS
Hasan et al., 2014	Case series	PSP	14, 10M, 4F, 57 (median)	M1	10 Hz/80%–90%RMT	5 sessions	Modest but significant pain relief by NRS
Kobayashi et al., 2015	Cross-over	PSP	18, 12M, 6F, 63.0 ± 9.9	M1	5 Hz/90%RMT	12 weeks	Pain relief by VAS
Matsumura et al., 2013	Cross-over	PSP	20, 12M, 8F, 63.6 ± 8.1	M1	5 Hz/100%RMT	1 day	Pain relief by VAS correlated well with morphine test
Galhardoni et al., 2019	Cross-over	PSP	98, Gender not, 55.02 ± 12.13	ACC/PSI	10 Hz/90%RMT	5 sessions	No significant pain relief by NRS
Ohn et al., 2012	Case series	PSP	22, 13M, 9F, 54.0 ± 9	M1	10 Hz/90%RMT	5 days	Significant pain relief by VAS
Sun et al., 2019	Sham-control	SCI	17, 15M, 2F, 23.0–54.5	M1	10 Hz/80%RMT	6 weeks	More pain relief from 2 to 6 weeks by NRS
Lefaucheur et al., 2004	Cross-over	SCI	12, Gender/age not	M1	10 Hz/80%RMT	1 session	Significant but transient pain relief by VAS
Defrin et al., 2007	Randomized control	SCI	11, 7M, 4F, 54.0 ± 6	vertex	5 Hz/115%RMT	10 days	Continued pain relief by MPQ
Kang et al., 2009	Cross-over	SCI	11, 6M, 5F, 54.8 ± 13.7	M1	10 Hz/85%RMT	5 days	No Significant pain relief by NRS and BPI
Jetté et al., 2013	Cross-over	SCI	16, 11M, 6F, 50.0 ± 9	motor cortex (hand / leg area)	10 Hz/90%RMT (hand area) 110%RMT (leg area)	3 sessions	Significant but equivalent pain relief by NRS
Yılmaz et al., 2014	Randomized control	SCI	16, 16M, 38.6 ± 6.5	motor cortex	10 Hz/110%RMT	10 days	Middle-term (over 6 weeks) pain relief by VAS
Centonze et al., 2007	Randomized control	MS	19, 5M, 14F, Age not	M1	5 Hz/100%RMT	2 weeks	Long-lasting spasticity pain relief

CNP, central neuropathic pain; PSP, post-stroke pain; CPSP, central post-stroke pain; SCI, spinal cord injury; MS, multiple sclerosis; M, male; F, female; rTMS, repetitive transcranial magnetic stimulation; Hz, hertz; RMT, resting motor threshold; ACC, anterior cingulate cortex; PSI, posterior superior insula; M1, primary motor cortex; DLPFC, dorsolateral prefrontal cortex; PMC, premotor cortex; VAS, visual analog scale; NRS, numerical rating scale; BPI, brief pain inventory; MPQ, McGill pain questionnaire; LANSS, Leeds assessment of neuropathic symptoms and signs.

and coordination, as well as emotional and psychiatric symptoms (Xie et al., 2015; Brys et al., 2016; Dagan et al., 2017). rTMS has antidepressant efficacy and can improve motor function (Xie et al., 2015). Studies showed that PD with NP was associated with depression and dyskinesia; thus, treating depression to improve motor symptoms can relieve the pain of patients with PD (Yang et al., 2014). rTMS usually targets the left DLPFC in the treatment of depression but regulates the excitability of pain circuits in related brain regions by stimulating the M1 region to achieve analgesia (Moseley and Flor, 2012; Martin et al., 2013). Therefore, the study of the analgesic effect of rTMS on patients with PD still needs more research input in terms of stimulation site, as well as the frequency and intensity of stimulation.

Repetitive Transcranial Magnetic Stimulation for Central Neuropathic Pain Associated With Multiple Sclerosis

Multiple sclerosis is a disease caused by an inflammatory demyelinating process in the central nervous system (CNS) and a leading cause of disability in young adults with substantial economic and social burdens (Patwardhan et al., 2005; Yamout and Alroughani, 2018). Many common symptoms of MS, such as spasticity, pain, depression, and cognitive impairment, cannot be fully managed by medication (Kesselring and Beer, 2005). The first clinical application of rTMS in MS patients was to manage spasms (Centonze et al., 2007). HF-rTMS can significantly reduce spasticity, compared to sham stimulation. Some studies supported a more durable effect in reducing pain and fatigue following HF-rTMS (Mori et al., 2011; Korzhova et al., 2019). According to the recent evidence-based guidelines (Lefaucheur et al., 2014), no recommendations still exist for the use of rTMS in the treatment of patients with MS, even though rTMS has few promising results for sensory and motor symptoms (Iodice et al., 2017).

Mechanisms of Repetitive Transcranial Magnetic Stimulation for Central Neuropathic Pain

Currently, the mechanism of rTMS is found to be related to synaptic plasticity, neural regulation, and response (**Figure 2**).

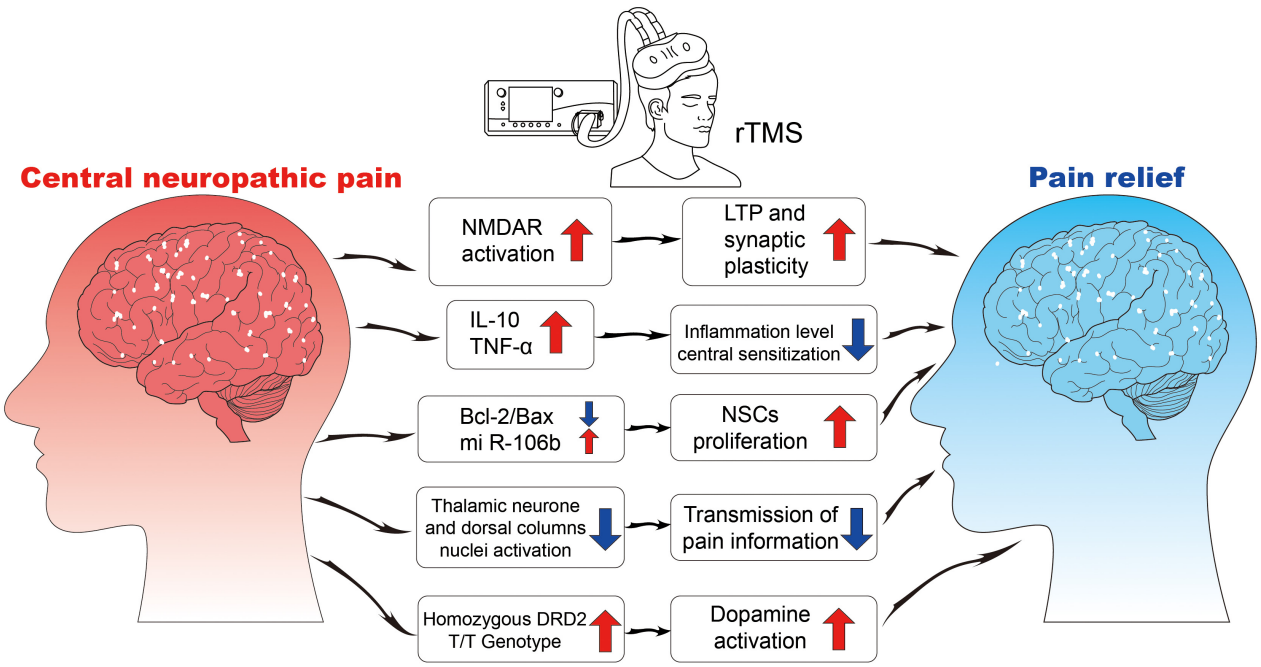

FIGURE 2 | The neurophysiological mechanisms of rTMS. NMDA, N-methyl-D-aspartate receptor; LTP, long-term potentiation; IL, interleukin; TNF, tumor necrosis factor; Bcl, B-cell lymphoma; Bax, Bcl2-associated X; NSCs, neural stem cells; DRD2, dopamine receptor D2.

Brain Plasticity

Repetitive transcranial magnetic stimulation acts on the synapses of neurons and causes axons to be depolarized and transmitted down-line, which then leads to changes in the nerve cell body, cell permeability, and excitability and results in brain plasticity. Esser et al. (2006) found that HF-rTMS induces long-term potentiation (LTP), which is a change in information transmission resulting from the emergence of central neurologic transsynaptic/trans-presynaptic nerve fibers and is also one of the important cellular and molecular mechanisms of human memory and learning. HF-rTMS can remarkably increase the level of serum brain-derived neurotrophic factor (BDNF) by enhancing cortical excitability and brain plasticity, which may be the basis of NP treatment by HF-rTMS (Dockx et al., 2018). Blocking signaling between BDNF and Tyrosine receptor kinase B (TrkB) was found to reduce abnormal pain caused by nerve injury (Coull et al., 2005). But rTMS has been found to enhance this signaling in the cerebral cortex (Wang et al., 2011). rTMS may induce the increase of BDNF level in the motor cortex or frontal lobe to cause neuroplasticity changes and thus achieve the analgesic effect.

Ghosh et al. (2010) found that rTMS may regulate the balance of inhibitory neurotransmitters and excitatory glutamate neurotransmitters in the cerebral cortex to achieve pain relief. Gamma-aminobutyric acid (GABA) is an inhibitory neurotransmitter because it inhibits certain interneuronal synaptic signals, thereby preventing or reducing the risk of CNP (Gwak and Hulsebosch, 2011). Some studies found that single rTMS protocol increased phrenic motoneuron excitability at 10 Hz through the mediation of a local GABA ergic disinhibition (Barr et al., 2013; Michel-Flutot et al., 2021). rTMS (10 Hz) alleviated acute CNP in the early stages of SCI by improving motor-evoked potential (MEP) parameters and modulating BDNF and nerve growth factor (NGF) secretion (Zhao et al., 2020). Some studies have found that rTMS can promote dopamine release and dopamine activity is affected by the DRD2 genotype (Strafella et al., 2001, 2003; Hagelberg et al., 2002). When navigated rTMS targeted M1, the participants with homozygous DRD2 T/T genotype were remarkably more likely to experience pain relief than those with other genotypes (Ojala et al., 2021). Therefore, the plasticity-related gene polymorphisms of DRD2 may play a key role in CNP regulation.

Central Sensitization Reduction

Central sensitization refers to the abnormal increase in the excitability or synaptic transmission of central pain-related neurons, including the increase in the spontaneous discharge activity of neurons, the expansion of the sensory domain, the reduction of threshold value to external stimuli, and the enhancement of response to suprathreshold stimuli, which amplify the transmission of pain signals (Dooley et al., 2007; Latremoliere and Woolf, 2009; Quintero et al., 2011; Nickel et al., 2012). The maintenance of NP depends on central sensitization. Cioni and Meglio (2007) used functional magnetic resonance imaging to find that rTMS can inhibit the transmission of pain information in the spinothalamic pathway. HF-rTMS may reduce central sensitization and relieve NP by down-regulating the overexpression of neuronal nitric oxide synthase in ipsilateral dorsal root ganglions and inhibiting the activity and proliferation of astrocytes in L4–6 spinal dorsal horn ipsilateral to the NP (Yang et al., 2018).

Neuroinflammation Modulation

The exudation of mast cells, macrophages, and other immune cells; sympathetic nerve excitation; and vascular dilation after nerve injury or disease make the peripheral nervous system and CNS produce histamine, NGF, IL-10, tumor necrosis factor (TNF)-α, and other pro-inflammatory cytokines and then cause NP (Vallejo et al., 2010; Li et al., 2011). Mechanical ectopic pain and hyperalgesia were partially reversed by rTMS, which may be related to increased levels of TNF-α, and IL-10 in the prefrontal cortex (Toledo et al., 2021).

Tumor necrosis factor-α expression in the central nervous system contributes to the induction of NP in rats (Andrade et al., 2011). The classical anti-inflammatory effects of IL-10 may be involved in the development of NP (Moore et al., 2001). rTMS has been shown to alter IL-10 levels in a variety of situations. rTMS reduced the activation of microglia and increased the level of IL-10 in the cortex, alleviating neurological abnormalities in rats with MS-induced neurological injury (Yang et al., 2020). The reduction of neurotoxic astrocyte polarization through IL-10 effects has been proposed as a mechanism by which rTMS (5-10 Hz) is effective in nerve regeneration induced by stroke in rats (Hong et al., 2020). Changes in IL-10 levels observed in NP rats treated with rTMS are reflected in increased TNF-α, contributing to central homeostasis. A link between pain and microglia TNF-α has been proposed because it improves long-term synaptic enhancement in spinal horn C fibers in animal models of nerve injury (Liu et al., 2017).

Cell Proliferation

Repetitive transcranial magnetic stimulation could promote nerve cell proliferation in healthy, depressed, and stroke rat models. Ueyama et al. (2011) stimulated rats with HF-rTMS (25 Hz) for 2 weeks and found that 5-bromo-2-deoxyuridine-positive cells in the subventricular zone increased remarkably in the rTMS group. The proliferative cells were later identified as neural stem cells (NSCs), but the proliferative mechanism remains unclear. The anti-apoptotic effect of rTMS may cause NSC proliferation. Yoon et al. (2011) treated cerebral ischemia rats with HF-rTMS (10 Hz) for 14 days, and the Bcl-2/Bax ratio increased and apoptosis decreased after treatments. In addition, Guo et al. (2014) found that 10 Hz rTMS can promote the secretion of the miR-106B family in cerebral ischemia rats and regulate the NSC cycle by regulating the downstream target gene, P57, which indicates that HF-rTMS can affect the cell cycle and stimulate cell proliferation. The in vitro stimulation of NSCs by HF-rTMS (10 Hz) can increase the mIR-106B expression of NSCs and promote the proliferation of NSCs (Liu et al., 2015). However, no relevant experimental study has been conducted on whether rTMS can promote NSC differentiation.

TRANSCRANIAL DIRECT CURRENT STIMULATION FOR CENTRAL NEUROPATHIC PAIN

Transcranial direct current stimulation is an approach that induces neuroplasticity and modulates cortical excitability by applying a weak direct current over the scalp of subjects (Stagg and Nitsche, 2011). tDCS is a noninvasive neuromodulatory technique that reduces bidirectional polarity-dependent changes in underlying cortical areas (Fregni et al., 2006). Five studies, which collectively included 95 NP cases, also found that tDCS can effectively manage NP (Antal et al., 2010; Soler et al., 2010; Bolognini et al., 2013; Attal et al., 2016; Houde et al., 2020). In the included studies, the M1 area plays a key role in the analgesic effect of tDCS. tDCS's cathode stimulation of the M1 and PMC can improve the hand motor function of patients with stroke, as well as the pain perception and pain-related symptoms induced by chronic pain (Andrade et al., 2017; Zortea et al., 2019). tDCS is a safe technique and has slight adverse reactions, such as headache, discomfort on the scalp, and a slight burning sensation under the electrode sheet (Nitsche et al., 2009; Brunoni et al., 2011; Fagerlund et al., 2015). Compared with rTMS, tDCS does not have the risk of convulsions and only has a brief and mild tingling sensation, whereas rTMS causes tingling throughout the process (Hummel et al., 2005).

The tDCS guidelines published by the International Society for Neuropsychopharmacology indicated that the use of tDCS to stimulate the left M1 region was highly effective in improving NP and was therefore a level B recommendation (Fregni et al., 2021). The guideline of the International Federation of Clinical Neurophysiology pointed out that tDCS in M1 (contralateral to pain side) in chronic lower limb NP following SCI was a level C recommendation (possible efficacy) (Lefaucheur et al., 2017). The commonly used tDCS parameter was an intensity of 2 mA, which was performed continuously for at least 5 consecutive days with a duration of 20 min each time. Although the current level of evidence suggests that tDCS was less effective than rTMS in relieving pain when stimulating the M1 area, the most surprising point was that tDCS appeared to be more effective for NP following SCI in the lower extremities (Lefaucheur et al., 2004, 2006, 2014, 2017). This point was reinforced by the treatment of a patient with chronic refractory NP who did not respond to the HF-rTMS but gradually improved by the tDCS over a long period (Hodaj et al., 2016). More research information about the effect of tDCS on CNP is shown in **Table 2**.

Transcranial Direct Current Stimulation for Post-stroke Pain

Patients with CPSP may have skin temperature changes because of autonomic nervous system dysfunction. Therefore, the physiological changes in patients with CPSP can be evaluated by measuring the skin temperature difference between the pain area and contralateral area (Klit et al., 2009; Kim, 2014). Bae et al. (2014) found a 1.15 reduction in pain intensity through VAS after 3 weeks of treatment in the tDCS group, as well as changes in warm sensation and cold pain threshold, some of which lasted up to 3 weeks after stimulation. This result means that tDCS improved sensory identification and exerted analgesic effects in patients with stroke and PSP. The decreased skin temperature also reduces the sensitivity of patients to pain and

TABLE 2 | Major findings of transcranial direct current stimulation (tDCS) in central neuropathic pain (CNP) studies.

Author, Year	Study type	CNP type	Sample (size, sex, age)	tDCS site	Intensity/Current flow time	Duration	Analgesic effect
Bae et al., 2014	Randomized control	PSP	14, 7M, 7F, 45–55	M1	2 mA/20 min	3 weeks	Pain relief by VAS
Hassan et al., 2021	Case report	PSP	1, Gender not, 45	DLPFC	2 mA/20 min	2 weeks	Immediate but transient pain relief by VAS
Molero-Chamizo et al., 2021	3 cases report	PSP	3, 2W:43, 72, 1M:54	M1	1.5 mA/20 min	5 sessions	Significant pain relief by AVAS
Fregni et al., 2006	Randomized control	SCI	17, 14M, 3F, 35.7 ± 13.3	M1	2 mA/20 min	16 days	Significant pain relief by VAS, CGI and PGA
Soler et al., 2010	Randomized control	SCI	39, 30M, 9F, 44.1 ± 11.6	M1	2 mA/20 min	10 sessions	Effective relief for continuous and paroxysmal pain by NRS and BPI
Wrigley et al., 2013	Cross-over	SCI	10, 8M, 2F, 56.1 ± 14.9	M1	2 mA/20 min	5 days	Effective relief for recent pain by NRS
Yoon et al., 2014	Prospective control	SCI	16, 12M, 4F, 44.1 ± 8.6	M1	2 mA/20 min	10 days	Significant pain relief by NRS
Ngernyam et al., 2015	Cross-over	SCI	20, 15M, 5F, 44.5 ± 9.16	M1	2 mA/20 min	1 session	Significant pain relief by NRS
Thibaut et al., 2017	Two-phase randomized control	SCI	Phase I: 33, 24M, 9F, 51.2 ± 12.5 Phase II: 9, 7M, 2F, 49.0 ± 14.38	M1	2 mA/20 min	5 days (Phase I) 10 days (Phase II)	Long-lasting pain relief by VAS
Mori et al., 2010	Randomized, sham-control	MS	19, 8M, 11F, 23–68	motor cortex	2 mA/20 min	5 days	Significant pain relief by VAS and MPQ
Ayache et al., 2016a	Cross-over	MS	16, 3M, 13F, 48.9 ± 10.0	DLPFC	2 mA/20 min	3 days	Significant pain relief by VAS and BPI
González-Zamorano et al., 2021	Randomized control	PD	32, Gender not, Age not	M1	2 mA/20 min	2 weeks (10 sessions)	Pain relief by BPI, KPDPS, PPT, TS and CPM

CNP, central neuropathic pain; PSP, post-stroke pain; CPSP, central post-stroke pain; SCI, spinal cord injury; MS, multiple sclerosis; PD, Parkinson's disease; M, male; F, female; tDCS, transcranial direct current stimulation; RMT, resting motor threshold; mA, milliampere; min, minute; M1, primary motor cortex; DLPFC, dorsolateral prefrontal cortex; VAS, visual analog scale; AVAS, adaptive visual analog scale; NRS, numerical rating scale; BPI, brief pain inventory; MPQ, McGill pain questionnaire; CGI, clinical global impression; PGA, patient global assessment; PPT, pain pressure threshold; KPDPS, King's Parkinson's disease pain scale; TS, temporal summation; CPM, conditioned pain modulation.

thus contributes to analgesia (Tan and Knight, 2018; Madden and Morrison, 2019). Ramger et al. (2019) also suggested that tDCS on M1 has positive effects on CPSP.

Transcranial Direct Current Stimulation for Central Neuropathic Pain Associated With Spinal Cord Injury

The increased excitability and reactivity of spinal dorsal horn neurons caused by the dysregulation of the central inhibitory mechanism is an important cause of pain following SCI (Tung et al., 2015). Fregni et al. (2006) first reported the effect of tDCS on NP after SCI. Subjects were randomly divided into the tDCS group (2 mA, 20 min) and the sham stimulation group to receive motor cortex stimulation. After 5 days of stimulation, the pain was remarkably reduced in the tDCS group according to the VAS, whereas no considerable change was observed in the sham stimulation group. More recently, Murray et al. (2015) investigated the effect of different current intensities on tDCS in treating NP after SCI. The subjects were randomly assigned to different groups (1 mA, 2 mA, and sham stimulation of the motor cortex). They found that MEP increased considerably in minutes only after 2 mA tDCS motor cortex stimulation. From this result, we can speculate that current intensity may influence the clinical outcome of tDCS stimulation. In addition, Soler et al. (2010) applied visual illusion technology and tDCS to patients with CNP after SCI, and the combination of the two can relieve pain more effectively than monotherapy.

Some evidence showed that tDCS did not provide any pain relief to longstanding NP after SCI (Wrigley et al., 2013). The analgesic effect of tDCS was not superior to exercise alone after 12 sessions of intervention, and the beneficial effect was not maintained at follow-up (Mehta et al., 2015; Yeh et al., 2021). However, not enough evidence could suggest that the analgesic effect of tDCS on NP following SCI over the M1 region is effective compared with medication treatments because of the lack of high-quality studies and sufficient sample size and control groups (Boldt et al., 2014; Nardone et al., 2014; Mehta et al., 2015; Ngernyam et al., 2015; David et al., 2018; Shen et al., 2020; Li et al., 2021). Fagerlund et al. (2015) found that pain reduction after the tDCS stimulation of the motor cortex was closely associated with increased peak spectral density in the θ-α range of electroencephalogram, but no corresponding association was found with sham stimulation. This finding may become a measurement tool to quantify the effect of tDCS management on NP to better compare analgesic effects.

Transcranial Direct Current Stimulation for Central Neuropathic Pain Associated With Parkinson's Disease

Transcranial direct current stimulation manages PD through brain stimulation by very weak currents to activate neurons into an excitable state (Shigematsu et al., 2013). A growing number of studies have shown that tDCS can improve motor and cognitive symptoms, but the results suggest that a fully optimized tDCS protocol has not been established (Biundo et al., 2016; Elsner et al., 2016; Putzolu et al., 2018; Broeder et al., 2019; Orru et al., 2019). Few studies have been conducted on tDCS for PD-related pain, but home-isolated patients with PD are experiencing increased pain frequency because of the reduction of movement due to the protocols for the coronavirus 2019 (COVID-19) pandemic. Approximately 49.7% of Spanish patients with PD reported pain every day during the COVID-19 pandemic (Santos-García et al., 2020). González-Zamorano et al. (2021) proposed a new method based on pain psychological expression techniques and tDCS in patients with pain following PD. Finally, after the configuration and explanation, the treatment can be applied at home to promote independence and self-management and maximize the time out of medical centers.

Transcranial Direct Current Stimulation for Central Neuropathic Pain Associated With Multiple Sclerosis

Transcranial direct current stimulation has been gradually used in the clinical of spasticity and pain in MS (Mori et al., 2010; Dubbioso et al., 2015; Iodice et al., 2015; Rossini et al., 2015; Saturnino et al., 2015; Ayache et al., 2016b). Poorly managed spasticity can lead to pain and limited mobility. Mori et al. (2010) researched the effect of the application of tDCS (2 mA, 20 min/day, 5 sessions) over M1 contralateral to the affected side on chronic, drug-fast pain. Nineteen patients with MS were randomized to receive sham stimulation or tDCS. Remarkable pain relief was found following tDCS but not sham stimulation as measured by VAS and McGill questionnaire, and a total improvement in quality of life was observed within 3 weeks after the end of treatment. tDCS could have acted on the pain matrix networks where the prefrontal cortex mainly contributed (Ayache et al., 2016b). And anodal tDCS over the DLPFC appeared to increase the pain threshold to produce analgesic effects, especially NP. Overall, data for the treatment of NP following MS with tDCS is sparse (Palm et al., 2014).

Mechanisms of Transcranial Direct Current Stimulation for Neuropathic Pain

The effect of tDCS in reducing CNP may be related to increased sympathetic nerve activity, decreased blood flow, and decreased or interrupted transmission of the connection between sympathetic nerve fibers and pain-transmitting nerve fibers (**Figure 3**).

Selective Excitability of Neurons

Transcranial direct current stimulation is thought to work by changing the excitability of nerve cells as electricity passes through brain tissue (Nitsche et al., 2008; To et al., 2016; Stagg et al., 2018). The current intensity used by tDCS is weak, does not cause action potential, only changes the resting membrane potential of nerve cells, and regulates the excitability of nerve cells (Bikson et al., 2004). tDCS affects the opening and closing of ion channels in the stimulated region and induces the flow of intracranial ions. Anodic stimulation leads to the depolarization of the nerve membrane, whereas cathodic stimulation leads to the hyperpolarization of the nerve membrane, both of which change the excitability of neurons (Zaghi et al., 2010). This effect can occur a few seconds after tDCS stimulation; therefore, it is often referred to as the immediate effect of tDCS stimulation (Chang et al., 2015). Notably, the cortical excitatory effect of tDCS is related to the direction and intensity of the stimulus current, but the relationship is not linear, that is, a greater current intensity has a better stimulus effect, but sometimes, the effect will be reversed with the increase in current intensity (Batsikadze et al., 2013; Benwell et al., 2015). The excitatory effect of tDCS on neurons is selective to some extent, that is, tDCS only acts on neurons that are already in an active state. This feature of tDCS can effectively avoid the side effects of excitatory toxicity caused by traditional nerve stimulation techniques (Fertonani and Miniussi, 2017).

Synaptic Plasticity and Connectivity

The subsequent effects of the cessation of tDCS stimulation may be related to the regulation of synaptic plasticity and connect ability by regulating neurotransmitter activity (Nitsche et al., 2008; To et al., 2016). Synaptic plasticity involves glutamate and GABAergic neurons, which produce glutamate and GABA, respectively. Glutamate N-methyl-D-aspartate (NMDA) receptor agonist, D-cycloserine, prolongs the effect of tDCS on M1 excitability (Nitsche et al., 2004a). GABA receptor agonist, lorazepam, enhances and extends the subsequent effects of tDCS in a short period (Nitsche et al., 2004b). tDCS can induce long-term enhancement or inhibition in the stimulated region, which leads to synaptic remodeling, by regulating NMDA expression and GABA release (Antonenko et al., 2017). tDCS also has a network effect that can alter the structure and functional connections between different brain regions. Lin et al. (2017) found that the analgesic effect of tDCS is associated with the structural connections between the left DLPFC and the left thalamus. Cummiford et al. (2016) found that applying anode stimulation to the left M1 reduces the functional connection of the left abdominal extrinsic thalamus to the inner frontal lobe and the left auxiliary movement area, as well as the functional connection between the right abdominal extrinsic thalamus and the lower chin and the left auxiliary movement area, which play an important role in pain processing and regulation.

Regulation of Pain Receptor Expression

The activation of purinoceptor 4 (P2X4) receptors in the microglia is a sufficient and necessary condition for NP (Wasserman and Koeberle, 2009; Gritsch et al., 2016). The P2X4 receptor is expressed in the spinal cord ganglion and brain microglia, and its upregulation is the key process for the microglia to participate in NP (Baroja-Mazo et al., 2013). Microglia in the posterior horn of the ipsilateral spinal cord is activated

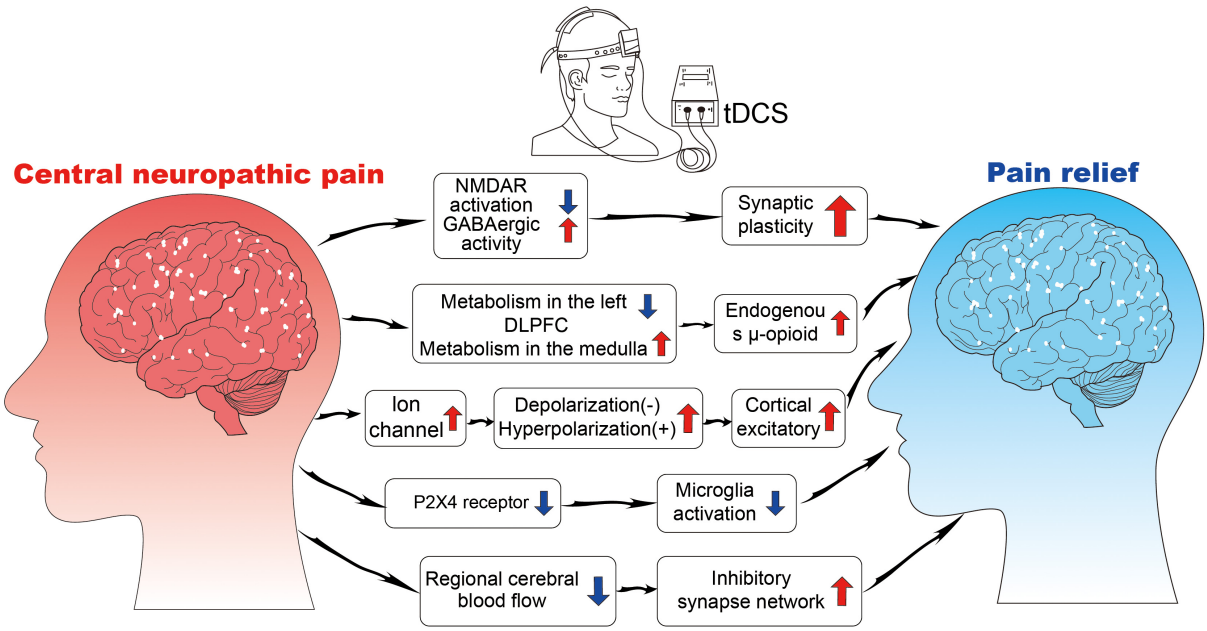

FIGURE 3 | The neurophysiological mechanisms of tDCS. NMDAR, N-methyl-D-aspartate receptor; GABA, gamma-aminobutyric acid; P2X4, purinoceptor 4.

rapidly, the expression of the P2X4 receptor is upregulated, and the change in P2X4 receptor expression is consistent with the timeline of mechanical pain sensitivity (Nasu-Tada et al., 2006; Beggs et al., 2012). tDCS can improve NP while inhibiting neuronal sensitivity and microglial activity after peripheral nerve injury (Zhang et al., 2020). This outcome may be due to the downregulation of P2X4 receptor expression by tDCS, which in turn inhibits microglia activity. Therefore, P2X4 can be used as a therapeutic target to treat NP in future studies.

Changes in Brain Blood Flow and Metabolism

Transcranial direct current stimulation modulates the activities of brain regions directly under the stimulating electrode, as well as a network of brain regions that are functionally related to the stimulated area. Zheng et al. (2011) found that the effect of tDCS is related to changes in cerebral blood flow, and blood flow is remarkably reduced and continues for a period after cathodic stimulation; these effects may also be a key mechanism of tDCS's therapeutic role. Yoon et al. (2014) found increased metabolism in the medulla and decreased metabolism in the left DLPFC after active tDCS stimulation compared with sham tDCS. In addition, an increase in metabolism after active tDCS was observed in the subgenual anterior cingulate cortex and insula. An instant increase in the endogenous μ-opioid release may occur during acute motor cortex neuromodulation with tDCS (DosSantos et al., 2012).

LIMITATIONS AND RECOMMENDATIONS

The relevant NIBS studies still have several shortcomings, which may be important causes of the inconsistency in research results and difficulties in clinical application. First, most studies have small sample sizes (typically less than 40 people per group). Studies with a limited sample size may lead to the poor stability of the results and the inability to reliably reveal the true analgesic effect of NIBS because of the subjective characteristics of pain scores and differences in pain sensitivity among individuals. Future research should gradually carry out large-scale, multicenter studies to test the stability and reliability of the analgesic effects of NIBS.

Second, the current research on the analgesic effect of brain stimulation is not sufficient and in-depth. The analgesic research of rTMS is limited to CPSP, and the attention to other pain types is insufficient. The parameters used in the study of tDCS are relatively single, and the effect of stimulus parameters on analgesia is not clear. The effect of stimulation parameters on the regulation of analgesic effect should be comprehensively investigated. Micro-neuron discharge and neurotransmitter release can be integrated, as well as macro-brain response signal and somatic nervous system signal changes, through cross-species studies.

Third, understanding analgesic mechanisms rely on comparisons with analgesic loops found in other analgesic areas in the past without substantial evidence. Additionally, the influence of the placebo effect cannot be excluded because some experimental designs did not set a placebo group and only examined the changes in pain indexes before and after stimulation. Scale measurement or behavioral experiments can be carried out in multi-experimental and placebo groups to reveal the analgesic circuits of NIBS. In addition, the current assessment of the analgesic effect of different combinations of technologies is insufficient, and the interaction between NIBS and analgesic drugs is less considered. Combining different approaches may enhance analgesic effects by considering differences in pain-avoidance mechanisms.

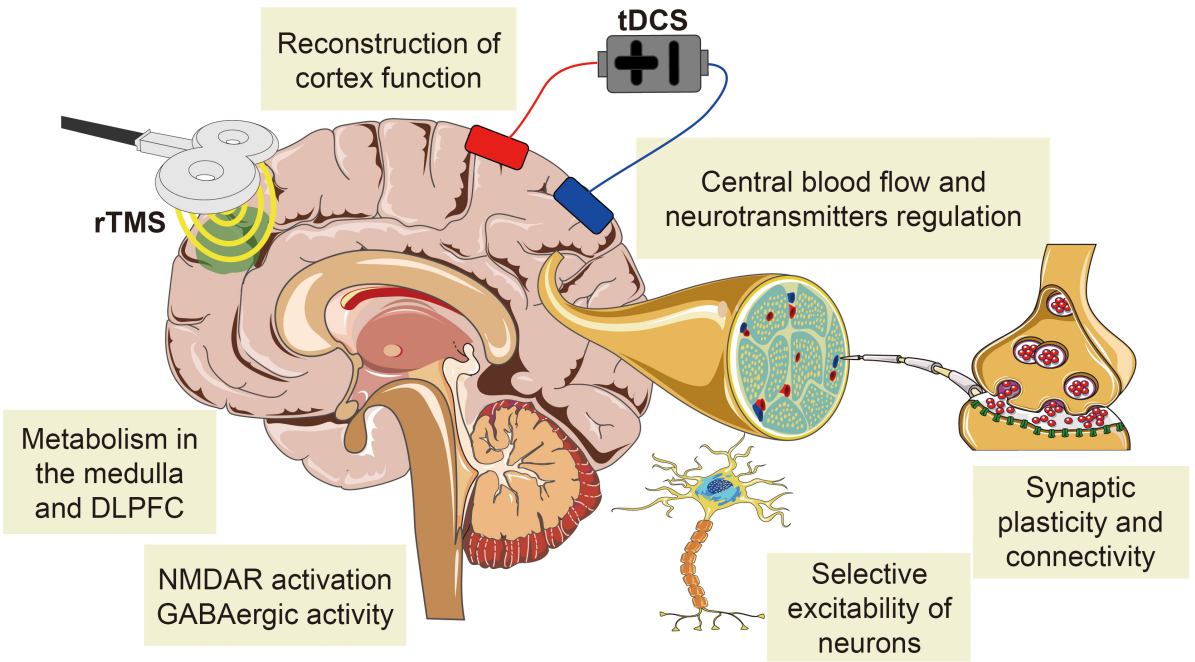

FIGURE 4 | The common mechanisms of NIBS analgesia on CNP. The analgesic mechanism of rTMS is similar to that of tDCS, both of which change cortical excitability and synaptic plasticity, regulate the release of related neurotransmitters, and affect the structural and functional connections of brain regions associated with pain processing and regulation.

DISCUSSION AND CONCLUSION

In this article, the analgesic effects of common NIBS techniques on CNP are described in detail, and their respective analgesic mechanisms are discussed. The stimulation parameters for rTMS to produce an analgesic effect are stimulation frequency of 5–10 Hz, RMT of 80–90%, 5–10 times, and current intensity of 2 mA, 20–30 mins a time, 5–10 times is the common parameter of tDCS. The most popular stimulation area of analgesia is the M1 region for rTMS and tDCS. In addition, DLPFC has also been used as a target for NP improvement for tDCS. Although tDCS stimulation of the DLPFC region has been found to reduce pain caused by MS, current guidelines do not mention improving NP by stimulating DLPFC. tDCS with different parameters acting on the DLPFC region to reduce NP induced by various diseases needs further study.

Repetitive transcranial magnetic stimulation analgesic research has been relatively mature and applied to a variety of CNP treatments (Lefaucheur et al., 2001; Lefaucheur, 2006; Ayache et al., 2016a; Nardone et al., 2017; Quesada et al., 2018; Sun et al., 2019). The analgesic mechanisms of rTMS and tDCS are similar, which both alter cortical excitability and synaptic plasticity, regulate the release of related neurotransmitters, and affect the structural and functional connections of brain regions associated with pain processing and regulation (**Figure 4**; Zheng et al., 2011; Thibaut et al., 2017; Hassan et al., 2021; Molero-Chamizo et al., 2021). tDCS has been studied in several studies and was able to manage pain effectively, but its optimal stimulation targets, stimulation intensity, and stimulation time for each type of CNP are still difficult to identify (Iodice et al., 2017; Wen et al., 2017; Young et al., 2020). NIBS not only affects the cerebral cortex at the stimulated site but also affects the related functional areas of the brain based on the pain matrix. The selection of optimal stimulation sites and parameters depends on the role of the primary disease-causing NP and its associated homologous brain regions in pain reduction. Revealing the interaction between NIBS with different parameters and cerebral cortex has great practical value for the selection of clinical analgesic methods to ultimately relieve pain and reduce the health and economic burden of pain on patients, families, and society.

AUTHOR CONTRIBUTIONS

X-QW and YF conceived the review. Q-HY drafted the manuscript and searched the literature to identify eligible trials. S-HD and Y-CW extracted and analyzed the data. Y-HZ revised the tables in the drafted manuscript. All authors approved the final manuscript.

FUNDING

The authors disclosed receipt of financial support from the following for the research, authorship, and/or publication of this article: Fok Ying-Tong Education Foundation of China (fund number: 161092), the Scientific and Technological Research Program of the Shanghai Science and Technology Committee

(fund number: 19080503100), and the Shanghai Key Lab of Human Performance (Shanghai University of Sport, fund number: 11DZ2261100). Shanghai Frontiers Science Research Base of Exercise and Metabolic Health, Talent Development Fund of Shanghai Municipal (2021081), and Shanghai Clinical Research Center for Rehabilitation Medicine (21MC1930200).

ACKNOWLEDGMENTS

The authors thank all the participants and clinical researchers involved in the publications cited in this review and peer reviewers who contributed to the continuous improvement of this article.

REFERENCES

Andrade, P., Visser-Vandewalle, V., Hoffmann, C., Steinbusch, H. W., Daemen, M. A., and Hoogland, G. (2011). Role of TNF-alpha during central sensitization in preclinical studies. *Neurol. Sci. offi. J. Ital. Neurol. Soc. Ital. Soc. Clin. Neurophysiol.* 32, 757–771. doi: 10.1007/s10072-011-0599-z

Andrade, S. M., Batista, L. M., Nogueira, L. L. R. F., de Oliveira, E. A., de Carvalho, A. G. C., Lima, S. S., et al. (2017). Constraint-induced movement therapy combined with transcranial direct current stimulation over premotor cortex improves motor function in severe stroke: a pilot randomized controlled trial. *Rehabili. Res. Pract.* 2017:6842549. doi: 10.1155/2017/6842549

Antal, A., Terney, D., Kühnl, S., and Paulus, W. (2010). Anodal transcranial direct current stimulation of the motor cortex ameliorates chronic pain and reduces short intracortical inhibition. *J. Pain Sympt. Manage.* 39, 890–903. doi: 10.1016/j.jpainsymman.2009.09.023

Antonenko, D., Schubert, F., Bohm, F., Ittermann, B., Aydin, S., Hayek, D., et al. (2017). tDCS-induced modulation of GABA Levels and Resting-State Functional Connectivity in Older Adults. *The Journal of neuroscience : the official journal of the Society for Neuroscience* 37, 4065–4073. doi: 10.1523/JNEUROSCI.0079-17.2017

Attal, N., Ayache, S. S., Ciampi De Andrade, D., Mhalla, A., Baudic, S., Jazat, F., et al. (2016). Repetitive transcranial magnetic stimulation and transcranial direct-current stimulation in neuropathic pain due to radiculopathy: a randomized sham-controlled comparative study. *Pain* 157, 1224–1231. doi: 10.1097/j.pain.0000000000000510

Attal, N., Poindessous-Jazat, F., De Chauvigny, E., Quesada, C., Mhalla, A., Ayache, S. S., et al. (2021). Repetitive transcranial magnetic stimulation for neuropathic pain: a randomized multicentre sham-controlled trial. *Brain J. Neurol.* 144, 3328–3339. doi: 10.1093/brain/awab208

Ayache, S. S., Ahdab, R., Chalah, M. A., Farhat, W. H., Mylius, V., Goujon, C., et al. (2016a). Analgesic effects of navigated motor cortex rTMS in patients with chronic neuropathic pain. *Eur. J. Pain (London, England)* 20, 1413–1422. doi: 10.1002/ejp.864

Ayache, S. S., Palm, U., Chalah, M. A., Al-Ani, T., Brignol, A., Abdellaoui, M., et al. (2016b). Prefrontal tDCS decreases pain in patients with multiple sclerosis. *Front. Neurosci.* 10:147. doi: 10.3389/fnins.2016.00147

Bae, S. H., Kim, G. D., and Kim, K. Y. (2014). Analgesic effect of transcranial direct current stimulation on central post-stroke pain. *Tohoku J. Exp. Med.* 234, 189–195. doi: 10.1620/tjem.234.189

Baroja-Mazo, A., Barberà-Cremades, M., and Pelegrín, P. (2013). The participation of plasma membrane hemichannels to purinergic signaling. *Biochim Biophys Acta* 1828, 79–93. doi: 10.1016/j.bbamem.2012.01.002

Baron, R., Binder, A., and Wasner, G. (2010). Neuropathic pain: diagnosis, pathophysiological mechanisms, and treatment. *Lancet. Neurol.* 9, 807–819. doi: 10.1016/S1474-4422(10)70143-5

Barr, M. S., Farzan, F., Davis, K. D., Fitzgerald, P. B., and Daskalakis, Z. J. (2013). Measuring GABAergic inhibitory activity with TMS-EEG and its potential clinical application for chronic pain. *J. Neuro. Pharmacol. Offi. J. Soc. Neuro. Pharmacol.* 8, 535–546. doi: 10.1007/s11481-012-9383-y

Batsikadze, G., Moliadze, V., Paulus, W., Kuo, M. F., and Nitsche, M. A. (2013). Partially non-linear stimulation intensity-dependent effects of direct current stimulation on motor cortex excitability in humans. *J. Physiol.* 591, 1987–2000. doi: 10.1113/jphysiol.2012.249730

Beggs, S., Trang, T., and Salter, M. W. (2012). P2X4R+ microglia drive neuropathic pain. *Nature neuroscience* 15, 1068–1073. doi: 10.1038/nn.3155

Benwell, C. S. Y., Learmonth, G., Miniussi, C., Harvey, M., and Thut, G. (2015). Non-linear effects of transcranial direct current stimulation as a function of individual baseline performance: evidence from biparietal tDCS influence on lateralized attention bias. *Cortex J. Dev. Study Nervous Syst. Behav.* 69, 152–165. doi: 10.1016/j.cortex.2015.05.007

Beydoun, A. (2003). Neuropathic pain: from mechanisms to treatment strategies. *J. Pain Sympt. Manage.* 25, S1–S3. doi: 10.1016/s0885-3924(03)00063-0

Bikson, M., Inoue, M., Akiyama, H., Deans, J. K., Fox, J. E., Miyakawa, H., et al. (2004). Effects of uniform extracellular DC electric fields on excitability in rat hippocampal slices in vitro. *J. Phys.* 557, 175–190. doi: 10.1113/jphysiol.2003.055772

Biundo, R., Weis, L., and Antonini, A. (2016). tDCS effect on cognitive performance in Parkinson's disease. *Movement Dis. Offi. J. Movement Dis. Soc.* 31, 1253–1254. doi: 10.1002/mds.26685

Boldt, I., Eriks-Hoogland, I., Brinkhof, M. W., de Bie, R., Joggi, D., and von Elm, E. (2014). Non-pharmacological interventions for chronic pain in people with spinal cord injury. *Cochrane Database Syst. Rev.* 2014:Cd009177. doi: 10.1002/14651858.CD009177.pub2

Bolognini, N., Olgiati, E., Maravita, A., Ferraro, F., and Fregni, F. (2013). Motor and parietal cortex stimulation for phantom limb pain and sensations. *Pain* 154, 1274–1280. doi: 10.1016/j.pain.2013.03.040

Borckardt, J. J., Reeves, S. T., Beam, W., Jensen, M. P., Gracely, R. H., Katz, S., et al. (2011). A randomized, controlled investigation of motor cortex transcranial magnetic stimulation (TMS) effects on quantitative sensory measures in healthy adults: evaluation of TMS device parameters. *Clin. J. Pain* 27, 486–494. doi: 10.1097/AJP.0b013e31820d2733

Broeder, S., Nackaerts, E., Cuypers, K., Meesen, R., Verheyden, G., and Nieuwboer, A. (2019). tDCS-enhanced consolidation of writing skills and its associations with cortical excitability in parkinson disease: a pilot study. *Neurorehabili. Neur. Rep.* 33, 1050–1060. doi: 10.1177/1545968319887684

Brunoni, A. R., Amadera, J., Berbel, B., Volz, M. S., Rizzerio, B. G., and Fregni, F. (2011). A systematic review on reporting and assessment of adverse effects associated with transcranial direct current stimulation. *Int. J. Neuropsychopharmacol.* 14, 1133–1145. doi: 10.1017/S1461145710001690

Brys, M., Fox, M. D., Agarwal, S., Biagioni, M., Dacpano, G., Kumar, P., et al. (2016). Multifocal repetitive TMS for motor and mood symptoms of parkinson disease: a randomized trial. *Neurology* 87, 1907–1915. doi: 10.1212/WNL.0000000000003279

Canavero, S., Bonicalzi, V., Dotta, M., Vighetti, S., Asteggiano, G., and Cocito, D. (2002). Transcranial magnetic cortical stimulation relieves central pain. *Stereot. Funct. Neurosurg.* 78, 192–196. doi: 10.1159/000068965

Centonze, D., Koch, G., Versace, V., Mori, F., Rossi, S., Brusa, L., et al. (2007). Repetitive transcranial magnetic stimulation of the motor cortex ameliorates spasticity in multiple sclerosis. *Neurology* 68, 1045–1050. doi: 10.1212/01.wnl.0000257818.16952.62

Chang, M. C., Kim, D. Y., and Park, D. H. (2015). Enhancement of cortical excitability and lower limb motor function in patients with stroke by transcranial direct current stimulation. *Brain Stimulat.* 8, 561–566. doi: 10.1016/j.brs.2015.01.411

Chisari, C., Fanciullacci, C., Lamola, G., Rossi, B., and Cohen, L. G. (2014). NIBS-driven brain plasticity. *Arch Ital Biol.* 152, 247–258. doi: 10.12871/00039829201445

Choi, G. S., and Chang, M. C. (2018). Effects of high-frequency repetitive transcranial magnetic stimulation on reducing hemiplegic shoulder pain in patients with chronic stoke: a randomized controlled trial. *Int. J. Neurosci.* 128, 110–116. doi: 10.1080/00207454.2017.1367682

Choi, G. S., Kwak, S. G., Lee, H. D., and Chang, M. C. (2018). Effect of high-frequency repetitive transcranial magnetic stimulation on chronic central pain after mild traumatic brain injury: a pilot study. *J. Rehabili. Med.* 50, 246–252. doi: 10.2340/16501977-2321

Choi-Kwon, S., Choi, S. H., Suh, M., Choi, S., Cho, K. H., Nah, H. W., et al. (2017). Musculoskeletal and central pain at 1 year post-stroke: associated factors and

impact on quality of life. *Acta Neurol. Scand.* 135, 419–425. doi: 10.1111/ane.12617

Cioni, B., and Meglio, M. (2007). Motor cortex stimulation for chronic non-malignant pain: current state and future prospects. *Acta Neurochirurgica. Suppl.* 97, 45–49. doi: 10.1007/978-3-211-33081-4_5

Colloca, L., Ludman, T., Bouhassira, D., Baron, R., Dickenson, A. H., Yarnitsky, D., et al. (2017). Neuropathic pain. *Nat. Rev. Dis. Primers* 3:17002.

Costa, B., Ferreira, I., Trevizol, A., Thibaut, A., and Fregni, F. (2019). Emerging targets and uses of neuromodulation for pain. *Exp. Rev. Neurother.* 19, 109–118. doi: 10.1080/14737175.2019.1567332

Coull, J. A., Beggs, S., Boudreau, D., Boivin, D., Tsuda, M., Inoue, K., et al. (2005). BDNF from microglia causes the shift in neuronal anion gradient underlying neuropathic pain. *Nature* 438, 1017–1021. doi: 10.1038/nature04223

Cruccu, G., Aziz, T. Z., Garcia-Larrea, L., Hansson, P., Jensen, T. S., Lefaucheur, J. P., et al. (2007). EFNS guidelines on neurostimulation. *Eur. J. Neurol.* 14, 952–970. doi: 10.1111/j.1468-1331.2007.01916.x

Cruccu, G., Garcia-Larrea, L., Hansson, P., Keindl, M., Lefaucheur, J. P., Paulus, W., et al. (2016). EAN guidelines on central neurostimulation therapy in chronic pain conditions. *Eur. J. Neurol.* 23, 1489–1499. doi: 10.1111/ene.13103

Cummiford, C. M., Nascimento, T. D., Foerster, B. R., Clauw, D. J., Zubieta, J.-K., Harris, R. E., et al. (2016). Changes in resting state functional connectivity after repetitive transcranial direct current stimulation applied to motor cortex in fibromyalgia patients. *Arthritis Res Ther* 18, 40. doi: 10.1186/s13075-016-0934-0

Dagan, M., Herman, T., Mirelman, A., Giladi, N., and Hausdorff, J. M. (2017). The role of the prefrontal cortex in freezing of gait in Parkinson's disease: insights from a deep repetitive transcranial magnetic stimulation exploratory study. *Exp. Brain Res.* 235, 2463–2472. doi: 10.1007/s00221-017-4981-9

David, M., Moraes, A. A., Costa, M. L. D., and Franco, C. I. F. (2018). Transcranial direct current stimulation in the modulation of neuropathic pain: a systematic review. *Neurol. Res.* 40, 555–563. doi: 10.1080/01616412.2018.1453190

de Oliveira, R. A. A., de Andrade, D. C., Mendonça, M., Barros, R., Luvisoto, T., Myczkowski, M. L., et al. (2014). Repetitive transcranial magnetic stimulation of the left premotor/dorsolateral prefrontal cortex does not have analgesic effect on central poststroke pain. *J. Pain* 15, 1271–1281. doi: 10.1016/j.jpain.2014.09.009

Defrin, R., Grunhaus, L., Zamir, D., and Zeilig, G. (2007). The effect of a series of repetitive transcranial magnetic stimulations of the motor cortex on central pain after spinal cord injury. *Arch. Phys. Med. Rehabili.* 88, 1574–1580. doi: 10.1016/j.apmr.2007.07.025

Delpont, B., Blanc, C., Osseby, G. V., Hervieu-Begue, M., Giroud, M., and Bejot, Y. (2018). Pain after stroke: a review. *Revue Neurol.* 174, 671–674.

Dockx, R., Baeken, C., Duprat, R., De Vos, F., Saunders, J. H., Polis, I., et al. (2018). Changes in canine cerebral perfusion after accelerated high frequency repetitive transcranial magnetic stimulation (HF-rTMS): a proof of concept study. *Vet J.* 234, 66–71. doi: 10.1016/j.tvjl.2018.02.004

Dooley, D. J., Taylor, C. P., Donevan, S., and Feltner, D. (2007). Ca2+ channel alpha2delta ligands: novel modulators of neurotransmission. *Trends Pharmacol. Sci.* 28, 75–82. doi: 10.1016/j.tips.2006.12.006

DosSantos, M. F., Love, T. M., Martikainen, I. K., Nascimento, T. D., Fregni, F., Cummiford, C., et al. (2012). Immediate effects of tDCS on the μ-opioid system of a chronic pain patient. *Frontiers in psychiatry* 3:93. doi: 10.3389/fpsyt.2012.00093

Dubbioso, R., Pellegrino, G., Antenora, A., De Michele, G., Filla, A., Santoro, L., et al. (2015). The effect of cerebellar degeneration on human sensori-motor plasticity. *Brain Stimulat.* 8, 1144–1150. doi: 10.1016/j.brs.2015.05.012

Dworkin, R. H., O'Connor, A. B., Kent, J., Mackey, S. C., Raja, S. N., Stacey, B. R., et al. (2013). Interventional management of neuropathic pain: NeuPSIG recommendations. *Pain* 154, 2249–2261. doi: 10.1016/j.pain.2013.06.004

Elefant, C., Baker, F. A., Lotan, M., Lagesen, S. K., and Skeie, G. O. (2012). The effect of group music therapy on mood, speech, and singing in individuals with Parkinson's disease–a feasibility study. *J. Music Ther.* 49, 278–302. doi: 10.1093/jmt/49.3.278

Elsner, B., Kugler, J., Pohl, M., and Mehrholz, J. (2016). Transcranial direct current stimulation (tDCS) for idiopathic Parkinson's disease. *Cochrane Database Syst. Rev.* 7:CD010916. doi: 10.1002/14651858.CD010916.pub2

Esser, S. K., Huber, R., Massimini, M., Peterson, M. J., Ferrarelli, F., Tononi, G., et al. (2006). demonstration of cortical LTP in humans: a combined TMS/EEG study. *Brain Res. Bull.* 69, 86–94. doi: 10.1016/j.brainresbull.2005.11.003

Fagerlund, A. J., Hansen, O. A., and Aslaksen, P. M. (2015). Transcranial direct current stimulation as a treatment for patients with fibromyalgia: a randomized controlled trial. *Pain* 156, 62–71. doi: 10.1016/j.pain.0000000000000006

Fertonani, A., and Miniussi, C. (2017). Transcranial electrical stimulation: what we know and do not know about mechanisms. *Neurosci. Rev. J. Bring. Neurobiol. Neurol. Psychiatry* 23, 109–123. doi: 10.1177/1073858416631966

Finnerup, N. B., Jensen, M. P., Norrbrink, C., Trok, K., Johannesen, I. L., Jensen, T. S., et al. (2016). A prospective study of pain and psychological functioning following traumatic spinal cord injury. *Spinal Cord* 54, 816–821. doi: 10.1038/sc.2015.236

Flaster, M., Meresh, E., Rao, M., and Biller, J. (2013). Central poststroke pain: current diagnosis and treatment. *Top Stroke Rehabil.* 20, 116–123. doi: 10.1310/tsr2002-116

Fregni, F., Boggio, P. S., Lima, M. C., Ferreira, M. J., Wagner, T., Rigonatti, S. P., et al. (2006). A sham-controlled, phase II trial of transcranial direct current stimulation for the treatment of central pain in traumatic spinal cord injury. *Pain* 122, 197–209. doi: 10.1016/j.pain.2006.02.023

Fregni, F., El-Hagrassy, M. M., Pacheco-Barrios, K., Carvalho, S., Leite, J., Simis, M., et al. (2021). Evidence-based guidelines and secondary meta-analysis for the use of transcranial direct current stimulation in neurological and psychiatric disorders. *Int. J. Neuropsychopharmacol.* 24, 256–313. doi: 10.1093/ijnp/pyaa051

Galhardoni, R., Aparecida da Silva, V., García-Larrea, L., Dale, C., Baptista, A. F., Barbosa, L. M., et al. (2019). Ciampi de Andrade, insular and anterior cingulate cortex deep stimulation for central neuropathic pain: disassembling the percept of pain. *Neurology* 92, e2165–e2175.

Garcia-Larrea, L., and Bastuji, H. (2018). Pain and consciousness. *Prog. Neuro Psychopharmacol. Biol. Psychiatry* 87, 193–199.

Garcia-Larrea, L., and Peyron, R. (2013). Pain matrices and neuropathic pain matrices: a review. *Pain* 154, S29–S43. doi: 10.1016/j.pain.2013.09.001

Ghosh, A., Haiss, F., Sydekum, E., Schneider, R., Gullo, M., Wyss, M. T., et al. (2010). Rewiring of hindlimb corticospinal neurons after spinal cord injury. *Nat. Neurosci.* 13, 97–104. doi: 10.1038/nn.2448

González-Zamorano, Y., Fernández-Carnero, J., Sánchez-Cuesta, F. J. S., Arroyo-Ferrer, A., Vourvopoulos, A., Figueiredo, P., et al. (2021). New approaches based on non-invasive brain stimulation and mental representation techniques targeting pain in Parkinson's disease patients: two study protocols for two randomized controlled trials. *Brain sciences* 11, 65. doi: 10.3390/brainsci11010065

Gritsch, S., Bali, K. K., Kuner, R., and Vardeh, D. (2016). Functional characterization of a mouse model for central post-stroke pain. *Molecular pain* 12, doi: 10.1177/1744806916629049

Gu, S. Y., and Chang, M. C. (2017). The effects of 10-Hz repetitive transcranial magnetic stimulation on depression in chronic stroke patients. *Brain Stimul.* 10, 270–274. doi: 10.1016/j.brs.2016.10.010

Guo, F., Han, X., Zhang, J., Zhao, X., Lou, J., Chen, H., et al. (2014). Repetitive transcranial magnetic stimulation promotes neural stem cell proliferation *via* the regulation of MiR-25 in a rat model of focal cerebral ischemia. *PLoS One* 9:e109267. doi: 10.1371/journal.pone.0109267

Gwak, Y. S., and Hulsebosch, C. E. (2011). GABA and central neuropathic pain following spinal cord injury. *Neuropharmacology* 60, 799–808. doi: 10.1016/j.neuropharm.2010.12.030

Haanpää, M., Attal, N., Backonja, M., Baron, R., Bennett, M., Bouhassira, D., et al. (2011). NeuPSIG guidelines on neuropathic pain assessment. *Pain* 152, 14–27. doi: 10.1016/j.pain.2010.07.031

Hagelberg, N., Martikainen, I. K., Mansikka, H., Hinkka, S., Någren, K., Hietala, J., et al. (2002). Dopamine D2 receptor binding in the human brain is associated with the response to painful stimulation and pain modulatory capacity. *Pain* 99, 273–279. doi: 10.1016/s0304-3959(02)00121-5

Hallett, M. (2007). Transcranial magnetic stimulation: a primer. *Neuron* 55, 187–199. doi: 10.1016/j.neuron.2007.06.026

Hasan, M., Whiteley, J., Bresnahan, R., MacIver, K., Sacco, P., Das, K., et al. (2014). Somatosensory change and pain relief induced by repetitive transcranial magnetic stimulation in patients with central poststroke pain. *Neuromodul. J. Int. Neuromodul. Soc.* 17, 731–736; discussion 736. doi: 10.1111/ner.12198

Hassan, A. B., Danazumi, M. S., Abdullahi, A., and Yakasai, A. M. (2021). Effect of transcranial direct current stimulation (tDCS) delivered *via* dorsolateral prefrontal cortex on central post-stroke pain and depression: a case report. *Phys. Theory Pract.* 2021, 1–8. doi: 10.1080/09593985.2021.1891591

Hemond, C. C., and Fregni, F. (2007). Transcranial magnetic stimulation in neurology: what we have learned from randomized controlled studies. *Neuromodul. J. Int. Neuromodula. Soc.* 10, 333–344. doi: 10.1111/j.1525-1403.2007.00120.x

Hodaj, H., Payen, J.-F., Lefaucheur, J.-P., and Case, A. (2016). Long-term treatment of chronic pain syndrome by anodal tDCS of the motor cortex, previously resistant to high-frequency rTMS and implanted spinal cord stimulation. *Brain Stimul.* 9, 618–620. doi: 10.1016/j.brs.2016.02.008

Hong, Y., Liu, Q., Peng, M., Bai, M., Li, J., Sun, R., et al. (2020). High-frequency repetitive transcranial magnetic stimulation improves functional recovery by inhibiting neurotoxic polarization of astrocytes in ischemic rats. *J. Neuroinflam.* 17:150. doi: 10.1186/s12974-020-01747-y

Hosomi, K., Kishima, H., Oshino, S., Hirata, M., Tani, N., Maruo, T., et al. (2013). Cortical excitability changes after high-frequency repetitive transcranial magnetic stimulation for central poststroke pain. *Pain* 154, 1352–1357. doi: 10.1016/j.pain.2013.04.017

Houde, F., Harvey, M.-P., Tremblay Labrecque, P.-F., Lamarche, F., Lefebvre, A., and Leonard, G. (2020). Combining transcranial direct current stimulation and transcutaneous electrical nerve stimulation to relieve persistent pain in a patient suffering from complex regional pain syndrome: a case report. *J. Pain Res.* 13, 467–473. doi: 10.2147/JPR.S226616

Hummel, F., Celnik, P., Giraux, P., Floel, A., Wu, W.-H., Gerloff, C., et al. (2005). Effects of non-invasive cortical stimulation on skilled motor function in chronic stroke. *Brain J. Neurol.* 128, 490–499. doi: 10.1093/brain/awh369

Iodice, R., Dubbioso, R., Ruggiero, L., Santoro, L., and Manganelli, F. (2015). Anodal transcranial direct current stimulation of motor cortex does not ameliorate spasticity in multiple sclerosis. *Restorat. Neurol. Neurosci.* 33, 487–492. doi: 10.3233/RNN-150495

Iodice, R., Manganelli, F., and Dubbioso, R. (2017). The therapeutic use of non-invasive brain stimulation in multiple sclerosis - a review. *Restorat. Neurol. Neurosci.* 35, 497–509. doi: 10.3233/RNN-170735

Jetté, F., Côté, I., Meziane, H. B., and Mercier, C. (2013). Effect of single-session repetitive transcranial magnetic stimulation applied over the hand versus leg motor area on pain after spinal cord injury. *Neurorehabili. Neural Rep.* 27, 636–643. doi: 10.1177/1545968313484810

Kang, B. S., Shin, H. I., and Bang, M. S. (2009). Effect of repetitive transcranial magnetic stimulation over the hand motor cortical area on central pain after spinal cord injury. *Arch. Phys. Med. Rehabili.* 90, 1766–1771. doi: 10.1016/j.apmr.2009.04.008

Kesselring, J., and Beer, S. (2005). Symptomatic therapy and neurorehabilitation in multiple sclerosis. *Lancet. Neurol.* 4, 643–652. doi: 10.1016/s1474-4422(05)70193-9

Khedr, E. M., Kotb, H., Kamel, N. F., Ahmed, M. A., Sadek, R., and Rothwell, J. C. (2005). Longlasting antalgic effects of daily sessions of repetitive transcranial magnetic stimulation in central and peripheral neuropathic pain. *J. Neurol. Neurosurg. Psychiatry* 76, 833–838. doi: 10.1136/jnnp.2004.055806

Kim, J. S. (2014). Pharmacological management of central post-stroke pain: a practical guide. *CNS Drugs* 28, 787–797. doi: 10.1007/s40263-014-0194-y

Klit, H., Finnerup, N. B., and Jensen, T. S. (2009). Central post-stroke pain: clinical characteristics, pathophysiology, and management. *Lancet. Neurol.* 8, 857–868. doi: 10.1016/S1474-4422(09)70176-0

Knotkova, H., Hamani, C., Sivanesan, E., Le Beuffe, M. F. E., Moon, J. Y., Cohen, S. P., et al. (2021). Neuromodulation for chronic pain. *Lancet (London, England)* 397, 2111–2124.

Kobayashi, M., Fujimaki, T., Mihara, B., and Ohira, T. (2015). Repetitive transcranial magnetic stimulation once a week induces sustainable long-term relief of central poststroke pain. *Neuromodul. J. Int. Neuromodul. Soc.* 18, 249–254. doi: 10.1111/ner.12301

Korzhova, J., Bakulin, I., Sinitsyn, D., Poydasheva, A., Suponeva, N., Zakharova, M., et al. (2019). High-frequency repetitive transcranial magnetic stimulation and intermittent theta-burst stimulation for spasticity management in secondary progressive multiple sclerosis. *Eur. J. Neurol.* 26:680. doi: 10.1111/ene.13877

Kumru, H., Murillo, N., Samso, J. V., Valls-Sole, J., Edwards, D., Pelayo, R., et al. (2010). Reduction of spasticity with repetitive transcranial magnetic stimulation in patients with spinal cord injury. *Neurorehabili. Neural Rep.* 24, 435–441. doi: 10.1177/1545968309356095

Latremoliere, A., and Woolf, C. J. (2009). Central sensitization: a generator of pain hypersensitivity by central neural plasticity. *J. Pain* 10, 895–926. doi: 10.1016/j.jpain.2009.06.012

Lefaucheur, J. P. (2006). The use of repetitive transcranial magnetic stimulation (rTMS) in chronic neuropathic pain. *Neurophysiol. Clin. Clin. Neurophysiol.* 36, 117–124. doi: 10.1016/j.neucli.2006.08.002

Lefaucheur, J. P., Aleman, A., Baeken, C., Benninger, D. H., Brunelin, J., Di Lazzaro, V., et al. (2020). Evidence-based guidelines on the therapeutic use of repetitive transcranial magnetic stimulation (rTMS): an update (2014-2018). *Clin. Neurophysiol. Offi. J. Int. Federat. Clin. Neurophysiol.* 131, 474–528.

Lefaucheur, J. P., Drouot, X., Keravel, Y., and Nguyen, J. P. (2001). Pain relief induced by repetitive transcranial magnetic stimulation of precentral cortex. *Neuroreport* 12, 2963–2965. doi: 10.1097/00001756-200109170-00041

Lefaucheur, J. P., Drouot, X., Menard-Lefaucheur, I., Zerah, F., Bendib, B., Cesaro, P., et al. (2004). Neurogenic pain relief by repetitive transcranial magnetic cortical stimulation depends on the origin and the site of pain. *J. Neurol. Neurosurg. Psychiatry* 75, 612–616. doi: 10.1136/jnnp.2003.022236

Lefaucheur, J. P., Hatem, S., Nineb, A., Ménard-Lefaucheur, I., Wendling, S., Keravel, Y., et al. (2006). Somatotopic organization of the analgesic effects of motor cortex rTMS in neuropathic pain. *Neurology* 67, 1998–2004. doi: 10.1212/01.wnl.0000247138.85330.88

Lefaucheur, J.-P., André-Obadia, N., Antal, A., Ayache, S. S., Baeken, C., Benninger, D. H., et al. (2014). Evidence-based guidelines on the therapeutic use of repetitive transcranial magnetic stimulation (rTMS). *Clin. Neurophysiol. Offi. J. Int. Federat. Clin. Neurophysiol.* 125, 2150–2206.

Lefaucheur, J.-P., Antal, A., Ayache, S. S., Benninger, D. H., Brunelin, J., Cogiamanian, F., et al. (2017). Evidence-based guidelines on the therapeutic use of transcranial direct current stimulation (tDCS). *Clin. Neurophysiol. Offi. J. Int. Federat. Clin. Neurophysiol.* 128, 56–92.

Leo, R. J., and Latif, T. (2007). Repetitive transcranial magnetic stimulation (rTMS) in experimentally induced and chronic neuropathic pain: a review. *J. Pain* 8, 453–459. doi: 10.1016/j.jpain.2007.01.009

Li, C., Jirachaipitak, S., Wrigley, P., Xu, H., and Euasobhon, P. (2021). Transcranial direct current stimulation for spinal cord injury-associated neuropathic pain. *Korean J. Pain* 34, 156–164. doi: 10.3344/kjp.2021.34.2.156

Li, F., Fang, L., Huang, S., Yang, Z., Nandi, J., Thomas, S., et al. (2011). Hyperbaric oxygenation therapy alleviates chronic constrictive injury-induced neuropathic pain and reduces tumor necrosis factor-alpha production. *Anesthesia Anal.* 113, 626–633. doi: 10.1213/ANE.0b013e31821f9544

Lin, R. L., Douaud, G., Filippini, N., Okell, T. W., Stagg, C. J., and Tracey, I. (2017). Structural Connectivity Variances Underlie Functional and Behavioral Changes During Pain Relief Induced by Neuromodulation. *Scientific reports* 7, 41603. doi: 10.1038/srep41603

Liu, H., Han, X.-H., Chen, H., Zheng, C.-X., Yang, Y., and Huang, X.-L. (2015). Repetitive magnetic stimulation promotes neural stem cells proliferation by upregulating MiR-106b in vitro. *J. Huazhong Univ. Sci. Technol. Med. Sci.* 35, 766–772. doi: 10.1007/s11596-015-1505-3

Liu, Y., Zhou, L. J., Wang, J., Li, D., Ren, W. J., Peng, J., et al. (2017). TNF-α differentially regulates synaptic plasticity in the hippocampus and spinal cord by microglia-dependent mechanisms after peripheral nerve injury. *J. Neurosci. Offi. J. Soc. Neurosci.* 37, 871–881. doi: 10.1523/jneurosci.2235-16.2016

Lundström, E., Smits, A., Terént, A., and Borg, J. (2009). Risk factors for stroke-related pain 1 year after first-ever stroke. *Eur. J. Neurol.* 16, 188–193. doi: 10.1111/j.1468-1331.2008.02378.x

Madden, C. J., and Morrison, S. F. (2019). Central nervous system circuits that control body temperature. *Neurosci. Lett.* 696, 225–232. doi: 10.1016/j.neulet.2018.11.027

Margot-Duclot, A., Tournebise, H., Ventura, M., and Fattal, C. (2009). What are the risk factors of occurence and chronicity of neuropathic pain in spinal cord injury patients? *Ann. Phys. Rehabili. Med.* 52, 111–123. doi: 10.1016/j.rehab.2008.12.003

Martin, L., Borckardt, J. J., Reeves, S. T., Frohman, H., Beam, W., Nahas, Z., et al. (2013). A pilot functional MRI study of the effects of prefrontal rTMS on pain perception. *Pain Med. (Malden, Mass.)* 14, 999–1009. doi: 10.1111/pme.12129

Matsumura, Y., Hirayama, T., and Yamamoto, T. (2013). Comparison between pharmacologic evaluation and repetitive transcranial magnetic stimulation-induced analgesia in poststroke pain patients. *Neuromodul. J. Int. Neuromodul. Soc.* 16, 349–354; discussion 354. doi: 10.1111/ner.12019

Mehta, S., McIntyre, A., Guy, S., Teasell, R. W., and Loh, E. (2015). Effectiveness of transcranial direct current stimulation for the management of neuropathic pain after spinal cord injury: a meta-analysis. *Spinal Cord* 53, 780–785. doi: 10.1038/sc.2015.118

Michel-Flutot, P., Zholudeva, L. V., Randelman, M. L., Deramaudt, T. B., Mansart, A., Alvarez, J. C., et al. (2021). High frequency repetitive transcranial magnetic stimulation promotes long lasting phrenic motoneuron excitability *via* GABAergic networks. *Res. Physiol. Neurobiol.* 292:103704. doi: 10.1016/j.resp.2021.103704

Moisset, X., Bouhassira, D., vez Couturier, J. A., Alchaar, H., Conradi, S., Delmotte, M. H., et al. (2020). Pharmacological and non-pharmacological treatments for neuropathic pain: systematic review and French recommendations. *Revue Neurol.* 176, 325–352. doi: 10.1016/j.neurol.2020.01.361

Molero-Chamizo, A., Salas Sanchez, A., Alvarez Batista, B., Cordero Garcia, C., Andujar Barroso, R., Rivera-Urbina, G. N., et al. (2021). Bilateral motor cortex tDCS effects on post-stroke pain and spasticity: a three cases study. *Front. Pharmacol.* 12:624582. doi: 10.3389/fphar.2021.624582

Moore, K. W., de Waal Malefyt, R., Coffman, R. L., and O'Garra, A. (2001). Interleukin-10 and the interleukin-10 receptor. *Ann. Rev. Immunol.* 19, 683–765. doi: 10.1146/annurev.immunol.19.1.683

Moreno-Duarte, I., Morse, L. R., Alam, M., Bikson, M., Zafonte, R., and Fregni, F. (2014). Targeted therapies using electrical and magnetic neural stimulation for the treatment of chronic pain in spinal cord injury. *NeuroImage* 85, 1003–1013. doi: 10.1016/j.neuroimage.2013.05.097

Mori, F., Codecà, C., Kusayanagi, H., Monteleone, F., Buttari, F., Fiore, S., et al. (2010). Effects of anodal transcranial direct current stimulation on chronic neuropathic pain in patients with multiple sclerosis. *J. Pain* 11, 436–442. doi: 10.1016/j.jpain.2009.08.011

Mori, F., Ljoka, C., Magni, E., Codeca, C., Kusayanagi, H., Monteleone, F., et al. (2011). Transcranial magnetic stimulation primes the effects of exercise therapy in multiple sclerosis. *J. Neurol.* 258, 1281–1287. doi: 10.1007/s00415-011-5924-1

Moseley, G. L., and Flor, H. (2012). Targeting cortical representations in the treatment of chronic pain: a review. *Neurorehabili. Neural Rep.* 26, 646–652. doi: 10.1177/1545968311433209

Mouraux, A., Diukova, A., Lee, M. C., Wise, R. G., and Iannetti, G. D. (2011). A multisensory investigation of the functional significance of the "pain matrix". *NeuroImage* 54, 2237–2249. doi: 10.1016/j.neuroimage.2010.09.084

Murray, L. M., Edwards, D. J., Ruffini, G., Labar, D., Stampas, A., Pascual-Leone, A., et al. (2015). Intensity dependent effects of transcranial direct current stimulation on corticospinal excitability in chronic spinal cord injury. *Arch. Phys. Med. Rehabili.* 96, S114–S121. doi: 10.1016/j.apmr.2014.11.004

Naess, H., Lunde, L., and Brogger, J. (2012). The effects of fatigue, pain, and depression on quality of life in ischemic stroke patients: the bergen stroke study. *Vasc Health Risk Manag* 8, 407–413. doi: 10.2147/VHRM.S32780

Nardone, R., Holler, Y., Langthaler, P. B., Lochner, P., Golaszewski, S., Schwenker, K., et al. (2017). rTMS of the prefrontal cortex has analgesic effects on neuropathic pain in subjects with spinal cord injury. *Spinal Cord* 55, 20–25. doi: 10.1038/sc.2016.87

Nardone, R., Höller, Y., Leis, S., Höller, P., Thon, N., Thomschewski, A., et al. (2014). Invasive and non-invasive brain stimulation for treatment of neuropathic pain in patients with spinal cord injury: a review. *J. Spinal Cord Med.* 37, 19–31. doi: 10.1179/2045772313Y.0000000140

Nasu-Tada, K., Koizumi, S., Tsuda, M., Kunifusa, E., and Inoue, K. (2006). Possible involvement of increase in spinal fibronectin following peripheral nerve injury in upregulation of microglial P2X4, a key molecule for mechanical allodynia. *Glia* 53, 769–775. doi: 10.1002/glia.20339

Ngernyam, N., Jensen, M. P., Arayawichanon, P., Auvichayapat, N., Tiamkao, S., Janjarasjitt, S., et al. (2015). The effects of transcranial direct current stimulation in patients with neuropathic pain from spinal cord injury. *Clin. Neurophysiol. Offi. J. Int. Federat. Clin. Neurophysiol.* 126, 382–390. doi: 10.1016/j.clinph.2014.05.034

Nickel, F. T., Seifert, F., Lanz, S., and Maihöfner, C. (2012). Mechanisms of neuropathic pain. *Eur. Neuropsychopharmacol. J. Eur. College Neuropsychopharmacol.* 22, 81–91.

Nitsche, M. A., Boggio, P. S., Fregni, F., and Pascual-Leone, A. (2009). Treatment of depression with transcranial direct current stimulation (tDCS): a review. *Exp. Neurol.* 219, 14–19. doi: 10.1016/j.expneurol.2009.03.038

Nitsche, M. A., Cohen, L. G., Wassermann, E. M., Priori, A., Lang, N., Antal, A., et al. (2008). Transcranial direct current stimulation: state of the art 2008. *Brain Stimulat.* 1, 206–223. doi: 10.1016/j.brs.2008.06.004

Nitsche, M. A., Jaussi, W., Liebetanz, D., Lang, N., Tergau, F., and Paulus, W. (2004a). Consolidation of human motor cortical neuroplasticity by D-cycloserine. *Neuropsychopharmacol. Offi. Publi. Am. College Neuropsychopharmacol.* 29, 1573–1578. doi: 10.1038/sj.npp.1300517

Nitsche, M. A., Liebetanz, D., Schlitterlau, A., Henschke, U., Fricke, K., Frommann, K., et al. (2004b). GAB aergic modulation of DC stimulation-induced motor cortex excitability shifts in humans. *Eur. J. Neurosci.* 19, 2720–2726. doi: 10.1111/j.0953-816X.2004.03398.x

Oh, H., Seo, W., and Comprehensive Review, A. (2015). Central post-stroke pain. *Pain Manage. Nurs.* 16, 804–818.

Ohn, S. H., Chang, W. H., Park, C.-H., Kim, S. T., Lee, J. I., Pascual-Leone, A., et al. (2012). Neural correlates of the antinociceptive effects of repetitive transcranial magnetic stimulation on central pain after stroke. *Neurorehabili. Neural Rep.* 26, 344–352. doi: 10.1177/1545968311423110

Ojala, J., Vanhanen, J., Harno, H., Lioumis, P., Vaalto, S., Kaunisto, M. A., et al. (2021). A Randomized, sham-controlled trial of repetitive transcranial magnetic stimulation targeting M1 and S2 in central poststroke pain: a pilot trial. *Neuromodul. J. Int. Neuromodul. Soc.* doi: 10.1111/ner.13496

Orru, G., Baroni, M., Cesari, V., Conversano, C., Hitchcott, P. K., and Gemignani, A. (2019). The effect of single and repeated tDCS sessions on motor symptoms in Parkinson's disease: a systematic review. *Arch. Ital. Biol.* 157, 89–101. doi: 10.12871/00039829201925

Palm, U., Ayache, S. S., Padberg, F., and Lefaucheur, J. P. (2014). Non-invasive brain stimulation therapy in multiple sclerosis: a review of tDCS, rTMS and ECT results. *Brain Stimulat.* 7, 849–854. doi: 10.1016/j.brs.2014.09.014

Paolucci, S., Iosa, M., Toni, D., Barbanti, P., Bovi, P., Cavallini, A., et al. (2016). Prevalence and time course of post-stroke pain: a multicenter prospective hospital-based study. *Pain Med. (Malden, Mass.)* 17, 924–930. doi: 10.1093/pm/pnv019

Patwardhan, M. B., Matchar, D. B., Samsa, G. P., McCrory, D. C., Williams, R. G., and Li, T. T. (2005). Cost of multiple sclerosis by level of disability: a review of literature. *Mult. Sclerosis (Houndmills, Basingstoke, England)* 11, 232–239. doi: 10.1191/1352458505ms1137oa

Peng, M. S., Wang, R., Wang, Y. Z., Chen, C. C., Wang, J., Liu, X. C., et al. (2022). Efficacy of therapeutic aquatic exercise vs physical therapy modalities for patients with chronic low back pain: a randomized clinical trial. *JAMA Network Open* 5:e2142069. doi: 10.1001/jamanetworkopen.2021.42069

Putzolu, M., Pelosin, E., Ogliastro, C., Lagravinese, G., Bonassi, G., Ravaschio, A., et al. (2018). Anodal tDCS over prefrontal cortex improves dual-task walking in parkinsonian patients with freezing. *Movement Dis. Offi. J. Movement Dis. Soc.* 33, 1972–1973. doi: 10.1002/mds.27533

Quesada, C., Pommier, B., Fauchon, C., Bradley, C., Creac'h, C., Vassal, F., et al. (2018). Robot-Guided Neuronavigated Repetitive Transcranial Magnetic Stimulation (rTMS) in Central Neuropathic Pain. *Archives of physical medicine and rehabilitation* 99, 2203–2215.e1. doi: 10.1016/j.apmr.2018.04.013

Quintero, J. E., Dooley, D. J., Pomerleau, F., Huettl, P., and Gerhardt, G. A. (2011). Amperometric measurement of glutamate release modulation by gabapentin and pregabalin in rat neocortical slices: role of voltage-sensitive Ca2+ α2δ-1 subunit. *J. Pharmacol. Exp. Ther.* 338, 240–245. doi: 10.1124/jpet.110.178384

Ramger, B. C., Bader, K. A., Davies, S. P., Stewart, D. A., Ledbetter, L. S., Simon, C. B., et al. (2019). Effects of non-invasive brain stimulation on clinical pain intensity and experimental pain sensitivity among individuals with central post-stroke pain: a systematic review. *J. Pain Res.* 12, 3319–3329. doi: 10.2147/JPR.S216081

Reimer, M., Helfert, S. M., and Baron, R. (2014). Phenotyping neuropathic pain patients: implications for individual therapy and clinical trials. *Curr. Opin. Support. Palliat. Care* 8, 124–129. doi: 10.1097/SPC.0000000000000045

Rekand, T., Hagen, E. M., and Gronning, M. (2012). Chronic pain following spinal cord injury. *Tidsskr Nor Laegeforen* 132, 974–979.

Rossini, P. M., Burke, D., Chen, R., Cohen, L. G., Daskalakis, Z., Di Iorio, R., et al. (2015). Non-invasive electrical and magnetic stimulation of the brain, spinal cord, roots and peripheral nerves: basic principles and procedures for routine clinical and research application. an updated report from an I.F.C.N. committee. *Clin. Neurophysiol. Offi. J. Int. Federat. Clin. Neurophysiol.* 126, 1071–1107. doi: 10.1016/j.clinph.2015.02.001

Sacco, P., Prior, M., Poole, H., and Nurmikko, T. (2014). Repetitive transcranial magnetic stimulation over primary motor vs non-motor cortical targets; effects on experimental hyperalgesia in healthy subjects. *BMC Neurol.* 14:166. doi: 10.1186/s12883-014-0166-3

Saitoh, Y., and Yoshimine, T. (2007). Stimulation of primary motor cortex for intractable deafferentation pain. *Acta Neurochirur. Suppl.* 97, 51–56. doi: 10.1007/978-3-211-33081-4_6

Santos-García, D., Oreiro, M., Pérez, P., Fanjul, G., Paz González, J. M., Feal Painceiras, M. J., et al. (2020). Impact of coronavirus disease 2019 pandemic on Parkinson's disease: a cross-sectional survey of 568 spanish patients. *Movement Dis. Offi. J. Movement Dis. Soc.* 35, 1712–1716. doi: 10.1002/mds.28261

Saturnino, G. B., Antunes, A., and Thielscher, A. (2015). On the importance of electrode parameters for shaping electric field patterns generated by tDCS. *NeuroImage* 120, 25–35. doi: 10.1016/j.neuroimage.2015.06.067

Shen, Z., Li, Z., Ke, J., He, C., Liu, Z., Zhang, D., et al. (2020). Effect of non-invasive brain stimulation on neuropathic pain following spinal cord injury: a systematic review and meta-analysis. *Medicine* 99:e21507. doi: 10.1097/MD.0000000000021507

Shigematsu, T., Fujishima, I., and Ohno, K. (2013). Transcranial direct current stimulation improves swallowing function in stroke patients. *Neurorehabili. Neur. Rep.* 27, 363–369. doi: 10.1177/1545968312474116

Soler, M. D., Kumru, H., Pelayo, R., Vidal, J., Tormos, J. M., Fregni, F., et al. (2010). Effectiveness of transcranial direct current stimulation and visual illusion on neuropathic pain in spinal cord injury. *Brain J. Neurol.* 133, 2565–2577. doi: 10.1093/brain/awq184

Stagg, C. J., and Nitsche, M. A. (2011). Physiological basis of transcranial direct current stimulation. *Neuroscientist* 17, 37–53. doi: 10.1177/1073858410386614

Stagg, C. J., Antal, A., and Nitsche, M. A. (2018). Physiology of transcranial direct current stimulation. *J. ECT* 34, 144–152.

Strafella, A. P., Paus, T., Barrett, J., and Dagher, A. (2001). Repetitive transcranial magnetic stimulation of the human prefrontal cortex induces dopamine release in the caudate nucleus. *J. Neurosci. Offi. J. Soc. Neurosci.* 21:RC157. doi: 10.1523/JNEUROSCI.21-15-j0003.2001

Strafella, A. P., Paus, T., Fraraccio, M., and Dagher, A. (2003). Striatal dopamine release induced by repetitive transcranial magnetic stimulation of the human motor cortex. *Brain J. Neurol.* 126, 2609–2615. doi: 10.1093/brain/awg268

Sun, X., Long, H., Zhao, C., Duan, Q., Zhu, H., Chen, C., et al. (2019). Analgesia-enhancing effects of repetitive transcranial magnetic stimulation on neuropathic pain after spinal cord injury:an fNIRS study. *Restorat. Neurol. Neurosci.* 37, 497–507. doi: 10.3233/RNN-190934

Tan, C. L., and Knight, Z. A. (2018). Regulation of body temperature by the nervous system. *Neuron* 98, 31–48. doi: 10.1016/j.neuron.2018.02.022

Terney, D., Chaieb, L., Moliadze, V., Antal, A., and Paulus, W. (2008). Increasing human brain excitability by transcranial high-frequency random noise stimulation. *J. Neurosci. Offi. J. Soc. Neurosci.* 28, 14147–14155. doi: 10.1523/JNEUROSCI.4248-08.2008

Thibaut, A., Carvalho, S., Morse, L. R., Zafonte, R., and Fregni, F. (2017). Delayed pain decrease following M1 tDCS in spinal cord injury: a randomized controlled clinical trial. *Neurosci. Lett.* 658, 19–26. doi: 10.1016/j.neulet.2017.08.024

To, W. T., Hart, J., De Ridder, D., and Vanneste, S. (2016). Considering the influence of stimulation parameters on the effect of conventional and high-definition transcranial direct current stimulation. *Exp. Rev. Med. Dev.* 13, 391–404. doi: 10.1586/17434440.2016.1153968

Toledo, R. S., Stein, D. J., Sanches, P. R. S., da Silva, L. S., Medeiros, H. R., Fregni, F., et al. (2021). rTMS induces analgesia and modulates neuroinflammation and neuroplasticity in neuropathic pain model rats. *Brain Res.* 1762, 147427. doi: 10.1016/j.brainres.2021.147427

Treister, A. K., Hatch, M. N., Cramer, S. C., and Chang, E. Y. (2017). Demystifying poststroke pain: from etiology to treatment. *PMR* 9, 63–75. doi: 10.1016/j.pmrj.2016.05.015

Tung, K.-W., Behera, D., and Biswal, S. (2015). Neuropathic pain mechanisms and imaging. *Sem. Muscul. Rad.* 19, 103–111.

Ueyama, E., Ukai, S., Ogawa, A., Yamamoto, M., Kawaguchi, S., Ishii, R., et al. (2011). Chronic repetitive transcranial magnetic stimulation increases hippocampal neurogenesis in rats. *Psychiatry and Clinical Neurosci.* 65, 77–81. doi: 10.1111/j.1440-1819.2010.02170.x

Vallejo, R., Tilley, D. M., Vogel, L., and Benyamin, R. (2010). The role of glia and the immune system in the development and maintenance of neuropathic pain. *Pain Pract. Offi. J. World Inst. Pain* 10, 167–184. doi: 10.1111/j.1533-2500.2010.00367.x

Vonloh, M., Chen, R., and Kluger, B. (2013). Safety of transcranial magnetic stimulation in Parkinson's disease: a review of the literature. *Parkins. Related Dis.* 19, 573–585. doi: 10.1016/j.parkreldis.2013.01.007

Wagner, T., Valero-Cabre, A., and Pascual-Leone, A. (2007). Noninvasive human brain stimulation. *Ann. Rev. Bio. Eng.* 9, 527–565.

Wang, H. Y., Crupi, D., Liu, J., Stucky, A., Cruciata, G., Di Rocco, A., et al. (2011). Repetitive transcranial magnetic stimulation enhances BDNF-TrkB signaling in both brain and lymphocyte. *J. Neurosci. Offi. J. Soc. Neurosci.* 31, 11044–11054. doi: 10.1523/JNEUROSCI.2125-11.2011

Wasserman, J. K., and Koeberle, P. D. (2009). Development and characterization of a hemorrhagic rat model of central post-stroke pain. *Neuroscience* 161, 173–183. doi: 10.1016/j.neuroscience.2009.03.042

Wen, H. Z., Gao, S. H., Zhao, Y. D., He, W. J., Tian, X. L., and Ruan, H. Z. (2017). Parameter optimization analysis of prolonged analgesia effect of tDCS on neuropathic pain rats. *Front. Behav. Neurosci.* 11:115. doi: 10.3389/fnbeh.2017.00115

Wrigley, P. J., Gustin, S. M., McIndoe, L. N., Chakiath, R. J., Henderson, L. A., and Siddall, P. J. (2013). Longstanding neuropathic pain after spinal cord injury is refractory to transcranial direct current stimulation: a randomized controlled trial. *Pain* 154, 2178–2184. doi: 10.1016/j.pain.2013.06.045

Wu, B., Zhou, L., Chen, C., Wang, J., Hu, L. I., and Wang, X. (2022). Effects of exercise-induced hypoalgesia and its neural mechanisms. *Med. Sci. Sports Exerc.* 54, 220–231. doi: 10.1249/MSS.0000000000002781

Xie, C. L., Chen, J., Wang, X. D., Pan, J. L., Zhou, Y., Lin, S. Y., et al. (2015). Repetitive transcranial magnetic stimulation (rTMS) for the treatment of depression in parkinson disease: a meta-analysis of randomized controlled clinical trials. *Neurol. Sci. offi. J. Ital. Neurol. Soc. Ital. Soc. Clin. Neurophysiol.* 36, 1751–1761. doi: 10.1007/s10072-015-2345-4

Yamout, B. I., and Alroughani, R. (2018). Multiple sclerosis. *Sem. Neurol.* 38, 212–225.

Yang, L., Su, Y., Guo, F., Zhang, H., Zhao, Y., Huang, Q., et al. (2020). Deep rTMS mitigates behavioral and neuropathologic anomalies in cuprizone-exposed mice through reducing microglial proinflammatory cytokines. *Front. Integrat. Neurosci.* 14:556839. doi: 10.3389/fnint.2020.556839

Yang, L., Wang, S. H., Hu, Y., Sui, Y. F., Peng, T., and Guo, T. C. (2018). Effects of repetitive transcranial magnetic stimulation on astrocytes proliferation and nNOS expression in neuropathic pain rats. *Curr. Med. Sci.* 38, 482–490. doi: 10.1007/s11596-018-1904-3

Yang, Z. Y., Lü, Q., Chen, X. T., Zhang, W. Q., Wang, H., and Zhao, S. J. (2014). Investigation on the features and the relevant factors of pain in patients with Parkinson disease. *J. Clin. Neurol.* 27, 94–96.

Yeh, N. C., Yang, Y. R., Huang, S. F., Ku, P. H., and Wang, R. Y. (2021). Effects of transcranial direct current stimulation followed by exercise on neuropathic pain in chronic spinal cord injury: a double-blinded randomized controlled pilot trial. *Spinal Cord* 59, 684–692. doi: 10.1038/s41393-020-00560-x

Yılmaz, B., Kesikburun, S., Yaşar, E., and Tan, A. K. (2014). The effect of repetitive transcranial magnetic stimulation on refractory neuropathic pain in spinal cord injury. *J. Spinal Cord Med.* 37, 397–400. doi: 10.1179/2045772313Y.0000000172

Yoon, E. J., Kim, Y. K., Kim, H.-R., Kim, S. E., Lee, Y., and Shin, H. I. (2014). Transcranial direct current stimulation to lessen neuropathic pain after spinal cord injury: a mechanistic PET study. *Neurorehabilitation and neural repair* 28, 250–259. doi: 10.1177/1545968313507632

Yoon, K. J., Lee, Y.-T., and Han, T. R. (2011). Mechanism of functional recovery after repetitive transcranial magnetic stimulation (rTMS) in the subacute cerebral ischemic rat model: neural plasticity or anti-apoptosis? *Exp. Brain Res.* 214, 549–556. doi: 10.1007/s00221-011-2853-2

Young Blood, M. R., Ferro, M. M., Munhoz, R. P., Teive, H. A., and Camargo, C. H. (2016). Classification and characteristics of pain associated with Parkinson's disease. *Parkinsons Dis.* 2016:6067132. doi: 10.1155/2016/6067132

Young, J., Zoghi, M., Khan, F., and Galea, M. P. (2020). The effect of transcranial direct current stimulation on chronic neuropathic pain in patients with multiple sclerosis: randomized controlled trial. *Pain Med. (Malden, Mass.)* 21, 3451–3457. doi: 10.1093/pm/pnaa128

Zaghi, S., Acar, M., Hultgren, B., Boggio, P. S., and Fregni, F. (2010). Noninvasive brain stimulation with low-intensity electrical currents: putative mechanisms of action for direct and alternating current stimulation. *Neurosci. Rev. J. Bring. Neurobiol. Neurol. Psychiatry* 16, 285–307. doi: 10.1177/1073858409336227

Zhang, K. L., Yuan, H., Wu, F. F., Pu, X. Y., Liu, B. Z., Li, Z., et al. (2021). Analgesic effect of noninvasive brain stimulation for neuropathic pain patients: a systematic review. *Pain Therapy* 10, 315–332. doi: 10.1007/s40122-021-00252-1

Zhang, K. Y., Rui, G., Zhang, J. P., Guo, L., An, G. Z., Lin, J. J., et al. (2020). Cathodal tDCS exerts neuroprotective effect in rat brain after acute ischemic stroke. *BMC neuroscience* 21:21. doi: 10.1186/s12868-020-00570-8

Zhao, C. G., Sun, W., Ju, F., Jiang, S., Wang, H., Sun, X. L., et al. (2021). Analgesic effects of navigated repetitive transcranial magnetic stimulation in patients with acute central poststroke pain. *Pain Therapy* 10, 1085–1100. doi: 10.1007/s40122-021-00261-0

Zhao, C. G., Sun, W., Ju, F., Wang, H., Sun, X. L., Mou, X., et al. (2020). Analgesic effects of directed repetitive transcranial magnetic stimulation in acute neuropathic pain after spinal cord injury. *Pain Med. (Malden, Mass.)* 21, 1216–1223. doi: 10.1093/pm/pnz290

Zheng, K., Chen, C., Yang, S., and Wang, X. (2021). Aerobic exercise attenuates pain sensitivity: an event-related potential study. *Front. Neurosci.* 15:735470. doi: 10.3389/fnins.2021.735470

Zheng, X., Alsop, D. C., and Schlaug, G. (2011). Effects of transcranial direct current stimulation (tDCS) on human regional cerebral blood flow. *NeuroImage* 58, 26–33. doi: 10.1016/j.neuroimage.2011.06.018

Zortea, M., Ramalho, L., Alves, R. L., Alves, C.F.d.S., Braulio, G., Torres, I.L.d.S., et al. (2019). Transcranial direct current stimulation to improve the dysfunction of descending pain modulatory system related to opioids in chronic non-cancer pain: an integrative review of neurobiology and meta-analysis. *Front. Neurosci.* 13:1218. doi: 10.3389/fnins.2019.01218

Conflict of Interest: The authors declare that the research was conducted in the absence of any commercial or financial relationships that could be construed as a potential conflict of interest.

Publisher's Note: All claims expressed in this article are solely those of the authors and do not necessarily represent those of their affiliated organizations, or those of the publisher, the editors and the reviewers. Any product that may be evaluated in this article, or claim that may be made by its manufacturer, is not guaranteed or endorsed by the publisher.

frontiers | Frontiers in Molecular Neuroscience

ORIGINAL RESEARCH
published: 20 May 2022
doi: 10.3389/fnmol.2022.856299

The Development of Mechanical Allodynia in Diabetic Rats Revealed by Single-Cell RNA-Seq

*Han Zhou†, Xiaosheng Yang†, Chenlong Liao, Hongjin Chen, Yiwei Wu, Binran Xie, Fukai Ma and WenChuan Zhang**

Department of Neurosurgery, Ninth People Hospital Affiliated to Shanghai Jiao Tong University School of Medicine, Shanghai, China

Mechanical allodynia (MA) is the main reason that patients with diabetic peripheral neuropathy (DPN) seek medical advice. It severely debilitates the quality of life. Investigating hyperglycemia-induced changes in neural transcription could provide fundamental insights into the complex pathogenesis of painful DPN (PDPN). Gene expression profiles of physiological dorsal root ganglia (DRG) have been studied. However, the transcriptomic changes in DRG neurons in PDPN remain largely unexplored. In this study, by single-cell RNA sequencing on dissociated rat DRG, we identified five physiological neuron types and a novel neuron type MAAC (*Fxyd7*$^{+}$/*Atp1b1*$^{+}$) in PDPN. The novel neuron type originated from peptidergic neuron cluster and was characterized by highly expressing genes related to neurofilament and cytoskeleton. Based on the inferred gene regulatory networks, we found that activated transcription factors *Hobx7* and *Larp1* in MAAC could enhance *Atp1b1* expression. Moreover, we constructed the cellular communication network of MAAC and revealed its receptor-ligand pairs for transmitting signals with other cells. Our molecular investigation at single-cell resolution advances the understanding of the dynamic peripheral neuron changes and underlying molecular mechanisms during the development of PDPN.

Keywords: mechanical allodynia, neuropathic pain, painful diabetic peripheral neuropathy, somatosensory neurons, single-cell RNA sequencing

OPEN ACCESS

Edited by:
Fengxian Li,
Southern Medical University, China

Reviewed by:
Temugin Berta,
University of Cincinnati, United States
Junguk Hur,
University of North Dakota, United States

***Correspondence:**
WenChuan Zhang
zhangwench88@sjtu.edu.cn

†These authors share first authorship

Specialty section:
This article was submitted to Pain Mechanisms and Modulators, a section of the journal Frontiers in Molecular Neuroscience

Received: *17 January 2022*
Accepted: *14 April 2022*
Published: *20 May 2022*

Citation:
Zhou H, Yang X, Liao C, Chen H, Wu Y, Xie B, Ma F and Zhang W (2022) The Development of Mechanical Allodynia in Diabetic Rats Revealed by Single-Cell RNA-Seq. Front. Mol. Neurosci. 15:856299. doi: 10.3389/fnmol.2022.856299

INTRODUCTION

Diabetic peripheral neuropathy (DPN) is a common complication of diabetes with variable clinical presentations. Patients can suffer from a painless syndrome with loss of sense of touch and temperature, or neuropathic pain manifested by mechanical allodynia (MA) (Berti-Mattera et al., 2008). The latter is the main reason for patients to seek medical advice as it severely debilitates patients' life quality (Quattrini and Tesfaye, 2003). The pathogenesis of painful DPN (PDPN) is complex. Diabetes can lead to multiple damage to the peripheral nervous system, including abnormal activation of multiple metabolic pathways and imbalance of mitochondrial redox state (Feldman et al., 2017). In addition, nerve swelling caused by metabolic disturbances can result in nerve compression injury (Best et al., 2019). In the central nervous system, neuroplastic changes that involve the spinal cord and thalamus were observed in patients or experimental models (Selvarajah et al., 2014; Marshall et al., 2017). The dorsal root ganglia (DRG) contains most of cell bodies of primary sensory neurons, which transmits sensory neural signals through the

peripheral nerves to the central nervous system (Maatuf et al., 2019). Due to exposure outside the blood-brain barrier, DRG is particularly vulnerable in diabetes and could be an important trigger for neuropathic pain (Sloan et al., 2018). Overall, the diversity of mechanisms determines that PDPN is difficult to cure. Current first-line treatment for PDPN is nonspecific, and serious adverse effects limit their clinical use (Todorovic, 2015; Snyder et al., 2016). Hence, deeper knowledge in molecular and cellular mechanisms of PDPN is urgently needed to provide a basis for pharmaceutical development.

Single-cell RNA sequencing (scRNA-seq) has progressed at a rapid pace for its advantages in determining tissue heterogeneity and identifying novel cell types (Rodriguez-Meira et al., 2019). Previous transcriptomic studies characterized changes that could contribute to PDPN or DPN in DRG or sural nerves (Hur et al., 2011, 2016; Yamazaki et al., 2013; Guo et al., 2020). These sequenced RNA samples were from whole tissue that inevitably contained mixed cell types. Meanwhile, the "average" gene expression profiles could possibly lead to the confounding interpretation of the results. The difference is that scRNA-seq can sequence thousands of cells in an unbiased manner to uncover both known and novel cell types. We can simultaneously classify and analyze numerous DRG neuron types to know which one is most associated with PDPN. Furthermore, thousands of cell sequencing data would help to investigate whether and how the dynamic DRG neuron type changes in response to hyperglycemia. In the current study, we performed scRNA-seq on rat DRG from PDPN models induced by streptozotocin (STZ) injection (Morrow, 2004). Our work established an unbiased classification of rat DRG neuronal types and identified a novel neuron type MAAC. MAAC was marked by Na, K -ATPase (NKA)-related genes *Fxyd7,* and *Atp1b1*. Compared with other neurons, MAAC was characterized by highly expressing genes related to neurofilaments and cytoskeletons. We inferred that it was derived from peptidergic neurons based on correlation analysis and used pseudo-time analysis to identify the gene expression kinetics in neuron type transitions. Furthermore, we studied the transcriptional regulatory networks and communication networks of MAAC. Our results provide comprehensive landscape to uncover the alteration of genes, cell types, and intercellular communication. These results advance our understanding of neuropathic pain in diabetes and provide a basis for the development of pain therapy.

MATERIALS AND METHODS

Rat

All animal studies were approved by the Shanghai Jiao Tong University Animal Care and Use Committee and conducted in accordance with the animal policies of the Shanghai Jiao Tong University and the guidelines established by the National Health and Family Planning Commission of China. Sprague Dawley rats were obtained from Shanghai Lab Animal Research Center. Rats were housed in specific pathogen-free conditions with free access to water and rat chow.

Diabetes

To induce diabetes, male Sprague-Dawley rats (200–220 g) were injected intraperitoneally with 60 mg/kg STZ (Solarbio, China) dissolved in 1% citrate buffer (pH = 4.5). The control group received equal volumes of the vehicle. Three days after the injections, the glucose concentration was measured in tail vein blood samples using a blood glucose meter (Bayer HealthCare, USA). Only rats with the glucose concentration higher than 11.1 mmol/l were considered diabetic (Dominguez et al., 2015). All the animals were weekly weighed and daily observed during the study.

Mechanical Allodynia

Mechanical nociception was weekly evaluated using the von Frey filaments (North Coast, USA). Rats were separately placed in transparent plexiglass chambers on an elevated metal grid floor with 1 cm holes and probed from below. After a 15-min adaptation period, the hind paws were stimulated with varying forces (in this case 1.4, 2, 4, 6, 8, 10, 15, and 26 grams-force). Every stimulation delivered a constant pre-determined force for 5 s, and the interval of every stimulation was 15 s. The depression in the center of the rats' paws was accurately stimulated. Sensation in this area is within the innervation range of the tibial nerve, of which most fibers originate from L5 DRG in rats (Rigaud et al., 2008; Laedermann et al., 2014). The 50% paw withdrawal threshold (PWT) was determined by the up–down method of Chaplan et al. (1994). The experiment begins by testing the response to the 6 g filament. If a positive response occurred, the next filament with a lower force was applied. Conversely, if a negative response occurred, the next filament with a higher force was applied. This continues until at least four readings are obtained after different reactions appear for the first time. If the force to be used is higher than 15 g or lower than 1.4 g, the threshold on this side is directly recorded as 15 g or 1.4 g, respectively (Deuis et al., 2017). Finally, diabetic rats were divided into groups on day 28 after STZ injection. Diabetic rats with the PWT $\leq$ 8 g were considered to develop MA. Rats with the PWT $\geq$ 15 g were selected into the group without MA, and other diabetic rats were excluded from subsequent experiments.

Tissue Dissociation and Cell Purification

In total, 24 rats (eight in each group) were sacrificed 28 days after STZ injection. Among these animals, two control group rats, four diabetic rats with MA, and two diabetic rats without MA were used for scRNA-seq. DRGs, dissected from rats of the abovementioned groups, were washed with Hanks Balanced Salt Solution (HBSS; Sigma-Aldrich, USA) three times. Then, the tissue pieces were transferred into a 15 ml centrifuge tube and digested with 2 ml GEXSCOPE^{TM} Tissue Dissociation Solution (Singleron, China) at 37°C for 15 min under sustained agitation. After digestion, the samples were filtered using 40 μm sterile strainers and centrifuged at 1,000 rpm for 5 min. The supernatant was discarded and the sediment was resuspended in 1 ml phosphate-buffered saline (PBS; HyClone, USA). Two milliliters of GEXSCOPE^{TM} red blood cell lysis buffer (Singleron, China) was added to remove the red blood cells for 10 min at 25°C. The solution was then centrifuged at 500 × g for 5 min

and suspended in PBS. The sample was stained with trypan blue (Sigma-Aldrich, USA) and microscopically evaluated.

Library Construction and Sequencing

The scRNA-seq libraries were constructed following the protocol of GEXSCOPE^{TM} Single-Cell RNA Library Kit (Singleron, China) (Dura et al., 2019). Briefly, the single-cell suspensions were loaded onto microfluidic devices. Then, millions of beads with unique cell barcodes and unique molecular identifiers (UMIs) were loaded similar to cells. Only one bead was loaded in each microwell. Following lysis, mRNA was captured onto the beads. More than 95% of the beads were recovered, and the captured mRNA was reverse-transcribed. After cDNA amplification and enrichment, the resulting scRNA-seq libraries were sequenced on Illumina HiSeq X10 instrument with 150 bp paired end reads. Sequencing data of cell populations was conserved in the National Center for Biotechnology Information (NCBI) database with the Gene Expression Omnibus (GEO) accession number GSE176017.

Pre-Processing of scRNA-Seq Data

The raw reads were processed to generate gene expression profiles by an internal pipeline, namely, FastQC for quality evaluation, fastp for trimming, STAR aligner (2.5.3a) for alignment, and featureCounts (1.6.2) for transcript counting (Dobin et al., 2013; Liao et al., 2014; Chen et al., 2018; Wingett and Andrews, 2018). Briefly, after filtering read 1 without polyT tails, cell-barcode and UMI were extracted. Adapters and polyA tails were trimmed before read 2 was mapped to RGSC rn6 reference genome with ensemble version 92 gene annotation (http://www.ensembl.org). Reads with the same cell barcode, UMI, and gene were grouped to calculate the number of UMIs per gene per cell. UMI count tables of each cellular barcode were used for further analysis.

Data Integration and the Dimensionality Reduction

The data were processed by the Seurat (version 4. 0. 4) (Hao et al., 2021) in R software (version 4. 1. 1). According to quality control metrics (Ilicic et al., 2016), cells with genes >2,500 or <200 and the cells that have >10% mitochondrial genes were filtered out. A total of 6,693 cells that were obtained (2,543 in the control group, 1,192 in diabetic rats without MA, and 2,958 in diabetic rats with MA) were used for further bioinformatics analysis. Gene expression of each cell was normalized by total expression, multiplied by a scale factor of 10,000, and log-transformed (NormalizeData function). The 2,000 highly variable genes (HVGs) were selected (FindVariableGenes). Then, we integrated different samples (IntegrateData), and the technical or batch effect was eliminated by canonical correlation analysis (CCA). The expression of each gene that was scaled to shift its mean/variance across cells is 0 and 1 (ScaleData). These results were used as input for dimensionality reduction *via* principal component analysis (PCA).

Unsupervised Clustering and Cell Type Identification

The top 30 principal components were chosen for cell clustering. The clustering analysis was performed based on FindClusters function after building the nearest neighbor graph using FindNeighbors function. The main cell clusters were identified and visualized with t-distributed stochastic neighbor embedding (t-SNE) plots or uniform manifold approximation and projection (UMAP) plots. Due to differences in algorithms, the distance between two points in the two-dimensional plane of UMAP plots can represent the difference in gene expression information between two cells of the high-dimensional space better. To annotate the cell clusters, cluster biomarkers with high discrimination abilities were identified (FindMarkers function). The cell groups were annotated based on SingleR (Aran et al., 2019) and conventional markers described in previous studies (Fallon, 1985; Arroyo et al., 1998; Le et al., 2005; Dhaka et al., 2007; Schroeter and Steiner, 2009; Usoskin et al., 2015; Li et al., 2016; Oikari et al., 2016; Urban-Ciecko and Barth, 2016; Wu et al., 2017; Donovan et al., 2018; Hockley et al., 2019; Ronning et al., 2019; Zhang et al., 2019; Avraham et al., 2020; Gerber et al., 2021). Similar procedures were applied in the subclusters identification of neurons.

Enrichment Analysis

The gene ontology (GO) enrichment analysis was explored in Database for Annotation, Visualization, and Integrated Discovery (DAVID) (Ashburner et al., 2000).

Pseudo-Time Trajectory Analysis

To discover the gene expression kinetics in neuron type transition in PDPN development, the pseudo-time trajectories were generated with the Monocle package (version 2.18.0) (Trapnell et al., 2014). It can arrange cells along the pseudo-time trajectory, where each cell corresponds to a distinct time point, showing their developmental trajectories such as cell differentiation and other biological processes. The gene expression matrix derived from the Seurat processed data were used as the inputs. The differentially expressed genes (DEGs) were identified (q-value < 0.1) to sort cells in a pseudo-time order. Dimension reduction was performed using the DDRTree method. DEGs were clustered into different categories according to the gene expression patterns along the pseudo-time (Plot_pseudotime_heatmap function). Biological processes were revealed using GO enrichment analysis in DAVID.

Transcription Factor Inference

The analysis of the single-cell gene regulatory network was performed using the single-cell regulatory network inference and clustering (SCENIC) package (Aibar et al., 2017). Rat gene symbols were converted in the corresponding mouse homologous genes using the homologene R package (github.com/oganm/homologene; www.ncbi.nlm.nih.gov/homologene). After initializing settings, the expression matrix was loaded onto GENIE3 for building the initial co-expression gene regulatory networks (GRN). The regulon data were analyzed using the RcisTarget package and

the network activity was evaluated. The transcriptional network of TF and predicted target genes were visualized by Cytoscape (Shannon et al., 2003).

Cell Communications Analysis

Cell communications were analyzed based on CellChat (Jin et al., 2021). The ligand-receptor interaction database can be found at http://www.cellchat.org/. All the rat gene names were converted to the mouse ortholog using the homologene R package. The communication network was generated to discover the number of ligand and receptor (L-R) pairs and the signaling strength between each cell cluster. The strength was defined by the communication probability, which was calculated by a specific algorithm using the geometric mean of the normalized expression of receptors and ligands as input data. Outgoing and incoming interaction strength was calculated to compare the communication ability of each neuronal cluster as senders and receivers. The communication probabilities mediated by L-R pairs were compared and visualized in the bubble plot.

Statistical Analysis

All statistical analyses and the graph generation were performed in R (version 4. 1. 1).

Code Availability

The analysis codes are available on GitHub: https://github.com/SJTU-ZhouHan/SJTU-ZhouHan.

RESULT

Cellular Constitution of Rat DRG

In the present work, we intended to investigate the cell diversity of DRG neurons in the adult rat under PDPN conditions. A conspicuous MA typically becomes steady 4 weeks after diabetes induction in rats. We performed scRNA-seq on the cells dissociated from bilateral lumbar (L) 5 DRGs of diabetic rats with and without MA and normal control groups (**Figure 1A**; **Supplementary Figure 1**). After quality control, 6,693 cells, including 3,979 neurons, were obtained. Visualization of single-cell transcriptomes in t-SNE space was able to separate cells into clusters which we mapped to eight major cell types with distinct markers (**Figure 1B**). These cells included neurons, satellite glial cells (SGC), proliferating SGC (PSGC), Schwann cells, fibroblasts, vascular smooth muscle cells (VSMC), vascular endothelial cells (VEC), and microglia. SGC were identified due to highly expressed *Fabp7* (**Figure 1C**) (Goncalves et al., 2017). PSGC specifically expressed *Fabp7* and proliferation markers *Top2a* (**Figure 1C**) (Gerber et al., 2021). The cell population that highly expressed *Mpz* was annotated as Schwann cells (**Figure 1C**) (Le et al., 2005). Microglia highly expressed *Lyz2* (**Figure 1C**) (Donovan et al., 2018; Ronning et al., 2019). In addition, we identified VEC marked by *Cldn5* and VSMC by *Tpm2* (**Figure 1C**) (Jang et al., 2011; Kalluri et al., 2019).

Subclusters-Specific Analysis of Neurons

To detect discrete neuron subclusters, we reclassified neurons based on the canonical DRG neuron markers (Usoskin et al., 2015; Liguz-Lecznar et al., 2016; Kupari et al., 2021). Eleven neuron clusters and their DEGs were unbiasedly identified by Seurat program (**Figures 1D,E**). These clusters were annotated as non-peptidergic nociceptors (NP), peptidergic nociceptors (PEP), somatostatin-positive neurons (SOM), C-fiber low-threshold mechanoreceptors (C-LTMR), and *Trpm8*-positive neurons (TRPM8) (**Figure 2A**). We identified MA-associated clusters (MAAC) for the obviously increased cell number in diabetic rats with MA (**Figure 2A**). The specific neuron number for each cluster is given in **Supplementary Table 1**. Neuron clusters were matched with a previous scRNA-seq study of macaques DRG (**Figure 2B**) (Kupari et al., 2021). NP was named based on Purinergic receptor P2X3 (*P2rx3*), and PEP was named based on tropomyosin receptor kinase A (TRKA, *Ntrk1*). SOM was identified using somatostatin (*Sst*) and interleukin 31 receptor A (*Il31ra*). Although SOM contains markers for both peptidergic and nonpeptidergic neurons (*Tac1* and *P2rx3*), this cluster was named NP3 in previous literature (Usoskin et al., 2015). *Exoc1l*, *P2ry1,* and *Gfra2* were used to assign C-LTMR. *Trpm8* expression was used for naming the TRPM8 neuron cluster.

Emerging Novel Neuron Cluster Associated With MA

The t-SNE plot was split based on different groups to present the progression of the emerging novel neuron cluster MAAC (**Figure 2A**). Neurons in other clusters were evenly distributed in different groups (**Figure 2A**). Hundreds of DEGs of MAAC were identified (log2FC $>$ 0.25 and adj. p-value $<$ 0.05) (**Figure 2C**; **Supplementary Table 2**). Among these genes, *Fxyd7* and *Atp1b1* were highly expressed in MAAC. The paralog of *Fxyd7*, *Fxyd1,* and the paralog of *Atp1b1* and *Atp2b4* were also included (**Supplementary Table 2**). We next annotated the DEGs with biological processes [false discovery rate (FDR) $<$ 0.3] from GO databases to obtain transcriptomic characteristics of MAAC. These cell-type specific genes recapitulated neurofilament, axon, synapse, and receptor-related biological processes (**Figure 2D**; **Supplementary Table 3**). "Regulation of cell shape," "receptor internalization," and "neurofilament bundle assembly" were the most significant enrichment terms. "Neurofilament bundle assembly" was the most enriched biological process with the highest fold enrichment.

The Origin and Transition of MAAC

To explore the origin of MAAC, we calculated the transcriptomic correlations of different neuron clusters. The heatmap showed that the gene expression of MAAC was close to PEP (**Figure 3A**), and the distance between these two clusters on the UMAP plot also provides corroborative evidence (**Supplementary Figure 2**). Then, we reconstructed the pseudo-time trajectories and identify genes whose expression changed as the neurons underwent transition (**Figures 3B,C**). Genes in the neuronal switch process from PEP to MAAC were classified into four modules based on their expressing patterns (**Figure 3C**). GO enrichment analysis were used to analyze the biological processes of each gene module. Upregulated genes in Module 1 were associated with "cell morphogenesis," including *Tgfb2*, *Tenm4*, *Hgf*, and *Atp2b2*.

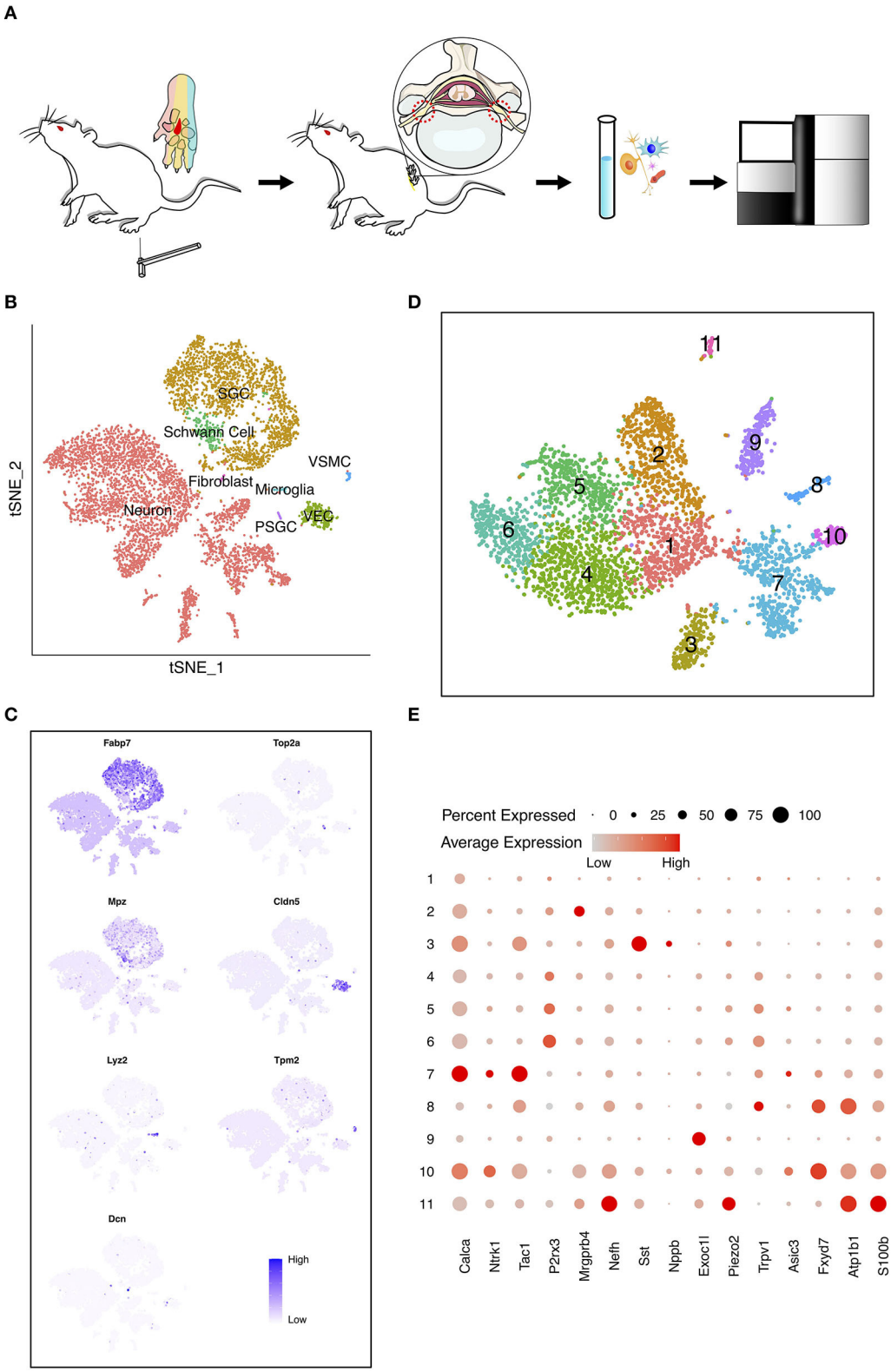

FIGURE 1 | The heterogeneity of dorsal root ganglia (DRG) cells in the painful diabetic peripheral neuropathy (PDPN) model. **(A)** Workflow of the pain threshold evaluation, sample preparation, sequencing, and bioinformatic analysis. The red region in the center of the rats' paws was stimulated by von Frey filaments. Sensation

(Continued)

FIGURE 1 | in this area is within the innervation range of the tibial nerve, originating from L5 DRG in rat. **(B)** t-distributed scholastic neighbor embedding (t-SNE) plot of single cells profiled in the presenting work colored by cell types. Each colored dot represents a cell. **(C)** Feature heatmap shows the marker genes in each cell type. The color represents the gene expression level after batch effect correction and normalization. **(D)** t-SNE plot shows the unsupervised clustering DRG neurons. Dots, individual cells; colors, neuron clusters. **(E)** Dot plot shows the differentially expressed genes (DEGs) of each DRG neuron cluster. The size of the dot means the percentage of cells expressing the gene, and the color indicates the average expression level.

Module 2 reflected the genes that were upregulated from a lower level across pseudo-time. These genes were enriched in "cell adhesion" and "regulation of neuron projection development." Comparatively, the expression of genes related to "inflammatory response" eventually decreased. Notably, some genes involved in "sensory perception of pain" were downregulated, including *Ndn*, *Trpv1*, *Asic1*, *Aqp1* (Module 3), *Adcyap1*, *Trpa1*, *Npy1r*, *Oprk1*, *Tac1* (Module 4).

Pivotal Regulons Involved in Neuron Type Transition

The SCENIC analysis was performed to identify the critical regulators and to reconstruct gene regulatory network. The binary regulon activity matrix was generated and two MAAC-specific regulons, *Hobx7* and *Lar1p,* were identified (**Figure 4A**). The binary t-SNE plot showed that these TFs were expressed and activated in MAAC (**Figure 4B**). Other TFs like *Fosb*, *Cebpd*, *Fosl1*, *Junb,* and *Ddit3* had broad expression patterns. They were mainly expressed and activated in PEP and MAAC. In addition, we constructed the gene regulatory network of *Hobx7* and *Lar1p* (**Figure 4C**). We observed that *Hobx7* regulated the most DEGs of MAAC, including genes with high expression level, like *Atp1b1* and *S100b*. However, *Larp1* only regulated the expression of *Gap43* and *Arid5b*. Thus, *Hobx7* could serve as a critical regulator in the formation of MAAC.

Intercellular Communication Analysis of MAAC

The intercellular communication was inferred based on the information of L-R pairs in CellChat database (Jin et al., 2021). The numbers of interactions between cell clusters were calculated (**Figures 5A,B**). There is a close link between MAAC and SGC, but not between other neuron clusters (**Figures 5A,B**). Then, we compared the outgoing and incoming interaction strength of each cell type (**Figure 5C**). The interaction strength of glia appeared to be greater than other cells, and the strength of MAAC was obviously greater than their PEP cluster origin. To identify the ligands or receptors involved, we respectively compared the communication probabilities mediated by L-R pairs between MAAC and other cells (**Figures 5D,E**). Only the L-R pairs with the most pronounced changes (p-value < 0.05) were displayed. When MAAC served as the signal source, communication probabilities of PTN ligand were prominent. MAAC may communicate with SGC and PSGC *via Ptn-Sdc4*, *Ptn-Ptprz1*, *Ptn-Ncl,* and *Bdnf-Ntrk2*. The communication between MAAC and VEC was mediated by *Calcb-Calcrl* and *Calca-Calcrl* in low communication probabilities. Besides, MAAC could communicate with microglia and VSMC by *Ptn-Ncl*. When MAAC served as the signal target, the *Ncl* receptor was playing an important role. The biologic behavior of MAAC may be regulated by *Ptn-Ncl* and *Mdk-Ncl*.

DISCUSSION

Dorsal root ganglia are vulnerable in diabetes due to lack of the protection of blood-nerve barrier. Injured somatosensory neurons could be an important trigger for pain. Here, using scRNA-seq, we generated a cell-type specific transcriptome atlas and revealed the complexity of the cellular landscape inside DRG tissues. Then, we identified a PDPN-related cluster MAAC and their origin. The transcriptomic characteristics of neuron type transition and pivotal regulons were demonstrated. Finally, we constructed the intercellular communication networks and revealed associated L-R pairs.

In the current study, we used STZ-induced diabetic rats to evoke MA. The extent of nerve damage exhibited individual differences among diabetic rodent models. In detail, in the same batch, the PWT of some rats dropped below 1.4 g, while some still stayed above 15 g on Day 28 after STZ injection. We compared L5 DRG cells from mechanically sensitive (diabetes with MA; PWT $\leq$ 8 g), insensitive rats (diabetes without MA; PWT $\geq$ 15 g), and normal rats.

Traditionally, DRG neuron classification was based on size and neuron-type genetic marker, but they were not always consistent with the functional heterogeneity of DRG neurons (Murray and Cheema, 2003). In contrast, comprehensive transcriptome analysis of scRNA-seq data can classify neurons in an unbiased manner. Usoskin et al. (2015) clustered mice L4-L6 DRG neurons into PEP, NP, and neurofilament-containing and tyrosine hydroxylase-containing clusters. Subsequently, these clusters were further classified into 11 subtypes including thermosensitive, itch sensitive, low-threshold mechanosensitive, and nociceptive neurons, etc. Compared with this study, we also identified cold thermoreceptors (TrpM8), C-LTMR, and SOM neurons which expressed the itch-related biomarker Il31ra. The SOM was named NP3 in the study of Usoskin et al. (2015). Because it expressed both peptidergic and non-peptidergic neuronal markers, and the distance in space is relatively independent in the t-SNE plot, we think it is more reasonable to label it as SOM. Kupari et al. (2021) classified macaques' primate DRG sensory neurons. The results of their neuron subtypes identification were broadly consistent Usoskin et al.'s (2015). A difference was that $Nefh^{+}$ neurons were not clustered into one subcluster as NF cluster in the latter, which was closer to our classification result.

In previous single-cell or single-nucleus sequencing studies of different models of pain, injury-related subpopulations of neurons have been reported (Nguyen et al., 2019; Renthal

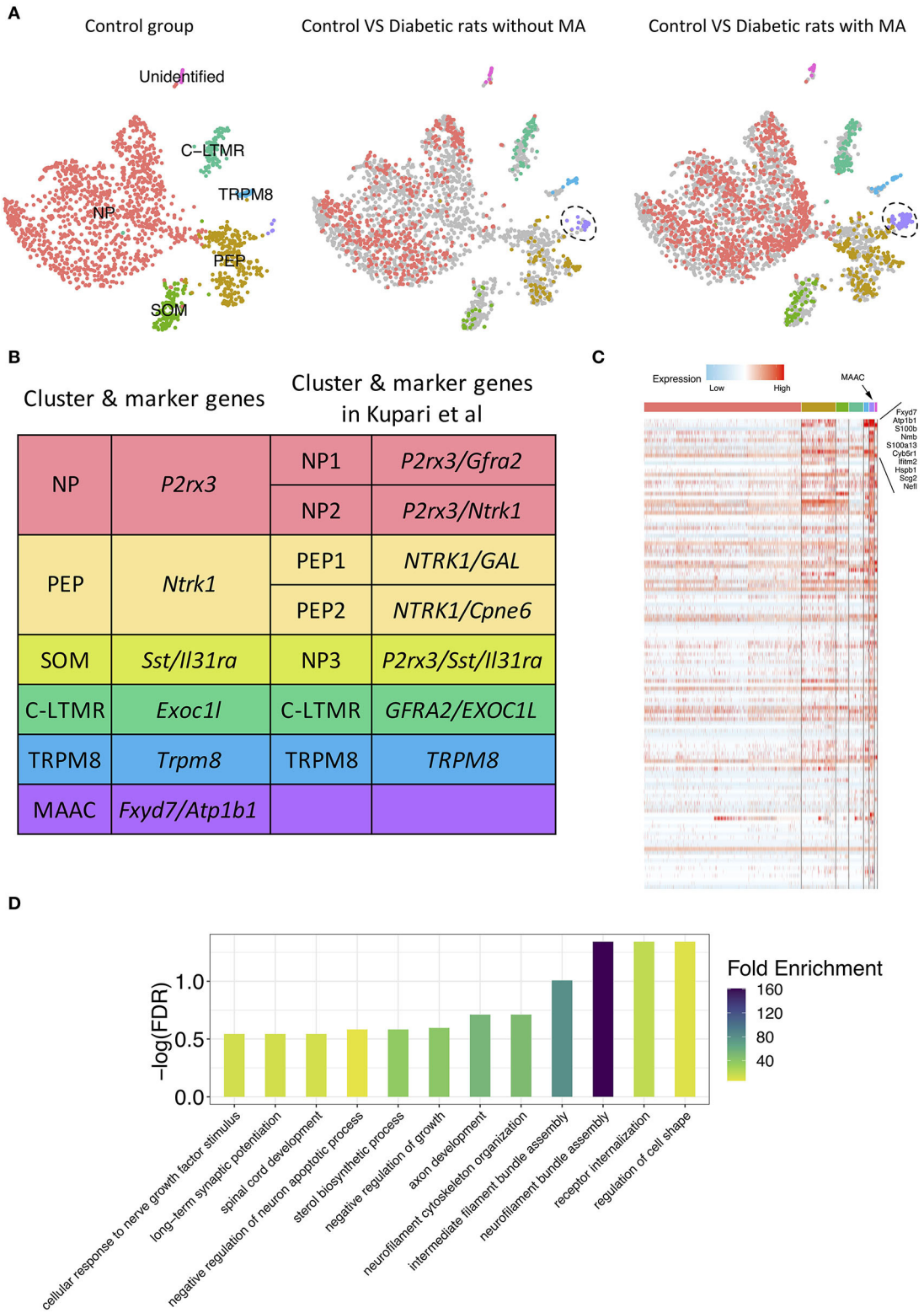

FIGURE 2 | Novel neuron cluster mechanical allodynia-associated cluster (MAAC) appeared in the development of PDPN. **(A)** t-SNE plot shows somatosensory neuron clusters in control versus in diabetic rats without or with mechanical allodynia (MA). The dots in the control group are grayed out when they are compared with the dots in the other two groups. Dots, individual cells; colors, neuron clusters. **(B)** Summary of neuron type classification in this work and previous study. **(C)** Heatmap shows the DEGs of MAAC. The genes with the largest fold difference are marked. Color, expression level. **(D)** Bar plot shows gene ontology (GO) terms of biological processes [false discovery rate (FDR) <0.3] enriched for the DEGs of MAAC.

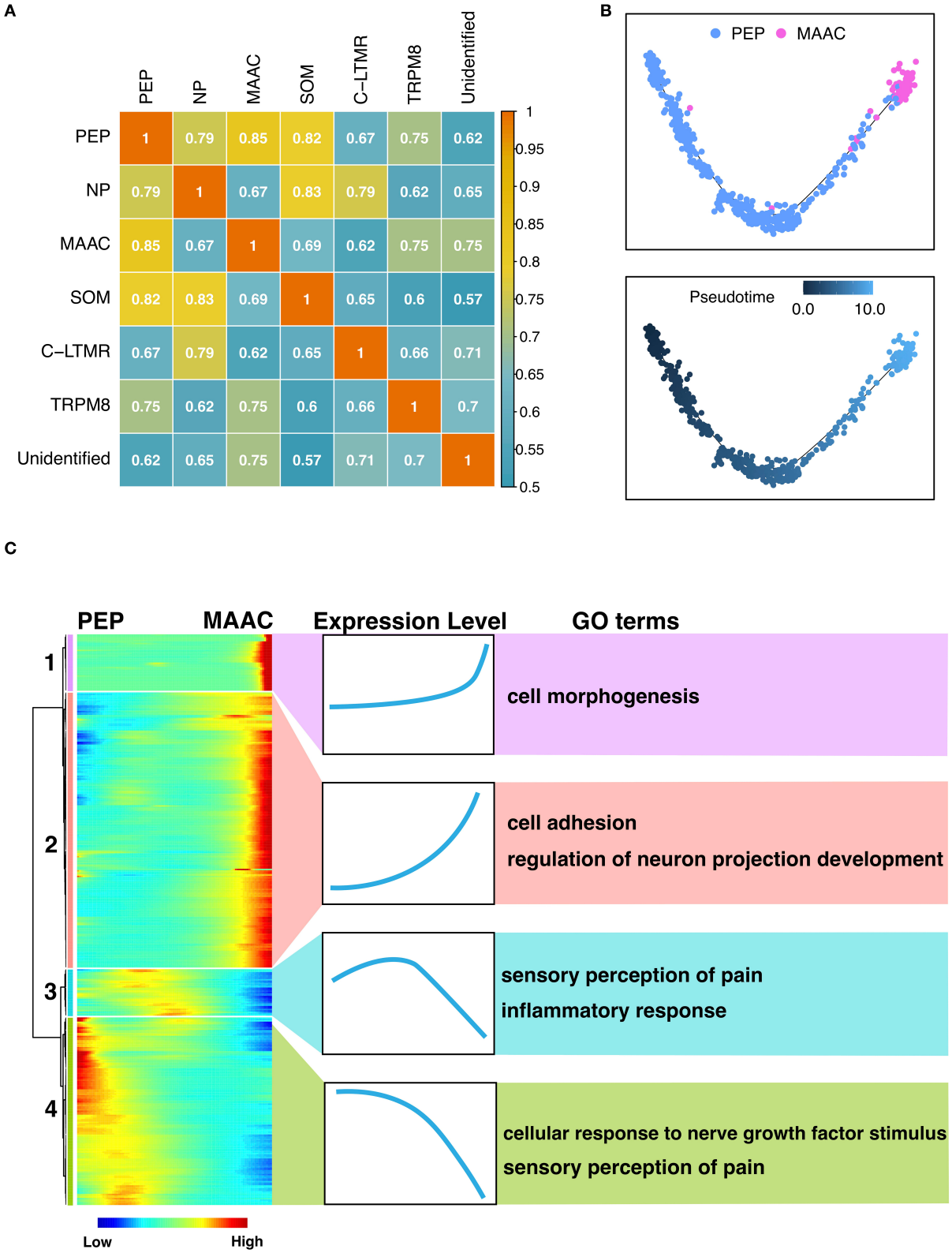

FIGURE 3 | The origin and transition of MAAC. **(A)** Heatmap shows the Pearson correlation of each neuron cluster based on their genes expression files. **(B)** Pseudo-time trajectories show the fate of MAAC originated from peptidergic nociceptors (PEP). Dot, cells; colors, neuron clusters or pseudotime. **(C)** Heatmaps show the DEGs clustered based on their dynamic expression characteristic, which were shown in pseudo-time from PEP to MAAC.

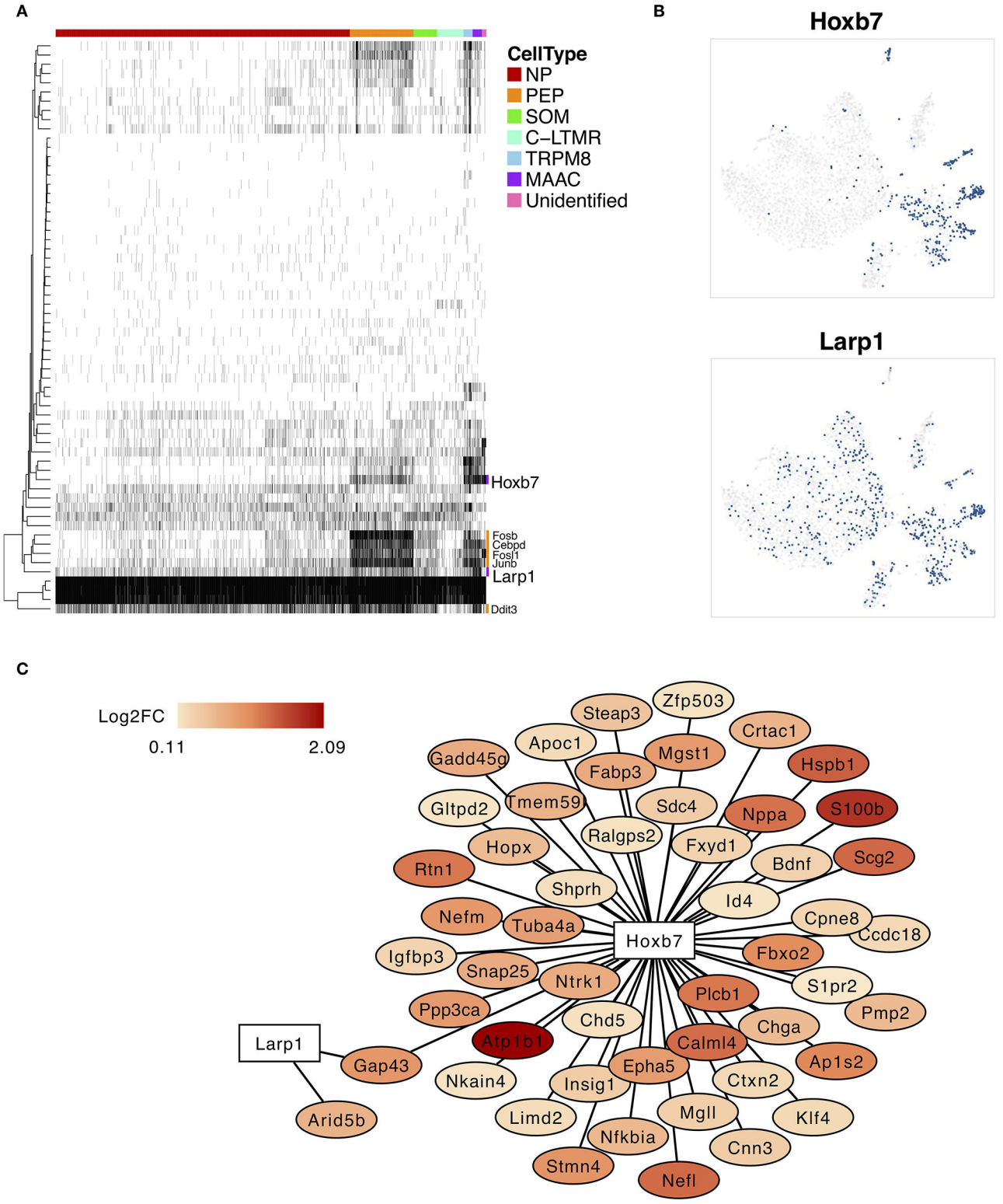

FIGURE 4 | Specifically expressed transcription factors and regulatory network of MAAC. **(A)** The binary heatmap shows the activity of inferred transcription factors in different neuron clusters. **(B)** t-SNE plots show the activities cells distribution of two specific expressed regulons of MAAC. Dots, individual cells; colors, activated cells. **(C)** Gene regulatory networks of *Hobx7* and *Larp1* inferred by single-cell regulatory network inference and clustering (SCENIC). Colors indicated the log2FC of DEGs of MAAC.

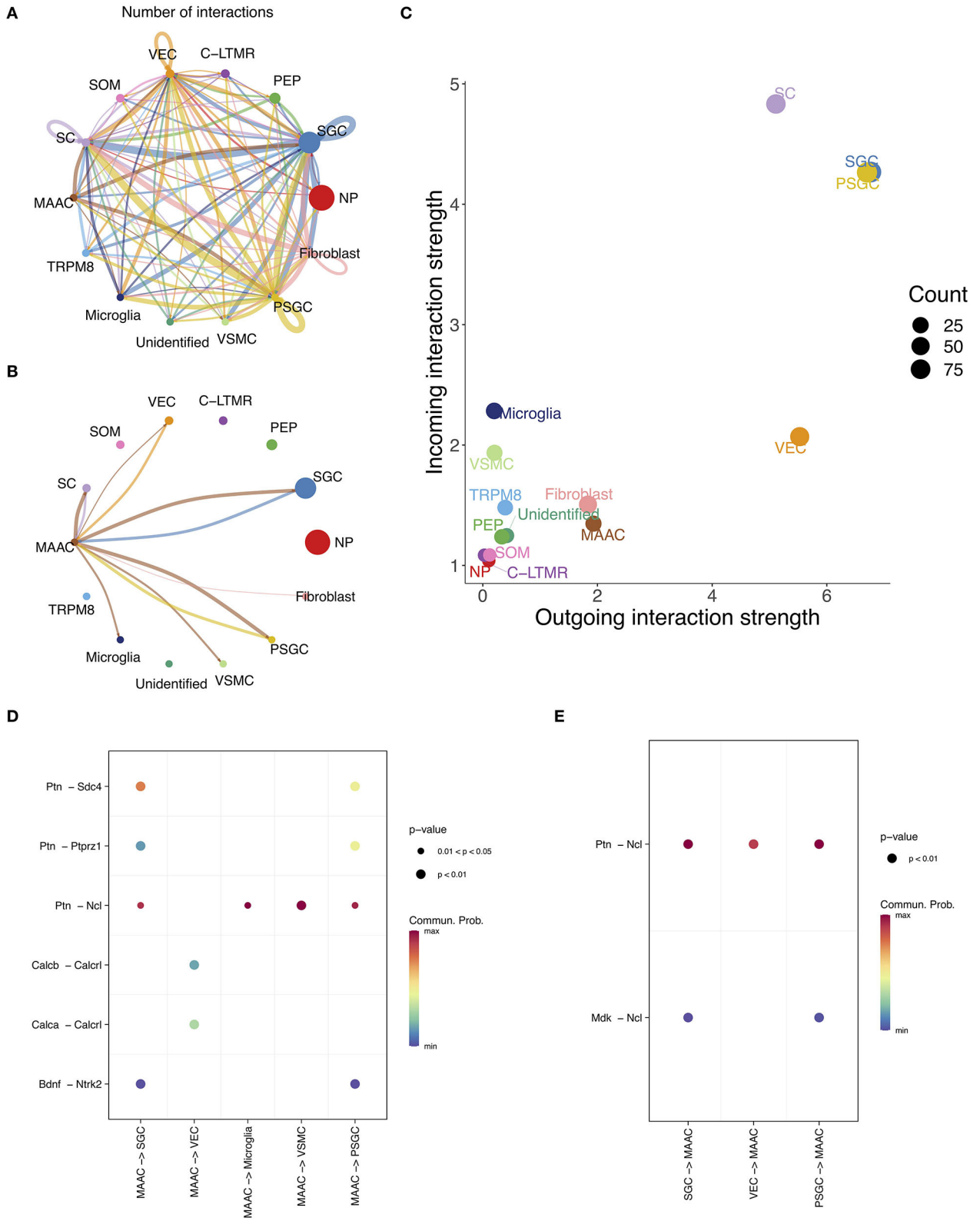

FIGURE 5 | The intercellular communication of MAAC. **(A)** Intercellular communication network reflects the number of interactions between clusters. Nodes, neuronal clusters; node size, cell counts; edge width, number of interactions. **(B)** Intercellular communication network shows the number of interactions between MAAC and

(Continued)

FIGURE 5 | other neuron clusters. Nodes, neuronal clusters; node size, cell counts; edge width, number of interactions. **(C)** Dot plot shows the incoming and outgoing strength of each cell type. The outgoing /incoming interaction strength is defined by the comprehensive communication probability between the signal sending /target cells and all cell types. **(D)** Dot plot shows the communication probabilities of ligand-receptor pairs when MAAC are sender cells. Only the ligand-receptor pairs with significant changes (p <0.05) are shown in the picture. Commun. Prob, communication probability. The communication probability here equals to the interaction strength and is not exactly a probability. Dot color means communication probabilities and dot size represents computed p-values. **(E)** Dot plot shows the communication probabilities of ligand-receptor pairs when MAAC serves as target cells.

et al., 2020; Wang et al., 2021). In the present study, we found that a new neuron type appeared in the development of PDPN, namely, MAAC (*Fxyd7*$^+$/*Atp1b1*$^+$), and identified the transcriptomic characteristics, origin, transition, and intercellular communication of them. Two DEGs with the highest fold change were considered as the biomarkers of MAAC. Interestingly, they are both closely associated with the NKA, and the dysfunction of NKA has been reported in patients with DPN (Vague et al., 1997; Krishnan et al., 2008). *Fxyd7* proven to be a regulator of NKA isozymes, which could significantly affect the apparent affinity for extracellular K^+ of NKA α1–β1 complexes (Béguin et al., 2002). The paralog of *Fxyd7* and *Fxyd2* could regulate neuronal activity by modulating NKA activity, which may be a fundamental mechanism underlying the persistent hypersensitivity to pain (Wang et al., 2015). *Atp1b1* encodes the protein of NKA family. Its paralog, *Atp1b3,* has been reported to be involved in the formalin pain behavior (LaCroix-Fralish et al., 2009).

The enrichment analysis investigated multiple processes of MAAC. Some processes with high significance were involved in neurofilament and cytoskeleton, including "regulation of cell shape," "neurofilament bundle assembly," and "neurofilament cytoskeleton organization." The mechanisms of how the cytoskeleton affects mechanical nociception are not fully understood, but it is known that through cytoskeleton force, it can be transmitted to cell membrane receptors, making them more responsive to pressure (Ingber, 2006). Bhattacherjee et al. (2017) reported that ganglion cytoskeletal genes were critical in determining mechanosensory properties in Rett syndrome. In addition, Dina et al. (2003) suggested that inflammatory mediator-induced MA was differentially dependent on the neuron cytoskeleton and that cytoskeletal disruptors could attenuate epinephrine-induced hyperalgesia in rat paws. Thus, activated cytoskeletal genes are another important feature of MAAC.

Our results suggested MAAC could originate from PEP by the alteration of gene expression profiles. The similar cellular transition was found in spared nerve injury (SNI) models. Wang et al. (2021) found three novel neuronal clusters induced by SNI. Most of them originate from the peptidergic neuron cluster. Then, through tracing the inferred trajectories, the dynamic characteristics were revealed. Notably, some enriched genes in sensory perception of pain were downregulated during MAAC formation. A similar phenomenon was also present after SNI injury (Wang et al., 2021). Further, based on the binary heatmap of regulon activity, we found the fate of MAAC could be determined by *Hobx7* and *Larp1*. *Hobx7* played a dominant role and was involved in the regulation of many DEGs of MAAC.

Next, the cellular communication activity of MAAC was inferred, and we found abundant communication relationships between MAAC and SGC and endothelial cells and microglia. Soma of neurons could not form synaptic contact with one another (Pannese, 1981), and each soma is tightly enwrapped by SGC. Therefore, the interactions of MAAC with other neurons were not found, and how hyperglycemia influences the signaling between SGC and neurons should be of particular concern. Both MAAC and SGC can send or receive signals to or from each other *via Ptn-Ncl*. SGC can also influence MAAC *via Mdk-Ncl*. *Ncl* encodes nucleolin, which is involved in the synthesis and maturation of ribosomes (Hirano et al., 2005). Previous studies have pointed out that nucleolin in neuronal cell bodies can restrict axon growth (Perry et al., 2016). Hence, we hypothesize that SGC may regulate abnormal axon growth through *Ptn-Ncl* and *Mdk-Ncl* in PDPN.

In summary, the present study reveals the single-cell transcriptomic alterations of somatosensory neurons in PDPN, identifies a novel neuron type MAAC, and investigates the novel neuron type's transcriptomic characteristics, origin, transition trajectory, regulons, and cellular communication. Thus, the study's findings advanced our current understanding of PDPN and neuropathic pain, which can be a resource for developing pain therapy. However, there were some limitations in the present study. For example, further basic experiments are needed to validate our results, and how the novel cluster MAAC induces pain symptom remains to be further clarified.

DATA AVAILABILITY STATEMENT

The datasets presented in this study can be found in online repositories. The names of the repository/repositories and accession number(s) can be found in the article/**Supplementary Material**.

ETHICS STATEMENT

The animal study was reviewed and approved by the Ethics Committee, Ninth People Hospital Affiliated to Shanghai Jiao Tong University School of Medicine.

AUTHOR CONTRIBUTIONS

HZ and XY built models, collected specimens, analyzed data, and wrote the manuscript. CL and HC analyzed data. YW, BX, and FM contributed to the discussion. WZ reviewed the manuscript. All authors contributed to the article and approved the submitted version.

FUNDING

This work was supported by the National Natural Science Foundation of China (Grant No. 81771320).

ACKNOWLEDGMENTS

We sincerely thank Dr. Jie Yu (Ninth People Hospital, Shanghai Jiao Tong University School of Medicine) for helpful discussion and Dr. Peng Jin (Ruijin Hospital, Shanghai Jiao Tong University School of Medicine) for his bioinformatics advice.

SUPPLEMENTARY MATERIAL

The Supplementary Material for this article can be found online at: https://www.frontiersin.org/articles/10.3389/fnmol.2022.856299/full#supplementary-material

REFERENCES

Aibar, S., González-Blas, C. B., Moerman, T., Huynh-Thu, V. A., Imrichova, H., Hulselmans, G., et al. (2017). SCENIC: single-cell regulatory network inference and clustering. *Nat Methods*. 14, 1083–1086. doi: 10.1038/nmeth.4463

Aran, D., Looney, A. P., Liu, L., Wu, E., Fong, V., Hsu, A., et al. (2019). Reference-based analysis of lung single-cell sequencing reveals a transitional profibrotic macrophage. *Nat Immunol*. 20, 163–172. doi: 10.1038/s41590-018-0276-y

Arroyo, E. J., Bermingham, J. R. Jr., Rosenfeld, M. G., and Scherer, S. S. (1998). Promyelinating Schwann cells express Tst-1/SCIP/Oct-6. *J Neurosci*. 18, 7891–7902. doi: 10.1523/jneurosci.18-19-07891.1998

Ashburner, M. M., Ball, C. A. C., Blake, J. A. J., Botstein, D. D., Butler, H. H., Cherry, J. M. J., et al. (2000). Gene ontology: tool for the unification of biology Consortium TGO. *Nat Genet.* 25, 25–29. doi: 10.1038/75556

Avraham, O., Deng, P. Y., Jones, S., Kuruvilla, R., Semenkovich, C. F., Klyachko, V. A., et al. (2020). Satellite glial cells promote regenerative growth in sensory neurons. *Nat Commun*. 11, 4891. doi: 10.1038/s41467-020-18642-y

Béguin, P., Crambert, G., Monnet-Tschudi, F., Uldry, M., Horisberger, J. D., Garty, H., et al. (2002). FXYD7 is a brain-specific regulator of Na,K-ATPase alpha 1-beta isozymes. *Embo j*. 21, 3264–3273. doi: 10.1093/emboj/cdf330

Berti-Mattera, L. N., Kern, T. S., Siegel, R. E., Nemet, I., and Mitchell, R. (2008). Sulfasalazine blocks the development of tactile allodynia in diabetic rats. *Diabetes*. 57, 2801–2808. doi: 10.2337/db07-1274

Best, T. J., Best, C. A., Best, A. A., and Fera, L. A. (2019). Surgical peripheral nerve decompression for the treatment of painful diabetic neuropathy of the foot—A level 1 pragmatic randomized controlled trial. *Diabetes Res Clin Pract*. 147, 149–156. doi: 10.1016/j.diabres.2018.08.002

Bhattacherjee, A., Mu, Y., Winter, M. K., Knapp, J. R., Eggimann, L. S., Gunewardena, S. S., et al. (2017). Neuronal cytoskeletal gene dysregulation and mechanical hypersensitivity in a rat model of Rett syndrome. *Proc Natl Acad Sci USA*. 114, E6952–e6961. doi: 10.1073/pnas.1618210114

Chaplan, S. R., Bach, F. W., Pogrel, J. W., Chung, J. M., and Yaksh, T. L. (1994). Quantitative assessment of tactile allodynia in the rat paw. *J Neurosci Methods*. 53, 55–63. doi: 10.1016/0165-0270(94)90144-9

Chen, S., Zhou, Y., Chen, Y., and Gu, J. (2018). fastp: an ultra-fast all-in-one FASTQ preprocessor. *Bioinformatics*. 34, i884–i890. doi: 10.1093/bioinformatics/bty560

Deuis, J. R., Dvorakova, L. S., and Vetter, I. (2017). Methods used to evaluate pain behaviors in rodents. *Front Mol Neurosci*. 10, 284. doi: 10.3389/fnmol.2017.00284

Dhaka, A., Murray, A. N., Mathur, J., Earley, T. J., Petrus, M. J., and Patapoutian, A. (2007). TRPM8 is required for cold sensation in mice. *Neuron*. 54, 371–378. doi: 10.1016/j.neuron.2007.02.024

Dina, O. A., McCarter, G. C., de Coupade, C., and Levine, J. D. (2003). Role of the sensory neuron cytoskeleton in second messenger signaling for inflammatory pain. *Neuron*. 39, 613–624. doi: 10.1016/s0896-6273(03)00473-2

Dobin, A., Davis, C. A., Schlesinger, F., Drenkow, J., Zaleski, C., Jha, S., et al. (2013). STAR: ultrafast universal RNA-seq aligner. *Bioinformatics*. 29, 15–21. doi: 10.1093/bioinformatics/bts635

Dominguez 2nd J. M., Yorek, M. A., and Grant, M. B. (2015). Combination therapies prevent the neuropathic, proinflammatory characteristics of bone marrow in streptozotocin-induced diabetic rats. *Diabetes*. 64, 643–653. doi: 10.2337/db14-0433

Donovan, K. M., Leidinger, M. R., McQuillen, L. P., Goeken, J. A., Hogan, C. M., Harwani, S. C., et al. (2018). Allograft inflammatory factor 1 as an immunohistochemical marker for macrophages in multiple tissues and laboratory animal species. *Comp Med*. 68, 341–348. doi: 10.30802/aalas-cm-18-000017

Dura, B., Choi, J. Y., Zhang, K., Damsky, W., Thakral, D., Bosenberg, M., et al. (2019). scFTD-seq: freeze-thaw lysis based, portable approach toward highly distributed single-cell 3' mRNA profiling. *Nucleic Acids Res*. 47, e16. doi: 10.1093/nar/gky1173

Fallon, J. R. (1985). Neurite guidance by non-neuronal cells in culture: preferential outgrowth of peripheral neurites on glial as compared to nonglial cell surfaces. *J Neurosci*. 5, 3169–3177. doi: 10.1523/jneurosci.05-12-03169.1985

Feldman, E. L., Nave, K. A., Jensen, T. S., and Bennett, D. L. H. (2017). New horizons in diabetic neuropathy: mechanisms, bioenergetics, and pain. *Neuron*. 93, 1296–1313. doi: 10.1016/j.neuron.2017.02.005

Gerber, D., Pereira, J. A., Gerber, J., Tan, G., Dimitrieva, S., Yángüez, E., et al. (2021). Transcriptional profiling of mouse peripheral nerves to the single-cell level to build a sciatic nerve ATlas (SNAT). *Elife*.10doi: 10.7554/eLife.58591

Goncalves, N. P., Vaegter, C. B., Andersen, H., Ostergaard, L., Calcutt, N. A., and Jensen, T. S. (2017). Schwann cell interactions with axons and microvessels in diabetic neuropathy. *Nat Rev Neurol*. 13, 135–147. doi: 10.1038/nrneurol.2016.201

Guo, K., Eid, S. A., Elzinga, S. E., Pacut, C., Feldman, E. L., and Hur, J. (2020). Genome-wide profiling of DNA methylation and gene expression identifies candidate genes for human diabetic neuropathy. *Clin Epigenetics*. 12, 123. doi: 10.1186/s13148-020-00913-6

Hao, Y., Hao, S., Andersen-Nissen, E., Mauck, W. M. 3rd, Zheng, S., Butler, A., Lee, M. J., et al. (2021). Integrated analysis of multimodal single-cell data. *Cell*. 184, 3573-3587.e3529. doi: 10.1016/j.cell.2021.04.048

Hirano, K., Miki, Y., Hirai, Y., Sato, R., Itoh, T., Hayashi, A., et al. (2005). A multifunctional shuttling protein nucleolin is a macrophage receptor for apoptotic cells. *J Biol Chem*. 280, 39284–39293. doi: 10.1074/jbc.M505275200

Hockley, J. R. F., Taylor, T. S., Callejo, G., Wilbrey, A. L., Gutteridge, A., Bach, K., et al. (2019). Single-cell RNAseq reveals seven classes of colonic sensory neuron. *Gut*. 68, 633–644. doi: 10.1136/gutjnl-2017-315631

Hur, J., O'Brien, P. D., Nair, V., Hinder, L. M., McGregor, B. A., Jagadish, H. V., et al. (2016). Transcriptional networks of murine diabetic peripheral neuropathy and nephropathy: common and distinct gene expression patterns. *Diabetologia*. 59, 1297–1306. doi: 10.1007/s00125-016-3913-8

Hur, J., Sullivan, K. A., Pande, M., Hong, Y., Sima, A. A., Jagadish, H. V., et al. (2011). The identification of gene expression profiles associated with progression of human diabetic neuropathy. *Brain*. 134, 3222–3235. doi: 10.1093/brain/awr228

Ilicic, T., Kim, J. K., Kolodziejczyk, A. A., Bagger, F. O., McCarthy, D. J., Marioni, J. C., et al. (2016). Classification of low quality cells from single-cell RNA-seq data. *Genome Biol*. 17, 29. doi: 10.1186/s13059-016-0888-1

Ingber, D. E. (2006). Cellular mechanotransduction: putting all the pieces together again. *Faseb j*. 20, 811–827. doi: 10.1096/fj.05-5424rev

Jang, A. S., Concel, V. J., Bein, K., Brant, K. A., Liu, S., Pope-Varsalona, H., et al. (2011). Endothelial dysfunction and claudin 5 regulation during acrolein-induced lung injury. *Am J Respir Cell Mol Biol*. 44, 483–490. doi: 10.1165/rcmb.2009-0391OC

Jin, S., Guerrero-Juarez, C. F., Zhang, L., Chang, I., Ramos, R., Kuan, C. H., et al. (2021). Inference and analysis of cell-cell communication using CellChat. *Nat Commun*. 12, 1088. doi: 10.1038/s41467-021-21246-9

Kalluri, A. S., Vellarikkal, S. K., Edelman, E. R., Nguyen, L., Subramanian, A., Ellinor, P. T., et al. (2019). Single-cell analysis of the normal mouse aorta reveals functionally distinct endothelial cell populations. *Circulation*. 140, 147–163. doi: 10.1161/circulationaha.118.038362

Krishnan, A. V., Lin, C. S., and Kiernan, M. C. (2008). Activity-dependent excitability changes suggest Na+/K+ pump dysfunction in diabetic neuropathy. *Brain*. 131, 1209–1216. doi: 10.1093/brain/awn052

Kupari, J., Usoskin, D., Parisien, M., Lou, D., Hu, Y., Fatt, M., et al. (2021). Single cell transcriptomics of primate sensory neurons identifies cell types associated with chronic pain. *Nat Commun*. 12, 1510. doi: 10.1038/s41467-021-21725-z

LaCroix-Fralish, M. L., Mo, G., Smith, S. B., Sotocinal, S. G., Ritchie, J., Austin, J. S., et al. (2009). The beta3 subunit of the Na+,K+-ATPase mediates variable nociceptive sensitivity in the formalin test. *Pain*. 144, 294–302. doi: 10.1016/j.pain.2009.04.028

Laedermann, C. J., Pertin, M., Suter, M. R., and Decosterd, I. (2014). Voltage-gated sodium channel expression in mouse DRG after SNI leads to re-evaluation of projections of injured fibers. *Mol Pain*. 10, 19. doi: 10.1186/1744-8069-10-19

Le, N., Nagarajan, R., Wang, J. Y., Araki, T., Schmidt, R. E., and Milbrandt, J. (2005). Analysis of congenital hypomyelinating Egr2Lo/Lo nerves identifies Sox2 as an inhibitor of Schwann cell differentiation and myelination. *Proc Natl Acad Sci USA*. 102, 2596–2601. doi: 10.1073/pnas.0407836102

Li, C. L., Li, K. C., Wu, D., Chen, Y., Luo, H., Zhao, J. R., et al. (2016). Somatosensory neuron types identified by high-coverage single-cell RNA-sequencing and functional heterogeneity. *Cell Res*. 26, 83–102. doi: 10.1038/cr.2015.149

Liao, Y., Smyth, G. K., and Shi, W. (2014). featureCounts: an efficient general purpose program for assigning sequence reads to genomic features. *Bioinformatics*. 30, 923–930. doi: 10.1093/bioinformatics/btt656

Liguz-Lecznar, M., Urban-Ciecko, J., and Kossut, M. (2016). Somatostatin and somatostatin-containing neurons in shaping neuronal activity and plasticity. *Front Neural Circuits*. 10, 48. doi: 10.3389/fncir.2016.00048

Maatuf, Y., Geron, M., and Priel, A. (2019). The role of toxins in the pursuit for novel analgesics. *Toxins (Basel) 0.11*. doi: 10.3390/toxins11020131

Marshall, A. G., Lee-Kubli, C., Azmi, S., Zhang, M., Ferdousi, M., Mixcoatl-Zecuatl, T., et al. (2017). Spinal disinhibition in experimental and clinical painful diabetic neuropathy. *Diabetes*. 66, 1380–1390. doi: 10.2337/db16-1181

Morrow, T. J. (2004). Animal models of painful diabetic neuropathy: the STZ rat model. *Curr. Protoc. Neurosci*. Chapter 9, Unit 9.18. doi: 10.1002/0471142301.ns0918s29

Murray, S. S., and Cheema, S. S. (2003). Constitutive expression of the low-affinity neurotrophin receptor and changes during axotomy-induced death of sensory neurones in the neonatal rat dorsal root ganglion. *J Anat*. 202, 227–238. doi: 10.1046/j.1469-7580.2003.00151.x

Nguyen, M. Q., Le Pichon, C. E., and Ryba, N. (2019). Stereotyped transcriptomic transformation of somatosensory neurons in response to injury. *Elife*. 8:e49679. doi: 10.7554/eLife.49679

Oikari, L. E., Okolicsanyi, R. K., Qin, A., Yu, C., Griffiths, L. R., and Haupt, L. M. (2016). Cell surface heparan sulfate proteoglycans as novel markers of human neural stem cell fate determination. *Stem Cell Res*. 16, 92–104. doi: 10.1016/j.scr.2015.12.011

Pannese E. (1981). The satellite cells of the sensory ganglia. *Adv. Anat. Embryol. Cell. Biol*. 65, 1–111. doi: 10.1007/978-3-642-67750-2

Perry, R. B., Rishal, I., Doron-Mandel, E., Kalinski, A. L., Medzihradszky, K. F., Terenzio, M., et al. (2016). Nucleolin-mediated RNA localization regulates neuron growth and cycling cell size. *Cell Rep*. 16, 1664–1676. doi: 10.1016/j.celrep.2016.07.005

Quattrini, C., and Tesfaye, S. (2003). Understanding the impact of painful diabetic neuropathy. *Diabetes Metab Res Rev*. 19, S2–8. doi: 10.1002/dmrr.360

Renthal, W., Tochitsky, I., Yang, L., Cheng, Y. C., Li, E., Kawaguchi, R., et al. (2020). Transcriptional reprogramming of distinct peripheral sensory neuron subtypes after axonal injury. *Neuron*. 108, 128-144.e129. doi: 10.1016/j.neuron.2020.07.026

Rigaud, M., Gemes, G., Barabas, M. E., Chernoff, D. I., Abram, S. E., Stucky, C. L., et al. (2008). Species and strain differences in rodent sciatic nerve anatomy: implications for studies of neuropathic pain. *Pain*. 136, 188–201. doi: 10.1016/j.pain.2008.01.016

Rodriguez-Meira, A., Buck, G., Clark, S. A., Povinelli, B. J., Alcolea, V., Louka, E., et al. (2019). Unravelling intratumoral heterogeneity through high-sensitivity single-cell mutational analysis and parallel RNA sequencing. *Mol Cell*. 73, 1292–1305.e1298. doi: 10.1016/j.molcel.2019.01.009

Ronning, K. E., Karlen, S. J., Miller, E. B., and Burns, M. E. (2019). Molecular profiling of resident and infiltrating mononuclear phagocytes during rapid adult retinal degeneration using single-cell RNA sequencing. *Sci Rep*. 9, 4858. doi: 10.1038/s41598-019-41141-0

Schroeter, M. L., and Steiner, J. (2009). Elevated serum levels of the glial marker protein S100B are not specific for schizophrenia or mood disorders. *Mol Psychiatry*. 14, 235–237. doi: 10.1038/mp.2008.85

Selvarajah, D., Wilkinson, I. D., Maxwell, M., Davies, J., Sankar, A., Boland, E., et al. (2014). Magnetic resonance neuroimaging study of brain structural differences in diabetic peripheral neuropathy. *Diabetes Care*. 37, 1681–1688. doi: 10.2337/dc13-2610

Shannon, P., Markiel, A., Ozier, O., Baliga, N. S., Wang, J. T., Ramage, D., et al. (2003). Cytoscape: a software environment for integrated models of biomolecular interaction networks. *Genome Res*. 13, 2498–2504. doi: 10.1101/gr.1239303

Sloan, G., Shillo, P., Selvarajah, D., Wu, J., Wilkinson, I. D., Tracey, I., et al. (2018). A new look at painful diabetic neuropathy. *Diabetes Res Clin Pract*. 144, 177–191. doi: 10.1016/j.diabres.2018.08.020

Snyder, M. J., Gibbs, L. M., and Lindsay, T. J. (2016). Treating painful diabetic peripheral neuropathy: an update. *Am Fam Physician*. 94, 227–234.

Todorovic, S. M. (2015). Is Diabetic Nerve Pain Caused by Dysregulated Ion Channels in Sensory Neurons? *Diabetes*. 64, 3987–3989. doi: 10.2337/dbi15-0006

Trapnell, C., Cacchiarelli, D., Grimsby, J., Pokharel, P., Li, S., Morse, M., et al. (2014). The dynamics and regulators of cell fate decisions are revealed by pseudotemporal ordering of single cells. *Nat Biotechnol*. 32, 381–386. doi: 10.1038/nbt.2859

Urban-Ciecko, J., and Barth, A. L. (2016). Somatostatin-expressing neurons in cortical networks. *Nat Rev Neurosci*. 17, 401–409. doi: 10.1038/nrn.2016.53

Usoskin, D., Furlan, A., Islam, S., Abdo, H., Lönnerberg, P., Lou, D., et al. (2015). Unbiased classification of sensory neuron types by large-scale single-cell RNA sequencing. *Nat Neurosci*. 18, 145–153. doi: 10.1038/nn.3881

Vague, P., Dufayet, D., Coste, T., Moriscot, C., Jannot, M. F., and Raccah, D. (1997). Association of diabetic neuropathy with Na/K ATPase gene polymorphism. *Diabetologia*. 40, 506–511. doi: 10.1007/s001250050708

Wang, F., Cai, B., Li, K. C., Hu, X. Y., Lu, Y. J., Wang, Q., et al. (2015). FXYD2, a γ subunit of Na^+, K^+-ATPase, maintains persistent mechanical allodynia induced by inflammation. *Cell Res*. 25, 318–334. doi: 10.1038/cr.2015.12

Wang, K., Wang, S., Chen, Y., Wu, D., Hu, X., Lu, Y., et al. (2021). Single-cell transcriptomic analysis of somatosensory neurons uncovers temporal development of neuropathic pain. *Cell Res*. 31, 904–918. doi: 10.1038/s41422-021-00479-9

Wingett, S. W., and Andrews, S. (2018). FastQ Screen: A tool for multi-genome mapping and quality control. *F1000Res*. 7, 1338. doi: 10.12688/f1000research.15931.2

Wu, Y. E., Pan, L., Zuo, Y., Li, X., and Hong, W. (2017). Detecting Activated Cell Populations Using Single-Cell RNA-Seq. *Neuron*. 96, 313-329.e316. doi: 10.1016/j.neuron.2017.09.026

Yamazaki, S., Yamaji, T., Murai, N., Yamamoto, H., Matsuda, T., Price, R. D., et al. (2013). FK1706, a novel non-immunosuppressive immunophilin ligand, modifies gene expression in the dorsal root ganglia during painful diabetic neuropathy. *Neurol Res*. 34, 469-477. doi: 10.1179/1743132812Y.0000000029

Zhang, M., Wang, Y., Geng, J., Zhou, S., and Xiao, B. (2019). Mechanically Activated Piezo Channels Mediate Touch and Suppress Acute Mechanical Pain Response in Mice. *Cell Rep*. 26, 1419–1431.e1414. doi: 10.1016/j.celrep.2019.01.056

Conflict of Interest: The authors declare that the research was conducted in the absence of any commercial or financial relationships that could be construed as a potential conflict of interest.

Publisher's Note: All claims expressed in this article are solely those of the authors and do not necessarily represent those of their affiliated organizations, or those of the publisher, the editors and the reviewers. Any product that may be evaluated in this article, or claim that may be made by its manufacturer, is not guaranteed or endorsed by the publisher.

frontiers | Frontiers in Molecular Neuroscience

METHODS
published: 01 June 2022
doi: 10.3389/fnmol.2022.859988

Study Protocol of tDCS Based Pain Modulation in Head and Neck Cancer Patients Under Chemoradiation Therapy Condition: An fNIRS-EEG Study

Brenda de Souza Moura[1,2†‡], *Xiao-Su Hu*[1†‡], *Marcos F. DosSantos*[2*†] and *Alexandre F. DaSilva*[1*†]

[1] Headache & Orofacial Pain Effort (H.O.P.E.), Department of Biologic and Materials Sciences, School of Dentistry, University of Michigan, Ann Arbor, MI, United States, [2] Laboratório de Propriedades Mecânicas e Biologia Celular (PropBio), Departamento de Prótese e Materiais Dentários, Faculdade de Odontologia, Universidade Federal do Rio de Janeiro (UFRJ), Rio de Janeiro, Brazil

Background: Multiple therapeutic strategies have been adopted to reduce pain, odynophagia, and oral mucositis in head and neck cancer patients. Among them, transcranial direct current stimulation (tDCS) represents a unique analgesic modality. However, the details of tDCS mechanisms in pain treatment are still unclear.

Aims: (1) to study the analgesic effects of a protocol that encompassed supervised-remote and in-clinic tDCS sessions applied in head and neck patients undergoing chemoradiation therapy; (2) to explore the underlining brain mechanisms of such modulation process, using a novel protocol that combined functional near-infrared spectroscopy (fNIRS), and electroencephalograph (EEG), two distinct neuroimaging methods that bring information regarding changes in the hemodynamic as well as in the electrical activity of the brain, respectively.

Methods: This proof-of-concept study was performed on two subjects. The study protocol included a 7-week-long tDCS stimulation procedure, a pre-tDCS baseline session, and two post-tDCS follow-up sessions. Two types of tDCS devices were used. One was used in the clinical setting and the other remotely. Brain imaging was obtained in weeks 1, 2, 5, 7, 8, and after 1 month.

Results: The protocol implemented was safe and reliable. Preliminary results of the fNIRS analysis in weeks 2 and 7 showed a decrease in functional connections between the bilateral prefrontal cortex (PFC) and the primary sensory cortex (S1) ($p < 0.05$, FDR corrected). Changes in EEG power spectra were found in the PFC when comparing the seventh with the first week of tDCS.

Conclusion: The protocol combining remote and in-clinic administered tDCS and integrated fNIRS and EEG to evaluate the brain activity is feasible. The preliminary results suggest that the mechanisms of tDCS in reducing the pain of head and neck cancer patients may be related to its effects on the connections between the S1 and the PFC.

Keywords: head and neck cancer, chemoradiotherapy, transcranial direct current stimulation, functional near-infrared spectroscopy, electroencephalograph

OPEN ACCESS

Edited by:
Wen Wu,
Southern Medical University, China

Reviewed by:
Antonio Chiarelli,
University of Studies G. d'Annunzio Chieti and Pescara, Italy
Fares Al-Shargie,
American University of Sharjah, United Arab Emirates
Rihui Li,
Stanford University, United States

***Correspondence:**
Alexandre F. DaSilva
adasilva@umich.edu
Marcos F. DosSantos
santosmfh@gmail.com;
marcos.fabio@odonto.ufrj.br

†ORCID:
Brenda de Souza Moura
orcid.org/0000-0003-1550-7907
Xiao-Su Hu
orcid.org/0000-0003-1401-000X
Marcos F. DosSantos
orcid.org/0000-0002-5997-9693
Alexandre F. DaSilva
orcid.org/0000-0003-3138-7781

‡These authors share first authorship

Specialty section:
This article was submitted to Pain Mechanisms and Modulators, a section of the journal Frontiers in Molecular Neuroscience

Received: *22 January 2022*
Accepted: *27 April 2022*
Published: *01 June 2022*

Citation:
de Souza Moura B, Hu X-S, DosSantos MF and DaSilva AF (2022) Study Protocol of tDCS Based Pain Modulation in Head and Neck Cancer Patients Under Chemoradiation Therapy Condition: An fNIRS-EEG Study. Front. Mol. Neurosci. 15:859988. doi: 10.3389/fnmol.2022.859988

INTRODUCTION

Head and neck cancer affects annually more than 50.000 in the USA (Siegel et al., 2012). Pain is an important symptom reported by head and neck cancer patients. Therefore, the pathophysiology of cancer-related pain and the mechanisms of novel therapies used to ameliorate cancer pain must be explored in deep. It has been widely recognized that patients with locally advanced head and neck cancer undergoing definitive chemoradiotherapy (CRT) frequently experience severe pain due to the side effects related to cancer therapies. In this regard CRT has been combined with clinical guidelines such as symptomatic treatment and individualized pain medication, including opioids, to treat oral mucositis (OM) and tumor pain (Ling and Larsson, 2011; Elad et al., 2020).

In many cases, this leads to opioid overuse and, as a result, to drug-associated side effects, including tolerance, dependence, and addiction (Elting et al., 2008; Ling and Larsson, 2011; Schaller et al., 2015; Hu et al., 2016). Hence, it is imperative to elucidate not only the peripheral but also the central mechanisms associated with cancer-related pain. It is also necessary to explore the neuromechanisms by which different therapies are applied to ameliorate pain in cancer patients. Such information will be crucial to tailoring more specific therapies in a precision medicine context. This knowledge may help physicians improve the quality of life and reduce the side effects associated with CRT treatment.

Among the several novel adjuvant therapies that have been used in the treatment of cancer-related pain, the modulation of the neural activity of the primary motor cortex through transcranial direct current stimulation (M1-tDCS) has been proved to be a promising therapy. In fact, according to some preliminary results, tDCS can provide significant relief of pain in head and neck cancer patients under CRT treatment (Hu et al., 2016). However, the specific mechanisms by which tDCS acts to control cancer-related pain are still uncertain. Therefore, more studies adopting protocols that permit the evaluation of changes in the brain activity associated with tDCS must be developed to understand better its mechanisms in controlling cancer-related pain.

tDCS has been proven to be safe and very effective in treating different types of pain (Fregni et al., 2006; Dossantos et al., 2012; Donnell et al., 2015). Moreover, due to its safety aspects, it is a potential therapy for treating cancer pain. Due to its portability and easy handling, it would be reasonable to include tDCS as an additional tool in the palliative clinical setting. Supporting this concept, one case report demonstrated the feasibility and the benefits of tDCS therapy in patients with pancreatic cancer. According to the reported results, tDCS relieves pain and decreases the need for rescue medication (Silva et al., 2007). These effects of tDCS in the modulation of cancer-related pain may be at least in part explained by a significant electric current that flows not only through outer but also through inner cortical structures, as previously demonstrated by the so-called forward model analyses (Dasilva et al., 2012, 2015).

Nonetheless, other functional mechanisms must also be considered (Dossantos et al., 2016). In this regard, new devices that use several different configurations have been introduced in recent years. Such modifications of the original apparatus permitted researchers to study the effects of tDCS on brain activity using different neuroimaging methods, including electroencephalography (EEG) and functional near-infrared spectroscopy (fNIRS).

As a matter of fact, clinicians and researchers have sought objective pain assessment solutions *via* neuroimaging techniques for many years. They focused on the brain to detect how nociceptive signals and pain are processed in the human brain. Technological advances have made it possible to obtain responses to many old questions and to have more detailed information on the brain functioning under different conditions. In some cases, it is possible to extract real-time information about the brain activity during painful stimuli (Hu et al., 2019), which was unthinkable until some years ago. This accurate pain assessment is crucial across a wide range of acute and chronic pain conditions. It provides proper diagnosis and treatment, especially when patients have limitations in expressing their ongoing suffering. This is the case for many patients with head and neck cancer.

Multimodal integration, which combines multiple neurophysiological signals, has brought more attention in the last few years, primarily because of its potential to supplement a single modality's drawbacks and yield reliable results by extracting complementary features. One example is the integration of EEG with fNIRS which is cost-effective and, therefore, a fascinating approach to brain-computer interface (BCI) (Ahn and Jun, 2017; Hong et al., 2018; Ge et al., 2019). Overall, the integration of EEG and fNIRS provides us with two different sources of information about the brain, e.g., the electrical activities through EEG, and the hemodynamic responses, through fNIRS. This integration has the advantages of non-invasiveness, portability, and the previously mentioned cost-effectiveness (Ahn and Jun, 2017; Li et al., 2020a,b; Ghafoor et al., 2021).

More recently, simultaneous tDCS/EEG evaluation of cortical mechanisms provided information regarding the immediate effects of tDCS on the brain. Furthermore, an emerging technology called fNIRS has been used for brain imaging. fNIRS has become a reliable and objective tool to evaluate the cortical activity of patients by measuring changes in the blood oxygenation within different layers of the nervous tissue likewise functional magnetic resonance imaging (fMRI) (Schestatsky et al., 2013; Liang et al., 2014; Racek et al., 2015). Interestingly, a recent study reported the use of concurrent EEG/fNIRS to clarify hemodynamic changes in children that presented spasms in clusters (Bourel-Ponchel et al., 2017).

In our previous study, we applied tDCS pain neuromodulation in patients with head and neck cancer under CRT (Hu et al., 2016). We found that tDCS could offer significant symptoms relief for mucositis and odynophagia. Thereby, it helped reduce weight loss, improve performance status, and decrease narcotics intake. At the same time, tDCS induced the prefrontal cortex (PFC), the motor cortex (MC), and precuneus activations, as revealed by EEG data. However, the detailed brain mechanism was not well-understood at that

time due to the limited number of EEG electrodes and the lack of spatial resolution of this method.

In the current study, we designed a new protocol that optimizes the one from our previous paper. More specifically, we added fNIRS to our study protocol. Also, we employed a tDCS device that can be administered remotely so that the tDCS sessions could be supervised and conducted in the patient's own place daily. fNIRS has become a reliable and objective tool to evaluate the cortical activity of patients by measuring changes in blood oxygenation, similar to fMRI (Ferrari and Quaresima, 2012; Curtin et al., 2019). The EEG/fNIRS combination has been proved to be effective in investigating the neurovascular coupling in the brain (Chiarelli et al., 2017; Pinti et al., 2021). On the other hand, the remotely supervised tDCS (RS-tDCS) has been an extension of in-clinic tDCS sessions that improve patients' compliance (Charvet et al., 2015; Kasschau et al., 2015; Shaw et al., 2017). Besides that, it has been shown that RS-tDCS represents an advance in the tDCS field, especially for patients with neurodegenerative diseases, including patients with multiple sclerosis and palliative care patients (Charvet et al., 2015; Kasschau et al., 2015, 2016; Shaw et al., 2017).

Hence, to provide a broader understanding of the central analgesic mechanisms linked to non-invasive neuromodulation in cancer-related pain, the protocol of the current study combined a 6-channel EEG with a 16-channel fNIRS system to investigate the effects of 20 sessions (remote and in clinic) of tDCS in head and neck cancer patients undergoing CRT.

METHODS

Subjects

Patients with head and neck cancer undergoing definitive CRT treatment were recruited through the University of Michigan health system (UMHS), department of medical oncology. The CRT protocol included two Gray (Gy) per day, 5 days a week, for a total of 7 weeks. Subjects were screened by a group of clinical oncologists and further approached by the H.O.P.E. lab team members to discuss the study protocol and read the informed consent form.

The designed study protocol comprised a 7-week-long tDCS stimulation procedure, a pre-tDCS baseline session (pre-1 week), and two post-tDCS follow-up sessions (the first after 1 week and the second after 1 month). We used two types of tDCS devices. One of them was applied in our facility by our research staff, and the other one was a remotely supervised tDCS. The subjects visited our research facility every week. We used neuroimaging techniques to scan their brains during those sessions, which occurred in weeks 1, 2, 5, 7, 8, and after 1 month of tDCS treatment. We did two neuroimaging techniques in the current study, fNIRS and EEG.

This protocol (HUM00078942) was approved by the University of Michigan Institutional Review Board. Written informed consent was obtained from all participants.

TABLE 1 | Questionnaires and clinical measurements in the current study.

Assessment purpose	Questionnaire(s) used
Pain	VAS, McGill, Geo-Pain
Emotion	PANAS-x
Oral mucositis	World Health Organization (WHO) scale, Oral Mucositis Weekly Questionnaire for Head and Neck Cancer
Weight	Clinical evaluation
Narcotic pain medication	Clinical evaluation
Diet	Clinical evaluation
Quality of Life	Head and Neck Quality of Life Weekly Questionnaire, University of Washington Quality of Life Questionnaire

Inclusion Criteria

A. Subjects with head and neck malignancy were scheduled for CRT and were capable of understanding and adhering to the protocol requirements.
B. Subjects willing to comply with the study procedures and visits.
C. Subjects aged 18–75 years old.

Exclusion Criteria

A. Substantial dementia.
B. Patients are being actively treated for another cancer at the time of enrollment.
C. Any condition that would prevent the use of tDCS and EEG, including any skull abnormality, implanted metals, implanted electronic devices, seizure disorders, neurologic conditions.
D. Use of an investigational drug or device within 30 days of study screening.

Questionnaire

We used multiple questionnaires in the current study to evaluate patients' status along the study process. These questionnaires assessed pain, emotion, oral mucositis, weight, narcotic pain medication requirement, diet, and quality of life. A summary of the questionnaires used in this study can be found in **Table 1**.

In this proof-of-concept study, we recruited two participants. Both subjects received tDCS on the day of their CRT appointments. tDCS was applied before CRT when doing tDCS sessions in-clinic or after CRT when tDCS was self-administered at home. tDCS was applied daily (5 days per week) during the second and third weeks of CRT, three times per week during the fourth and fifth weeks of CRT, and twice per week during the sixth and seventh weeks of CRT (5/5/3/3/2/2 per week). The tDCS stimulation protocol was designed to accommodate the patient's CRT schedule in this study.

In-clinic Procedures

The in-clinic tDCS protocol followed the methodology published in previous articles (Dasilva et al., 2011; Schestatsky et al., 2013). Briefly, the procedure was divided into seven steps: (1) check if all materials were available before starting the entire procedure.

The checking items included the cap quality, the device battery, and the USB and Bluetooth connections between the device and the computer. Our study used C3 or C5 as references; (2) prepare the skin for tDCS stimulation. We inspected the skin for any pre-existing lesions—to avoid electrical stimulation/EEG recording over damaged skin or skull lesions. To increase conductance, we moved the hair away from the site of the electrical stimulation/EEG registering and placed plastic hair clips to keep hair away and cleaned the skin's surface to remove any signs of lotion, dirt, and grease. Furthermore, we allowed it to dry; (3) obtained patients' head measurements to decide the size of the cap in use. We marked the fiducial points, Cz, Fp1, and Fp2; (4) mount the electrodes onto the cap. We put conducting gel on the tDCS electrodes and embedded both EEG, and the tDCS electrodes into the cap; (5) patients wear the cap. We confirmed that the subject was seated comfortably and placed the cap in a way that the vertex of the cap matched the Cz point on the cap, while the Fp1 and Fp2 points were aligned as well. (6) configure the stimulation and data acquisition software (NeuroElectric, Spain) on the computer. (7) Finally, start the stimulation simultaneously with EEG data recording. We used a 2-mA current for the tDCS stimulation with a duration of 20 min per session.

Remote Procedures

We used physical mini-CT tDCS devices (Soterix, NY) and online management software ElectraRx (Soterix, NY). At the end of the first in-clinic session, the patient received proper training on the remotely supervised tDCS using the ElectraRx website (https://www.soterixmedical.com/electrarx/login) and was provided with a mini-CT device and written guidelines. Then the patients were able to complete their stimulation sessions at home. In each remote session, the patients filled out the steps through the ElectraRx website ahead of the remote session start and then were provided with a code that allowed the participant to start the stimulation (**Figure 1**). We used a 2-mA current for the tDCS stimulation with a duration of 20 min per session.

Patients were asked to properly follow the steps to ensure correct electrode preparation and placement, low impedance, and safe device removal. During the remote sessions, the patients were instructed to abort the RS-tDCS session in case of any significant discomfort or other adverse events, or if a study team member determined that the session should be discontinued. Also, they were aware of the designated "stop criteria." If the stop criteria were met at any time throughout the study, the session and/or ongoing study participation were reviewed.

Finally, the subjects completed a "tDCS side effects form" after each stimulation. This assessment objectively gauged any adverse events that the patient underwent as a direct result of the stimulation.

Neuroimaging

We used an NE EEG/tDCS device (Neutralelectrics, Spain) combined with NIRx fNIRS (NIRx Medical Technologies, Germany) device for the neuroimaging data collection. The montage for the EEG/fNIRS/tDCS probes can be found in **Figure 2**. Our neuroimaging probe cap design was based on the international 10-10 system reference map. The **Table 2** provides the relevant fiducial markers in the 10-10 system and MNI coordinates (Koessler et al., 2009). We placed the tDCS anode at the right F4 fiducial mark, while the cathode was placed at the left C5 fiducial mark. Then we placed the EEG electrodes, respectively, at Fpz, Fz, Cz, Pz, F3, and C6 fiducial marks, yielding 6 EEG data channels. Our EEG data were collected at a sample rate of 500 Hz. Finally, our fNIRS setup employed 8 by 8 source-detector combinations (3 cm apart), yielding 16 data measurement channels. The data channels, respectively, covered the bilateral prefrontal cortices and bilateral somatosensory/motor cortices. Our fNIRS data were sampled at a rate of 7.81 Hz. The localization process was validated *via* a photogrammetry-based localization process (Hu et al., 2020).

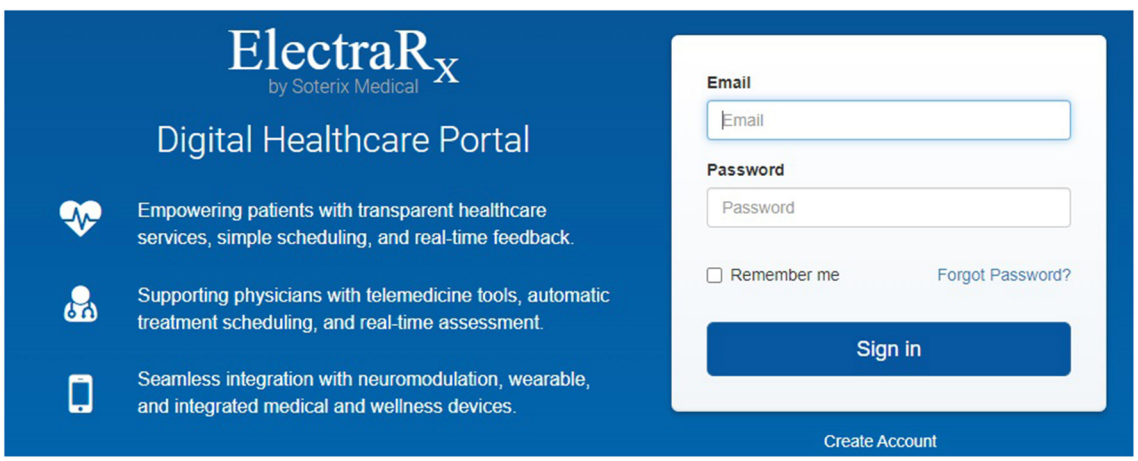

FIGURE 1 | Remote tDCS website set-up. Further details can be found at: https://soterixmedical.com/research/remote/electrarx.

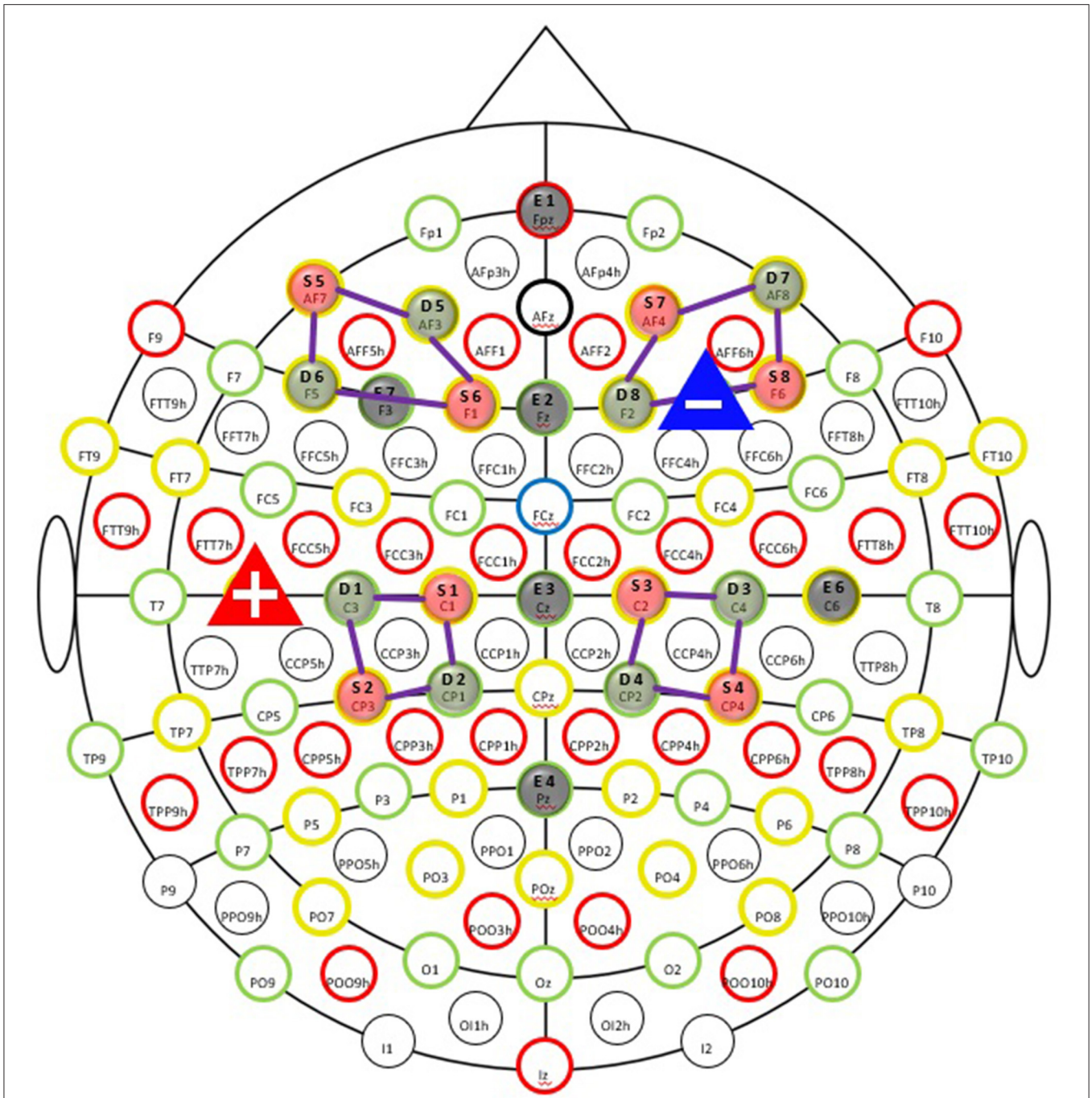

FIGURE 2 | Simultaneous EEG-fNIRS-tDCS multimodal scanning and stimulation setup EEG evaluation of cortical mechanisms can elucidate valuable information regarding the immediate tDCS effects on the brain. EEG recording was taked at the pre-study visit, the first stimulation visit, last stimulation on first week of tDCS session, and the fifth and seventh week of treatment (both on the last session on week), as well as the follow-up appointment. The fNIRS is an important tool for clinical monitoring of tissue oxygenation and measurement of cortical activity, thereby appear that an advancement in brain imaging. fNIRS was taked at the pre-study visit, first stimulation visit, at the fifth week of treatment and the last stimulation visit.

Optodes and Electrodes Registration

We designed the cap in three sizes, 56, 58, and 60, respectively, to account for head size variation, following the international 10-10 transcranial system positioning. We then applied a photogrammetry method to register all the optodes and data channels onto the cortical surface. Our previous article described the detailed method (Hu et al., 2020). Briefly, we used the Structure Sensor (Occipital Inc, CO) with an iPad (Apple Inc,

TABLE 2 | The neuroimaging localization results for fNIRS optodes, channels, EEG, and tDCS electrodes.

Type	Modality	10-10 location	MNI coordinates		
			X	Y	Z
Source 1	fNIRS	C1	−25.1	−22.5	70.1
Source 2	fNIRS	CP3	−46.9	−47.7	49.7
Source 3	fNIRS	C2	26.7	−20.9	69.5
Source 4	fNIRS	CP4	49.5	−45.5	50.7
Source 5	fNIRS	AF7	−41.7	52.8	11.3
Source 6	fNIRS	F1	−22.1	26.8	54.9
Source 7	fNIRS	AF4	35.1	50.1	31.1
Source 8	fNIRS	F6	52.9	28.7	25.2
Detector 1	fNIRS	C3	−49.1	−20.7	53.2
Detector 2	fNIRS	CP1	−24	−49.1	66.1
Detector 3	fNIRS	C4	50.3	−18.8	53
Detector 4	fNIRS	CP2	25.8	−47.1	66
Detector 5	fNIRS	AF3	−32.7	48.4	32.8
Detector 6	fNIRS	F5	−51.4	26.7	24.7
Detector 7	fNIRS	AF8	43.9	52.7	9.3
Detector 8	fNIRS	F2	23.6	28.2	55.6
Electrode 1	EEG	Fpz	1.4	65.1	11.3
Electrode 2	EEG	Fz	0	26.8	60.6
Electrode 3	EEG	Cz	0.8	−21.9	77.4
Electrode 4	EEG	Pz	0.7	−69.3	56.9
Electrode 5	EEG	F3	−39.7	25.3	44.7
Electrode 6	EEG	C6	65.2	−18	26.4
Anode	tDCS	F4	41.9	27.5	43.9
Cathode	tDCS	C5	−63.6	−18.9	25.8
Type	**Modality**	**Estimated brain region**	**MNI coordinates**		
	Source-detector		**X**	**Y**	**Z**
Channel 1	fNIRS S1-D1	BA* 6	−37.1	−21.6	61.65
Channel 2	fNIRS S1-D2	BA 2|BA 4|BA 1|BA 6|BA 3	−24.55	−35.8	68.1
Channel 3	fNIRS S2-D1	BA 3|BA 4|BA 6|BA 1|BA 2	−48	−34.2	51.45
Channel 4	fNIRS S2-D2	BA 5|BA 2|BA 1|BA 3	−35.45	−48.4	57.9
Channel 5	fNIRS S3-D3	BA 6	38.5	−19.85	61.25
Channel 6	fNIRS S3-D4	BA 6|BA 1|BA 2|BA 4|BA 3	26.25	−34	67.75
Channel 7	fNIRS S4-D3	BA 3|BA4|BA 1|BA 2|BA 6	49.9	−32.15	51.85
Channel 8	fNIRS S4-D4	BA 1|BA 2|BA 3	37.65	−46.3	58.35
Channel 9	fNIRS S5-D5	BA 9|BA 8	−37.2	50.6	22.05
Channel 10	fNIRS S5-D6	BA 9|BA 46|BA 8|BA 10	−46.55	39.75	18
Channel 11	fNIRS S6-D5	BA 8	−27.4	37.6	43.85
Channel 12	fNIRS S6-D6	BA 8|BA 6	−36.75	26.75	39.8
Channel 13	fNIRS S7-D7	BA 9|BA 10	39.5	51.4	20.2
Channel 14	fNIRS S7-D8	BA 8	29.35	39.15	43.35
Channel 15	fNIRS S8-D7	BA 46|BA 9|BA 10	48.4	40.7	17.25
Channel 16	fNIRS S8-D8	BA 8	38.25	28.45	40.4

*BA stands for Brodmann Area.

CA) to capture the 3D photos of the optodes and electrodes on the participants' heads. We then loaded the 3-D photo in the MATLAB software (Mathworks, MA, USA) and pinpointed the locations of fNIRS optodes and EEG/tDCS electrodes with five fiducial markers (Nasion, Inion, Cz, AR, and AL in the 10-10 system). The derived optodes coordinates were affinely transferred into the MNI space using the MATLAB-based AtlasViewerGUI toolbox (Aasted et al., 2015). The mid-points

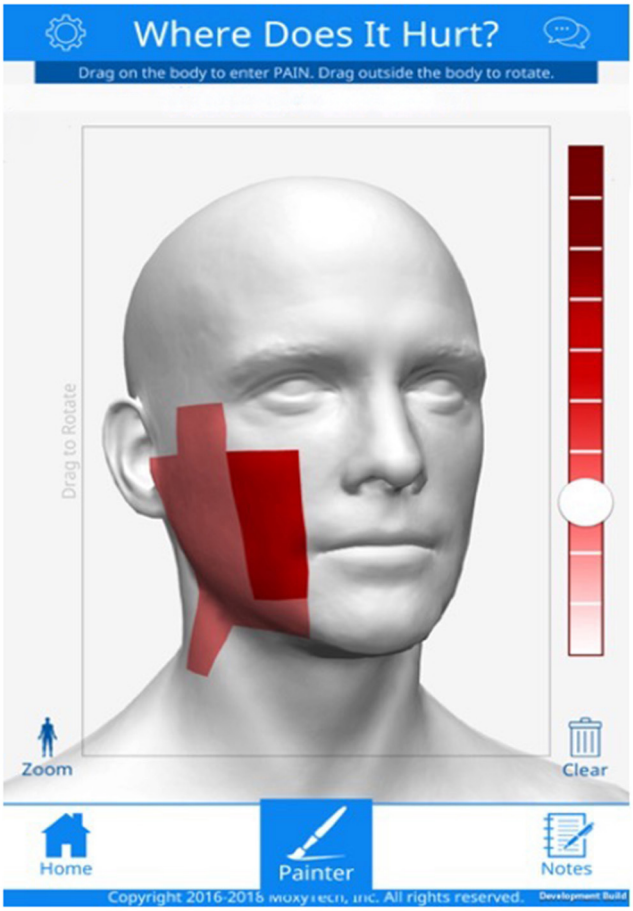

FIGURE 3 | Geo-pain software graphical user interface, MoxyTech Inc, MI.

between the source-detector (optodes) pairs were used as the coordinates for the fNIRS channels. Finally, we estimated the regions under each fNIRS channel and EEG electrode by matching their MNI coordinates with locations in the neurosynth.org database. Also, we evaluated the brain regions with a voxel size of 10 mm using the WFU_pick atlas in XJview toolbox (https://www.alivelearn.net/xjview).

Pain Level Evaluation

Patients' pain levels were evaluated immediately before and after the stimulation through the McGill Pain Questionnaire (MPQ)—Short Form (Melzack, 1975) and through the GeoPain App (Kaciroti et al., 2020). GeoPain is a free stand-alone and embedded mobile app developed in collaboration with the Headache and Orofacial Pain Effort (HOPE) at the University of Michigan and is currently licensed by the spinoff MoxyTech Inc (Kaciroti et al., 2020). GeoPain provides a 3D body map for pain tracking based on a squared grid system with vertical and horizontal coordinates using anatomical landmarks (an example can be found in **Figure 3**).

Neuroimaging Data Analysis

fNIRS and EEG data collected in the current study were analyzed separately and then interpreted jointly. The fNIRS data were analyzed using the NIRSAnalyzer toolbox (Santosa et al., 2018), while the EEG data were analyzed using the EEGLAB toolbox (Delorme and Makeig, 2004) in MATLAB (Mathworks, MA).

We conducted functional connectivity analysis on the collected fNIRS data to study the brain mechanism induced by tDCS. The calculation process was described in a previous method paper (Santosa et al., 2017). Briefly, the raw fNIRS data was first downsampled to 4 Hz. Then we converted the raw data into oxy- and deoxy-hemoglobin using the modified Beer-Lambert law (Kocsis et al., 2006). We then used bandpass filters to filter that HbO data into two frequency bands, namely, high (0.5–1 Hz) and low (0.01–0.08) frequency bands. These two frequency bands were selected to avoid the physiological signal bandwidth, including Mayer's wave (0.1 Hz), respiratory (0.3–0.5 Hz), and cardiac (1–1.5 Hz) relevant fluctuations. Next, we calculated the between-channel correlation at the individual level using the connectivity method in the toolbox. This method used prewhitening *via* the autoregressive filter and the weighted least-squares fit during the FC calculation to account for physiological noises, motion, and other artifacts in the fNIRS signal (Santosa et al., 2017). Then, the individual-level correlation coefficients were converted to Z-score using Fisher's Z-transform. Finally, a linear mixed-effect (LME) model was applied to obtain the group-level connectivity effect. We applied the LME analysis using the MixedEffectsConnectivity function in the NIRSAnalyzer toolbox. Briefly, the LME estimated the group-level correlation effects based on the individual Z scores. The model consists of two parts, fixed effects and random effects. We used the individual subject as random effects to account for between-subject variability so that the fixed effects can be estimated as the group-level correlation effects. This calculation was implemented on the data collected from both subjects during the two lab visits. It is worth noting that we included a relatively high-frequency band (0.5–1 Hz) connectivity analysis in this study for exploratory EEG-fNIRS network comparison on the delta frequency band (0–4 Hz).

For EEG data, we conducted a dipole source localization analysis on the collected EEG signal. First, we visually inspected the EEG data to reject artifact-affected segments. The inspected EEG signals were first filtered using a bandpass filter with cut-off frequencies at 0.01–40 Hz. Then, the data was cleaned using the automatic data cleaning pipeline in the EEGLab toolbox and re-referenced. We ran an independent component analysis (ICA) on the preprocessed signal. The calculated independent components were then entered into the DIPFIT plug-in in the EEGLAB toolbox for the source localization (Kavanagh et al., 1978; Oostendorp and Van Oosterom, 1989). The head model used for the DIPFIT was the BEM DIPFIT head model with MNI coordinates. In addition, we used the phase-lag index (PLI) to analyze the functional connectivity between the electrodes. The PLI measures the phase synchronization of EEG signals recorded from different electrodes [CITATION]. In this study, we

calculated the PLI using the following equation:

$$PLI = \left| \frac{\sum_{t=1}^{K} sign(Im[e^{-i(\theta^x - \theta^y)_t}])}{K} \right| \quad (1)$$

Where K is the number of the phase differences, t is the time from 1 to K, x and y are, respectively, the electrode indices, and *sign* is the sign function. The PLI value ranges from 0 to 1, where 0 means inconsistent phase lag (volume conduction), while 1 means perfectly consistent phase lag.

Finally, the fNIRS and EEG analysis results were gathered for a qualitative and quantitative comparison and correlation. For qualitative comparison, we plotted the possible tDCS induced brain mechanism in a network consisting of (1) cortico-cortical connections revealed by the fNIRS signal, (2) cortico-deep-brain connections revealed by the EEG signal, if available. Also, the collected questionnaire data and preprocessed neuroimaging data were entered into a canonical correlation analysis model for brain-behavior correlation change in EEG power spectra. For quantitative analysis, we calculated the correlation between the fNIRS connectivity at low/high-frequency bands and the EEG power spectral density at different frequencies (respectively, at 4/8/16/24 Hz). The Pearson's and Spearman's correlation coefficients were calculated, and the relative p-values were examined to reveal the potential relationship between the fNIRS signal and EEG signal.

Preliminary Results

The data presented in this section were collected from two subjects who have participated in the study. We first presented the demographic and questionnaire data in **Table 1**. **Figure 4** illustrates the results of neuroimaging data analysis during tDCS stimulation, respectively, for Subjects #8 and #11. Panels (a) and (c) present the significant connections between bilateral prefrontal and sensory cortices revealed by fNIRS data ($p < 0.05$, FDR corrected). Differences in EEG power spectra in the

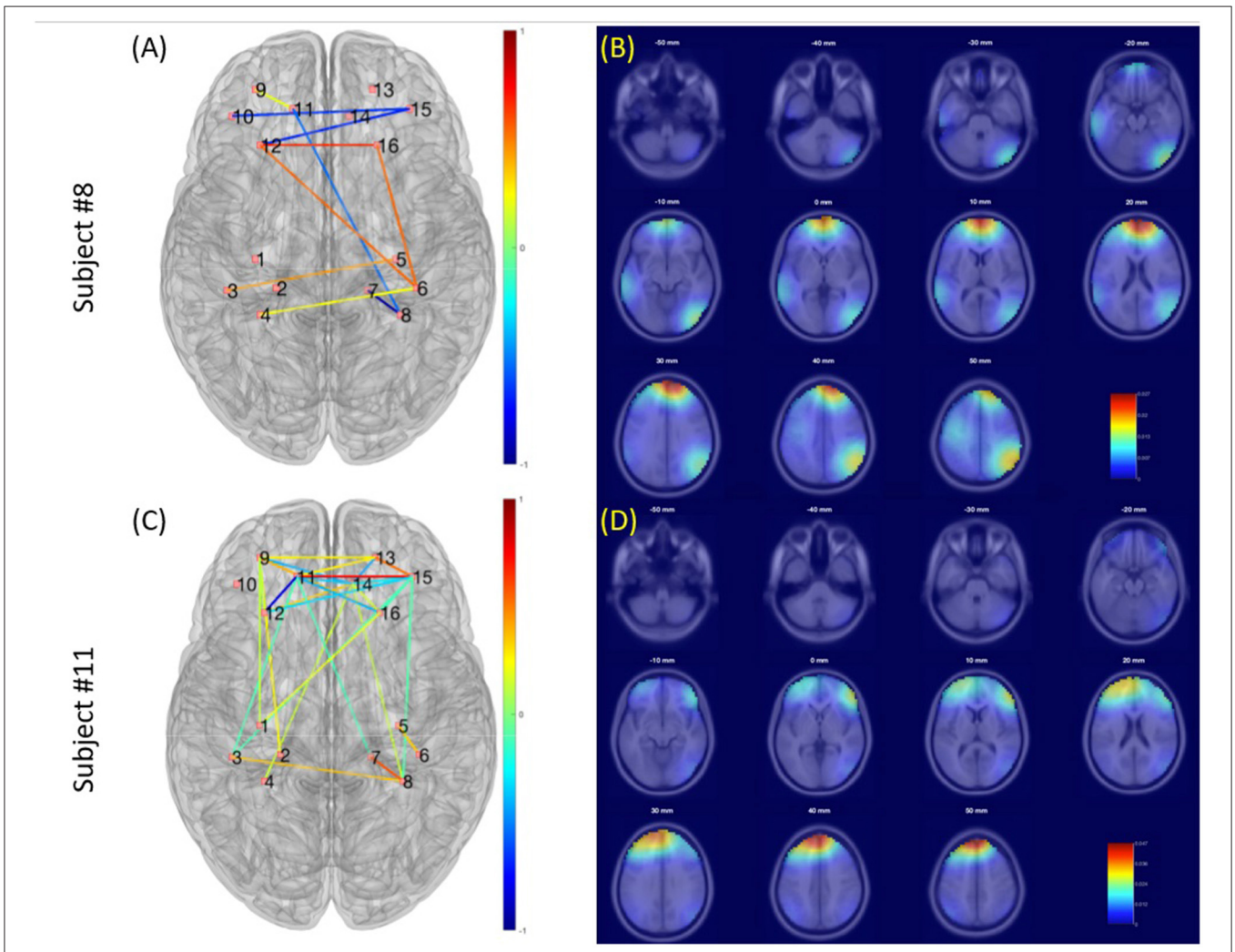

FIGURE 4 | Brain activations during tDCS stimulation (Week 2, 5, and 7 combined). **(A,C)** Functional connectivity revealed by fNIRS. **(B,D)** Source localization of EEG signal.

PFC were found when comparing the seventh with the first week of tDCS. Panels (b) and (d) show the results of the EEG source localization analysis, presented as a transverse view at different slicing. **Figure 5** shows the connectivity patterns of the resting state before tDCS stimulation at week 2, week 7, and one-month follow-up, respectively, for subjects #8 and #11. Panels (a) and (b) show the significant connections between bilateral prefrontal and sensory cortices revealed by the fNIRS data ($p<0.05$, FDR corrected) in week 2 and week 7. Panel (c), (d), and (e) demonstrate the power map of EEG data at 4/8/16/24 Hz, respectively, in week 2, week 7, and month 1 follow-up for subjects #8 and #11.

DISCUSSION

The current study presented a preliminary protocol that applies tDCS modulation of pain in head and neck cancer patients under CRT. Furthermore, patient-bedside neuroimaging techniques, e.g., fNIRS and EEG, were used to monitor the associated underlining brain mechanisms. tDCS was able to decrease the functional connections between the PFC and S1 according to the fNIRS data. The EEG data revealed that the 7 weeks of tDCS activated the right PFC compared to the first week of stimulation (week 2).

The collected visual analog scale (VAS) score and amount of narcotic use (**Table 3**) indicated that both patients suffered from the worst pain in the weeks 5–week 8 along the CRT treatment process. Such severe pain was probably due to the side effects of the CRT treatment since both patients presented little pain and no narcotic use at the beginning of the treatment. We then analyzed the resting state data collected as baseline data before tDCS sessions in weeks 2, 7, and 1-month follow-up. The EEG power maps at different frequency bands (4/8/16/24 Hz) demonstrated a similar pattern of right prefrontal cortical activation after 7 weeks of tDCS. fNIRS data obtained from both participants demonstrated less PFC-S1 connection after 7 weeks of tDCS stimulation. In addition, we found that both participants developed PFC activation during the tDCS modulation, as revealed by the EEG signal. Participant # 8 also demonstrated right parietal activation, while participant # 11 demonstrated some very weak activation in bilateral parietal cortices. Previous studies have confirmed that the PFC, including the anterior PFC and the dorsal lateral prefrontal cortex (DLPFC), play a key role in pain perception (Peng et al., 2018). Our observations revealed by the preliminary data also indicated that the PFC was activated during the tDCS modulation (**Figure 5**). Also, the PFC decreased in connection with the motor and sensory parts of the brain, as indicated in **Figure 5**, panels (a) and (b). We also found that the 7-week tDCS modulation protocol increased the broadband (4/8/16/24 Hz) EEG power at the right PFC region in both the subjects enrolled in this study. While in Subject # 8, we observed a decrease in the activation in the anterior PFC after 7-week stimulation, consistent with the findings of a previous study (Roy et al., 2014). Unfortunately, we have not collected data from a standard of care (control) group to make further conclusions.

During the experiment protocol designed and data collection, we experienced several challenges that presented limitations to the study. The first challenge in this study is designing a

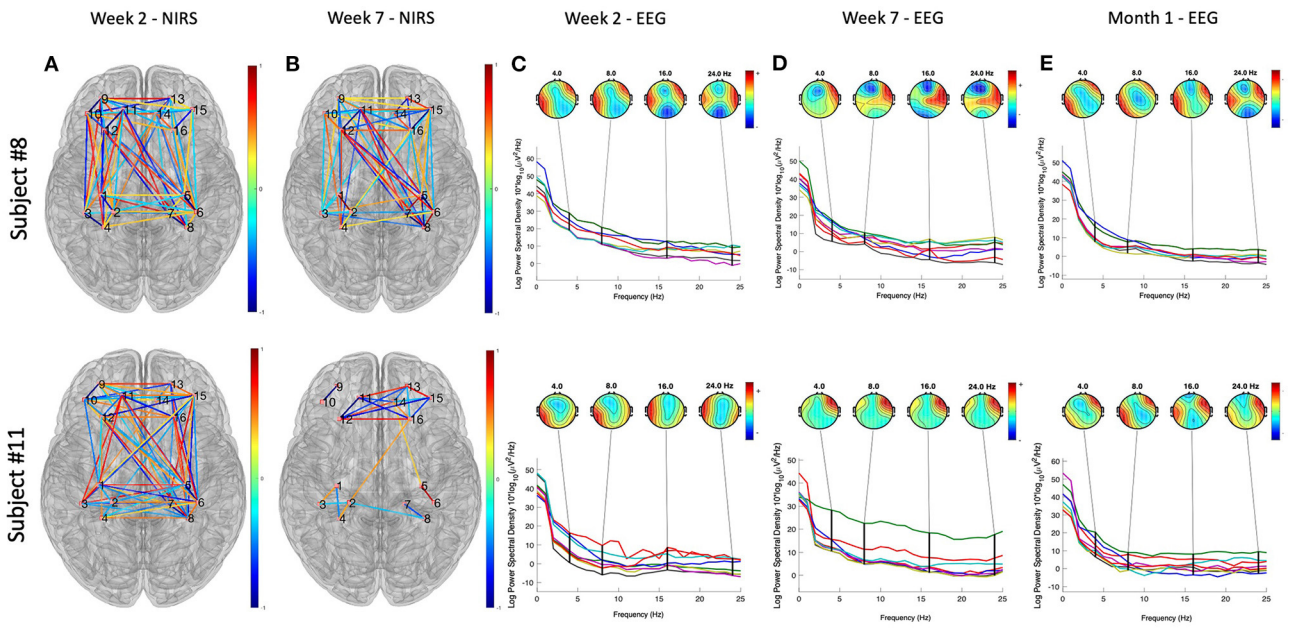

FIGURE 5 | Neuroimaging data analysis results of the resting state before tDCS stimulation at week 2, week 7, and 1-month follow-up, respectively, for subjects #8 and #11. **(A,B)** Show the significant connections between bilateral prefrontal and sensory cortices revealed by the fNIRS data ($p < 0.05$, FDR corrected) in week 2 and week 7. The color bar represent the correlation coefficient levels, ranges from −1 to 1. **(C–E)** Demonstrate the power spectra map of EEG data, separately at 4/8/16/24 Hz, in week 2, week 7, and month 1 follow-up. The color bars represent the power of the spectral density at different frequencies, ranges from 0 to 60.

TABLE 3 | Preliminary demographic and clinical measurement data collected from two patients.

	VAS (0–5)	VAS (0–100)	pre-PANASx -PA	pre-PANASx -NA	Narcotic _use	Weight	Mucositis	QoL WA pain gen	QoL H&N	PPI _Mcgill
Subject # 8 Age = 62 Gender = M										
Wk0	0	0			0	276	0	20	0	0
Wk1	0	0	29	24	0	276	0			0
Wk2	3	40	27	25	0	272	1			0
Wk3	2	20	30	21	0	260	4			2
Wk4	3	25	20	21	0	257	0			
Wk5	2	40	25	20	25	239	3			3
Wk6	2	80	24	23	300	242	3			
Wk7	2	20	23	23	420	240	2	30	0	2
Wk8	3	60	24	25	840	240	4	30	5	
Mo1	1	30	34	23	630	232	4	30	1	2
Subject # 11 Age = 60 Gender = M										
Wk0	0	0			0	211		10	1	0
Wk1	0	0	36	10	0	211				0
Wk2	2	20	43	10	0	212				5
Wk3	4	60	49	10	0	208	4			2
Wk4	2	20	46	10	70	208	3			3
Wk5	1	10	42	10	70	209	1			2
Wk6	2	20	44	10	140	203	4			4
Wk7	3	70	44	10	140	204	4	40	3	2
Wk8	3	40	43	10	140	208	3	40	1	3
M	3	40	43	10	0	208	3	30	1	2

PANAS, Positive and Negative Affect Schedule; PA, Positive Affects; NA, Negative Affexts; QoL, Quality of Life; WA, Washington; H&N, Head and Neck; PPI, Present Pain Intensity.

probe holding cap that holds both EEG electrodes and fNIRS optodes. The two neuroimaging techniques required placement of their probes on the head surface, and thus the space for each probe could be very limited (Chiarelli et al., 2017). The cap design included two regions of interest, the PFC and the S1. Therefore, we used the F7, F8, C3, and C4, in the international 10-20 system as the centers to deploy fNIRS/EEG probes. Specifically, we used four fNIRS optodes (two sources and two detectors, forming up 4 channels) to surround one EEG electrode, as illustrated in **Figure 4**. In addition, the number of EEG electrodes was not sufficient. The electrodes employed as anode/cathode for tDCS stimulation cannot record EEG signals. Therefore, we only had 6 electrodes for EEG signal recording, which may lead to less-optimal source localization analysis for EEG data.

Moreover, the fNIRS and EEG signal analysis do not have a standard pipeline (Pinti et al., 2021). The advantage of the dual-modality measurement was to detect both hemodynamic responses and neurophysiology signals using an entire portable setup. fNIRS has balanced spatial and temporal resolutions. However, it detects only the cortical response. Thus, EEG is a supplementary imaging technique not only to measure neuronal signals that couples hemodynamic responses but also from both cortical and deep brain regions. We combined the two imaging techniques and investigated both cortico-cortical and cortico-deep brain networks.

Nonetheless, the joint data analysis is challenging due to the neurovascular coupling (Huneau et al., 2015; Phillips et al., 2016). Previous studies analyzed the two types of data separately and then correlated the preprocessed signals (Pinti et al., 2021). Recently, a novel study recorded EEG signal as the stimulus function for the hemodynamic response modeling and then used the model to fit the fNIRS data from different channels (Zhang and Zhu, 2019). By fitting the hemodynamic response model to the fNIRS data, future studies will be able to obtain both cortico-cortical and cortico-deep-brain connections based on the two types of signals.

Finally, the large amount of clinical data collected through the questionnaires pose challenges on clinical information-brain correlation. Such correlation is a key step that associates the collected neuroimage data with the clinical data acquired from the questionnaires and clinical measurements. Along with the protocol in the current study, we collected eight categories of clinical measures or questionnaires along with the study at multiple time points. On the other hand, we collected fNIRS data from 16 data channels, 3 sessions (75 min in total), and EEG data from 6 channels, 5 sessions (125 min in total) from each participant. The large amount of data posed challenges to associating neuroimaging with clinical measures. Existing studies proved that methods like canonical correlation analysis (CCA) (Wang et al., 2020) or artificial intelligence (machine learning) analysis (Mihalik et al., 2020) could be used to solve such "big

data" correlation issues. In the current study, we condensed the neuroimaging data by finding the connectivity between the brain regions of interest. In future studies, we will use a method like CCA or un-supervised artificial intelligence algorithms to find precisely which "clinical score" correlates mainly with the specific "connection" revealed by the neuroimaging data analysis.

Our understanding of tDCS-based head and neck pain modulation is very limited. In this article, we proposed a novel protocol to study (1) the effect of tDCS-based pain modulation (remote-supervised and in-clinic) in head and neck patients undergoing CRT and (2) the underlining brain mechanisms of such modulation process. The study results will enhance understanding of the mechanisms by which tDCS modulates cancer-related pain. We also expect that our study and data will represent a starting point for more complicated protocols of tDCS-based cancer-pain modulation.

DATA AVAILABILITY STATEMENT

The original contributions presented in the study are included in the article/supplementary material, further inquiries can be directed to the corresponding authors.

ETHICS STATEMENT

The studies involving human participants were reviewed and approved by University of Michigan Institutional Review Board. The patients/participants provided their written informed consent to participate in this study.

AUTHOR CONTRIBUTIONS

AD conceived the project. BS collected the data. X-SH analyzed the data. BS, X-SH, MD, and AD led the writing. All authors read and accepted the final version of the manuscript. All authors contributed to the article and approved the submitted version.

FUNDING

We thank the MCubed Award–University of Michigan and the Brazilian Government Agencies: CNPQ (Conselho Nacional de Desenvolvimento Científico e Tecnológico), Fundação de Amparo à Pesquisa do Estado do Rio de Janeiro (FAPERJ), for their financial support. This research did not receive any grants from funding agencies in the commercial sectors.

REFERENCES

Aasted, C. M., Yücel, M. A., Cooper, R. J., Dubb, J., Tsuzuki, D., Becerra, L., et al. (2015). Anatomical guidance for functional near-infrared spectroscopy: AtlasViewer tutorial. *Neurophotonics* 2, 020801. doi: 10.1117/1.NPh.2.2.020801

Ahn, S., and Jun, S. C. (2017). Multimodal integration of EEG-fNIRS for brain-computer interfaces - current limitations and future directions. *Front. Hum. Neurosci.* 11, 503. doi: 10.3389/fnhum.2017.00503

Bourel-Ponchel, E., Mahmoudzadeh, M., Delignieres, A., Berquin, P., and Wallois, F. (2017). Non-invasive, multimodal analysis of cortical activity, blood volume and neurovascular coupling in infantile spasms using EEG-fNIRS monitoring. *Neuroimage Clin.* 15, 359–366. doi: 10.1016/j.nicl.2017.05.004

Charvet, L. E., Kasschau, M., Datta, A., Knotkova, H., Stevens, M. C., Alonzo, A., et al. (2015). Remotely-supervised transcranial direct current stimulation (tDCS) for clinical trials: guidelines for technology and protocols. *Front. Syst. Neurosci.* 9, 26. doi: 10.3389/fnsys.2015.00026

Chiarelli, A. M., Zappasodi, F., Di Pompeo, F., and Merla, A. (2017). Simultaneous functional near-infrared spectroscopy and electroencephalography for monitoring of human brain activity and oxygenation: a review. *Neurophotonics* 4, 041411. doi: 10.1117/1.NPh.4.4.041411

Curtin, A., Tong, S., Sun, J., Wang, J., Onaral, B., and Ayaz, H. (2019). A Systematic Review Of Integrated Functional Near-Infrared Spectroscopy (fNIRS) and transcranial magnetic stimulation (TMS) studies. *Front. Neurosci.* 13, 84. doi: 10.3389/fnins.2019.00084

Dasilva, A. F., Mendonca, M. E., Zaghi, S., Lopes, M., Dossantos, M. F., Spierings, E. L., et al. (2012). tDCS-induced analgesia and electrical fields in pain-related neural networks in chronic migraine. *Headache* 52, 1283–1295. doi: 10.1111/j.1526-4610.2012.02141.x

Dasilva, A. F., Truong, D. Q., Dossantos, M. F., Toback, R. L., Datta, A., and Bikson, M. (2015). State-of-art neuroanatomical target analysis of high-definition and conventional tDCS montages used for migraine and pain control. *Front. Neuroanat.* 9, 89. doi: 10.3389/fnana.2015.00089

Dasilva, A. F., Volz, M. S., Bikson, M., and Fregni, F. (2011). Electrode positioning and montage in transcranial direct current stimulation. *J. Vis. Exp.* 51:2744. doi: 10.3791/2744

Delorme, A., and Makeig, S. (2004). EEGLAB: an open source toolbox for analysis of single-trial EEG dynamics including independent component analysis. *J. Neurosci. Methods* 134, 9–21. doi: 10.1016/j.jneumeth.2003.10.009

Donnell, A. D., Nascimento, T., Lawrence, M., Gupta, V., Zieba, T., et al. (2015). High-definition and non-invasive brain modulation of pain and motor dysfunction in chronic TMD. *Brain Stimul.* 8, 1085–1092. doi: 10.1016/j.brs.2015.06.008

Dossantos, M. F., Ferreira, N., Toback, R. L., Carvalho, A. C., and Dasilva, A. F. (2016). Potential mechanisms supporting the value of motor cortex stimulation to treat chronic pain syndromes. *Front. Neurosci.* 10, 18. doi: 10.3389/fnins.2016.00018

Dossantos, M. F., Love, T. M., Martikainen, I. K., Nascimento, T. D., Fregni, F., Cummiford, C., et al. (2012). Immediate effects of tDCS on the mu-opioid system of a chronic pain patient. *Front. Psychiatry* 3, 93. doi: 10.3389/fpsyt.2012.00093

Elad, S., Cheng, K. K. F., Lalla, R. V., Yarom, N., Hong, C., Logan, R. M., et al. (2020). MASCC/ISOO clinical practice guidelines for the management of mucositis secondary to cancer therapy. *Cancer* 126, 4423–4431. doi: 10.1002/cncr.33100

Elting, L. S., Keefe, D. M., Sonis, S. T., Garden, A. S., Spijkervet, F. K., Barasch, A., et al. (2008). Patient-reported measurements of oral mucositis in head and neck cancer patients treated with radiotherapy with or without chemotherapy: demonstration of increased frequency, severity, resistance to palliation, and impact on quality of life. *Cancer* 113, 2704–2713. doi: 10.1002/cncr.23898

Ferrari, M., and Quaresima, V. (2012). A brief review on the history of human functional near-infrared spectroscopy (fNIRS) development and fields of application. *Neuroimage* 63, 921–935. doi: 10.1016/j.neuroimage.2012.03.049

Fregni, F., Gimenes, R., Valle, A., Ferreira, M., Rocha, R., Natalle, L., et al. (2006). A randomized, sham-controlled, proof of principle study of transcranial direct current stimulation for the treatment of pain in fibromyalgia. *Arthritis Rheum.* 54, 3988–3998. doi: 10.1002/art.22195

Ge, S., Wang, P., Liu, H., Lin, P., Gao, J., Wang, R., et al. (2019). Neural activity and decoding of action observation using combined EEG and fNIRS measurement. *Front. Hum. Neurosci.* 13, 357. doi: 10.3389/fnhum.2019.00357

Ghafoor, U., Yang, D., and Hong, K. S. (2021). Neuromodulatory effects of HD-tACS/tDCS on the prefrontal cortex: a resting-state fNIRS-EEG study. *IEEE J. Biomed. Health Inform.* 1. doi: 10.1109/JBHI.2021.3127080. [Epub ahead of print].

Hong, K. S., Khan, M. J., and Hong, M. J. (2018). Feature extraction and classification methods for hybrid fNIRS-EEG brain-computer interfaces. *Front. Hum. Neurosci.* 12, 246. doi: 10.3389/fnhum.2018.00246

Hu, X. S., Fisher, C. A., Munz, S. M., Toback, R. L., Nascimento, T. D., Bellile, E. L., et al. (2016). Feasibility of non-invasive brain modulation for management of pain related to chemoradiotherapy in patients with advanced head and neck cancer. *Front. Hum. Neurosci.* 10, 466. doi: 10.3389/fnhum.2016.00466

Hu, X. S., Nascimento, T. D., Bender, M. C., Hall, T., Petty, S., O'malley, S., et al. (2019). Feasibility of a Real-time clinical augmented reality and artificial intelligence framework for pain detection and localization from the brain. *J. Med. Internet Res.* 21:e13594. doi: 10.2196/13594

Hu, X. S., Wagley, N., Rioboo, A. T., Dasilva, A., and Kovelman, I. (2020). Photogrammetry-based stereoscopic optode registration method for functional near-infrared spectroscopy. *J. Biomed. Opt.* 25, 095001. doi: 10.1117/1.JBO.25.9.095001

Huneau, C., Benali, H., and Chabriat, H. (2015). Investigating human neurovascular coupling using functional neuroimaging: a critical review of dynamic models. *Front. Neurosci.* 9, 467. doi: 10.3389/fnins.2015.00467

Kaciroti, N., Dossantos, M. F., Moura, B., Bellile, E. L., Nascimento, T. D., Maslowski, E., et al. (2020). Sensory-discriminative three-dimensional body pain mobile app measures versus traditional pain measurement with a visual analog scale: validation study. *JMIR Mhealth Uhealth* 8, e17754. doi: 10.2196/17754

Kasschau, M., Reisner, J., Sherman, K., Bikson, M., Datta, A., and Charvet, L. E. (2016). Transcranial direct current stimulation is feasible for remotely supervised home delivery in multiple sclerosis. *Neuromodulation* 19, 824–831. doi: 10.1111/ner.12430

Kasschau, M., Sherman, K., Haider, L., Frontario, A., Shaw, M., Datta, A., et al. (2015). A protocol for the use of remotely-supervised transcranial direct current stimulation (tDCS) in multiple sclerosis (MS). *J. Vis. Exp.* e53542. doi: 10.3791/53542

Kavanagh, R. N., Darcey, T. M., Lehmann, D., and Fender, D. H. (1978). Evaluation of methods for three-dimensional localization of electrical sources in the human brain. *IEEE Trans. Biomed. Eng.* 25, 421–429. doi: 10.1109/TBME.1978.326339

Kocsis, L., Herman, P., and Eke, A. (2006). The modified Beer-Lambert law revisited. *Phys. Med. Biol.* 51, N91–N98. doi: 10.1088/0031-9155/51/5/N02

Koessler, L., Maillard, L., Benhadid, A., Vignal, J. P., Felblinger, J., Vespignani, H., et al. (2009). Automated cortical projection of EEG sensors: anatomical correlation via the international 10-10 system. *Neuroimage* 46, 64–72. doi: 10.1016/j.neuroimage.2009.02.006

Li, R., Li, S., Roh, J., Wang, C., and Zhang, Y. (2020a). Multimodal neuroimaging using concurrent EEG/fNIRS for poststroke recovery assessment: an exploratory study. *Neurorehabil. Neural Repair* 34, 1099–1110. doi: 10.1177/1545968320969937

Li, R., Zhao, C., Wang, C., Wang, J., and Zhang, Y. (2020b). Enhancing fNIRS analysis using EEG rhythmic signatures: an EEG-informed fNIRS analysis study. *IEEE Trans. Biomed. Eng.* 67, 2789–2797. doi: 10.1109/TBME.2020.2971679

Liang, W. K., Lo, M. T., Yang, A. C., Peng, C. K., Cheng, S. K., Tseng, P., et al. (2014). Revealing the brain's adaptability and the transcranial direct current stimulation facilitating effect in inhibitory control by multiscale entropy. *Neuroimage* 90, 218–234. doi: 10.1016/j.neuroimage.2013.12.048

Ling, I. S., and Larsson, B. (2011). Individualized pharmacological treatment of oral mucositis pain in patients with head and neck cancer receiving radiotherapy. *Support. Care Cancer* 19, 1343–1350. doi: 10.1007/s00520-010-0955-1

Melzack, R. (1975). The McGill Pain Questionnaire: major properties and scoring methods. *Pain* 1, 277–299. doi: 10.1016/0304-3959(75)90044-5

Mihalik, A., Ferreira, F. S., Moutoussis, M., Ziegler, G., Adams, R. A., Rosa, M. J., et al. (2020). Multiple holdouts with stability: improving the generalizability of machine learning analyses of brain-behavior relationships. *Biol. Psychiatry* 87, 368–376. doi: 10.1016/j.biopsych.2019.12.001

Oostendorp, T. F., and Van Oosterom, A. (1989). Source parameter estimation in inhomogeneous volume conductors of arbitrary shape. *IEEE Trans. Biomed. Eng.* 36, 382–391. doi: 10.1109/10.19859

Peng, K., Steele, S. C., Becerra, L., and Borsook, D. (2018). Brodmann area 10: collating, integrating and high level processing of nociception and pain. *Prog. Neurobiol.* 161, 1–22. doi: 10.1016/j.pneurobio.2017.11.004

Phillips, A. A., Chan, F. H., Zheng, M. M., Krassioukov, A. V., and Ainslie, P. N. (2016). Neurovascular coupling in humans: physiology, methodological advances and clinical implications. *J. Cereb. Blood Flow Metab.* 36, 647–664. doi: 10.1177/0271678X15617954

Pinti, P., Siddiqui, M. F., Levy, A. D., Jones, E. J. H., and Tachtsidis, I. (2021). An analysis framework for the integration of broadband NIRS and EEG to assess neurovascular and neurometabolic coupling. *Sci. Rep.* 11, 3977. doi: 10.1038/s41598-021-83420-9

Racek, A. J., Hu, X., Nascimento, T. D., Bender, M. C., Khatib, L., Chiego, D. Jr., et al. (2015). Different brain responses to pain and its expectation in the dental chair. *J. Dent. Res.* 94, 998–1003. doi: 10.1177/0022034515581642

Roy, A., Baxter, B., and He, B. (2014). High-definition transcranial direct current stimulation induces both acute and persistent changes in broadband cortical synchronization: a simultaneous tDCS-EEG study. *IEEE Trans. Biomed. Eng.* 61, 1967–1978. doi: 10.1109/TBME.2014.2311071

Santosa, H., Aarabi, A., Perlman, S. B., and Huppert, T. J. (2017). Characterization and correction of the false-discovery rates in resting state connectivity using functional near-infrared spectroscopy. *J. Biomed. Opt.* 22, 55002. doi: 10.1117/1.JBO.22.5.055002

Santosa, H., Zhai, X., Fishburn, F., and Huppert, T. (2018). The NIRS brain AnalyzIR toolbox. *Algorithms* 11, 73. doi: 10.3390/a11050073

Schaller, A., Larsson, B., Lindblad, M., and Liedberg, G. M. (2015). Experiences of pain: a longitudinal, qualitative study of patients with head and neck cancer recently treated with radiotherapy. *Pain Manag. Nurs.* 16, 336–345. doi: 10.1016/j.pmn.2014.08.010

Schestatsky, P., Morales-Quezada, L., and Fregni, F. (2013). Simultaneous EEG monitoring during transcranial direct current stimulation. *J. Vis. Exp.* 76:50426. doi: 10.3791/50426

Shaw, M. T., Kasschau, M., Dobbs, B., Pawlak, N., Pau, W., Sherman, K., et al. (2017). Remotely supervised transcranial direct current stimulation: an update on safety and tolerability. *J. Vis. Exp.* 128:56211. doi: 10.3791/56211

Siegel, R., Naishadham, D., and Jemal, A. (2012). Cancer statistics, 2012. *CA Cancer J. Clin.* 62, 10–29. doi: 10.3322/caac.20138

Silva, G., Miksad, R., Freedman, S. D., Pascual-Leone, A., Jain, S., Gomes, D. L., et al. (2007). Treatment of cancer pain with noninvasive brain stimulation. *J. Pain Symptom Manage.* 34, 342–345. doi: 10.1016/j.jpainsymman.2007.06.002

Wang, H. T., Smallwood, J., Mourao-Miranda, J., Xia, C. H., Satterthwaite, T. D., Bassett, D. S., et al. (2020). Finding the needle in a high-dimensional haystack: canonical correlation analysis for neuroscientists. *Neuroimage* 216, 116745. doi: 10.1016/j.neuroimage.2020.116745

Zhang, Y., and Zhu, C. (2019). Assessing brain networks by resting-state dynamic functional connectivity: an fNIRS-EEG study. *Front. Neurosci.* 13, 1430. doi: 10.3389/fnins.2019.01430

Conflict of Interest: AD is the co-creator of GeoPain and cofounder of MoxyTech Inc, which licensed the technology from the University of Michigan.

The remaining authors declare that the research was conducted in the absence of any commercial or financial relationships that could be construed as a potential conflict of interest.

Publisher's Note: All claims expressed in this article are solely those of the authors and do not necessarily represent those of their affiliated organizations, or those of the publisher, the editors and the reviewers. Any product that may be evaluated in this article, or claim that may be made by its manufacturer, is not guaranteed or endorsed by the publisher.

frontiers | Frontiers in Molecular Neuroscience

TYPE Original Research
PUBLISHED 13 September 2022
DOI 10.3389/fnmol.2022.956797

OPEN ACCESS

EDITED BY
Fengxian Li,
Southern Medical University, China

REVIEWED BY
Daniele Corbo,
University of Brescia, Italy
Katherine N. Theken,
University of Pennsylvania,
United States
Yuefeng Li,
Jiangsu University, China

*CORRESPONDENCE
Junrong Li
ljry612@163.com
Hong Zhang
jnyyfsk@126.com

†These authors have contributed equally to this work

SPECIALTY SECTION
This article was submitted to Pain Mechanisms and Modulators, a section of the journal Frontiers in Molecular Neuroscience

RECEIVED 30 May 2022
ACCEPTED 22 August 2022
PUBLISHED 13 September 2022

CITATION
Wei H-L, Yang W-J, Zhou G-P, Chen Y-C, Yu Y-S, Yin X, Li J and Zhang H (2022) Altered static functional network connectivity predicts the efficacy of non-steroidal anti-inflammatory drugs in migraineurs without aura.
Front. Mol. Neurosci. 15:956797.
doi: 10.3389/fnmol.2022.956797

Altered static functional network connectivity predicts the efficacy of non-steroidal anti-inflammatory drugs in migraineurs without aura

Heng-Le Wei[1†], Wen-Juan Yang[2†], Gang-Ping Zhou[1], Yu-Chen Chen[3], Yu-Sheng Yu[1], Xindao Yin[3], Junrong Li[2]* and Hong Zhang[1]*

[1]Department of Radiology, Nanjing Jiangning Hospital, Nanjing, China, [2]Department of Neurology, Nanjing Jiangning Hospital, Nanjing, China, [3]Department of Radiology, Nanjing First Hospital, Nanjing Medical University, Nanjing, China

Brain networks have significant implications for the understanding of migraine pathophysiology and prognosis. This study aimed to investigate whether large-scale network dysfunction in patients with migraine without aura (MwoA) could predict the efficacy of non-steroidal anti-inflammatory drugs (NSAIDs). Seventy patients with episodic MwoA and 33 healthy controls (HCs) were recruited. Patients were divided into MwoA with effective NSAIDs (M-eNSAIDs) and with ineffective NSAIDs (M-ieNSAIDs). Group-level independent component analysis and functional network connectivity (FNC) analysis were used to extract intrinsic networks and detect dysfunction among these networks. The clinical characteristics and FNC abnormalities were considered as features, and a support vector machine (SVM) model with fivefold cross-validation was applied to distinguish the subjects at an individual level. Dysfunctional connections within seven networks were observed, including default mode network (DMN), executive control network (ECN), salience network (SN), sensorimotor network (SMN), dorsal attention network (DAN), visual network (VN), and auditory network (AN). Compared with M-ieNSAIDs and HCs, patients with M-eNSAIDs displayed reduced DMN-VN and SMN-VN, and enhanced VN-AN connections. Moreover, patients with M-eNSAIDs showed increased FNC patterns within ECN, DAN, and SN, relative to HCs. Higher ECN-SN connections than HCs were revealed in patients with M-ieNSAIDs. The SVM model demonstrated that the area under the curve, sensitivity, and specificity were 0.93, 0.88, and 0.89, respectively. The

widespread FNC impairment existing in the modulation of medical treatment suggested FNC disruption as a biomarker for advancing the understanding of neurophysiological mechanisms and improving the decision-making of therapeutic strategy.

KEYWORDS

migraine, functional network connectivity, non-steroidal anti-inflammatory drugs, efficacy, machine learning

Introduction

Migraine is a persistent, disabling neurological disorder involving moderate-to-severe headache attacks, which can last up to 72 h, and related unpleasant symptoms (Headache Classification Committee of the International Headache Society [IHS], 2013). It is the second leading cause of neuronal disability in the world, which may lead to personal suffering and impaired quality of life with significant socioeconomic burdens (Feigin et al., 2019; Abrams et al., 2020). In the United States alone, its estimated healthcare cost is about $1 billion annually (Mennini et al., 2008). Migraine affects approximately 15% of the general population worldwide (Abrams et al., 2020). Given the health and socio-economic burden caused by migraine, exploring effective treatments for the disorder is one of the key areas of clinical research. Several studies have continuously proposed, developed, and tested more specific drugs for migraine treatment. Although several pharmacological choices are available to treat migraines, none of such treatments are ideal for most people. Regardless of that, non-steroidal anti-inflammatory drugs (NSAIDs) are still the first-line drugs for the acute treatment of migraines (Ashina, 2020). Currently, the selection strategy for NSAIDs is still mainly based on trial and error. Possible explanations include various pathophysiological mechanisms with complexity in migraine. The trial-and-error approach not only prolongs the treatment time but also increases the ineffective cost. Recent studies have focused on understanding the pathophysiological mechanism of migraine to develop new theories for improving the treatment efficacy. For instance, neuroimaging studies have transformed the understanding of migraine from a vascular to a neurovascular, and most recently, to a central neural system disorder (Schwedt et al., 2015). However, the effect of brain functional alterations on migraine treatment remains unknown.

The resting-state functional magnetic resonance imaging (rs-fMRI), a non-invasive neuroimaging examination, has therefore attracted considerable attention. It is reported that neurogenic inflammation resulting from activation of the trigeminovascular pathway is the main cause of migraine attacks (Goadsby et al., 2017). Various studies have suggested that the cortical feed-forward system originates from the trigeminal neurovascular pathway and connects to the higher-sensory cortex (Brennan and Pietrobon, 2018; Tu et al., 2020). Yu et al. (2017) and Chen et al. (2019) revealed the alterations in either regional brain activity or functional connectivity among core cognitive networks located in the trigeminovascular pathway, such as the default mode network (DMN), executive control network (ECN), and salient network (SN), and their correlations with clinical characteristics in patients with migraine. Nonetheless, they only focused on regional and seed-based functional changes, or a limited number of prior selected networks, and have not done a comprehensive analysis of the abnormal connections among the large-scale functional networks in migraine. Some studies have linked complex subjective experiences like perception and processing of pain in patients with migraine to functional integration among intrinsic large-scale functional networks and reported significant differences (Zhang et al., 2016; Coppola et al., 2018; Wei et al., 2020). These studies provided initial evidence regarding abnormal interactions among the functional networks in migraine. Although these rs-fMRI studies have proved that functional alterations between different large-scale networks were associated with the neurophysiological mechanism of migraine, less is known about the interactions among the large-scale networks and their influence on the treatment efficacy in migraine.

Additionally, machine learning models based on clinical and neuroimaging data have shown great potential in constructing automatic predictors in the field of classification and treatment of migraine (Pérez Benito et al., 2019; Kwon et al., 2020; Liu et al., 2020; Mu et al., 2020). However, predictors for the efficacy of NSAIDs are still in their infancy. It has been revealed that migraine subtypes can have various influences on the efficacy of drugs because of their diverse pathophysiological mechanisms. Therefore, this study attempted to investigate the possible neural mechanisms for underpinning the efficacy of NSAIDs in patients with migraine without aura (MwoA) using a combination of functional network connectivity (FNC) analysis and a support vector machine (SVM) algorithm. We hypothesized that patients with MwoA and showing an effective response to NSAIDs (M-eNSAIDs) may display significant FNC differences among large-scale networks involved in modulating

nociception and predicting efficacy, compared to patients with ineffective response to NSAIDs (M-ieNSAIDs). Substantive differences, as revealed in this study, may be linked with clinical characteristics, and provide novel insights into elucidating the pathophysiological mechanism and developing treatment strategies for migraine.

Materials and methods

Participants

A total of 73 patients diagnosed with episodic MwoA in the neurological outpatient clinic were prospectively and continuously enrolled. The diagnosis of patients with MwoA was based on the International Classification of Headache Disorders, 3rd edition (ICHD-3) (Headache Classification Committee of the International Headache Society [IHS], 2013). To control the potential pharmacological and physiological effects, the inclusion criteria were: (1) patients were drug-free for at least 1 month before being enrolled; (2) patients in the interictal phase were headache-free for at least 3 days before and after scanning, ascertained by a structured telephonic interview. Thirty-three healthy subjects (all right-handed) matched for age, sex, and education level were recruited as healthy controls (HCs). The general exclusion criteria included: (1) comorbidity with other forms of headache and neuropsychological or neurological diseases, (2) a history of previous brain injury or psychoactive medication use, (3) a history of alcohol or drug abuse, (4) pregnant or lactating women, and (5) any contraindications to MRI scanning.

Clinical characteristics

All migraine participants underwent comprehensive questionnaires during the first visit and were followed up via telephone. The questionnaires primarily include demographic data (e.g., age, sex, and education level) and migraine characteristics (e.g., disease duration, frequency and attack duration, headache intensity, the extent of the impact, and burden on quality of life). Namely, headache intensity was recorded on the Visual Analog Scale (VAS); impact and disability on an individual were assessed by Headache Impact Test-6 item (HIT-6) and Migraine Disability Assessment Scale (MIDAS), respectively. We also applied the Montreal Cognitive Assessment (MoCA) to evaluate cognitive impairment (all participants' MoCA scores were > 25). Patients were asked to record a headache diary about headache intensity (VAS score) before and 2 h after drug intake within 3 months after scanning. According to the criteria, the complete response, partial response, minimal response, and no response were classified as $>$ 75% reduction, 50–75% reduction, 25–50% reduction, and $<$ 25% reduction in VAS scores, respectively (Yadav et al., 2020). The response to NSAIDs was defined as a 50% or greater reduction in pain intensity from pre-treatment level to post-treatment level at least 2 times.

Magnetic resonance imaging acquisition

All MRI data were acquired on a 3.0-Tesla Philips MRI scanner (Ingenia) with an eight-channel head coil. For this analysis, the functional images were acquired axially using a gradient echo-planar imaging sequence as follows: repetition time (TR) = 2,000 ms; echo time (TE) = 30 ms; slices = 36; thickness = 4 mm; gap = 0 mm; field of view (FOV) = 240 mm × 240 mm; acquisition matrix = 64 × 64; and flip angle (FA) = 90°. Moreover, structural images were obtained using a three-dimensional turbo fast echo T1WI sequence with the following parameters: TR/TE = 8.1/3.7 ms; slices = 170; thickness = 1 mm; gap = 0 mm; FA = 8°; acquisition matrix = 256 × 256; FOV = 256 mm × 256 mm. During the scanning, scanner noise and head motion were reduced using earplugs and foam padding, and the participants were instructed to reflex and lie with their eyes closed but not fall asleep.

Data pre-processing

Image preprocessing was performed using the Resting-state fMRI Data Analysis Toolkit plus V1.24 (RESTplus V1.24).[1] The preprocessing included the following steps: discarding the first 10 volumes, slice timing correction with the 35th slice as the reference, realignment of head motion, and normalizing corrected images to the Montreal Neurological Institute space ($3 \times 3 \times 3$ mm^3) using the diffeomorphic anatomical registration through exponentiated lie (DARTEL) algebra, and spatial smoothing with a 6-mm full-width half-maximum (FWHM) Gaussian kernel. Moreover, subjects with excessive head motion in any direction ($>$2 mm or 2°) were excluded from the analysis.

Independent component analysis and static functional network connectivity analysis

The Group ICA of fMRI Toolbox (GIFT 4.0a)[2] was used to extract independent networks. The preprocessed data were automatically decomposed into spatial independent

1 http://restfmri.net/forum/
2 http://icatb.sourceforge.net/

components (ICs) by the minimum description length (MDL) criteria. Then the data were concatenated and reduced by subject-level and group-level principal component analysis, using the Infomax algorithm. Subsequently, the GICA-3 back reconstruction step was used to separate single-subject components from the set of aggregate components. Finally, the spatial component maps were acquired and the value of connectivity strength within each IC was converted into a z-score.

After the ICA, the individual-level time courses of recognized components were deduced via the spatio-temporal double regression method. The relationship between the time courses of different pairwise networks was determined using static FNC analysis. Briefly, a band-pass filter (band-pass 0.01–0.15 Hz) was used to reduce the potential influence of low-and high-frequency noise on the time course. Then, the Pearson correlation coefficient between the ICs was performed to calculate the FNC strength. An FNC matrix with the dimensions of 12 times 12 (selected ICs) times 103 (participants) was realized.

Prediction for non-steroidal anti-inflammatory drugs efficacy

Migraineurs were randomly divided into the training and testing cohorts, in the ratios of 80%/20%, 75%/25%, and 70%/30%, respectively. To classify the efficacy of NSAIDs, the SVM model based on abnormal FNC patterns between two migraine subgroups was trained by a fivefold cross-validation strategy in the training cohort. Subsequently, the model was tested on the internal testing cohort. The receiver operating characteristic (ROC) curve was plotted to determine the area under the curve (AUC). Calculations to determine sensitivity and specificity were also measured.

Statistical analysis

The SPSS 25.0 software was used for statistical analyses and the level of significance was set at $p < 0.05$. The demographic characteristics of the three groups were compared using one-way analyses of variance (ANOVA) for the normally distributed continuous variables, while the Kruskal–Wallis test was employed for the non-normally distributed continuous variables. The clinical characteristics of the two migraine groups were compared using a two-sample *t*-test for the normally distributed continuous variables and the Mann–Whitney test for the non-normally distributed continuous variables. Comparisons between categorical variables were determined using the Chi-square test.

For FNC analysis, the correlation coefficients of each pairwise component among the three groups were compared. All *post hoc* tests were corrected by the Bonferroni correction method ($p < 0.05/3$). Furthermore, the partial correlation analysis between the FNC strength and migraine-related characteristics was calculated at a significant level of $p < 0.05$, controlling for age, sex, and education level.

Results

Demographics and clinical characteristics

After the fMRI data head motion check, three patients were excluded because of excessive head motion artifacts. Therefore, the final cohort consisted of patients with seventy MwoA and 33 healthy participants. There was no significant difference in the demographic and clinical data among the three groups ($p > 0.05$) (**Table 1**).

Independent component analysis and component selection

In this study, 26 ICs were automatically extracted, and 12 components of them were selected as the resting-state networks for further analysis (**Figure 1**). Afterward, seven large-scale networks within the 12 components were labeled (Li et al., 2019, 2020). The first was the ECN (IC8, IC11, and IC16). This mainly focused on the dorsolateral prefrontal cortex, inferior parietal lobule, and superior parietal lobule. The second was the DMN (IC14, IC20), which includes the medial prefrontal cortex, posterior cingulate cortex (PCC), precuneus, inferior parietal gyrus, and angular gyrus. The third was the SN (IC1), which mainly consists of the anterior cingulate cortex (ACC), anterior insular cortex, and part of the prefrontal areas. The fourth was the sensorimotor network (SMN) (IC4), which included the supplementary motor area, the paracentral lobule, the precentral gyrus, and the postcentral gyrus. The fifth was the dorsal attention network (DAN) (IC19) which mainly includes the bilateral intraparietal sulcus, frontal eye field, and middle temporal lobe. The DAN was followed by the auditory network (AN) (IC15). The auditory network includes the temporal lobe and the surrounding temporal-parietal association cortex. Finally, was the visual network (VN) (IC5, IC24, IC26), which includes the primary visual cortex and extra-visual cortex.

Group-level differences in functional network connectivity analysis

For the FNC analysis between all patients and HCs, patients with MwoA had increased connections, including SN (IC1)-

TABLE 1 The demographic and clinical characteristics of MwoA patients and HCs.

	M-eNSAIDs	M-ieNSAIDs	HCs	$F/t/\chi$ 2	*P*-value
Age (years)	33.91 ± 10.75	35.69 ± 11.47	36.30 ± 10.38	0.445	0.642
Sex (male/female)	3/32	4/31	2/31	0.669	0.907
Education (years)	13.54 ± 2.81	13.11 ± 3.08	12.39 ± 4.06	1.020	0.364
Disease duration (years)	7.94 ± 6.15	11.60 ± 10.08	/	−1.832	0.071
Frequency (days/month)	4.77 ± 3.15	5.23 ± 5.76	/	−0.412	0.682
Attack duration (hours)	17.31 ± 13.81	17.03 ± 15.05	/	0.083	0.934
VAS score	6.40 ± 1.54	5.97 ± 1.65	/	1.123	0.265
MIDAS score	38.97 ± 32.26	37.29 ± 31.78	/	0.220	0.826
HIT-6 score	57.57 ± 8.86	60.34 ± 9.41	/	−1.269	0.209
Drug types (Ibuprofen/Aspirin)	30/5	28/7	/	0.402	0.752

Values for continuous variables are mean ± standard deviation. HCs, healthy controls; HIT, headache impact test; MIDAS, migraine disability assessment scale; M-eNSAIDs, MwoA with effective NSAIDs; M-ieNSAIDs, MwoA with ineffective NSAIDs; MwoA, migraine without aura; NSAIDs, non-steroid anti-inflammatory drugs; VAS, visual analogue scale.

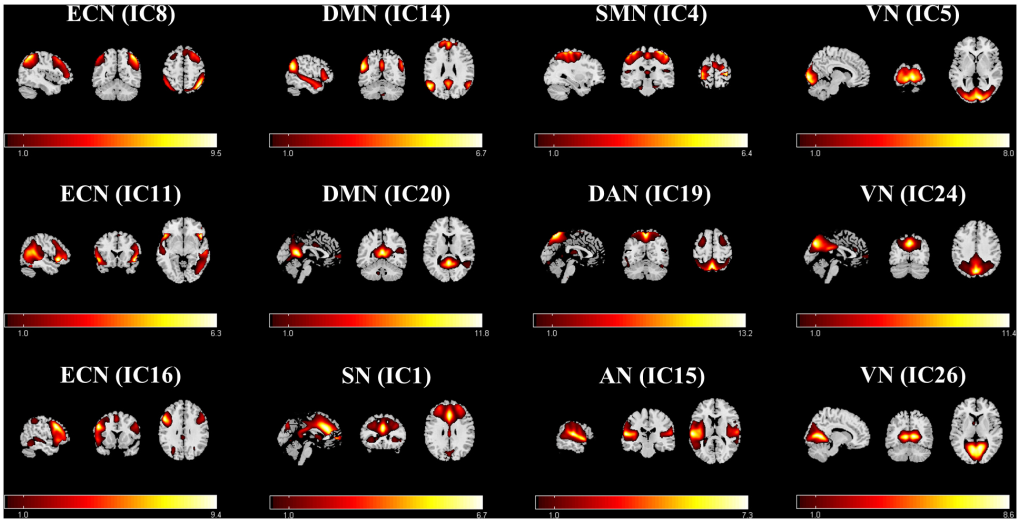

FIGURE 1
Functional relevant resting-state networks. The spatial maps of the 12 independent components were selected for further analysis. AN, auditory network; DAN, dorsal attention network; DMN, default mode network; ECN, executive control network; SMN, sensorimotor network; SN, salient network; VN, visual network.

ECN (IC8), SN (IC1)-ECN (IC16), SN (IC1)-DAN (IC19), and ECN (IC16)-DAN (IC19) (Figure 2A). For the FNC analysis among the three groups, nine FNC patterns were shown to be significantly altered (Figures 2B–D). Relative to patients with M-ieNSAIDs, patients with M-eNSAIDs exhibited significantly opposite interactions in three networks, including the decreased DMN (IC14)-VN (IC5, IC26) and increased VN (IC5)-AN (IC15) connections. Moreover, compared with HCs, patients with M-eNSAIDs showed significantly increased FNC patterns for SN (IC1)-ECN (IC16), SN (IC1)-DAN (IC19), VN (IC5)-AN (IC15), and ECN (IC16)-DAN (IC19) connections. On the contrary, there was revealed a decreased connection between SMN (IC4)-VN (IC26). In addition, SN (IC1)- ECN (IC8) connection was also found to be significantly increased in patients with M-ieNSAIDs, compared with HCs.

Correlation analysis

There were significant correlations between the SMN-VN connection and frequency ($r = -0.424$, $p = 0.016$), as well as between the ECN-SN connection and frequency ($r = 0.565$, $p = 0.001$) in patients with M-eNSAIDs (Figure 3). However, there was no correlation between migraine-related characteristics and abnormal FNC patterns, neither in all patients with MwoA nor in patients who did not respond to NSAIDs.

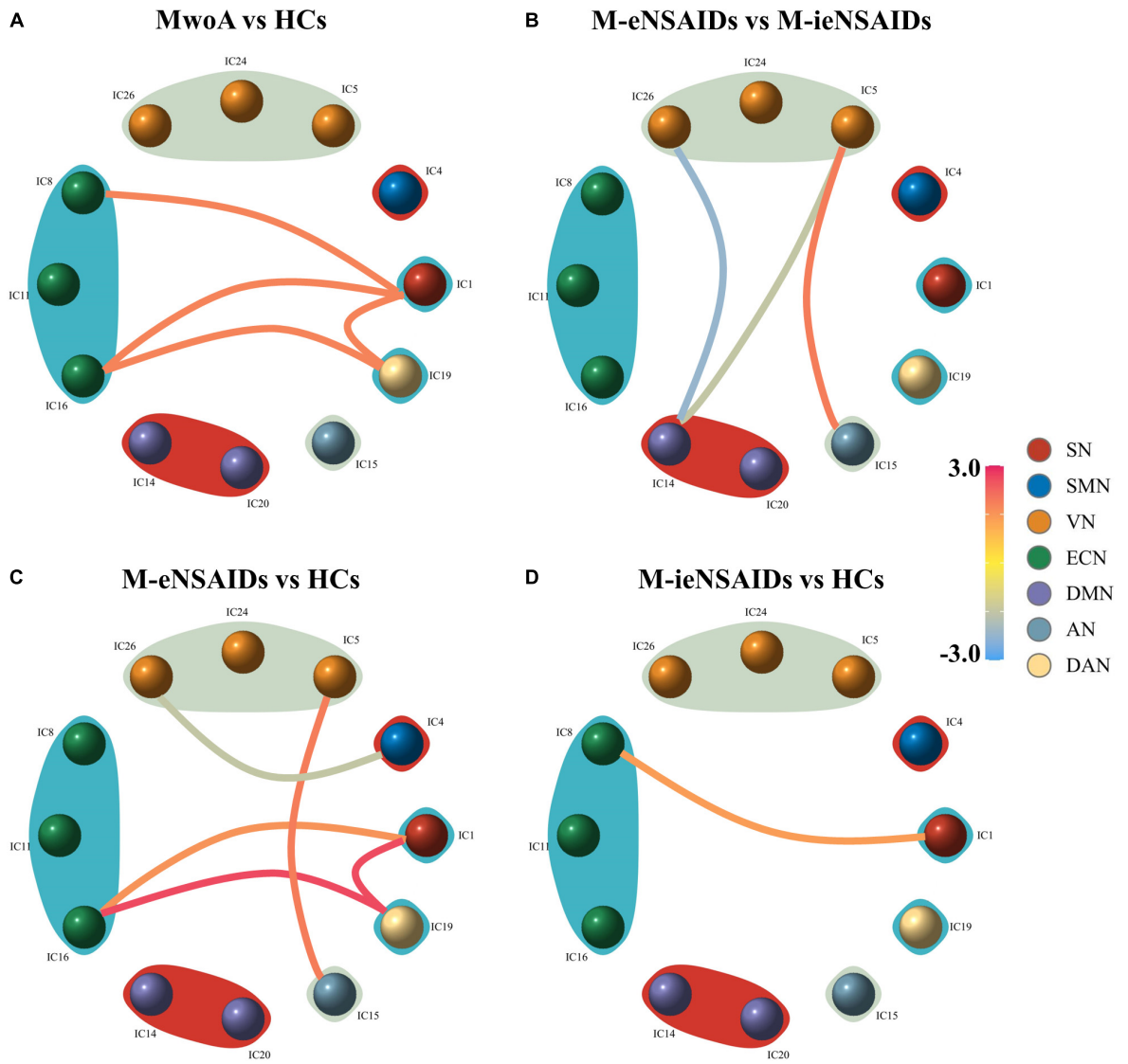

FIGURE 2
Group-level differences in static functional network connectivity patterns. **(A–D)** AN, auditory network; DAN, dorsal attention network; DMN, default mode network; ECN, executive control network; SMN, sensorimotor network; SN, salient network; VN, visual network; M-eNSAIDs, MwoA with effective NSAIDs; M-ieNSAIDs, MwoA with ineffective NSAIDs; MwoA, migraine without aura; NSAIDs, non-steroid anti-inflammatory drugs.

Support vector machine model performance

The SVM model with an allocation ratio of 75%/25% demonstrated a better predictive capacity, with an AUC of 0.93, the sensitivity of 0.88, and a specificity of 0.89 (Figure 4).

Discussion

To our knowledge, this study is the first time through the ICA approach to explore the inter-network connectivity and the relationship with the efficacy of NSAIDs in patients with MwoA. The DMN and several somatosensory-associated networks, including the VN, AN, and SMN, were detected to be abnormal in patients with M-eNSAIDs. Meanwhile, the two migraine subgroups also showed increased alterations of the inter-network functional coupling in the higher-level executive areas, such as SN, ECN, and DAN, when compared with HCs. Interestingly, only SN-ECN functional abnormality was found between both two subgroups and HCs, which may indicate that the executive control function of the SN and ECN is mainly manifested in the potential neuroimaging features for migraine. These results reveal evidence of aberrant connectivity patterns

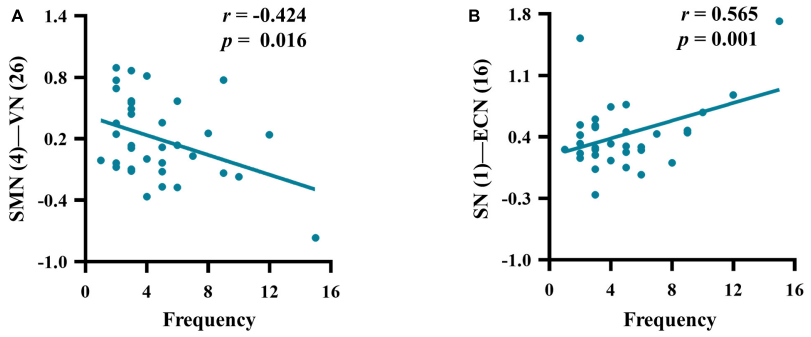

FIGURE 3
Correlations between the mean z-scores of functional network connectivity and headache frequency **(A–B)** in migraineurs with effective NSAIDs (for other abbreviations see **Figure 2** legend).

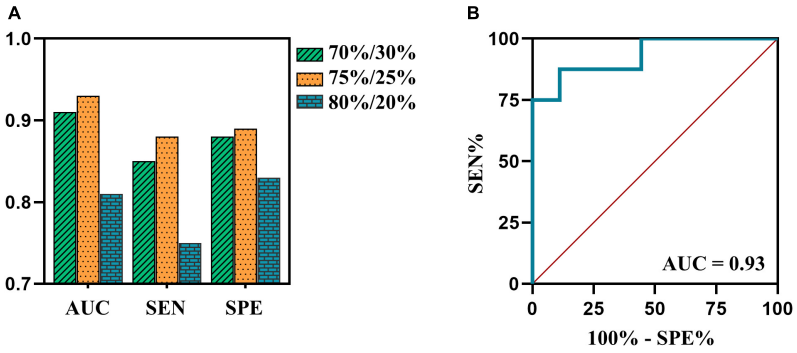

FIGURE 4
(A) The AUCs, sensitivity and specificity of SVM model in testing cohort of 70%/30%, 75%/25%, and 80%/20% datasets are 0.91, 0.85, and 0.88 (green bar); 0.93, 0.88, and 0.89 (orange bar); 0.81, 0.75, and 0.83 (blue bar), respectively. **(B)** The ROC curve of SVM model in testing cohort of 75%/25% dataset. AUC, area under the curve; ROC, receiver operating characteristic; SEN, sensitivity; SPE, specificity; SVM, support vector machine.

across core neurocognitive networks in migraineurs and provide a proposition complementary to the point that migraine involves dysfunctional cortical-subcortical circuitry. Moreover, the observed correlations between FNC abnormalities and clinical parameters may not only improve the understanding of the pathophysiologic features of migraine but also further highlight neuroimaging characteristics in migraine treatment.

Visual and auditory discomforts are the most common complaints of migraine patients during both ictal and interictal periods. Thus, the visual and auditory cortex may play an important role in the neurophysiological mechanisms and treatment strategies. Moreover, the visual and auditory cortices have been demonstrated to be abnormal neural activity in the acupuncture treatment of migraine patients (Yang et al., 2012; Liu et al., 2020). An acupuncture study showed that the visual-related regions could predict the therapeutic efficacy of acupuncture in migraineurs without aura (Liu et al., 2020). In the present study, the functional connectivity strength of VN-AN in patients with M-eNSAIDs was significantly higher than that of patients with M-ieNSAIDs and HCs. It may imply that this connection pattern could play an important role in the development and treatment of migraine. Also, the pattern may be a neuroimaging marker for predicting the treatment efficacy for migraine. Moreover, a decreased FNC pattern between SMN and VN showed a significant negative correlation with headache frequency in the present study. Similarly, a prior study revealed that there was a bidirectional connection between SMN and VN in patients with MwoA (Wei et al., 2020). Furthermore, it was reported that the activity of SMN is positively correlated with headache frequency, which is contrary to our results. However, another study showed that multiple increased VN-related functional connections were negatively correlated with headache frequency in patients with MwoA (Wei et al., 2021). Although consistency has been maintained in the migraine population according to the ICHD-3, the controversial results of these studies may be caused by the patients of different subtypes and complex pathological mechanisms of migraine. Long-term and repeated migraine attacks could lead to somatosensory and visual cortex changes. When this happens, it may result in dysfunctional relief of pain and modulation of mental disorders,

as well as the efficacy of NSAIDs. These findings suggest that altered intrinsic FNC architecture could provide a novel perspective to understand the neural circuits of NSAIDs in migraine, providing a more appropriate therapeutic strategy.

Results of the FNC abnormality of patients with M-eNSAIDs showed evidence of several prominent networks in the high cognitive and sensory networks. These included FNC pairs associated with DMN regions extending to sensory functional nodes (visual cortex and auditory cortex). The DMN is active in the resting condition and has a salient function in the functional network architecture of the resting-state brain. The main functions of the DMN are to maintain the steady state of the endogenous environment and exclude the interference of exogenous stimuli. When stimulated by endogenous or exogenous stimuli, the trigeminovascular pathway enters into an active status to suppress the DMN function and activates the executive regions to inhibit the pain signals. However, disrupted brain-network circuits contribute to inefficient control performance and headache attacks (Menon, 2019). A growing body of evidence (Zhang et al., 2016; Lo Buono et al., 2017) indicates similar results that, compared with HCs, migraine patients showed significantly increased spontaneous neuronal activity in the DMN. Also, the functional coupling between the DMN and other pain inhibitory cortex is associated with pain inhibition efficiency. Previous task-state fMRI studies (Hougaard et al., 2014; Wang et al., 2017) have reported greater visual-induced DMN activation in patients with migraine, indicating correlations and synchronizations between the DMN and VN. Hence, the disrupted DMN-VN connection may be involved in the information transfer and multimodal integration dysfunction affecting the clinical efficacy of NSAIDs for migraineurs.

A PET study (Di et al., 2013) also showed similar cerebral glucose hypermetabolism in the DMN in chronic migraine patients with analgesic overuse relative to patients without overuse. The ability of DMN to enhance functional hyperresponsiveness is possibly associated with pathogenesis and drug overuse. Similar to the aforementioned studies, the results of the current study reflected elevated functional connectivity in the static state involving the DMN in migraine patients. Additionally, Kong et al. (2010) studied the effect of pain intensity on DMN activation and deactivation in a healthy cohort, demonstrating an intriguing result that moderate-intensity nociception decreased DMN activity to a lesser extent than did severity-intensity nociception. The report suggested that deactivation of DMN may be a compensatory physiological response to the pain perception and higher intensity of painful stress exceeding the regulatory threshold of pain stimuli, leading to dysfunctional deactivation. On the basis of the current study, compared with the M-ieNSAIDs patients, only patients with M-eNSAIDs demonstrated lower connectivity strength between DMN and VN. These results suggest that NSAIDs may exert analgesic effects by depressing the activity of the DMN, but excessive DMN activity may eventually result in invalid efficacy. Nevertheless, an ASL study (Hodkinson et al., 2015) attended to explore the activation in response to NSAIDs-induced analgesia. The study concluded that there was significantly enhanced cerebral blood flow in the PCC and nearby limbic system, and significant negative analgesic interaction in the SN and prefrontal cortex in post-surgery patients. The completely opposite findings may be due to variations in methodology and heterogeneity of populations between post-surgery patients and headache-free migraineurs. On the other hand, similar to the current study, the ASL study verified that the functional imbalance of task-free and task-positive networks may be the substrate neuromechanism in the perception and modulation of pain.

The present findings further showed that enhanced FNC connections among the large-scale networks including ECN, DAN, and SN are important for efficient therapy. ECN and DAN are dubbed the "task-positive networks," well-characterized by the performance of cognitive control and attention-demanding tasks. The previous study has called attention to the presence of anticorrelations between the DMN and the task-positive networks in pain perception (Ter Minassian et al., 2013). The study reported that during pain perception, the DMN was activated, as was the DAN, showing the anticorrelation between DMN and DAN disappears in chronic pain patients. This findings of this study are in agreement with our results that revealed lower DMN-related and higher task-related connections in migraineurs with an effective response to NSAID treatment. Moreover, the present study indicated that there was a significant increase in the connections between ECN-SN and DAN-SN. The SN, consisting of the insula and dorsal ACC, responds to the perception and chronification of pain (Lu et al., 2016), modulation of emotion (Gasquoine, 2014), and making of decisions (Chand and Dhamala, 2016). Furthermore, the SN, related to gating the nociceptive hypersensitivity pathway (Tan et al., 2017), performs its function as a switch to deactivate the DMN and activate the ECN when a salient stimulus is ongoing (Menon, 2019). These three components (DMN, ECN, and SN) constituted a "triple-network model," mapping the salient aberrance and cognitive deficits across neurological disorders (Menon, 2011), including the migraine. Additionally, a nociceptive-task study displayed opposite functional patterns between the DMN and ECN observed in healthy subjects, confirming this functional coupling model is an effective physiological modulation for inhibiting nociception (Kong et al., 2010).

The results of this study showed similar anti-correlations among the three core networks, which may provide a new perspective on investigating the potential mechanisms underlying migraine treatment. Besides, the functional imbalance of the triple-network model in this study induced significant and potential correlations with headache frequency.

Recently, gradually increasing evidence has suggested that clinical characteristics are strongly linked with inter-network functional deficits (Russo et al., 2012; Lo Buono et al., 2017; Coppola et al., 2018). Reciprocally, these migraine-related features may be potentially vital for influencing the progression of the disease and the quality of therapy (Zou et al., 2019). This result of association with headache frequency implies understanding of the neural mechanisms facilitating the transition from episodic to chronic migraine.

These results demonstrated that abnormal FNC patterns were associated with neurophysiological mechanisms of migraine and NSAID treatment, and represented a novelty approach to predicting NSAIDs efficacy, since to our knowledge network-level neuroimaging characteristics had never been considered predictive variables. We believe that our findings provide a foundation for a new line of research oriented to individually predicting NSAIDs efficacy in patients with MwoA, as well as its significant interaction with neuroimaging FNC characteristics. These neuroimaging variables could be taken into account for the selection and implementation of improving NSAIDs efficacy and enhancing the quality of life in patients with MwoA.

Although the study was to examine targeted relationships between FNC patterns and the efficacy of NSAIDs, some limitations need to be addressed. First, the large-scale brain networks involved in this study are limited. Other brain networks may also play a vital role in the neurophysiology of drug treatment in migraineurs, thus exploring the extending FNC abnormalities among the multiple networks may give insight into the neural mechanism. Second, cause-and-effect relationships between altered FNC patterns and the efficacy of NSAIDs should be cautiously interpreted using a longitudinal study in the future. Third, despite not taking any medication for 1 month before the scanning, the effect of other analgesic drugs on neurological function cannot be ruled out completely. Fourth, the models in this work underwent only internal tests, future work should focus on additional validation using external data to confirm the robustness. Moreover, no significant results persisted after Bonferroni correction for multiple comparisons in the FNC analyses due to the relatively strict method. Nonetheless, our research is still meaningful as it forms a basis upon which future novel studies can be developed. Finally, this study only explored the non-directional FNC interactions between static networks using the ICA approach. Further studies are needed to reflect the characteristics of temporal and directional function in the coupling between brain networks.

Conclusion

The major strength and novelty of this study are that inter-static FNC patterns participate in the pain processing and medicine treatment in patients with migraine. The present data support the notion that the development of the antinociceptive effects of NSAIDs is mediated via the triple-network model, involving the descending pain inhibitory pathway, which provides meaningful insights for further understanding the neural mechanism of migraine treatment.

Data availability statement

The original contributions presented in this study are included in the article/supplementary material, further inquiries can be directed to the corresponding author/s.

Ethics statement

The studies involving human participants were reviewed and approved by the Ethics Committee of Nanjing Jiangning Hospital, affiliated with Nanjing Medical University. The patients/participants provided their written informed consent to participate in this study.

Author contributions

H-LW, W-JY, and HZ designed the study. G-PZ and Y-SY acquired the data. H-LW, Y-CC, and Y-SY performed the data analysis. W-JY, Y-CC, and XY interpreted the results. H-LW and W-JY prepared the manuscript. JL and HZ revised the manuscript and corrected the English. All authors contributed to manuscript revision and approved the submitted version.

Funding

This work was supported by the Science and Technology Development Project, Nanjing of China (YKK20202) and Science and Technology Development Project of Nanjing Medical University (NMUB2020168).

Acknowledgments

We thank the participants for sharing their time.

Conflict of interest

The authors declare that the research was conducted in the absence of any commercial or financial relationships that could be construed as a potential conflict of interest.

Publisher's note

References

Abrams, E. M., Akombi, B., Alam, S., Alcalde-Rabanal, J. E., Allebeck, P., Amini-Rarani, M., et al. (2020). Global burden of 369 diseases and injuries in 204 countries and territories, 1990–2019: A systematic analysis for the Global Burden of Disease Study 2019. *Lancet* 396, 1204–1222. doi: 10.1016/S0140-6736(20)30925-9

Ashina, M. (2020). Migraine. *New Engl. J. Med.* 383, 1866–1876. doi: 10.1056/NEJMra1915327

Brennan, K. C., and Pietrobon, D. (2018). A systems neuroscience approach to migraine. *Neuron* 97, 1004–1021. doi: 10.1016/j.neuron.2018.01.029

Chand, G. B., and Dhamala, M. (2016). The salience network dynamics in perceptual decision-making. *Neuroimage* 134, 85–93. doi: 10.1016/j.neuroimage.2016.04.018

Chen, C., Yan, M., Yu, Y., Ke, J., Xu, C., Guo, X., et al. (2019). Alterations in regional homogeneity assessed by fMRI in patients with migraine without aura. *J. Med. Syst.* 43:298. doi: 10.1007/s10916-019-1425-z

Coppola, G., Di Renzo, A., Tinelli, E., Di Lorenzo, C., Scapeccia, M., Parisi, V., et al. (2018). Resting state connectivity between default mode network and insula encodes acute migraine headache. *Cephalalgia* 38, 846–854. doi: 10.1177/0333102417715230

Di, W., Shi, X., Zhu, Y., Tao, Y., Qi, W., Luo, N., et al. (2013). Overuse of paracetamol caffeine aspirin powders affects cerebral glucose metabolism in chronic migraine patients. *Eur. J. Neurol.* 20, 655–662. doi: 10.1111/ene.12018

Feigin, V. L., Nichols, E., Alam, T., Bannick, M. S., Beghi, E., Blake, N., et al. (2019). Global, regional, and national burden of neurological disorders, 1990–2016: A systematic analysis for the Global Burden of Disease Study 2016. *Lancet Neurol.* 18, 459–480. doi: 10.1016/S1474-4422(18)30499-X

Gasquoine, P. G. (2014). Contributions of the insula to cognition and emotion. *Neuropsychol. Rev.* 24, 77–87. doi: 10.1007/s11065-014-9246-9

Goadsby, P. J., Holland, P. R., Martins-Oliveira, M., Hoffmann, J., Schankin, C., and Akerman, S. (2017). Pathophysiology of migraine: A disorder of sensory processing. *Physiol. Rev.* 97, 553–622. doi: 10.1152/physrev.00034.2015

Headache Classification Committee of the International Headache Society [IHS] (2013). The International Classification of Headache Disorders, 3rd edition (beta version). *Cephalalgia* 33, 629–808. doi: 10.1177/0333102413485658

Hodkinson, D. J., Khawaja, N., O'Daly, O., Thacker, M. A., Zelaya, F. O., Wooldridge, C. L., et al. (2015). Cerebral analgesic response to nonsteroidal anti-inflammatory drug ibuprofen. *Pain* 156, 1301–1310. doi: 10.1097/j.pain.0000000000000176

Hougaard, A., Amin, F. M., Hoffmann, M. B., Rostrup, E., Larsson, H. B. W., Asghar, M. S., et al. (2014). Interhemispheric differences of fMRI responses to visual stimuli in patients with side-fixed migraine aura. *Hum. Brain Mapp.* 35, 2714–2723. doi: 10.1002/hbm.22361

Kong, J., Loggia, M. L., Zyloney, C., Tu, P., LaViolette, P., and Gollub, R. L. (2010). Exploring the brain in pain: Activations, deactivations and their relation. *Pain* 148, 257–267. doi: 10.1016/j.pain.2009.11.008

Kwon, J., Lee, H., Cho, S., Chung, C., Lee, M. J., and Park, H. (2020). Machine learning-based automated classification of headache disorders using patient-reported questionnaires. *Sci. Rep.* 10:14062. doi: 10.1038/s41598-020-70992-1

Li, C., Deng, Y., He, Y., Zhai, H., and Jia, F. (2019). The development of brain functional connectivity networks revealed by resting-state functional magnetic resonance imaging. *Neural Regen. Res.* 14:1419. doi: 10.4103/1673-5374.253526

Li, F., Lu, L., Shang, S., Hu, L., Chen, H., Wang, P., et al. (2020). Disrupted functional network connectivity predicts cognitive impairment after acute mild traumatic brain injury. *CNS Neurosci. Ther.* 26, 1083–1091. doi: 10.1111/cns.13430

Liu, M., Gao, Y., Sun, G., Dong, M., Yin, T., Tian, Z., et al. (2020). The spontaneous activity pattern of the middle occipital gyrus predicts the clinical efficacy of acupuncture treatment for migraine without aura. *Front. Neurol.* 11:588207. doi: 10.3389/fneur.2020.588207

Lo Buono, V., Bonanno, L., Corallo, F., Pisani, L. R., Lo Presti, R., Grugno, R., et al. (2017). Functional connectivity and cognitive impairment in migraine with and without aura. *J. Headache Pain* 18:72. doi: 10.1186/s10194-017-0782-6

Lu, C., Yang, T., Zhao, H., Zhang, M., Meng, F., Fu, H., et al. (2016). Insular cortex is critical for the perception, modulation, and chronification of pain. *Neurosci. Bull.* 32, 191–201. doi: 10.1007/s12264-016-0016-y

Mennini, F. S., Gitto, L., and Martelletti, P. (2008). Improving care through health economics analyses: Cost of illness and headache. *J. Headache Pain* 9, 199–206. doi: 10.1007/s10194-008-0051-9

Menon, B. (2019). Towards a new model of understanding -The triple network, psychopathology and the structure of the mind. *Med. Hypotheses* 133:109385. doi: 10.1016/j.mehy.2019.109385

Menon, V. (2011). Large-scale brain networks and psychopathology: A unifying triple network model. *Trends Cogn. Sci.* 15, 483–506. doi: 10.1016/j.tics.2011.08.003

Mu, J., Chen, T., Quan, S., Wang, C., Zhao, L., and Liu, J. (2020). Neuroimaging features of whole-brain functional connectivity predict attack frequency of migraine. *Hum. Brain Mapp.* 41, 984–993. doi: 10.1002/hbm.24854

Pérez Benito, F. J., Conejero, J. A., Sáez, C., García Gómez, J. M., Navarro Pardo, E., Florencio, L. L., et al. (2019). Subgrouping factors influencing migraine intensity in women: A semi-automatic methodology based on machine learning and information geometry. *Pain Pract.* 20, 297–309. doi: 10.1111/papr.12854

Russo, A., Tessitore, A., Giordano, A., Corbo, D., Marcuccio, L., De Stefano, M., et al. (2012). Executive resting-state network connectivity in migraine without aura. *Cephalalgia* 32, 1041–1048. doi: 10.1177/0333102412457089

Schwedt, T. J., Chiang, C., Chong, C. D., and Dodick, D. W. (2015). Functional MRI of migraine. *Lancet Neurol.* 14, 81–91. doi: 10.1016/S1474-4422(14)70193-0

Tan, L. L., Pelzer, P., Heinl, C., Tang, W., Gangadharan, V., Flor, H., et al. (2017). A pathway from midcingulate cortex to posterior insula gates nociceptive hypersensitivity. *Nat. Neurosci.* 20, 1591–1601. doi: 10.1038/nn.4645

Ter Minassian, A., Ricalens, E., Humbert, S., Duc, F., Aubé, C., and Beydon, L. (2013). Dissociating anticipation from perception: Acute pain activates default mode network. *Hum. Brain Mapp.* 34, 2228–2243. doi: 10.1002/hbm.22062

Tu, Y., Zeng, F., Lan, L., Li, Z., Maleki, N., Liu, B., et al. (2020). An fMRI-based neural marker for migraine without aura. *Neurology* 94, e741–e751. doi: 10.1212/WNL.0000000000008962

Wang, M., Su, J., Zhang, J., Zhao, Y., Yao, Q., Zhang, Q., et al. (2017). Visual cortex and cerebellum hyperactivation during negative emotion picture stimuli in migraine patients. *Sci. Rep.* 7:41919. doi: 10.1038/srep41919

Wei, H., Chen, J., Chen, Y., Yu, Y., Guo, X., Zhou, G., et al. (2020). Impaired effective functional connectivity of the sensorimotor network in interictal episodic migraineurs without aura. *J. Headache Pain* 21:111. doi: 10.1186/s10194-020-01176-5

Wei, H., Li, J., Guo, X., Zhou, G., Wang, J., Chen, Y., et al. (2021). Functional connectivity of the visual cortex differentiates anxiety comorbidity from episodic migraineurs without aura. *J. Headache Pain* 22:40. doi: 10.1186/s10194-021-01259-x

Yadav, M. P., Ballal, S., Meckel, M., Roesch, F., and Bal, C. (2020). [177Lu]Lu-DOTA-ZOL bone pain palliation in patients with skeletal metastases from various cancers: Efficacy and safety results. *EJNMMI Res.* 10, 1–13. doi: 10.1186/s13550-020-00709-y

Yang, J., Zeng, F., Feng, Y., Fang, L., Qin, W., Liu, X., et al. (2012). A PET-CT study on the specificity of acupoints through acupuncture treatment in migraine patients. *BMC Complement. Altern. Med.* 12:123. doi: 10.1186/1472-6882-12-123

Yu, D., Yuan, K., Luo, L., Zhai, J., Bi, Y., Xue, T., et al. (2017). Abnormal functional integration across core brain networks in migraine without aura. *Mol. Pain* 13:19341042. doi: 10.1177/1744806917737461

Zhang, J., Su, J., Wang, M., Zhao, Y., Yao, Q., Zhang, Q., et al. (2016). Increased default mode network connectivity and increased regional homogeneity in migraineurs without aura. *J. Headache Pain* 17:98. doi: 10.1186/s10194-016-0692-z

Zou, Y., Tang, W., Li, X., Xu, M., and Li, J. (2019). Acupuncture reversible effects on altered default mode network of chronic migraine accompanied with clinical symptom relief. *Neural Plast.* 2019, 1–10. doi: 10.1155/2019/5047463

Advantages of publishing in Frontiers

OPEN ACCESS
Articles are free to read for greatest visibility and readership

FAST PUBLICATION
Around 90 days from submission to decision

HIGH QUALITY PEER-REVIEW
Rigorous, collaborative, and constructive peer-review

TRANSPARENT PEER-REVIEW
Editors and reviewers acknowledged by name on published articles

Frontiers
Avenue du Tribunal-Fédéral 34
1005 Lausanne | Switzerland

Visit us: www.frontiersin.org
Contact us: frontiersin.org/about/contact

REPRODUCIBILITY OF RESEARCH
Support open data and methods to enhance research reproducibility

DIGITAL PUBLISHING
Articles designed for optimal readership across devices

FOLLOW US
@frontiersin

IMPACT METRICS
Advanced article metrics track visibility across digital media

EXTENSIVE PROMOTION
Marketing and promotion of impactful research

LOOP RESEARCH NETWORK
Our network increases your article's readership